WASTE BIOREFINERIES: FUTURE ENERGY, GREEN PRODUCTS AND WASTE TREATMENT

EDITED BY: Mohammad Rehan, Abdul-Sattar Nizami, Umer Rashid and Muhammad Raza Naqvi

PUBLISHED IN: Frontiers in Energy Research and Frontiers in Bioengineering and Biotechnology

frontiers Research Topics

ISSN 1664-8714
ISBN 978-2-88945-993-3
DOI 10.3389/978-2-88945-993-3

About Frontiers

Frontiers is more than just an open-access publisher of scholarly articles: it is a pioneering approach to the world of academia, radically improving the way scholarly research is managed. The grand vision of Frontiers is a world where all people have an equal opportunity to seek, share and generate knowledge. Frontiers provides immediate and permanent online open access to all its publications, but this alone is not enough to realize our grand goals.

Frontiers Journal Series

The Frontiers Journal Series is a multi-tier and interdisciplinary set of open-access, online journals, promising a paradigm shift from the current review, selection and dissemination processes in academic publishing. All Frontiers journals are driven by researchers for researchers; therefore, they constitute a service to the scholarly community. At the same time, the Frontiers Journal Series operates on a revolutionary invention, the tiered publishing system, initially addressing specific communities of scholars, and gradually climbing up to broader public understanding, thus serving the interests of the lay society, too.

Dedication to Quality

Each Frontiers article is a landmark of the highest quality, thanks to genuinely collaborative interactions between authors and review editors, who include some of the world's best academicians. Research must be certified by peers before entering a stream of knowledge that may eventually reach the public - and shape society; therefore, Frontiers only applies the most rigorous and unbiased reviews.
Frontiers revolutionizes research publishing by freely delivering the most outstanding research, evaluated with no bias from both the academic and social point of view. By applying the most advanced information technologies, Frontiers is catapulting scholarly publishing into a new generation.

What are Frontiers Research Topics?

Frontiers Research Topics are very popular trademarks of the Frontiers Journals Series: they are collections of at least ten articles, all centered on a particular subject. With their unique mix of varied contributions from Original Research to Review Articles, Frontiers Research Topics unify the most influential researchers, the latest key findings and historical advances in a hot research area! Find out more on how to host your own Frontiers Research Topic or contribute to one as an author by contacting the Frontiers Editorial Office: researchtopics@frontiersin.org

WASTE BIOREFINERIES: FUTURE ENERGY, GREEN PRODUCTS AND WASTE TREATMENT

Topic Editors:
Mohammad Rehan, King Abdulaziz University, Saudi Arabia
Abdul-Sattar Nizami, King Abdulaziz University, Saudi Arabia
Umer Rashid, Universiti Putra Malaysia, Malaysia
Muhammad Raza Naqvi, Karlstad University, Sweden

Energy recovery from waste resources holds a significant role in the sustainable waste management hierarchy to support the concept of circular economies and to mitigate the challenges of waste originated problems of sanitation, environment, and public health. Today, waste disposal to landfills is the most widely used methodology, particularly in developing countries, because of limited budgets and lack of efficient infrastructure and facilities to maintain efficient and practical global standards. As a consequence, the dump-sites or non-sanitary landfills have become the significant sources of greenhouse gases emissions, soil and water contamination, unpleasant odors, leachate, and disease spreading vectors, flies, and rodents. However, waste can be utilized to produce a range of potential products such as energy, fuels and value-added products under waste biorefineries.

A holistic and quantitative view, such as waste biorefinery, on waste management must be linked to the actual country, taking into account its socio-economic situation, local waste sources, and composition, as well as the available markets for the recovered energy and products. Therefore, it is critical to understand that solutions cannot be just copied from one region to the others. In fact, all waste handling, transportation, and treatment can represent a burden to the cities' environment and macro and micro economics, except for the benefits obtained from recovered materials and energy. Equally significant is a clear and quantitative understanding of the industrial, and public potential of utilizing recovered materials and energy in the markets as these can be reached without exacerbating the environmental issues using excessive transport.

The book explores new advancements and discoveries on the development of emerging waste-to-energy technologies, practical implementation, and lessons learned from sustainable wastemanagement practices under waste biorefinery concept, which will accelerate the growth of circular economies in the world. The articles presented in this book have been written by expert researchers and academics working in institutions at different countries across the world including Germany, Greece, Japan, South Korea, China, Saudi Arabia, Pakistan, Indonesia, Malaysia, Iran, and India. The research articles have been arranged into three main subject categories; 1) Resource recovery from waste, 2) Waste to energy technologies and 3) Waste biorefineries. This book will serve as an important resource for research students, academics, industry, policy makers, and government agencies working in the field of integrated waste management, energy and resource recovery, waste to energy technologies, waste biorefineries etc. The editorial team of this book is very grateful to all the authors for their excellent contributions and making the book successful.

Citation: Rehan, M., Nizami, A.-S., Rashid, U., Naqvi, M. R., eds. (2019). Waste Biorefineries: Future Energy, Green Products and Waste Treatment. Lausanne: Frontiers Media. doi: 10.3389/978-2-88945-993-3

Table of Contents

frontiers in Energy Research

EDITORIAL
published: 12 June 2019
doi: 10.3389/fenrg.2019.00055

Editorial: Waste Biorefineries: Future Energy, Green Products and Waste Treatment

Mohammad Rehan[1], Abdul-Sattar Nizami[1], Umer Rashid[2] and Muhammad Raza Naqvi[3]*

[1] Centre of Excellence in Environmental Studies (CEES), King Abdulaziz University, Jeddah, Saudi Arabia, [2] Institute of Advanced Technology, Universiti Putra Malaysia, Seri Kembangan, Malaysia, [3] Department of Engineering and Chemical Sciences, Karlstad University, Karlstad, Sweden

Keywords: waste-to-energy, waste biorefinery, green products, biofuels, bioenergy

Editorial on the Research Topic

Waste Biorefineries: Future Energy, Green Products and Waste Treatment

Energy recovery from waste resources holds a significant role in the sustainable waste management hierarchy to support the concept of circular economies and to mitigate the challenges of waste originated problems of sanitation, environment, and public health. Today, waste disposal to landfills is the most widely used methodology, particularly in developing countries, because of limited budgets and lack of efficient infrastructure and facilities to maintain efficient and practical global standards. As a consequence, the dump-sites or non-sanitary landfills have become the significant sources of greenhouse gases emissions, soil and water contamination, unpleasant odors, leachate, and disease spreading vectors, flies, and rodents. However, waste can be a potential source of energy, fuels, and value-added products, if appropriately and wisely managed.

This Frontiers Research Topic was designed to collect new advancements and discoveries on the development of emerging waste-to-energy technologies, practical implementation, and lessons learned from sustainable waste management practices under waste biorefinery concept (**Figure 1**), which will accelerate the growth of circular economies in the world. This Frontiers Research Topic has attracted and compiled 13 top quality research and review articles. The articles have been written by researchers and academics working in institutions at different countries across the world including Germany, Netherlands, Greece, South Korea, Japan, Hong Kong, Saudi Arabia, Pakistan, Indonesia, Malaysia, Iran, and India. The editorial team of this research topic is very grateful to all the authors for their excellent contributions and making the research topic successful.

RESOURCE RECOVERY FROM WASTE

A wide range of resources, such as energy, fuels, chemicals, and other by-products, can be recovered from waste using different technologies. The article Saghir et al. in this research topic demonstrates how energy deficient countries like Pakistan can generate significant amounts of renewable energy from biomass waste. The authors further discussed the two major classes of the techniques for the processing of biomass into bioenergy, such as (1) thermo-chemical conversion techniques including direct combustion, liquefaction, transesterification, gasification and pyrolysis; and (2) biochemical decomposition techniques including anaerobic decomposition and fermentation.

Biofuels are emerging as alternative clean fuels to replace the fossil fuels that contributed to huge environmental damage and climate change. An interesting study, Akhtar et al. showed the production of biodiesel from non-edible sterculia foetida (Bottle Tree) using CuO-CeO_2 and Fe_2O_3 nanocatalysts using transesterification technology. Organic residual streams, such as food waste,

Edited and reviewed by:
Uwe Schröder, Technische Universitat Braunschweig, Germany

****Correspondence:***
Mohammad Rehan
dr.mohammad_rehan@yahoo.co.uk

Specialty section:
This article was submitted to Bioenergy and Biofuels, a section of the journal Frontiers in Energy Research

Received: *04 May 2019*
Accepted: *23 May 2019*
Published: *12 June 2019*

Citation:
Rehan M, Nizami A-S, Rashid U and Naqvi MR (2019) Editorial: Waste Biorefineries: Future Energy, Green Products and Waste Treatment. Front. Energy Res. 7:55. doi: 10.3389/fenrg.2019.00055

FIGURE 1 | Waste biorefinery concept.

also have great potential as an alternative resource to produce chemicals and fuels, since they are renewable and do not compete with the human food chain. For example, medium chain fatty acids (MCFAs), such as n-caproate, are potential valuable platform chemicals that can be produced from low-grade organic residues. The study Roghair et al. focused on the production of MCFAs from food waste by anaerobic reactor microbiomes through two subsequent biological processes: hydrolysis combined with acidogenesis and chain elongation. The authors have claimed to set the record for producing the highest concentration of n-caproate (25.7 g/L) observed in a chain elongation process to date. Moreover, the study notably demonstrates that such high concentrations can be obtained from food waste under practical circumstances in a continuous process.

WASTE TO ENERGY TECHNOLOGIES

Energy can be recovered from waste in the form of fuels, heat, and electricity using a wide range of available waste to energy technologies. However, more research and development work is needed to optimize these technologies for achieving maximum economic, environmental and social benefits. A study Prajapati et al. published in this research topic proposed a new method for enhanced methane production from agriculture waste. The same idea can be tested and applied for other wastes such as food waste to produce cleaner biogas for energy applications.

Another study Hanum et al. highlighted the challenges and possible solutions of treating sewage sludge via anaerobic digestion. The authors presented the case study of Malaysia and how the energy can be recovered from huge waste in this country. The deep understanding of chemistry, thermodynamics, and kinetics of reactions involved in any process is crucial for process control and optimization. A study, Ali and Bahadar presented detailed kinetics of pyrolysis of macro-algae using a simple order-based model compared with the versatile Šesták-Berggren (SB) model considering combined and multiple reactions.

WASTE BIOREFINERIES

Waste biorefineries are attracting significant interest worldwide as sustainable waste management solutions as well as facilities to produce fuels, power, heat, and value-added products. This research topic attracted many articles on recent developments and challenges associated with waste biorefineries based on a range of waste. For example, authors have presented detailed experimental data of pyrolysis of plastic waste and way forward to develop pyrolysis based biorefineries using plastic, biomass, and other waste in Miandad et al.. The authors have also discussed the many technical, operational, and socio-economic challenges, and the potential of biorefineries to achieve circular economies.

Other interesting studies published on possibilities of waste biorefineries using waste sludge from water treatment plants (Cheng et al.), used cooking oil (Rahimzadeh et al.), co-digestion of plant biomass and poultry waste (Shah et al.), and co-digestion of catering and agro-industrial waste (Anjum et al.). These studies not only illustrate the possibilities of obtaining different products from a wide range of wastes, but some also showcase studies of corresponding countries.

There could be many ideas and prospects for optimizing waste based biorefineries. For example, the study Wambugu et al. showed the positive role of biochar in food waste based biorefineries. The biochar enhanced the performance of the anaerobic digestion system. The sustainable waste biorefinery facilities represent multifactorial systems that necessitate the organization, cooperation and the acceptance of different social stakeholders. A comprehensive study Kokkinos et al. was published in the research topic in which a novel Fuzzy Cognitive Map (FCM) modeling approach was proposed in order to analyze the socio-economic implications and to overcome multiple uncertainties occurring in sustainable WBF development and implementation.

OUTLOOK

Waste management in a sustainable and environment-friendly manner is a crucial issue to protect the environment and human health. This research topic highlights the potential and recent developments in waste biorefineries as a sustainable solution to treat waste. Multiple resources such as energy, fuels, chemicals, and other value-added products can be recovered from waste through waste biorefineries. The research topic also highlights the challenges and potential solutions in developing waste based biorefineries from treating different types of waste such as food waste, plastic waste, organic waste, biomass, and agriculture waste. One of the most essential area to work on is to figure out smart ways of integrating different technologies

under one platform of biorefinery for achieving maximum socio-economic and environmental benefits.

AUTHOR CONTRIBUTIONS

MR wrote the initial editorial draft. A-SN critically reviewed and corrected the initial draft. UR and MN read and approved the final draft. A-SN was responsible for editing 5 chapters, MR: 4 chapters, and MN: 1 chapter, in this research topic.

Conflict of Interest Statement: The authors declare that the research was conducted in the absence of any commercial or financial relationships that could be construed as a potential conflict of interest.

frontiers in Energy Research

REVIEW
published: 22 March 2019
doi: 10.3389/fenrg.2019.00024

Unlocking the Potential of Biomass Energy in Pakistan

Muhammad Saghir[1], Shagufta Zafar[2], Amiza Tahir[2], Miloud Ouadi[1], Beenish Siddique[1] and Andreas Hornung[1,3]*

[1] Department of Chemical Engineering, University of Birmingham, Birmingham, United Kingdom, [2] Department of Chemistry, Government Sadiq College Women University, Bahawalpur, Pakistan, [3] Fraunhofer Institute for Environmental, Safety, and Energy Technology UMSICHT, Sulzbach Rosenberg, Germany

Being a developing economy, Pakistan is facing a severe energy crisis that limits its economic development. Pakistan relies heavily on energy resources like natural gas, oil, hydropower, nuclear, coal and liquefied petroleum gas (LPG) which contribute as 48.3, 32.1, 11.3, 7.6, and 0.6% of the primary energy supply, respectively. Because of the rapidly growing population and economy, Pakistan's energy needs are huge; to accomplish these energy necessities, Pakistan is continually spending $7–9 billion on the import of fossil fuels. To resolve the serious issues of energy availability, the Alternative Energy Development Board (AEDB) of Pakistan is currently exploring the development of renewable energy technologies in Pakistan that will be beneficial for the developing economy so that Pakistan might be able to minimize the growing energy crisis. Out of all the renewable energy resources, biomass is considered the best and most easily accessible source of energy with its unique environmentally friendly nature, constant supply, wider availability, and ease of integration into existing infrastructure. Despite the presence of an abundance of biomass energy resources, there is still a need for work on the use of these sources to produce energy. This literature review explores the availability of biomass resources in Pakistan and their potential for addressing rapidly growing energy demand in the country, which can assist in the stabilization of a Pakistan's energy demand for challenged economic development.

Keywords: biomass, bioenergy, pyrolysis, gasificaiton, energy, biochar

OPEN ACCESS

Edited by:
Muhammad Raza Naqvi, Karlstad University, Sweden

Reviewed by:
Mohammad Zain Khan, Aligarh Muslim University, India
Lucian Toma, Politehnica University of Bucharest, Romania

****Correspondence:***
Muhammad Saghir
m.saghir@bham.ac.uk

Specialty section:
This article was submitted to Bioenergy and Biofuels, a section of the journal Frontiers in Energy Research

Received: *12 November 2018*
Accepted: *14 February 2019*
Published: *22 March 2019*

Citation:
Saghir M, Zafar S, Tahir A, Ouadi M, Siddique B and Hornung A (2019) Unlocking the Potential of Biomass Energy in Pakistan. Front. Energy Res. 7:24. doi: 10.3389/fenrg.2019.00024

INTRODUCTION

The current population of Pakistan is 198,139,348 (198 million) with an annual growth rate of 1.97% based on the most recent United Nations approximations.[1] Within various sectors of, such as domestic consumption, commercial consumption, agriculture, public lighting and bulk supply, the expenditure of energy is 45.7, 7.5, 28.1, 11.8, 0.5, and 6.4%, respectively (Aziz, 2013). Agriculture is the second largest sector of Pakistan's economy, comprising five subsectors with major crops, minor crops, livestock, fisheries, and forestry having a collective share of 21% of the total Gross Domestic Product (GDP) (Raza et al., 2012; Chandio et al., 2016). Major crops, minor crops, livestock, and forestry contribute 5.3, 2.3, 11.8, and 0.4%, respectively, to the total GDP (Chandio et al., 2016). Agriculture is the backbone of Pakistan's economy as most of the exports from Pakistan are based on agricultural products including rice, cotton, wheat, sugarcane, and many other major and minor

[1]Worldometer: Population. http://www.worldometers.info/world-population/pakistan-population/ 2017

products (Faridi, 2012). Presently, Pakistan is facing a severe and unmanageable energy crisis that is hindering socio-economic development (Mirza et al., 2008a; Aziz, 2013).

The Energy Situation in Pakistan

The industrial and agricultural sectors are the backbones of the economy, and the progress of the economy is directly linked to the constant availability of energy resources (Abbas, 2015). The main hindrance to the economic development of Pakistan is its poor division of risky energy resources. The power sector of Pakistan remains unsuccessful in overcoming the energy-related issues despite being rich in coal resources (Arif, 2011). Michael Kugelman (Javed et al., 2016) acknowledged in his remarks on Pakistan's energy situation in the National Bureau of Asian Research of America, "Pakistan is mired in an acute energy crisis, one with immense implications for both the nation's floundering economy and its volatile security situation." At periods of high demand in Pakistan, the electricity supply gap is ∼6,000 MW, which accounts for 33–35% of the total expenditures (Abbas, 2015; Saeed et al., 2015). Pakistan has more than 30% of its population (55 million) with no access to electricity (Harijan et al., 2008; Saeed et al., 2015). In urban and rural areas the duration of power outages is 6–12 and 12–18 h per day, respectively (Saeed et al., 2015).[2] Pakistan relies heavily on energy resources like natural gas, oil, hydro, nuclear, coal, and liquefied petroleum gas (LPG), each of which contributes 48.3, 32.1, 11.3, 7.6, and 0.6%, respectively, to the primary energy supply (Rehman et al., 2013). According to recent statistics by AEDB, the share of various resources of energy, along with a contribution of 2% from renewable energy, resources involve natural gas (21%), hydropower (31%), Oil (39%), LNG (4%), and nuclear power (3%).[2] Moreover, relevant figures for the energy mix have also been supported by the Hydrocarbon Development Institute of Pakistan (HDIP). During 2013, dependence on various sources made up an 80.8% share of natural resources [oil (30.8%), gas (49.5%), coal (87.4%), and liquefied petroleum gas (0.5%)], with a 12.5% share coming from the remaining sources [hydro-power (10.5%), nuclear electricity (1.9%) and imported electricity (0.1%)] (Shaikh et al., 2015). Widening power supply and demand gaps from 1980 to 2012 are shown in **Table 1** (Mahmood and Ayaz, 2018).[3] Kessides (2013) explored the entire energy scenario of Pakistan, developing a projection of the future stating that electricity outages are expected to increase to 13,000 MW by 2020 (**Figure 1**).

TABLE 1 | Energy Demand and Supply Share in Pakistan for the period 1980–2012[3].

Energy source	Energy demand (%)	Energy supply (%)
Coal	0.7	0.8
Electricity	10	14
Natural gas	44	51
Petroleum	39	27

Effects of Energy Crisis

The economic development of any country relies on energy availability as energy is the engine of the economy (Lee and Chang, 2008; Sadorsky, 2010; Kakar et al., 2011). Economical productivity exhibits an increase concomitant with that of the increase in available energy resources. Likewise, energy crisis leads to serious impacts on the economy of a country through its adverse impacts on employment, marketing, and poverty (Cleveland et al., 1984; Kessides, 2013). Because of the heavy shortfall in energy production vs. demand, not only domestic but also various dimensions of the industrial sectors are also badly affected (Khan and Ahmad, 2008; Aziz, 2013; Saeed et al., 2015). Sixty to seventy percent (60–70%) of industrial investors have shifted their businesses to other countries, such as China, India, and Bangladesh, which is attributed to the increase in the energy shortfall, which reaches 40% (Asif, 2009; Saeed et al., 2015). In this period of industrialization and globalization, increasing energy demand cannot be accompanied by only depending on natural resources. Since the mid-1970s, natural energy resources have been running low and considerable efforts have been made to produce energy through renewable energy technologies (Mohan et al., 2006). Not only is the industrial sector affected, but agricultural productivity is also adversely affected by the rapid decrease in affordable energy availability, as the proper functioning of all the tools for agriculture—i.e., for transportation, pesticides and irrigation—are based on the application of energy (Pimentel et al., 1973). Pakistan is not only facing this severe electricity crisis, but a shortage of petroleum products and water scarcity have also become serious issues (Khan et al., 2012). Kessides (2013) in his recent publication described the severe energy crisis in Pakistan. He related severe energy issues with the lack of proper forecasting and planning together with the increasing domestic necessity. Severe blackouts in Pakistan are pushing the country toward concerning levels of poverty and create a negative impact on employment, global competitiveness and exports. The effects of energy disruption and electrical failures are so intensive that they declined the growth rate of the economy by 2% of the original figure of 6.5% per annum (GOP, 2013; Komal and Abbas, 2015). Kugelman (2013) stated that the unavailability of indispensable energy to the various economical sectors has resulted in an annual decline of up to 4% in the total GDP. Siddiqui et al. (2008) reported a survey describing the impacts of power crisis on the employment, production cost, and supply orders. Employment demand for labor in the industrial sector of Pakistan is adversely impacted. The resulting unemployment and labor loss per day varies from industry to industry and the results for different industries are shown in **Figure 2**.

Energy or Electricity Theft in Pakistan

Of all the electricity generated every year in Pakistan, a large segment is either stolen or lost in the distribution process. Besides the transmission losses and electricity theft, a significant fraction of the electricity consumed remains unpaid for. Islamabad Electricity Supply Company (IESCO), Lahore Electricity Supply

[2]Alternative-Energy-Development-Board, Ministry of Water and Power, Government of Pakistan [http://www.aedb.org/].
[3]https://www.eia.gov/beta/international

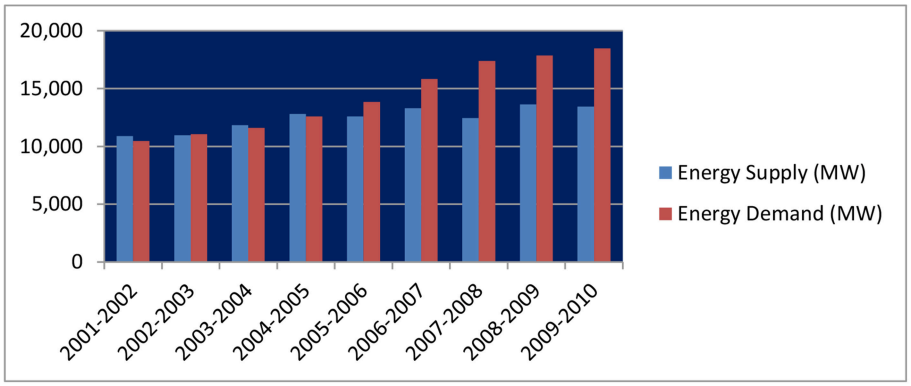

FIGURE 1 | Energy scenario of Pakistan with the supply and demand gap (Kessides, 2013; Khan et al., 2014).

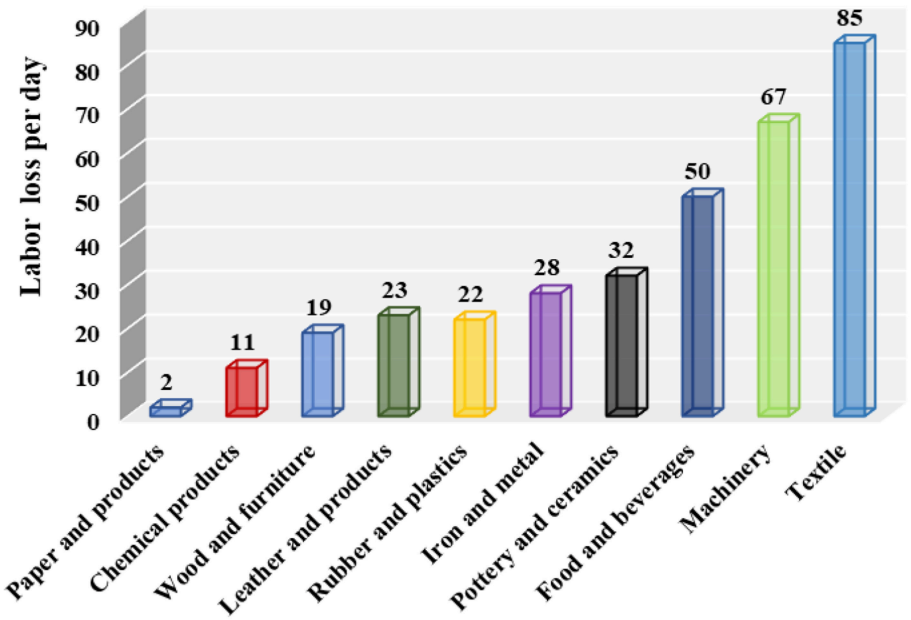

FIGURE 2 | Labor loss per day in different industries due to the energy crisis.

Company (LESCO), Gujranwala Electric Power Company (GEPCO), Faisalabad Electricity Supply Company (FESCO), Multan Electric Power Company (MEPCO), Peshawar Electricity Supply Company (PESCO), Quetta Electricity Supply Company (QESCO), Hyderabad Electricity Supply Company (HESCO), and Karachi Electric Supply Company (KESC) are the major power distribution companies in Pakistan (Jamil and Ahmad, 2014). The collective transmission loss of all the distributing companies was reported to be 20.4% by 2010, with the average loss exceeding 20–25% per year. Jamil and Ahmad (2014) submitted a detailed analysis of electricity theft and transmission losses throughout the country. During 201–13, the recorded transmission losses for the IESCO, PESCO, and KESC were 9.5, 36, and 40% respectively. They discovered that 17.8 million consumers were supplied with 92,480 GWh, and ∼18,919 GWh remained unpaid for in 2010. The illegal consumption and stealing of electrical power can be prevented by the implementation of strict laws of accountability, strategies and action plans alongside the establishment of good political governance.

Effects of Gas Shortage

In the previous decade, Pakistan was self-reliant in natural gas. However, currently, widespread utilization of natural gas in industry, domestic affairs, and transportation has led to a gas shortage in Pakistan. During 2001–2008, a significant elevation of 10% yearly in gas use was reported. Natural gas provides 31.9% of the overall national energy expenditure and 29% of electricity production (Awan and Rashid, 2012). The Ministry of Petroleum and Natural Resources reported that the growth rate

of production of natural gas increased by 2.6%, which occurred alongside a growth rate of 4.4% in the consumption of gas. The consumption of natural gas in various sectors of Pakistan is shown in **Figure 3** (Dawood et al., 2013). The textile industry of Pakistan is one of the biggest industries of the country, covering about 60% of total exports and having a net worth of $9 billion. This textile industry is also adversely affected by the gas crisis (Khan and Khan, 2010).

Effects of Oil-Shortage

The International Energy Agency has reported that the rise of oil consumption, on average, will be from 85 million barrels to 113 million barrels by 2030 (Howden, 2007). In Pakistan, the energy yearbook describes a 35.5% increase in the share of oil consumption, which surely can be a reason for oil depletion (**Figure 4**).[4] In Pakistan, oil utilization is equivalent to 490 kilograms, with the commercial share of oil in the production of electricity being 19% (Husain, 2010; Javaid et al., 2011). There is a huge gap between oil production and consumption, with production equaling 64,000 barrels per day and consumption surpassing 351,400 barrels per day (Sahir and Qureshi, 2008; Zuberi et al., 2013). The consumption of oil and gas has grown so fast that the remaining reserves are reported to last for 19 and 10 years respectively (Muneer et al., 2006; Asif, 2009). The depletion of natural gas and oil reserves not only affects agriculture and transport, but a reduction in industrial productivity has also been noticed (Asif, 2009). The majority of the natural oil reserves of Pakistan have been consumed, and due to this reason Pakistan is spent $6.7 billion on oil imports during 2005–06 with an increase in growth rate of 1% per year (Ashraf Chaudhry et al., 2009; Awan and Rashid, 2012).[5] Currently, studied sources of renewable energy in Pakistan are solar, wind, hydro and biomass. A great number of industries in Pakistan are at present dependent on liquid fuels to fulfill their electricity and heating requirements (Saeed et al., 2015). Unfortunately, accessing universal energy is also a large concern in the country. More than 20,920 villages in the country are so far to be electrified.[5] This energy dilemma is further exacerbated because there is no connection to the national electricity grid for some of these remote villages. Thus, decentralized electricity provision is the only cost-effective solution for them.

Reasons for Critical Power Outages

Continuous power interruptions negatively affect economic activities. The obvious reduction in Pakistan's economic productivity is due to power cuts that exceeded 8,000 MW until 2012. Experts analyzed various aspects of the critical power situation in Pakistan and provided reasons for these drastic shortfalls; one of these is that the relevant organizations and institutes have failed to enhance electricity generation and capacity according to supply demands, which leads to drastic energy deficits. Other major reasons include the decline in natural energy reserves, severe water shortfalls, rapidly increasing demand, excessive dependency on imported petroleum products, circular debt and other significant political and governance issues (Malik, 2012; Munir and Khalid, 2012; Nawaz et al., 2013; Rashid Amjad, 2015). Mismanagement and poor administration are also significant factors behind energy issues due to nepotism, corruption, incompetent generation or limited capacity addition, inefficient and outdated transmission systems, financial malefaction, non-optimal tariffs and reliance on expensive fuels (Malik, 2012; Nawaz et al., 2013; Ullah, 2013; Ahmed et al., 2015; Rashid Amjad, 2015). In general, the unskilled and undereducated political leaders and policymakers, low investments by the government, lacking proper vision and accountability, and instability of governance have all led to the power crisis in the country. Delays in payments by the government to the relevant power generation agencies is another huge issue that has lead to the growth of this crisis (Malik, 2012; Munir and Khalid, 2012; Kugelman, 2013; Rashid Amjad, 2015).

The Policy for Energy Production

Efficient policies and proper planning can prevent severe power outages and expanding crisis. Pakistan needs good and efficient governance for broad-based planning to overcome the energy shortfalls. In the designing of reliable policies, many factors are taken into consideration, such as valid and reliable forecast for future demand on the basis of past trends, appropriate development and assessment of technologies, energy conservation, improved policies of long-term and short-term planning to compensate for the energy demand and effective project management (Mathur, 2001; Chikkatur et al., 2009; Østergaard and Sperling, 2014). There are numerous concerns for policy-makers in the formation and management of long-term reliable energy policies, such as energy security, climate change and natural fuel depletion (Turton and Barreto, 2006; Østergaard and Sperling, 2014; Overland, 2016). Energy security refers to the availability of affordable energy without interruptions, which is crucial for economic development (Turton and Barreto, 2006; Hogan et al., 2007).

Reliable energy policy and planning take into account the following important factors, such as the following (Mathur, 2001; Qureshi, 2009; Balat, 2010; Valasai et al., 2017):

- Focusing on renewable energy sources
- Focusing on the cost-effective generation of electricity
- Increasing resources to overcome energy deficits
- Conservation of energy
- Reducing the energy vs. supply demand gaps
- Improving the energy infrastructure to reduce the system losses

Various past governments of Pakistan have also put forward a number of different policies which were reshaped occasionally, including the national energy policies of 1994, 1995, 1998, 2002, 2005, 2006, 2010–2012, and 2013 (**Table 2**) (Munir and Khalid, 2012; Dawood et al., 2013; Abbas, 2015; Valasai et al., 2017).

For bridging the supply and demand gap, the Government of Pakistan (GOP) has recognized alternative and renewable energy (ARE) sources as one of the best preference (Aziz, 2013; Saeed et al., 2015). Pakistan had made a strategy to add a minimum

[4]Pakistan Energy Year Book 2015 published by Hydrocarbon Development Institute of Pakistan (HDIP) MoPNR, Government of Pakistan.

[5]An overview of Fossil Fuels in Pakistan PEY, 2004 by Ministry of Petroleum and Natural Resources, Government of Pakistan.

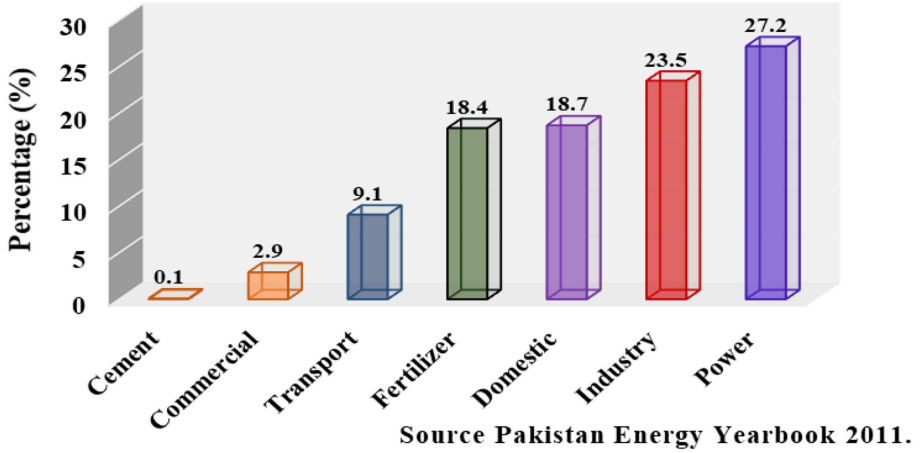

FIGURE 3 | Sector-based division of the consumption of natural gas in Pakistan (Dawood et al., 2013).

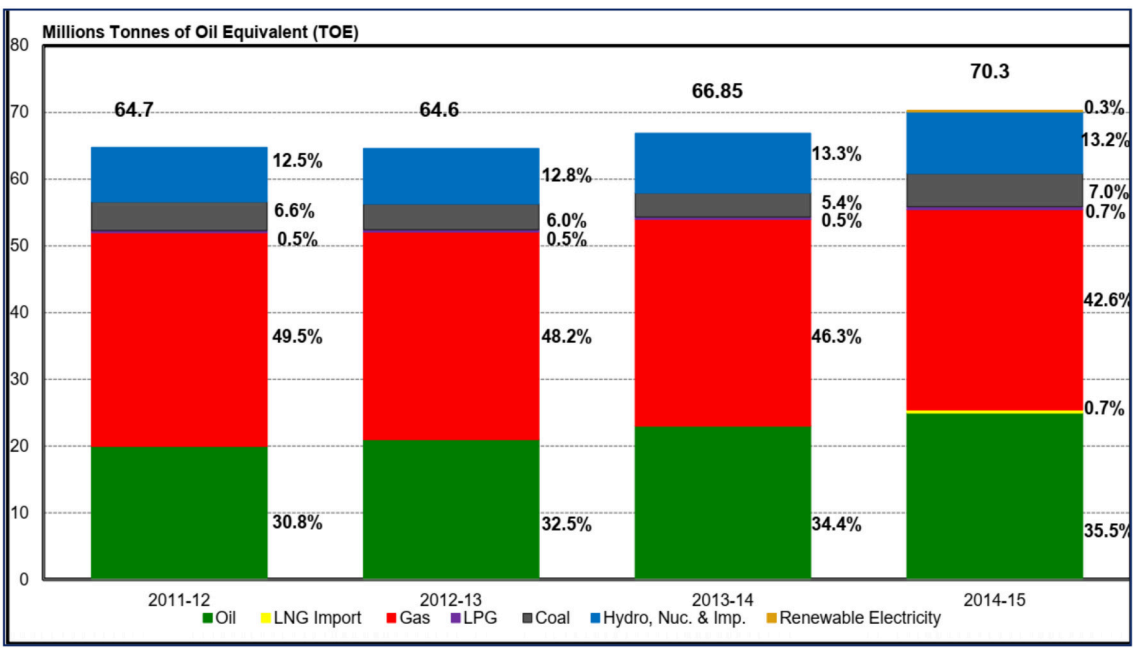

FIGURE 4 | Primary energy supplies by source[4].

of 9.7 GW of renewable energy by 2030 in the national energy mix. The industrial sector contributes about 40% of the country's GDP. But owing to the deficiency in energy, a large number of these industrial units are dependent on expensive and polluting diesel generation units to meet their energy demand.[5] Various industries, such as rice mills, wood processing mills, brick kilns, cement kilns, and metal processing are heavily dependent on heat energy. They frequently burn fossil fuels and some biomass to sustain their energy needs.[5] So now, Pakistan is in dire need of advanced conversion technologies, such as biomass combustion, gasification and pyrolysis. Such technologies have been effectively installed in various countries around the globe (Mirza et al., 2008a; Saeed et al., 2015).[5] The global daily expenditure of oil currently stands at 85 million barrels, which will be increased to 113 million barrels by 2030 (Howden, 2007). Energy resources that are used at present will not be able to cope with future energy necessities because Pakistan's fossil fuel reserves are diminishing rapidly and the demand of energy is expected to exceed 66,000 MW or 66 GW by 2030 (Howden, 2007; Zuberi et al., 2013). Modern society and economic development would not be realistic without energy; thus, a continuous decline in fossil fuels has forced the relevant agencies to plan alternative ways to produce sustainable energy (Qureshi, 2009; Valasai et al., 2017). The energy produced by renewable sources or

TABLE 2 | National energy policies of Pakistan with their major focus (Abbas, 2015; Valasai et al., 2017).

Year	Policy	Focus
1994	Energy Policy (First Formal Policy)	Introduced Independent Power Producers (IPPs) and emphasized energy conservation.
1995	Hydropower Power Policy	1994 Power Policy extended for Hydropower Generation.
1998	Revised Policy for New Private Independent Power Projects	Amended/Revised 1994 Policy with more rationalization i.e., introducing completion/bidding.
2000	Power Generation Policy	This policy encouraged investment from private, public-private and public sector organizations.
2005	Energy Security Action Plan (2005–2030)	The objectives of Pakistan's Vision 2030 for reliable and quality energy supplies are addressed in this policy.
2006	Development of Renewable Energy for Power Generation	Focused on development of small hydro, wind, and Solar and biofuel technologies.
2010–2012	National Energy Policy	This policy focused on energy conservation, short-term and long-term plans for generation of electricity and included RPPs and the rehabilitation of existing public sector power plants and investment by IPPs to cater to the energy needs of the country.
2013	National Power Policy	Focuses on the development of electricity generation and energy conservation projects to overcome the energy crisis.

inexhaustible natural resources is usually referred to as renewable or sustainable energy (Howden, 2007; Ashraf Chaudhry et al., 2009).[2] Renewable energy sources including solar, wind, biomass and others are prevalent in Pakistan (Raja and Abro, 1994; Farooq and Kumar, 2013).[2] As stated in a recent survey, the extent of power generation by renewable energy sources in Pakistan is accounted for by wind (340,000 MW), solar (2,900,000 MW), hydro (small/mini, 3,000 MW), and bagasse cogeneration (2,000 MW) (Syed et al., 2014).[2]

RENEWABLE OR SUSTAINABLE ENERGY RESOURCES IN PAKISTAN

Pakistan can resolve energy-related concerns by utilizing renewable energy resources rather than relying on conventional fossil energy resources (non-renewable). Sheikh (2010) described in his study that Pakistan pays 60% of the foreign exchange on the import of expensive fuels, which can be saved by diverting to renewable energy resources. The renewable energy resources of Pakistan are solar, wind, hydro, geothermal and biomass (Sheikh, 2009, 2010; Rafique and Rehman, 2017).

Wind-Power

The coastal area of Pakistan is spread over 1,050 km (250 km in Sindh and 800 km in Balochistan) from the Indian border in the east to the Iranian border in the west (Bhutto et al., 2013).[6] According to an estimation of AEDB, Pakistan has the potential to produce 360 GW, but currently, Pakistan ranks 44th in generating wind power, with a total installed capacity of 106 MW (Bhutto et al., 2013; Khahro et al., 2014a). The estimated wind speed on the coastlines of Pakistan ranges between 5 and 7 m/s which leads to wind power generation at the coastal areas of Sindh and Balochistan (Karachi, Ormara, Jivani, Pasni, Baburband, Kati Bandar, Gharo, and many others), and wind power plants have been installed (Ahmed et al., 2006; Sheikh, 2009; Ullah and Chipperfield, 2010; Khahro et al., 2014a,b; Siddique and Wazir, 2016). Wind power plants with energy capacities of 4 KW and 20 KW have been installed at various locations on the coastline of Sindh and Balochistan (Ahmed et al., 2006). Ahmed et al. (2006) reported that the generators of 4 kW capacities work efficiently throughout the year, but there are only a few locations, such as Pasni and Jivani where the 20 KW plants can work because they need high wind speed for operation. The Pakistan Meteorological Department has reported the wind power potential of 45 different Pakistani locations on the coastline. The resulting measures are shown in **Table 3** (Harijan, 2008; Harijan et al., 2009, 2011). Despite having considerable wind power generation capacity, regrettably the wind power share has no significant contribution to the total energy mix, but wind energy can be employed in the development of various rural and remote areas in Pakistan (Ahmed et al., 2006). Wind power generation can be enhanced by the formation and proper implementation of long-term productive policies, significant investment and proper vision (Mirza et al., 2007).

Solar-Power

Pakistan possesses exceptional solar potential, which is suitable for decentralized commercial utilization of energy. Therefore, solar energy could be the best option to balance the increasing supply and demand energy gap (Khalil and Zaidi, 2014). Solar rays occur on 95% of the surface of Pakistan, which is about 1,500–3,000 h per annum with 5–7 kWh/m^2/day of annual average solar radiation, accounting for 200–250 watt/m^2 or 6,840–8,280 MJ/m^2/day (Mirza et al., 2003; Ashraf Chaudhry et al., 2009; Solangi et al., 2011; Harijan et al., 2015). According to the solar map of Pakistan issued by NREL and USAID, the province of Balochistan shares more than 5–7 kWh/m^2/day of annual average global insolation, with an energy potential of 18–25 MJ/m^2/day as the sun warms the surface of Balochistan for 6–8 h daily (Sheikh, 2009). Adnan et al. (2012) presented a report stating that solar irradiation intensity was observed to be varied, as the irradiation intensity exceeded 200 W/m from February–October in province of Sindh, March–October in Balochistan, April–September in the various regions of KPK, Gilgit-Baltistan, Azad Kashmir, and March–October in the areas of Punjab. Solar energy resources can be exploited in rural and urban areas for an assortment of applications in two major fields, including photovoltaic (PV) and solar

[6] Wildlife of Pakistan. Introduction to Pakistan: Coastline WoP: Available online at: http://www.wildlifeofpakistan.com/IntroductiontoPakistan/coastlineofPakistan.htm

TABLE 3 | Estimated wind power generation capacity of Pakistan (Harijan et al., 2009, 2011).

Sindh	Power generation		Balochistan	Power generation	
	GWh	FLH		GWh	FLH
Jamshoro	1.89	3,154	Ramra	0.4	669
Hyderabad	1.59	2,643	Ormara	0.83	1,375
Gharo	1.7	2,827	Jiwani	0.75	1,257
Ketibander	1.83	3,044	Pasni	0.65	1,090
Nooriabad	1.74	2,895	Gawadar	0.63	1,044
Shahbander	1.32	2,192	Turbat	0.37	610
Mirpursakro	1.36	2,267	Aghore	1.1	1,835
Jati	1.37	2,280	Basol	0.67	1,110
Badin	1.06	1,766	Gaddani	1.06	1,758
Baghan	1.39	2,309	Hoshab	0.66	1,098
Chohar Jamali	1.35	2,255	Hubchoki	0.91	1,517
Golarchi	1.23	2,048	Liari	0.99	1,650
Kadhan	0.94	1,561	Makola	0.53	885
Matli	1.34	2,226	Managi	0.84	1,400
Sajawal	1.32	2,198	Mand	0.35	574
Talhar	1.51	2,524	Nalent	0.36	592
Thano Bula Khan	1.31	2,182	Othal	0.69	1,142
Thatta	1.73	2,886	Phore	0.77	1,287
DHA Karachi	1.41	2,358	Pishukan	0.59	987
Hawksbay	1.08	1,798	Winder	0.77	1,285

thermal (for instance solar water heating, steam generation, solar cookers, solar dryers and solar desalination) (Mirza et al., 2003; Ashraf Chaudhry et al., 2009). Solangi et al. (2011) reviewed the complete profile of solar power units' installment in Pakistan. They stated that since the 1990s, Pakistan had established 18 photovoltaic projects with 440 kW capacities that afterward diminished due to the inadequacy of technical expertise and mismanagement. Other solar power units of photovoltaic and solar thermal were installed by the relevant companies, with <1,000 kW in photovoltaic and 10,000 kW solar thermal power, which is considerably less than the estimated potential of solar energy generation in Pakistan. There are many reasons behind the current regrettable solar energy scenario in Pakistan, for instance lack of managing and operating proficiency, appropriate policies, awareness in remote areas and lack of sufficient investment together with the extravagant PV technology (Sheikh, 2010; Solangi et al., 2011); (Khan and Pervaiz, 2013).

Hydropower

Hydropower, as the name suggests, is the form of energy that is interconnected with the force of flowing water (potential energy), which can be converted into electricity for diversified applications (Wagner and Mathur, 2011). Globally, hydro-power shares a great deal of about 20% contribution in the total electricity production (Boyle, 2004; Asif, 2009). Total water resources (such as rivers, glaciers, snow melt, etc.) of Pakistan have been estimated to be 400,000 Km^2 with an anticipated potential of about 42 GW (Ashraf Chaudhry et al., 2009; Sheikh, 2009). Regardless of being rich in natural water resources, the contribution of hydropower to the total energy mix of the country is declining day after day due to many reasons (such as climate change, short-term policies, proper execution of project, land clearance, resettlement site development, long construction periods and many other financial and political issues). Until now, only 15% of the total hydropower potential, accounting for 6.5 GW, has been installed (Asif, 2009; Bhutto et al., 2012). The generation and exploitation of hydropower have reduced since the 1970s, from 70 to 33% in 2006. Various major hydropower projects are operational, for instance Tarbela, Mangla, Warsak, Chashma, Ghazi, and Barotha contributing about 6,355 MW (Mirza et al., 2008b). The major hydropower projects including Tarbela, Mangla, and Chashma have recently been reported as displaying declines in their storage capacity by 20%, yet alternate undertakings, for instance Ghazi and Barotha (introduced in 2004), are noteworthy contributors toward the complete hydropower capability of Pakistan (Asif, 2009; Bhutto et al., 2012). Hydropower development in Pakistan is shown in **Figure 5**.[7] In the Indus basin of Pakistan, 800 potential sites have been recognized, with a hydroelectric power of 60 GW. Only the hydropower plants at 134 sites are operational, amounting to 11% (6,720 MW) of the total, but the remaining 89% of this project are under implementation and completely undeveloped (Siddiqi et al., 2012). Pakistan can boost the hydroelectric share of the nation's overall energy output by effectively working on the following major projects: Kalabagh, Bhasha, Bunji, Dasu, Kohala, Patan, Neelam-Jhelum, Thakot, Munda, and Ahori, with energy generation capacities of about 3,600–3,800, 4,500–4,600, 5,400, 3,800, 1,100, 2,800, 950, 2,800, 750, and 600 MW, respectively (Asif, 2009; Malik and Sukhera, 2012). Besides these major projects, there are many mini- and micro-hydropower sites in Pakistan, with an identified potential of <5%, which can be employed to harness <1,000 MW of hydroelectric power (Sheikh, 2009, 2010).

Geothermal

Geothermal energy is another form of clean, renewable energy that is obtained from the heat energy available on the earth. There are various sources of geothermal energy, such as hot springs, volcanoes, fumaroles, and geysers. Pakistan also has great potential for electricity production from geothermal energy. There are numerous hot springs with temperatures of 30–170°C in the regions of Balochistan, Sindh, Karachi, Azad Kashmir, and KPK that can be exploited for the generation of geothermal energy. Despite having plentiful geothermal resources, there is no substantial work or planning to produce usable energy from these resources in Pakistan (Sheikh, 2009, 2010; Awan and Rashid, 2012; Malik and Sukhera, 2012).

[7]Hydropower Development in Pakistan [http://www.wapda.gov.pk/index.php/projects/hydropower-development-in-pakistan].

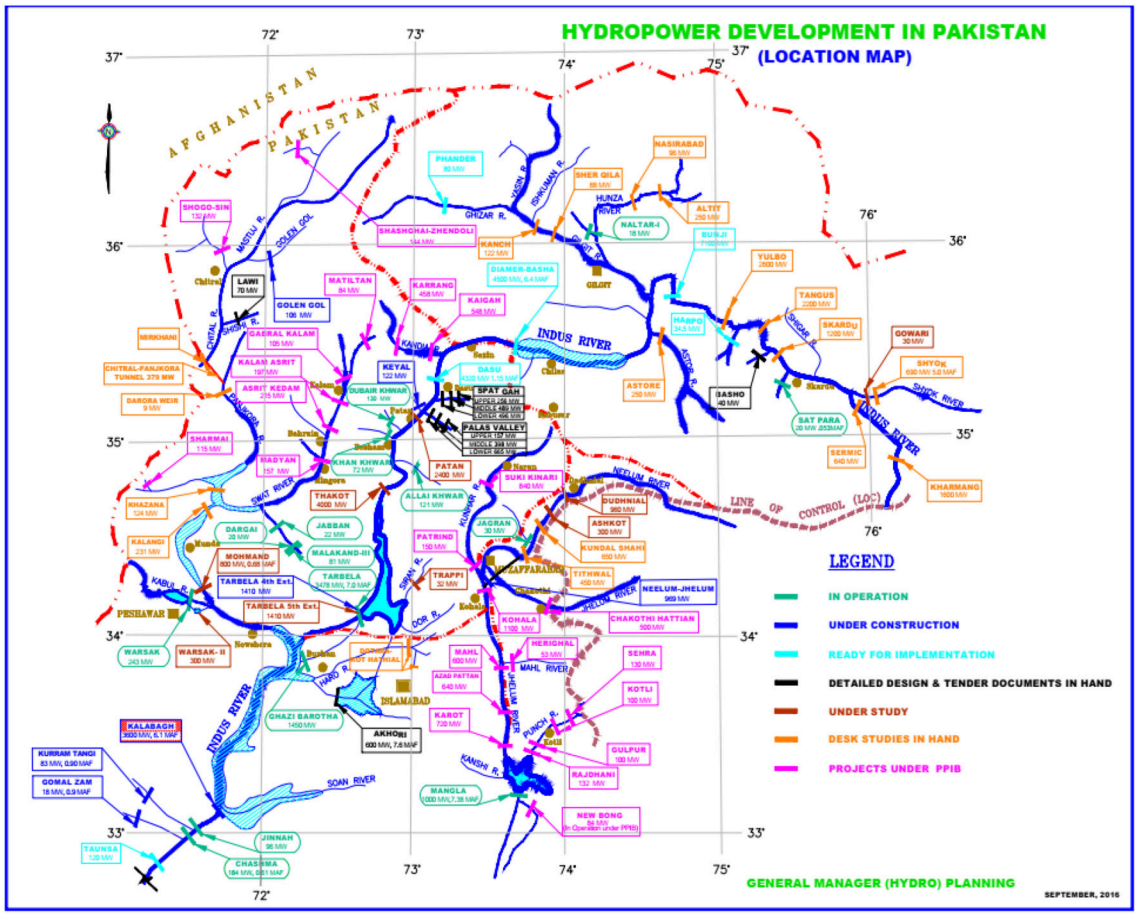

FIGURE 5 | Hydroelectric power development in Pakistan[7].

ENERGY FROM BIOMASS

Biomass energy has the potential to play a substantial role in combating the expanding energy crisis in Pakistan owing to the massive and diversified biomass potential of the country. Biomass is counted as a clean energy source since it recycles carbon dioxide through photosynthesis during biomass growth (Mirza et al., 2008a). Biomass can be used to produce electricity, thermal energy, and various chemicals. Zuberi et al. (2013) depicted the diverse advantageous aspects of the biomass resources in Pakistan including economic, environmental and employment benefits. Understanding the different properties of the biomass resources is crucial for the success of a biomass-to-energy project. The properties include calorific value, moisture content, ash content, carbon content, hydrogen content, cellulose, hemicellulose and lignin (McKendry, 2002a).

Indigenous Biomass Resources in Pakistan

Pakistan is gifted with biomass resources; however, its overall energy potential is yet to be scientifically determined. Biomass is not only limited to habitat and animal waste but also includes feedstocks, such as agricultural stalk, straw and trash, agro-industrial bagasse, paddy husks and shells, forestry and woodchips, barks and trims, and riverside greens (Farooq and Kumar, 2013; Naqvi et al., 2018).[2] Agricultural waste, agro-industrial waste or lignocellulosic waste and wood-based residues are presently estimated to be around 20,494, 25,271, and 1,121 million tons, respectively (Anwar et al., 2014).[2] The total estimated biomass potential of Pakistan is 50,000 GW h/year (Farooqui, 2014), which contributes up to 36% of the total nation's energy scenario (Asif, 2009). The various types of biomass feedstock/sources available for power generation are shown in the following **Figure 6** (Asif, 2009; Naqvi et al., 2018).[2]

Potential of Agricultural Residues

Owing to the huge agricultural sector, Pakistan produces a large number of agricultural residues including wheat husks, rice husks, cotton sticks and sugar cane residues. In addition to non-woody agricultural residues, the woody portion also contributes a great share to the production of energy (Mirza et al., 2008a; Aziz, 2013; Zuberi et al., 2013). The total land structure of Pakistan is presented in **Figure 7** (Book, 2017).

Cotton is being planted on a large scale with an average crop production of 2,00,000 tons, 2.67 million hectares (11% of the

agricultural land) during 2011–12. From 2011 to 2012, the cotton stalks obtained were about 5,898,771 tons, containing an energy potential of 614 GWh. Pakistan is positioned as the fourth largest sugarcane producing country. According to a survey from 2011 to 2012, Pakistan's sugar cane crop cultivation was measured to be 63,920,000 tons, with 5,752,800 tons of residue possessing a power potential of 9,475 GWh (**Table 4**) (Naqvi et al., 2018). Sugar mills contribute ~2,000 MW in the total national energy (Naqvi et al., 2018).

Regarding the cultivation of wheat, Pakistan is listed as the world's third largest country in the production of wheat, with its total share of the agricultural sector reaching 10.1%, and it has been identified as a potential source to produce clean energy, such as bio-oil (Iqbal et al., 2018). Together with these major crops, other crop residues (maize, rice, gram, etc.) also encompass a significant share of the total of agricultural residues that are available for energy conversion (Farooq and Kumar, 2013). The total residue production from the agriculture sector was estimated to be 62 million tons, with 2% growth rate per annum since 2000, which became 81 million tons per annum in 2012–13 (Farooq and Kumar, 2013; Ghafoor et al., 2016). Woody residues are utilized extensively in the household and cottage industries. Forest covers 5.2% (4.224 million hectares) of the available land and provides about 80% of the total generated bio-energy (Sheikh, 2009; Naqvi et al., 2018). Banana production is also considered as a source of renewable energy in Pakistan. According to one estimation, there are 173,000 banana trees per km^2 countrywide, with an average caloric value of 17.8 MJ/k. Cutting of the banana trees is usually carried out three times per annum, resulting 7 kg of heavy residues per tree (Saeed et al., 2015). Saeed et al. (2015) presented a comprehensive study on the estimated energy production from banana cultivation in Pakistan (**Table 5**). They stated that the share of banana tree remains in the annual consumption of electricity is 2.4% and, by efficiently processing agricultural waste materials, 56% of the total electricity requirement of the nation can be achieved.

FIGURE 6 | Types of biomass feedstocks.

Potential of Animal Manure

The bovine population of Pakistan is estimated to be 67,294,000 (**Table 6**) with an annual growth rate of 4% (Amjid et al., 2011; Aziz, 2013; Sakib Sherani, 2009-10). The resulting animal manure measures at 368,434,650 kg, which is deployed in the production of biogas with an energy potential of 23,654 GWh (Aziz, 2013; Naqvi et al., 2018). Livestock animals (such as cows, buffaloes, sheep, cattle, etc.) account for 55.3% of the total agricultural sector, which was elevated to 55.4% a year later, with total contributions of 11.9 and 12.1% to the GDP, respectively (Uddin et al., 2016).

Potential of Municipal Solid Waste (MSW)

Being a populous country, urban areas of Pakistan produce more than 64,000 tons of municipal solid waste daily, which comprises

TABLE 4 | Major crop contributions to Pakistan's total energy content.

Crop	Crop productionl (tons)	Residuesl (tons)	Power potential (GWh)
Cotton	200,000	5,898,771	614
Sugar cane	63,920,000	5,752,800	9,475

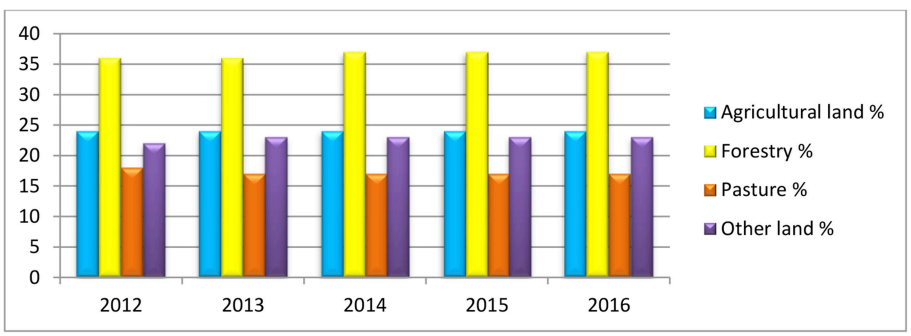

FIGURE 7 | Total land structure of Pakistan.

TABLE 5 | Energy production from banana crop per year (Saeed et al., 2015).

Area Km^2	No of banana tree per Km^2	Frequency of cutting per year	Weight of air dried banana tree Kg	Total banana tree waste ($\times 10^6$)Kg/y	Calorific value "MJ/Kg"	Energy content from banana tree waste ($\times 10^6$) MJ/y
296	173,000	3	7	1,075	17.8	1,908
Total heat contents from banana tree residue "GWh/y"						5,300
With 32% efficiency "GWh/y"						1,696
Contribution of banana tree residue toward annual consumption of electricity						2.4%

TABLE 6 | Livestock population (in millions) in Pakistan from 2010 to 2013 (Uddin et al., 2016).

Species	2010–11	2011–12	2012–13
Cattles	35.6	36.9	38.3
Buffalo	31.7	32.7	33.7
Sheep	28.1	28.4	28.8
Goat	61.5	63.1	64.9
Camels	1	1	1
Horses	0.4	0.4	0.4
Asses	4.7	4.8	4.9
Mules	0.2	0.2	0.2

both organic and inorganic components and can be efficiently processed into various energy forms with an average calorific value of 6.89 MJ/kg (Harijan et al., 2008; Aziz, 2013; Valasai et al., 2017). In the major cities of Pakistan (such as Karachi, Islamabad, Lahore, Multan, Faisalabad, Peshawar, Gujranwala, Rawalpindi, and Quetta), the estimated MSW production is about 7,121,626 tons (Aziz, 2013). MSW can contribute 13,900 GWh of energy production (Naqvi et al., 2018). Pakistan is confronting issues of waste (damped papers, plastics, metals, rubbers, glass, textile effluents, cardboards, bones, leaves, grass, straws, wood, fodder, and so on) mismanagement as the effluent is not disposed of properly. The typical composition of the MSW is shown in **Figure 8** (Zuberi and Ali, 2015). According to an approximation, 9.8 million tons of MSW were produced in 2005, 57% of which was collected for utilization in the production of electricity (Farooq and Kumar, 2013). Muhammad Khalid Farooq and S. Kumar (Farooq and Kumar, 2013) reported the complete scenario of MSW in Pakistan shown in **Table 7**.

METHODOLOGIES FOR BIOMASS-TO-ENERGY CONVERSION

There are two major classes of the techniques for processing of biomass into bioenergy, such as (i) thermo-chemical conversion techniques including direct combustion, liquefaction, trans-esterification, gasification and pyrolysis; and (ii) biochemical decomposition techniques including anaerobic decomposition and fermentation, as shown in **Figure 9** (McKendry, 2002a,b; Naqvi et al., 2018). Another unique set of techniques receiving attention is bioelectrochemical systems (BES). In bioelectrochemical techniques, microbes are utilized to yield valuable inorganic and organic byproducts along with power generation by oxidization of biological substratum (Pant et al., 2012; Kelly and He, 2014; Wang et al., 2015; Bajracharya et al., 2016; Khan et al., 2017). BES is a potential platform for producing sustainable bio-energy by minimum power consumption and it can also be applied as a robust tool for remediation of contaminants, such as carbon dioxide, nitrates, phosphates, and micropollutants in wastewater, etc. (Jin and Fallgren, 2014; Kelly and He, 2014; Sultana et al., 2015; Wang et al., 2015). Amongst various thermo-chemical processes, the most preferable are gasification and pyrolysis. Biomass pyrolysis has drawn much consideration recently owing to the production of bio-oil, biochar, and hydrogen-rich fuel gas (Ferdous et al., 2001; Li et al., 2004; Goyal et al., 2008). Pyrolysis of biomass takes place at elevated temperatures above 400°C in the absence of oxygen or air, and the nature of the resulting products is determined by the chemical composition of the biomass and reaction conditions of the pyrolysis (Li et al., 2004; Naqvi et al., 2018). The efficiency of the pyrolysis process mainly depends upon various factors, such as particle size, temperature, heating rate, residence time, biopolymer composition, and type of catalyst (Li et al., 2004). The process of pyrolysis has certain limitations including the production of unstable crude bio-oil, which is comprised of high contents of water and oxygen and needs to be further upgraded for direct use in combustible engines. Moreover, an air decontamination installation is essential as the pyrolysis process generates a high concentration of detrimental gases, such as carbon dioxide, carbon monoxide, etc. As a result of pyrolysis, the delivered ashes are reported to have high heavy metal content that is regarded as hazardous waste (Zaror and Pyle, 1982; Serio et al., 2001; Yaman, 2004; Jahirul et al., 2012). Sometimes, biochemical conversion methodology is applied to wet biomass (anaerobic digestion, ethanol fermentation, lignocellulosic conversions) for biomass energy conversions (Goyal et al., 2008; Naqvi et al., 2018).[2] The anaerobic digestion process is well-recognized in the generation of biogas from biomass including MSW, remnants of fruits, vegetables, leaves, grasses, woods, weeds, as well as marine and freshwater biomass. As an outcome of this process, the biogas obtained is rich in methane (60%) together with hydrogen and carbon dioxide, which can be utilized for numerous applications, such as transportation fuel, heating fuel, as a substitute to natural gas and so on (Jones and Ogden, 1984; Chynoweth, 1987; Gunaseelan, 1997; Chynoweth et al., 2001). Almost all types of dry biomass can be effectively utilized as fuel in combustion-based processes with the limited end-use of products. For gasification, woody

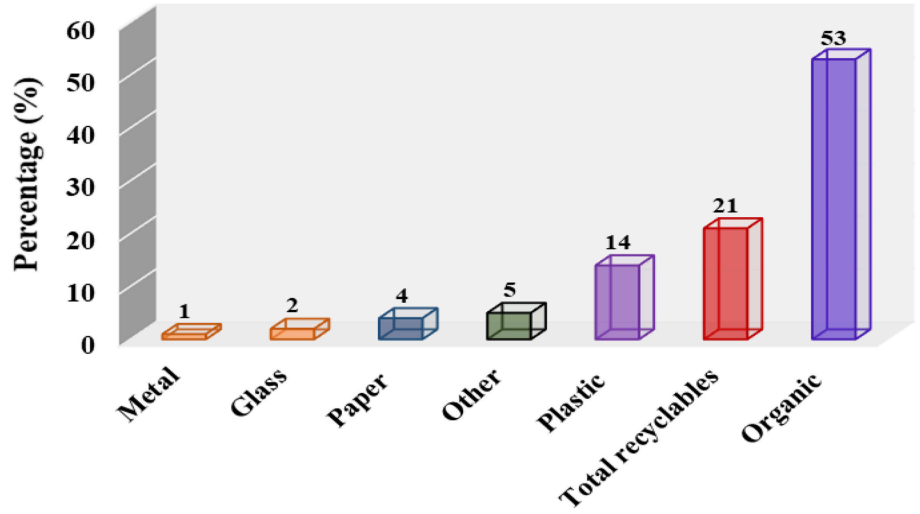

FIGURE 8 | Composition of municipal waste (Zuberi and Ali, 2015).

biomass—for example husks and wood chips—are good fuels in dry form. Gasification of biomass is carried out in the presence of oxygen, air and/or steam at temperatures exceeding 700°C with or without a catalyst, which subsequently generates a syngas consisting of hydrogen, methane, carbon dioxide, carbon monoxide, nitrogen and water vapor (Nunes et al., 2016). Various reactor configurations are utilized, such as fixed bed (updraft or downdraft) and fluidized bed (bubbling or circulation) reactors. Moreover, with the application of gas turbines or diesel generators, the generated gases can be converted into electricity (Chynoweth et al., 2001). The complete process of biomass conversion to syngas consists of different steps (**Figure 10**) (Kumar et al., 2009). Some of the semi-woody biomass, such as corncobs and corn stalks, can also be used for gasification. Leafy biomass, such as straw and stalks need to be densified (pellet) for gasification (Demirbas et al., 2009; Kumar et al., 2009; Farooq and Kumar, 2013).[2] An alternative sustainable solution of solid waste management including agricultural waste materials and animal manure is composting, which is frequently practiced in various underdeveloped countries including Pakistan. In the process of composting, the organic matter is subjected to aerobic or anaerobic decomposition by microbes, which act as an effective fertilizer or soil conditioner for the agricultural land. Moreover, composting results in the production of harmful greenhouse gases—for instance, methane, ammonia, nitrous oxide, and carbon dioxide—which, together with deteriorating the atmosphere, emits an unpleasant odor and causes contamination of the underground water sources (Inbar et al., 1993; Smet et al., 1999; Alfano et al., 2008; Ngoc and Schnitzer, 2009; Shen et al., 2011).

Biomass Composition

The woody biomass is categorized into three types—softwood, hardwood, and eucalypt. Lignocellulosic biomass primarily consists of three natural polymers (lignin, cellulose, and hemicelluloses). The chemical composition of different biopolymers of wood is given in **Table 8** (Papari and Hawboldt, 2015).

TABLE 7 | The potential of Municipal Solid Waste (MSW) in Pakistan (Farooq and Kumar, 2013; Valasai et al., 2017).

Technology	Technical potential (MW)			Technical potential (GWh)		
	2010	2030	2050	2010	2030	2050
Waste	199	672	1933	1134	3826	11,004

Biomass Products

The final product of pyrolysis of biomass depends on feedstock that can be sourced from agricultural waste, such as rice, wheat, sugar cane, and forestry residues, such as sawdust, bark, wood chips, shavings, and algae. Three main products obtained from biomass are bio-oil, biochar, and non-condensable fuel gas, in addition to solid pellets, chemicals and biofuels (Papari and Hawboldt, 2015).

Bio-Oils

During pyrolysis, the breakage of bonds between the biopolymers (lignin, cellulose, and hemi-cellulose) leads to volatile vapors being produced. These vapors are condensed to form a liquid called bio-oil. Fast pyrolysis leads to higher bio-oil yields and slow pyrolysis to lower yields. Bridgwater (2012) and Duman et al. (2011) describe the bio-oil as a complex mixture of different organic compounds, which requires blending with conventional fuels or hydro-deoxygenation to make it usable as a liquid fuel. Bio-oil is a complex mixture of around 300 different compounds as stated by Zhang (Zhang et al., 2007). Various researchers (Oasmaa and Kuoppala, 2003; Oasmaa and Meier, 2005; Mullen et al., 2010) have described the weighted

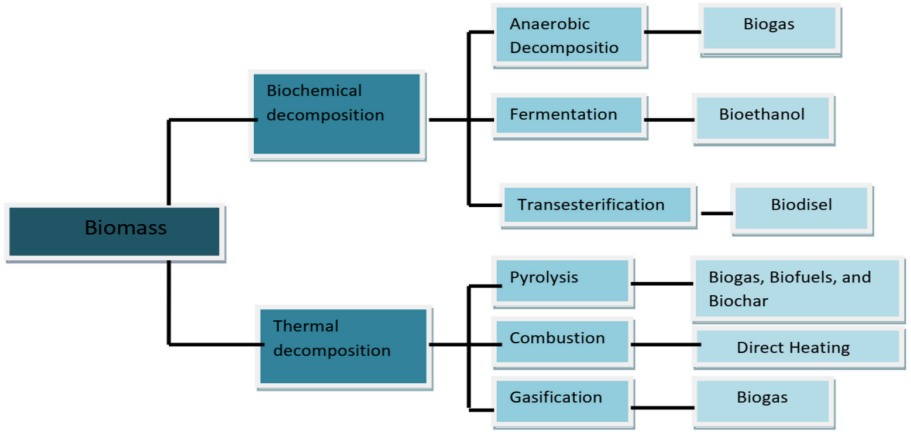

FIGURE 9 | Various techniques for biomass conversion into bio-fuels (Naqvi et al., 2018).

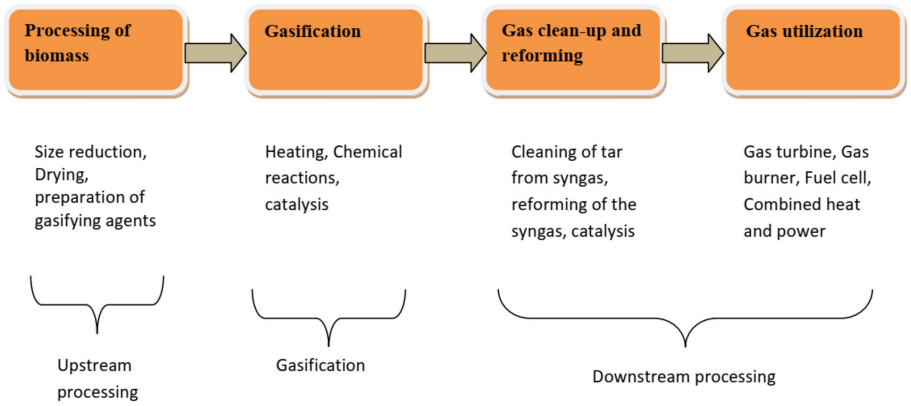

FIGURE 10 | Steps involved in gasification of biomass (Kumar et al., 2009).

percentage of compounds present in bio-oil to include water (10–30%), aldehydes (1–17%), acids (3–10%), carbohydrates (3–34%), phenolics (2–15%), alcohols (<4%), ketones (2–11%), and other unclassified compounds (5–58%). Calorific value, pH and viscosity of bio-oil are shown by Zhang (Zhang et al., 2007) to vary between 16 and 30 MJ/kg, 2.5–3.4 and 40–100 (cP), which makes it an inferior fuel compared to diesel.

Pyrolysis of biomass generates bio-oil which is a CO_2-neutral fuel with limited contents of sulfur oxide gases and can be readily stored and transported (Mohan et al., 2006). Bio-oils have been catalytically improved to high-quality hydrocarbon fuels and can be used as an alternative to petroleum fuels, which are of exceptionally high cost (Czernik and Bridgwater, 2004; Mohan et al., 2006). Iqbal et al. (2018) presented a study based on the production of bio-oil from the wheat residues by using the fast pyrolysis methodology. They studied the energy products of the fast pyrolysis of wheat stalks under a temperature range of 300–650 degree Celsius, which resulted in the phenolics, linear ketones, anhydrosugars, ketones, furan, anhydrosugar and acids, with percentage shares of 27.32, 8.53, 7.66, 8.53, 10.74, and 11.12%, respectively (Iqbal et al., 2018).

TABLE 8 | Chemical composition of different biopolymers of wood (Papari and Hawboldt, 2015).

Feed stock type	Cellulose (%)	Hemicellulose (%)	Lignin (%)
Hardwood	40–45	25–30	25–30
Softwood	40–45	30–35	20–25
Eucalypt	45	20	30

Biofuels

Biofuels are harnessed from food crops that require, for instance, bio-ethanol from corn, wheat or sugar beet, and biodiesel from oil seeds (such as rapeseed, soybean, palm, sunflower, and so forth) (Demirbas, 2011; Naqvi et al., 2018). Some of the biofuels are highly controversial as they use land that is used for growing food. Forestry and agricultural remains along with the MSW can also be exploited in the production of biofuels (Balat, 2007). Another classification of bio-fuels presented based on the conversion technology including first generation biofuels,

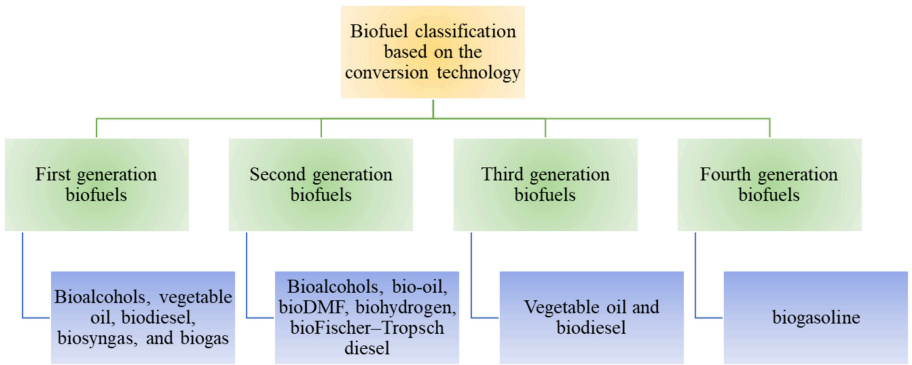

FIGURE 11 | Classification of bio-fuels presented based on the conversion technology.

second-generation biofuels, third generation biofuels, and fourth generation biofuels as shown in **Figure 11**. Variant products obtained by using first-generation biofuels are bio-alcohols, vegetable oil, biodiesel, bio-syngas, and biogas. Bio-alcohols, bio-oil, bioDMF, biohydrogen, and bio-Fischer–Tropsch diesel are generated by employing the second-generation biofuel technology. Third-generation biofuel technology results in the production of vegetable oil and biodiesel, and the fourth-generation technology gives bio-gasoline (Demirbas, 2011).

Vegetable oils and animal fats are also frequently deployed nowadays in the production of biodiesels (a biofuel) through trans-esterification, which is used in compression–ignition engines or diesel engines. Low sulfur content, flash point, aromatic content, and biodegradability make biodiesel superior to diesel fuel (Mirza et al., 2008a). Currently, Pakistan possesses the largest stocks of the methanol and ethanol, which react with vegetable oil to form bio-diesels. Pakistan is estimated to have the potential to produce 56 million tons of bio-diesels, which is far greater than the required amount (8.5 million tons). It has been reported in the literature that Pakistan has the potential to produce ∼930,000 tons of edible oils, which is expected to be elevated in the future (Khan and el Dessouky, 2009).

Biogas

Biogas is generated by using the microbially-controlled anaerobic digestion process from waste byproducts including animal dung, urban waste, and crop residues with high moisture content. On average, biogas contains methane (50 to 70%), carbon dioxide (30 to 50%) and traces of other gases, such as hydrogen, hydrogen sulfides, moisture, and siloxanes. Biogas plants of varying scales are deployed in domestic biogas production for cooking and in industrial installations to generate electricity. In the literature, the reported calorific value of biogas is 21–24 MJ/m^3 (Sheikh, 2010; Amjid et al., 2011; Jiang et al., 2011; Saleh, 2012). Rural areas of Pakistan are replete with a variety of biomass resources (animal dung waste, MSW, agri-industrial, and agricultural waste), which can be used to produce about 12 million cubic meters of biogas per day, which is enough to fulfill the energy requirements of 28 million rural people. Currently, Pakistan possesses ∼5,357 operational biogas units, with a varying production capacity of 3–15 m^3/day; however, the targeted total biogas potential is 12–16 million m^3/day (Mirza et al., 2008a; Sheikh, 2010; Javed et al., 2016; Naqvi et al., 2018). In Pakistan, the installment of biogas plants was started in 1974, and from then 4,137 plants were installed until 1987, but the growth rate of this technology became extremely slow, resulting in an increase of the figure to only 6,000 installations by 2006. Nevertheless, new policies are being developed by the government to install 3,00,000 biogas units throughout Pakistan within 10 years. This program was initiated in 2009, but only 5,360 plants have been successfully installed as of 2014 (Saleh, 2012).[8,9] Biogas is also used to produce electricity in Pakistan on a small scale, as 92 biogas plants are working in this regard resulting in the generation of 790 KW electricity (Uddin et al., 2016). There is significant potential that remains to be explored to install biogas plants for electricity production.

Biochar

Biochar is a charcoal-like substance (Chynoweth et al., 2001) produced by the thermochemical conversion of organic matter, such as crop residues, various grasses, and agricultural plant residues. Char can be produced either by heating biomass with or without air or oxygen (pyrolysis) by processes known as gasification and pyrolysis (run in the regime that leaves charcoal residue) (Jones and Ogden, 1984; Chynoweth et al., 2001).

Carbon is found in all living organisms. It is the major building block for life on Earth. Carbon exists in many forms, predominately as plant biomass, soil organic matter and as the gas carbon dioxide (CO_2) in the atmosphere and dissolved in seawater (Demirbas et al., 2009). Carbon dioxide (CO_2) is a potent greenhouse gas along with other gases, such as methane (CH_4) and nitrous oxide (NO_x) (Jones and Ogden,

[8]EKN-RSPN Pakistan Domestic Biogas Programme (PDBP): [http://www.rspn.org/index.php/projects/completed/ekn-pdbp/].

[9](PDBP) E-RPDBP: [http://www.rspn.org/wp-content/uploads/2014/09/Newsletter-Jan-Mar-2012.pdf].

TABLE 9 | Potentials for worldwide carbon sequestration via biochar production and dispersion over agricultural land (Jones and Ogden, 1984).

Items	Value	Comments
Net primary production (NPP)	60.6 GtC/yr	
Percentage of NPP for biochar	10.00%	
Resultant biochar production	3 GtC/yr	Assume 50% biomass carbon is converted into biochar
Carbon offset via combustible products (60 of 50% biomass)	1.8 GtC/yr	Assume 60% emission displacement efficiency of the combustion portion (50% of biomass). The remaining 40% (1.3 GtC/yr) is used up for running pyrolysis
Annual increase in atmospheric C due to fossil fuels and cement industry	4.1 GtC/yr	Amount of CO_2 that remains in the atmosphere, out of the total of 7.2 GtC/yr released by humans

1984; Demirbas et al., 2009; Kumar et al., 2009; Ngoc and Schnitzer, 2009; Nunes et al., 2016). CO_2 is released through natural processes; for example via respiration and volcano eruptions or by human activities, such as the burning of fossil and biomass fuels. It has been reported that in the last 150 years, the amount of carbon in the atmosphere has increased by 30% (Alfano et al., 2008). According to the World Meteorological Organization (WMO) "concentrations of carbon dioxide in the atmosphere surged at a record-breaking speed in 2016 to the highest level in 800,000 years." This high level of CO_2 in the atmosphere affects the global climate. The scientists believe that the rising global temperature has a direct relationship with the increased level of CO_2 (Alfano et al., 2008). It is estimated that global temperatures will rise for decades to come, largely due to greenhouse gases emitted by human activities. At present, Pakistan contributes <1% of the total global greenhouse gas emission on a per-capita basis. However, due to the geographical location of Pakistan, average temperatures are predicted to rise faster than elsewhere, increasing 7.2°F (4°C) by the year 2100 (2012 World Wildlife Fund report) (Inbar et al., 1993). Pakistan's per capita energy consumption and cumulative CO_2 emissions are extremely low (Inbar et al., 1993). However, the situation will not remain so as Pakistan is projected to add nearly 100 million people by 2050, causing great strains on its resources. According to projections, the country will increase carbon emissions by 300 percent in the next 15 years due to more cars which clog roads and an increased demand for electricity (Inbar et al., 1993). Hence, it is high time for Pakistan to focus on using renewable sources for energy production that will lead the country to a low-carbon pathway. In this direction, biochar production via pyrolysis of biomass is a carbon-negative system that leads to the production of energy products and biochar for carbon sequestration. This technology is carbon-negative as it removes net carbon dioxide from the atmosphere and can store CO_2 in the soil via a process known as carbon sequestration. Electrochemical reduction of the carbon dioxide is also actualized by deploying modified microbial electrochemical technologies (METs) including microbial fuel cells (MFCs), which aim to convert of biomass into electrical power using micro-organisms (Rabaey and Verstraete, 2005; Logan et al., 2006; Oh and Logan, 2007; Wang et al., 2010). In low-cost microbial electrochemical technologies (METs) or bioelectrochemical systems (BES), such as microbial electrolysis cells (MECs), the biological substrate is oxidized at the surface of the anode by utilizing bacteria that act as exoelectrogens, leading to electron generation and also CO_2 (Aelterman et al., 2006; Logan, 2009; Qiao et al., 2010; Villano et al., 2010; Zhao et al., 2012). Then, these electrons are captured by the cathode. On the cathode surface, the electron and diffused protons cause a reduction process of CO_2 and produce valuable products; for example, hydrogen gas or water and methane [$CO_2 + 8H^+ + 9e^{-1} \rightarrow CH_4 + 2H_2O$] (Call and Logan, 2008; Sun et al., 2008; Cheng et al., 2009; Villano et al., 2010; Wang et al., 2010; Kim and Logan, 2011; Logan and Rabaey, 2012; Zhao et al., 2012; Khan et al., 2017). It is estimated that biochar has the potential to sequester almost 400 billion tons of carbon by 2100 and to lower atmospheric CO_2 concentrations by 37 parts per million (Ngoc and Schnitzer, 2009). Overall, it seems reasonable to conclude that biochar production from biomass has the potential to offset the entire annual CO_2 increase in the atmosphere (4.8 vs. 4.1 GtC/yr), as shown in **Table 9** (Jones and Ogden, 1984).

CONCLUSION

Being a developing country, Pakistan is facing a severe energy crisis that limits its economy. Because of the rapidly growing population and economy, Pakistan's energy needs become potentially huge; to resolve these serious issues, AEDB is currently functioning on the development of recent renewable energy technologies in Pakistan, which will be beneficial for the developing economy of Pakistan to minimize the growing energy crisis. The sources of renewable energy are hydel, solar, wind and biomass, which has significant potential to compete with growing energy requirements. Thus far, Pakistan envisions setting up plants to generate 10,000 MW through renewable resources by 2030. These plants will be installed with a 50% share of the beneficiary. Out of all the renewable energy resources, biomass is considered the best and most easily accessible source of energy with its unique environmentally friendly nature. Despite the bountiful presence of biomass energy resources, there is still a need to work on the use of these sources to produce energy.

AUTHOR CONTRIBUTIONS

All authors listed have made a substantial, direct and intellectual contribution to the work, and approved it for publication.

REFERENCES

Abbas, M. N. (2015). *Energy Crisis in Pakistan*. Monterey, CA: Naval Postgraduate School.

Adnan, S., Hayat Khan, A., Haider, S., and Mahmood, R. (2012). Solar energy potential in Pakistan. *J. Renew. Sustain. Energy* 4:032701. doi: 10.1063/1.4712051

Aelterman, P., Rabaey, K., Pham, H. T., Boon, N., and Verstraete, W. (2006). Continuous electricity generation at high voltages and currents using stacked microbial fuel cells. *Environ. Sci. Technol.* 40, 3388–3394. doi: 10.1021/es0525511

Ahmed, M., Riaz, K., Khan, A. M., and Bibi, S. (2015). Energy consumption–economic growth nexus for Pakistan: taming the untamed. *Renew. Sustain. Energy Rev.* 52, 890–896. doi: 10.1016/j.rser.2015.07.063

Ahmed, M. A., Ahmed, F., and Akhtar, M. W. (2006). Assessment of wind power potential for coastal areas of Pakistan. *Turk. J. Phys.* 30, 127–135.

Alfano, G., Belli, C., Lustrato, G., and Ranalli, G. (2008). Pile composting of two-phase centrifuged olive husk residues: technical solutions and quality of cured compost. *Bioresour. Technol.* 99, 4694–4701. doi: 10.1016/j.biortech.2007.09.080

Amjid, S. S., Bilal, M. Q., Nazir, M. S., and Hussain, A. (2011). Biogas, renewable energy resource for Pakistan. *Renew. Sustain. Energy Rev.* 15, 2833–2837. doi: 10.1016/j.rser.2011.02.041

Anwar, Z., Gulfraz, M., and Irshad, M. (2014). Agro-industrial lignocellulosic biomass a key to unlock the future bio-energy: a brief review. *J. Radiat. Res. Appl. Sci.* 7, 163–173. doi: 10.1016/j.jrras.2014.02.003

Arif, M. (2011). *Energy Crisis in Pakistan*. Karachi: Oxford University Press.

Ashraf Chaudhry, M., Raza, R., and Hayat, S. A. (2009). Renewable energy technologies in Pakistan: prospects and challenges. *Renew. Sustain. Energy Rev.* 13, 1657–1662. doi: 10.1016/j.rser.2008.09.025

Asif, M. (2009). Sustainable energy options for Pakistan. *Renew. Sustain. Energy Rev.* 13, 903–909. doi: 10.1016/j.rser.2008.04.001

Awan, K. Y., and Rashid, A. (2012). *Overview of Pakistan's Electricity Crisis, Generation-Mix and Renewable Energy Scenarios*.

Aziz, N. (2013). *Biomass Potential in Pakistan*. European Energy Center Online verfügbar unter.

Bajracharya, S., Sharma, M., Mohanakrishna, G., Benneton, X. D., Strik, D. P., Sarma, P. M., et al. (2016). An overview on emerging bioelectrochemical systems (BESs): technology for sustainable electricity, waste remediation, resource recovery, chemical production and beyond. *Renew. Energy* 98, 153–170. doi: 10.1016/j.renene.2016.03.002

Balat, M. (2007). Global bio-fuel processing and production trends. *Energy Explor. Exploit.* 25, 195–218. doi: 10.1260/014459807782009204

Balat, M. (2010). Security of energy supply in Turkey: challenges and solutions. *Energy Conv. Manage.* 51, 1998–2011. doi: 10.1016/j.enconman.2010.02.033

Bhutto, A. W., Bazmi, A. A., and Zahedi, G. (2012). Greener energy: issues and challenges for Pakistan-hydel power prospective. *Renew. Sustain. Energy Rev.* 16, 2732–2746. doi: 10.1016/j.rser.2012.02.034

Bhutto, A. W., Bazmi, A. A., and Zahedi, G. (2013). Greener energy: issues and challenges for Pakistan—wind power prospective. *Renew. Sustain. Energy Rev.* 20, 519–538. doi: 10.1016/j.rser.2012.12.010

Book, S. Y. (2017). *Statistical Year Book*. Available online at: www.instat.gov.al/media/3658/statistical-yearbook-2017.pdf

Boyle, G. (2004). *Renewable Energy, Power for a Sustainable Future*. Oxford: Oxford University Press, The Open University.

Bridgwater, A. V. (2012). Review of fast pyrolysis of biomass and product upgrading. *Biomass Bioenergy* 38, 68–94. doi: 10.1016/j.biombioe.2011.01.048

Call, D., and Logan, B. E. (2008). Hydrogen production in a single chamber microbial electrolysis cell lacking a membrane. *Environ. Sci. Technol.* 42, 3401–3406. doi: 10.1021/es8001822

Chandio, A. A., Yuansheng, J., and Magsi, H. (2016). Agricultural sub-sectors performance: an analysis of sector-wise share in agriculture GDP of Pakistan. *Int. J. Econ. Finance* 8:156. doi: 10.5539/ijef.v8n2p156

Cheng, S., Xing, D., Call, D. F., and Logan, B. E. (2009). Direct biological conversion of electrical current into methane by electromethanogenesis. *Environ. Sci. Technol.* 43, 3953–3958. doi: 10.1021/es803531g

Chikkatur, A. P., Sagar, A. D., and Sankar, T. (2009). Sustainable development of the Indian coal sector. *Energy* 34, 942–953. doi: 10.1016/j.energy.2008.12.014

Chynoweth, D. P. (1987). *Anaerobic Digestion of Biomass*. Springer.

Chynoweth, D. P., Owens, J. M., and Legrand, R. (2001). Renewable methane from anaerobic digestion of biomass. *Renew. Energy* 22, 1–8. doi: 10.1016/S0960-1481(00)00019-7

Cleveland, C. J., Costanza, R., Hall, C. A., and Kaufmann, R. (1984). Energy and the US economy: a biophysical perspective. *Science* 225, 890–897. doi: 10.1126/science.225.4665.890

Czernik, S., and Bridgwater, A. (2004). Overview of applications of biomass fast pyrolysis oil. *Energy Fuels* 18, 590–598. doi: 10.1021/ef034067u

Dawood, Y., Saeed, A., Ata, M. G., and Nawaz, M. T. (2013). *Impact of International Politics on Pakistans Energy Crisis*. Vol. 3, International Journal of Developing Country Studies.

Demirbas, A. (2011). Competitive liquid biofuels from biomass. *Appl. Energy* 88, 17–28. doi: 10.1016/j.apenergy.2010.07.016

Demirbas, M. F., Balat, M., and Balat, H. (2009). Potential contribution of biomass to the sustainable energy development. *Energy Conv. Manage.* 50, 1746–1760. doi: 10.1016/j.enconman.2009.03.013

Duman, G., Okutucu, C., Ucar, S., Stahl, R., and Yanik, J. (2011). The slow and fast pyrolysis of cherry seed. *Bioresour. Technol.* 102, 1869–1878. doi: 10.1016/j.biortech.2010.07.051

Faridi, M. Z. (2012). Contribution of agricultural exports to economic growth in Pakistan. *Pak. J. Comm. Soc. Sci.* 6, 133–146. Available online at: https://www.econstor.eu/bitstream/10419/188047/1/pjcss079.pdf

Farooq, M. K., and Kumar, S. (2013). An assessment of renewable energy potential for electricity generation in Pakistan. *Renew. Sustain. Energy Rev.* 20, 240–254. doi: 10.1016/j.rser.2012.09.042

Farooqui, S. Z. (2014). Prospects of renewables penetration in the energy mix of Pakistan. *Renew. Sustain. Energy Rev.* 29, 693–700. doi: 10.1016/j.rser.2013.08.083

Ferdous, D., Dalai, A., Bej, S., Thring, R., and Bakhshi, N. (2001). Production of H2 and medium Btu gas via pyrolysis of lignins in a fixed-bed reactor. *Fuel Process. Technol.* 70, 9–26. doi: 10.1016/S0378-3820(00)00147-8

Ghafoor, A., ur Rehman, T., Munir, A., Ahmad, M., and Iqbal, M. (2016). Current status and overview of renewable energy potential in Pakistan for continuous energy sustainability. *Renew. Sustain. Energy Rev.* 60, 1332–1342. doi: 10.1016/j.rser.2016.03.020

GOP (2013). *Economic Survey 2012–2013 FDEAsW*. Islamabad: Government of Pakistan.

Goyal, H., Seal, D., and Saxena, R. (2008). Bio-fuels from thermochemical conversion of renewable resources: a review. *Renew. Sustain. Energy Rev.* 12, 504–517. doi: 10.1016/j.rser.2006.07.014

Gunaseelan, V. N. (1997). Anaerobic digestion of biomass for methane production: a review. *Biomass and bioenergy* 13, 83–114. doi: 10.1016/S0961-9534(97)00020-2

Harijan, K. (2008). *Mode Lung and Analysis of Tile Potential Demand for Renewable Sources of Energy in Pakistan*. Jamshoro: Mehran University of Engineering and Technology.

Harijan, K., Uqaili, M. A., and Memon, M. (2008). "Renewable energy for managing energy crisis in Pakistan," in *International Multi Topic Conference: 2008* (Berlin; Heidelberg: Springer), 449–455. doi: 10.1007/978-3-540-89853-5_48

Harijan, K., Uqaili, M. A., Memon, M., and Mirza, U. K. (2009). Assessment of centralized grid connected wind power cost in coastal area of Pakistan. *Renew. Energy* 34, 369–373. doi: 10.1016/j.renene.2008.05.001

Harijan, K., Uqaili, M. A., Memon, M., and Mirza, U. K. (2011). Forecasting the diffusion of wind power in Pakistan. *Energy* 36, 6068–6073. doi: 10.1016/j.energy.2011.08.009

Harijan, K., Uqaili, M. A., and Mirza, U. K. (2015). Assessment of solar PV power generation potential in Pakistan. *J. Clean Energy Technol.* 3, 54–56. doi: 10.7763/JOCET.2015.V3.168

Hogan, L., Curtotti, R., and Austin, A. (2007). *APEC Energy Security and Sustainable Development Through Efficiency and Diversity: Economic Issues in Technology RandD, Adoption and Transfer*. Canberra, ACT: ABARE.

Howden, D. (2007). *World Oil Supplies Are Set to Run Out Faster Than Expected, Warn Scientists*. The Independent.

Husain, T. (2010). Pakistan's energy sector issues: energy efficiency and energy environmental links. *Lahore J. Econ.* 15, 33–59. Available online at: http://www.lahoreschoolofeconomics.edu.pk/EconomicsJournal/Journals/Volume%2015/Issue%20SP/03%20Dr%20Tariq%20Husain%20EDITED%20TTC%2011-10-10.pdf

Inbar, Y., Hadar, Y., and Chen, Y. (1993). Recycling of cattle manure: the composting process and characterization of maturity. *J. Environ. Qual.* 22, 857–863. doi: 10.2134/jeq1993.00472425002200040032x

Iqbal, T., Lu, Q., Dong, C.-Q., Zhou, M.-X., Arain, Z., Ali, Z., et al. (2018). "A study of product distribution under fast pyrolysis of wheat stalk while producing bio-oil," in *Computing, Mathematics and Engineering Technologies (iCoMET), 2018 International Conference on: 2018* (Sukkur: IEEE), 1–6.

Jahirul, M. I., Rasul, M. G., Chowdhury, A. A., and Ashwath, N. (2012). Biofuels production through biomass pyrolysis—a technological review. *Energies* 5, 4952–5001. doi: 10.3390/en5124952

Jamil, F., and Ahmad, E. (2014). An empirical study of electricity theft from electricity distribution companies in Pakistan. *Pak. Dev. Rev.* 239–254. doi: 10.30541/v53i3pp.239-254

Javaid, M. A., Hussain, S., Maqsood, A., Arshad, Z., Arshad, A., and Idrees, M. (2011). Electrical energy crisis in Pakistan and their possible solutions. *Int. J. Basic Appl. Sci.* 11, 26–35. Available online at: http://climateinfo.pk/frontend/web/attachments/data-type/Javaid%20et%20al%20(2011)%20Electrical%20Energy%20Crisis%20in%20Pakistan%20and%20Their%20Possible%20Solutions.pdf

Javed, M. S., Raza, R., Hassan, I., Saeed, R., Shaheen, N., Iqbal, J., et al. (2016). The energy crisis in Pakistan: a possible solution via biomass-based waste. *J. Renew. Sustain. Energy* 8:043102. doi: 10.1063/1.4959974

Jiang, X., Sommer, S. G., and Christensen, K. V. (2011). A review of the biogas industry in China. *Energy Policy* 39, 6073–6081. doi: 10.1016/j.enpol.2011.07.007

Jin, S., and Fallgren, P. H. (2014). "Feasibility of using bioelectrochemical systems for bioremediation," in *Microbial Biodegradation and Bioremediation*, ed S. Das (Rourkila: Elsevier), 389–405.

Jones, Jr. H. B., and Ogden, E. (1984). Biomass energy potential from livestock and poultry wastes in the Southern United States. *Biomass* 6, 25–35. doi: 10.1016/0144-4565(84)90005-2

Kakar, Z. K., Khilji, B. A., and Khan, M. J. (2011). Financial development and energy consumption: empirical evidence from Pakistan. *Int. J. Trade Econ. Finance* 2:469. doi: 10.7763/IJTEF.2011.V2.150

Kelly, P. T., and He, Z. (2014). Nutrients removal and recovery in bioelectrochemical systems: a review. *Bioresour. Technol.* 153, 351–360. doi: 10.1016/j.biortech.2013.12.046

Kessides, I. N. (2013). Chaos in power: Pakistan's electricity crisis. *Energy Policy* 55, 271–285. doi: 10.1016/j.enpol.2012.12.005

Khahro, S. F., Tabbassum, K., Soomro, A. M., Dong, L., and Liao, X. (2014b). Evaluation of wind power production prospective and Weibull parameter estimation methods for Babaurband, Sindh Pakistan. *Energy Conv. Manage.* 78, 956–967. doi: 10.1016/j.enconman.2013.06.062

Khahro, S. F., Tabbassum, K., Soomro, A. M., Liao, X., Alvi, M. B., Dong, L., et al. (2014a). Techno-economical evaluation of wind energy potential and analysis of power generation from wind at Gharo, Sindh Pakistan. *Renew. Sustain. Energy Rev.* 35, 460–474. doi: 10.1016/j.rser.2014.04.027

Khalil, H. B., and Zaidi, S. J. H. (2014). Energy crisis and potential of solar energy in Pakistan. *Renew. Sustain. Energy Rev.* 31, 194–201. doi: 10.1016/j.rser.2013.11.023

Khan, A. A., and Khan, M. (2010). Pakistan textile industry facing new challenges. *Res. J. Int. Stud.* 14, 21–29. Available online at: https://www.researchgate.net/profile/Aftab_Alam18/publication/258351787_Pakistan_textile_industry_facing_new_challenges/links/0deec52808bf9271ff000000.pdf

Khan, A. A., Mehmood, Z., Shahzad, A., Chughtai, K. A., and Javed, A. (2014). Evaluation of wind energy potential alongside motorways of Pakistan. *Asian J. Appl. Sci. Eng.* 3, 375–381. doi: 10.15590/ajase

Khan, A. N., Begum, T., and Sher, M. (2012). *Energy Crisis in Pakistan: Causes and Consequences*.

Khan, H. A., and Pervaiz, S. (2013). Technological review on solar PV in Pakistan: scope, practices and recommendations for optimized system design. *Renew. Sustain. Energy Rev.* 23, 147–154. doi: 10.1016/j.rser.2013.02.031

Khan, M., Nizami, A., Rehan, M., Ouda, O., Sultana, S., Ismail, I., et al. (2017). Microbial electrolysis cells for hydrogen production and urban wastewater treatment: a case study of Saudi Arabia. *Appl. Energy* 185, 410–420. doi: 10.1016/j.apenergy.2016.11.005

Khan, M. A., and Ahmad, U. (2008). Energy demand in Pakistan: a disaggregate analysis. *Pak. Dev. Rev.* 47, 437–455. doi: 10.30541/v47i4IIpp.437-455

Khan, N. A., and el Dessouky, H. (2009). Prospect of biodiesel in Pakistan. *Renew. Sustain. Energy Rev.* 13, 1576–1583. doi: 10.1016/j.rser.2008.09.016

Kim, Y., and Logan, B. E. (2011). Microbial reverse electrodialysis cells for synergistically enhanced power production. *Environ. Sci. Technol.* 45, 5834–5839. doi: 10.1021/es200979b

Komal, R., and Abbas, F. (2015). Linking financial development, economic growth and energy consumption in Pakistan. *Renew. Sustain. Energy Rev.* 44, 211–220. doi: 10.1016/j.rser.2014.12.015

Kugelman, M. (2013). *Pakistan's Energy Crisis*. Washington, DC: National Bureau of Asian Research.

Kumar, A., Jones, D., and Hanna, M. (2009). Thermochemical biomass gasification: a review of the current status of the technology. *Energies* 2, 556–581. doi: 10.3390/en20300556

Lee, C.-C., and Chang, C-P. (2008). Energy consumption and economic growth in Asian economies: a more comprehensive analysis using panel data. *Resour. Energy Econ.* 30, 50–65. doi: 10.1016/j.reseneeco.2007.03.003

Li, S., Xu, S., Liu, S., Yang, C., and Lu, Q. (2004). Fast pyrolysis of biomass in free-fall reactor for hydrogen-rich gas. *Fuel Process. Technol.* 85, 1201–1211. doi: 10.1016/j.fuproc.2003.11.043

Logan, B. E. (2009). Exoelectrogenic bacteria that power microbial fuel cells. *Nat. Rev. Microbiol.* 7:375. doi: 10.1038/nrmicro2113

Logan, B. E., Hamelers, B., Rozendal, R., Schröder, U., Keller, J., Freguia, S., et al. (2006). Microbial fuel cells: methodology and technology. *Environ. Sci. Technol.* 40, 5181–5192. doi: 10.1021/es0605016

Logan, B. E., and Rabaey, K. (2012). Conversion of wastes into bioelectricity and chemicals by using microbial electrochemical technologies. *Science* 337, 686–690. doi: 10.1126/science.1217412

Mahmood, T., and Ayaz, M. T. (2018). Energy security and economic growth in Pakistan. *Pak. J. Appl. Econ.* 28, 47–64. Available online at: http://www.aerc.edu.pk/wp-content/uploads/2018/04/Paper-759-TAHIR-IV-1.pdf

Malik, A. (2012). *Power Crisis in Pakistan: A Crisis in Governance?* Islamabad: Pakistan Institute of Development Economics.

Malik, S. N., and Sukhera, O. R. (2012). Management of natural gas resources and search for alternative renewable energy resources: a case study of Pakistan. *Renew. Sustain. Energy Rev.* 16, 1282–1290. doi: 10.1016/j.rser.2011.10.003

Mathur, J. (2001). *Development of a Modified Dynamic Energy and Greenhouse Gas Reduction Planning Approach Through the Case of Indian Power Sector*. Essen: Universität GH Essen.

McKendry, P. (2002a). Energy production from biomass (part 1): overview of biomass. *Bioresour. Technol.* 83, 37–46. doi: 10.1016/S0960-8524(01)00118-3

McKendry, P. (2002b). Energy production from biomass (part 2): conversion technologies. *Bioresour. Technol.* 83, 47–54. doi: 10.1016/S0960-8524(01)00119-5

Mirza, U. K., Ahmad, N., and Majeed, T. (2008a). An overview of biomass energy utilization in Pakistan. *Renew. Sustain. Energy Rev.* 12, 1988–1996. doi: 10.1016/j.rser.2007.04.001

Mirza, U. K., Ahmad, N., Majeed, T., and Harijan, K. (2007). Wind energy development in Pakistan. *Renew. Sustain. Energy Rev.* 11, 2179–2190. doi: 10.1016/j.rser.2006.03.003

Mirza, U. K., Ahmad, N., Majeed, T., and Harijan, K. (2008b). Hydropower use in Pakistan: past, present and future. *Renew. Sustain. Energy Rev.* 12, 1641–1651. doi: 10.1016/j.rser.2007.01.028

Mirza, U. K., Maroto-Valer, M. M., and Ahmad, N. (2003). Status and outlook of solar energy use in Pakistan. *Renew. Sustain. Energy Rev.* 7, 501–514. doi: 10.1016/j.rser.2003.06.002

Mohan, D., Pittman, C. U., and Steele, P. H. (2006). Pyrolysis of wood/biomass for bio-oil: a critical review. *Energy Fuels* 20, 848–889. doi: 10.1021/ef0502397

Mullen, C. A., Boateng, A. A., Goldberg, N. M., Lima, I. M., Laird, D. A., and Hicks, K. B. (2010). Bio-oil and bio-char production from corn cobs and stover by fast pyrolysis. *Biomass Bioenergy* 34, 67–74. doi: 10.1016/j.biombioe.2009.09.012

Muneer, T., Maubleu, S., and Asif, M. (2006). Prospects of solar water heating for textile industry in Pakistan. *Renew. Sustain. Energy Rev.* 10, 1–23. doi: 10.1016/j.rser.2004.07.003

Munir, K. A., and Khalid, S. (2012). *Pakistan's Power Crisis: How Did We Get Here?*

Naqvi, S. R., Jamshaid, S., Naqvi, M., Farooq, W., Niazi, M. B. K., Aman, Z., et al. (2018). Potential of biomass for bioenergy in Pakistan based on present case and future perspectives. *Renew. Sustain. Energy Rev.* 81, 1247–1258. doi: 10.1016/j.rser.2017.08.012

Nawaz, S., Iqbal, N., and Anwar, S. (2013). Electricity demand in Pakistan: a nonlinear estimation. *Pak. Dev. Rev.* 52, 479–491. doi: 10.30541/v52i4Ipp.479-492

Ngoc, U. N., and Schnitzer, H. (2009). Sustainable solutions for solid waste management in Southeast Asian countries. *Waste Manage.* 29, 1982–1995. doi: 10.1016/j.wasman.2008.08.031

Nunes, L., Matias, J., and Catalão, J. (2016). Biomass combustion systems: a review on the physical and chemical properties of the ashes. *Renew. Sustain. Energy Rev.* 53, 235–242. doi: 10.1016/j.rser.2015.08.053

Oasmaa, A., and Kuoppala, E. (2003). Fast pyrolysis of forestry residue. 3. Storage stability of liquid fuel. *Energy Fuels* 17, 1075–1084. doi: 10.1021/ef030011o

Oasmaa, A., and Meier, D. (2005). Norms and standards for fast pyrolysis liquids: 1. Round robin test. *J. Anal. Appl. Pyrol.* 73, 323–334. doi: 10.1016/j.jaap.2005.03.003

Oh, S.-E., and Logan, B. E. (2007). Voltage reversal during microbial fuel cell stack operation. *J. Power Sources* 167, 11–17. doi: 10.1016/j.jpowsour.2007.02.016

Østergaard, P. A., and Sperling, K. (2014). Towards sustainable energy planning and management. *Int. J. Sustain. Energy Plan. Manage.* 1, 1–5. doi: 10.5278/ijsepm.2014.1.1

Overland, I. (2016). *Energy: The Missing Link in Globalization*. Vol. 14, ScienceDirect.

Pant, D., Singh, A., Van Bogaert, G., Irving Olsen, S., Singh Nigam, P., Diels, L., et al. (2012). Bioelectrochemical systems (BES) for sustainable energy production and product recovery from organic wastes and industrial wastewaters. *RSC Adv.* 2, 1248–1263. doi: 10.1039/C1RA00839K

Papari, S., and Hawboldt, K. (2015). A review on the pyrolysis of woody biomass to bio-oil: focus on kinetic models. *Renew. Sustain. Energy Rev.* 52, 1580–1595. doi: 10.1016/j.rser.2015.07.191

Pimentel, D., Hurd, L., Bellotti, A., Forster, M., Oka, I., Sholes, O., et al. (1973). Food production and the energy crisis. *Science* 182, 443–449. doi: 10.1126/science.182.4111.443

Qiao, Y., Bao, S.-J., and Li, C. M. (2010). Electrocatalysis in microbial fuel cells—from electrode material to direct electrochemistry. *Energy Environ. Sci.* 3, 544–553. doi: 10.1039/b923503e

Qureshi, M. N. (2009). *Energy Crisis in Pakistan: A Threat to National Security*. Islamabad: ISSRA.

Rabaey, K., and Verstraete, W. (2005). Microbial fuel cells: novel biotechnology for energy generation. *Trends Biotechnol.* 23, 291–298. doi: 10.1016/j.tibtech.2005.04.008

Rafique, M. M., and Rehman, S. (2017). National energy scenario of Pakistan–current status, future alternatives, and institutional infrastructure: an overview. *Renew. Sustain. Energy Rev.* 69, 156–167. doi: 10.1016/j.rser.2016.11.057

Raja, I. A., and Abro, R. S. (1994). Solar and wind energy potential and utilization in Pakistan. *Renew. Energy* 5, 583–586. doi: 10.1016/0960-1481(94)90439-1

Rashid Amjad, S. J. B. (Ed.). (2015). *Pakistan Moving the Economy Forward*. New Delhi: Cambridge University Press.

Raza, S. A., Ali, Y., and Mehboob, F. (2012). *Role of Agriculture in Economic Growth of Pakistan*. Euro Journals.

Rehman, M. S. U., Rashid, N., Saif, A., Mahmood, T., and Han, J-I. (2013). Potential of bioenergy production from industrial hemp (Cannabis sativa): Pakistan perspective. *Renew. Sustain. Energy Rev.* 18, 154–164. doi: 10.1016/j.rser.2012.10.019

Sadorsky, P. (2010). The impact of financial development on energy consumption in emerging economies. *Energy Policy* 38, 2528–2535. doi: 10.1016/j.enpol.2009.12.048

Saeed, M., Irshad, A., Sattar, H., Andrews, G., Phylaktou, H., and Gibbs, B. (2015). "Agricultural waste biomass energy potential in Pakistan," in *Proceedings of the International Conference held in Shanghai, PR China: 2015* (Leeds).

Sahir, M. H., and Qureshi, A. H. (2008). Assessment of new and renewable energy resources potential and identification of barriers to their significant utilization in Pakistan. *Renew. Sustain. Energy Rev.* 12, 290–298. doi: 10.1016/j.rser.2006.07.002

Sakib Sherani, M. O. F. (2009-10). *Growth and Development, Pakistan Economic Survey*. Government of Pakistan.

Saleh, A. (2012). *Biogas Potential in Pakistan*. Lahore: Biomass Conversion Research Centre, Department of Chemical Engineering, COMSATS Institute of information Technology.

Serio, M. A., Kroo, E., Bassilakis, R., Wójtowicz, M. A., and Suuberg, E. M. (2001). *A Prototype Pyrolyzer for Solid Waste Resource Recovery in Space*. SAE Technical Paper. doi: 10.4271/2001-01-2349

Shaikh, F., Ji, Q., and Fan, Y. (2015). The diagnosis of an electricity crisis and alternative energy development in Pakistan. *Renew. Sustain. Energy Rev.* 52, 1172–1185. doi: 10.1016/j.rser.2015.08.009

Sheikh, M. A. (2009). Renewable energy resource potential in Pakistan. *Renew. Sustain. Energy Rev.* 13, 2696–2702. doi: 10.1016/j.rser.2009.06.029

Sheikh, M. A. (2010). Energy and renewable energy scenario of Pakistan. *Renew. Sustain. Energy Rev.* 14, 354–363. doi: 10.1016/j.rser.2009.07.037

Shen, Y., Ren, L., Li, G., Chen, T., and Guo, R. (2011). Influence of aeration on CH_4, N_2O and NH_3 emissions during aerobic composting of a chicken manure and high C/N waste mixture. *Waste Manage.* 31, 33–38. doi: 10.1016/j.wasman.2010.08.019

Siddiqi, A., Wescoat Jr., J. L., Humair, S., and Afridi, K. (2012). An empirical analysis of the hydropower portfolio in Pakistan. *Energy Policy* 50, 228–241. doi: 10.1016/j.enpol.2012.06.063

Siddique, S., and Wazir, R. (2016). A review of the wind power developments in Pakistan. *Renew. Sustain. Energy Rev.* 57, 351–361. doi: 10.1016/j.rser.2015.12.050

Siddiqui, R., Jalil, H. H., Nasir, M., Malik, W. S., and Khalid, M. (2008). The cost of unserved energy: evidence from selected industrial cities of Pakistan. *Pak. Dev. Rev.* 47, 227–246. Available online at: https://www.jstor.org/stable/23234709?seq=1#page_scan_tab_contents

Smet, E., Van Langenhove, H., and De Bo, I. (1999). The emission of volatile compounds during the aerobic and the combined anaerobic/aerobic composting of biowaste. *Atmos. Environ.* 33, 1295–1303. doi: 10.1016/S1352-2310(98)00260-X

Solangi, K., Islam, M., Saidur, R., Rahim, N., and Fayaz, H. (2011). A review on global solar energy policy. *Renew. Sustain. Energy Rev.* 15, 2149–2163. doi: 10.1016/j.rser.2011.01.007

Sultana, S., Khan, M. D., Sabir, S., Gani, K. M., Oves, M., and Khan, M. Z. (2015). Bio-electro degradation of azo-dye in a combined anaerobic–aerobic process along with energy recovery. *New J. Chem.* 39, 9461–9470. doi: 10.1039/C5NJ01610J

Sun, M., Sheng, G. P., Zhang, L., Xia, C. R., Mu, Z. X., Liu, X. W., et al. (2008). An MEC-MFC-coupled system for biohydrogen production from acetate. *Environ. Sci. Technol.* 42, 8095–8100. doi: 10.1021/es801513c

Syed, M. S., Chaudhry, I. A., Farooq, M., and Qamar, A. (2014). Modeling and forecasting of energy scenario in Pakistan with application of decentralized energy planning. *J. Faculty Eng. Technol.* 21, 11–24. Available online at: http://111.68.103.26/journals/index.php/jfet/article/view/399

Turton, H., and Barreto, L. (2006). Long-term security of energy supply and climate change. *Energy Policy* 34, 2232–2250. doi: 10.1016/j.enpol.2005.03.016

Uddin, W., Khan, B., Shaukat, N., Majid, M., Mujtaba, G., Mehmood, A., et al. (2016). Biogas potential for electric power generation in Pakistan: a survey. *Renew. Sustain. Energy Rev.* 54, 25–33. doi: 10.1016/j.rser.2015.09.083

Ullah, I., and Chipperfield, A. J. (2010). An evaluation of wind energy potential at Kati Bandar, Pakistan. *Renew. Sustain. Energy Rev.* 14, 856–861. doi: 10.1016/j.rser.2009.10.014

Ullah, K. (2013). Electricity infrastructure in Pakistan: an overview. *Int. J. Energy Inform. Commun.* 4, 11–26. Available online at: https://www.researchgate.net/profile/Kafait_Ullah/publication/304826505_Electricity_infrastructure_in_Pakistan_an_overview/links/59b0d4efa6fdcc3f8889b977/Electricity-infrastructure-in-Pakistan-an-overview.pdf

Valasai, G. D., Uqaili, M. A., Memon, H. R., Samoo, S. R., Mirjat, N. H., and Harijan, K. (2017). Overcoming electricity crisis in Pakistan: a review of sustainable electricity options. *Renew. Sustain. Energy Rev.* 72, 734–745. doi: 10.1016/j.rser.2017.01.097

Villano, M., Aulenta, F., Ciucci, C., Ferri, T., Giuliano, A., and Majone, M. (2010). Bioelectrochemical reduction of CO_2 to CH_4 via direct and indirect

extracellular electron transfer by a hydrogenophilic methanogenic culture. *Bioresour. Technol.* 101, 3085–3090. doi: 10.1016/j.biortech.2009.12.077

Wagner, H.-J., and Mathur, J. (2011). *Introduction to Hydro Energy Systems: Basics, Technology and Operation*. Heidelberg; Dordrecht; London; New York, NY: Springer Science and Business Media.

Wang, H., Luo, H., Fallgren, P. H., Jin, S., and Ren, Z. J. (2015). Bioelectrochemical system platform for sustainable environmental remediation and energy generation. *Biotechnol. Adv.* 33, 317–334. doi: 10.1016/j.biotechadv.2015.04.003

Wang, X., Feng, Y., Liu, J., Lee, H., Li, C., Li, N., et al. (2010). Sequestration of CO_2 discharged from anode by algal cathode in microbial carbon capture cells (MCCs). *Biosens. Bioelectron.* 25, 2639–2643. doi: 10.1016/j.bios.2010.04.036

Yaman, S. (2004). Pyrolysis of biomass to produce fuels and chemical feedstocks. *Energy Conv. Manage.* 45, 651–671. doi: 10.1016/S0196-8904(03)00177-8

Zaror, C., and Pyle, D. (1982). The pyrolysis of biomass: a general review. *Proc. Indian Acad. Sci. Sect. C Eng. Sci.* 5:269.

Zhang, Q., Chang, J., Wang, T., and Xu, Y. (2007). Review of biomass pyrolysis oil properties and upgrading research. *Energy Conv. Manage.* 48, 87–92. doi: 10.1016/j.enconman.2006.05.010

Zhao, H., Zhang, Y., Zhao, B., Chang, Y., and Li, Z. (2012). Electrochemical reduction of carbon dioxide in an MFC–MEC system with a layer-by-layer self-assembly carbon nanotube/cobalt phthalocyanine modified electrode. *Environ. Sci. Technol.* 46, 5198–5204. doi: 10.1021/es300186f

Zuberi, M. J. S., and Ali, S. F. (2015). Greenhouse effect reduction by recovering energy from waste landfills in Pakistan. *Renew. Sustain. Energy Rev.* 44, 117–131. doi: 10.1016/j.rser.2014.12.028

Zuberi, M. J. S., Hasany, S. Z., Tariq, M. A., and Fahrioglu, M. (2013). "Assessment of biomass energy resources potential in Pakistan for power generation," in *Power Engineering, Energy and Electrical Drives (POWERENG), 2013 Fourth International Conference on: 2013* (Istanbul: IEEE), 1301–1306. doi: 10.1109/PowerEng.2013.6635801

Conflict of Interest Statement: The authors declare that the research was conducted in the absence of any commercial or financial relationships that could be construed as a potential conflict of interest.

frontiers in Energy Research

ORIGINAL RESEARCH
published: 01 March 2019
doi: 10.3389/fenrg.2019.00004

Comparative Study of Liquid Biodiesel From *Sterculia foetida* (Bottle Tree) Using CuO-CeO_2 and Fe_2O_3 Nano Catalysts

Maryam Tanveer Akhtar[1], Mushtaq Ahmad[2], Anjuman Shaheen[1], Muhammad Zafar[2], Riaz Ullah[3], Maliha Asma[1], Shazia Sultana[2], Mamoona Munir[2], Neelam Rashid[2], Khafsa Malik[2], Muhammad Saeed[4] and Amir Waseem[4]*

[1] *Department of Environmental Science, International Islamic University, Islamabad, Pakistan,* [2] *Biodiesel Lab, Department of Plant Sciences, Quaid-i-Azam University, Islamabad, Pakistan,* [3] *Medicinal Aromatic and Poisonous Plants Research Center, College of Pharmacy, King Saud University, Riyadh, Saudi Arabia,* [4] *Analytical Lab, Department of Chemistry, Quaid-i-Azam University, Islamabad, Pakistan*

OPEN ACCESS

Edited by:
Umakanta Jena, New Mexico State University, United States

Reviewed by:
Mohammad Zain Khan, Aligarh Muslim University, India
JunLi Ren, South China University of Technology, China
Jabbar Gardy, University of Leeds, United Kingdom

***Correspondence:**
Mushtaq Ahmad
mushtaqahmadqau@gmail.com

Specialty section:
This article was submitted to Bioenergy and Biofuels, a section of the journal Frontiers in Energy Research

Received: *29 October 2018*
Accepted: *17 January 2019*
Published: *01 March 2019*

Citation:
Akhtar MT, Ahmad M, Shaheen A, Zafar M, Ullah R, Asma M, Sultana S, Munir M, Rashid N, Malik K, Saeed M and Waseem A (2019) Comparative Study of Liquid Biodiesel From Sterculia foetida (Bottle Tree) Using CuO-CeO_2 and Fe_2O_3 Nano Catalysts. Front. Energy Res. 7:4. doi: 10.3389/fenrg.2019.00004

This study examined the potential of nanocatalyst CuO-CeO_2 and Fe_2O_3 for efficient conversion of *Sterculia foetida* seed Oil into biodiesel. *S. foetida* contains 40% oil content and low free fatty acid value (0.18 mg KOH/g). The synthesized nanocatalyst was characterized using X-Ray Diffraction (XRD), Fourier Transform Infrared Spectroscopy (FT-IR), and Scanning Electron Microscopy (SEM) techniques. The maximum conversion was achieved (92% yield) using CuO-CeO_2 at 0.25% catalyst loading. The optimized reaction was carried out by experimental variables included molar ratio (1:9), temperature (70°C), reaction time (3 h) and stirring rate (600 rpm) using reflux transesterification method. The XRD results showed the size of crystals with order 54.4 nm for CuO-CeO_2 and 31.3 nm for Fe_2O_3. The SEM images of CuO-CeO_2 showed spherical structure having an average particle size of 32.3 nm. SEM images of Fe_2O_3 showed the size ranges from 46.27 to 28.76 nm having regular morphology, including spherical shape. The FT-IR analysis of this nanocatalyst also reinforced the results of this study. Gas Chromatography Mass Spectroscopy (GC-MS) and Fourier Transform Infrared Spectroscopy (FT-IR) confirmed the efficient conversion of *S. foetida* seed oil into biodiesel using prepared nanocatalysts. The prepared nanocatalysts are cheaper, readily available and can be used for industrial scale biofuel production assembly, making it economically feasible and more cost effective.

Keywords: *Sterculia foetida*, biodiesel, nanocatalyst, conversion efficiency, XRD, SEM, FT-IR, GC-MS

INTRODUCTION

Sterculia foetida, commonly known as Bottle tree, Java Olive, Bastard Poon Tree, Jangli Badam, Hazel *Sterculia*, and Wild Almond tree, belongs to the genus *Sterculiae.* The family *Sterculiaceae* is considered one of the non-drying and non-edible oil yielding species. It is considered as a potential non-edible feed stock for biodiesel production amongst the previously studied framework of non-edible seed oil. This family represents 10 genera and 20 species in Pakistan. Most of them are introduced as a decorative plant (Rao et al., 2015). *S. foetida* is planted in many parts of the world,

such as Ethiopia, Australia, Bangladesh, India, Indonesia, Malaysia, Oman, Uganda, Thailand, Somalia, Sri Lanka as well as Pakistan. It is a wild plant that is modified by tropical and sub-tropical areas (30 North Latitude to 35 South Latitude). The plant has an average life span of more than 100 years (Heyne, 1987; Munarso, 2010). *S. feotida* is a large, straight and deciduous tree which can grow up to 40 m in height and 3 m in width. It is commonly grown across roadsides and in parks for shadow, variegating flashy flowers. The fruit is 10 m long, woody red, nearly smooth in appearance. The single large seed is enclosed by a shell and a thin 1–2 mm layer of pulp. Each fruit contains 10–15 seeds, giving about 250–300 kg seeds annually (Munarso, 2010). Seed collection from the fruit is somewhat problematic due to the presence of harsh curls in it. The main compositions of *S. foetida* seeds are fats and protein which are 51.78 and 21.61%, respectively (Heyne, 1987; Munarso, 2010).

Alternative fuel has acquired more attention over the past twenty-five years due to fossil fuel depletion, climate change and human health hazards (Gardy et al., 2018). Biodiesel, being eco-friendly, non-toxicity, and biodegradability are gaining popularity. Worldwide, 90% of biodiesel is produced by a homogeneous catalyzed transesterification process, using edible feedstock (Rehan et al., 2018). Substantial amount of fresh water and arable land are required for its cultivation, which could lead to food security problems in developing countries (Salam et al., 2016). The above mentioned issues can be overwhelmed by using non-edible feedstock, such as waste cooking oil, Jatropha oil, Neem, Pongamia, Karanja, Rocket seed oil, Chinese wild tallow tree, Castor beans, Hemp, Milo, etc. (Rashid et al., 2015). This non-edible feedstock contain large amount of Free Fatty Acids (FFA) resulting in soap formation. Therefore, the nanocatalyst is currently used for synthesis of biodiesel to overcome such problems. These materials have significant permeability, high contact area, high thermal stability, and good chemical properties, culminating in a more effective participation in the chemical reactions to produce biodiesel.

To the best of our knowledge based on detail literature reviewed, qualitative, and quantitative analysis of fatty acid methyl esters (FAMESs) profile of non-edible seed oils has been the focus of many advanced publications. This study focused, for the first time, on a detailed investigation on seed oil source of *S. feotida* as a new addition in the list of non-edible feedstock for biodiesel synthesis using application of nano-catalysts. Biodiesel can be defined as fuel consisting of mono alkyl esters of long chain fatty acids derived from renewable sources. Biodiesel have various reigns over conventional diesel, such as biodegradability, non-toxicity, renewability, environment friendly, high flash point, and lubricity (Kumar et al., 2011; Okitsu et al., 2014). There are several problems related to biodiesel production, i.e., expensive raw material, shortage of food supply and high energy consumption. Recently, an increase in energy consumption causes a steady depletion of conventional petrol-diesel reserves. According to this theory, the higher demand for oil will require its exceeded the supplies, (Fusco, 2006; Ashnani et al., 2014; Datta and Mandal, 2014; Ullah et al., 2015). To fill this gap, it is significant to investigate the potential of appropriate feedstock like *S. feotida* as non-edible seed oil production which must be increased significantly if biodiesel possesses the potential impact to contribute in solving energy crises.

Different approaches have been used to reduce the viscosity of oil such as dilution, micro emulsions with short chain alcohols, pyrolysis, catalytic cracking, and transesterification (Farobie and Matsumura, 2015). Transesterification is one of the viable processes used for biodiesel synthesis at industrial scale (Edward and Peggy, 2013) because it gives high yield with low temperature and pressure at short reaction time (Shikha and Chauhan, 2012).

Transesterification method is used for biodiesel production. In this process triglycerides first convert into diglycerides followed by the conversion of diglycerides into monoglycerides in presence of methanol and suitable catalyst (Farobie and Matsumura, 2015). Homogeneous catalysts are typically used at large scale for biodiesel production. Although, they show good catalytic activity with several inadequacies, such as high production cost, difficulty in product isolation and requirement of large quantity of water. A new drift in biodiesel production is the use of heterogeneous alkali catalysts. Heterogeneous catalytic methods are time consuming, low catalytic stability with significant escape of catalyst components to the deactivation of the catalyst, incompetent, and robust to mass transfer. In contrast, nanocatalysts are gaining much more attention in biodiesel production due to its latent role to overcome the disadvantages associated with the use of homogeneous and heterogeneous catalyst. Nanocatalysts show several advantages such as large surface to volume ratio, high catalytic efficiency due to its Nano dimension and morphological structure, good rigidity, low separation cost, and reusability, resistance to saponification, simple operational procedures, and decrease in pollution regeneration.

Among nano-catalysts, transition metals catalysts are more effective than alkali or acid catalyst for biodiesel production (Hu et al., 2011). In the development of nanoparticles, transition metals are intensively perused because of their prominence in the field of applications in science and technology (Aparna et al., 2012). The selected metal oxide nanocatalysts CuO-CeO_2 and Fe_2O_3 have high catalytic efficiency, higher stability, and lower cost as compared to noble metals. Due to turbulent flow and shock waves, metal particles can move toward each other at high-speed and may also melt at collision point. The suspension solution occurs because of very quick Inter-particle collisions; as a result, the mass of the particle is formed. Collisions can cause a crushing blow between particles, and so, increased specific surface, and finally to achieve high reactivity and good conversion (Karimi et al., 2013).

In recent years, several mixed oxide catalysts have been practiced for synthesizing biodiesel owing to their highest catalytic activity during transesterification reaction. Since mixed oxides possess strong basic sites that increases catalytic surface area which increases catalytic stability and activity during the process. This also helps in the reutilization of catalysts after the completion of its reaction. For instance, $CaCeO_3$ gives 80% biodiesel yield during transesterification reaction with the reusability of about 5 to 7 times (Okoronkwo et al., 2012). CuO-CeO_2 gives 92.59% biodiesel via transesterification of waste

cooking oil and proves to be stable during the process (Tajammul Hussain et al., 2013). In the methonolysis of *Pistaciachinensis seed oil* via CuO-CeO_2 gives 91% biodiesel yield and can be used with five times consecutively, while Fe-Zn double metal cyanide gives 92% biodiesel yield with the reusability of five times(Chouhan and Sarma, 2011). On the basis of reported work, transition metal mixed oxide Nano catalysts (CuO-CeO_2 and Fe_2O_3) are therefore, selected for the present work on the basis of its stability, reusability, and highest catalytic performance under mild reaction conditions.

Previously, several mixed oxide catalysts have been practiced for synthesizing biodiesel owing to their highest catalytic activity during transesterification reaction. Since mixed oxides possess strong basic sites that increase the catalytic surface area which increases catalytic stability and activity during the process. This also helps in the reutilization of catalysts after the completion of its reaction. For instance $CaCeO_3$ gives 80% biodiesel yield during transesterification reaction with the reusability of about 5–7 times (Okoronkwo et al., 2012). CuO-CeO_2 gives 92.59% biodiesel via transesterification of waste cooking oil and proves to be stable during the process (Tajammul Hussain et al., 2013). In the methonolysis of *Pistacia chinensis seed oil* via CuO-CeO_2 gives 91% biodiesel yield and can be used with five times consecutively, while Fe-Zn double metal cyanide gives 92% biodiesel yield with the reusability of five times (Chouhan and Sarma, 2011). On the basis of reported work transition metal mixed oxide Nanocatalysts (CuO-CeO_2 and Fe_2O_3) is therefore, selected for the present work on the basis of its stability, reusability, and highest catalytic performance under mild reaction conditions.

Several studies focused on the Biodiesel production using nano-catalysts. On the other hand, comparative studies are very limited. In the present study, comparative evaluation has been made to deliberate the effects of two different nano-catalysts (CuO-CeO_2, Fe_2O_3) in terms of their characterization i.e., X-ray powder diffraction (XRD), Scanning Electron Microscopy (SEM), Fourier transfer Infrared spectroscopy (FT-IR), on FAMEs synthesis using non-edible seed oil of *S. feotida*. In addition to this, synthesized FAMEs have been quantitatively analyzed using analytical techniques such as Gas Chromatography-Mass Spectrometry (GC-MS), FT-IR.

METHODS

The experimental work was conducted at Wet Lab, Department of Environmental Science, International Islamic University Islamabad and Nano Science and Technology research lab of the National Centre for Physics, Quad-i-Azam University Islamabad, Pakistan. Shells of *S. feotida* plant was collected through several field trips across the country. The collected shells were placed in sun light to remove insects and moisture, then processes for seed separation. Seeds were washed with soft warm distilled water to eradicate the dirt then dried in an oven at 55°C. The Soxhlet apparatus was used to determine seed oil contents. Crude oil was extracted using an electric oil expeller (KEK P0015-10127) from Germany.

Equipment and Chemicals

Digital Weighing Balance (GF-3000), Teflon Magnetic Stirrer (AM4, VELP, SCIENTIFICA), Thermometer, pH Paper, Conical Flasks, Beakers (100 and 500 ml), Filter Paper (Wattman 42), Aluminum Foil, Pipette (10 ml), Iron Stand, Electric Oil Expeller (KEK P0015, 10127 Germany), Burette, Soxhlet Assembly (Behr Labor – Technik), Magnetic Stirrers, Pestle mortar, Drying Oven (DHG-9053A), Calcination Furnance (Neycraft), Sodium hydroxide (NaOH), Methanol 99.9% purity, Cerium (IV) oxide, Iron Sulfate, Copper Oxide, Sulfuric acid. All the reagents used were of analytical grade and purchased from Merck (Germany), Scharlau (Spain), and Sigma Aldrich (USA).

Oil Extraction

Soxhlet apparatus was used for solvent extraction. It is a sequence by which chemical constituents are removed from sample by using organic solvent. Dried seeds were wrinkled into fine powder using pestle and mortar. Round bottom flask was filled with 250 ml of n-hexane. Thimble was filled with 5 g of seeds powder and heated up to 60°C for 5 h. In this process, solvent is continually recovered and reused. Oil droplets were also visible in the round bottom flask. The resulting wet sample was again oven dried at 60°C to evaporate the solvent and weigh the sample. The reduction in the sample weight was determined to calculate the amount of oil extracted.

$$\text{Percentage of oil content} = \mathbf{W4} = [(\mathbf{W3} - \mathbf{W1})/\mathbf{W2}] \times \mathbf{100} \quad (1)$$

Where **W1** = Weight of Empty Flask
W2 = Weight of Empty Flask + powdered Sample
W3 = Weight of Sample Used
W4 = Weight of Extracted Oil

The collected oil was pre-treated by filtration and titrated using acid base titration method to determine its FFAs contents. The resulting crude oil contained 3.7 wt% FFA.

Synthesis of Nanocatalyst (CuO-CeO_2) and Fe_2O_3

CuO-CeO_2 composite was synthesized by top down approach through the ball mill method. Equivalent amount of CuO (2 g) and CeO_2 (2 g) were weighed through analytical balance and then placed in ball mill apparatus. It was made airtight with the help of a rubber piece. At room temperature the revolution per minute was 200 for 8 h. The powder was subjected to high energy collision from the balls. Then, these processed nanoparticles were calcined for 3 h at 500°C in the muffle furnace. After calcinations, the composite of CuO and $CeO_2$was ready for characterization.

Fe_2O_3 was prepared by co-precipitation route. 0.1 M solution of $FeSO_4$ was prepared. Then, 0.1 M solution of NaOH was prepared and put into the burette. Take 100 ml of Iron Sulfate into beaker and titrate it against 0.1 M NaOH, to get its basic pH i.e., 10–12. NaOH solution dropped very slowly to produce fine nanoparticles. The color of solution turns to reddish brown Iron (II) oxide, due to oxidation. The solution was frequently stirred at 600 rpm till its pH reached up to 10. When the solution pH

reached 10, titration was stopped. The solution was left over night for phase separation then washed with distilled water to remove impurities of NaOH. After washing, the sample was oven dried at 90°C for 10–12 h to evaporate extra water then calcined in muffle furnace for 3 h at 500°C. Following calcination, the $FeSO_4$ nanoparticles were ready for characterization.

Characterization of Nanocatalyst

X-Ray Diffraction

The Nanocatalyst was characterized using XRD Model No. D8 Advance Bruker, to confirm the formation of crystallite size. The Scherer Debye equation was used to calculate crystallite size. XRD measurement was performed at 2^{θ} value between 10 and 80°C.

Scanning Electron Microscopy (SEM)

SEM was performed using scanning electron microscopy Model JEOL JSM-5910 to understand the morphology of nanocatalyst. Field emission electron microscopy with 5 kV accelerating voltage was used to attain SEM image. This allows the qualitative characterization of catalyst and support, to understand the phenomena occurring in calcination and pretreatment.

Fourier Transform Infrared (FT-IR) Analysis

FT-IR spectroscopic technique was used to identify and measure organic functional groups and inorganic ions of *S. feotida* biodiesel using MODEL BRUKER-TENSOR 27 in the range from 3,500 to 400 cm^{-1}. The resolution was 1 cm^{-1} and 15 scans for biodiesel analysis. FT-IR of seed oil, biodiesel and catalysts were analyzed.

Biodiesel Synthesis Using Reflux Transesterification

Reflux transesterification method was used for biodiesel production from seed oil. Materials used for transesterification were Nanocatalyst, seed oil, hot plate, magnetic stirrer, thermometer, reflux condenser. The reaction was carried out in a 250 ml round bottom flask equipped with thermometer, reflux condenser and magnetic stirrer. 0.1 g Nanocatalyst was refluxed with 1:3 oil to methanol ratio for 1 h at 70°C. After cooling, preheated oil was added into flask and refluxed again at 70°C for 2 h. Then mixture was allowed to cool down and transferred into separating funnel for phase separation. The upper liquid phase was crude ester and the lower liquid phase was the glycerol. Biodiesel yield was calculated using the equation

$$\% \text{ Yield } = \frac{Grams\ of\ biodiesel\ produced}{Grams\ of\ oil\ used} \times 100 \qquad (2)$$

Characterization of Synthesized Fatty Acid Methyl Esters/Biodiesel

FT-IR Analysis

FT-IR spectroscopic technique was used to determine structural composition of *Sterculia feotida* biodiesel using FT-IR MODEL BRUKER-TENSOR 27 in the range of 4,000 to 600 cm^{-1}. The resolution was 1 cm^{-1} and 15 scans for biodiesel analysis. FT-IR of seed oil, biodiesel, and catalysts were analyzed.

GC-MS Analysis

It was used to determine the chemical composition of fatty acids in *S. foetida* oil biodiesel. The synthesized biodiesel was subjected to GC-MS model QP 210 ultra (Shimadzu, Japan). A sample volume of 1 ml was dissolved with 5 ml chloroform and stirred for 3 min. One microliter of this sample was injected into GC-MS model using a split mode with split ratio of 1:3. Helium was used as a vector with a flow rate of 1.44 mL/min. The column temperature was set from 50 to 300°C at the rate of 80°C/min. The temperature of detector and injector was set at 250 and 120°C.

Physico-Chemical Properties of Biodiesel

Fuel properties of synthesized biodiesel from *Sterculia* Oil were determined quantitatively from Pakistan State Oil (PSO) and Rawalpindi, and were compared to ASTM ;biodiesel standards. Flash point (°C) was recorded at ASTM D-93,Pour point at ASTM D-97, Cloud Point °C at ASTM D-2500, Density @ 15°C kg/L at D-1298, Kinematic Viscosity @ 40°C at ASTM D-445, Sulfur % ASTM D-4294 and Total Acid Number (mg KOH/mg) at ASTM D-974 (Atabani et al., 2013) was recorded and compared to the ASTM.

RESULTS AND DISCUSSION

Biodiesel Synthesis From *S. foetida* Seed Oil

S. foetida seed oil was converted into biodiesel, and oil content and FFA contents were determined. Based on dry biomass, the extracted oil percentage was 40% which is higher as compared to other edible and non-edible oil sources studied in previous literature, such as *Pongamia* oil (37%) (Baskar et al., 2016), *Melia Azedarch* fruit oil (39%) (Stavarache et al., 2008), Rocket seed (35%) (Chakrabarti et al., 2011), Soybean (18–22%) (Williams, 2005; Moser, 2010). Biodiesel quality and yield highly depend upon the FFA contents. As reported in literature, FFA content of crude oil up to 2.5% is suitable for biodiesel synthesis. Efficiency of crude oil gradually decreases outside the prescribed limit, and soap formation occurs which ultimately causes difficulty in separation process (Naik et al., 2010; Shikha and Chauhan, 2012).

Two nano-catalysts $CuO\text{-}CeO_2$ and Fe_2O_3 in different concentrations were used for efficient conversion of *S. foetida* seed oil (SFSO) into biodiesel. Data presented in **Table 1** depicts that conversion rate of oil is mainly dependent on type and amount of catalyst. At 0.25% of said catalysts concentration, the conversion rate is relatively high, up to 92%. While, by increasing the catalyst amount shows declining trends in biodiesel yield, keeping all the variables constant. Loss in biodiesel yield is proportional to the catalyst amount as shown in **Table 1**. Higher amount of catalyst emulsification which hampers the glycerin separation that results low ester yield (Vicente et al., 1998; Gurunathan and Ravi, 2015). As reported in literature, different nanocatalysts were used for biodiesel production from non-edible feedstock. Hashmi et al. (2016) investigated the use of $CaO\text{-}Al_2O_3$ nano-catalyst for biodiesel production from Jatropha oil. The highest 82.3 %

TABLE 1 | Effect of nanocatalyst on biodiesel production of *S. foetida* oil using molar ratio (1:6), temperature (70°C), reaction time (3 h), and stirring speed (600 rpm).

S. No	Nanocatalyst (gm)	Biodiesel yield using $CuO\text{-}CeO_2$ (%)	Glycerine yield using $CuO\text{-}CeO_2$ (%)	Biodiesel yield using Fe_2O_3 (%)	Glycerine yieldk2 using Fe_2O_3 (%)
1	0.1	80 ± 0.03	20 ± 0.01	70.6 ± 0.11	29.4 ± 0.08
2	0.15	87 ± 0.02	13 ± 0.05	73.5 ± 0.01	26.5 ± 0.10
3	0.2	87.6 ± 0.02	12.4 ± 0.05	84 ± 0.02	16 ± 0.01
4	0.25	92 ± 0.06	08 ± 0.01	84 ± 0.02	16 ± 0.03
5	0.3	78.4 ± 0.03	21.6 ± 0.02	66 ± 0.01	34 ± 0.03
6	0.35	89.8 ± 0.01	10.2 ± 0.1	81.5 ± 0.05	18.5 ± 0.1

biodiesel yield was obtained. Baskar et al. (2017) demonstrated the biodiesel production from Pongame oil using magnetic composite of Zinc oxide nano-catalyst. Transesterification of Pongame oil yielded 93% of biodiesel. In this study, $CuO\text{-}CeO_2$ showed the highest conversion efficacy of crude oil into FAMEs that is 92%.

Characterization of $CuO\text{-}CeO_2$ and Fe_2O_3 Nano-Catalysts

XRD of $CuO\text{-}CeO_2$ and Fe_2O_3

X-Ray Diffraction pattern of $CuO\text{-}CeO_2$ nano-catalyst (**Figure 1**) shows strong diffraction peaks at 2θ angles i.e., 28.6, 33.1, 47.4, and 56.3 with diffraction pattern (1 1 1), (2 0 0), (2 2 0), and (3 1 1), respectively. The peak appears at 2θ angles 28.6, 33.1, 47.4, and 56.3 confirms the cubic fluorite structure of CeO_2. The peak observed at 2θ angles 35.7, 38.7 with diffraction pattern (1 1 1), and (0 2 2), respectively shows the hexagonal structure of CuO. The average crystalline size of $CuO.CeO_2$ 54.4 nm was determined by Debye-Scherer equation ($D=K\lambda/\beta\cos\theta$) (Mustafa et al., 2013). Where D is the crystallite size in nm, λ stands for X-ray wavelength = 0.154095 nm, θ is the half diffraction angle, K stands for the factor shape which takes a value of 0.89 and β stands for full width at half maximum (Pathaka et al., 2017). crystallite size of $CuO\text{-}CeO_2$ nano-particles in literature was 40 nm (Amaniampong et al., 2018). XRD pattern of Fe_2O_3 nano catalyst (**Figure 2**) shows strong diffraction peaks at 2θ angles 33.1, 35.6, 40.6, 49.5, 54.0, 62.5, and 64.16 with diffraction pattern of (1 0 4), (1 1 0), (1 1 3), (0 2 4), 1 1 6), (2 1 0), and (3 0 0), respectively. These peaks indicate the rhombohedral structure of Fe_2O_3 which is confirmed from (JCPDS File No. 24-0072) with particle size 32 nm.

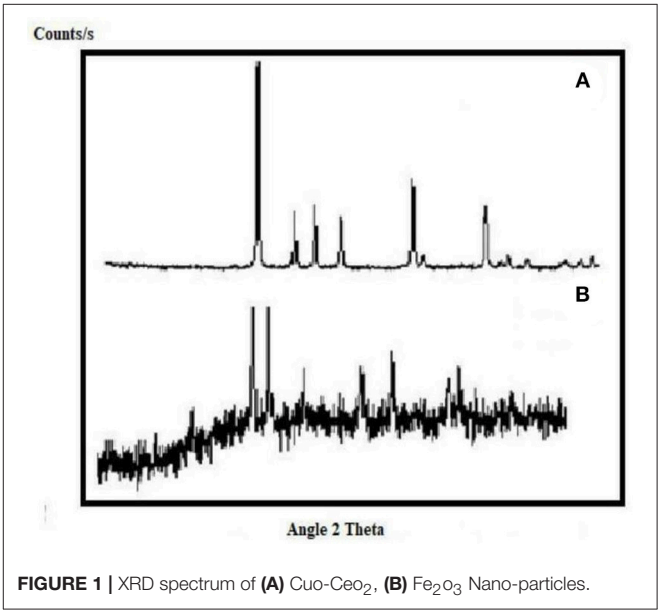

FIGURE 1 | XRD spectrum of **(A)** $Cuo\text{-}Ceo_2$, **(B)** Fe_2o_3 Nano-particles.

Scanning Electron Microscopy (SEM)

SEM was used to see the morphology and particle size of synthesized nano-catalysts. The SEM images have been shown in different magnifications. The SEM results showed that $CuO\text{-}CeO_2$ nanoparticles have average crystalline size 32.3 nm. The results showed that the nanoparticles have spherical shape with no agglomeration (**Figure 2**).

The SEM study of Fe_2O_3 nano-catalyst demonstrated the average size and morphology. The average size ranged from 46.27 to 28.76 nm. The shape of Iron oxide nanoparticles appeared to be spherical with no agglomeration. The larger iron oxide aggregated particles remained visible may be due to the aggregation of the smaller particles (**Figure 3**).

FTIR of $CuO\text{-}CeO_2$

FT-IR spectroscopic analysis is used to determine characteristic peaks in functional group (4,000–1,400 cm^{-1}) and finger print (400–1,400 cm^{-1}) region. FT-IR spectrum of $CuO\text{-}CeO_2$ shows characteristic absorption peaks in functional group region at 3648.13, 3565.93, 1738.54, 1558.63, 1540.72, 1507.07, 1456.98, 1365.10 cm^{-1} and in finger print region at 1229.86, 1217.11, 715.05, 690.37, 681.98, 668.78 cm^{-1} which is shown as (**Figure 5**). The peak observed at 3648.13 and 3565.93 cm^{-1} due to –OH stretch of water molecule present in sample as a moisture. The peak appears in spectra at 1738.51 and 1558 cm^{-1} is due to bending vibrations of H-O-H molecule present in sample. The C-H stretching and bending vibration appears at 2,969 and 1456, 1365 cm^{-1}, respectively. The peak appears at 690 and 681 cm^{-1} is due to of Cu-O particles, but an additional peak is observed at 1,229 cm^{-1} , which is due to stretching mode of Cu^{+2} and O^{-2}. The peak appearing at 668 cm^{-1} is due to CeO_2 vibration. These peaks confirm the formation of $CuO\text{-}CeO_2$ (Karimi et al., 2013) (**Figure 4**).

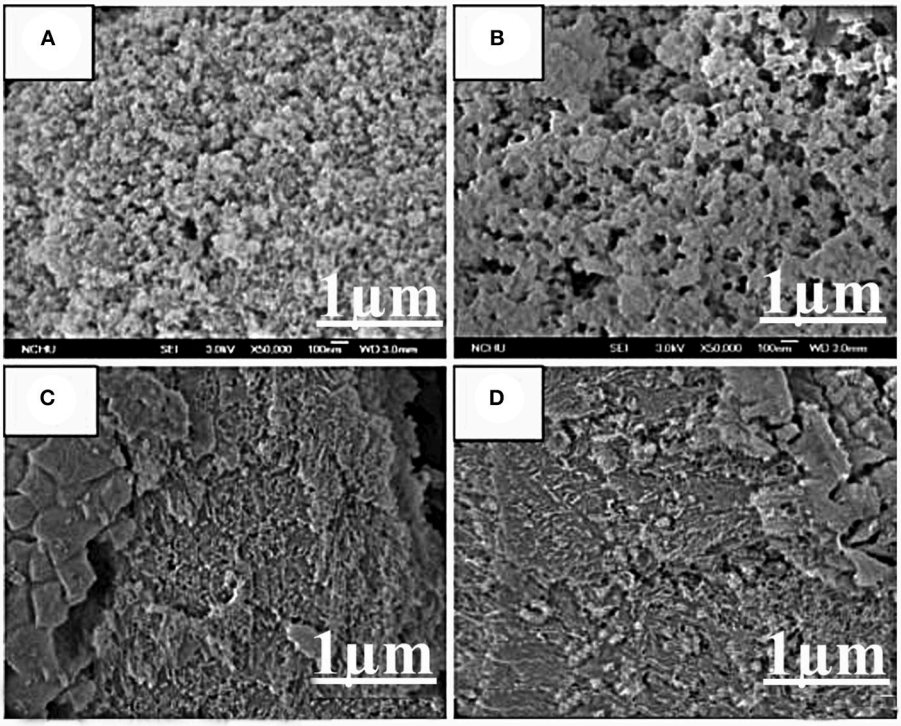

FIGURE 2 | (A–D) 1 μm. SEM image of $CuO\text{-}CeO_2$ nano-catalyst at different resolution.

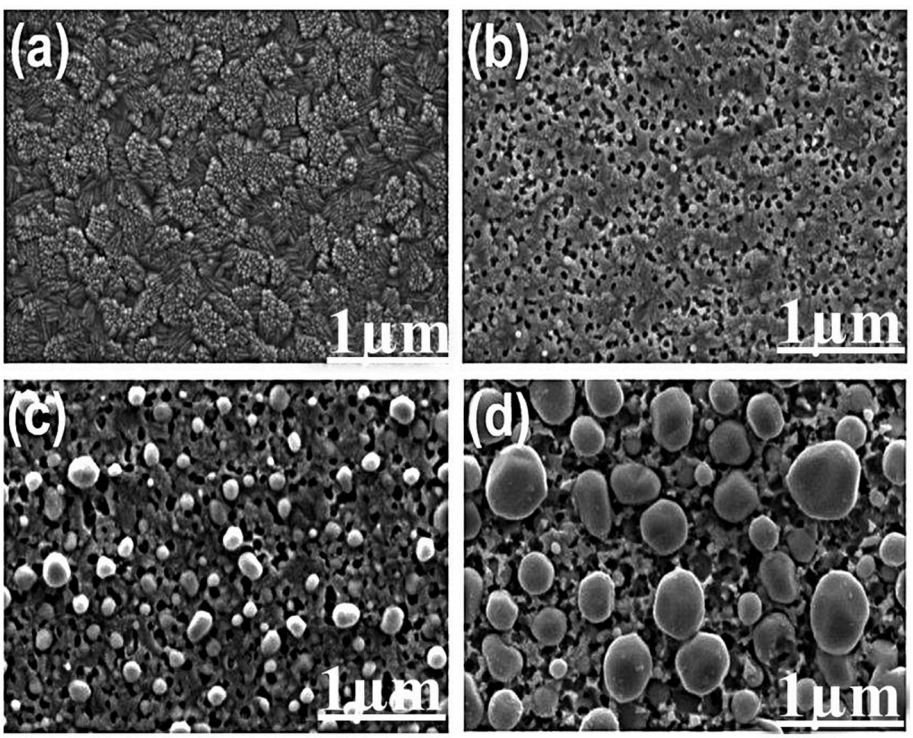

FIGURE 3 | (A–D) 1 μm. SEM image of Fe_2O_3 nano-catalyst at different resolution.

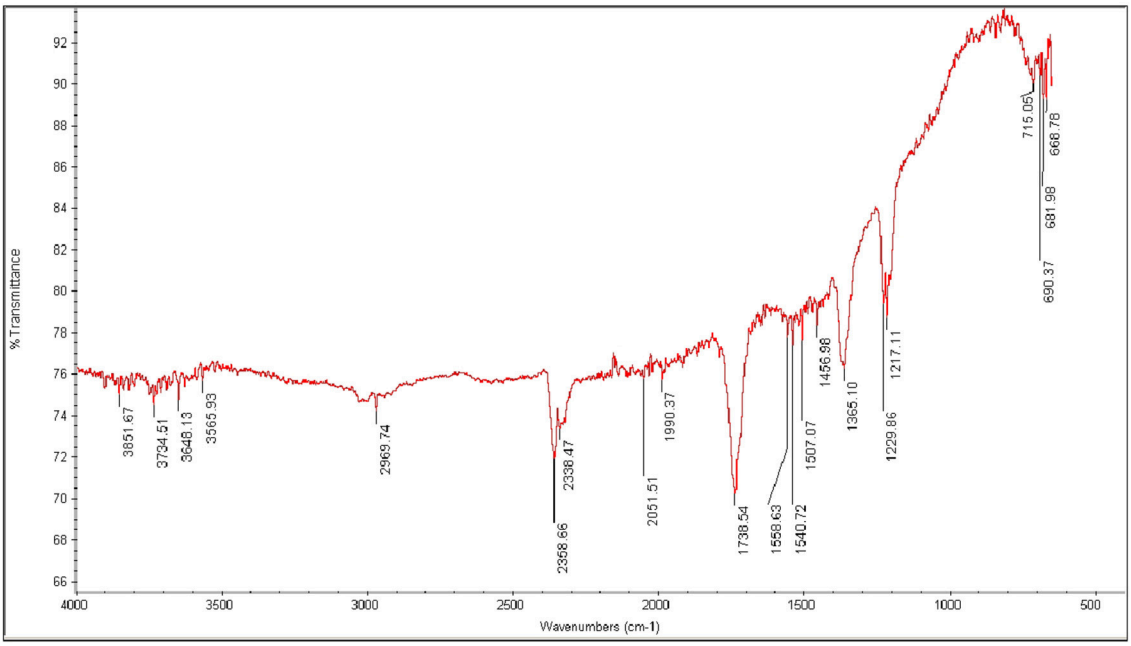

FIGURE 4 | FT-IR spectra of $CuO.CeO_2$.

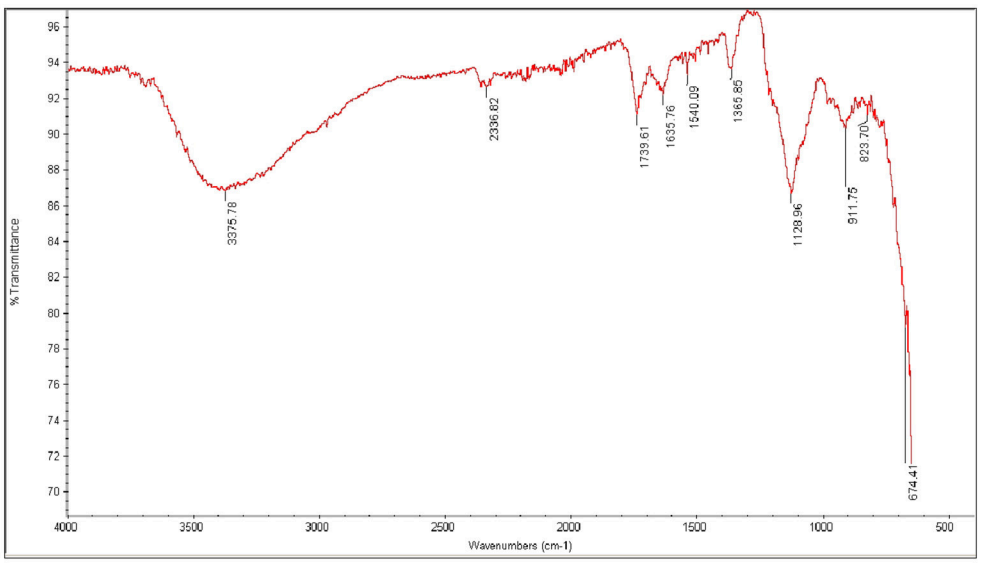

FIGURE 5 | FT-IR spectra of Fe_2O_3.

FT-IR of Fe_2O_3

The peak appearing in the spectra of Fe_2O_3 at 3,375 cm^{-1} is due to –OH stretching vibration of water molecule present in sample as moisture. The peak observed at 1,635 cm^{-1} is due to bending vibration of H-O-H. The characteristic peak appears at 674 cm^{-1} is due to Fe-O stretching vibration mode. An additional stretching mode of Fe-O is observed at 911 cm^{-1} in spectra.The previous study also supports the results. Farahmandjou and Soflaee (2015) Synthesize and Characterize Fe_2O_3 nanoparticles by simple co-precipitation method (Farahmandjou and Soflaee, 2015). These peaks confirm the formation of Fe_2O_3 (**Figure 5**).

Characterization of Synthesized FAMEs

GC-MS Analysis of *S. foetida* FAMEs

GC-MS analysis is an extensively used analytical technique to quantify chemical composition, structure and type of FAMEs present in biodiesel. The given hierarchy shows the efficiency of

TABLE 2 | Comparative analysis of fatty acid methyl ester profile of *S. foetida* using nano-catalysts.

Peak number	Compound name (FAMEs)	Molecular formula	Retention time
(A) $CuO.CeO_2$			
1–6	Methyl Alcohol	CH_3OH	0.363, 0.397, 0.402, 1.167, 1.242, 1.316
7	Myristic Acid (Tetradecanoic acid)	$C_{15}H_{30}O_2$	10.31
8	Palmitic Acid (Hexadecanoic Acid),	$C_{17}H_{34}O_2$	10.40
10	Hexanedioic Acid	$C_8H_{13}O_4$	10.59
11	9-Octadecaenoic Acid , Methyl Ester	$C_{19}H_{36}O_2$	11.77
12	7,10-Octadecadienoic Acid	$C_{19}H_{34}O_2$	11.88
13	Heptadecanoic Acid	$C_{19}H_{36}O_2$	12.07
14	1-Azuleneethanol, Acetate	$C_{14}H_{14}O_2$	15.48
15	Sterculic acid 8-(-2-Octacyclopropen)octanoic acid	$C_{19}H_{34}O_2$	14.59
(B) Fe_2O_3			
1	Trichloromethane	$CHCl_3$	0.046
2	Ethanol	C_2H_6O	1.257
3	Dodecanoic acid	$C_{12}H_{24}O_2$	0.81
4	Myristic acid (Tetradecanoic acid)	$C_{14}H_{28}O_2$	2.33
5	Palmitic acid (Hexadecanoic acid)	$C_{17}H_{34}O_2$	5.90
6	Eurcic acid (Docosenoic acid)	$C_{22}H_{42}O_2$	2.44
7	Hexadecanoic acid	$C_{17}H_{34}O_2$	10.06
8	Sterculic acid (Octadecadienoic acid)	$C_{19}H_{34}O_2$	4.34
9	9-Octadecenoic, methyl ester	$C_{19}H_{36}O_2$	6.50
10	Octadecanoic acid	$C_{19}H_{38}O_2$	1.21

synthesized Nanocatalyst i.e., $CuO\text{-}CeO_2$ $>Fe_2O_3$ on biodiesel synthesis, the percentage of synthesized methyl esters was in the order of 92 > 84%. The catalytic efficiency of $CuO\text{-}CeO_2$ was highest due to its specific characteristics. GC spectrum of $CuO\text{-}CeO_2$ catalyzed biodiesel showed 9 different peaks (**Figure 6**). Each peak corresponds to Methyl Ester and identified from the library match software (NO. NIST II). The major FAMES were found to be tetradecanoic acid, Hexadecanoic acid, 6- Nonezal, 9-Octadecaenoic Acid, Methyl Ester, 7,10-Octadecadienoic Acid, Heptadecanoic Acid, 1-Azuleneethanol, Acetate, Sterculic acid 8-(-2-Octacyclopropen-1-yl) octanoic acid. The retention time of these methyl esters is illustrated in **Tables 2A,B**. FAMEs were identified by arranging the retention time data; moreover, verification was made by GC internal standards (**Figures 7**, **8**).

FT-IR of *S. foetida* Seed Oil

FT-IR spectroscopic analysis is used to determine characteristic peaks in functional group (4,000–1,400 cm^{-1}) and finger print (400–1,400 cm^{-1}) region. The peak appearing at 3007.82 cm^{-1} confirms the presence of aromatic compounds. Strong peaks at 2923.91, 2852.93 cm^{-1} confirm the (sp^3 and sp^2C-H) stretch. An intense peak in FT-IR spectrum is observed at 1743.67, 1710.28 cm^{-1} due to C=O stretching vibrations that confirmed the presence of saturated aliphatic Esters. A medium peak at 1458.49 and 1377.20 cm^{-1} appears in spectra due to bending vibrations of CH_2 and CH_3. A peak appeared at 1236.01 cm^{-1} shows C-H deformation vibration, whereas, at 1162.02 cm^{-1} stretching vibration of C-C bond was observed. Peak observed at 1099.06 cm^{-1} confirm the presence of cyclic compound shows C-O stretching vibration as shown in **Figure 9**.

BIODIESEL OPTIMIZATION

The conversion rate of *Sterculia* oil to biodiesel depends on various parameters, such as molar ratio, reaction temperature, reaction time, catalyst loading. A series of experiments were performed to achieve the maximum conversion of crude oil into biodiesel. Five variables were selected to check out their effect on biodiesel yield (**Figure 10**).

Molar Ratio

It is one of the most important variables in biodiesel production. Stoichiometrically 3 mole of methanol is required for 1 mole of triglyceride but practically, a large amount of methanol is required to shift the equilibrium favorably(Khan and El Dessouky, 2009) when other variables were kept constant methanol to all ratio shows positive influence on the biodiesel yield as it increases from 1:3 to 1:9. But as the molar ratio increase from 1:9 to 1:15, the incremental decrease in the yield was observed (Atapour and Kariminia, 2013). The maximum biodiesel yield was obtained at 1:9 oil to methanol ratio. Biodiesel yield was reduced at 1:15 oil to methanol ratio, due to decrease in density difference between the two phases obtained after transesterification reaction. High amount of methanol was used to minimize the contact of triglyceride on the catalyst active sites, ultimately decreasing the catalyst activity.

Reaction Temperature

The reaction temperature is one of the main parameters which affects the biodiesel yield. At certain range, elevated temperatures will speed up the reaction rate. The transesterification proceeded slowly at 45°C because at lower temperatures, only small numbers of molecules were able to get over the required energy barrier. Based off of the literature, the maximum conversion results acquired at the range of 60–70°C were studied (Chelladurai and Rajamanickam, 2014). In this study, the reaction temperature was kept at 60, 65, 70, 75, and 80°C by keeping other variables constant. Maximum conversion of esters was obtained at 70°C. At lower temperature, the energy is not enough to promote the collisions among reactant molecules. Whereas at higher temperature the possibility of collision among reactant molecules becomes greater and the activation energy is easily reached (Sivakumar et al., 2012).

Reaction Time

Reaction time has great influence on the rate of transesterification reaction. Oil must be stirred at constant rate to convert it into biodiesel. The conversion increased progressively with increasing

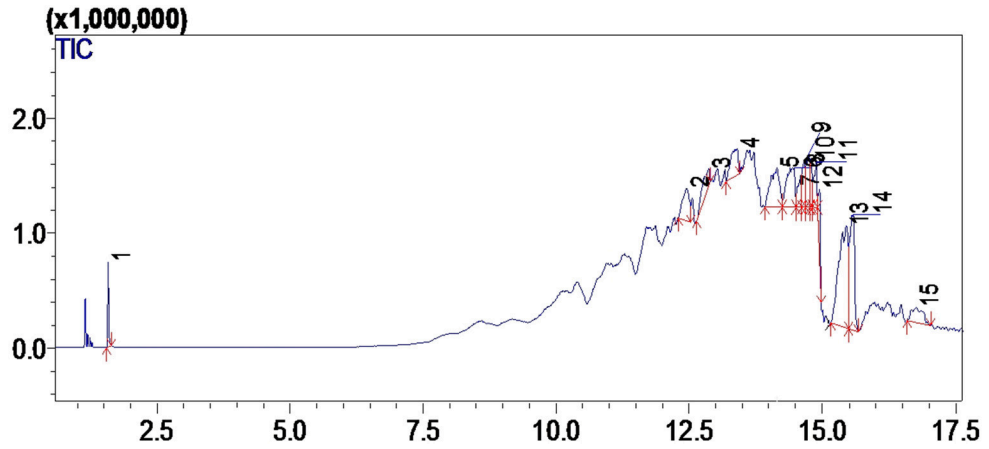

FIGURE 6 | Gas chromatogram of SOB using $CuO\text{-}CeO_2$ nano-catalyst.

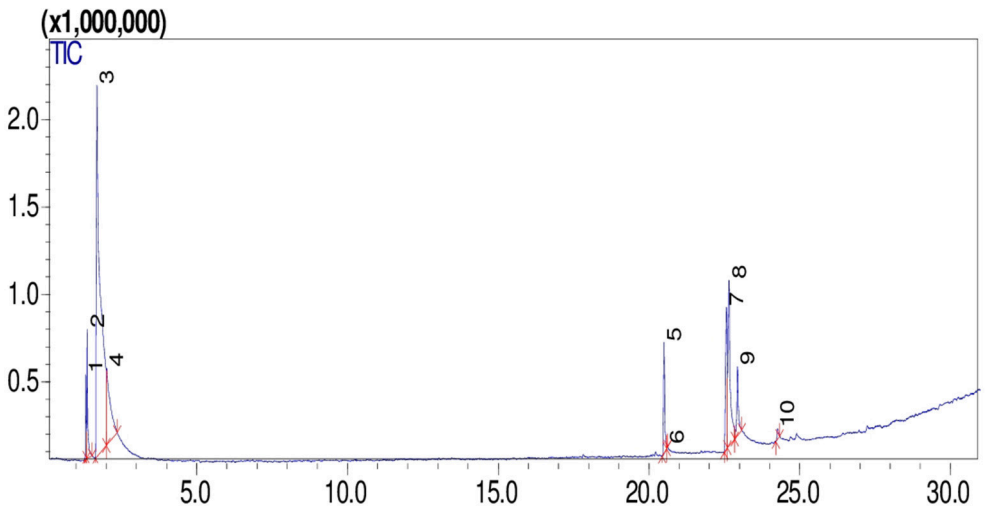

FIGURE 7 | Gas chromatogram of SOB using Fe_2O_3 nanocatalyst.

reaction time and then reached a plateau value that represents the equilibrium (Pathaka et al., 2017). By keeping all other variables constant, the reaction time was kept from 1 to 3 h at the optimal reaction conditions. The results show the maximum conversion of biodiesel was obtained at 3 h. After that, further increase in time, up to 5 h, showed the decrease in yield of biodiesel. This decrease in yield is due to the backward reaction. Results show that increasing reaction time has influence on FAME yield production (Feyzi et al., 2013) (**Figure 11**).

Catalyst Loading

The concentration of fatty acid methyl ester decreases with the increase in catalyst concentration (Gupta and Agrawal, 2015). The catalyst concentration used in transesterification reaction was 0.1, 0.15, 0.2, 0.25, 0.3, and 0.35 gm by keeping other variables such as reaction time, reaction temperature, oil to methanol ratio and catalyst type constant. The results showed a decrease in biodiesel yield with increase in catalyst concentration up to 0.25 gm because emulsification process hampers the glycerine separation and decreases the ester yields. The maximum biodiesel yield is obtained by using low catalyst concentration (Leung et al., 2010).

Physico-Chemical Properties of *Sterculia* Oil Biodiesel (Sob)

Physico-chemical properties of SOB were quantitatively determined and compared with the American Society for Testing and Materials (ASTM) standards for biodiesel testing (Atadashi et al., 2010). Fuel properties of pure biodiesel was tested where its density, cloud point, viscosity, density, sulfur content, Flash point, and total acid number were determined. The obtained values were then compared with the research and with the standard values of ASTM. The results for B-100 are mentioned in **Table 3**.

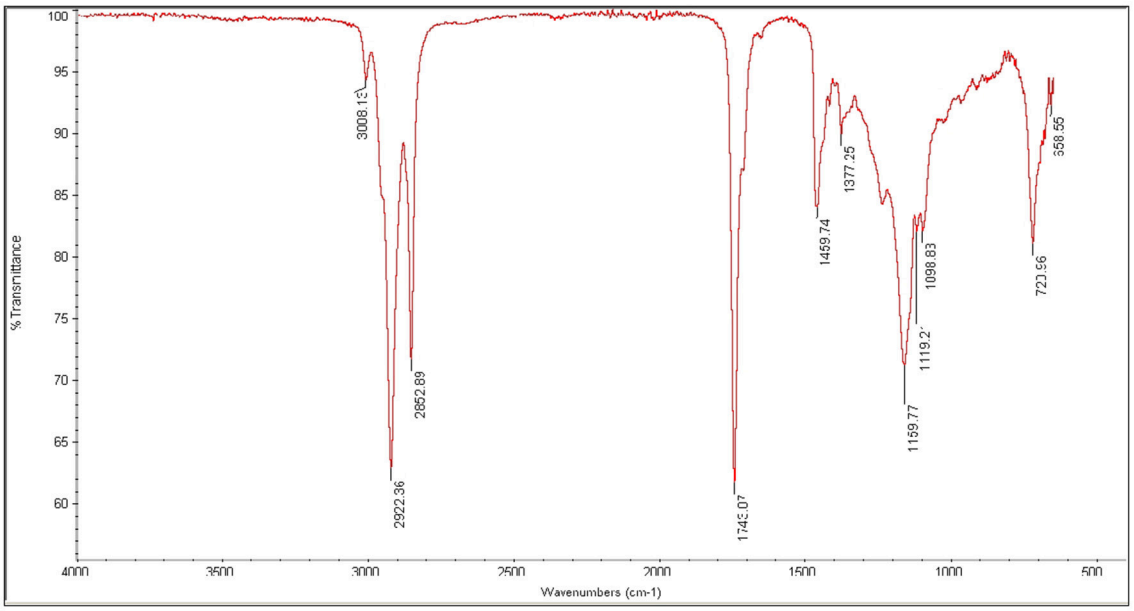

FIGURE 8 | FT-IR spectrum of sterculia oil biodiesel using $CuO\text{-}CeO_2$ nano-catalyst.

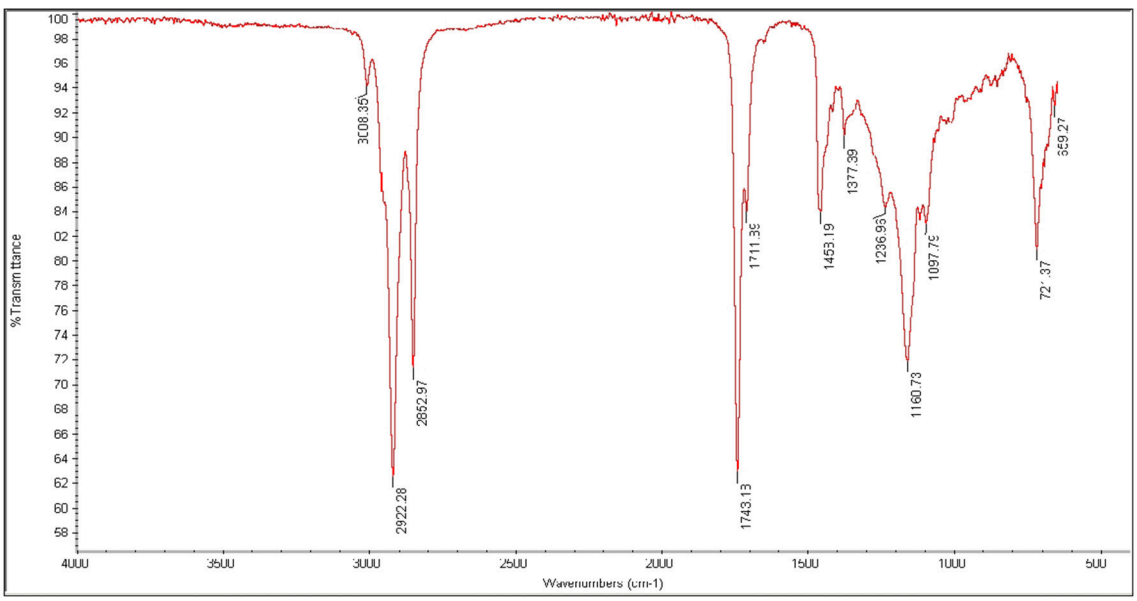

FIGURE 9 | FT-IR spectrum of sterculia oil biodiesel using Fe_2O_3 nano-catalyst.

Color

The color of *Sterculia* biodiesel is on visual 2 according to ASTM standards.

Flash Point°C

The temperature at which fuel can ignite, is known as a flash point. It is the measure of affinity of a material to form a flammable mixture in the presence of air. Fuel having high flash point is safe during handling, transportation and storage (Candeia et al., 2009). Karmee and Chadha (2005) reported the flash point value of *Pongamia pinnata* i.e., 150°C using ASTM D-93. In this sample, the flash point was recorded as 73°C within the range of ASTM D-93 standards, which makes it safer fuel. High Speed Diesel (HSD) have flash point in the range of 60–80°C.

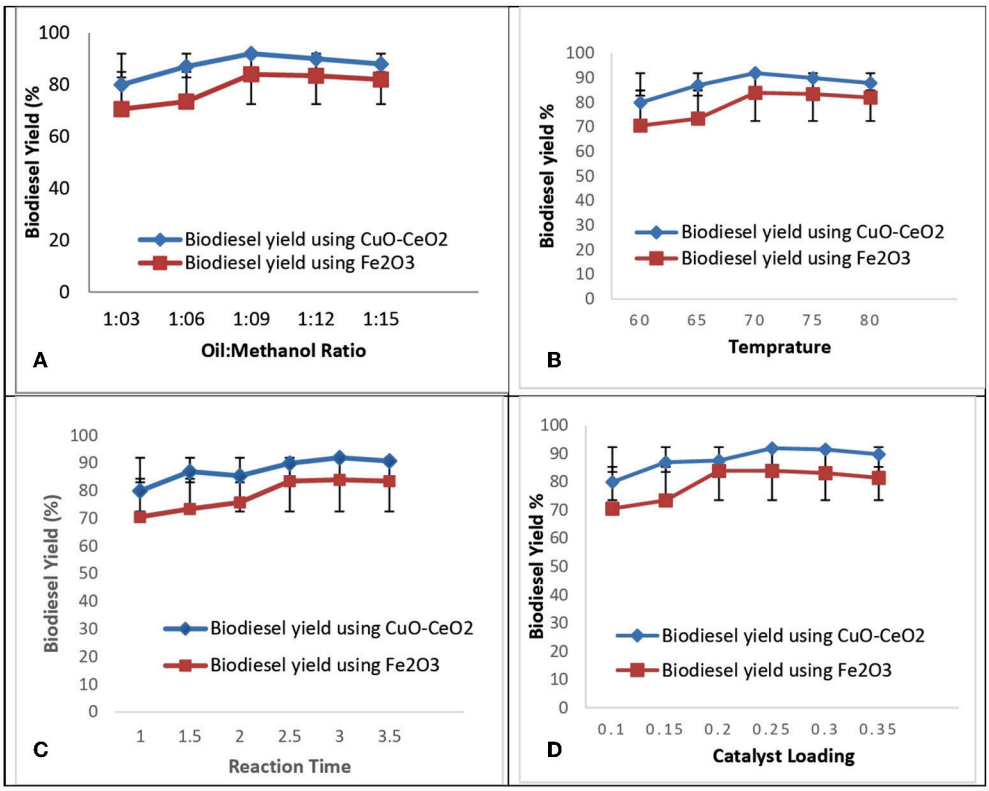

FIGURE 10 | Optimization ofbiodiesel **(A)** oil-methanol ration, **(B)** temperature, **(C)** reaction time, **(D)** catalyst loading.

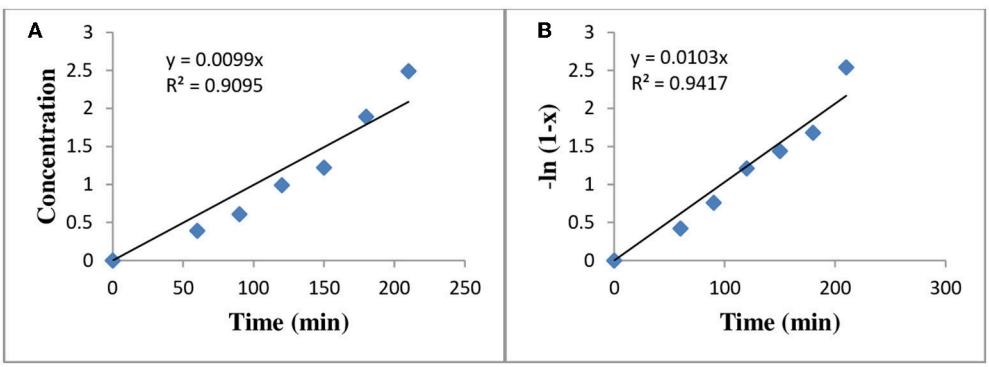

FIGURE 11 | Reaction kinetics for transesterification **(A)** zero order reaction (Cone. vs. time), **(B)** Pseudo first order reaction (-ln(l-x) vs. time).

Density @ 15°C Kg/L

Fuel density is defined as the mass per unit of volume that measures in a vacuum. It plays a vital role in the determination of biodiesel quality. Fuel density has direct effect on fuel efficiency. Cetane number and viscosity are strongly linked with density. Small mass and speed of less viscous fuel make very accurate spray (Candeia et al., 2009). The density of Sterculia Oil Biodiesel was analyzed at ASTM D-1298 and the result was 0.0832 kg/L (**Table 3**), while High Speed Diesel has a density of 0.834. It confirms that SOB has less density than that of High Speed Diesel (HSD).

Kinematic Viscosity @ 40°C

Kinematic viscosity provides the indication of the ability of a material to flow. Engine efficiency becomes reduced due to the deposition of higher viscosity fuel (Gunstone and Hamilton, 2001; Sarin et al., 2007). Esterification process helped to reduce the viscosity (Sarin et al., 2007). Less viscous oil is easier to pump and to achieve fine droplets of fuel (Goodrum, 2002). (Morshed et al., 2011)studied that rubber oil biodiesel have kinematic viscosity of 4.5 @ 40°C which was greater as compared to HSD viscosity i.e., 4.223. The kinematic viscosity of SOB was analyzed at ASTM D-445 and result was 4.15 @ 40°C which lie within the

range of ASTM standards. The value is also higher than that of HSD value i.e., 4.22.

Pour Point°C and Cloud Point°C

The lowest temperature at which the fuel can flow in chilled conditions is known as Pour point. While the cold point is a temperature at which paraffin becomes crystallize or begin to separate from solution. When the fuel is ice cold under suggested conditions, (Rashid et al., 2013) discovered that the Pour point and Cloud Point value of Rocket seed oil was −15 and −3°C, respectively. The Pour point and Cloud point of SOB was analyzed at ASTM D-97 and ASTM D-2500. Pour point value was −8°C which were according to ASTM standards whereas its cloud point value is −13°C which is higher than HSD.

Sulfur Contents % (wt)

Fuel with decreasing number of sulfur contents is ideal for most polluted areas. Low sulfur is considered more effective for the environment and for the engine's life (Candeia et al., 2009). Rashid et al. (2011) found that Muskmelon seed oil biodiesel contains 0.02% sulfated ash. Ahmad et al. (2009) reported that the 0.01% of sulfated ash present in Sesame oil biodiesel. The sulfur contents in SOB were found to be 0.0002% by weight, which was very low by comparing with ASTM D-4294 standard. It is stated that biodiesel is superior to HSD due to its decreasing number of sulfur contents.

Total Acid Number mg KOH/gm

Total acid number or Acid Value is termed as the number of free fatty acids present in fuel samples. It is expressed in mg KOH/gm for neutralizing 1 gm of FAMEs (Raj and Sahayaraj, 2010). Biodiesel is not acidic in nature but presence of FFAs in the diesel can make it acidic. High number of acid value is not good for engine efficiency. It results in severe corrosion in fuel supply system and internal engine combustion (Atabani et al., 2013). Rashid et al. (2011) studied that the acid value of Cotton Seed oil is 0.45 mg KOH/gm. According to ASTM D-974 standard, the acid value of SOB was 0.173 mg/KOH.

TABLE 3 | Fuel properties of SOB.

S. No	Fuel properties	Methods	ALM B-100	ASTM standards
1	Color	Visual	2	2
2	Flash point (°C)	ASTM D-93	73	60-100
3	Density @ 15°C Kg/L	ASTM D-1298	0.0832	0.86-0.90
4	Kinematic viscosity @ 40°C	ASTM D-445	4.15	1.9-6.0
5	Pour Point (°C)	ASTM D-97	−8	−15 to −16
6	Cloud Point (°C)	ASTM D-2500	−13	−3 to −12
7	Sulfur % wt	ASTM D-4294	0.0002	0.05
8	Total Acid No. mg KOH/gm	ASTM D-974	0.173	0.5

Kinetic Study of Biodiesel

Rate of Chemical reaction is the decrease in reactants concentration and increase in product concentration and was calculated experimentally. The order of reaction for the transesterification process to produce biodiesel was calculated by: second order (1/Conc. vs. time), first order (-(ln(conc.) vs. time), zero order (conc. vs. time) (Shu et al., 2011). The R^2-values calculated from the graph is given in the table below. The zero order reaction rate of the chemical reaction was calculated from Equation (1);

$$\frac{d[P]}{dt} = \frac{Kpdx}{dt}$$

Where *[P]* is the product concentration, *Kp* is reaction rate constant, *x* is the fraction of biodiesel.

The pseudo first order was calculated from Equation (2);

$$r = \frac{-dp}{dt} = k[P]$$

Where *K* is the rate constant of pseudo first order of reaction and was calculated from Equation (3);

$$K = \frac{\ln(1-x)}{time}$$

Where *x* is the methanol content and the Reaction rate constant of various kinetic study at different temperatures for zero and pseudo first order reaction, are given in **Table 4**. The activation energy was calculated from Arrhenius equation (Aransiola et al., 2013) and value of R^2 calculated from graph of (conc. vs. time) and (-ln (1-x) vs. time) and is given in **Table 5**. By comparing R^2-values of different models via Arrhenius equation, pseudo first order reaction appeared to be well fit with experimental yield because it has greater value of ($R^2 = 0.9417$) as compared to zero order reaction rate.

TABLE 4 | Rate constant values at different temperature.

Temperature (°C)	Rate constant of reaction (K), (min^{-1})		Biodiesel yield (%)
	Zero order	Pseudo first order	
60	9.9	18.8	70.6
65	15.9	25.6	73.5
70	20.2	41.9	84
75	27.1	33.4	83.5
80	29.2	52.3	82

TABLE 5 | Activation energy for the reaction.

S. No	Reaction order	R^2-value	Activation energy (Ea) in KJ/mol
1	Zero order	0.9095	890.98
2	Pseudo first order	0.9417	229.30

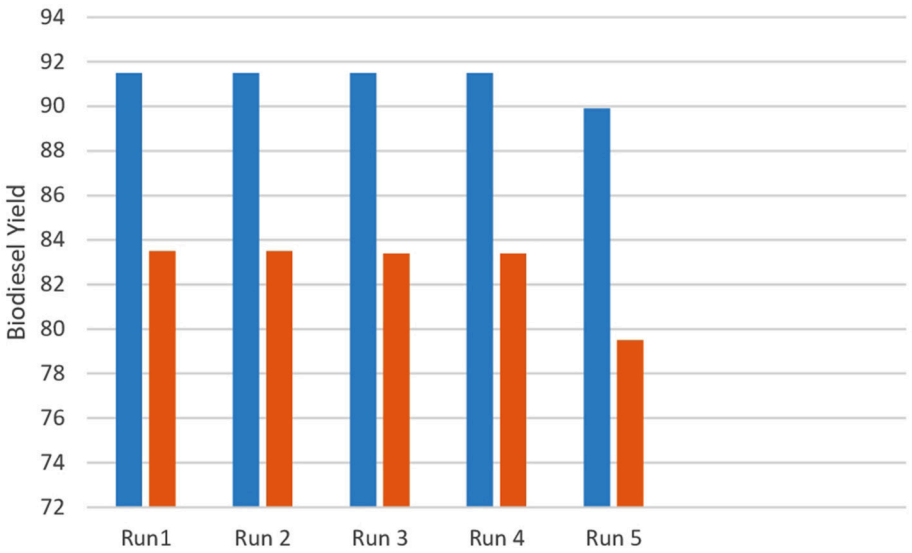

FIGURE 12 | Catalyst reusability via transesterification of *S. foetida*.

The reusability of transition metal mixed oxide Nano catalysts (CuO-CeO_2 and Fe_2O_3) was checked by collecting catalyst after each round of reaction through reflux system. It was noted that CuO-CeO_2 and Fe_2O_3 can be used four times without decrease in their catalytic activity. This fact was supported by the literature values, where CuO-CeO_2 and Fe-Zn double metal cyanide can be used five times (Chouhan and Sarma, 2011). Therefore, CuO-CeO_2 and Fe_2O_3 are stable and active catalysts for large scale biodiesel synthesis.

Long term use and feasibility of catalysts can be checked by examining the reusability of transition metal mixed oxide Nano catalysts (CuO-CeO_2 and Fe_2O_3) on biodiesel yield at optimum operating conditions. **Figure 12** shows the reusability of (CuO-CeO_2 and Fe_2O_3) under optimum conditions of 0.25% catalyst loading with oil to methanol ratio of 1:9 at 70°C for 3 h. After each cycle of catalyst used, it was washed with absolute ethanol followed by oven drying (100°C) for 4 h. The catalysts were found to be active over four times without decrease in their catalytic activity. However, after the fifth round of catalyst testing, their activity significantly decreased. This fact was supported by the literature values where CuO-CeO_2 and Fe-Zn double metal cyanide can be used five times (Chouhan and Sarma, 2011). Therefore, CuO-CeO_2 and Fe_2O_3 are stable and active catalysts. The decrease in biodiesel yield might be attributed to the deactivation of active sites and leaching of catalyst in reaction media (**Figure 12**).

CONCLUSION

This study focused on the comparative analysis of nano-catalysts on biodiesel production from *S. foetida*. Nanocatalysts (CuO-CeO_2 and Fe_2O_3) were synthesized chemo-mechanically, then characterized and applied for biodiesel production from SSO to SOB. Among these two catalysts, CuO-CeO_2 showed the auspicious results; highest conversion efficiency was achieved 92%, using CuO-CeO_2 followed by Fe_2O_3 at 0.25% catalyst loading. The best optimized variables were: alcohol to oil molar ratio (1:6), reaction time (3 h), temperature (70°C) and stirring rate (600 rpm) using reflux transesterification method. Moreover, pseudo first order reaction appeared fit with experimental yield with greater $R^2 = 0.9417$ as compared to zero order reaction rate. The synthesized nanocatalyst exhibit good stability and reusability during the reaction. The encouraging results of this study strongly recommended *S. foetida* an economically feasible potential feedstock for biodiesel production as a renewable energy on industrial level.

AUTHOR CONTRIBUTIONS

MA, RU, MZ, and MTA designed the whole experiment and methodology. AS collected the seeds. MTA, MAs, and SS performed the whole experiment. MM, MS, and AW revised the whole manuscript carefully to its present form, and assisted with checking the consistency of the data. NR and KM drafted manuscript with contribution from all co-authors. All authors read the final manuscript and agreed to its submission.

ACKNOWLEDGMENTS

The authors extend their appreciation to Deanship of Scientific Research at King Saud University for funding their group through research Group No (RG 1440–100). Authors are also thankful to Chengdu Institute of Biology for providing lab facilities.

REFERENCES

Ahmad, M., Khan, M., Zafar, M., and Sultana, S. (2009). Environment-friendly renewable energy from sesame biodiesel. *Energy Sour Part A* 32, 189–196. doi: 10.1080/15567030802467480

Amaniampong, P. N., Trinh, Q. T., Li, K., Mushrif, S. H., Hao, Y., and Yang, Y. (2018). Porous structured CuO-CeO2 nanospheres for the direct oxidation of cellobiose and glucose to gluconic acid. *Catal. Today* 306, 172–182. doi: 10.1016/j.cattod.2017.01.009

Aparna, Y., Rao, K. E., and Subbarao, P. S. (2012). "Synthesis and characterization of CuO nano particles by novel sol-gel method," in *Proceedings of the 2nd International Conference on Environment Science and Biotechnology* (Singapore).

Aransiola, E. F., Daramola, M. O., Ojumu, T. V., Solomon, B. O., and Layokun, S. K. (2013). Homogeneously catalyzed transesterification of Nigerian *Jatropha curcas* oil into biodiesel: a kinetic study. *Modern Res. Catal.* 2:83. doi: 10.4236/mrc.2013.23012

Ashnani, M. H. M., Johari, A., Hashim, H., and Hasani, E. (2014). A source of renewable energy in Malaysia, why biodiesel? *Renew. Sustain. Energy Rev.* 35, 244–257. doi: 10.1016/j.rser.2014.04.001

Atabani, A., Silitonga, A., Ong, H., Mahlia, T., Masjuki, H., Badruddin, I. A., et al. (2013). Non-edible vegetable oils: a critical evaluation of oil extraction, fatty acid compositions, biodiesel production, characteristics, engine performance and emissions production. *Renew. Sustain. Energy Rev.* 18, 211–245. doi: 10.1016/j.rser.2012.10.013

Atadashi, I., Aroua, M., and Aziz, A. A. (2010). High quality biodiesel and its diesel engine application: a review. *Renew. Sustain. Energy Rev.* 14, 1999–2008. doi: 10.1016/j.rser.2010.03.020

Atapour, M., and Kariminia, H.-R. (2013). Optimization of biodiesel production from Iranian bitter almond oil using statistical approach. *Waste Biomass Valorizat.* 4, 467–474. doi: 10.1007/s12649-013-9203-5

Baskar, G., Gurugulladevi, A., Nishanthini, T., Aiswarya, R., and Tamilarasan, K. (2017). Optimization and kinetics of biodiesel production from Mahua oil using manganese doped zinc oxide nanocatalyst. *Renew. Energy* 103, 641–646. doi: 10.1016/j.renene.2016.10.077

Baskar, G., Soumiya, S., and Aiswarya, R. (2016). Biodiesel production from pongamia oil using magnetic composite of zinc oxide nanocatalyst. *Int. J. Modern Sci. Technol.* 1, 129–137. doi: 10.1016/j.renene.2016.02.068

Candeia, R., Silva, M., Carvalho Filho, J., Brasilino, M., Bicudo, T., Santos, I., et al. (2009). Influence of soybean biodiesel content on basic properties of biodiesel–diesel blends. *Fuel* 88, 738–743. doi: 10.1016/j.fuel.2008.10.015

Chakrabarti, M., Ali, M., Baroutian, S., and Saleem, M. (2011). Techno-economic comparison between B10 of *Eruca sativa* L. and other indigenous seed oils in Pakistan. *Process Safety Environ. Protect.* 89, 165–171. doi: 10.1016/j.psep.2010.11.006

Chelladurai, K., and Rajamanickam, M. (2014). Environmentally benign neem biodiesel synthesis using nano-Zn-Mg-Al hydrotalcite as solid base catalysts. *J. Catal.* 2014:326575. doi: 10.1155/2014/326575

Chouhan, A. S., and Sarma, A. (2011). Modern heterogeneous catalysts for biodiesel production: a comprehensive review. *Renew. Sustain. Energy Rev.* 15, 4378–4399. doi: 10.1016/j.rser.2011.07.112

Datta, A., and Mandal, B. K. (2014). Use of *Jatropha* biodiesel as a future sustainable fuel. *Energy Technol. Policy* 1, 8–14. doi: 10.1080/23317000.2014.930723

Edward, N., and Peggy, A. (2013). Optimization of biodiesel production from non-edible seeds of *Delonix regia* (Gul. Mohr). *Int. J. Bioresou. Technol.* 1, 2327–7734. Available online at: www.acascipub.com

Farahmandjou, M., and Soflaee, F. (2015). Synthesis and characterization of α-Fe2O3 nanoparticles by simple co-precipitation method. *Phys. Chem. Res.* 3, 191–196. doi: 10.22036/pcr.2015.9193

Farobie, O., and Matsumura, Y. (2015). A comparative study of biodiesel production using methanol, ethanol, and tert-butyl methyl ether (MTBE) under supercritical conditions. *Bioresour. Technol.* 191, 306–311. doi: 10.1016/j.biortech.2015.04.102

Feyzi, M., Hassankhani, A., and Rafiee, H. R. (2013). Preparation and characterization of Cs/Al/Fe3O4 nanocatalysts for biodiesel production. *Energy Conver. Manage.* 71, 62–68. doi: 10.1016/j.enconman.2013.03.022

Fusco, L. (2006). *Peak Oil Theory*. St. John's: Memorial University of Newfoundland Recuperado de. Available online at: http://www.ucs.mun.ca/~oilpower/documents/Peakoil2-1.doc.pdf

Gardy, J., Osatiashtiani, A., Céspedes, O., Hassanpour, A., Lai, X., Lee, A. F., et al. (2018). A magnetically separable SO4/Fe-Al-TiO2 solid acid catalyst for biodiesel production from waste cooking oil. *Appl. Catal. B* 234, 268–278. doi: 10.1016/j.apcatb.2018.04.046

Goodrum, J. (2002). Volatility and boiling points of biodiesel from vegetable oils and tallow. *Biomass Bioenergy* 22, 205–211. doi: 10.1016/S0961-9534(01)00074-5

Gunstone, F. D., and Hamilton, R. J. (2001). *Oleochemical Manufacture and Applications*. Sheffield, UK: CRC Press.

Gupta, G., and Agrawal, M. (2015). "Preparation and Characterization of CaO Nanoparticle for Biodiesel Production," in *2nd International Conference on Emerging Technologies* (AIP Publishing), 1–10. doi: 10.1063/1.4945186

Gurunathan, B., and Ravi, A. (2015). Biodiesel production from waste cooking oil using copper doped zinc oxide nanocomposite as heterogeneous catalyst. *Bioresou. Technol.* 188, 124–127. doi: 10.1016/j.biortech.2015.01.012

Hashmi, S., Gohar, S., Mahmood, T., Nawaz, U., and Farooqi, H. (2016). Biodiesel production by using $CaO\text{-}Al_2O_3$ Nano catalyst. *Int. J. Eng. Res. Sc.* 2:3.

Heyne, K. (1987). The useful Indonesian plants. *Res. Dev. Agency Ministry Forestry, Jakarta, Indonesia* 845.

Hu, S., Guan, Y., Wang, Y., and Han, H. (2011). Nano-magnetic catalyst KF/CaO–Fe3O4 for biodiesel production. *Appl. Energy* 88, 2685–2690. doi: 10.1016/j.apenergy.2011.02.012

Karimi, A., Fatehifar, E., and Alizadeh, R. (2013). Synthesis and characterization of nanostructured CuO/CeO_2 catalysts via ultrasound assisted techniques used for selective oxidation of CO. *Iran. J. Chem. Eng.* 10, 51–59.

Karmee, S. K., and Chadha, A. (2005). Preparation of biodiesel from crude oil of *Pongamia pinnata*. *Bioresour. Technol.* 96, 1425–1429. doi: 10.1016/j.biortech.2004.12.011

Khan, N. A., and El Dessouky, H. (2009). Prospect of biodiesel in Pakistan. *Renew. Sustain. Energy Rev.* 13, 1576–1583. doi: 10.1016/j.rser.2008.09.016

Kumar, G., Kumar, D., Johari, R., and Singh, C. (2011). Enzymatic transesterification of Jatropha curcas oil assisted by ultrasonication. *Ultrasonics Sonochem.* 18, 923–927. doi: 10.1016/j.ultsonch.2011.03.004

Leung, D. Y., Wu, X., and Leung, M. (2010). A review on biodiesel production using catalyzed transesterification. *Appl. Energy* 87, 1083–1095. doi: 10.1016/j.apenergy.2009.10.006

Morshed, M., Ferdous, K., Khan, M. R., Mazumder, M., Islam, M., and Uddin, M. T. (2011). Rubber seed oil as a potential source for biodiesel production in Bangladesh. *Fuel* 90, 2981–2986. doi: 10.1016/j.fuel.2011.05.020

Moser, B. R. (2010). Camelina (*Camelina sativa* L.) oil as a biofuels feedstock: Golden opportunity or false hope? *Lipid Technol.* 22, 270–273. doi: 10.1002/lite.201000068

Munarso, J. (2010). *Plantation of Sterculia feotida. L as vegetable oil. Information technology agriculture*. Jakarta: Indonesia Agency for Agricultural Research and Development. 13–15.

Mustafa, G., Tahir, H., Sultan, M., and Akhtar, N. (2013). Synthesis and characterization of cupric oxide (CuO) nanoparticles and their application for the removal of dyes. *African J. Biotechnol.* 12, 6650–6660. doi: 10.5897/AJB2013.13058

Naik, S. N., Goud, V. V., Rout, P. K., and Dalai, A. K. (2010). Production of first and second generation biofuels: a comprehensive review. *Renew. Sustain. Energy Rev.* 14, 578–597. doi: 10.1016/j.rser.2009.10.003

Okitsu, K., Maeda, Y., and Bandow, H. (2014). Ultrasound assisted production of fatty acid methyl esters from transesterification of triglycerides with methanol in the presence of KOH catalyst: Optimization, mechanism and kinetics. *Ultrasonics Sonochem.* 21, 467–471. doi: 10.1016/j.ultsonch.2013.09.015

Okoronkwo, M., Galadima, A., and Leke, L. (2012). Advances in Biodiesel synthesis: from past to present. *Elixir Appl. Chem.* 43, 6924–6945.

Pathaka, P. K., Rajb, J., Saxena, G., and Uma, S. A. (2017). A review on production of biodiesel by transesterification using heterogeneous nanocatalyst. *Int. J. Sci. Res. Dev.* 5, 631–636.

Raj, F. R. M. S., and Sahayaraj, J. W. (2010). "A comparative study over alternative fuel (biodiesel) for environmental friendly emission," in *Recent Advances in*

Space Technology Services and Climate Change (RSTSCC) (Chennai: IEEE), 80–86.

Rao, P., Ramesh, S., and Kumar, S. (2015). Study of CI engine performance with diesel-biodiesel (*Sterculia foetida*) blend as fuel. *Intl. J. Trend Res. Dev.* 2, 76–79.

Rashid, U., Anwar, F., Ashraf, M., Saleem, M., and Yusup, S. (2011). Application of response surface methodology for optimizing transesterification of Moringa oleifera oil: Biodiesel production. *Energy Conver. Manage.* 52, 3034–3042. doi: 10.1016/j.enconman.2011.04.018

Rashid, U., Anwar, F., Yunus, R., and Al-Muhtaseb, A. H. (2015). Transesterification for biodiesel production using *Thespesia populnea* seed oil: an optimization study. *Int. J. Green Energy* 12, 479–484. doi: 10.1080/15435075.2013.853177

Rashid, U., Ibrahim, M., Yasin, S., Yunus, R., Taufiq-Yap, Y., and Knothe, G. (2013). Biodiesel from *Citrus reticulata* (mandarin orange) seed oil, a potential non-food feedstock. *Indus. Crops Products* 45, 355–359. doi: 10.1016/j.indcrop.2012.12.039

Rehan, M., Gardy, J., Demirbas, A., Rashid, U., Budzianowski, W., Pant, D., et al. (2018). Waste to biodiesel: a preliminary assessment for Saudi Arabia. *Bioresour Technol.* 250, 17–25. doi: 10.1016/j.biortech.2017.11.024

Salam, K. A., Velasquez-Orta, S. B., and Harvey, A. P. (2016). Surfactant-assisted direct biodiesel production from wet Nannochloropsis occulata by *in situ* transesterification/reactive extraction. *Biofuel Res. J.* 3, 366–371. doi: 10.18331/BRJ2016.3.1.6

Sarin, R., Sharma, M., Sinharay, S., and Malhotra, R. K. (2007). Jatropha–palm biodiesel blends: an optimum mix for Asia. *Fuel* 86, 1365–1371. doi: 10.1016/j.fuel.2006.11.040

Shikha, K., and Chauhan, Y. R. (2012). Biodiesel production from non edible-oils: a review. *J. Chem. Pharmaceut. Res.* 4, 4219–4230.

Shu, Q., Gao, J., Liao, Y., and Wang, J. (2011). Reaction kinetics of biodiesel synthesis from waste oil using a Carbon-based solid acid catalyst. *Chinese J. Chem. Eng.* 19, 163–168. doi: 10.1016/S1004-9541(09)60193-2

Sivakumar, P., Parthiban, K. S., Sivakumar, P., Vinoba, M., and Renganathan, S. (2012). Optimization of extraction process and kinetics of *Sterculia foetida* seed oil and its process augmentation for biodiesel production. *Indus. Eng. Chem. Res.* 51, 8992–8998. doi: 10.1021/ie300882t

Stavarache, C. E., Morris, J., Maeda, Y., Oyane, I., and Vinatoru, M. (2008). Syringa (*Melia azedarach* L.) berries oil: a potential source for biodiesel fuel. *Revista de Chimie* 59, 672–677.

Tajammul Hussain, S., Ahmed, W., Saeed, M., Danish Ali, S., and Asma, M. (2013). Fatty acid methyl ester production from waste cooking oil catalyzed by CuO-CeO2/NiO mixed oxides. *J. Renew. Sustain. Energy* 5:023104. doi: 10.1063/1.4794437

Ullah, K., Ahmad, M., and Qiu, F. (2015). Assessing the experimental investigation of milk thistle oil for biodiesel production using base catalyzed transesterification. *Energy* 89, 887–895. doi: 10.1016/j.energy.2015.06.028

Vicente, G., Coteron, A., Martinez, M., and Aracil, J. (1998). Application of the factorial design of experiments and response surface methodology to optimize biodiesel production. *Indus. Crops Products* 8, 29–35. doi: 10.1016/S0926-6690(97)10003-6

Williams, M. A. (2005). Recovery of oils and fats from oilseeds and fatty materials. *Bailey's Indus. Oil Fat Prod.* doi: 10.1002/047167849X.bio066

Conflict of Interest Statement: The authors declare that the research was conducted in the absence of any commercial or financial relationships that could be construed as a potential conflict of interest.

frontiers in Bioengineering and Biotechnology

ORIGINAL RESEARCH
published: 27 April 2018
doi: 10.3389/fbioe.2018.00050

Development of an Effective Chain Elongation Process From Acidified Food Waste and Ethanol Into n-Caproate

Mark Roghair[1], Yuchen Liu[1], David P. B. T. B. Strik[1], Ruud A. Weusthuis[2], Marieke E. Bruins[3] and Cees J. N. Buisman[1]*

[1] Sub-department of Environmental Technology, Wageningen University and Research, Wageningen, Netherlands, [2] Bioprocess Engineering, Wageningen University and Research, Wageningen, Netherlands, [3] Wageningen Food and Biobased Research, Wageningen University and Research, Wageningen, Netherlands

OPEN ACCESS

Edited by:
Abdul-Sattar Nizami, King Abdulaziz University, Saudi Arabia

Reviewed by:
Qaisar Mahmood, COMSATS Institute of Information Technology, Pakistan
Baskar Gurunathan, St. Joseph's College of Engineering, India
Weichao Wang, Purdue University, United States

***Correspondence:**
David P. B. T. B. Strik
david.strik@wur.nl

Specialty section:
This article was submitted to Bioenergy and Biofuels, a section of the journal Frontiers in Bioengineering and Biotechnology

Received: *10 March 2018*
Accepted: *13 April 2018*
Published: *27 April 2018*

Citation:
Roghair M, Liu Y, Strik DPBTB, Weusthuis RA, Bruins ME and Buisman CJN (2018) Development of an Effective Chain Elongation Process From Acidified Food Waste and Ethanol Into n-Caproate. Front. Bioeng. Biotechnol. 6:50. doi: 10.3389/fbioe.2018.00050

Introduction: Medium chain fatty acids (MCFAs), such as n-caproate, are potential valuable platform chemicals. MCFAs can be produced from low-grade organic residues by anaerobic reactor microbiomes through two subsequent biological processes: hydrolysis combined with acidogenesis and chain elongation. Continuous chain elongation with organic residues becomes effective when the targeted MCFA(s) are produced at high concentrations and rates, while excessive ethanol oxidation and base consumption are limited. The objective of this study was to develop an effective continuous chain elongation process with hydrolyzed and acidified food waste and additional ethanol.

Results: We fed acidified food waste (AFW) and ethanol to an anaerobic reactor while operating the reactor at long (4 d) and at short (1 d) hydraulic retention time (HRT). At long HRT, n-caproate was continuously produced (5.5 g/L/d) at an average concentration of 23.4 g/L. The highest n-caproate concentration was 25.7 g/L which is the highest reported n-caproate concentration in a chain elongation process to date. Compared to short HRT (7.1 g/L n-caproate at 5.6 g/L/d), long HRT resulted in 6.2 times less excessive ethanol oxidation. This led to a two times lower ethanol consumption and a two times lower base consumption per produced MCFA at long HRT compared to short HRT.

Conclusions: Chain elongation from AFW and ethanol is more effective at long HRT than at short HRT not only because it results in a higher concentration of MCFAs but also because it leads to a more efficient use of ethanol and base. The HRT did not influence the n-caproate production rate. The obtained n-caproate concentration is more than twice as high as the maximum solubility of n-caproic acid in water which is beneficial for its separation from the fermentation broth. This study does not only set the record on the highest n-caproate concentration observed in a chain elongation process to date, it notably demonstrates that such high concentrations can be obtained from AFW under practical circumstances in a continuous process.

Keywords: food waste, chain elongation, caproate, HRT, sludge, ethanol, sodium hydroxide

INTRODUCTION

Organic residual streams, like food waste, have great potential as alternative resource for production of fuels and chemicals because they are renewable and because they do not compete with the human food chain (Coma et al., 2017). The challenge is to convert these mixed residues into the desired products and purify them in an energy-efficient and economically viable process. An emerging technology that facilitates conversion of (derivatives of) organic residues into (precursors of) fuels and chemicals is chain elongation. Chain elongation is an anaerobic open-culture biotechnological process that converts volatile fatty acids (VFAs) and an electron donor into more valuable medium chain fatty acids (MCFAs) (Angenent et al., 2016). The conversion of VFAs into MCFAs with ethanol as electron donor is done by chain elongating micro-organisms (e.g., *Clostridium kluyveri*) that use the reverse β-oxidation pathway. In this pathway, 1 additional mole of ethanol is oxidized into acetate for every 5 chain elongation reactions (Equation 1) (Seedorf et al., 2008).

$$\text{Reverse } \beta - \text{ oxidation pathway } \quad 5C_xH_{2x-1}O_2^- + 6C_2H_6O \rightarrow 5C_{x+2}H_{2x+3}O_2^- + C_2H_3O_2^- + 4H_2O + H^+ + 2H_2 \quad (1)$$

VFAs can be obtained through hydrolysis and acidogenesis of organic residues. Electron donors that are suitable for chain elongation processes, such as ethanol (Steinbusch et al., 2011), hydrogen (Steinbusch et al., 2011), methanol (Chen et al., 2016b), and lactic acid (Zhu et al., 2015), can also be produced from organic residues (e.g., lignocellulosic bioethanol). Particularly, MCFAs can be used for production of aviation fuels (Harvey and Meylemans, 2014; Khor et al., 2017) and for other end-products such as solvents, lubricants, feed additives for poultry (Evans et al., 2017) and piglets (Hanczakowska et al., 2013), plastics and dyes (Angenent et al., 2016). The main advantage of chain elongation is that it is catalyzed by an anaerobic open-culture reactor microbiome (i.e., sludge). Open-culture microbiomes can tolerate mixtures of residual streams while they convert the residues under mild and non-sterile conditions. Chain elongation, therefore, does not need a chemical catalyst and proceeds under mild and non-sterile conditions. Although inhibition of competing processes is important, it is not necessary to do this by adding bioactive chemicals such as antibiotics or methanogenic inhibitors such as 2-bromoethanesulfonate (e.g., Roghair et al., 2018). As such, solid residual streams from the chain elongation process itself could be used as soil fertilizer upon composting.

MCFA production from organic residues through biomass hydrolysis, acidogenesis and chain elongation can be executed in a single-stage system (Agler et al., 2012) as well as in a two-stage system (Grootscholten et al., 2014). In a two-stage system, hydrolysis and acidogenesis are done in one stage and chain elongation in a subsequent stage. The advantage of a two-stage system over a single-stage system is that both stages can be optimized independently. Grootscholten et al. (2014) concluded that MCFA production from the organic fraction of municipal solid waste and additional ethanol in a two-stage system resulted in higher MCFA production rates and concentrations compared to a single-stage system. Another advantage of a two-stage system is that it allows easier control of the hydrogen partial pressure (pH_2) in the chain elongation stage by e.g., manipulating CO_2 loading rate (Grootscholten et al., 2014; Roghair et al., 2018). The pH_2 is important because it can thermodynamically inhibit competing processes such as anaerobic oxidation of MCFAs and anaerobic oxidation of ethanol, also known as excessive ethanol oxidation (EEO; Equation 2).

$$\text{Excessive ethanol oxidation (EEO)} \quad C_2H_6O + H_2O \rightarrow C_2H_3O_2^- + H^+ + 2H_2 \quad (2)$$

$$\text{Hydrogenotrophic methanogenesis} \quad 2H_2 + 0.5CO_2 \rightarrow 0.5CH_4 + H_2O \quad (3)$$

$$\text{Syntrophic ethanol oxidation} \quad C_2H_6O + 0.5\,CO_2 \rightarrow C_2H_3O_2^- + H^+ + 0.5\,CH_4 \quad (4)$$

Suppression of EEO is essential to make efficient use of ethanol because ethanol is a major cost factor. EEO is considered to be performed by ethanol-oxidizing microorganisms which do not perform chain elongation (Roghair et al., 2018). Earlier work demonstrated that ethanol is oxidized due to hydrogenotrophic methanogenesis (Equation 3) (Agler et al., 2014) and that the overall reaction can be referred to as syntrophic ethanol oxidation (Roghair et al., 2018) (Equation 4). By limiting the CO_2 loading rate to a chain elongation process, EEO was reduced from 28.8 to 15.9% of total ethanol consumption (Roghair et al., 2018). No CO_2 addition resulted in low and decreasing MCFA production rates. When working with organic residues, however, CO_2 loading rate may be more difficult to control because CO_2 is also a product of acidogenesis. Even though acidogenesis and chain elongation can be separated, dissolved CO_2 could still complicate the control over the actual CO_2 supply to the chain elongation process. In such a case, alternative strategies than CO_2 loading rate to suppress EEO are needed. Although EEO can be beneficial for ethanol upgrading processes to n-caproate (*in situ* ethanol oxidation into acetate and subsequent chain elongation into even-numbered fatty acids), one can consider ethanol upgrading as an inefficient use of ethanol per produced MCFA (Roghair et al., 2018). Furthermore, EEO acidifies the fermentation broth and this requires extra base addition for pH correction. Because the use of both ethanol and base cause major environmental impact over the life cycle of chain elongation processes (Chen et al., 2017), their consumption should be reduced in the development of this technology.

A high MCFA concentration in chain elongation processes would be beneficial because this improves its separation from the fermentation broth (López-Garzón and Straathof, 2014). Grootscholten et al. (2014) achieved a maximum n-caproate concentration of 12.6 g/L in a two-stage MCFA production

Abbreviations: VFAs, Volatile Fatty Acids; MCFAs, Medium Chain Fatty Acids; HRT, Hydraulic Retention Time; AFW, Acidified Food Waste; FW, Food Waste; NaOH, Sodium Hydroxide; EEO, Excessive Ethanol Oxidation; VS, Volatile Solids; VSS, Volatile Suspended Solids; TS, Total Solids; COD, Chemical Oxygen Demand; UASB, Upflow Anaerobic Sludge Blanket.

system from organic waste. Recently, considerably higher concentrations of n-caproate (>20 g/L) have been reported from chain elongation processes which were conducted in batch at near-neutral pH (Zhu et al., 2015; Liu et al., 2017). These studies suggest that such high concentrations can also be reached in a continuous chain elongation process as long as the hydraulic retention time (HRT) is long enough to allow product accumulation. The HRT, however, was also shown to influence the volumetric MCFA productivity as the highest reported MCFA production rate was achieved at a short HRT of 4 h (57 g/L/d) (Grootscholten et al., 2013a). A high MCFA productivity is desired to make effective use of the bioreactor; though MCFA production by chain elongation (62.4 g COD/L/d, Grootscholten et al., 2014) already exceeds the rate of methane production by anaerobic digestion (6.7–11.2 g COD/L/d[1], Syngellakis, 2015). Chain elongation studies that operated at near neutral pH usually maintained an HRT shorter than 1 d (Grootscholten et al., 2013b,c, 2014; Roghair et al., 2016, 2018). To date, however, there are no studies that report the effect of a long HRT in combination with a near-neutral pH in a chain elongation process from acidified organic waste and ethanol.

The objective of this study was to develop an effective continuous biological chain elongation process from acidified food waste (AFW) and ethanol to produce n-caproate at a high concentration while EEO is limited. The effect of 2 HRTs (1 and 4 d) was compared and evaluated based on an extensive set of performance indicators including MCFA production rates, MCFA concentrations, MCFA production efficiency, substrate consumption efficiency, rate of EEO and base consumption. Finally, an outlook is given on the potential of the developed bioprocess.

MATERIALS AND METHODS

Preparation of Food Waste

Food waste was collected from Rotie, a recycling company in Lijnden, the Netherlands. The waste consisted of outdated food scraps and had a total solids (TS) content of 15.5 ± 0.2% (w/w), a volatile solids (VS) content of 13.8 ± 0.4% (w/w) and a sodium content of 2.7 ± 0.01 g/L. The waste was stored at −20°C until further use. Before use as fermentation feed, the waste was thawed at 4°C, diluted until ∼4.0% VS (w/w) with tap water and the pH was adjusted to 5.5 with 5 M NaOH.

First Stage: Hydrolysis and Acidogenesis of Food Waste

Hydrolysis and acidogenesis of food waste was executed in a batch reactor with a working volume of 20 L as described by Chen et al. (2016a). After loading 20 L diluted food waste into the reactor, the reactor content was sparged with N_2 for 10 min to remove oxygen. Thereafter, 200 mL inoculum (derived from a previous hydrolysis and acidogenesis run that used the same substrate and reactor configuration) and 5 mL Antifoam B Emulsion (Sigma-Aldrich, the Netherlands) were added. The reactor was then operated at 35°C, 1 atm, stirred at 44 rpm while the pH was maintained at 5.5 using a pH sensor (model QP-635-E275-S8, ProSense BV - QiS, Oosterhout, The Netherlands) and 5M NaOH. The slightly acidic pH was selected to inhibit methanogenesis (Agler et al., 2012; Ge et al., 2015). After 18 days of operation, reactor content (acidified food waste; AFW) was centrifuged (15,000 rpm for 15 min) and decanted to remove solids and sieved (1 mm) to remove floating particles (e.g., lipids). This was performed for in total four 20 L batches to generate sufficient AFW as feedstock for the chain elongation stage. The resulting centrifuged and sieved AFW from the four batches was pooled together and stored at 4°C until further use. The following compounds in the pooled AFW were measured (concentration in g/L): inorganic carbon (0.011), sodium (4.8), ethanol (0.1), butanol (0.2), acetate (8.1), propionate (1.7), isobutyrate (0.6), n-butyrate (9.3), isovalerate (0.4), valerate (0.4) and n-caproate (1.4). The mentioned organic compounds account for a chemical oxygen demand (COD) of 35 g_{O2}/L. AFW had a soluble COD of 37.1 g_{O2}/L (LCK 014 COD, Hach Lange GMBH, Germany).

Average VS consumption in the hydrolysis and acidogenesis stage was determined based on the mean VS content at the beginning of two batches ($n = 6$) and on the mean VS content at the end of these two batches ($n = 6$). Average NaOH consumption in the hydrolysis and acidogenesis stage was determined based on the difference between the mean sodium content of diluted food waste ($n = 3$) and the mean sodium content of AFW ($n = 3$).

Seconds Stage: Chain Elongation of Acidified Food Waste and Ethanol

Chain elongation of AFW and ethanol was performed in one single process using a continuously stirred anaerobic reactor as described by Roghair et al. (2016). In short, a continuous reactor with a working volume of 1 L was operated at 30°C, 1 atm, stirred at 100 rpm while the pH was maintained at 6.8 using a pH sensor (Applisens model Z001023551, Schiedam, The Netherlands) and 2M NaOH. Gaseous CO_2 was supplied with a mass-flow controller (Brooks Instruments 5850S, the Netherlands) at 1 L_{CO2}/L/d. The reactor was started with a synthetic medium that contained 13.8 g/L propionic acid (≥99.5%, Sigma-Aldrich) and 32.2 g/L ethanol (Absolute, VWR). These starting conditions have formerly shown to induce formation of granular sludge (Roghair et al., 2016) and can also be used to distinguish the carbon flux of ethanol upgrading from VFA upgrading (Roghair et al., 2018). The composition of other components (salts, yeast extract, vitamins and trace elements) were as previously described (Roghair et al., 2016). The reactor was inoculated in batch mode on day 1 with 50 mL chain elongation sludge from a previous run; the inoculum contained chain elongating micro-organisms, ethanol oxidizers and hydrogenotrophic methanogens (Roghair et al., 2018). On day 9, the reactor operation mode was set from batch to continuous with an HRT of 4 d. From day 19 onwards, the reactor was fed with AFW to which 32.2 g/L ethanol was added. On day 58, the HRT was set from 4 to 1 d. On day 103, the HRT was set back from 1 to 4 d.

Liquid samples were taken from the reactor content and from the influent tank 1-3 times per week. Gas samples were taken

[1a] Based on 5–6 m^3/m^3/d with a methane content of 50–70% Syngellakis, 2015

from the headspace 1-3 times per week. The reactor was assumed to be in steady state when n-caproate production rates were similar (with a maximum relative standard deviation of 16%) over a period of at least 7 HRTs. Average concentrations and rates and their corresponding standard deviations were based on at least nine measurements within a steady state. Average NaOH consumption in the chain elongation stage was determined based on the difference between average sodium concentration in the effluent ($n = 3$ different samples during a steady state) and on the average sodium concentration in the influent tank ($n = 3$ different samples during a steady state).

Analytical Procedures

Alcohols (C2-C6) and fatty acids (C2-C8) were analyzed by gas chromatography using an Agilent 7890B (USA), equipped with HP-FFAP capillary column (l = 25 m, ID = 0.32 mm, film = 0.5 μm). 1 μl from a diluted sample was injected into a liner with glass wool at 250°C. Vaporized compounds entered the column, along with helium as carrier gas, with a flow rate of 1.25 mL/min (first 3 min) and 2 mL/min (until the end of the run). The oven temperature program was as follows: 60°C for 3 min; 21°C/min up to 140°C; 8°C/min up to 150°C and constant for 1.5 min; 120°C/min up to 200°C and constant for 1.25 min; 120°C/min up to 240°C and constant for 3 min. Compounds were detected with a flame ionization detector at 240°C, fed with 30 mL/min hydrogen and 400 mL/min air.

Gaseous compounds (N_2, H_2, CO_2, CH_4, and O_2) were analyzed by gas chromatography using an Agilent Varian CP4900 μGC (USA) equipped with a thermal conductivity detector and two parallel columns: a Mol Sieve 5A PLOT column (l = 10 m, ID = 0.32 mm, film = 0.15 μm) and a PoraPlot U column (l = 10 m). The oven temperature was 80°C for the Mol Sieve 5A PLOT column and 65°C for the PoraPLOT U column. The carrier gas was argon and had a flow rate of 1.47 mL/min.

Sodium was measured by ion chromatography using a Metrohm Compact IC Flex 930 (Schiedam, the Netherlands) equipped with a pre-column (Metrohm Metrosep RP 2 Guard/3.6), a cation column (Metrosep C 4-150/4.0) and a conductivity detector. The mobile phase was 3mM nitric acid.

TS, VS, and VSS were determined following Standard Methods (APHA, 1998). The filter for VSS measurements (Whatman GF/F 0.7 μm) was preheated at 450°C prior to filtration. Inorganic carbon was measured using a total organic carbon analyser (Shimadzu TOC-VCPH, Japan).

Mathematical Expressions

The volumetric production or consumption rate of aqueous compounds is based on the difference between effluent concentration and influent concentration divided by the HRT:

Rate [g/L/d] = (effluent concentration [g/L] – influent concentration [g/L]) / HRT [d]

Excessive ethanol oxidation is the difference between total ethanol consumption and ethanol consumption through the reverse β-oxidation pathway:

Excessive ethanol oxidation (EEO) [g/L/d] = rate total ethanol consumption [g/L/d] – rate ethanol consumption through the reverse β-oxidation pathway [g/L/d] (Roghair et al., 2018)

Ethanol consumption through the reverse β-oxidation pathway (g/L/d) = ethanol use for elongation of fatty acids through the reverse β-oxidation pathway (g/L/d) + ethanol oxidation into acetate through the reverse β-oxidation pathway (g/L/d)

Ethanol use for elongation of fatty acids through the reverse β-oxidation pathway (g/L/d) = (rate n-butyrate [mmol/L/d] + rate valerate [mmol/L/d] + 2· rate n-caproate [mmol/L/d] + 2· rate n-heptanoate [mmol/L/d] + 3 · rate n-caprylate [mmol/L/d]) · 46.05 / 1000

Ethanol oxidation into acetate through the reverse β-oxidation pathway (g/L/d) = Ethanol use for elongation of fatty acids through the reverse β-oxidation pathway (g/L/d) · 0.2

Selectivity is defined as product produced relative to substrates consumed on an electron basis (Grootscholten et al., 2014):

Selectivity [mol e %] = product formation rate [mol e/L/d] / total substrate consumption rate (mol e / L/d) · 100

Selectivity values that are based on a carbon basis are reported in the supplementary material but are not presented and discussed in the results and discussion section.

Substrate consumption efficiency is defined as substrate consumed relative to the organic loading rate on an electron basis:

Substrate consumption efficiency [mol e %] = (|substrate consumption rate [mol e/L/d]| / organic loading rate [mol e/L/d] · 100

Product production efficiency is defined as product produced relative to the organic loading rate on an electron basis

Product production efficiency [mol e %] = product formation rate [mol e/L/d] / organic loading rate [mol e/L/d] · 100

RESULTS

Higher MCFA Concentrations and Selectivities at Long HRT Than at Short HRT

Acidified food waste (AFW) and ethanol were fed to a continuous biological chain elongation process, resulting in production of MCFAs (n-caproate, isocaproate, n-heptanoate and n-caprylate). n-Caproate, the dominant MCFA, was produced (5.5 ± 0.4 g/L/d) at a high steady state concentration of 23.4 ± 1.0 g/L. This was observed at long HRT (4 d) from day 28 through day 58 (**Figure 1**). After the HRT was decreased from 4 to 1 d (short HRT), another steady state was observed from day 79 through day 103. Here, n-caproate was produced at a similar rate (5.6 ± 0.9 g/L/d) but at a lower concentration (7.1 ± 0.9 g/L). On day 103, the HRT was increased from 1 to 4 d. Again, n-caproate was continuously produced at a high steady state concentration (23.2 ± 1.9 g/L). This was observed from day 114 through day 147. The maximum n-caproate concentration was 25.7 g/L on day 120. Reactor performance of the first steady state at long HRT was similar as the reactor performance of the second steady state at long HRT. This shows that the effect of HRT on reactor performance is reversible. From here on, however, "long HRT"

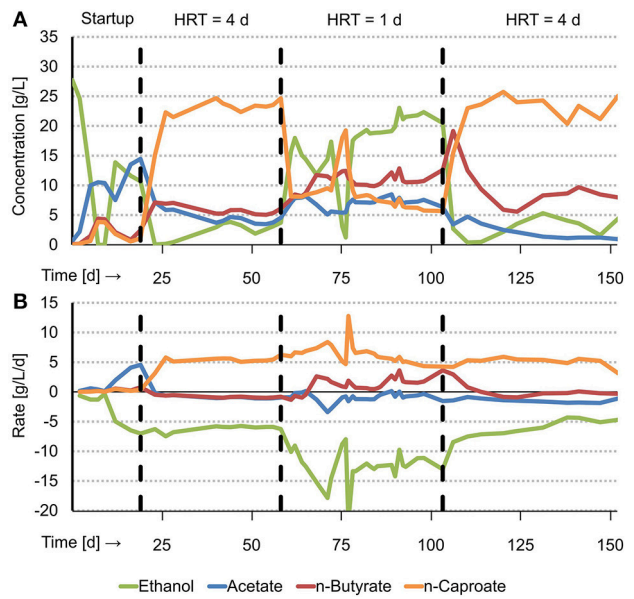

FIGURE 1 | Graphical summary of experimental results with concentrations over time **(A)** and net production and consumption rates over time **(B)**. T = 30°C, pH = 6.8, V = 1 L, CO_2 loading rate = 1.0 L_{CO2}/L/d.

refers to the first steady state (day 28–58). Mean steady state rates, concentrations and selectivities of all identified substrates and products at long and at short HRT are reported in Tables S1 and S2 respectively. A summary of reactor performance indicators and properties of the steady states at both long and short HRT are reported in **Table 1** for comparison.

At long HRT, n-heptanoate and n-caprylate were both produced at a low rate (∼0.15 g/L/d) and concentration (∼0.6 g/L) compared to n-caproate. At short HRT, however, these MCFAs were produced at insignificant amounts (<0.1 g/L). Isocaproate was produced in trace amounts at both long and short HRT. The selectivity of MCFAs was 81.6 mol e % at long HRT and 46.3 mol e % at short HRT. The remaining consumed carbon ended up as VSS (biomass), VFAs, methane, propanol, and unidentified products as given in Tables S1 and S2. The MCFA productivity at both long and short HRT (∼12.5 g COD/L/d) was somewhat higher compared to the typical methane productivity in an anaerobic digester (6.7–11.2 g COD/L/d[1], Syngellakis, 2015).

Excessive Ethanol Oxidation, Methane Production and NaOH Consumption

Long HRT did not only result in higher MCFA concentrations and selectivities compared to short HRT, it also resulted in less EEO and in less sodium hydroxide (NaOH) consumption per MCFA produced. EEO occurred at a 6.3 times lower rate at long HRT (0.9 ± 0.4 g/L/d) than at short HRT (5.6 ± 1.4 g/L/d). This process was also relative to the total ethanol consumption rate lower at long HRT (14.7 ± 5.5%) than at short HRT (45.0 ± 9.7%). Methane production was 3.4 times lower at long HRT (12.8 ± 2.6 mmol/L/d) than at short HRT (43.8 ± 2.5 mmol/L/d). A previous study showed that hydrogenotrophic methanogenesis and EEO are coupled and that the overall reaction can be referred to as syntrophic ethanol oxidation (Roghair et al., 2018). In syntrophic ethanol oxidation, the stoichiometric ratio between methane production and ethanol oxidation is 0.5 mol/mol (Equation 4). The present study shows a similar ratio at long HRT (0.7 ± 0.3) and at short HRT (0.4 ± 0.1) which implies that EEO, like in the previous study, was a result of syntrophic ethanol oxidation. Less EEO also led to fewer NaOH consumption for pH correction because EEO is an acidifying process that releases a proton (Equation 2). NaOH consumption per produced MCFA was two times lower at long HRT (0.92 ± 0.04 mol_{NaOH}/mol_{MCFA}) than at short HRT (1.93 ± 0.31 mol_{NaOH}/mol_{MCFA}). These results not only show that EEO can be limited at long HRT but also that consumption of NaOH is hereby reduced.

Consumption of VFAs and Ethanol

Acetate, propionate and ethanol were consumed at both long and short HRT. However, whereas butyrate was consumed at long HRT (−0.9 ± 0.1 g/L/d), it was produced at short HRT (1.6 ± 1.1 g/L/d). This resulted in a lower n-butyrate concentration in the reactor at long HRT (5.6 ± 0.6 g/L) than at short HRT (10.8 ± 1.0 g/L). A net consumption of n-butyrate instead of production indicates that caproate production is more efficient in ethanol-use. This is because n-butyrate consumption (i.e., elongation) requires less ethanol than acetate elongation to caproate or ethanol upgrading. Whereas ethanol upgrading requires 3 moles of ethanol to produce 1 mole of n-caproate, VFA upgrading requires only 1.2 moles of ethanol from n-butyrate or 2.4 moles of ethanol from acetate (Roghair et al., 2018). Indeed, the chain elongation process at long HRT was more efficient in ethanol-use than at short HRT. Approximately two times less ethanol was consumed per produced MCFA at long HRT (0.87 ± 0.07 mol C/mol C) than at short HRT (1.83 ± 0.31 mol C/mol C). The VFA consumption per produced MCFA at both long (0.29 ± 0.04 mol C/mol C) and short HRT (0.20 ± 0.07 mol C/mol C) were found to be similar.

The concentration of ethanol in the reactor (and thus also in the effluent) was much lower at long HRT (2.8 ± 1.1 g/L) than at short HRT (20.1 ± 1.6 g/L). The ethanol consumption efficiency, therefore, defined as consumed ethanol relative to supplied ethanol, was higher at long HRT (98.6 ± 5.4 mol e %) than at short HRT (40.3 ± 3.5 mol e %). A high ethanol consumption efficiency (or a low ethanol concentration in the effluent) is desired because any unconsumed ethanol requires an additional recovery or treatment step after the chain elongation stage which makes the overall process more expensive. The VFA consumption efficiency was also higher at long HRT (45.8 ± 6.9 mol e %) than at short HRT (7.2 ± 2.3 mol e %). Although VFAs are not as costly as ethanol, it is evident that a higher VFA consumption efficiency is preferred because the remaining VFAs (e.g., after selective extraction of the MCFAs) also have to be recovered or treated with a waste water treatment system.

VSS

The mean VSS concentration in the reactor at long HRT (0.34 ± 0.23 g/L) was similar compared to the mean VSS concentration

TABLE 1 | Performance indicators and properties of the chain elongation process at long and at short HRT.

Performance indicator	Unit	Long HRT [4 d]	Short HRT [1 d]
STEADY STATE CHARACTERISTICS			
Steady state interval	d	28–58	79–103
Number of HRTs	–	7.5	24.3
PRODUCTS			
n-Caproate concentration	g/L	23.4 ± 1.0	7.1 ± 0.9
n-Caproate rate	g/L/d	5.5 ± 0.4	5.6 ± 0.9
n-Caproate selectivity	mol e %	76.5 ± 5.0	44.6 ± 7.8
MCFA selectivity	mol e %	81.6 ± 5.0	46.3 ± 8.0
Methane rate	mmol/L/d	12.8 ± 2.6	43.8 ± 2.5
SUBSTRATES			
Ethanol loading rate	g/L/d	6.1 ± 0.2	30.6 ± 1.3
Ethanol concentration	g/L	2.8 ± 1.1	20.1 ± 1.6
Ethanol rate	g/L/d	−6.0 ± 0.3	−12.3 ± 1.1
EEO	g/L/d	0.9 ± 0.4	5.6 ± 1.4
EEO	% of total ethanol use	14.7 ± 5.5	45.0 ± 9.7
Acetate rate	g/L/d	−1.0 ± 0.2	−0.8 ± 0.5
Propionate rate	g/L/d	−0.3 ± 0.0	−0.7 ± 0.1
n-Butyrate rate	g/L/d	−0.9 ± 0.1	1.6 ± 1.1
SUBSTRATE TO PRODUCT CONVERSIONS			
Consumed VFA per produced MCFA	mol C/mol C	0.29 ± 0.04	0.20 ± 0.07
Consumed Ethanol per produced MCFA	mol C/mol C	0.87 ± 0.07	1.83 ± 0.31
CONSUMPTION/PRODUCTION EFFICIENCY			
Ethanol consumption efficiency	mol e %	98.6 ± 5.4	40.3 ± 3.5
VFA consumption efficiency	mol e %	45.8 ± 6.9	7.2 ± 2.3
n-Caproate production efficiency	mol e %	58.7 ± 2.9	12.8 ± 2.1
MCFA production efficiency	mol e %	62.6 ± 2.9	13.3 ± 2.2
NaOH USE			
Sodium concentration in influent [AFW]	g/L	4.9 ± 0.1	4.8 ± 0.1
Sodium concentration in reactor	g/L	9.1 ± 0.5	7.0 ± 0.0
Consumed NaOH per produced MCFA	mol/mol	0.92 ± 0.04	1.93 ± 0.31
VSS			
VSS concentration	g/L	0.34 ± 0.23	0.33 ± 0.03
VSS rate	g/L/d	0.02 ± 0.05	0.18 ± 0.33
Growth rate	g/g/d	0.07 ± 0.16	0.54 ± 1.00

in the reactor at short HRT (0.33 ± 0.03 g/L). These reactor concentrations were in the same order of magnitude as the VSS concentrations in the effluent (0.43 ± 0.32 g/L at long HRT and 0.35 ± 0.20 g/L at short HRT), implying that the reactor was ideally stirred with no biomass retention (i.e., CSTR). Formation of granular sludge, however, was observed like in the earlier experiment with the same set-up while using a synthetic medium (Roghair et al., 2016). The earliest observation of granules (by eye visible) was on day 82, at short HRT. Granules disappeared within a few days after the HRT was increased on day 103. Because the formation of granular sludge coincided with high-rate syntrophic ethanol oxidation (at short HRT) it is likely that this syntrophic process attributed to sludge granulation. Syntrophic processes may benefit from granulation because granules could facilitate a more efficient interspecies hydrogen transfer due to the decreased intermicrobial distances (Kouzuma et al., 2015).

The mean VSS concentration in the influent was 0.25 ± 0.06 g/L. From the mentioned values the VSS production rate and VSS specific growth rate were calculated (**Table 1**). Although one could expect a four times lower growth rate at long HRT (0.07 ± 0.16 g/g/d) than at short HRT (0.54 ± 1.0 g/g/d), there was no significant difference due to the large standard deviations.

DISCUSSION

Continuous n-Caproate Production at a High Concentration From Acidified Food Waste

In this study, an effective two-stage MCFA production process from food waste and ethanol was developed. The microbiome in the second stage (chain elongation) was able to continuously produce n-caproate at 23.4 ± 1.0 g/L while EEO was limited to

TABLE 2 | Overview of comparable studies that report high n-caproate concentrations and/or rates using open cultures.

Reactor type	Substrate(s)	pH	HRT	n-Caproate			References
				Concentration [g/L]	Rate [g/L/d]	Selectivity [mol e%]	
Continuously stirred anaerobic reactor	AFW and ethanol	6.8	4 d	23.4	5.5	76.5	This study
Continuously stirred anaerobic reactor	AFW and ethanol	6.8	1 d	7.1	5.6	44.6	This study
Batch reactor	Lactate	∼6.5	N.A.	23.4	1.1	81.4	Zhu et al., 2015
Batch reactor	Acetate and ethanol	∼6.5	N.A.	21.1	N.D.	65.0	Liu et al., 2017
Continuous upflow anaerobic filter	Acetate and ethanol	6.5–7.2	4 h	9.3	55.8	∼78.0	Grootscholten et al., 2013a
Continuous upflow anaerobic filter	Acidified food/garden waste and ethanol	6.5–7.0	11 h	12.6	26.0	72.0	Grootscholten et al., 2014
Continuous upflow anaerobic filter	Acetate and ethanol	6.5–7.0	17 h	11.1	15.7	85.0	Grootscholten et al., 2013c

N.A., Not applicable.
N.D., Not determined.

14.7 ± 5.5% of total ethanol consumption. This was achieved at long HRT (4 d) and at near-neutral pH (6.8) but without in-line product extraction. Thus, a long HRT was shown to be effective for this specific waste stream. The n-caproate production rate was similar for both long and short HRT (∼5.5 g/L/d) and was much lower compared to the highest reported n-caproate production rate to date (55.8 g/L/d) (Grootscholten et al., 2013a). This high production rate, however, occurred at a substantially lower n-caproate concentration (9.3 g/L) than obtained in the present study. An overview of comparable studies that reported high n-caproate concentrations and/or rates using open cultures is shown in **Table 2**.

A high n-caproate concentration is beneficial for its separation from the fermentation broth. The obtained n-caproate concentration in the present study is more than twice as high as the maximum solubility of the undissociated form of n-caproate, n-caproic acid, in water (∼10.8 g/L, Yalkowsky et al., 2016). Thus, in theory, the high n-caproate concentration allows it to be separated from the effluent by phase separation after lowering the pH to 4.9 or lower. A recent study, executed by Zhu et al. (2015), also reported a high n-caproate concentration (23.4 g/L) using an anaerobic reactor microbiome. The n-caproate was produced from lactate as the sole carbon source in a batch process using an inoculum that was derived from mature pit mud, a microbiome used for the production of Chinese strong-flavored liquor. Their process reached a higher n-caproate selectivity (81.4 mol e %) than the process in the present study at long HRT (76.5 mol e %). However, the process in the present study achieved a slightly higher MCFA selectivity (81.6 mol e %) because it also produced other MCFAs (isocaproate, n-heptanoate and caprylate).

Liu et al. (2017) also reported a high n-caproate concentration (21.2 g/L) from ethanol and acetate using an anaerobic reactor microbiome. They were able to produce this in a batch process upon addition of biochar and 2-bromoethanesulfonate (Liu et al., 2017). The maximum n-caproate selectivity was lower (65.0 mol e %) than the maximum n-caproate selectivity in the present study (76.5 mol e %).

The studies by Zhu et al. (2015), and by Liu et al. (2017) already showed that high n-caproate concentrations (>20 g/L) can be reached using anaerobic reactor microbiomes. However, they were using synthetic media and batch systems. As such, the present study does not only show that such high concentrations can be obtained from organic residues, it also shows that this can be obtained in a continuous process and without the use of bioactive compounds such as 2-bromoethanesulfonate. The organic residue that was used, food waste, is a suitable substrate for MCFA production not only because such conversion was recently subjected to a life cycle assessment (Chen et al., 2017) but also because it is currently being developed to a demonstration factory, processing ∼40 ton/day, by ChainCraft in Amsterdam, the Netherlands.

Why Was Reactor Performance so Much Better at Long HRT Than at Short HRT?

The performance of the chain elongation process was far better at long HRT than at short HRT. A long HRT did not only result in a higher concentration of MCFAs, it also led to a lower rate of syntrophic ethanol oxidation, a net n-butyrate consumption instead of production, and to less NaOH consumption for pH correction. Why was reactor performance so much better at long HRT?

The difference in MCFA concentration can be explained as follows: at long HRT, the microbiome had sufficient time to accumulate MCFAs while these products were washed out (as effluent) at a relatively low rate. This resulted in a high caproate concentration (23.4 ± 1.1 g/L). Vice versa, at short HRT, the microbiome had little time to accumulate MCFAs while these products were washed out at a relatively high rate. This resulted in a considerably lower caproate concentration (7.1

± 0.9 g/L). Because production of n-caproate occurred at the same volumetric production rate at both long and short HRT (∼5.5 g/L/d), it is a logical consequence that n-caproate reached a higher concentration at long HRT than at short HRT. The high n-caproate concentration could also be achieved because the process was not limited by availability of substrates as sufficient ethanol (2.8 ± 1.1 g/L), acetate (4.2 ± 0.8 g/L) and n-butyrate (5.6 ± 0.6 g/L) was observed in the reactor. At short HRT, however, substantially more ethanol (20.1 ± 1.6 g/L), acetate (7.3 ± 0.5 g/L) and n-butyrate (10.8 ± 1.0 g/L) was observed but no higher MCFA production rates. This seems to be limited by the biomass concentration or by the high (i.e., inhibitory) ethanol concentration (Lonkar et al., 2016).

Syntrophic ethanol oxidation was more limited at long HRT than at short HRT. Two explanations can be given: firstly, the low ethanol concentration at long HRT may have resulted in a low rate of EEO. Vice versa, the high ethanol concentration at short HRT may have resulted in a high rate of EEO. However, a previous chain elongation study showed that ethanol loading rate and ethanol concentration does not substantially influence reactor performance as long as ethanol is not depleted (Roghair et al., 2018). Secondly, the high MCFA concentration may have caused an inhibitory effect on (one of) the involved competing syntrophs (i.e., ethanol oxidizers and hydrogenotrophic methanogens). It is known that undissociated MCFAs are toxic to microorganisms because they can damage the cell membrane (Royce et al., 2013). The average undissociated MCFA concentration at long HRT (at pH 6.8) was 0.27 g/L. Ge et al. (2015) determined that chain elongation proceeds until a toxic limit of 0.87 g/L undissociated n-caproic acid is reached (Ge et al., 2015) although recent work demonstrated chain elongation activity up to 1.46 g/L undissociated n-caproic acid (Andersen et al., 2017). Because chain elongating microorganisms were producing MCFAs at ∼5.8 g/L/d in the present study, evidently these organisms were not rigorously inhibited by the undissociated MCFAs. It is well possible, however, that these undissociated MCFAs (at 0.27 g/L) were selectively inhibitory to either ethanol oxidizers or hydrogenotrophic methanogens. This would explain the limited rate of syntrophic ethanol oxidation at long HRT compared to a short HRT while chain elongation could proceed at a similar rate at both HRTs. It is also possible that the dissociated form of n-caproate was selectively inhibitory to one of the syntrophs. This means that dissociated n-caproate (i.e., the conjugate base) becomes toxic to ethanol oxidizers or hydrogenotrophic methanogens at a concentration around 20 g/L.

The data is not consistent to point out whether hydrogenotrophic methanogens or ethanol oxidizers were more inhibited at long HRT: whereas the first steady state at long HRT (day 28 to day 58) had a pH_2 below the detection limit of the gas chromatograph (<0.1%), the second steady state at long HRT (day 138–147) had a pH_2 of up to 30%. This means that the data from the first steady state suggests that ethanol oxidizers were more inhibited whereas data from the second steady state suggests that hydrogenotrophic methanogens were more inhibited. To what extent n-caproic acid and n-caproate is toxic to hydrogenotrophic methanogens and ethanol oxidizers could be elucidated in further studies. In any way, irrespective how syntrophic ethanol oxidation was limited, it is clear from the results that longer HRTs should be applied in chain elongation processes at near-neutral pH to allow n-caproate accumulation and to limit the rate of syntrophic ethanol oxidation. This limited rate of syntrophic ethanol oxidation results in a more efficient use of ethanol, more VFA consumption and in less base addition for pH control and as such, in a more effective chain elongation process.

Methanogenic UASB Sludge Can Acclimate Into a Reactor Microbiome That Is Able to Produce n-Caproate at High Concentrations

This study can be compared with a previous study (Grootscholten et al., 2014). Both studies focused on two-stage MCFA production from organic residues and ethanol using anaerobic reactor microbiomes. In the previous study, a continuous chain elongation process was operated at similar pH (6.5–7.0) but at shorter HRT than in the present study (11 h instead of 1 and 4 d). This resulted in a lower maximum n-caproate concentration (12.6 g/L) and selectivity (72.0 mol e %). Besides, n-butyrate was produced instead of consumed, indicating that the process was not efficient in ethanol use. A hypothesis is that the process in the previous study could have performed better, including a high n-caproate concentration, if both the HRT and the ethanol concentration in the influent were increased. Of course, the origin of the inoculum may also have an effect on reactor performance because this determines which pathways or microorganisms are introduced and to what extent the initial microbiome is acclimated. The inoculum used by Grootscholten et al. (2014) and also the inoculum used in the present study were both eventually derived from a study executed by Steinbusch et al. (2011), who used granular sludge from an upflow anaerobic sludge blanket (UASB) reactor treating brewery wastewater (Steinbusch et al., 2011). This shows that high n-caproate concentrations can be obtained using various types of inocula and not only with mature pit mud (e.g., Zhu et al., 2015) or with mesophilic sludge from an anaerobic reactor treating paper mill wastewater (e.g., Liu et al., 2017). Under the right circumstances (e.g., as described in this study), UASB sludge from a methanogenic reactor will likely acclimate within a matter of weeks to a reactor microbiome that is able to produce n-caproate at high concentrations (>20 g/L).

Consumption of Food Waste, Ethanol and Base in the Overall Two-Stage System

In this study, MCFAs were produced from food waste and ethanol using a two-stage system. In the hydrolysis and acidogenesis stage, part of the food waste was converted into VFAs while some MCFAs were also produced. In the chain elongation stage, a part of the VFAs from the hydrolysis and acidogenesis stage were converted with additional ethanol into MCFAs while some ethanol was also used for ethanol upgrading. Both stages required NaOH addition to keep the pH constant in the reactors. Based

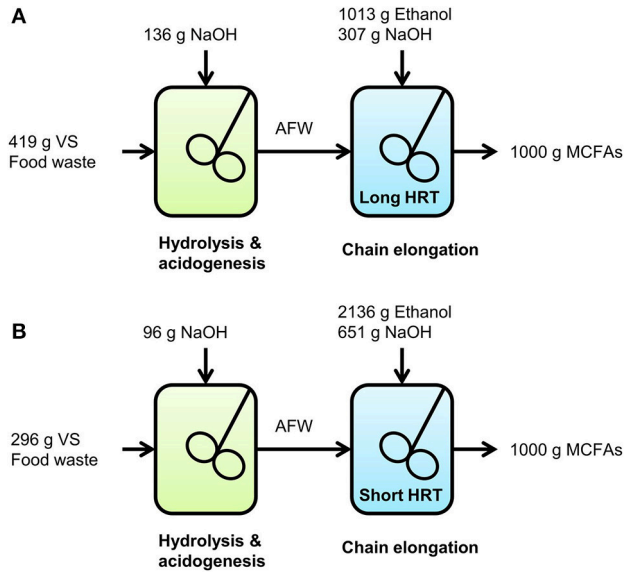

FIGURE 2 | Graphical representation on how much food waste (g VS), ethanol and NaOH would be consumed to yield 1,000 g MCFAs in the two-stage system at long HRT **(A)** and at short HRT **(B)** in the chain elongation stage.

on the results of this study it was possible to calculate how much food waste (expressed as g VS), ethanol and NaOH would be consumed to yield 1,000 g MCFAs. This was done for two scenarios; at long and at short HRT in the chain elongation stage. Equations are shown in Table S3. Parameters that were used as input for the equations are shown in Table S4 and were based on:

- Observed conversions and average NaOH consumption in the hydrolysis and acidogenesis stage (VFA yield on VS, MCFA yield on VS, consumed NaOH per consumed VS).
- Observed steady state conversions and NaOH consumption in the chain elongation stage (consumed VFAs per produced MCFAs, consumed ethanol per produced MCFAs, consumed NaOH per consumed ethanol).
- Average MCFA composition in the chain elongation stage (average carbon atoms per produced MCFAs, average molar weight of produced MCFAs).

A graphical representation on how much food waste (in g VS), ethanol and NaOH would be consumed to yield 1,000 g MCFAs at long and short HRT in the chain elongation stage is shown in **Figure 2**.

To produce 1,000 g MCFAs, the two-stage system with a long HRT in the chain elongation stage would consume 53% less ethanol, 41% less NaOH and 42% more VS compared to a two-stage system with a short HRT in the chain elongation stage. This does not only show that a long HRT in the chain elongation stage result in a more efficient consumption of ethanol and base in the chain elongation stage itself, it also shows that base consumption is hereby reduced in the overall two-stage system. Unfortunately, such quantification on waste-use and chemical-use is not common in chain elongation studies to date.

Addition of ethanol could be minimized or even completely avoided by steering the hydrolysis and acidogenesis stage to MCFAs and/or lactate production. In this study, for example, 1.6 g/L n-caproate was produced in the hydrolysis and acidogenesis stage without addition of an external electron donor. Lim et al. (2008) also demonstrated production of n-caproate (up to 5 g/L) from food waste without an external electron donor (Lim et al., 2008). Xu et al. (2017) demonstrated conversion of acid whey waste into MCFAs via lactate (Xu et al., 2017) using a two-stage system; also without an external electron donor. This shows that the effectiveness of MCFA production processes from diverse organic waste streams can be further improved by optimizing the hydrolysis and acidogenesis stage. Studies should also report on how much base or acid or electricity was used for pH control for a better comparison in terms of effectiveness.

Chemical base consumption could be fully eliminated through membrane electrolysis using electricity and separation of fatty acids, as was demonstrated by Andersen et al. (2015). They fermented thin stillage into VFAs and MCFAs using a membrane electrolysis system and no chemical pH control. Such system, however, consumes a substantial amount of energy. Based on their experiments, they estimated a power input of 2 kWh per produced kg $COD_{fatty\ acids}$. The developed two-stage system in the present study, at long HRT, consumed 0.22 kg NaOH per produced kg $COD_{fatty\ acids}$. Assuming an electricity consumption of 3 kWh/kg NaOH via the chloralkali process (Euro Chlor, 2010), the two-stage system would require less energy for pH control per produced kg COD (0.67 kWh/kg $COD_{fatty\ acids}$) compared to the in-site membrane electrolysis system. However, whereas the membrane electrolysis system already separated fatty acids from the fermentation broth, the two-stage system would require an additional product separation step to be comparable in electricity consumption.

Effective MCFA production from organic waste can be further developed by reducing the need for chemicals and/or electricity. Possibly, also water-use can be reduced too since the two-stage system used a substantial amount of water to dilute the waste before use as fermentation feed. The presented scenario in the present study, as well as the mentioned alternative scenarios (e.g., Lim et al., 2008; Andersen et al., 2015; Xu et al., 2017) can be optimized and assessed with a case-specific life cycle assessment to make a complete justified discussion on the total environmental impact.

Future Outlook

In a previous study, it was shown that EEO in a chain elongation process can be limited to 15.9% of total ethanol consumption by reducing the CO_2 loading rate to 0.5 L_{CO2}/L/d (Roghair et al., 2018). In the present study, an alternative strategy to suppress EEO is provided: by applying a long HRT, EEO was limited to a similar extent (14.7%). A major advantage of this strategy is that the n-caproate concentration can become much higher. By further increasing the HRT possibly higher n-caproate concentrations can be reached. This could potentially lead to

even more limited rate of EEO and thus base consumption in the chain elongation process. Of course, this is only feasible when the process is not limited in substrates (ethanol and VFAs) and CO_2.

Based on this study and the availability of 88 million ton wet food waste per year in the European Union (Stenmarck et al., 2017), the developed process has the prospects to produce 29 million ton MCFAs per year. This was calculated using the ratios in **Figure 2** (at long HRT) and by assuming that wet food waste has the same VS content as in this study; calculations are shown in the supplementary material. The required ethanol (∼311 million barrels) would be 37% of total annual global ethanol production (∼844 million barrels, Renewable Fuels Association, 2017). The required electrical power for NaOH production (38.4 tWh) would be 13% of total annual wind energy production in Europe (305.8 tWh, International Energy Agency, 2015).

After selective extraction of the MCFAs, they can be further processed into a fuel (i.e., a mixture of hydrocarbons) via Kolbe electrolysis (Khor et al., 2017; Urban et al., 2017). Assuming no losses during extraction and a theoretical efficiency of 0.61 $g_{hydrocarbons}/g_{MCFA}$ in the Kolbe electrolysis process and a fuel density of 0.73 g/cm^3, it is possible to produce ∼202 million barrels of fuel per year. This is approximately 7% of the nowadays annual aviation fuel consumption (∼2,710 million barrels, International Air Transport Association, 2017).

AUTHOR CONTRIBUTIONS

MR planned and performed the experiments, analyzed the results, and wrote the manuscript. YL assisted in experimental work and analytical work. DS assisted in the design of the study and revised the manuscript. MB, RW, and CB revised the manuscript. All authors read and approved the final manuscript.

FUNDING

This work has been carried out with a grant from the BE-BASIC program FS 01.006 (www.be-basic.org).

SUPPLEMENTARY MATERIAL

The Supplementary Material for this article can be found online at: https://www.frontiersin.org/articles/10.3389/fbioe.2018.00050/full#supplementary-material

REFERENCES

Agler, M. T., Spirito, C. M., Usack, J. G., Werner, J. J., and Angenent, L. T. (2012). Chain elongation with reactor microbiomes: upgrading dilute ethanol to medium-chain carboxylates. *Energy Environ. Sci.* 5, 8189–8192. doi: 10.1039/c2ee22101b

Agler, M. T., Spirito, C. M., Usack, J. G., Werner, J. J., and Angenent, L. T. (2014). Development of a highly specific and productive process for n-caproic acid production: applying lessons from methanogenic microbiomes. *Water Sci. Technol.* 69, 62–68. doi: 10.2166/wst.2013.549

Andersen, S. J., Candry, P., Basadre, T., Khor, W. C., Roume, H., Hernandez-Sanabria, E., et al. (2015). Electrolytic extraction drives volatile fatty acid chain elongation through lactic acid and replaces chemical pH control in thin stillage fermentation. *Biotechnol. Biofuels* 8:221. doi: 10.1186/s13068-015-0396-7

Andersen, S. J., De Groof, V., Khor, W. C., Roume, H., Props, R., Coma, M., et al. (2017). A clostridium group IV species dominates and suppresses a mixed culture fermentation by tolerance to medium chain fatty acids products. *Front. Bioeng. Biotechnol.* 5:8. doi: 10.3389/fbioe.2017.00008

Angenent, L. T., Richter, H., Buckel, W., Spirito, C. M., Steinbusch, K. J. J., Plugge, C. M., et al. (2016). Chain elongation with reactor microbiomes: open-culture biotechnology to produce biochemicals. *Environ. Sci. Technol.* 50, 2796–2810. doi: 10.1021/acs.est.5b04847

APHA (1998). *Standard Methods for the Examination of Water and Wastewater, 20th Edn*. Washington, DC: APHA American Public Health Association.

Chen, W. S., Huang, S., Strik, D. P. B. T. B., and Buisman, C. J. N. (2016a). Isobutyrate biosynthesis via methanol chain elongation: converting organic wastes to platform chemicals. *J. Chem. Technol. Biotechnol.* 92, 1370–1379. doi: 10.1002/jctb.5132

Chen, W.-S., Strik, D. P. B. T. B., Buisman, C. J. N., and Kroeze, C. (2017). Production of caproic acid from mixed organic waste- an environmental life cycle perspective. *Environ. Sci. Technol.* 51, 7159–7168. doi: 10.1021/acs.est.6b06220

Chen, W. S., Ye, Y., Steinbusch, K. J. J., Strik, D. P. B. T. B., and Buisman, C. J. N. (2016b). Methanol as an alternative electron donor in chain elongation for butyrate and caproate formation. *Biomass Bioenergy* 93, 201–208. doi: 10.1016/j.biombioe.2016.07.008

Coma, M., Martinez-Hernandez, E., Abeln, F., Raikova, S., Donnelly, J., Arnot, T. C., et al. (2017). Organic waste as a sustainable feedstock for platform chemicals. *Faraday Discuss.* 202, 175–195. doi: 10.1039/C7FD00070G

Euro Chlor (2010). *The European Chlor-Alkali industry: An Electricity Intensive Sector Exposed to Carbon Leakage*. Available online at: http://www.eurochlor.org/media/9385/3-2-the_european_chlor-alkali_industry_-_an_electricity_intensive_sector_exposed_to_carbon_leakage.pdf (Accessed October 24, 2017).

Evans, N. P., Collins, D. A., Pierson, F. W., Mahsoub, H. M., Sriranganathan, N., Persia, M. E., et al. (2017). Investigation of medium chain fatty acid feed supplementation for reducing Salmonella typhimurium colonization in Turkey poults. *Foodborne Pathog. Dis.* 14, 531–536. doi: 10.1089/fpd.2016.2273

Ge, S., Usack, J. G., Spirito, C. M., and Angenent, L. T. (2015). Long-term n-caproic acid production from yeast-fermentation beer in an anaerobic bioreactor with continuous product extraction. *Environ. Sci. Technol.* 49, 8012–8021. doi: 10.1021/acs.est.5b00238

Grootscholten, T. I. M., Steinbusch, K. J. J., Hamelers, H. V. M., and Buisman, C. J. N. (2013a). Improving medium chain fatty acid productivity using chain elongation by reducing the hydraulic retention time in an upflow anaerobic filter. *Bioresour. Technol.*, 136, 735–738. doi: 10.1016/j.biortech.2013.02.114

Grootscholten, T. I. M., Steinbusch, K. J. J., Hamelers, H. V. M., and Buisman, C. J. N. (2013b). High rate heptanoate production from propionate and ethanol using chain elongation. *Bioresour. Technol.*, 136, 715–718. doi: 10.1016/j.biortech.2013.02.085

Grootscholten, T. I. M., Steinbusch, K. J. J., Hamelers, H. V. M., and Buisman, C. J. N. (2013c). Chain elongation of acetate and ethanol in an upflow anaerobic filter for high rate MCFA production. *Bioresour. Technol.* 135, 440–445. doi: 10.1016/j.biortech.2012.10.165

Grootscholten, T. I. M., Strik, D. P. B. T. B., Steinbusch, K. J. J., Buisman, C. J. N., and Hamelers, H. V. M. (2014). Two-stage medium chain fatty acid (MCFA) production from municipal solid waste and ethanol. *Appl. Energy* 116, 223–229. doi: 10.1016/j.apenergy.2013.11.061

Hanczakowska, E., Szewczyk, A., Swiatkiewicz, M., and Okon, K. (2013). Short- and medium-chain fatty acids as a feed supplement for weaning and nursery pigs. *Pol. J. Vet. Sci.* 16, 647–654. doi: 10.2478/pjvs-2013-0092

Harvey, B. G., and Meylemans, H. A. (2014). 1-Hexene: a renewable C6 platform for full-performance jet and diesel fuels. *Green Chem.* 16, 770–776. doi: 10.1039/C3GC41554F

International Air Transport Association (2017). *(IATA) Economic Performance of the Airline Industry: 2017 Mid-Year Report. (2017).* Available online at: https://www.iata.org/whatwedo/Documents/economics/IATA-Economic-Performance-of-the-Industry-mid-year-2017-report.pdf (Accessed October 25, 2017).

International Energy Agency (2015). *(IEA) OECD Europe: Electricity and Heat for 2015 Statistics [Online*]. Available online at: http://www.iea.org/statistics/statisticssearch/report/?year=2015andcountry=OECDEURandproduct=ElectricityandHeat (Accessed October 26, 2017).

Khor, W. C., Andersen, S., Vervaeren, H., and Rabaey, K. (2017). Electricity-assisted production of caproic acid from grass. *Biotechnol. Biofuels* 10:180. doi: 10.1186/s13068-017-0863-4

Kouzuma, A., Kato, S., and Watanabe, K. (2015). Microbial interspecies interactions: recent findings in syntrophic consortia. *Front. Microbiol.* 6:477. doi: 10.3389/fmicb.2015.00477

Lim, S.-J., Kim, B. J., Jeong, C.-M., Choi, J.-,d-r, Ahn, Y. H., and Chang, H. N. (2008). Anaerobic organic acid production of food waste in once-a-day feeding and drawing-off bioreactor. *Bioresour. Technol.* 99, 7866–7874. doi: 10.1016/j.biortech.2007.06.028

Liu, Y., He, P., Shao, L., Zhang, H., and Lü, F. (2017). Significant enhancement by biochar of caproate production via chain elongation. *Water Res.* 119, 150–159. doi: 10.1016/j.watres.2017.04.050

Lonkar, S., Fu, Z., and Holtzapple, M. (2016). Optimum alcohol concentration for chain elongation in mixed-culture fermentation of cellulosic substrate. *Biotechnol. Bioeng.* 113, 2597–2604. doi: 10.1002/bit.26024

López-Garzón, C. S., and Straathof, A. J. J. (2014). Recovery of carboxylic acids produced by fermentation. *Biotechnol. Adv.* 32, 873–904. doi: 10.1016/j.biotechadv.2014.04.002

Renewable Fuels Association (2017). *Industry Statistics: World Fuel Ethanol Production 2016.* Available online at: https://www.ethanolrfa.org/resources/industry/statistics/ (Accessed October 24, 2017).

Roghair, M., Hoogstad, T., Strik, D. P. B. T. B., Plugge, C. M., Timmers, P. H. A., Weusthuis, R. A., et al. (2018). Controlling ethanol use in chain elongation by CO2 loading rate. *Environ. Sci. Technol.* 52, 1496–1505. doi: 10.1021/acs.est.7b04904

Roghair, M., Strik, D. P. B. T. B., Steinbusch, K. J. J., Weusthuis, R. A., Bruins, M. E., and Buisman, C. J. N. (2016). Granular sludge formation and characterization in a chain elongation process. *Process Biochem.* 51, 1594–1598. doi: 10.1016/j.procbio.2016.06.012

Royce, L. A., Liu, P., Stebbins, M. J., Hanson, B. C., and Jarboe, L. R. (2013). The damaging effects of short chain fatty acids on Escherichia coli membranes. *Appl. Microbiol. Biotechnol.* 97, 8317–8327. doi: 10.1007/s00253-013-5113-5

Seedorf, H., Fricke, W. F., Veith, B., Brüggemann, H., Liesegang, H., Strittmatter, A., et al. (2008). The genome of Clostridium kluyveri, a strict anaerobe with unique metabolic features. *Proc. Natl. Acad. Sci. U.S.A.* 105, 2128–2133. doi: 10.1073/pnas.0711093105

Steinbusch, K. J. J., Hamelers, H. V. M., Plugge, C. M., and Buisman, C. J. N. (2011). Biological formation of caproate and caprylate from acetate: fuel and chemical production from low grade biomass. *Energy Environ. Sci.* 4, 216–224. doi: 10.1039/C0EE00282H

Stenmarck, Å., Jensen, C., Quested, T., and Moates, G. (2017). *Estimates of European Food Waste Levels 2016.* Available online at: https://www.eu-fusions.org/phocadownload/Publications/Estimates%20of%20European%20food%20waste%20levels.pdf (Accessed October 25, 2017).

Syngellakis, S. (2015). *Biomass to Biofuels.* Southampton; Boston: WIT Press.

Urban, C., Xu, J., Strauber, H., dos Santos Dantas, T. R., Muhlenberg, J., Hartig, C., et al. (2017). Production of drop-in fuels from biomass at high selectivity by combined microbial and electrochemical conversion. *Energy Environ. Sci.* 10, 2231–2244. doi: 10.1039/C7EE01303E

Xu, J., Hao, J., Guzman, J. J. L., Spirito, C. M., Harroff, L. A., and Angenent, L. (2017). Temperature-phased conversion of acid whey waste into medium-chain carboxylic acids via lactic acid: no external e-donor. *Joule* 2, 280–295. doi: 10.1016/j.joule.2017.11.008

Yalkowsky, S. H., He, Y., and Jain, P. (2016). *Handbook of Aqueous Solubility Data.* Boca Raton, FL: CRC press.

Zhu, X., Tao, Y., Liang, C., Li, X., Wei, N., Zhang, W., et al. (2015). The synthesis of n-caproate from lactate: a new efficient process for medium-chain carboxylates production. *Sci. Rep.* 5:14360. doi: 10.1038/srep14360

Conflict of Interest Statement: The authors declare that the research was conducted in the absence of any commercial or financial relationships that could be construed as a potential conflict of interest.

frontiers in Energy Research

ORIGINAL RESEARCH
published: 23 October 2018
doi: 10.3389/fenrg.2018.00111

Pretreatment and Multi-Feed Anaerobic Co-digestion of Agro-Industrial Residual Biomass for Improved Biomethanation and Kinetic Analysis

Kishan Kumar Prajapati[1], *Nidhi Pareek*[2] *and Vivekanand Vivekanand*[1]*

[1] Centre for Energy and Environment, Malaviya National Institute of Technology, Jaipur, India, [2] Department of Microbiology, School of Life Sciences, Central University of Rajasthan Bandarsindri, Kishangarh, India

Batch biochemical methane potential (BMP) test of agro-industrial, agricultural, and municipal solid waste (MSW) individuals like groundnut straw, rice bran, and guar husk, mung bean husk (MBH), wheat straw (WS), and organic fraction of municipal solid waste (OFMSW), under mesophilic conditions, were performed to evaluate the biogas potential. BMP test for multi-feed anaerobic co-digestion (AcoD) of WS, OFMSW, and MBH at five mixing ratio was performed to evaluate the synergistic effect of multi feed-stocks of blending the feedstocks. Mixture ratio having OFMSW:WS:MBH of 25:5:70% composition resulted into 37, 20, and 4% higher methane yield up to 280 ml/g Volatile solid (VS) in comparison with mono-digestion of OFMSW, WS and MBH. Ultrasonic pretreatment was also performed and the experimental results showed that varying the sonication time have a significant improvement on substrate's biodegradation and solubilization augmenting the methane yield from OFMSW, WS, and MBH by 71, 75, and 46%, respectively at sonication period of 60 min. Effect of pretreatment on the substrate studied through Scanning electron microscopy (SEM), XRD and FT-IR analysis. Cone and Exponential models showed an average coefficient of determination R^2 = 0.9855 and R^2 = 0.9893, respectively, and RMSE values for cone model was lower than that of Exponential model showing Cone model was more précised.

Keywords: agricultural waste, agro-industrial waste, organic fraction of municipal solid waste, anaerobic digestion, ultrasonic pretreatment, kinetics

OPEN ACCESS

Edited by:
Mohammad Rehan, King Abdulaziz University, Saudi Arabia

Reviewed by:
Qaisar Mahmood, COMSATS University Islamabad, Pakistan
Samir Jaiwantrao Deshmukh, Prof.Ram Meghe Institute of Technology & Research, India

***Correspondence:**
Vivekanand Vivekanand
vivekanand.cee@mnit.ac.in

Specialty section:
This article was submitted to Bioenergy and Biofuels, a section of the journal Frontiers in Energy Research

Received: *30 June 2018*
Accepted: *02 October 2018*
Published: *23 October 2018*

Citation:
Prajapati KK, Pareek N and Vivekanand V (2018) Pretreatment and Multi-Feed Anaerobic Co-digestion of Agro-Industrial Residual Biomass for Improved Biomethanation and Kinetic Analysis. Front. Energy Res. 6:111. doi: 10.3389/fenrg.2018.00111

INTRODUCTION

Developing country India facing energy security problem and striving to fulfill its energy demand by natural resources like coal, crude oil, and natural gas. Renewable energy sources like wind, solar, hydro, biomass, and geothermal have huge potential to wipe out this problem of energy demand with sustainability and an excellent alternative to declining fossil fuel reserves. Biomass is considered as carbon neutral for energy production through biogas, ethanol, and pellets production, still, its direct burning practiced over the country, its conversion to renewable bio-energy production is a sustainable way. As 686 MT (million tons) biomass is generated in the country annually (Hiloidhari et al., 2014; Wang et al., 2017; Kumar et al., 2018). Agricultural crops residues, organic fraction of municipal solid waste (OFMSW), food wastes, agro-industrial wastes, aquatic plants, and algae, animal dung etc. all are considered as biomass.

Agriculture, MSW, and agro-industrial waste materials embody potential sources of renewable energy production and making a contribution toward energy production independent from fossil fuels.

Organic Waste Generation

Agriculture biomass or waste are alternative feedstock to energy and chemical production. Leftover straw, stalk and husk of a crop plant are the crop residues after its harvesting (Devi et al., 2017). Agricultural wastes are agriculture crop residues i.e. residues from group of cereals, oilseeds, pulses, horticulture, and other crops. Most of the agricultural residues used for animal feeding, fuel for domestic application or gasification (Hiloidhari et al., 2014; Report RRECL, 2017).

Around 25% of biomass from crop residues is burnt on a global basis (Devi et al., 2017). Its on-farm burning, categorized as underutilization of resources and leading to environmental impacts (Hiloidhari et al., 2014; Kumar et al., 2018). Agricultural crop residues can be utilized into biogas production, textile making process, fuel and manure, etc. to mitigate the problem of on farm *in-situ* burning of surplus crop residues which is a source of GHG, smoke, aerosols, and particulate matters etc. (Nguyen et al., 2016; Devi et al., 2017). Animal dung from cattle, goats, ships, and poultry are highly loaded from organic matter content and having huge pollution potential of methane gas. It is utilized as potential substrate or inoculum in co-digestion in the biogas plants (Bundhoo et al., 2016). Also, Shah et al. (2015) has reported the anaerobic co-digestion of blends of maize residues, water hyacinth, giant reed, and poultry litter for biogas production at community scale.

India generates crop residues 686 MT annually, out of which 34% of crop residue is estimated as surplus (Hiloidhari et al., 2014). For Rajasthan state, agricultural activity generates 52.6 MT/year residues out of which 9.25% remain surplus (Report RRECL, 2017). The surplus fraction of residue availability from cereals is 29%, from oilseeds is 18%, and 23% from pulses crop in Rajasthan (Hiloidhari et al., 2014). **Wheat** (*Triticum*) crops cultivation is 2nd highest among cereals in the country, and 5th highest in the Rajasthan state. Wheat straw [Crop Residue Ratio (CRR) = 1.5] production is 15.8 MT/year having 30% share to total biomass generation in the state (Annual Report MA FW, 2017; Report RRECL, 2017). Wheat straw has composition of 30.1–39.2% cellulose, 22.2–34.0% hemicellulose, and 6.5–22.1% lignin (Chandra et al., 2012a,b; Bolado-Rodríguez et al., 2016; Yadav et al., 2018).

MSW generation is increasing in almost all cities with urbanization and population growth, accompanied by its economy. MSW handling is one of the chief issue facing Indian cities. Its poor and incautious management entails enormous impacts on public health, environment, and climate change (Shekdar, 2009; Yadav and Samadder, 2017; Gollapalli and Kota, 2018). Currently, India generates 62 MT MSW per year where collection and treatment efficiency is around 90 and 27%, respectively, which means 79% MSW directly goes to unsanitary landfilling (Planning Commission Report, 2014; MSW Report, 2017; Yadav and Samadder, 2017). Jaipur, one of the metro cities of India, generates 1,000 tons per day (TPD) MSW, 31% share alone in total state MSW generation with ∼3.04 million population (Census, 2011; Municipal solid waste, 2017). Waste to energy potential in India with organic and inorganic portions are open for conversion to biofuel and for power generation. Presently, India has 2,554 MW potential as renewable energy potential from waste generated i.e., MSW and waste water (Kalyani and Pandey, 2014; MNRE Annual Report, 2017).

Improved income and population in a city led to a changed lifestyle of urban dwellers, and also causing an escalation in waste quantity and MSW composition altered. Knowledge of the composition of MSW is important for selecting the suitable waste processing and disposal practices since MSW volume and its composition differs considerably with the places having changes in food habits, cultural traditions, lifestyles, socio-economic conditions, and climate (Yay, 2015; Mboowa et al., 2017). OFMSW has composition around 17.5% cellulose, 10.7% hemicellulose, 9.6% lignin, 37.8% raw fiber, 7.7% protein, and 9.6% fat or oil (Rao and Singh, 2004). However, its composition varies with their nutrient content due to its heterogeneous nature with respect to place to place even in the same city. Through AD process, OFMSW is capable of generating 300–400 m^3 biogas/ ton of VS of OFMSW (Dhar et al., 2017).

The **agro-industrial** sector represents one of the important sectors of the economy, responsible for processing or production of different foodstuffs and meanwhile also generating large quantity of waste. Major agro-industrial waste comes from food processing, juice and wine industry, edible oil refineries, slaughterhouse, and dairy processing. Many food processing wastes are sent to animal feeding, and chemical production and rest goes to landfilling (Bundhoo et al., 2016; Pellera and Gidarakos, 2017). Although glycerine as ideal co-substrate being pure and 100% degradability, other products like cheese whey, olive mill waste, sugar by-products, have been used for co-digestion with positive results (Mata-Alvarez et al., 2014). Here, Mung bean husk, groundnut shell, guar husk and rice bran have been studied as agro-industrial waste for biogas potential.

Mung bean (*Vigna radiata*) production is 4,77,245 tons sharing 20% of pulse production as 2nd highest production after gram pulse which has 44% share in pulses production in the state (Rajasthan Agri-Statistics Report, 2017). **Groundnut** (*Arachis hypogea*) crop production is 8,08,143 tons production in Rajasthan with 15.56% share to country (Rajasthan Agri-Statistics Report, 2017). Its shells (CRR = 0.3) are discarded waste, which is a carbohydrate rich biomass having composition 25.57% carbohydrate, crude protein 4.43% and lipid 0.50%, crude fiber 59%, ash content 2.5%, and moisture 8% (Abdulrazak et al., 2014; Hiloidhari et al., 2014). **Guar** or cluster bean, with the botanical name *Cyamopsis tetragonoloba* drought tolerant legume grown in the Rajasthan state of India. Guar meal is a protein and fiber rich nutritional food for livestock containing germ and hull part of it (Janampet et al., 2016). Rajasthan produces Guar crop 2,204,931 tons annually in 2014–15. Its residues are stalks and husk. **Rice** (*Oryza sativa*) crop is most widely consumed food grain in the world. This cereal has 103.73 MT cultivation in India being 2nd highest in India after sugarcane crop. Its production is 2,84,131 tons annually in Rajasthan state. Residues from rice

milling industry are rice husk and bran. (Rajasthan Agri-Statistics Report, 2017). Rice bran has composition around 4.6% cellulose, 8.4% hemicellulose, 2.8% lignin, 28.5% starch, and 13.9% protein (Favaro et al., 2017).

Anaerobic Digestion

The AD is biological process categorized in the effective waste management as well as waste to energy technologies. As it avoids the natural emission of greenhouse gases like CH_4 and CO_2 from self-degradation of organic waste. Main products of AD process are CH_4 for renewable energy production and a digestate as bio-fertilizer for soil amendment (Vivekanand et al., 2013; Bundhoo et al., 2016). As AD owing several benefits concerning environment, economy and maintenance, also have been used for processing agricultural waste, MSW, sewage sludge, livestock effluents, agro-industrial waste, therefore AD process being dealt in this study.

The AD consists of four consecutive processes i.e., Hydrolysis, acidogenesis, acetogenesis, and methanation as shown in **Figure 1**. In first phase, large polymers breakdown into monomers, carbohydrates into simple sugar, fat into fatty acid, and glycerol, protein into amino acid and peptide. In second phase, these monomers break down into carbonic acid, alcohols, H_2, CO_2, NH_3. In this phase, O_2 and CO_2 consumed by facultative bacteria to create the anaerobic condition. In third phase i.e., acetogenesis, previous phase products are converted into acetic acid, H_2 and CO_2. This acetic acid and hydrogen are converted into methane by different methanogens i.e. archea in the last phase of AD i.e., methanogenesis (Kumar et al., 2018; Negi et al., 2018).

Nutritional imbalance and operating factors like biodegradability and chemical composition of single substrate make its direct utilization tough. Therefore, different nutrition composition substrates are digested together, also biogas yield gets improved. Anaerobic co-digestion provides benefits like process stabilization, pH and buffer capacity, avoid inhibitory or toxic compounds (formation of Volatile fatty acids (VFA)/ammonia), microorganism's good synergistic effect (Mata-Alvarez et al., 2014; Hagos et al., 2017; Pellera and Gidarakos, 2017). AcoD is a technique for simultaneous treatment of different organic residues proving better synergism through diverse co-substrates and microbial activity by improving methane yield in process. Suitable co-substrate is that which compensate with excess metabolites produced by another substrate which inhibit the methanogens in AD (Zhang et al., 2016). In simple words, AcoD is performed to balance the C/N ratio of the feedstock.

BMP test is a batch experiment of AD determining the biomethane potential of a substrate. This test is performed in laboratory for examining the biodegradability and methane conversion efficiency of organic substrates, assessing different combination of co-substrates, feasibility of different biomasses for AD, also helps in achieving optimal condition for AD process (Cho et al., 2013; Vivekanand et al., 2013; Hagos et al., 2017). A feasibility study of organic waste energy potential in college campus shows mixed food and green waste has biogas potential of 400–660 ml/g VS of the mixed substrate (Paritosh et al., 2018).

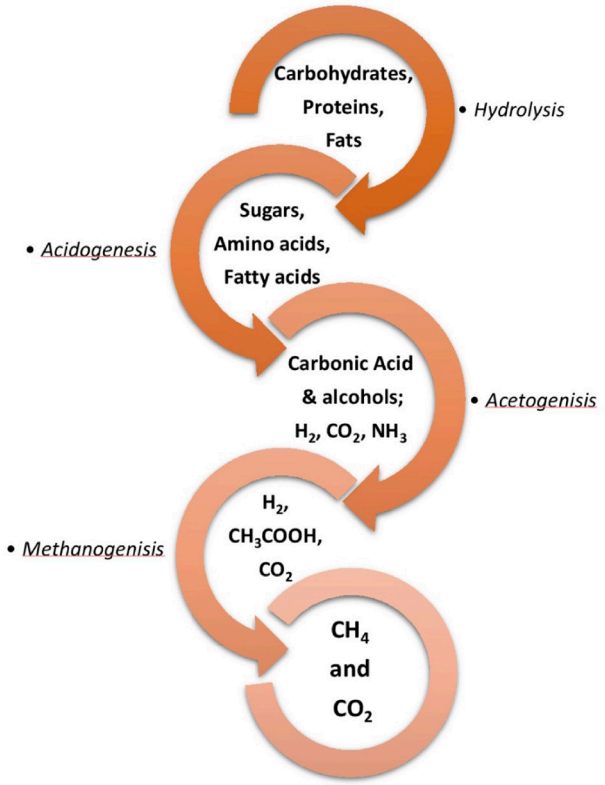

FIGURE 1 | Four stages of the anaerobic digestion process.

Kacprzak et al. (2010), experimented combination of agriculture waste (corn silage, carrot residues), agro-industrial waste (beet pulp silage and cheese whey) with industrial waste: glycerine (waste from biodiesel production), resulting highest methane yield with mixture of corn silage, cheese whey and glycerine (Kacprzak et al., 2010; Mata-Alvarez et al., 2014). Blending of few agro-industrial waste i.e. brewery spent grain, carbonated soft drink sludge, with either powdered rice husk or soya bean cake resulted into enhanced biogas production than individuals (Uzodinma et al., 2007). Vivekanand et al. (2018) co-digested manure, fish ensilage and whey as multi feed-stocks and produced 84% higher methane production than individual substrate digestion. Food waste co-digestion with straw (containing straw of wheat, maize, and sorgos) showed 39.5 and 149.7% augmented methane yield at 5:1 mixing ratio as compared to mono-digestion of food waste and straw, respectively (Yong et al., 2015). Co-digestion of OFMSW and rice straw in the ratio of 2:1 yielded 57% higher methane (403 ml/g VS) than the other combinations (Negi et al., 2018). Batch test of co-digestion of OFMSW with pretreated sludge and rice straw experimented at different blending ratio, and ratio 3:0.5:0.5 yields maximum biogas 558 ml/g VS (Abudi et al., 2016). Shekdar (2009) has reported the different treatment methods for improving the biogas production from OFMSW. MSW, bovine slaughterhouse, manure and crop residues were mixed and evaluated for methane production in mesophilic

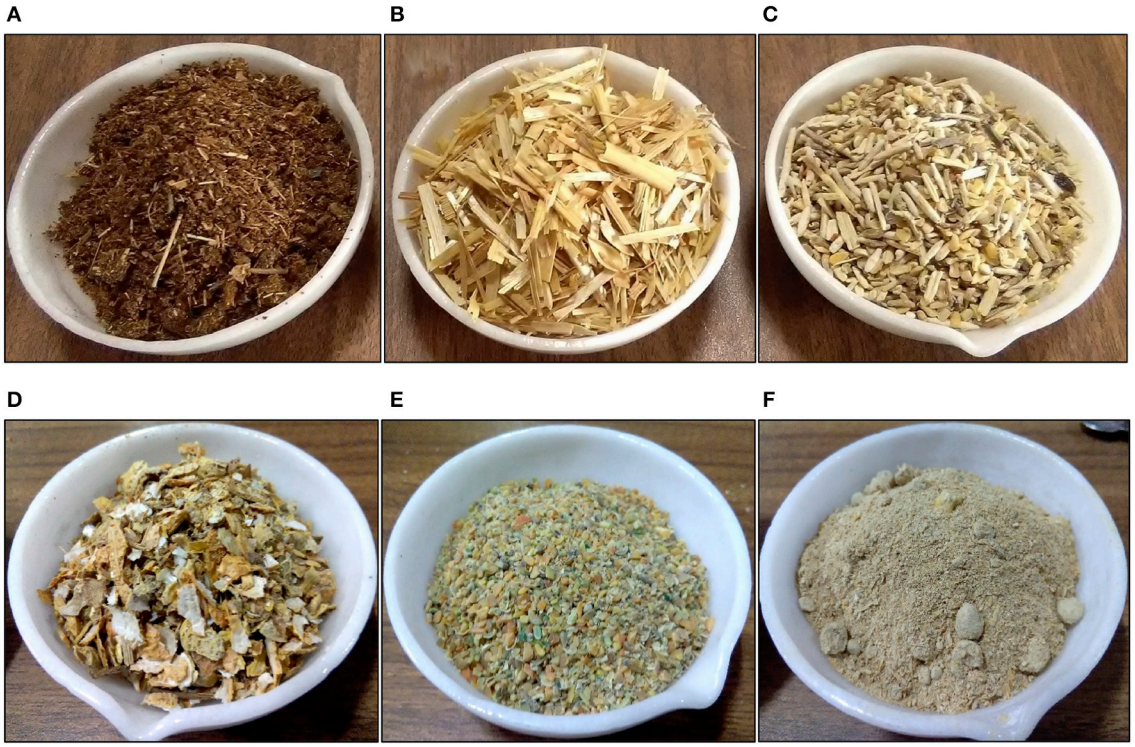

FIGURE 2 | Substrates. **(A)** Organic fraction of MSW, **(B)** Wheat straw, **(C)** Mung bean husk, **(D)** Groundnut shell, **(E)** Guar husk and **(F)** Rice bran.

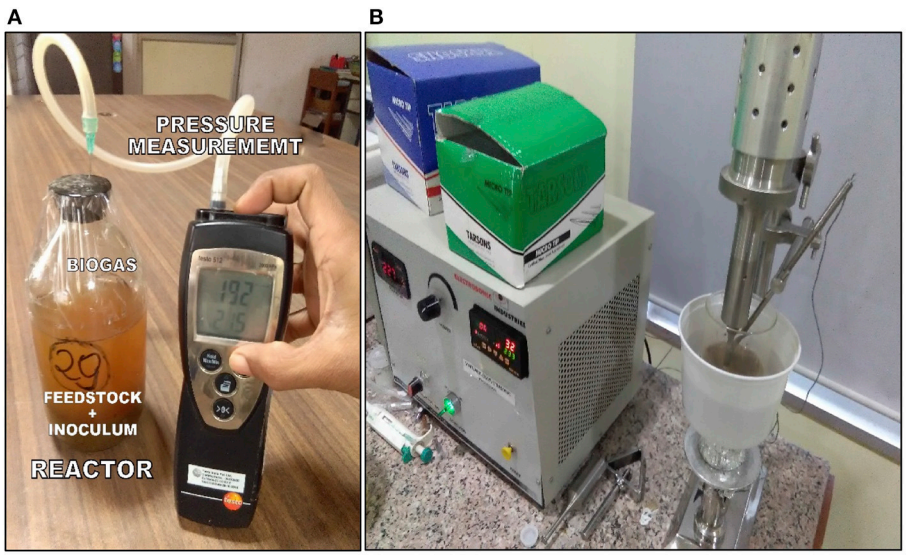

FIGURE 3 | (A) Digital pressure meter and **(B)** Ultrasonicator with probe and temperature sensor.

and thermophilic condition and mesophilic condition results showed 57% lower methane in comparison with the thermophilic condition (Pagés-Díaz et al., 2013). Methane yield from corn straw and manure get increased up to 22.4% by means of mixing another substrate i.e., fruit and vegetable waste (Wang et al., 2018).

The organic fraction of municipal waste and agro-industrial waste are mostly investigated and used for co-substrates with manure (Mata-Alvarez et al., 2014; Abudi et al., 2016). Selection of suitable co-substrates and the ratio of mixing are key factors aiming synergism to enhanced methane production. Municipal, agro-industrial and agricultural waste have been individually

TABLE 1 | Characterization of feed-stocks.

Feedstocks Parameters (unit)	Wheat straw	Organic fraction of MSW	Mung bean husk	Guar husk	Rice bran	Groundnut shell
Moisture (% of dry wt.)	5.6	47.1	9.5	8.0	10.1	4.7
TS (% of dry wt.)	94.4	52.9	90.5	92.0	89.9	95.3
VS (% of TS)	93.1	91.7	95.6	94.6	87.7	95.8
Ash (% of TS)	6.9	8.3	4.4	5.4	12.3	4.2
Calorific value (Cal./g)	4381.4	2524.5	4157.3	NA	NA	NA
C (%)	41.5	26.8	42.2	NA	NA	NA
H (%)	8.03	8.6	5.6	NA	NA	NA
N (%)	0.3	1.2	0.8	NA	NA	NA
O* (%)	43.2	55.1	45.8	NA	NA	NA
C/N	118.6	22.6	52.7	NA	NA	NA

**O estimated by deducting other constituents from 100%, NA-Not Analyzed.*

utilized as a source of energy through this technique. So far little work performed regarding synergistic effect from these three different sector waste or biomass (Sharholy et al., 2008; Vivekanand et al., 2018).

Pretreatment Process

Utilizing bioenergy from biomass with higher efficiency is also a major concern, for this different pretreatment techniques are applied. Lignocellulosic biomass composed of cellulose, hemicellulose, and lignin, where lignin has the amorphous 3D structure of phenylpropanoid units covering cellulose fibers hindering access from enzymes. For deconstructing lignin structure, biological, physical or chemical, or physiochemical pretreatment techniques are available (Bussemaker and Zhang, 2013; Kumar et al., 2018; Yadav et al., 2018).

Ultrasonic Pretreatment

Sound waves or energy having frequency beyond 20 kHz, inaudible to human beings, called as ultrasonic waves. These waves are responsible for producing vibration in the suspension leading the formation of cavitation bubbles of vapor. The formation of microbubbles and its growth and collapse called cavitation effect, it occurs only due to more ultrasonic energy (e.g., 1 W/cm^3 for water) than molecular attractive forces. Microbubbles collapse during wave compression generating high temperature and pressure spot on the biomass disrupting the outer structure. This cavitation delivers physical effects on the substrate due to shear forces to the surface of the substrate leading its structure lysis (Nakashima et al., 2016; Rodriguez et al., 2017; Wang et al., 2017).

Depending on the ultrasonication condition, effective physical disintegration can be achieved augmenting AD yield. It was also proven to be effective and versatile in comparison with other pretreatment such as acid, base thermal and bacterial for fat-rich solid substrates especially waste coming from meat processing (Cesaro and Belgiorno, 2014). Pretreatment parameters should require to be near at room temperature and pressure, mild severity with significant delignification. Ultrasonication exclusiveness is due to its parameters ranges near to atmospheric conditions i.e., room temperature, atmospheric pressure, no chemicals required (Nakashima et al., 2016; Xiong et al., 2017). Factors influencing cavitation effect are vibration frequency, ultrasound power (or amplitude), temperature and viscosity of liquid (solvent), surface tension, and time duration (Clark and Nujjoo, 2000; Bussemaker and Zhang, 2013; Rasapoor et al., 2016).

Deepanraj et al. (2017) found that the ultrasonication (20 kHz, 130 W, 30 min) as more effective pretreatment than autoclave and microwave for biogas production from food waste. Castrillón et al. (2011) analyzed ultrasound (20 kHz, 100 W, 4 min) pretreatment and co-digestion of cattle manure with 4% glycerin both showing 121 and 400% increment, respectively on biogas production in mesophilic and thermophilic condition. Cesaro et al. (2012) sonicated mixture of organic solid waste and sewage sludge for 30 and 60 min duration at different energy densities (0.1, 0.2 and 0.4 W/ml). Twenty-four percent enhanced biogas from the sonicated mixture due to enhanced solubilization and enhanced biodegradability of organic matter enhanced during the AD. Cho et al. (2013) conducted sonication for microalgae at different power amplitude for 15 and 30 min duration without temperature control on microalgae *Scenedesmus,* and methane increment was around 14–75%. Effect of ultrasonic power density and sonication time was analyzed by performing ultrasonic pretreatment of OFMSW on biogas production and proving low power density and higher sonication time give better results than high power density and low sonication time due to simultaneously temperature increment with respect to time making more effective. Effect of sonication on municipal sludge has widely investigated, however, there is an inadequate study on different organic residues (Cesaro et al., 2014; Rasapoor et al., 2016; Zeynali et al., 2017).

As such this study investigates the feasibility and potential of energy production from AcoD of multi feed-stocks from different waste sectors i.e., agricultural, agro-industrial, and municipal solid waste, through BMP tests to alleviate the energy as well as waste management problem. Also exploring the ultrasonic pretreatment for organic residues from above-mentioned sectors at controlled temperature condition and to validate experimental

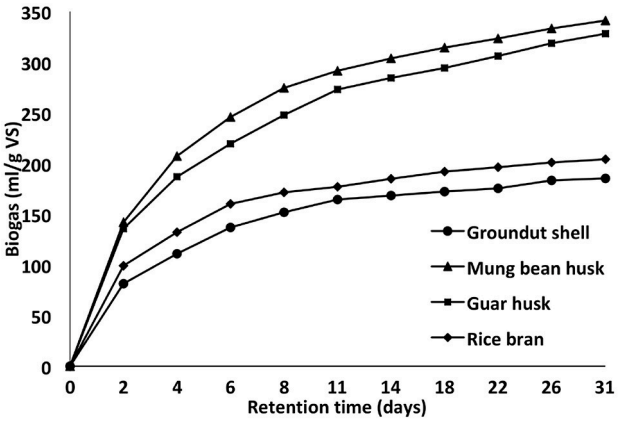

FIGURE 4 | Accumulated biogas production from agro-industrial residues.

pretreatment results with two classical kinetic models which can be used to describe and evaluate the batch BMP test for AD process.

MATERIALS AND METHODS

Feed Stocks Collection and Preparation

Inoculum

Microbial inoculum used in this study was collected from the continuous Durgapura biogas plant feeding cow dung as substrate. The inoculum was incubated anaerobically at 37°C for a week to reduce endogenous biogas production. Inoculum has 7.5% TS and VS content as 59.3% of TS. The inoculum was diluted to a TS content of 1.2% with water. Furthermore, divided into 400 mL aliquots in 610 mL batch serum bottles. This diluted inoculum has pH 7.4 and conductivity 2.3 mS.

Feed-Stocks or Substrates

The organic fraction of MSW was collected from MNIT campus and two residence of Malviya Nagar, which is a source segregated waste i.e. without any contamination of non-biodegradable waste**.** This waste is mainly composed of leftover cooked food, vegetable peelings, dry green waste of fallen leaves, grass trimmings. With the help of household blender organic wastes were comminuted and mixed homogenously to have better solubility shown in **Figure 2A**, then stored at 4°C till use (Izumi et al., 2010; Negi et al., 2018).

Wheat straw as an agricultural waste collected from Jaisinghpura village, Jaipur, the collected WS sample shown in **Figure 2B**. Agro-industrial waste: (i) Mung bean husk sample shown in **Figure 2C** is procured from Sunny Daal Mill industry, Sitapura, Jaipur, MBH residue from mill contains almost equal amount of broken small beans and husk, (ii) Groundnut shell waste sample (**Figure 2D**) collected from groundnut processing industry (Rajasthan Agro Product, Sikar Road, Jaipur), which is latter being burnt or disposed, (iii) Guar husk and (iv) Rice bran samples shown in **Figures 2E, F,** respectively which were

TABLE 2 | Accumulated biogas and methane in BMP tests.

I- Anaerobic digestion (RT-30)												
Agro-industrial waste	Groundnut shell			MBH			Guar husk			Rice bran		
Accumulated biogas (ml/g VS)	185.4 ± 3.5			341.1 ± 8.1			328.1 ± 5.4			204.0 ± 4.5		
II-Anaerobic co-digestion (RT-60)												
Mixtures (M= OFMSW: WS: MBH)												
Substrates	WS	MBH	OFMSW	M1(90:03:07)	M2(66:05:29)	M3(42:7.5:50.5)	M4(25:05:70)	M5(12:03:85)				
Accumulated methane (ml/g VS)	224.71 ± 3.6	267.44 ± 5.7	202.66 ± 5.2	256.49 ± 4.4	225.55 ± 5.8	274.59 ± 7.0	279.62 ± 9.2	83.96 ± 2.4				
Methane fraction (%)	52	57	51	54	52	56	59	23				
Accumulated biogas (ml/g VS)	430.60 ± 6.8	467.79 ± 7.9	397.04 ± 7.5	477.51 ± 7.1	430.21 ± 8.2	487.91 ± 10.9	470.83 ± 16.2	361.51 ± 8.3				
C/N ratio	118.6	52.7	22.6	27.6	36.1	45	48.5	51.1				
III-BMP test for pretreatment analysis (RT-45)												
Substrates	WS	WS-30	WS-60	WS-90	MBH	MBH-30	MBH-60	MBH-90	OFMSW	OFMSW-30	OFMSW-60	OFMSW-90
Accumulated biogas (ml/g VS)	406.85 ± 7.2	469.36 ± 9.8	551.0 ± 8.5	518.43 ± 4.6	460.82 ± 8.6	518.13 ± 4.8	551.70 ± 7.2	586.43 ± 9.0	386.24 ± 8.2	474.85 ± 4.7	504.78 ± 9.4	493.21 ± 9.3
Methane fraction (%)	50%	67%	65%	61%	57%	68%	69%	65%	50%	61%	66%	58%
Accumulated methane (ml/g VS)	204.23 ± 3.6	314.17 ± 7.3	356.94 ± 5.5	314.12 ± 3.0	261.10 ± 6.1	350.44 ± 3.9	381.77 ± 5.7	379.25 ± 6.3	193.17 ± 5.6	291.23 ± 3.4	331.09 ± 6.7	287.27 ± 6.1

RT, Retention time in days; MBH, Mung bean husk; OFMSW, Organic fraction of MSW; WS, Wheat straw; 30, 60, and 90 represents sonication (pretreatment) time (minutes) for respective substrates.

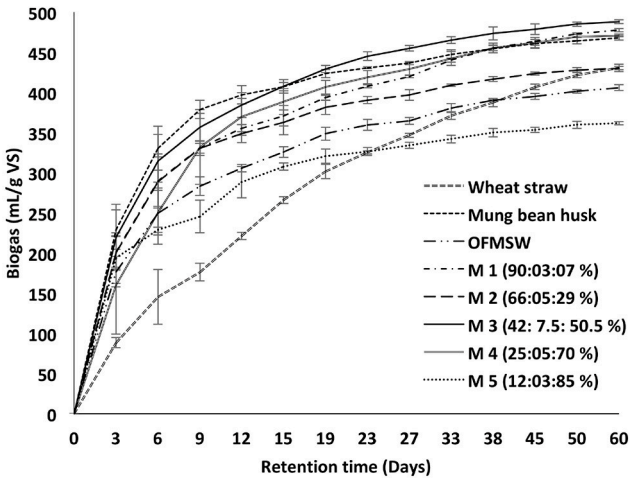

FIGURE 5 | Accumulative biogas production of mixture.

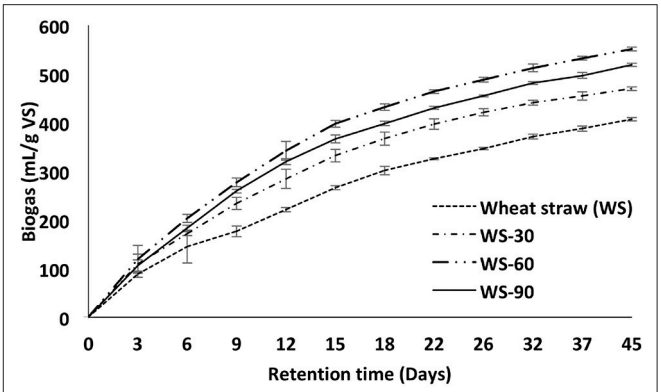

FIGURE 6 | Accumulated Biogas and Methane yield from pretreated WS samples.

collected from Unique Organic Ltd, Sitapura Industrial Area, Jaipur.

Biochemical Methane Potential Test

A BMP test for biogas production was performed in triplicates of each 6 different substrates, with control bottles i.e., negative control having inoculum alone, and positive control having cellulose as substrates. Subsequently, total 24 bottles flushed with nitrogen and closed with a rubber cap, and transferred to the shaker (REMI CIS 24, India) for incubation (37 °C, 90 rpm, 30 days) to figure out best agro-industrial substrate for co-digestion. 1.55 g substrate VS was added to diluted inoculum bottles (610 ml) having a working volume of 400 ml (Vivekanand et al., 2013; Paritosh et al., 2018).

Biogas Volume and Methane Composition

Pressure measurement in head space of each batch reactors was made periodically through Digital pressure meter (TESTO model 512, Germany, shown in **Figure 3A**) for biogas volume measurement. After this, biogas was released, reducing head space pressure to atmospheric pressure. The ideal gas law was used for calculating the biogas volume in the headspace volume of the batch reactors. Biogas production from inoculum control bottles is subtracted from biogas production by each substrate (Donoso-Bravo et al., 2010; Vivekanand et al., 2018).

Ten millimeters gas-tight glass syringe used for sampling of biogas for methane composition analysis. Methane composition was analyzed by Gas chromatography (Thermo SCIENTIFIC Trace 1110) equipped with Porapak column and Thermal Conductivity Detector (TCD) where helium gas was used as carrier gas (Zhen et al., 2016).

BMP Test of Mixtures

Five ratios were selected based on nutritional content (C/N ratio) of individual substrates and mixed on VS basis (Mata-Alvarez et al., 2014; Pellera and Gidarakos, 2017; Vivekanand et al., 2018). BMP test of these mixtures was performed for an incubation period of 60 days at 37°C with shaking of 90 rpm.

Ultrasonic Pretreatment

Each selected substrate suspension (10 g in 200 mL of water) in a beaker (500 mL) was sonicated (Wang et al., 2017; Xiong et al., 2017). Ultrasonic pretreatment was carried out in a probe-type sonicator (Ultrasonic Processor-sonicator EI-250UP, Electrosonic Industries, Mumbai, India) equipped with a probe of 15 mm diameter (shown in **Figure 3B**) operating at frequency 22 kHz and power of 250 W.

Ultrasonication pretreatment was performed by immersing probe to a half depth of suspension. Here, only pretreatment time is accounted as pretreatment variable i.e., for 30, 60, and 90 min (Nakashima et al., 2016). The temperature of suspension was maintained constant at 32 ± 1°C by recirculating cold water in the provided water bath and manual stirring is performed to have uniform pretreatment effect on substrates. Here, the project aims to investigate the influence of ultrasonic pretreatment duration without temperature effect on methane production.

Afterward, BMP test was performed to evaluate the effect of ultrasonic pretreatment on methane production from different substrates.

Analytical Studies

Proximate analysis i.e. Moisture content, Total solids (TS) and VS of the inoculum and substrates were determined by standard methods from American Public Health Association (APHA, 1999). Ultimate analysis i.e. carbon, hydrogen and nitrogen content were determined by CHNS analyser (Thermo Finnigan, FLASH EA 1112 series, Italy). pH of batch bottles was measured by a pH meter (LMPH 10, Labman Scientific Instruments Pvt. Ltd. India) in the beginning and end of the BMP test. The proximate and ultimate results of selected substrates are shown in **Table 1**.

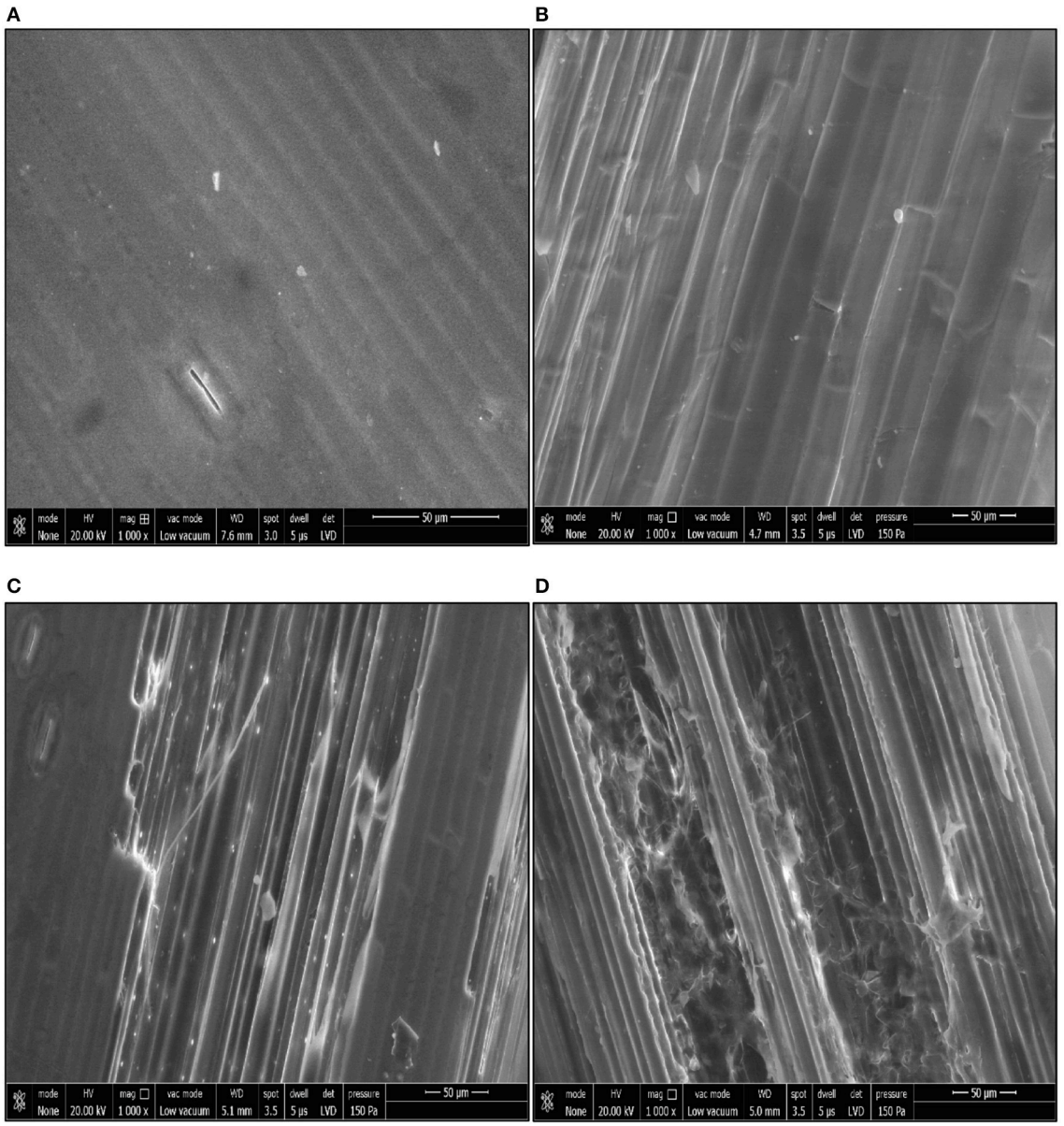

FIGURE 7 | The SEM images of **(A)** Untreated WS, **(B)** WS-30, **(C)** WS-60, and **(D)** WS-90.

Surface Morphology

Surface morphology of different pretreatment level of the respective substrate was observed by morphological change through scanning electron microscope SEM (Nova NanoSEM 450, Netherland) observation.

Crystallinity

Crystallinity index of untreated and pretreated substrates was examined through X-ray diffraction test using a XPERT-PRO X-ray diffractometer (XRD), and the samples were scanned in 2θ ranged from 5–50° with a step size of 0.02° (Liu et al., 2015; Wang et al., 2017). The decrease in CrI ascribed to disruption of crystalline structure, whereas an increase in CrI ascribed to removal of lignin and remained crystalline cellulose (Nakashima et al., 2016).

The crystallinity index (CrI) is calculated by following equation (1):

$$CrI = \frac{I_{cr} - I_{amor}}{I_{cr}} * 100\ \% \quad (1)$$

I_{cr} = Diffraction intensity from 002 plane of crystalline part (cellulose) at $2\theta = 22.6°$, and I_{amor} = Diffraction intensity of amorphous part (cellulose, hemicellulose, and lignin) $2\theta = 18°$ (Kumar et al., 2009; Liu et al., 2015; Wang et al., 2017).

Chemical Structure

Effect of pretreatment on different substrates can be observed by a change in chemical compositions through Spectrum 10.4.00 FTIR spectrophotometer (PerkinElmer, USA). FT-IR can be used to characterize the intrinsic biodegradability of a biomass. FT-IR spectroscopy analysis of selected samples of untreated and pretreated FW was performed in the range of 4000–400 cm^{-1} to characterize the effect of treatment on the functional groups and the chemical structure.

Kinetics Study

The different kinetics models have been used in previous studies to determine the methane yield by fitting the measured and predicted methane yield. Cone model and Exponential kinetic (or First order kinetic) model were chosen to fit the methane yield. Principal kinetic patterns (digestion mechanism of the organic substrate) of methane production from BMP test can be described through these models. Both models have an assumption of methane production in the batch test is proportional to methanogenic bacteria growth rate. These two models were used to compare and understand the kinetics of methane production from AD (El-Mashad, 2013; Zhen et al., 2016; Syaichurrozi, 2018).

Hydrolysis process as rate limiting step is the basis for using Exponential kinetic model describing the AD assuming no accumulation of intermediary elements (Veeken and Hamelers, 1999; Li K. et al., 2015). And, cone model gives better fit with methane production than other models reported by El-Mashad (2013), Li K. et al. (2015) and Paritosh et al. (2017). The equations of Cone model (Equation 2), and Exponential model (Equation 3) were shown below:

$$\text{Exponential model}: B = P \times (1 - exp^{-k \times t}) \quad (2)$$

$$\text{Cone model}: B = \frac{P}{1 + (k \times t)^{-n}} \quad (3)$$

B = Accumulative methane yield (ml/g VS), P = Final methane yield (ml/g VS), k = hydrolysis rate constant (1/day), n = shape factor, t = digestion time (day) for $t \geq 0$. With the help of non-linear least square fitting of accumulative methane yield, parameter "k" and "n" were estimated (Syaichurrozi, 2018).

The coefficient of determination (R^2) and Root mean square error (RMSE) were used as indicators for model fitness, and to compare the accuracy of both models. R^2 is an index for the goodness of fit, and RMSE gives standard deviation between measured and predicted values, the better fit model shows low RMSE (Li K. et al., 2015). RMSE can be calculated through following formula:

$$RMSE = \sqrt{\frac{\sum_{i=1}^{n} \left(Y_p - Y_m\right)^2}{n}}$$

Where, Y_p and Y_m are predicted and measured methane yield (ml/g VS), respectively, and n is a number of measurements performed (El-Mashad, 2013).

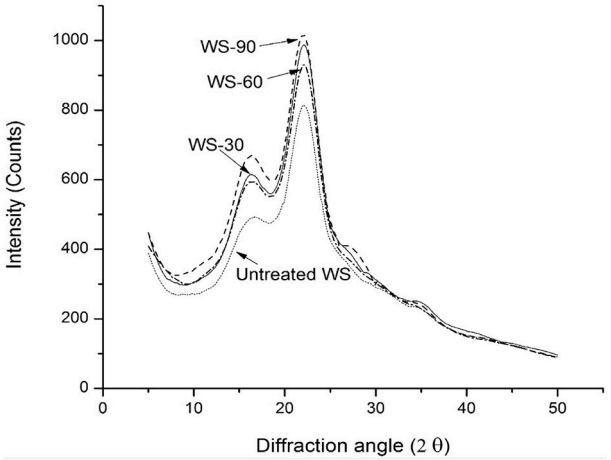

FIGURE 8 | The XRD patterns of WS samples.

RESULTS AND DISCUSSION

BMP Test of Different Agro-Industrial Waste

The results of I-BMP test of individual substrates showing biogas production are shown in **Figure 4** of different agro-industrial waste for digestion time of 30 days. Accumulated biogas production in 30 days of digestion period from raw Groundnut shell, Mung bean husk, Guar husk, and Rice bran are also defined in **Table 2**. Mung bean husk showed maximum potential of biogas among other agro-industrial waste (i.e., groundnut shell, guar husk, and rice bran) therefore it was selected as co-substrate with wheat straw and OFMSW for the multi feed-stock AD. Biogas production from rice bran was low due to its high protein content making unstable AD process (Favaro et al., 2017).

BMP Test of Selected Substrates and Their Mixtures

The II-BMP test of selected substrate i.e., OFMSW, WS, and MBH, and anaerobic co-digestion of five different mixing ratio shown in **Table 2** of these substrates were performed for a retention time of 60 days. Accumulative biogas production in 60 days from above-mentioned substrates and mixtures are shown in **Figure 5**. Biogas production of OFMSW, WS, and MBH in mono-digestion mode were 397, 431, and 468 ml/g VS, respectively. AcoD having mixture M3 having a composition of OFMSW, WS, and MBH at 42, 7.5, and 50.5%, respectively ratios produced maximum biogas production in comparison with other mixing ratios.

Comparison of biogas and methane production of substrates in mono-digestion and co-digestion mode with total methane fraction are shown in **Table 2**. Methane produced and its total fraction in biogas from WS, OFMSW, and MBH are 225 (52%), 203 (51%), and 267 (57%) ml/g VS. WS cellulosic enzymatic hydrolysis is the slow due presence of hemicellulose and lignin can be seen from accumulative biogas production curve in

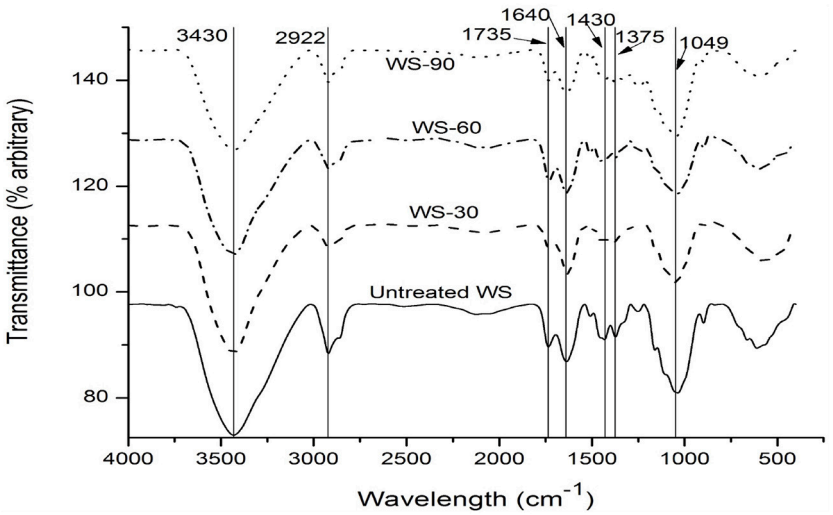

FIGURE 9 | The FT-IR spectra of WS samples.

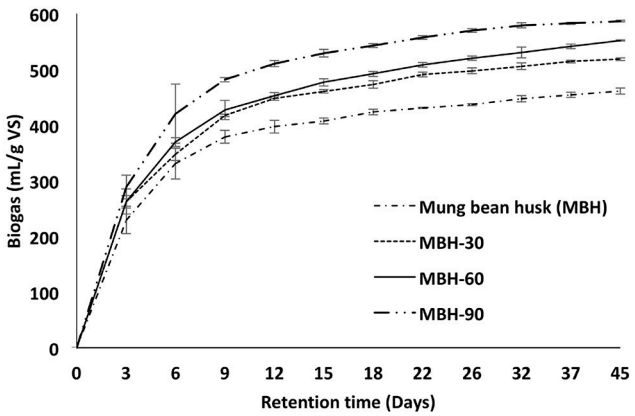

FIGURE 10 | Accumulated biogas and Methane yield from pretreated MBH.

Figure 5 (Zheng et al., 2018). Methane production through AcoD of mixtures were 256 (M1), 226 (M2), 275 (M3), 280 (M4), and 84 (M5) ml/g VS. Mixture M4 showed maximum methane production with 280 ml/g VS with methane fraction of 59%, whereas mixture M5 has minimum methane production 84 ml/g VS, due to the nutritional imbalance i.e., high C/N ratio of 52 which led to the accumulation of VFA inhibiting the methanogens.

The enhanced methane yield from mixtures M1-M4 showed the good synergistic effect of co-digestion. For better methane yield mixture of such substrates should have a composition of OFMSW and MBH in the range of 25–42%, and 50–70%, respectively. The synergistic effect of co-digestion can be strengthened by optimizing the above-mentioned range of specific substrate fractions. The mixture M4 methane yield showed 37, 20, and 4% higher methane yield in comparison with mono-digestion of OFMSW, WS, and MBH.

Analytical Study of Ultrasonic Pretreatment on Different Substrates

Untreated and pretreated substrates were digested anaerobically at mesophilic conditions, for which III-BMP test was performed whose results were shown in **Table 2**. The effect of pretreatment was evaluated by analyzing following sections of respective substrates.

Wheat Straw (WS)

Methane yield

Ultrasonication enhance biogas and methane yield due to improved solubility of organic matters. This can be validated with enhancement of accumulative biogas yield from WS are shown in **Figure 6**. Biogas yield due to pretreatment are similar with results from previous pretreatment studies on WS (Li Y. et al., 2015). Methane yield and methane fraction in biogas from pretreated WS samples 314 (67%), 357 (65%), and 314 (61%) ml/g VS at sonication time of 30, 60, and 90 min, respectively. Highest methane yield (357 ml/g VS) was obtained at 60 min of sonication pretreatment. The increment of 75% was observed in methane yield of ultrasonic pretreated WS at sonication period of 60 min than untreated WS. After 60 min sonication, methane yield decreases in WS, it was due to an increased particle size of samples because of reflocculation phenomena so lowered the hydrolysis rate. Re-flocculation occurred due to excess radical formation in the suspension (Rasapoor et al., 2016; Zeynali et al., 2017).

Surface morphology

The morphological changes induced by ultrasonic pretreatment on Wheat straw samples with increment in sonication time were observed by SEM images which are shown in **Figures 7A–D**. The untreated sample has smooth surface whereas pretreated samples showing erosion on the surfaces which can be recognized as the action of ultrasound pretreatment caused by the cavitation

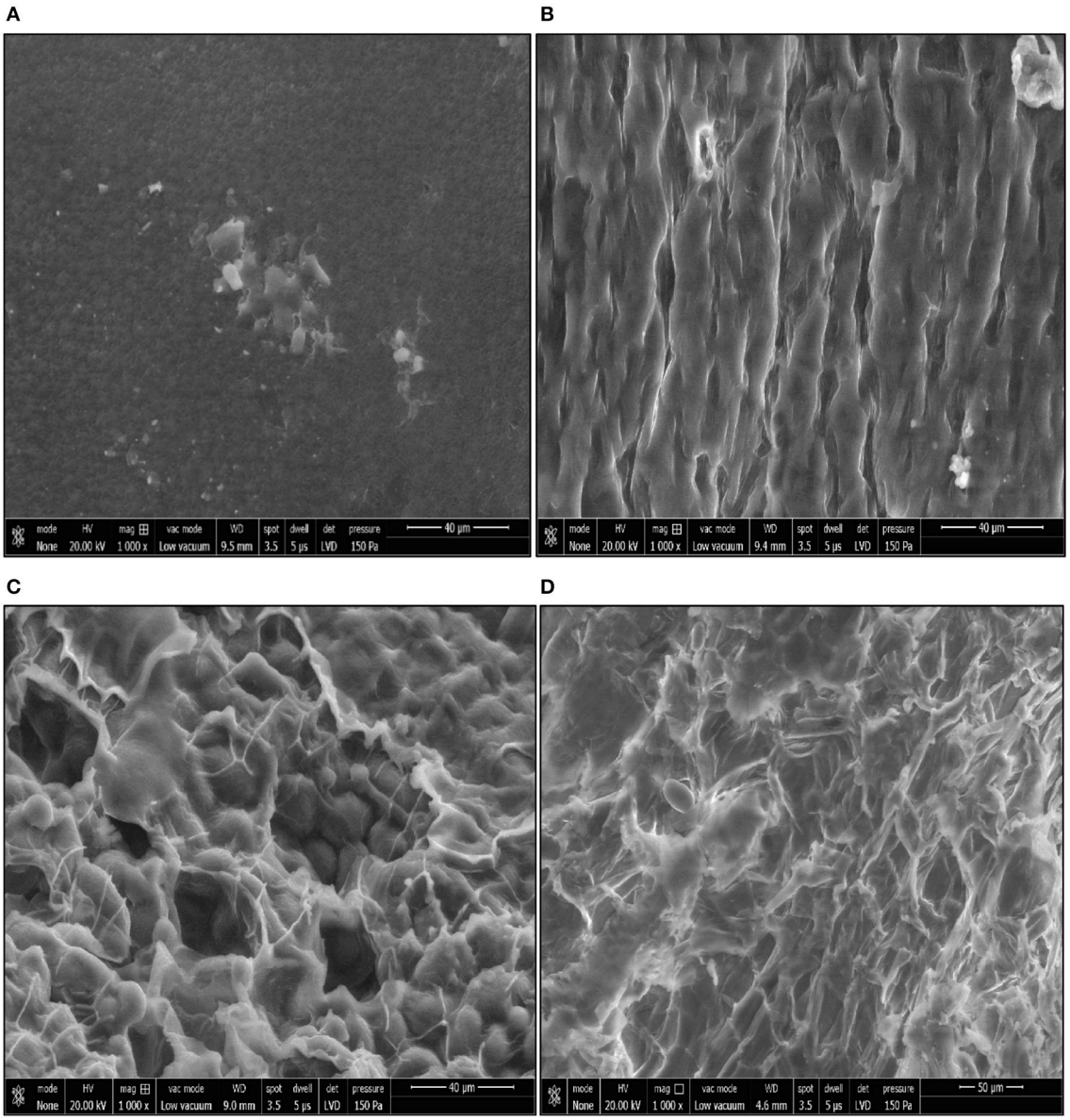

FIGURE 11 | The SEM images of **(A)** Untreated MBH, **(B)** MBH-30, **(C)** MBH-60, and **(D)** MBH-90.

effect of sonication. As sonication time increases more surface erosion occurs on the outer surface of the WS samples which can be observed from **Figures 7A–D**. Also, images **Figures 7B–D** of pretreated WS samples reflecting some of the lignin cover on the surface are removed and broken resulting into the more accessible area of microfibrils for faster enzymatic hydrolysis, leading methane augmentation (Wang et al., 2016; Zheng et al., 2018).

Crystallinity

Crystallinity is a factor affecting hydrolysis significantly, its higher value represents better pretreatment effect if the purpose is to destroy amorphous fraction i.e. hemicellulose and lignin structure (Wang et al., 2017). Untreated and pretreated WS samples have similar XRD patterns shown in **Figure 8**, revealing significant disruption in the structure of WS samples. The crystallinity index (CrI) of pretreated WS samples calculated according to equation (1) whose values for untreated WS, WS-30, WS-60, and WS-90 are 39.9, 40.8, 38.7, and 37.4, respectively. Here, crystallinity increases from 39.9 to 40.8 after 30 min sonication showing deconstruction the lignin cover of WS samples due to cavitation effect induced by ultrasound frequency in water. Afterward, as sonication time is increases resulted in decreased crystallinity. The decrease in CrI may be ascribed as partial disruption of crystalline cellulose structure (Zheng et al., 2018). This shows pretreatment destroys concurrently lignin,

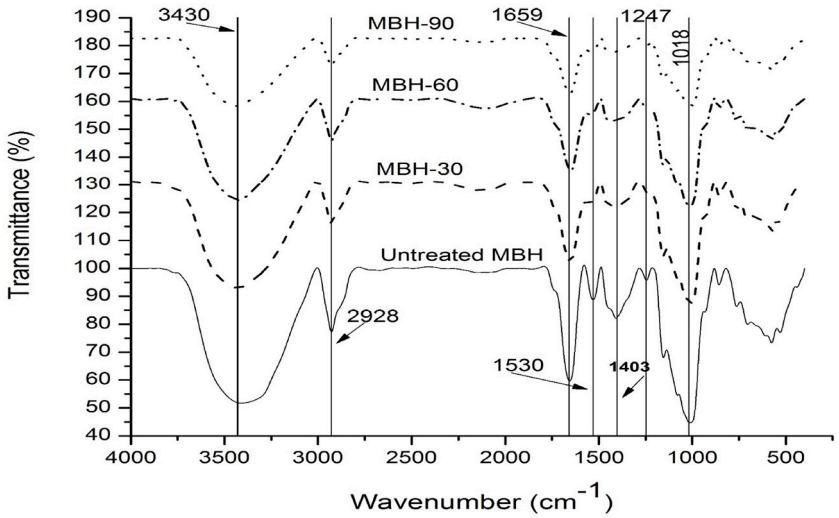

FIGURE 12 | The FT-IR spectra of MBH samples.

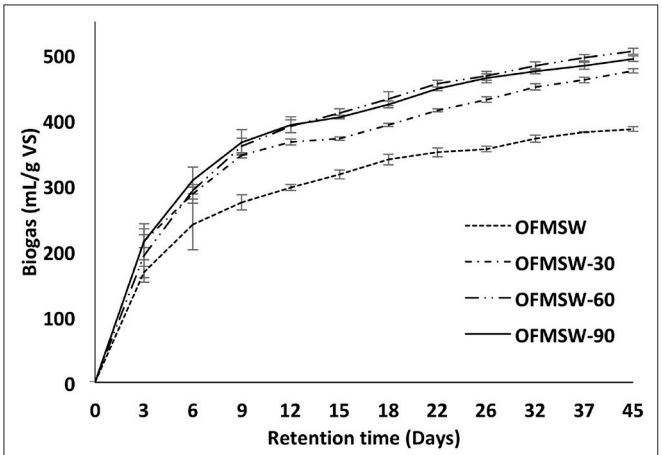

FIGURE 13 | Accumulated biogas and Methane yield from pretreated OFMSW.

hemicellulose, and cellulose structure i.e., in a non-selective manner (Xiong et al., 2017).

Chemical structure

The FT-IR spectra of untreated and pretreated WS samples are shown in **Figure 9**. The absorbance band of 3350–3450 cm^{-1} assigned to the –OH stretching vibrations, peak intensity is weakened as pretreatment increases showed cellulose content in pretreated samples is higher than untreated one (Zheng et al., 2018). In FT-IR spectroscopy, 1400–1700 cm^{-1} band shows the presence of C=C of aromatic rings which are found in lignin. In this spectra, the peak near 1430 and 1640 cm^{-1} are diminishing in pretreated samples that indicates the degradation of lignin. The peak at 1735 cm^{-1} which represents ester bond C=O also diminishing with pretreatment indicating degradation of ester linkages between lignin and carbohydrates corresponding to the hemicellulose (Liu et al., 2009). Apart from lignin and hemicellulose, the crystalline cellulose defined by peak 1049 cm^{-1} also degrades indicating reduction in crystalline cellulose part. The intensity of peak 2922 and 1375cm^{-1} which is related to asymmetric methylene stretching and CH_2 wagging, respectively of cellulose, becomes weaker with increasing pretreatment severity (Singh et al., 2011; Raj et al., 2015). The pretreatment effect is consistent with results of XRD analysis.

Mung Bean Husk (MBH)

The effect of pretreatment was evaluated by analyzing methane yield, changes in surface morphology and chemical structure of pretreated MBH samples.

Methane yield

Enhancement in accumulative biogas yield from pretreated MBH substrate are shown in **Figure 10**. Methane yield and methane fraction (% of biogas) of pretreated MBH samples were 350 (68%), 382 (69%), and 379 (65%) ml/g VS at sonication time of 30, 60, and 90 min, respectively. Highest methane yield (382 ml/g VS) was obtained at 60 min of sonication. Ultrasonication pretreatment enhanced methane fraction from 57 to 69% of biogas volume. In case of MBH pretreatment, biogas volume was consistently increasing with an increment of sonication time in performed pretreatment conditions. Ultrasonic pretreated MBH has a maximum increment of methane yield up to 46% at sonication 60 min.

Surface morphology

SEM images of different pretreated MBH samples were obtained shown in **Figure 11** to prove the substrate structural change caused by ultrasonication pretreatment. Before and after pretreatment SEM images show surfaces of MBH samples have significant changes can be observed. Untreated samples exhibit compact and regular surface structure, where microfibers

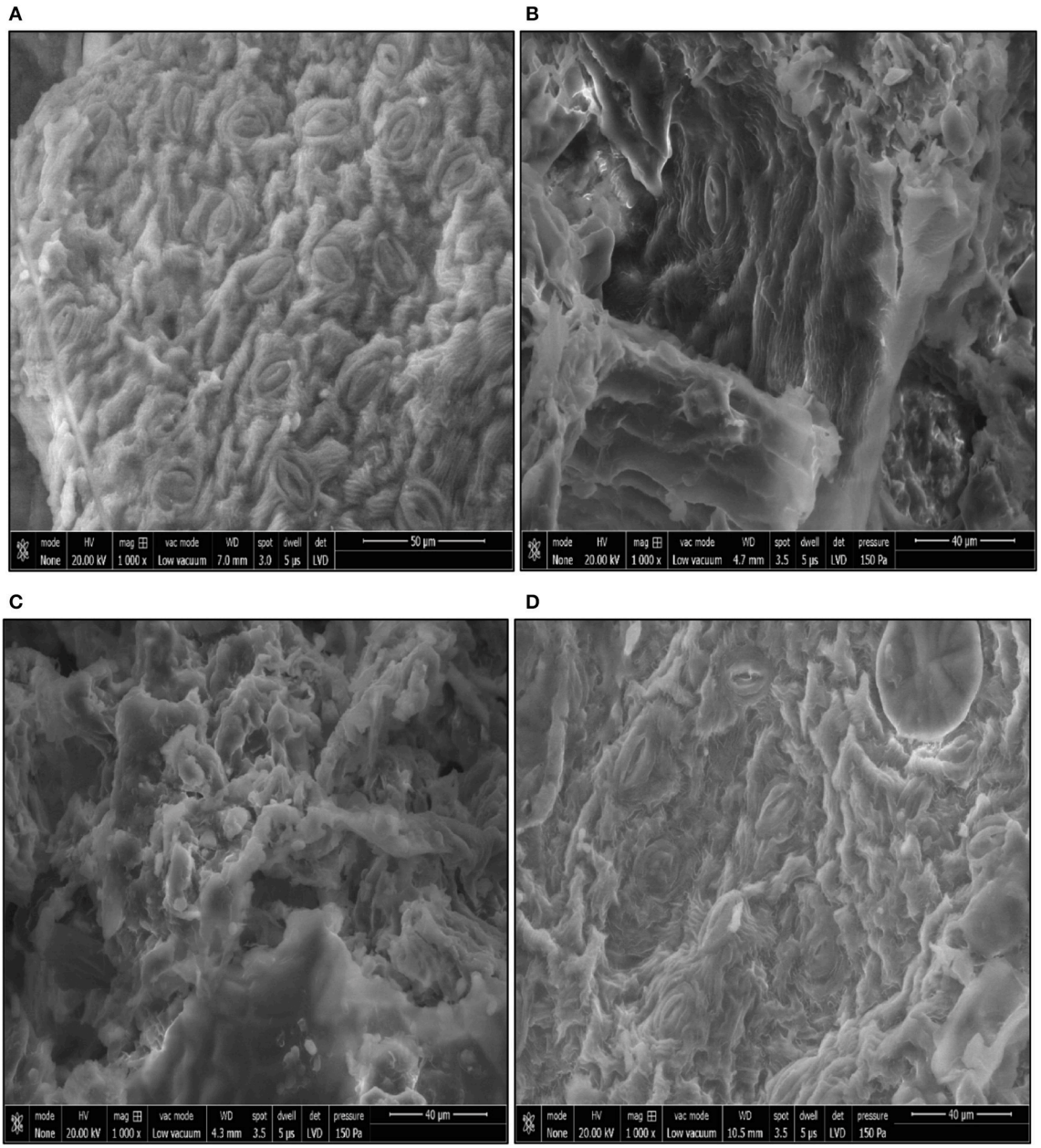

FIGURE 14 | The SEM images of **(A)** Untreated OFMSW, **(B)** OFMSW-30, **(C)** OFMSW-60, and **(D)** OFMSW-90.

can't be observed. After sonication pretreatment, MBH samples becomes coarse and scattered making microfibrils more porous compared to untreated MBH. Thus, pretreatment enhances surface defibrillation and coarseness as sonication time increases, confirming the positive effect in disrupting the structure of MBH samples.

Chemical structure

The FT-IR analysis demonstrates that untreated and pretreated samples of MBH have similar spectra pattern shown in **Figure 12**, showing the surface functional groups were significantly affected by pretreatment. The –OH bond at 3430 cm^{-1} represents the OH groups in cellulose whose degradation can be observed with pretreatment. As can be seen from FT-IR spectra, peak 1659 and 1530 cm^{-1} corresponds to C=C stretching of aromatic ring originated from lignin, were diminishing with pretreatment severity to MBH samples. Also, peak at 1247 cm^{-1} of ether bonds in pretreated MBH samples were almost disappearing in comparison to untreated MBH sample. This indicates ultrasonic pretreatment could disrupt or remove ether linkages between carbohydrates and lignin (Liu et al., 2009). Reduction in the peak of 1018 cm^{-1} of C-O stretching corresponding to hemicellulose

TABLE 3 | Parameters of Cone and Exponential kinetic model obtained from untreated and pretreated samples.

Substrates	Experimental methane (ml/g VS)	Cone model					Exponential model			
		Predicted methane (ml/g VS)	k (day^{-1})	*n*	R^2	RMSE	Predicted methane (ml/g VS)	k (day^{-1})	R^2	RMSE
Untreated MBH	261.1	251.8	0.21	1.47	0.9922	4.4	260.3	0.13	0.9793	9.7
MBH-30	350.4	338.3	0.24	1.4	0.9849	8.0	349.8	0.142	0.9892	11.6
MBH-60	381.7	364.1	0.22	1.32	0.9877	7.9	380.4	0.126	0.987	15.8
MBH-90	379.2	368.3	0.24	1.48	0.9929	6.4	378.8	0.15	0.9902	10.7
Untreated WS	204.2	188.3	0.064	2.34	0.9894	6.8	178.4	0.046	0.9918	16.6
WS-30	314.2	296.0	0.082	2.14	0.9918	9.5	293.0	0.06	0.996	17.8
WS-60	356.9	335.5	0.083	2.09	0.9921	10.0	332.9	0.06	0.9954	19.2
WS-90	314.1	292.8	0.078	2.09	0.9921	8.7	288.8	0.056	0.9973	18.1
Untreated OFMSW	193.2	181.2	0.135	1.51	0.9811	6.4	189.1	0.086	0.9933	3.9
OFMSW-30	291.2	267.3	0.156	1.24	0.9592	12.1	285.6	0.088	0.9723	14.9
OFMSW-60	331.1	311.8	0.15	1.46	0.9851	9.3	326.2	0.094	0.9931	7.8
OFMSW-90	287.2	269.5	0.16	1.38	0.9776	9.4	283.6	0.097	0.9868	9.9

showing degradation of hemicellulose. Also, the intensity at 2928 cm^{-1} of –CH aliphatic stretching represents CH_2 and CH_3 groups corresponding to cellulose and hemicellulose which were diminishing as sonication time increases for MBH samples. Also, peak of $–CH_2$ wagging at wavenumber 1403 cm^{-1} is also weakening than the untreated samples (Smidt et al., 2002; Chandra, 2015; Li et al., 2018). FT-IR spectra results showed pretreatment affect lignin, hemicellulose, and cellulose simultaneously.

Organic Fraction of Municipal Solid Waste (OFMSW)

The effect of pretreatment was evaluated by analyzing methane yield, and changes in surface morphology of pretreated OFMSW samples.

Methane yield

Accumulated biogas yield were measured for defined sonication time to OFMSW is shown in the **Figure 13**. **Table 2** also showing methane yield and methane fraction of pretreated OFMSW samples 291 (60%), 331 (66%), and 287 (58%) ml/g VS at sonication time of 30, 60, and 90 min, respectively with respect to 193 (50%) ml/g VS from untreated OFMSW. Highest methane yield (331 ml/g VS) was obtained at 60 min of sonication pretreatment. The increment of 71% in methane yield and methane fraction enhanced from 50 to 66% of biogas, were observed from ultrasonic pretreated OFMSW at sonication period of 60 min than untreated OFMSW. Methane yield resulted from ultrasound pretreatment of OFMSW were comparable with results of Cesaro and Belgiorno (2013). Methane yield from pretreated OFMSW samples increases with ultrasonication time due to the organic matter solubilization making the higher availability of substrate for digestion. After 60 min of ultrasonication, methane yield decreases in OFMSW, it was due to increased particle size of samples because of radical formation initiating the polymerization reaction during ultrasonic pretreatment (González-Fernández et al., 2012).

Surface morphology

SEM analysis of untreated and pretreated OFMSW samples helped to comprehend the ultrasonication effect. SEM images of OFMSW samples are shown in **Figures 14A–D**. Untreated OFMSW has more tight particles having composites of organic compounds having clusters of particles, whereas ultrasonicated OFMSW samples showed bigger particle cluster were rugged, and broken into smaller particles sizes, thereby augmenting surface area of pretreated samples and improving the organic matters solubility. Thus ultrasonication effect led changes in physical structure to OFMSW samples achieving better disintegration, so pretreated OFMSW samples have the more microbial accessibility of carbon for enzymatic hydrolysis than untreated one (Deepanraj et al., 2017).

Kinetic Study Results

The degradation kinetics of selected substrates were described by using Cone and Exponential kinetic models for III-BMP test. **Table 3** shows the experimental methane yield (ml/g VS) from BMP-III test and predicted methane yield (ml/g VS) for respective kinetic models with relevant kinetic parameters. For both models, hydrolysis rate constant "k" increasing with pretreatment duration of respective substrate samples with few exceptions. Hydrolysis rate constant "k" reflects biodegradability of substrates. High "k" refers to the faster rate of degradation of organic substrate, enhancing methane production (Veeken and Hamelers, 1999; Zhen et al., 2015; Mao et al., 2017).

The studied model results of OFMSW shows improvement in measured methane and maximum methane potential was independent of "k," that rise in "k" doesn't convey high methane production. This inference was similar to Zhen et al. (2016) and Keymer et al. (2013). In case of cone model, "k" ranges between 0.21 and 0.24 day^{-1} for MBH, 0.064–0.083 day^{-1} for WS, and 0.135–0.16 day^{-1} for OFMSW, in case of exponential kinetic model "k" ranges 0.13–0.15 day^{-1} for MBH, 0.046–0.06 day^{-1} for WS, and 0.086–0.097 day^{-1} for OFMSW. The "k" values are

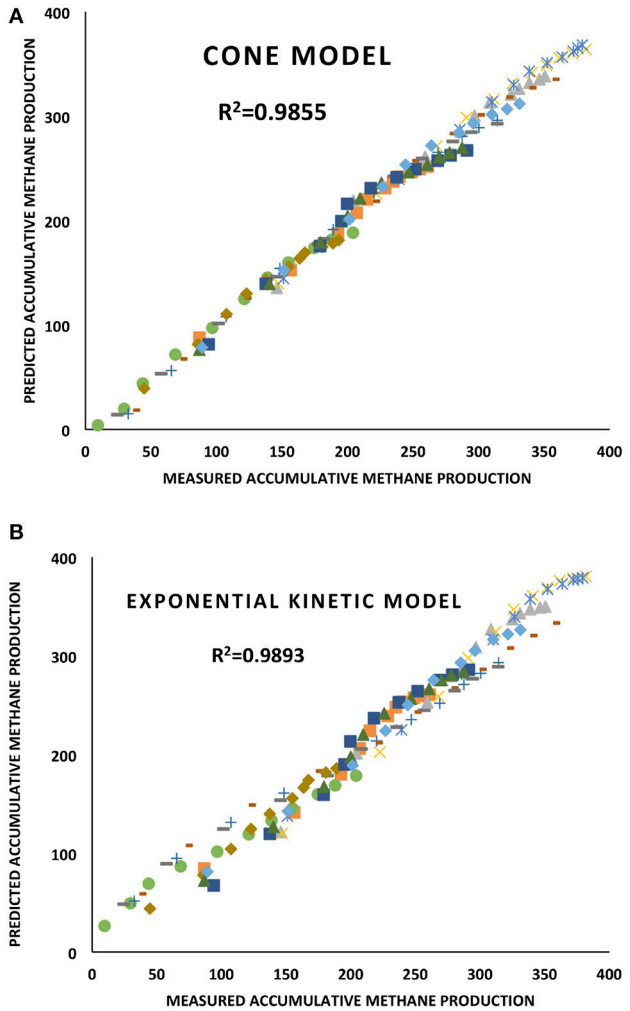

FIGURE 15 | Predicted methane yield against measured values for **(A)** cone model, **(B)** exponential kinetic model.

comparatively lower for lignocellulosic biomass, therefore lignin content is higher in WS, than substrate MBH, and OFMSW, as it contains green waste.

The calculated RMSE and R^2 values for both models are shown in **Table 3**, their lower values confirming the model's good agreement with experimental results. RMSE values vary in between 4.4–12.1 for Cone model and 3.9–19.2 for the Exponential model. This reflects Cone model with a lower range of RMSE, is more accurate than the Exponential kinetic model. The cone model (R^2: 0.9592–0.9929) and Exponential kinetic model (R^2: 0.9723–0.9973) showed a good fit to predicted and measured data of different untreated and pretreated substrates in mono-digestion. **Figure 15A,B** shows relation between predicted methane yield against measured values for both Cone and Exponential kinetic model through R^2.

CONCLUSION

This study shows multi-feed of wheat straw, mung bean husk, and OFMSW anaerobic co-digestion shows good synergy for enhanced methane production. Mixing of such co-substrates results into 37, 20, and 4% higher methane yield in comparison with mono-digestion of OFMSW, wheat straw and mung bean husk. The experimental results showed ultrasonic pretreatment with varying sonication time have a significant effect on methane yield from OFMSW, wheat straw, and Mung bean husk. Pretreatment significant effects on different substrates were validated through BMP test, SEM, XRD, and FTIR analysis. Ultrasonication time can be increased up to 60 min with stable temperature pretreatment constraint. Methane yield of ultrasonic pretreated wheat straw, mung bean husk and OFMSW have a maximum increment of 75, 46, and 71%, respectively at sonication period of 60 min. Two classical kinetic models i.e., Cone and Exponential were used for validating the experimental results of III-BMP test. Cone and Exponential model have an average coefficient of determination $R^2 = 0.9855$ and $R^2 = 0.9893$, respectively, but the range of RMSE for cone model results is lower than that of Exponential model showing Cone model is more précised.

AUTHOR CONTRIBUTIONS

KP performed the experiments and VV conceived and designed the experiments. KP carried out the experiments and wrote the manuscript. VV and NP worked on and corrected the manuscript critically.

ACKNOWLEDGMENTS

KP thanks MNIT for assistantship and SAIF, IIT Bombay for CHN characterization. Authors are thankful to Department of Biotechnology-GoI (Grant No. BT/RLF/Re-Entry/04/2013) and Department of Science and Technology-GoI (Grant No. ECR/2016/000989) for financial support.

REFERENCES

Abdulrazak, S., Otie, D., and Oniwapele, Y. A. (2014). Proximate analysis and anti-nutritional factors of groundnut and melon husk. *Online J. of Anim. Feed Res.* 4, 25–28.

Abudi, Z. N., Hu, Z., Sun, N., Xiao, B., Rajaa, N., Liu, C., et al. (2016). Batch anaerobic co-digestion of OFMSW (organic fraction of municipal solid waste), TWAS (thickened waste activated sludge) and RS (rice straw): influence of TWAS and RS pretreatment and mixing ratio. *Energy* 107, 131–140. doi: 10.1016/j.energy.2016.03.141

Annual Report MA and FW (2017). *Agricultural Statistics at a Glance 2016.* Ministry of Agriculture & Farmers Welfare (Govermentment. of India).

APHA, (1999). *Standard Methods for Examination of Water and Waste Water,* 17th edn. American Public Health Association, Washington, DC.

Bolado-Rodríguez, S., Toquero, C., Martín-Juárez, J., Travaini, R., and García-Encina, P. A. (2016). Effect of thermal, acid, alkaline and alkaline-peroxide

pretreatments on the biochemical methane potential and kinetics of the anaerobic digestion of wheat straw and sugarcane bagasse. *Bioresour. Technol.* 201, 182–190. doi: 10.1016/j.biortech.2015.11.047

Bundhoo, Z. M., Mauthoor, S., and Mohee, R. (2016). Potential of biogas production from biomass and waste materials in the Small Island Developing State of Mauritius. *Renew. Sustainable Energy Rev.* 56, 1087–1100. doi: 10.1016/j.rser.2015.12.026

Bussemaker, M. J., and Zhang, D. (2013). Effect of ultrasound on lignocellulosic biomass as a pretreatment for biorefinery and biofuel applications. *Indust. Eng. Chem. Res.* 52, 3563–3580. doi: 10.1021/ie3022785

Castrillón, L., Fernández-Nava, Y., Ormaechea, P., and Marañón, E. (2011). Optimization of biogas production from cattle manure by pre-treatment with ultrasound and co-digestion with crude glycerin. *Bioresour. Technol.* 102, 7845–7849. doi: 10.1016/j.biortech.2011.05.047

Census, (2011). *Census in India*. Available online at: http://www.census2011.co.in/ (Accessed November 17, 2017).

Cesaro, A., and Belgiorno, V. (2013). Sonolysis and ozonation as pretreatment for anaerobic digestion of solid organic waste. *Ultrasonics Sonochem.* 20, 931–936. doi: 10.1016/j.ultsonch.2012.10.017

Cesaro, A., and Belgiorno, V. (2014). Pretreatment methods to improve anaerobic biodegradability of organic municipal solid waste fractions. *Chemical Eng. J.* 240, 24–37. doi: 10.1016/j.cej.2013.11.055

Cesaro, A., Naddeo, V., Amodio, V., and Belgiorno, V. (2012). Enhanced biogas production from anaerobic codigestion of solid waste by sonolysis. *Ultrasonics Sonochem.* 19, 596–600. doi: 10.1016/j.ultsonch.2011.09.002

Cesaro, A., Velten, S., Belgiorno, V., and Kuchta, K. (2014). Enhanced anaerobic digestion by ultrasonic pretreatment of organic residues for energy production. *J. Clean. Prod.* 74, 119–124. doi: 10.1016/j.jclepro.2014.03.030

Chandra, R. (2015). *Advances in Biodegradation and Bioremediation of Industrial Waste*. Boca Raton, FL: CRC Press.

Chandra, R., Takeuchi, H., and Hasegawa, T. (2012b). Methane production from lignocellulosic agricultural crop wastes: a review in context to second generation of biofuel production. *Renew. Sustainable Energy Rev.* 16, 1462–1476. doi: 10.1016/j.rser.2011.11.035

Chandra, R., Takeuchi, H., Hasegawa, T., and Kumar, R. (2012a). Improving biodegradability and biogas production of wheat straw substrates using sodium hydroxide and hydrothermal pretreatments. *Energy* 43, 273–282. doi: 10.1016/j.energy.2012.04.029

Cho, S., Park, S., Seon, J., Yu, J., and Lee, T. (2013). Evaluation of thermal, ultrasonic and alkali pretreatments on mixed-microalgal biomass to enhance anaerobic methane production. *Bioresour. Technol.* 143, 330–336. doi: 10.1016/j.biortech.2013.06.017

Clark, P. B., and Nujjoo, I. (2000). Ultrasonic sludge pretreatment for enhanced sludge digestion. *Water Environ. J.* 14, 66–71. doi: 10.1111/j.1747-6593.2000.tb00228.x

Deepanraj, B., Sivasubramanian, V., and Jayaraj, S. (2017). Effect of substrate pretreatment on biogas production through anaerobic digestion of food waste. *Int. J. of Hydrogen Energy* 42, 26522–26528. doi: 10.1016/j.ijhydene.2017.06.178

Devi, S., Gupta, C., Jat, S. L., and Parmar, M. S. (2017). Crop residue recycling for economic and environmental sustainability: the case of India. *Open Agricult.* 2, 486–494. doi: 10.1515/opag-2017-0053

Dhar, H., Kumar, S., and Kumar, R. (2017). A review on organic waste to energy systems in India. *Bioresour. Technol.* 245, 1229–1237. doi: 10.1016/j.biortech.2017.08.159

Donoso-Bravo, A., Pérez-Elvira, S. I., and Fdz-Polanco, F. (2010). Application of simplified models for anaerobic biodegradability tests. Evaluation of pre-treatment processes. *Chemical Eng. J.* 160, 607–614. doi: 10.1016/j.cej.2010.03.082

El-Mashad, H. M. (2013). Kinetics of methane production from the codigestion of switchgrass and Spirulina platensis algae. *Bioresour. Technol.* 132, 305–312. doi: 10.1016/j.biortech.2012.12.183

Favaro, L., Cagnin, L., Basaglia, M., Pizzocchero, V., van Zyl, W. H., and Casella, S. (2017). Production of bioethanol from multiple waste streams of rice milling. *Bioresour. Technol.* 244, 151–159. doi: 10.1016/j.biortech.2017.07.108

Gollapalli, M., and Kota, S. H. (2018). Methane emissions from a landfill in north-east India: performance of various landfill gas emission models. *Environ. Pollut.* 234, 174–180. doi: 10.1016/j.envpol.2017.11.064

González-Fernández, C., Sialve, B., Bernet, N., and Steyer, J. P. (2012). Comparison of ultrasound and thermal pretreatment of Scenedesmus biomass on methane production. *Bioresour. Technol.* 110, 610–616. doi: 10.1016/j.biortech.2012.01.043

Hagos, K., Zong, J., Li, D., Liu, C., and Lu, X. (2017). Anaerobic co-digestion process for biogas production: progress, challenges and perspectives. *Renew. Sustainable Energy Rev.* 76, 1485–1496. doi: 10.1016/j.rser.2016.11.184

Hiloidhari, M., Das, D., and Baruah, D. C. (2014). Bioenergy potential from crop residue biomass in India. *Renew. Sustainable Energy Rev.* 32, 504–512. doi: 10.1016/j.rser.2014.01.025

Izumi, K., Okishio, Y. K., Nagao, N., Niwa, C., Yamamoto, S., and Toda, T. (2010). Effects of particle size on anaerobic digestion of food waste. *Int. Biodet. Biodegrad.* 64, 601–608. doi: 10.1016/j.ibiod.2010.06.013

Janampet, R. S., Malavath, K. K., Neeradi, R., Chedurupalli, S., and Thirunahari, R. (2016). Effect of feeding guar meal on nutrient utilization and growth performance in Mahbubnagar local kids. *Vet. World* 9:1043. doi: 10.14202/vetworld.2016.1043-1046

Kacprzak, A., Krzystek, L., and Ledakowicz, S. (2010). Co-digestion of agricultural and industrial wastes. *Chemical Papers* 64, 127–131. doi: 10.2478/s11696-009-0108-5

Kalyani, K. A., and Pandey, K. K. (2014). Waste to energy status in India: a short review. *Renew. Sustainable Energy Rev.* 31, 113–120. doi: 10.1016/j.rser.2013.11.020

Keymer, P., Ruffell, I., Pratt, S., and Lant, P. (2013). High pressure thermal hydrolysis as pre-treatment to increase the methane yield during anaerobic digestion of microalgae. *Bioresour. Technol.* 131, 128–133. doi: 10.1016/j.biortech.2012.12.125

Kumar, R., Mago, G., Balan, V., and Wyman, C. E. (2009). Physical and chemical characterizations of corn stover and poplar solids resulting from leading pretreatment technologies. *Bioresour. Technol.* 100, 3948–3962. doi: 10.1016/j.biortech.2009.01.075

Kumar, S., Paritosh, K., Pareek, N., Chawade, A., and Vivekanand, V. (2018). De-construction of major Indian cereal crop residues through chemical pretreatment for improved biogas production: an overview. *Renew. Sustainable Energy Rev.* 90, 160–170. doi: 10.1016/j.rser.2018.03.049

Li, G., Sun, Y., Guo, W., and Yuan, L. (2018). Comparison of various pretreatment strategies and their effect on chemistry and structure of sugar beet pulp. *J. Clean. Prod.* 181, 217–223. doi: 10.1016/j.jclepro.2018.01.259

Li, K., Liu, R., and Sun, C. (2015). Comparison of anaerobic digestion characteristics and kinetics of four livestock manures with different substrate concentrations. *Bioresour. Technol.* 198, 133–140. doi: 10.1016/j.biortech.2015.08.151

Li, Y., Merrettig-Bruns, U., Strauch, S., Kabasci, S., and Chen, H. (2015). Optimization of ammonia pretreatment of wheat straw for biogas production. *J. Chem. Technol. Biotechnol.* 90, 130–138. doi: 10.1002/jctb.4297

Liu, L., Sun, J., Li, M., Wang, S., Pei, H., and Zhang, J. (2009). Enhanced enzymatic hydrolysis and structural features of corn stover by FeCl3 pretreatment. *Bioresour. Technol.* 100, 5853–5858. doi: 10.1016/j.biortech.2009.06.040

Liu, X., Zicari, S. M., Liu, G., Li, Y., and Zhang, R. (2015). Pretreatment of wheat straw with potassium hydroxide for increasing enzymatic and microbial degradability. *Bioresour. Technol.* 185, 150–157. doi: 10.1016/j.biortech.2015.02.047

Mao, C., Zhang, T., Wang, X., Feng, Y., Ren, G., and Yang, G. (2017). Process performance and methane production optimizing of anaerobic co-digestion of swine manure and corn straw. *Sci. Rep.* 7, 9379. doi: 10.1038/s41598-017-09977-6

Mata-Alvarez, J., Dosta, J., Romero-Güiza, M. S., Fonoll, X., Peces, M., and Astals, S. (2014). A critical review on anaerobic co-digestion achievements between 2010 and 2013. Renew. *Sust. Energy Rev.* 36, 412–427. doi: 10.1016/j.rser.2014.04.039

Mboowa, D., Quereshi, S., Bhattacharjee, C., Tonny, K., and Dutta, S. (2017). Qualitative determination of energy potential and methane generation from municipal solid waste (MSW) in Dhanbad (India). *Energy* 123, 386–391. doi: 10.1016/j.energy,.2017.02.009

MNRE Annual Report (2017). *Waste to Energy Potential in India 2017*. Ministry of New and Renewable Energy. Available online at: http://mnre.gov.in/file-manager/annual-report/2016-2017/EN/pdf/1.pdf (Accessed December 15, 2017).

MSW Report (2017). *Annual Review Report 2014-15. Implementation of Municipal solid wastes (Management and Handling) Rules, 2000*. Central Pollution Control Board, Ministry of Environment, Forest and Climate Change, Govnerment of India.

Municipal solid waste, Central Pollution Control Board (2017). (CPCB), Ministry of Environment, Forest and Climate Change, Govnerment of India. Available online at: http://cpcb.nic.in/wast/municipalwast/trend_46_cities_list.pdf (Accessed November 17, 2017).

Nakashima, K., Ebi, Y., Kubo, M., Shibasaki-Kitakawa, N., and Yonemoto, T. (2016). Pretreatment combining ultrasound and sodium percarbonate under mild conditions for efficient degradation of corn stover. *Ultrasonics Sonochem*. 29, 455–460. doi: 10.1016/j.ultsonch.2015.10.017

Negi, S., Dhar, H., Hussain, A., and Kumar, S. (2018). Biomethanation potential for co-digestion of municipal solid waste and rice straw: a batch study. *Bioresour. Technol.* 254, 139–144. doi: 10.1016/j.biortech.2018.01.070

Nguyen, V. H., Topno, S., Balingbing, C., Nguyen, V. C. N., Röder, M., Quilty, J., et al. (2016). Generating a positive energy balance from using rice straw for anaerobic digestion. *Energy Reports* 2, 117–122. doi: 10.1016/j.egyr.2016.05.005

Pagés-Díaz, J., Sárvári-Horváth, I., Pérez-Olmo, J., and Pereda-Reyes, I. (2013). Co-digestion of bovine slaughterhouse wastes, cow manure, various crops and municipal solid waste at thermophilic conditions: a comparison with specific case running at mesophilic conditions. *Water Sci. Technol.* 67, 989–995. doi: 10.2166/wst.2013.647

Paritosh, K., Mathur, S., Pareek, N., and Vivekanand, V. (2017). Feasibility study of waste (d) potential: co-digestion of organic wastes, synergistic effect and kinetics of biogas production. *Int. J. Environmental Sci. Technol.* 15, 1009–1018. doi: 10.1007/s13762-017-1453-5

Paritosh, K., Yadav, M., Mathur, S., Balan, V., Liao, W., Pareek, N., et al. (2018). Organic fraction of municipal solid waste: overview of treatment methodologies to enhance anaerobic biodegradability. *Front. Energy Res.* 6, 75. doi: 10.3389/fenrg.2018.00075

Pellera, F. M., and Gidarakos, E. (2017). Anaerobic digestion of solid agroindustrial waste in semi-continuous mode: evaluation of mono-digestion and co-digestion systems. *Waste Management* 68, 103–119. doi: 10.1016/j.wasman.2017.06.026

Planning Commission Report (2014). *Reports of the Task Force on Waste to Energy (Vol-I) (in the context of Integrated MSW management)*. Available online at: http://planningcommission.nic.in/reports/genrep/rep_wte1205.pdf (Accessed September 15, 2017).

Raj, T., Kapoor, M., Gaur, R., Christopher, J., Lamba, B., Tuli, D. K., et al. (2015). Physical and chemical characterization of various Indian agriculture residues for biofuels production. *Energy Fuels* 29, 3111–3118. doi: 10.1021/ef5027373

Rajasthan Agri-Statistics Report. (2017). *Rajasthan Agricultural Statistics At A Glance 2015-16*. Jaipur: Commissionerate of Agriculture. Available online at: http://www.agriculture.rajasthan.gov.in/content/dam/agriculture/Agriculture%20Department/ecitizen/agriculture-statistics/agriculture_statistics_2015-16.pdf

Rao, M. S., and Singh, S. P. (2004). Bioenergy conversion studies of organic fraction of MSW: kinetic studies and gas yield–organic loading relationships for process optimisation. *Bioresour. Technol.* 95, 173–185. doi: 10.1016/j.biortech.2004.02.013

Rasapoor, M., Ajabshirchi, Y., Adl, M., Abdi, R., and Gharibi, A. (2016). The effect of ultrasonic pretreatment on biogas generation yield from organic fraction of municipal solid waste under medium solids concentration circumstance. *Energy Convers. Management* 119, 444–452. doi: 10.1016/j.enconman.2016.04.066

Report RRECL (2017). *Biomass Fuel Supply Study (Rajasthan) for Rajasthan Renewable Energy Corporation Limited (RRECL)*. ABI ENERGY Consultancy Services Pvt Ltd, Chennai.

Rodriguez, C., Alaswad, A., Benyounis, K. Y., and Olabi, A. G. (2017). Pretreatment techniques used in biogas production from grass. *Renew. Sustainable Energy Rev.* 68, 1193–1204. doi: 10.1016/j.rser.2016.02.022

Shah, F. A., Mahmood, Q., Rashid, N., Pervez, A., Iqbal, A., and Shah, M. M. (2015). Anaerobic digestion of water hyacinth, giant reed, maize and poultry waste for biogas generation. *EC Agriculture* 22, 277–284.

Sharholy, M., Ahmad, K., Mahmood, G., and Trivedi, R. C. (2008). Municipal solid waste management in Indian cities–A review. *Waste Manage* 28, 459–467. doi: 10.1016/j.wasman.2007.02.008

Shekdar, A. V. (2009). Sustainable solid waste management: an integrated approach for Asian countries. *Waste Manage* 29, 1438–1448. doi: 10.1016/j.wasman.2008.08.025

Singh, D., Zeng, J., Laskar, D. D., Deobald, L., Hiscox, W. C., and Chen, S. (2011). Investigation of wheat straw biodegradation by Phanerochaete chrysosporium. *Biomass Bioenergy* 35, 1030–1040. doi: 10.1016/j.biombioe.2010.11.021

Smidt, E., Lechner, P., Schwanninger, M., Haberhauer, G., and Gerzabek, M. H. (2002). Characterization of waste organic matter by FT-IR spectroscopy: application in waste science. *Appl. Spectroscopy* 56, 1170–1175. doi: 10.1366/000370202760295412

Syaichurrozi, I. (2018). Biogas production from co-digestion Salvinia molesta and rice straw and kinetics. *Renew. Energy* 115, 76–86. doi: 10.1016/j.renene.2017.08.023

Uzodinma, E. O. U., Ofoefule, A. U., Eze, J. I., and Onwuka, N. D. (2007). Biogas production from blends of agro-industrial wastes. *Trends in Appl. Sci. Res.* 2, 554–558. doi: 10.3923/tasr.2007.554.558

Veeken, A., and Hamelers, B. (1999). Effect of temperature on hydrolysis rates of selected biowaste components. *Bioresour. Technol.* 69, 249–254. doi: 10.1016/S0960-8524(98)00188-6

Vivekanand, V., Mulat, D. G., Eijsink, V. G. H., and Horn, S. J. (2018). Synergistic effects of anaerobic co-digestion of whey, manure and fish ensilage. *Bioresour. Technol.* 249, 35–41. doi: 10.1016/j.biortech.2017.09.169

Vivekanand, V., Olsen, E. F., Eijsink, V. G., and Horn, S. J. (2013). Effect of different steam explosion conditions on methane potential and enzymatic saccharification of birch. *Bioresour. Technol.* 127, 343–349. doi: 10.1016/j.biortech.2012.09.118

Wang, Q., Hu, J., Shen, F., Mei, Z., Yang, G., Zhang, Y., et al. (2016). Pretreating wheat straw by the concentrated phosphoric acid plus hydrogen peroxide (PHP): investigations on pretreatment conditions and structure changes. *Bioresour. Technol.* 199, 245–257. doi: 10.1016/j.biortech.2015.07.112

Wang, S., Li, F., Zhang, P., Jin, S., Tao, X., Tang, X., et al. (2017). Ultrasound assisted alkaline pretreatment to enhance enzymatic saccharification of grass clipping. *Energy Convers. Manage.* 149, 409–415. doi: 10.1016/j.enconman.2017.07.042

Wang, X., Li, Z., Bai, X., Zhou, X., Cheng, S., Gao, R., et al. (2018). Study on improving anaerobic co-digestion of cow manure and corn straw by fruit and vegetable waste: methane production and microbial community in CSTR process. *Bioresour. Technol.* 249, 290–297. doi: 10.1016/j.biortech.2017.10.038

Xiong, Z. Y., Qin, Y. H., Ma, J. Y., Yang, L., Wu, Z. K., Wang, T. L., et al. (2017). Pretreatment of rice straw by ultrasound-assisted Fenton process. *Bioresour. Technol.* 227, 408–411. doi: 10.1016/j.biortech.2016.12.105

Yadav, M., Paritosh, K., Chawade, A., Pareek, N., and Vivekanand, V. (2018). Genetic engineering of energy crops to reduce recalcitrance and enhance biomass digestibility. *Agriculture* 8, 1–15. doi: 10.3390/agriculture8060076

Yadav, P., and Samadder, S. R. (2017). A global prospective of income distribution and its effect on life cycle assessment of municipal solid waste management: a review. *Environ. Sci. Pollut. Res.* 24, 9123–9141. doi: 10.1007/s11356-017-8441-7

Yay, A. S. E. (2015). Application of life cycle assessment (LCA) for municipal solid waste management: a case study of Sakarya. *J. Clean. Prod.* 94, 284–293. doi: 10.1016/j.jclepro.2015.01.089

Yong, Z., Dong, Y., Zhang, X., and Tan, T. (2015). Anaerobic co-digestion of food waste and straw for biogas production. *Renew. Energy* 78, 527–530. doi: 10.1016/j.renene.2015.01.033

Zeynali, R., Khojastehpour, M., and Ebrahimi-Nik, M. (2017). Effect of ultrasonic pre-treatment on biogas yield and specific energy in anaerobic digestion of fruit and vegetable wholesale market wastes. *Sustain. Environ. Res.* 27, 259–264. doi: 10.1016/j.serj.2017.07.001

Zhang, Q., Hu, J., and Lee, D. J. (2016). Biogas from anaerobic digestion processes: research updates. *Renew. Energy* 98, 108–119. doi: 10.1016/j.renene.2016.02.029

Zhen, G., Lu, X., Kobayashi, T., Kumar, G., and Xu, K. (2016). Anaerobic co-digestion on improving methane production from mixed microalgae

(Scenedesmus sp., Chlorella sp.) and food waste: kinetic modeling and synergistic impact evaluation. *Chemical Eng. J.* 299, 332–341. doi: 10.1016/j.cej.2016.04.118

Zhen, G., Lu, X., Kobayashi, T., Li, Y. Y., Xu, K., and Zhao, Y. (2015). Mesophilic anaerobic co-digestion of waste activated sludge and Egeria densa: performance assessment and kinetic analysis. *Applied Energy* 148, 78–86. doi: 10.1016/j.apenergy.2015.03.038

Zheng, Q., Zhou, T., Wang, Y., Cao, X., Wu, S., Zhao, M., et al. (2018). Pretreatment of wheat straw leads to structural changes and improved enzymatic hydrolysis. *Scientific Reports* 8:1321 doi: 10.1038/s41598-018-19517-5

Conflict of Interest Statement: The authors declare that the research was conducted in the absence of any commercial or financial relationships that could be construed as a potential conflict of interest.

frontiers in Energy Research

MINI REVIEW
published: 05 March 2019
doi: 10.3389/fenrg.2019.00019

Treatment of Sewage Sludge Using Anaerobic Digestion in Malaysia: Current State and Challenges

*Farida Hanum[1,2], Lee Chang Yuan[1], Hirotsugu Kamahara[3], Hamidi Abdul Aziz[4], Yoichi Atsuta[1], Takeshi Yamada[1] and Hiroyuki Daimon[1,3]**

[1] Department of Environmental and Life Sciences, Toyohashi University of Technology, Toyohashi, Japan, [2] Department of Chemical Engineering, Universitas Sumatera Utara, Medan, Indonesia, [3] Institute for Global Network Innovation in Technology Education, Toyohashi University of Technology, Toyohashi, Japan, [4] School of Civil Engineering, Universiti Sains Malaysia, Nibong Tebal, Malaysia

Anaerobic digestion is widely considered as an environmentally friendly technology for various organic waste including sewage sludge. Although the implementation of anaerobic digestion as an alternative treatment method for sewage sludge can be seen in many countries, its status in Malaysia is not clear. This study reviewed the current state of sewage sludge treatment in Malaysia and discussed the challenges to promote anaerobic digestion in sewage sludge treatment. Other than the common constraints faced, namely technical, political and economic, the characteristics of sewage sludge in Malaysia are considered to be a factor regarding feasibility. Anaerobic co-digestion is the simultaneous anaerobic digestion of two or more substrates which is a promising possible option to overcome the disadvantages of mono-digestion, and improve the economic viability due to higher methane production. There are a variety of biomasses as co-substrates in Malaysia. However, the anaerobic co-digestion of food waste and sewage sludge might be the most feasible method to overcome such constraints. Adding food waste as co-substrate is suggested as the possible approach to not only improve the process's performance but also help to handle the increasing volume of food waste in Malaysia. This study aims to highlight the potential as well as to provide a starting point for further studies regarding the treatment of sewage sludge using anaerobic digestion in Malaysia.

Keywords: sewage sludge, anaerobic digestion, co-digestion, food waste, Malaysia

OPEN ACCESS

Edited by:
Mohammad Rehan, King Abdulaziz University, Saudi Arabia

Reviewed by:
Muzammil Anjum, Pir Mehr Ali Shah Arid Agriculture University, Pakistan
Muhammad Waqas, Kohat University of Science and Technology, Pakistan

***Correspondence:**
Hiroyuki Daimon
daimon@ens.tut.ac.jp

Specialty section:
This article was submitted to Bioenergy and Biofuels, a section of the journal Frontiers in Energy Research

Received: *02 July 2018*
Accepted: *11 February 2019*
Published: *05 March 2019*

Citation:
Hanum F, Yuan LC, Kamahara H, Aziz HA, Atsuta Y, Yamada T and Daimon H (2019) Treatment of Sewage Sludge Using Anaerobic Digestion in Malaysia: Current State and Challenges. Front. Energy Res. 7:19. doi: 10.3389/fenrg.2019.00019

INTRODUCTION

Sewage sludge is the residue produced by a wastewater treatment process and has the largest volume amongst all the components removed during the process. In global terms, the amount of sludge is expected to increase. This is due to an increase in the percentage of households connected to central wastewater treatment plants (WWTPs), increasingly tightening regulations on effluent discharges, as well as improved technologies in achieving higher efficiency in wastewater treatment (Werther and Ogada, 1999; Appels et al., 2008). As the sludge itself may contain concentrated levels of contaminants that were initially included in the wastewater, the increasing sewage sludge has become a growing concern. Current primary disposal methods for sewage sludge are agricultural use, landfill, and incineration. Nevertheless, each technique has its particular issues which relate to public health as well as its environmental impacts (Fytili and Zabaniotou, 2008).

Anaerobic digestion is generally considered to be an economical and environmentally-friendly technology for treating various organic waste, including sewage sludge (Appels et al., 2011; Nasir et al., 2012). In the absence of oxygen, the organic waste is biologically degraded and converted into a form of biogas, and other energy-rich organic compounds as end products. The biogas, which is generally composed of 48–65% methane, could be used for power generation (Ward et al., 2008). Since the introduction of both commercial and pilot plant designs during the early 1990s, anaerobic digestion has gained worldwide attention (Karagiannidis and Perkoulidis, 2009). Throughout the world, more than 1,300 anaerobic digestion systems, based on sewage sludge, are in operation or under construction (IEA Bioenergy, 2001). Although China and India lead the initiative among developing countries, the thrust in of the developed world mainly comes from Western Europe (Abbasi et al., 2012). The biogas generation from anaerobic digestion in Europe has reached 4.5–5.0% growth annually, with Germany being the largest biogas producer (Bodík et al., 2011). It is notable that a high proportion of the biogas produced in anaerobic digestion plants is from those situated in WWTPs and thus anaerobic digestion has become a major and essential part in modern WWTPs. The current trend has also seen the introduction of anaerobic co-digestion, in which two or more substrates are mixed and digested simultaneously, with successful examples reported from WWTPs in Denmark, Germany, and Switzerland dedicated to combined sewage sludge and biowaste (Braun and Wellinger, 2009).

As a developing country, Malaysia is no exception from the global *trends* of the volume of sewage sludge increasing annually. It is reported that about 3 million metric tons of sewage sludge is produced annually in Malaysia, and is expected to increase to 7 million metric tons by 2020 (Indah Water Konsortium Sdn Bhd, 2010). Almost 50 % of the sewerage systems in Malaysia uses mechanized plants while others still use septic tanks and oxidation ponds. Some modern mechanized plants have been upgraded with anaerobic digesters whereby the sewage sludge are treated anaerobically to produce CH_4 which is a valuable energy source to generate electricity (Kumaran et al., 2016).

Malaysia is the third-largest consumer of energy in Southeast Asia. Petroleum, natural gas, and coal are the primary fuel sources consumed in Malaysia. In 2014, Malaysia consumed 43% of natural gas, 37% of petroleum and other liquids, 17% of coal, 2% of other renewable, and 1% of hydroelectricity (EIA, 2017). The growing consumption of energy has resulted in becoming increasingly dependent on fossil fuels such as coal, oil, and gas. Fossil fuel depletion and environmental issues have encouraged the government and researchers to investigate renewable energy as alternative sustainable energy resources (Hosseini and Wahid, 2013). Recently, bioenergy sources like animal and agricultural wastes, municipal solid waste and wastewater effluents as the renewable energy sources, have attracted attention and applied for preparing a fraction of the global energy demand (Petinrin and Shaaban, 2015).

The main objective of this study is to assess the potential of treating sewage sludge in Malaysia using anaerobic digestion. The current state regarding sewage sludge in Malaysia was reviewed, with activities around other regions included for comparison. Challenges and tasks faced when treating sewage sludge using anaerobic digestion in Malaysia were discussed, with anaerobic co-digestion which would include food waste, suggested as a possible approach. This study aims to provide a greater understanding as well as a starting point for further study regarding the future aspect of utilizing sewage sludge in Malaysia.

OVERVIEW OF SEWERAGE SYSTEM AND PRODUCTION OF SEWAGE SLUDGE IN MALAYSIA

Malaysia's sewerage industry has expanded over the last half of the twentieth century. At the end of the 1960s, the Malaysian government launched a series of 5-year plans to construct appropriate sanitation facilities in both urban and rural areas. At that time septic tanks were used as the primary sewerage system. In the 1970s, the government started the "National Sewerage Development Program" to develop sewerage facilities in major cities with the aim of introducing modern sewerage systems in urban areas. During the 1980s, the government introduced a policy that obliged housing developers to build sewerage systems for regions comprising more than 30 households of a 150 population equivalent (PE). This resulted in the diffusion of many small-scale wastewater treatment facilities all over the country, which were gradually connected to large-scale sewerage systems to complete the public sewerage system (Japan Sanitation Consortium, 2011). A profile of sewerage systems in Malaysia can be seen in **Table 1**. Although the large-scale sewerage systems, or public sewage treatment plants in Malaysia have increased in number, as seen from **Table 1**, the amount of operational individual septic tanks constitutes an enormous part of the overall wastewater treatment in Malaysia. This current situation could be a crucial factor in the attempt to utilize sewage sludge, as the septic tanks only provide partial treatment of the sewage that flows into it and needs to be desludged on a regular basis (Suruhanjaya Perkhidmatan Air Negara, 2017).

Under the Environmental Quality (Scheduled Waste) Regulations 2005, the Department of Environment (DOE) categorizes sludge generated from WWTPs as scheduled waste, and shall be disposed of under a prescribed premise only. Since 1994, the management of wastewater in most of the states of Peninsular Malaysia, is undertaken by a private company named Indah Water Konsortium (IWK) Sdn Bhd. According to a recent sustainable report by IWK, it has been operating and maintaining 16,328 km of sewer pipelines, 5,997 public sewerage treatment plants and 926 network pump stations. On average, IWK assumes control of 300 treatment facilities and 1,000 km of sewer network yearly (Indah Water Konsortium Sdn Bhd, 2013). It was estimated that the total cost of managing sewage sludge is US$ 0.33 billion per year (Kadir and Mohd, 1998). Currently, the sewage sludge is commonly being disposed of either at landfill sites or being burned in incinerators (Bradley

TABLE 1 | Profile of sewerage systems in Malaysia.

Sewerage facilities	2015		2016	
	Quantity	Population Equivalent (PE)	Quantity	Population Equivalent (PE)
Public sewage treatment plant (a + b)	6,571	23,517,185	6,752	24,789,450
a. Multipoint plant	6,481	16,296,052	6,659	16,964,923
b. Regional plant	90	7,221,133	93	7,824,527
Private sewage treatment plant	3,158	2,795,877	3,338	3,009,095
Communal septic tank	4,386	532,051	4,386	532,076
Individual septic tank	1,321,856	6,747,774	1,343,439	6,859,823
Traditional system	1,369,609	6,848,045	1,154,592	5,772,960
Network pumping station	1,078	n.a.	1,117	n.a.
Length of sewer network (km)	18,689	n.a.	18,689	n.a.

n.a., Data not available.

and Dhanagunan, 2004). However, as mentioned before, the sewage sludge itself may contain particular contaminants, and in case of incineration, approximately 30% of the solids remain as ash. Hence, these current disposal methods remain a concern (Malerius and Werther, 2003).

IWK had begun planning to reuse the sewage by-products, yet this mainly occurs only at local plants with a PE of 100,000 (Kadir and Mohd, 1998). There are very few wastewater treatment plants where digestion system could be found operating, and in most cases, the biogas produced is not utilized for power generation but only for combustion (Liew, 2008; Indah Water Konsortium Sdn Bhd, 2013). Bunus Centralized Sewage Treatment Plant (Kuala Lumpur) generates 2,500 m^3/days of biogas. From that amount of biogas, 15,000 kWh/m^3 of power without conversion losses could be produced. In fact, to date, all methane gas has been burned without effective use. As the average plant consumes electricity of 43,503 kWh/day (David et al., 2014), which is about 40% of the overall operations and maintenance costs (Baki et al., 2005), then the power generated through biogas from anaerobic digestion could be helpful in reducing total energy consumption, as well as serving as an alternative power generation source for public use. Recently, Malaysia has three modern WWTPs which are equipped with anaerobic digestion. There are the Pantai 2 WWTP in Greater Kuala Lumpur, the Jelutong WWTP in Pe18nang, and the Langat WWTP in Selangor. Pantai 2 and Jelutong WWTP are in operation, but at Langat is due to be completed in 2018. Pantai 2 WWTP has been designed to produce up to 9,600 m^3/day of biogas. Presently, in 2018, they produce around 450–500 KW electricity (Pantai 2 regional sewage treatment plant Kuala Lumpur)[1]. The Jelutong WWTP is one of the largest plants in Malaysia. It operates to treat 800,000 PE (Jelutong WWTP-Malaysia).[2]

Overall, not many investigations or studies have been conducted in Malaysia regarding the treatment of sewage sludge using anaerobic digestion, which reflects that the focus and awareness of these issues are indeed not high amongst the general public.

TREATMENT OF SEWAGE SLUDGE USING ANAEROBIC DIGESTION

Anaerobic digestion is a proven technology for sewage sludge treatment, in which the high water content sewage sludge can be processed without any pretreatment (Ward et al., 2008). The properties of sewage sludge are modified during anaerobic digestion, with not only biogas being produced as a result, but also several positive consequences for the sludge management that follows the process. Anaerobic digestion enhances the stabilization of sewage sludge, reduces pathogens and odor emission, and dry matter of sludge is reduced, which leads to a significant reduction in the final sludge volume. These benefits of anaerobic digestion of sewage sludge are widely recognized, and the technology is well established in many countries. The total biogas production in several countries and biogas production from WWTPs are listed in **Table 2** based on the statistics of the International Energy Agency (IEA Bioenergy Task 37, 2017) and the World Bioenergy Association (2017). Germany dominates the worldwide biogas production with 10,431 biogas plants generating 55,108 GWh/y of electricity. It has 1, 258 sewerage plants generating 3,517 GWh/y of electricity. Although India has 83,540 biogas plants, bioenergy production is still at a household mode and has been limited to small size biogas plants which are used by the people especially in rural areas. On the other hand, in Malaysia, IWK has taken over 4,281 small plants for upgrading to large plants by 2013. Overall IWK has 35 large plants (Indah Water Konsortium Sdn Bhd, 2013) which is 247 GWh/y electricity generated in 2017 (Sustainable Energy Development Authority Malaysia, 2018)[3].

Meanwhile, in Japan, policies such as SPIRIT21 (Sewage Project, Integrated and Revolutionary Technology for Twenty First Century) and Sewerage Vision 2100 have been implemented over the last decade regarding the improvement of WWTPs and utilization of sewage sludge. Led to the active movements on the usage of sewage sludge, which included energy recovery by anaerobic digestion. According to the Japan Sewage Works Agency, 280 out of 2,150 WWTPs have anaerobic digestion system operating, with 0.4–0.6 m^3 CH_4/kg-VS produced averagely (Japan Ministry of Land, Infrastructure, Transport and Tourism).[4] One of the most successful WWTPs has sewage sludge treated using anaerobic digestion and is located in Yamagata Prefecture. The daily biogas produced is 4,082 m^3, in which 7,226 kWh/d of electricity is generated. This corresponds to 48.7% of the total energy consumption of the plant itself (Li and Kobayashi, 2010).

[1] English brochure. Published by IWK.
[2] Available online at: http://sfcu.at/portfolio_category/asia/?lang=en
[3] Available online at: http://www.seda.gov.my/
[4] Available online at: http://www.mlit.go.jp/index_e.html

TABLE 2 | Biogas production in several countries.

Country	Year	Total biogas production (From agricultural residues, industrial wastewater, bio-waste, landfills and sewage sludge)		Biogas production in WWTPs (Only from sewage sludge)	
		Number of plants	[GWh/y]	Number of plants	[GWh/y]
Australia	2017	242	1,587	52	381
Austria	2017	291	3,489	39	18
Argentine	2016	62	n.a.	n.a.	n.a.
Belgium	2015	184	955	n.a.	n.a.
Brazil	2016	165	5,219	10	210
China	2014	11,500	90	2,630	n.a.
Czech Republic	2015	554	2,611	n.a.	n.a.
Denmark	2015	156	1,763	52	281
Finland	2015	88	623	16	152
France	2017	687	3,527	88	442
Germany	2016	10,431	55,108	1,258	3,517
India	2015	83,540	22,140	n.a.	n.a.
Ireland	2015	28	202	n.a.	n.a.
Italy	2015	1,491	8,212	n.a.	n.a.
Japan	2015	n.a.	30,200	2,200	n.a.
Norway	2017	39	738	24	223
Korea	2016	110	2,798	49	1,234
Pakistan	2015	4,000	n.a.	n.a.	n.a.
Poland	2015	277	906	n.a.	n.a.
Switzerland	2017	634	1,409	475	620
Spain	2015	39	982	n.a.	n.a.
Sweden	2017	279	1,200	139	n.a
Sri Lanka	2013	6,000	n.a.	n.a.	n.a.
Thailand	2014	n.a.	1,500	n.a.	n.a.
Netherlands	2015	268	3,011	80	541
United Kingdom	2016	987	26,457	162	950
United States	2017	2,100	1,030	1,240	n.a.
Malaysia	2017	n.a.	482	35	247

n.a., Data not available.

CHALLENGES TO UTILIZE SEWAGE SLUDGE USING ANAEROBIC DIGESTION IN MALAYSIA

Technical, Political and Economic Issues for Sewage Sludge Anaerobic Digestion

Several issues are surrounding the water services industry that needs the attention of policymakers and stakeholders to ensure the success of restructuring the water industry and achieving the goal of a sustainable water services industry in Malaysia. Anaerobic digestion is a complex system which involved several stages of biotransformation of organic matter, which are hydrolysis, acidogenesis, acetogenesis, and methanogenesis. Each of these steps has operational requirements, especially for methanogenesis, where methanogenic bacteria convert acetate into CH_4 and CO_2. In term of the technical aspect, improper operation of the anaerobic digestion will lead to low biogas yield. Sun et al. (2014) showed that increasing fat content in municipal solid waste (< 60%) could increase CH_4 yield significantly. The study also observed a decrease in CH_4 yield when the fat content is higher than 65% and displayed inhibitory effect on biogas production. There is still a lack of research and development effort in this aspect. Besides, the operation and maintenance of the anaerobic digestion plant will require skillful engineers and technicians, which could be lacking in Malaysia as anaerobic digestion is still not a common practice (Ali et al., 2012).

Climate change and depletion of fossil fuel along with the rise in petroleum prices have forced the Malaysian Government to rethink strategies to be more effective including the decision to embark on renewable energy resources as a better energy source amongst the global energy mix. The Malaysian Government established policies, renewable energy programs, and incentives more effective to promote and develop the use of renewable energy. In 2000, under the eight Malaysia Plan (MP), the Fifth Fuel Diversification Policy was launched, and Renewable Energy was included to be the fifth primary energy source, following oil, gas, coal, and hydropower. Following this, there has been continuous implementation of renewable energy-promoting policies and actions, such as the Small Renewable Energy Program, National Green Policy 2009, National Renewable Energy Plan 2010, Renewable Energy Act 2011, Feed-in Tariff (FiT) mechanisms, renewable energy business fund and Green Technology Financial Schemes under different Malaysia Plans (Bong et al., 2017). On the other hand, regarding social aspect, the public is generally not aware of anaerobic digestion plant and can be reluctant to have the anaerobic digestion plant near residential area and city area.

Characteristics of Sewage Sludge in Malaysia

Despite producing a massive amount of sewage sludge annually, the utilization of sewage sludge in Malaysia did not get as much attention or progress as seen in other regions. The current state of sewage sludge treatment sees it primarily being used for landfill. Several studies had reported using sewage sludge to produce clay bricks (Liew et al., 2004), compost (Kala et al., 2009), as well as fuels (Abbas et al., 2011). Nevertheless, there are very few focused on anaerobic digestion. One aspect that should be considered regarding anaerobic digestion is the characteristics of sewage sludge. Characterization of sewage sludge is essential for determining a suitable rate of application of sewage and for investigating pollutant risks that may be associated with the use of sewage sludge. Sewage sludge is characterized by high concentrations of solid and organic matter, with a significant presence of pathogens, nutrients, organic and inorganic pollutants. In an anaerobic digester, proper carbon to nitrogen (C/N) ratio is essential for efficient digestion (Kim et al., 2012). Characterization of sewage sludge from wastewater treatment plants in Malaysia can be seen in **Table 3** (Abbas et al., 2011). The C/N ratio of sewage sludge is 6. However, in general, the suggested optimum C/N ratio for anaerobic digestion is

in the range of 20–30 (Parkin and Owen, 1986), but the C/N ratio of sewage sludge is ranged between 6 and 16 typically (Tchobanoglous et al., 1993). Similar research also reported by Rosenani et al. (2008) in which they analyzed sewage sludge samples taken from 10 WWTPs throughout Peninsular Malaysia, showed that the C/N ratio of sewage sludge ranged from 4.1 to 38.0 with a mean of 16.6. As the fermentation substrate, this low C/N in sewage sludge, which goes against the nutrition balance of microorganisms. The pH of sewage sludge was reported as acidic, ranging from 3.57 to 6.43 because no lime was added in WWTPs. While the optimum pH of anaerobic digestion is in the range 6.5–7.5 (Liu et al., 2008).

Besides, the concentration of nutrients, such as nitrogen, phosphorus, iron, nickel, etc., it is crucial as the bacteria needs them for optimum growth. Although these elements are needed in low concentrations, the lack of these nutrients interferes microbial growth and performance. Methanogenic archaea have relatively high internal concentrations of iron, nickel, and cobalt, which are 1,800, 100, and 75 mg/kg, respectively (Rajeshwari et al., 2000). Rosenani et al. (2008) determined the mean of the heavy metal content (mg/L) of 10 selected sewage sludge samples taken from different wastewater plants in Malaysia and found that elements like potassium, magnesium, iron and nickel were at significantly lower levels than the suggested concentration. Therefore, precise design and a good understanding of the anaerobic digestion process would be necessary to apply the process based on the different characteristic of each WWTPs sewage sludge.

On the other hand, Baki et al. (2005) reported that 85% of the WWTPs are serving <5,000 PE. Therefore, the volumes generated from those small size treatment plants might be too small to be considered for power generation, and even if the sludge were to be collected to one centralized location, it would be uneconomical concerning logistics and transportation costs. Under such circumstance, studies based on the small-scale WWTPs seen in Germany could be used as a reference when adopting anaerobic digestion in small-scale WWTPs in Malaysia (Dichtl et al., 2013). Therefore, the results determined may indicate that the current state of sewage sludge currently would be considered as low feasibility if anaerobic digestion is applied. To cope with the challenges mentioned above, more detailed studies as well as a different approach are needed.

Anaerobic Co-digestion of Sewage Sludge

The complex microstructure components such as extracellular polymeric substances make sewage sludge difficult to hydrolyze and digest. These components have low volatile solid degradation (30–50%) even at a long retention time (20–30 day), caused low methane yield (Appels et al., 2008; Pereira et al., 2015). To accelerate the hydrolysis and enhance subsequent methane productivity, a variety of sewage sludge pretreatment options, such as mechanical, thermal, chemical, biological process or integration of these, have been developed at laboratory or pilot level recently (Kim et al., 2010; Houtmeyers et al., 2014; Kinnunen et al., 2015; Zhen et al., 2017). Although pretreatment can increase methane yield but leads to high energy demand and capital cost, complex operation, and maintenance, as an aspect of uneconomically feasible, caused most of them were still in the research stage and could not be utilized in real or commercial scale.

Anaerobic co-digestion is the simultaneous digestion of a homogenous mixture of two or more substrates. By combining two or more substrates or biomass resources, anaerobic co-digestion could improve the economic viability of anaerobic digestion plants due to higher methane production (Alvarez et al., 2000), and hence is a well-known and feasible option to overcome the drawbacks of a conventional digestion process. Co-digestion can improve the C/N ratio, enhance biogas production, overcome the nutrient imbalance of substrate, and improve the stable condition of anaerobic digestion (Kumaran et al., 2016). Anaerobic co-digestion of sewage sludge with biomasses resources which is a municipal solid waste, livestock manure, industrial waste, forestry, and agriculture waste can be used as co-substrate in anaerobic co-digestion. Recently, different organic waste materials such as food waste with higher content of organic carbon have been mixed with sewage sludge in anaerobic co-digester to improve C/N ratio which is leading to an increase in biogas production (Tanimu et al., 2014).

Anaerobic co-digestion between sewage sludge and the organic fraction of municipal solid waste (OFMSW) is the most reported co-digestion research (Alvarez et al., 2014). It was found that the cumulative biogas production from mixtures of sewage sludge and the OFMSW increased with increasing proportions of the OFMSW (Sosnowski et al., 2003). One study which evaluated the economic and environmental suitability of using OFMSW as co-substrate in two WWTPs had concluded that using OFMSW as co-substrate with sewage sludge was the most advantageous solution when compared to OFMSW composting and conventional digestion (Krupp et al., 2005).

The introduction of anaerobic co-digestion would be an advantageous approach to the current situation of OFMSW treatment in Malaysia as well. Nearly half of the Malaysian municipal waste is made up of food waste, and by 2020 the amount of municipal waste is estimated to increase to 9,820,000 tons in Peninsular Malaysia only (Tarmudi et al., 2009). Conventionally this municipal waste is disposed through landfill, but most of the landfill sites are mere open dumpsites where capacity has been exceeded. The high amount of food waste at landfill sites would lead to issues such as foul odor, toxic leachate and vermin infestation (Lee et al., 2007). There is currently no

TABLE 3 | Characteristics of sewage sludge in Malaysia.

Moisture content (%)	Volatile matter (%)	Fixed carbon (%)	Ash content (%)	C (%)	N (%)	C/N	H (%)	S (%)	Heating value (MJ/Kg)
12	48.86	19.32	31.86	33.01	5.52	6	4.97	1.18	15.7

clear strategy regarding the increasing food waste in Malaysia. Thus, the co-digestion of sewage sludge and food waste might be the most feasible breakthrough method for handling both biomass resources problems in Malaysia. In this case, WWTPs with low PE could be benefited by including food waste collected from the surrounding area. A well-organized system or structure that includes collection and separation of municipal solid waste would certainly lead to a more feasible anaerobic digestion process of sewage sludge.

CONCLUSIONS

This this study we reviewed the current state of sewage sludge treatment in Malaysia and discussed the challenges to promote anaerobic digestion in sewage sludge treatment. Currently, the sewage sludge produced from WWTPs is mostly disposed of through landfill and incineration. Although noteworthy movements can be seen in many regions including developing countries, where sewage sludge is utilized using anaerobic digestion for energy recovery as well as alternative to replace conventional methods, the focus on sewage sludge within Malaysia is not strong. The increasing volume of sewage sludge produced, corresponding with the growth of population, should not be treated lightly as the process itself consumes a lot of energy. Furthermore, the majority of WWTPs in Malaysia are operated on a small scale, and so the feasibility of anaerobic digestion, if applied, would be a challenge. Though various technical, political, and economic factors constrain anaerobic digestion of sewage sludge, the anaerobic co-digestion of food waste and sewage sludge might be the most feasibility method to overcome such constraints. It would not only improve the performance of anaerobic digestion when applied on sewage sludge but also simultaneously solve the problem of the increasing food waste in Malaysia. Nevertheless, considering the lack of information as well as the complexity of anaerobic digestion itself, more research, especially with some demonstration projects, are needed to verify the proper design, suitable conditions, and practical approach for the utilization of sewage sludge using anaerobic digestion in Malaysia.

Overall anaerobic digestion is a proven technique and at present applied in a variety of waste streams. To cope with the increasing energy demand, as well as to mitigate the environmental impacts as a result of the present situation, immediate but effective actions have to be taken, both by the government and the private sectors in Malaysia. Promotion and application of utilizing sewage sludge using anaerobic digestion could be not only one of the solutions to various environmental problems, but also a breakthrough in the field of waste recycling for Malaysia, where the accumulation of knowledge and understanding about anaerobic digestion could be shared and used for other biomass resources.

AUTHOR CONTRIBUTIONS

FH and LY carried out the literature review and wrote the initial draft. HA, YA, and TY revised the manuscript. HK and HD revised the manuscript and provided over-all guidance for work and editing of the text.

ACKNOWLEDGMENTS

We would like to acknowledge financial support from the Indonesian Endowment Fund for Education (LPDP), Ministry of Finance; and the Directorate General of Higher Education (DIKTI), Ministry of Research, Technology and Higher Education, Republic of Indonesia.

REFERENCES

Abbas, A. H., Ibrahim, A. B. A., Nor, M. F. M., and Aris, M. S. (2011). "Characterization of Malaysian domestic sewage sludge for conversion into fuels for energy recovery plants," in *National Postgraduate Conference (NPC)* (Kuala Lumpur), 19–20.

Abbasi, T., Tauseef, S. M., and Abbasi, S. A. (2012). Biogas energy. *Springer Briefs Environ. Sci.* 2, 11–23. doi: 10.1007/978-1-4614-1040-9

Ali, R., Daut, I., and Taib, S. (2012). A review on existing and future energy sources for electrical power generation in Malaysia. *Renew. Sustain. Energy Rev.* 16, 4047–4055. doi: 10.1016/j.rser.2012.03.003

Alvarez, J. M., Dosta, J., Güiza, M. S. R., Fonoll, X., Peces, M., and Astals, S. (2014). A critical review on anaerobic co-digestion achievements between 2010-2013. *Renew. Sustain. Energy Rev.* 36, 412–427. doi: 10.1016/j.rser.2014.04.039

Alvarez, J. M., Macé, S., and Llabrés, P. (2000). Anaerobic digestion of organic solid wastes. an overview of research achievements and perspectives. *Bioresour. Technol.* 74, 3–16. doi: 10.1016/S0960-8524(00)00023-7

Appels, l., Baeyens, J., Degrève J., and Dewil, R. (2008). Principles and potential of the anaerobic digestion of waste-activated sludge. *Prog. Energy Combust.* 34, 755–781. doi: 10.1016/j.pecs.2008.06.002

Appels, L., Joost, L., Degrève, J., Helsen, L., Lievens, B., Willems, K., et al. (2011). Anaerobic digestion in global bio-energy production: potential and research challenges. *Renew. Sustain. Energy Rev.* 15, 4295–4301. doi: 10.1016/j.rser.2011.07.121

Baki, A., Talib, S. A., Hamid, M. H. A., and Chin, K. B. (2005). "Energy from sewage sludge: potential application in Malaysia," in *Proceedings of 3rd Workshop on Regional Network Formation for Enhancing Research and Education on Green Energy Technologies*.

Bodík, I., Sedláèek, S., Kubaská, M., and Hutòan, M. (2011). Biogas production in municipal wastewater treatment plants-current status in EU with a focus on the Slovak Republic. *Chem. Biochem. Eng. Q.* 25, 335–340.

Bong, C. P. C., Ho, W. S., Hashim, H., Lim, J. S., Ho, C. S., Tan, W. S. P., et al. (2017). Review on the renewable energy and solid waste management policies towards biogas development in Malaysia. *Renew. Sustain. Energy Rev.* 70, 988–998. doi: 10.1016/j.rser.2016.12.004

Bradley, R. M., and Dhanagunan, G. R. (2004). Sewage sludge management in Malaysia. *Int. J. Water* 2, 267–283. doi: 10.1504/IJW.2004.005526

Braun, R., and Wellinger, A. (2009). *Potential of Co-Digestion*. Vienna: IEA Bioenergy.

David, H., Palanisamy, K., and Normanbhay, S. (2014). "Pre-treatment of sewage sludge to enhance biogas production to generate green energy for reduction of carbon footprint in sewage treatment plant (STP)," in *International Conference and Utility Exhibition 2014 on Green Energy for Sustainable Development* (Pattaya).

Dichtl, N., Dellbrügge, R. I., and Morcali, B. (2013). "Sludge Treatment in Germany More than 50 Years of Experience Current Discussions-Future Prospects," in *18th European Biosolids and Organic Resources Conference and Exhibition*.

EIA (2017). *Country Analysis Brief: Malaysia*. U.S. Energy Information Administration.

Fytili, D., and Zabaniotou, A. (2008). Utilization of sewage sludge in EU application of old and new methods - a review. *Renew. Sustain. Energy Rev*. 12, 116–140. doi: 10.1016/j.rser.2006.05.014

Hosseini, S. E., and Wahid, M. A. (2013). Feasibility study of biogas production and utilization as a source of renewable energy in Malaysia. *Renew. Sustain. Energy Rev*. 19, 454–462. doi: 10.1016/j.rser.2012.11.008

Houtmeyers, S., Degreve, J., Willems, K., Dewil, R., Appels, L. (2014). Comparing the influence of low power ultrasonic and microwave pre-treatments on the solubilisation and semi-continuous anaerobic digestion of waste activated sludge. *Bioresour. Technol.* 171, 44–49. doi: 10.1016/j.biortech.2014.08.029

IEA Bioenergy (2001). *Biogas and More! Systems and Markets Overview of Anaerobic Digestion*. Abingdon: AEA Technology Environment.

IEA Bioenergy Task 37 (2017). *Country Reports Summaries 2017*. Berlin: IWK.

Indah Water Konsortium Sdn Bhd (2010). *A Potty History of Sewage Sludge and it Treatment*. Indah Water Konsortium Sdn Bhd.

Indah Water Konsortium Sdn Bhd (2013). *Sustainability Report 2012-2013*. Kuala Lumpur: IWK.

Japan Sanitation Consortium (2011). *Country Sanitation Assessment in Malaysia Report*. Japan Sanitation Consortium.

Kadir, M. A., and Mohd, H. D. (1998). The management of municipal wastewater sludge in Malaysia. *Tropics* 28, 109–120.

Kala, D. R., Rosenani, A. B., Fauziah, C.I., and Thohirah, L. A. (2009). Composting oil palm wastes and sewage sludge for use in potting media of ornamental plants. *Malays. J. Soil Sci*. 13, 77–91.

Karagiannidis, A., and Perkoulidis, G. (2009). A multi-criteria ranking of different technologies for the anaerobic digestion for energy recovery of the organic fraction municipal solid wastes. *Bioresour. Technol*. 100, 2355–2360. doi: 10.1016/j.biortech.2008.11.033

Kim, D. H., Jeong, E., Oh, S. E., and Shin, H. S. (2010). Combined (alkaline+ultrasonic) pretreatment effect on sewage sludge disintegration. *Water Res*. 44, 3093–3400. doi: 10.1016/j.watres.2010.02.032

Kim, M., Yang, Y., Morikawa-Sakura, M. S., Wang, Q., Lee, M. V., Lee, D., et al. (2012). Hydrogen production by anaerobic co-digestion of rice straw and sewage sludge. *Int. J. Hydrogen Energy* 37, 3142–3149. doi: 10.1016/j.ijhydene.2011.10.116

Kinnunen, V., Outinen, Y. A., and Rintala, J. (2015). Mesophilic anaerobic digestion of pulp and paper industry biosludgeelong-term reactor performance and effects of thermal pretreatment. *Water Res*. 87, 105–111. doi: 10.1016/j.watres.2015.08.053

Krupp, M., Schubert, J., and Widmann, R. (2005). Feasibility study for co-digestion of sewage with OFMSW on two wastewater treatment plants in Germany. *Waste Manage*. 25, 393–399. doi: 10.1016/j.wasman.2005.02.009

Kumaran, P., Hephzibah, D., Sivasankari, R., Saifuddin, N., and Shamsuddin, A. H. (2016). A review on industrial scale anaerobic digestion system deployment in Malaysia: opportunities and challenges. *Renew. Sustain. Energy Rev*. 56, 929–940. doi: 10.1016/j.rser.2015.11.069

Lee, S. H., Choi, K. I., Osako, M., and Dong, J. I. (2007). Evaluation of environmental burdens caused by changes of food waste management in Seoul, Korea. *Sci. Total Environ*. 387, 117–120. doi: 10.1016/j.scitotenv.2007.06.037

Li, Y. Y., and Kobayashi, T. (2010). "Applications and new development of biogas technology in Japan," in *Environmental Anaerobic Technology: Applications and New Development*, ed H. H. P. Fang (World Scientific Publishing), 35–58. doi: 10.1142/9781848165434_0003

Liew, A. G., Idris, A., Samad, A. A., Wong, C. H. K., Jaafar, M. S., and Baki, A. M. (2004). Reusability of sewage sludge in clay bricks. *J. Mater. Cycles Waste Manag*. 6, 41–47. doi: 10.1007/s10163-003-0105-7

Liew, R. (2008). *Malaysia: Water and Wastewater Treatment*. Asia-Pacific Economy Cooperation 2008.

Liu, C. F., Yuan, X. Z., Zeng, G. M., Li, W., and Li, J. (2008). Prediction of methane yield at optimum pH for anaerobic digestion of organic fraction of municipal solid waste. *Bioresour. Technol*. 99, 882–888. doi: 10.1016/j.biortech.2007.01.013

Malerius, O., and Werther, J. (2003). Modelling the adsorption of mercury in the flue gas of sewage sludge incineration. *Chem. Eng. J*. 96, 197–205. doi: 10.1016/j.cej.2003.08.018

Nasir, I. M., Tinia, I. M. G., and Rozita, O. (2012). Production of biogas from solid organic wastes through anaerobic digestion: a review. *Appl. Microbiol. Biotechnol*. 95, 321–329. doi: 10.1007/s00253-012-4152-7

Parkin, G. F., and Owen, W. F. (1986). Fundamentals of anaerobic digestion of wastewater sludges. *J. Environ. Eng*. 112, 867–920. doi: 10.1061/(ASCE)0733-9372(1986)112:5(867)

Pereira, A. J. M., Elvira, P. S. I., Oneto, S. J. Cruz, D. L. R., Portela, J.R., and Nebot, E. (2015). Enhancement of methane production in mesophilic anaerobic digestion of secondary sewage sludge by advanced thermal hydrolysis pretreatment. *Water Res*. 71, 330–340. doi: 10.1016/j.watres.2014.12.027

Petinrin, J. O., and Shaaban, M. (2015). Renewable energy for continuous energy sustainability in Malaysia. *Renew. Sustain. Energy Rev*. 50, 967–981 doi: 10.1016/j.rser.2015.04.146

Rajeshwari, K.V., Balakrishnan, M., Kansal, A., Lata, K., and Kishore, V. V. N. (2000). State-of-the-art of anaerobic digestion technology for industrial wastewater treatment. *Renew. Sustain. Energy Rev*. 4, 135–156. doi: 10.1016/S1364-0321(99)00014-3

Rosenani, A. B., Kala, D. R., and Fauziah, C. I. (2008). Characterization of Malaysia sewage sludge and nitrogen mineralization in three soils treated with sewage sludge. *Malays. J. Soil Sci*. 12, 103–112.

Sosnowski, P., Wieczorek, A., and Ledakowicz, S. (2003). Anaerobic co-digesiton of sewage sludge and organic municipal solid wastes. *Adv. Environ. Res*. 7, 609–616. doi: 10.1016/S1093-0191(02)00049-7

Sun, Y., Wang, D., Yan, J., Qiao, W., Wang, W., and Zhu, T. (2014). Effects of lipid concentration on anaerobic co-digestion of municipal biomass wastes. *Waste Manag*. 34, 1025–1034. doi: 10.1016/j.wasman.2013.07.018

Suruhanjaya Perkhidmatan Air Negara (2017). *Sewerage Statistic, Malaysia*. Available online at: https://www.span.gov.my/

Tanimu, M. S., Tinia, I. M. G., Razif, M. H., and Idris, A. (2014). Effect of carbon to nitrogen ratio of food waste on biogas methane production in a batch mesophilic anaerobic digester. *Int. J. Innovat. Manage. Technol.* 5, 116–119. doi: 10.7763/IJIMT.2014.V5.497

Tarmudi, Z., Abdullah, M. L., and Tap, A. O. M. (2009). An overview of municipal solid waste generation in Malaysia. *Jurnal Teknologi* 51, 1–15. doi: 10.11113/jt.v51.142

Tchobanoglous, G., Theisen, H., and Vigil, S. (1993). *Integrated Solid Waste Management*. New York, NY: McGraw-Hill Inc.

Ward, A. J., Hobbs, P. J., Holliman, P. J., and Jones, D. L. (2008). Optimization of the anaerobic digestion of agricultural resources. *Bioresour. Technol*. 99, 7928–7940. doi: 10.1016/j.biortech.2008.02.044

Werther, J., and Ogada, T. (1999). Sewage sludge combustion. *Prog. Energy Comb.* 25, 55–116. doi: 10.1016/S0360-1285(98)00020-3

World Bioenergy Association (2017). *WBA Global Bioenergy Statistics (2017)*. Published by WBA.

Zhen, G., Lu, X., Kato, H., Zhao, Y., and Li, Y. Y. (2017). Overview of pretreatment strategies for enhancing sewage sludge disintegration and subsequent anaerobic digestion: current advances, full-scale application and future perspectives. *Renew. Sustain. Energy Rev*. 69, 559–577. doi: 10.1016/j.rser.2016.11.187

Conflict of Interest Statement: The authors declare that the research was conducted in the absence of any commercial or financial relationships that could be construed as a potential conflict of interest.

frontiers in Energy Research

ORIGINAL RESEARCH
published: 13 February 2019
doi: 10.3389/fenrg.2019.00007

Thermogravimetric Characteristics and Non-isothermal Kinetics of Macro-Algae With an Emphasis on the Possible Partial Gasification at Higher Temperatures

Imtiaz Ali and Ali Bahadar*

Department of Chemical and Materials Engineering, King Abdulaziz University, Rabigh, Saudi Arabia

Pyrolysis of *Turbinaria ornata* was realized in a thermogravimetric analyzer. The process was crudely classified into primary and secondary reaction zones. In the primary reaction zone, the thermal decompositions of the low-thermal stable components produced volatiles and biochar. The solid products obtained from the primary decomposition reactions contained inorganics with heavy metals. At mild-to-high temperatures, the catalytic effects accompanied gasification using oxygen, which was partially supplied by the oxygen carriers present in the solids and evolved gases. In order to study the pyrolytic conversion, combined, and multiple reaction schemes were employed. While the model-free methods helped to provide the accurate activation energies and the initial value of the pre-exponential factor, the non-linear regression optimized the chosen model parameters. In this study, a simple order-based model was compared with the versatile Šesták-Berggren (SB) model considering combined and multiple reactions. The application of a multiple reaction scheme to the primary and secondary reaction zones concluded that a simple order-based model suffices for the kinetic analysis. The secondary decomposition was shown to start with a high activation energy, which decreased appreciably when the conversion proceeded toward completion.

Keywords: *Turbinaria ornata*, seaweed, pyrolysis, pseudo-components, independent parallel reactions

OPEN ACCESS

Edited by:
Mohammad Rehan, King Abdulaziz University, Saudi Arabia

Reviewed by:
Meisam Tabatabaei, Agricultural Biotechnology Research Institute of Iran, Iran
Vivekanand Vivekanand, Malaviya National Institute of Technology, Jaipur, India

****Correspondence:***
Imtiaz Ali
imtiaz_che@hotmail.com

Specialty section:
This article was submitted to Bioenergy and Biofuels, a section of the journal Frontiers in Energy Research

Received: *19 October 2018*
Accepted: *18 January 2019*
Published: *13 February 2019*

Citation:
Ali I and Bahadar A (2019) Thermogravimetric Characteristics and Non-isothermal Kinetics of Macro-Algae With an Emphasis on the Possible Partial Gasification at Higher Temperatures. Front. Energy Res. 7:7. doi: 10.3389/fenrg.2019.00007

INTRODUCTION

The last few decades have seen an increase in the use of biofuels and high-value biochemicals derived from biomass. Biomass is a renewable carbonaceous source, an alternative to fossil fuel, and a precursor of biochemicals. Non-food biomasses are widespread in nature and are also cultivated at ∼100 billion tons annually (Sheldon, 2014). According to an estimate, biofuels are expected to satisfy around 10% of the global energy demand by 2035, and they have the potential to replace 27% of global transportation fuel by 2050. The main reason for the growing interest in the use of biomass, besides its renewable nature, is its carbon-neutral and less polluting characteristics. The Paris climate agreement requires clean energy transformation in order to reach net zero emissions by 2060, which can only be achieved by scaling-up efficient energy conversion systems to generate bio-energy with carbon capture and storage (BECCS) (Agency, 2017).

Marine macro-algae or seaweeds are efficient photosynthetic organisms. Besides their use in the food, pharmaceutical, and cosmetic industries, they are also well-known for their use in bio-sequestration and bioremediation, thereby mitigating climate change (Maceiras et al., 2011; Oliveira, 2016). There has been increased interest in macro-algae as a renewable and sustainable energy source over the past decade among the scientific and industrial communities because of its high biomass productivity (Baghel et al., 2017). Macro-algae biomass is mainly produced from the harvesting of wild stocks, a recent report of FAO reveals that a volume of around 12 million tons is produced annually (Ferdouse et al., 2018). Its cultivation is normally carried out through ocean farming and thus does not require land or fresh water, allowing these to be used for food crops and aquaculture. Macro-algae is a cheap source of carbon with a varying chemical composition depending on the type and the environmental conditions. It can be crudely classified into four main groups depending on the stored nutrients, pigments and chemical composition, namely red seaweeds (Rhodophyceae), green seaweeds (Chlorophyceae), brown seaweeds (Phaeophyceae), and blue-green seaweeds (Cyanophyceae) (Manivannan et al., 2009).

Seaweeds, like terrestrial forms of biomass, are lignocellulosic in nature with a complicated embedding of cellulose, hemicellulose, lignin, and intracellular substances. However, compared to terrestrial biomass, they may have higher costs attached to their cultivation in conjunction with the presence and effects of heavy metal concentrations in aquatic environments, while the removal of harmful contents (sulfur and nitrogen) from the resulting fuel (Ghadiryanfar et al., 2016) is another problem. Furthermore, some studies have revealed that the transesterification of oil extracted from macro-algae is restricted due to low lipid contents, and they have suggested the conversion of carbohydrates into biofuel but with a higher gas yield (Roesijadi et al., 2010; Hong et al., 2017). Therefore, the most suited conversion technologies, such as anaerobic digestion and hydrous pyrolysis (Ross et al., 2008), are likely to be employed for macro-algal biomass containing high levels of ash and alkali metals. Macro-algae are rich in macro and micronutrients, but also display an uptake of heavy metals from the environment. The heavy metals in macro-algae may indicate the fractions of industrial effluents affecting the aquatic ecosystems, which is also a serious concern. These accumulations depend upon their biochemical composition, specifically the properties of the cell wall (Davis et al., 2003) and the constituents present in the macro-algae cell walls. The cell wall contains the fibers and matrix of polysaccharides (alginates and fucoidan). The alginates in brown algae have a high accumulation of divalent cations, while sulfated polysaccharides exhibit a tendency toward trivalent cations (Saha and Orvig, 2010; Ortiz-Calderon et al., 2017). **Figure 1** presents the various major constituents of the seaweed cell wall.

The uptake of heavy metals takes place in macro-algae through bio-sorption or ion exchange processes by the chemical constituents present in the cell wall. The Red Sea, with its diverse ecosystem, has over 500 species of seaweeds, which are spread over 1,900 km covering 438,000 km^2 of coral reef

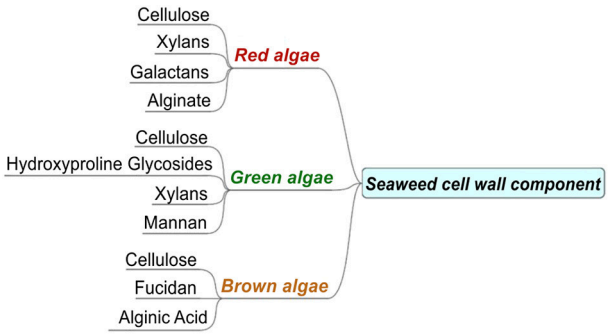

FIGURE 1 | Major chemical constituents of the seaweed cell wall, adapted from Bold and Wynne (1984).

stretching along its coasts and part of the Indian-Pacific Ocean (Spalding et al., 2001; Siddall et al., 2004; Bruckner et al., 2013). Red Sea seaweeds primarily consist of small green and brown algal filaments found in the northern and central parts, while the southern area of the Red Sea has large brown algal species like *Sargassum* and *Turbinaria* spp (Bruckner et al., 2013). *Turbinaria ornata* (*T. ornata*) is a well-known brown alga suitable for human consumption due to its antioxidant characteristics (Deepak et al., 2017a). Several studies have discussed its antibacterial, antioxidant, and anticancer properties (Omar et al., 2012; Ponnan et al., 2017; Stranska-Zachariasova et al., 2017; Tenorio-Rodriguez et al., 2017) as well as the biogenic synthesis of crystalline Ag/Au nanoparticles (Rajeshkumar et al., 2013; Kayalvizhi et al., 2014; Deepak et al., 2017b), but to the best of the authors' knowledge, no previous studies are available for its use as a source of biofuel. The mineral and heavy metal uptakes by different *Turbinaria* species are presented in **Table 1**.

Chemical looping pyrolysis gasification (CLPG) and chemical looping combustion (CLC) are proven concepts for syngas production and CO_2-capturing, respectively. The use of oxygen carriers such as the oxides of Ni, Mn, Cu, Fe, and Co have previously been investigated in these processes (Adanez et al., 2012; Huang et al., 2017). In the present study, the pyrolysis of *T. ornata* was realized in a thermogravimetric analyzer (TGA). The unique and novel concept of pyrolysis-gasification with the oxides of heavy metals already embedded in the matrix of polysaccharides of brown macro-algae (*T. ornata*) has also been considered besides the condensation of polymers at higher temperatures. The understanding of the role of inherent inorganic compounds of *T. ornata* and the investigation into evolved gases at high temperatures will lead to process optimization, efficient use, and the removal of heavy metals in the form of biochar.

MATERIALS AND METHODS

Macro-Algae Biomass

T. ornata is a brown alga that has phytochemical constituents like carbohydrates, proteins, flavonoids, alkaloids, and phenols as well as sulfated fucan-polymers like polysaccharide and alginate

TABLE 1 | Macro/micro mineral and heavy metal uptake by Turbinaria macroalgal species.

Macroalgae species	Micro/Macro minerals				Heavy metals								References
	K	Ca	Na	Mg	Fe	Zn	Mn	As	Cd	Cr	Hg	Ni	Pb	
Turbinaria ornata mg g^{-1} dw (mean ± SD)	112.2 ± 5.7	41.3 ± 1.2	19.3 ± 0.5	12.7 ± 0.5	0.891 ± 0.211	0.042 ± 0.007	0.015 ± 0.007	–	–	–	–	–	–	Zubia et al., 2005
	35.2 ± 0.7	29.40 ± 0.15	36.10 ± 0.16		0.49 ± 0.01	0.69 ± 0.01	0.58 ± 0.01	–	–	–	–	–	–	Mohamed Ali and Elnabawy Ward, 2016
Turbinaria. conoides mg g^{-1} dw (mean ± SD)	27.9 ± 1.1	14.8 ± 2.2	11.5 ± 0.5	5.7 ± 0.3	0.062 ± 0.017	0.006 ± 0.003	–	–	–	–	–	–	–	Santoso et al., 2006
Turbinaria triquetra (ppm)	–	–	–	–	–	–	–	7.79	0.06		4.65	0.55	0.89	El-Naggar and Al-Amoudi, 1989
Turbinaria triquetra (mg kg^{-1}, dry weight)	–	–	–	–	–	–	–	–	0.80 ± 0.3	0.10	6.2 ± 2.4	1.1 ± 0.2	3.1 ± 1.1	Abdallah et al., 2006
Turbinaria deccurens (ppb)	–	–	–	–	–	–	–	99.53	23.47	5.71	–	–	1.47	Roy et al., 2017
Turbinaria ornata (ppb)	–	–	–	–	–	–	–	129.37	3.07	2.04	–	–	1.92	Roy et al., 2017

structures that display tremendous potential for use in various applications. Its ability to bind heavy metals is of particular interest. Its biochar can also be used as a bio-indicator for identifying the type and quantity of heavy metals present in aquatic environments.

T. ornata was collected from the Red Sea coastal area (N22°48′32″, E38°56′37″). The fresh macro-algae was thoroughly washed to remove adherent dirt and sand with deionized water several times. The cleaned biomass was air-dried for 2 days, then crushed and sieved. A fine powder with a particle size of <0.147 mm (the fraction of the material passed through a 100 mesh sieve) was kept in an air-dried container for further use. **Table 2** shows the physicochemical properties of *T. ornata*.

Thermogravimetric Analysis

Pyrolysis is a promising process to convert biomass whereby the distribution of the product depends greatly on the conditions used. It has been reported that slow pyrolysis yields more biochar whereas fast pyrolysis produces more volatiles (Mohan et al., 2006). Extensive development in the pyrolysis process has been made recently and there has been a growing interest in its use because of its simplicity, flexibility, and efficiency. Biochar, a product of pyrolysis, finds in addition to volatiles potential application in the agricultural and environmental sectors. A thermogravimetric analyzer (TGA) is a commonly employed thermo-analytic instrument for the thermal degradation study of biomass. Under well-defined conditions of slow pyrolysis, it provides precise time and temperature-series mass loss data, which are used to estimate the kinetic parameters.

In the present study, the TGA experiments were performed on a Q5000 IR electro-balance analyzer (TA Instruments, USA). Approximately 15 mg of algal biomass sample was used for each run in triplicate to ensure accuracy and precision. The TGA temperature was raised from 50 to 900°C using different heating rates (5, 10, 15, and 30 °C·min^{-1}), while a flow of high purity N_2 gas was maintained at 70 ml min^{-1}. Additionally, an isothermal step was introduced before the heating ramp to achieve pyrolysis stabilization. The acquisition, diagnosis, and processing of curves were performed on Platinum™ software.

Kinetic Evaluation and Analysis

The devolatilization of algal biomass through pyrolysis is useful in understanding multi-component and multi-pyrolytic phases for process design, optimization, and scale-up (Ranzi et al., 2017).

TABLE 2 | Physicochemical properties of Turbinaria ornata.

Proximate analysis[a]		Ultimate analysis[b]	
Moisture	15.6%	C	30.38%
Volatile Matter	54.2%	H	6.03%
Ash	25.3%	N	0.89%
Fixed Carbon	4.9%		

[a] *ASTM standard methods (E1756, E1755-01, and D3174-12) were used except for fixed carbon, which was calculated from the difference.*

[b] *C, H, and N were measured with a CHN/O 2400 series II Perkin Elmer elemental analyzer.*

A global single-step reaction is always used in assessing the kinetic mechanism of pyrolysis. In a simplistic approach, the overall reaction process of *T. ornata* pyrolysis can be described with the following reaction:

$$\textit{Turbinaria ornata}\ (s) \rightarrow\ \textit{Volatiles}\ (g) +\ \textit{Biochar}\ (s) \qquad (1)$$

A non-isothermal TGA analysis technique is usually preferred over an isothermal technique for three main reasons. Firstly, the isothermal procedures are simply not possible to realize at higher temperatures because of the large non-isothermal heat-up and cool-down durations. Secondly, the estimation of the kinetic parameters at low heating rates is rather difficult due to weight loss during the heat-up time. Thirdly, there is the existence of the almost non-zero extent of conversions (Vyazovkin and Wight, 1998; Grigiante et al., 2016). For the aforementioned reasons, a non-isothermal technique was selected for this study. The process data recorded by TGA during non-isothermal pyrolysis can be expressed in terms of conversion (α) at any time (t) using the Arrhenius law [43]:

$$\frac{\mathrm{d}\alpha}{\mathrm{d}t} = \beta\frac{\mathrm{d}\alpha}{\mathrm{d}T} = A\cdot\exp\left(-\frac{E_a}{RT}\right)\cdot f(\alpha) \qquad (2)$$

where E_a ($\mathrm{J{\cdot}mol^{-1}}$) is the apparent activation energy, A ($\mathrm{s^{-1}}$) is the frequency factor, T is the absolute temperature, R is the ideal gas constant ($\mathrm{J{\cdot}mol^{-1}{\cdot}K^{-1}}$), β is the heating rate ($\mathrm{K{\cdot}s^{-1}}$), and $f(\alpha)$ represents the algebraic form of the reaction model. The conversion (α) is defined as the fractional mass loss expressed by the following equation:

$$\alpha = \frac{m_o - m_i}{m_o - m_f} \qquad (3)$$

where m_0, m_i, and m_f are the intial, instantaneous, and final mass, respectively.

Integrating Equation (1) with respect to conversion and temperature in the ranges $\alpha \in [0, \alpha]$ and $T \in [T_o, T]$ gives Equation (4):

$$g(\alpha) = \int_0^{\alpha}\frac{\mathrm{d}\alpha}{f(\alpha)} = \frac{A}{\beta}\int_{T_0}^{T}\exp\left(-\frac{E_a}{RT}\right)\mathrm{d}T \qquad (4)$$

Equation (4) can be used to describe the conversion when the temperature lag between the sample and its environment is very small. E_a is an important kinetic parameter, defined as the energy required to have a reaction, which is usually measured by model-free and model-fitting methods. Each method has its own advantages, and they are complementary and are not in competition. A model-free analysis can be performed without having specified the reaction mechanism, while the model-fitting analysis uses the approach of data-model best fitting to estimate E_a, A, and $f(\alpha)$ (Šesták and Berggren, 1971).

Model-Free Methods

Model-free kinetics methods are mostly isoconversional in nature. They provide an accurate estimation of E_a from isothermal and non-isothermal measurements and are most commonly employed in the pyrolytic kinetics of biomass (Opfermann et al., 2002). These methods have the capability to solve complex processes and are based on the fact that the reaction rate at a particular heating rate (β) is a function of temperature (T) alone at a specific conversion (α), while $f(\alpha)$ remains constant. Model-free methods provide a detailed kinetic analysis without knowledge of the reaction mechanism while indicating multiple processes if E_a varies strongly with α (Vyazovkin et al., 2011). Depending on the mathematical form of the kinetic equation, model-free methods can be differential or integral. The Friedman method (Friedman, 1964) is the most common differential while the Kissinger-Akahira-Sunose (KAS) method (Kissinger, 1957) is a widely used integral method. The Friedman method reveals the dependency of the conversion rate $\ln\left(\frac{d\alpha}{dt}\right)_{\alpha_i}$ over $1/T_{\alpha\mathrm{i}}$ as a straight line:

$$\textbf{Friedman}: \quad \ln\left(\frac{\mathrm{d}\alpha}{\mathrm{d}t}\right)_{\alpha_i} = \text{const} - \frac{E_\alpha}{R\cdot T_{\alpha_i}} \qquad (5)$$

The apparent activation energy (E_α) at a particular conversion (α) is estimated from the slope of the straight line. Integral methods are relatively less sensitive to data noise as compared to differential isoconversional methods and offer consistent E_α measurements. The KAS method is represented by the following linear Equation (6):

$$\textbf{KAS}: \qquad \ln\left(\frac{\beta_i}{T_{\alpha_i}^2}\right) = \text{const} - \frac{E_\alpha}{R\cdot T_{\alpha_i}} \qquad (6)$$

The slope of the linear fit of the $\ln\left(\frac{\beta_i}{T_{\alpha_i}^2}\right)$ vs. $1/T_{\alpha\mathrm{i}}$ is used to evaluate the apparent E_α.

Model-Fitting Methods

The model-fitting analysis is conventionally used for the pyrolytic assessment of biomass materials on the basis of their devolatilization weight loss measurements using 1st-order decomposition single-step reaction modeling or adding the weight of multiple pseudo-components like cellulose, hemicellulose, lignin, and others (Aboyade et al., 2012). The resulting characteristics from the kinetic analysis by model-fitting yield detailed simulations of biomass pyrolysis experiment data. Also, many studies have reported more precise simulations when using nth-order for specific reaction mechanisms where an optimization of the unknown constant is needed (Osman et al., 2017). Thus, in model-fitting procedures many models were applied to data collected from experiments to achieve the best fit to assess the kinetic parameters.

Combined Kinetics

The simple nth-order reaction has been used extensively to study the pyrolytic kinetics of biomass materials (Xu et al., 2017). The nth-order reaction mechanism for a solid state generally uses an

expression like $f(\alpha) = (1-\alpha)^n$, which when used in Equation (2) becomes:

$$\frac{\mathrm{d}\alpha}{\mathrm{d}t} = A \cdot \exp\left(-\frac{E_a}{RT}\right) \cdot (1-\alpha)^n \tag{7}$$

Another function is the Šesták—Berggren model (Šesták and Berggren, 1971), which was employed for the kinetic fitting of the experimental data. This is because of the high flexibility of the function to investigate the various types of physico-geometrical mechanism of the solid-state reaction (Kissinger, 1957; Opfermann et al., 2002; Vyazovkin et al., 2011; Aboyade et al., 2012), deviating cases with non-integral or fractal reaction geometry (Šimon, 2011; Dussan et al., 2017; Osman et al., 2017), the size distribution of the reactant particles (Orfão et al., 1999), and so on (Zubia et al., 2005). The high flexibility makes it difficult to interpret the physicochemical meanings of the kinetic exponent, but the SB model with the three parameters indicates the highest performance as a fitting function.

$$\mathbf{SB}: \qquad f(\alpha) = \alpha^m.(1-\alpha)^n \cdot \left[-\ln(1-\alpha)\right]^p \tag{8}$$

The SB model with three fit parameters (m, n, and p) is considered as one of the highest performing model-fitting methods, where m is accelerating behavior, n represents the order of the reaction and p shows the nuclei growth. By incorporating the SB model, Equation (7) becomes:

$$\frac{\mathrm{d}\alpha}{\mathrm{d}t} = A \cdot \exp\left(-\frac{E_a}{RT}\right) \cdot (1-\alpha)^n \cdot \alpha^m \cdot \left[-\ln(1-\alpha)\right]^p \tag{9}$$

The SB (m, n, p), for specific reaction model functions and other parameters like E_a and A can be optimized by employing a non-linear least square analysis, whereby the residual sum of squares, also known as the sum of squared errors (SSE), is minimized by fitting the data curve of $\left.\frac{d\alpha}{dt}\right|_{exp}$ from the predicted curve of $\left.\frac{d\alpha}{dt}\right|_{pred}$ against time.

$$SSE = \sum\left(\left.\frac{\mathrm{d}\alpha}{\mathrm{d}t}\right|_{exp} - \left.\frac{\mathrm{d}\alpha}{\mathrm{d}t}\right|_{pred}\right)^2 \tag{10}$$

A non-linear least square analysis always requires the initial values for SB (m, n, p), E_a and A for optimization. After fitting the data, the goodness of the fit was measured by *Fit* (%), as in Equation (11).

$$Fit\ (\%) = \left[1 - \frac{\sqrt{SSE}}{\left(\left.\frac{\mathrm{d}\alpha}{\mathrm{d}t}\right|_{exp}\right)_M}\right] \times 100 \tag{11}$$

where $\left(\left.\frac{d\alpha}{dt}\right|_{exp}\right)_M$ is the peak-maximum conversion rate.

Independent-Parallel Reactions

Independent reaction models are mainly employed to identify the roles of the components in the thermal decomposition process. Biomass consists of many components and each component behaves differently. Therefore, these models have a set of discrete multiple reactions and may be extended to continuous distribution, which is largely employed to study the degradation kinetics of lignocellulosic materials. It is commonly accepted that each pseudo-constituent degrades independently at a particular temperature range. The weight loss calculations are performed by taking the sum of the mass fractions from the individual pseudo-components' decomposition rates (Orfão et al., 1999). The polysaccharides of *T. ornata* are mainly hemicellulose, cellulose, and others. The proximate composition of different *Turbinaria* species is given in **Table 3** below.

T. ornata contains many components and each component can be divided into subcomponents. During decomposition, the components which degrade during a similar temperature range may be grouped together and termed as pseudo-component. Lignocellulosic materials are normally classified into three pseudo-components, whereby each pseudo-component is involved in an independent reaction (Orfão et al., 1999). Similarly, the pyrolysis of *T. ornata* can be presented in terms of three pseudo-independent components, as given in Equation (12).

$$\left.\begin{array}{ll} Pseudo-Hemicellulose & \xrightarrow{\frac{\mathrm{d}\alpha_1}{\mathrm{d}t}} \\ Pseudo-Cellulose & \xrightarrow{\frac{\mathrm{d}\alpha_2}{\mathrm{d}t}} \\ Others & \xrightarrow{\frac{\mathrm{d}\alpha_3}{\mathrm{d}t}} \end{array}\right\} Volatiles1 + Biochar1 \tag{12}$$

During the main stage of the pyrolysis process, the pseudo-components are subjected to the thermal splitting of chemical

TABLE 3 | Proximate composition of various Turbinaria species.

Composition	Ash	Total fiber	Crude lipid	Crude protein	Fat	Moisture	References
Turbinaria ornata % dw (mean ± SD)	39.8 ± 0.8	38.1±1.5	2.2 ± 1.1	9.2 ± 0.6	–	10.8 ± 3.9	Behairy and El-Sayed, 1983
Turbinaria conoides % dw (mean ± SD)	2.5 ± 0.1	9.5 ± 0.5	–	1.0 ± 0.1	0.8 ± 0.1	85.1 ± 0.3	Mohammadi et al., 2013
Turbinaria murrayana % dw	17.04	40.06	1.46	19.51	–	–	Santoso et al., 2006
Turbinaria triquetra % dw (mean ± SD)	29.573 ± 0.007	48.3 ± 0.007	1.62 ± 0.003	4.133 ± 0.009	–	23.62 ± 0.42	Zubia et al., 2005

bonds for the production of primary *Volatiles1*, gases (e.g., CH_4, CO_2, and CO), and condensates and yield biochar solids at <500°C, named as *Biochar1*. Biochar contains minerals and even trace elements which were present in parent biomass. The pyrolytic conversion of three pseudo-components (i.e., pseudo-hemicellulose, pseudo-cellulose, and others) mainly depends on the temperature, particle size, and reactor type. The decomposition of hemicellulose and cellulose usually occurs between 470 to 530 K and 510 to 620 K, respectively, while others like lignin degrade at 550–770 K (Wang et al., 2017). The decomposition of cellulosic materials is mainly induced by depolymerization reactions forming oligosaccharides an then levoglucosan, which is finally decomposed into smaller molecules (Patwardhan et al., 2011). Similarly, the hemicellulose pyrolysis is initiated by the depolymerization of polysaccharides into oligosaccharides and, subsequently, leads to the rearrangement of the molecules, producing 1,4-Anhydro-D-xylopyranose, which further disintegrates into smaller molecular weight components.

At high temperature, secondary decomposition leads to the formation of secondary volatiles (*Volatiles2*) and biochar (*Biochar2*). This may include cracking, reforming, condensation, polymerization, oxidation, and gasification (Di Blasi, 2008). During the secondary reactions, *Biochar1* forms *Volatiles2* and *Biochar2*, as presented in Equation (13).

$$Biochar1 \xrightarrow{\frac{d\alpha_4}{dt}} Volatiles2 + Biochar2 \tag{13}$$

Likewise, the inorganic compounds are also greatly affected during pyrolysis. These inorganic compounds, including heavy metals, may be accumulated in the cell wall and bind ionically and covalently to polysaccharides, which can initiate autocatalytic pyrolysis (Keown et al., 2005). Here, a concept of the partial gasification of *T. ornata* polluted with heavy metals from the Red Sea is presented in **Figure 2**.

These inorganic compounds may include macro/micro minerals (e.g., K, Ca, Na, Mg, Fe, Zn, and Mn) and heavy metals (e.g., Ag, Al, As, Cd, Cr, Co, Hg, Mo, Ni, Pb, and Ti). The pyrolysis process has been previously employed for processing these minerals and heavy metals for valuable products like biochar and bio-oil. For example, alkali and alkaline earth metals (such as K, Ca, and Mg) have notable catalytic effects on the pyrolytic conversion. Vaporization of K has been shown to take place at lower temperatures, while Ca and Mg vaporize at higher temperatures depending on their ionic or covalent bonding with organic molecules (Wei et al., 2012). Liu et al. (2017) reviewed biomass pyrolysis in the presence of inorganic elements including heavy metals and contributed a critical analysis for optimizing the pyrolytic mechanisms with productive resource utilization and a reduction in pyrolysis-based pollutants. Liu et al. (2017) also found that the prior literature has exhibited the enrichment of heavy metals in the solid biochar phase rather than being released into the volatile (gaseous/liquid) phase, and that there is no need to focus on the release of heavy metals in later research. Also, Ni and Cu have been previously used to enhance the quality of pyrolysis products (Richardson et al., 2013; Zhao et al., 2015). Hence, there is an urgent need to investigate the mechanisms for the use of inherited available inorganics and heavy metals to improve the processes and products (Liu et al., 2017). **Table 4** presents a few studies on biomass pyrolysis containing salts of heavy metals.

The summation of the rate equations in Equation (14) gives the overall degradation rate.

$$\frac{d\alpha}{dt} = \sum_{j=1}^{4} \frac{d\alpha_j}{dt} = \sum_{j=1}^{4} x_j \cdot A_j \cdot \exp\left(-\frac{E_{aj}}{RT}\right) \cdot f(\alpha) \tag{14}$$

The separation of the pseudo-component peaks was carried out assuming an asymmetric Fraser–Suzuki (FS) distribution with the following function (Perejón et al., 2011):

$$\frac{d\alpha_j}{dt} = a_0 exp\left[-ln2\left\{\frac{ln\left(1+2a_1\frac{T-T_m}{HW}\right)}{a_1}\right\}^2\right] \tag{15}$$

where a_0 is the amplitude, a_1 is the asymmetry, T_m is the peak maximum temperature and *HW* is the half width of the peak.

Initial values of kinetic parameters were obtained from model-free methods applied to the separated pseudo-components. The optimization of the kinetic parameters was performed by non-linear least square fitting using Equation (10).

RESULTS AND DISCUSSIONS

Thermal Behavior and Reactivity Analysis

Figure 3 shows the TG and DTG profiling of *T. ornata* against temperature at different heating rates. *T. ornata* biomass was pyrolyzed to 850°C at different heating rates. The DTG curves feature two prominent zones, as illustrated in **Figure 3B**: A primary pyrolysis zone and a secondary reaction zone. In the primary pyrolysis zone, more than 90% of the total amount of mass loss was observed, resulting from reactions such as depolymerization, decarboxylation, and cracking. The maximum mass loss rates increased from 0.043 to 0.290%·s^{-1} with an incremental increase in the heating rates of 5 to 30°C·min^{-1}. Secondary reaction zones (Zone II), initiated at 875 K, and the remaining mass was decomposed at a slower rate. This slow rate is caused by the trapped volatile matter present in the biochar and delays the decomposition (Richardson et al., 2013). The most common characteristic of all the DTG and TG curves is the increase in the conversion rate and the shifting of the peaks toward the higher temperatures when the heating rates are increased. This increase in conversion rates may be ascribed to the improved transport phenomenon. Meanwhile, the shifting of peaks is rendered to the slowing down of the pyrolysis process owing to the difficulty in the heat transfer from the surrounding to the sample for a shorter time and larger thermal lag (Shuping et al., 2010; Han et al., 2017; Özsin and Pütün, 2017). It can also be perceived from the DTG curves that the peaks in the secondary reaction zone (900–1,100 K) may be caused by the catalytic effect and gasification of the biochar due to the presence of inorganic oxides.

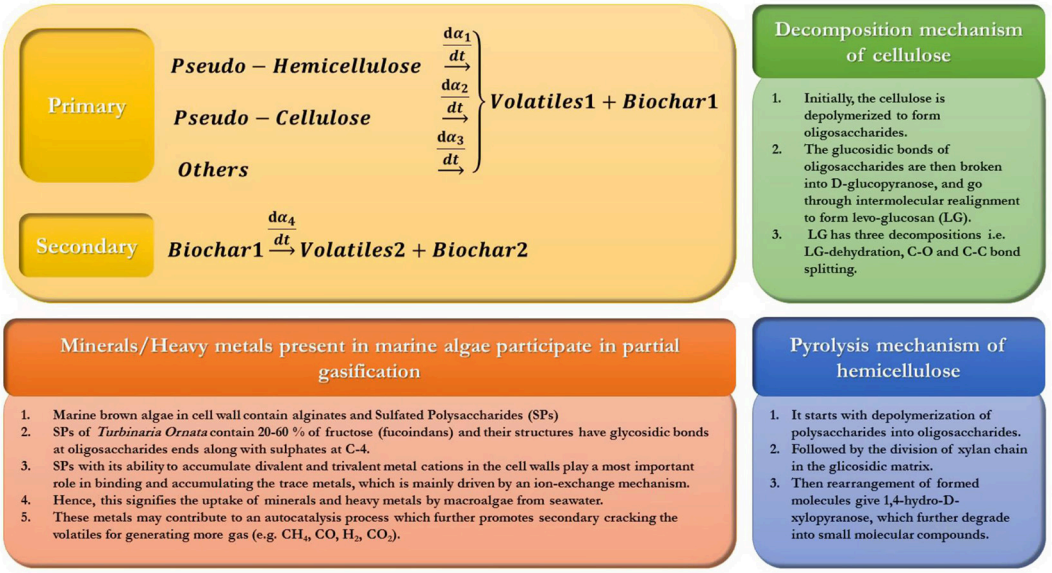

FIGURE 2 | Primary and secondary reactions during pyrolysis of Turbinaria ornata.

Isoconversional Methods

The pyrolytic characteristics were measured using the two isoconversional methods Friedman and KAS. **Figure 4** establishes the Arrhenius plot using Equations (5, 6) at different conversions. The data were fitted using linear regression lines for both differential and integral isoconversional methods at the progressive increase of conversion from 10 to 90% with a step size of 5%, as depicted in **Figure 4**.

The apparent activation energy E_a was measured from the slope of the straight lines from the plots. The quality of the regression models was estimated by the coefficient of determination (R^2), which strengthens our confidence in the estimation of E_a from the observed data. The mean apparent activation energy E_α, calculated from the Friedman and KAS isoconversional models, are 164.03 and 146.41 kJ·mol^{-1}, respectively.

Model-Fitting Methods

Model-fitting methods have two stages, namely (a) the estimation of the initial parameters and (b) the application of iterative routines to obtain the optimized values of the kinetic parameters.

Combined Kinetics

The average activation energies (E_a) obtained from the isoconversional methods (both differential and integral) were used to obtain the order-based and SB model parameters by optimizing Equations (7, 9) using MS Excel Solver. The differential best-fit curves of *T. ornata* with optimized order-based and SB model parameters at different heating rates (5, 10, 15, and 30°C·min^{-1}) are shown in **Figure 5**. It is worth noting here that this displays the fitting of the data to order-based and SB models through a single reaction. Moreover, a single heating rate may render inaccuracies; therefore, the mean values calculated at different heating rates are presented in **Table 5**.

The SB model is a powerful tool that allows the measurement of complex degradation mechanisms (Gámiz-González et al., 2017). As is evident from **Table 5** and has been previously found as well, one of the SB model parameters is numerically absent (Šesták and Berggren, 1971; Ali et al., 2018). In the present study for all heating rates, parameter m, which corresponds to the deceleration mechanism, was not involved and hence the pyrolysis of macro-algae (*T. ornata*) was most probably driven by random nucleation and growth (Wang et al., 2006; Li et al., 2010; Ye et al., 2010). **Table 5** shows a Fit% higher for the SB model, which indicates that the SB model can better explain thermal degradation than the order-based model. Thus, the parameters obtained from the SB model can better represent the pyrolysis mechanism. The average values of A obtained from the Friedman method were 6.4×10^{13} and 1.3×10^{14}, while for the KAS method these were 1.0×10^{12} and 2.3×10^{12} for the order-based and SB models, respectively. The values of n for the order-based and SB models were 7.47 and 8.08 for the Friedman method and 6.76 and 7.44 for the KAS method, respectively. The high value of n in the SB model with a higher Fit% (>92) highlights the roles of order-based, diffusion and geometrical contraction in *T. ornata* pyrolysis. The order-based mechanism can be attributed to the nucleation process in a solid state reaction where the nucleus growth is induced by nuclei collisions with each other (Poletto et al., 2012). The optimum p-values (0.40 and 0.43) signify that the degradation process is partially controlled by the random nucleation mechanism, which randomly promotes the generation of activation centers. It is highly likely that the presence of oxygen carriers (gases and inorganic salts containing heavy metals) could initiate partial gasification (Huang et al., 2013) and catalyze *T. ornata* pyrolysis. This would increase the

TABLE 4 | Influence of heavy metals present in biomass during pyrolysis.

Heavy metal polluted biomass	Heavy metal	Pyrolysis performance	Major findings	References
Fir sawdust	Cu	1) Increase in bio-oil yields 2) Decreased in the oxygen contents in bio-oil 3) Significant increase in HHV 4) Cu-FSD derived bio-oil have higher HHV of 13.42–14.79 MJ kg^{-1} as compared to HHV of FSD which range between 10.77 and 12.32 MJ kg^{-1} 5) Increase in biochar yields 6) Lower gas yields	The increase in yields of bio-oil and biochar attributes toward catalytic effects of Cu. The decrease in gas yields may be an indication of 1) More gas composition reactions like H_2 with lignin in the presence of Cu to form phenols 2) Cu may promote the production of aromatics to increase bio-oil yield than gas yield. A significant quantity of C7–C10 was formed because of the catalytic effect of Cu on breaking down lignin-chains.	Liu et al., 2012
Typha angustifolia	Pb	1) More than 98% Pb was distributed in biochar phase while only traces of Pb were present in bio-oil. 2) Decrease in biochar yield from 46.5 to 33.0 % whereas the gas yield increase with increase in temperature from 673 to 873 K	The quick decline in biochar yield with the elevation of temperature may be due to cracking of the volatiles, which shows improved decomposition of biomass. An economic analysis renders leaching methods to be expensive compared to pyrolysis. This shows bio-oil produced can be used for various applications without secondary pollution.	Liu et al., 2011
Wood	Ni	1) At below 500°C, the *in situ* Ni nanoparticles (Ni°NPs) were produced during pyrolysis which offers active sites to enhance the catalytic effect on biomass pyrolysis by adsorbing the aromatics. 2) Biochar supported NiNPs was produced, which was later used in secondary reactions as a catalyst to improve tar conversions and hydrogen production.	The catalytic effect for both *in-situ* Ni°NPs and synthesized Ni°NPs on secondary reactions were studied. Results of *in-situ* Ni°NPs pyrolysis, synthesized Ni°NPs, and catalyst-free wood pyrolysis was evaluated. The *in situ* Ni°NPs catalyst featured high production of aromatics than synthesized one. There was a clear difference in the performance of the pyrolysis when using the *in-situ* metal species present in the wood biomass because of their catalytic effect	Richardson et al., 2013
Arundo donax and *Broussonetia papyrifera*	Cd, Cu, Pb	1) Activation Energy (E_a) was calculated for both the biomasses having heavy metal salts. The E_a tends to decrease when pyrolysis was performed with these polluted biomasses. This may be because of the catalytic effect of these heavy metals. 2) Increase in bio-oil yields. The volatile metals increased when having these meals salts, from 55.13 to 59.81% for *Arundo donax* and from 44.62 to 52.12 % for *Broussonetia papyrifera*.	Cd, Cu, and Pd promoted the pyrolysis process by decreasing the activation energies of the biomasses. These metals could assist in producing more volatiles both in liquid and gas phase	Han et al., 2017

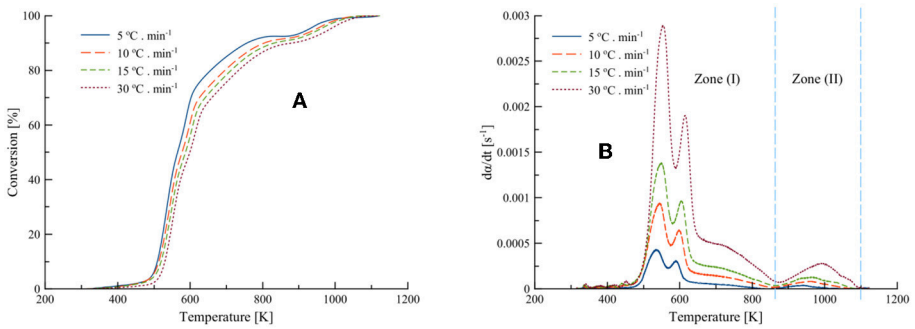

FIGURE 3 | (A) Conversion and **(B)** DTG curves of Turbinaria ornata at 5, 10, 15, and 30°C min^{-1}.

weight loss rate and increase the gases produced (like CH_4, H_2, and CO_2) from the pyrolysis of *T. ornata* and could remove lattice oxygen from the oxygen carriers. Depending upon the amount of inorganics accumulated by the marine algae *T. ornata*, the catalytic characteristics of heavy metals stimulating pyrolysis and partial gasification could vary.

Independent-Parallel Reactions

From the DTG curves of samples in **Figure 3B**, it is indicated that the degradation process is taking place in a multiple reaction scheme since the peaks are overlapping in the close temperature range. The thermal decomposition of hemicellulose in *T. ornata* biomass started at about 473 K, followed by a

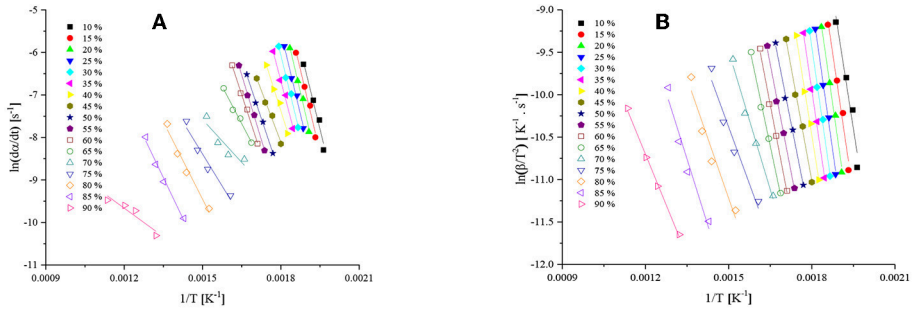

FIGURE 4 | (A) Friedman and **(B)** KAS graphs at the different extent of conversions.

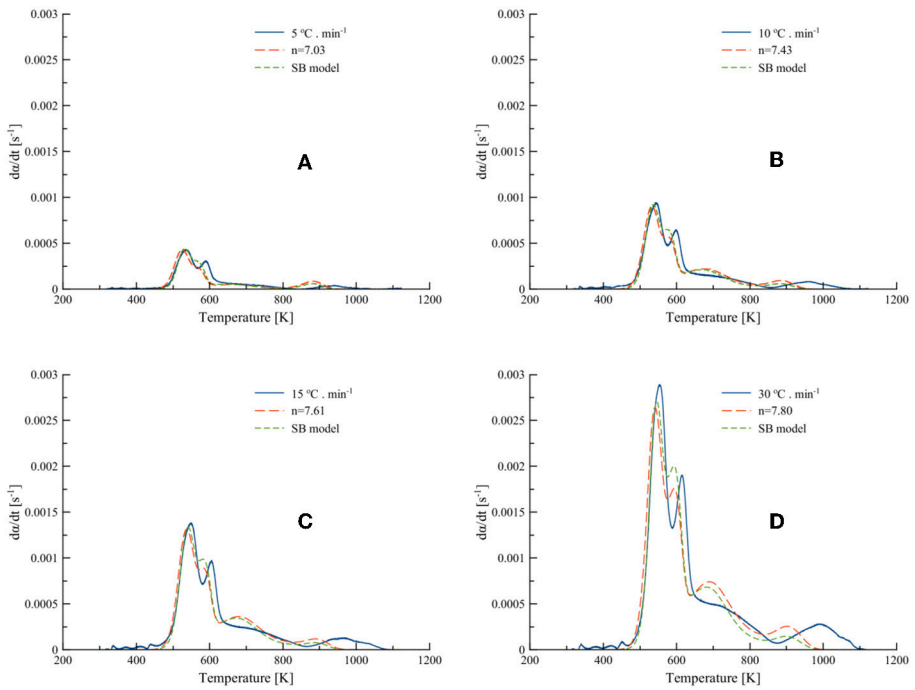

FIGURE 5 | Best-fit DTG curves of Turbinaria ornata with optimized order-based and SB model parameters at **(A)** 5, **(B)** 10, **(C)** 15, and **(D)** 30°C·min^{-1}.

major mass loss between 550 and 660 K and tailing up to 900 K; then there was a slight shoulder followed by a tail in the temperature range 880–1100 K, which could have induced the partial gasification mechanism using inherited minerals. Most of the mass loss occurs in Zone (I), as shown in **Figure 3B**, which takes the shape of a shoulder with overlapping peaks, which corresponds to hemicellulose and cellulosic material, followed by the contribution of other components with an interplay of the inherited minerals present in *T. ornata* collected from the Red Sea. The shoulder and tailing in Zone (II) may correspond to the decomposition of inorganics and could proceed further to a partial gasification process. Hence, it is necessary to apply three parallel-reaction models for the primary reactions in Zone (I) pertaining to the decomposition of pseudo-hemicellulose, pseudo-cellulose and pseudo-others. Overall, the DTG curves at 5, 10, 15, and 30°C·min^{-1} were decomposed into three primary and one secondary decomposition reactions by employing asymmetric Fraser-Suzuki (FS) distributions, as presented in **Figure 6**. Recent studies show have shown that the application of the FS function suits the thermal degradation of a solid state reaction into its individual processes (Millán et al., 2017). The mass loss contributions (x_j) of separated peaks obtained from **Figure 6** are presented in **Table 6**.

The average relative mass loss contribution (x_j) for pseudo-hemicellulose, pseudo-cellulose, pseudo-others, and biochar at 5, 10, 15, and 30°C·min^{-1} was 40.5, 13.0, 38.5, and 8.0%, respectively. It can also be seen from **Figure 5** that the degradation rates of pseudo-components increase with

TABLE 5 | Optimized order-based and SB model parameters at different heating rates with isoconversional methods.

β [°C·min^{-1}]		Order				*SB*					
		n **[–]**	***A*** **[s^{-1}]**	***SSE*** **[s^{-2}]**	**Fit [%]**	***A*** **[s^{-1}]**	***m*** **[–]**	***n*** **[–]**	***p*** **[–]**	***SSE*** **[s^{-2}]**	**Fit [%]**
Differential	5	7.03	4.6×10^{13}	1.6×10^{-5}	90.46	1.2×10^{14}	0	7.72	0.55	1.0×10^{-5}	92.60
	10	7.43	6.7×10^{13}	2.3×10^{-5}	92.47	1.3×10^{14}	0	8.00	0.36	1.7×10^{-5}	93.50
	15	7.61	6.8×10^{13}	3.2×10^{-5}	92.46	1.2×10^{14}	0	8.13	0.31	2.6×10^{-5}	93.29
	30	7.80	7.7×10^{13}	8.6×10^{-5}	91.28	1.6×10^{14}	0	8.34	0.36	6.4×10^{-5}	92.62
	Average (± SE)	7.47 (± 0.16)	6.4×10^{13} ($\pm 0.7 \times 10^{13}$)	–	–	1.3×10^{14} ($\pm 0.1 \times 10^{14}$)	0	8.08 (± 0.13)	0.40 (± 0.05)	–	–
Integral	5	6.35	6.7×10^{11}	1.6×10^{-5}	90.35	1.7×10^{12}	0	7.07	0.55	9.1×10^{-6}	92.93
	10	6.73	1.0×10^{12}	2.3×10^{-5}	92.19	2.2×10^{12}	0	7.38	0.41	1.6×10^{-5}	93.65
	15	6.89	1.1×10^{12}	3.3×10^{-5}	92.16	2.1×10^{12}	0	7.36	0.36	2.5×10^{-5}	93.41
	30	7.06	1.3×10^{12}	9.0×10^{-5}	90.88	1.6×10^{14}	0	7. 67	0.40	6.2×10^{-5}	92.70
	Average (± SE)	6.76 (± 0.15)	1.0×10^{12} ($\pm 0.1 \times 10^{12}$)	–	–	2.3×10^{12} ($\pm 0.3 \times 10^{12}$)	0	7.44 (± 0.12)	0.43 (± 0.04)	–	–

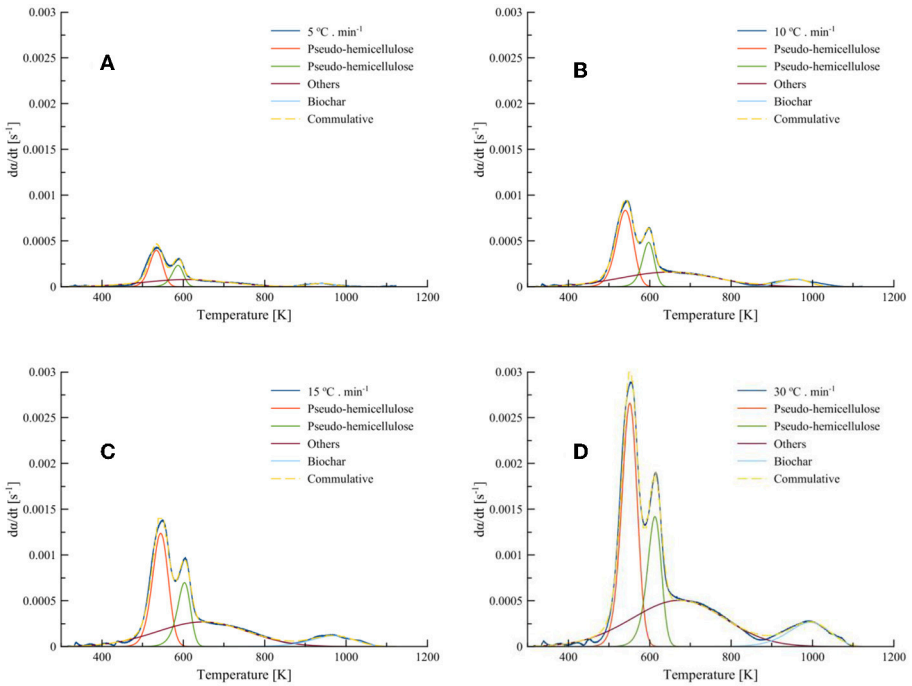

FIGURE 6 | Model-fitting of Turbinaria ornata with three pseudo-components and biochar degradation at **(A)** 5; **(B)** 10; **(C)** 15; and **(D)** 30°C·min^{-1}.

increasing heating rates. Furthermore, with increasing heating rates the Fit% increases.

The major mass loss comes from the degradation of pseudo-hemicellulose and others, accounting for relative mass loss contributions of 40.5 and 38.5%, respectively. The decomposition continues over wide temperature ranges. The secondary decomposition in Zone (II) contributes to an additional mass loss of 8%, which results in the evolution of more volatiles. Therefore, the remaining mass after secondary decomposition, termed as *Biochar2*, further decreases. The decompositions of carbohydrates, others, and *Biochar1* in the presence of inorganics indicates the cumulative effects of catalysts and gasification. This could encourage flash pyrolysis or rapid heating in order to fully utilize the gasification and catalytic effects of these inorganically rich marine biomasses.

The kinetic parameters of the pseudo-component degradations were estimated using the Friedman and KAS model-free methods on separated deconvoluted peaks. The E_a of the independent-parallel reactions were calculated from the regression plots of Friedman and KAS and the evolution of

TABLE 6 | Fractional mass loss (x_j) of deconvoluted Turbinaria ornata pseudo-components using FS distribution at different heating rates.

β [°C·min^{-1}]	*Pseudo-Hemicellulose* (Peak 1)	*Pseudo-Cellulose* (Peak 2)	*Others* (Peak 3)	*Biochar1* (Peak 4)	SSE [s^{-2}]	Fit [%]
5	0.425	0.147	0.361	0.067	2.3×10^{-7}	98.85
10	0.403	0.124	0.397	0.075	3.1×10^{-7}	99.14
15	0.397	0.107	0.411	0.085	4.4×10^{-7}	99.16
30	0.394	0.143	0.370	0.093	8.2×10^{-7}	99.23
Average (± SE)	0.405 (+ 0.007)	0.130 (+ 0.009)	0.385 (+ 0.012)	0.080 (+ 0.006)	–	–

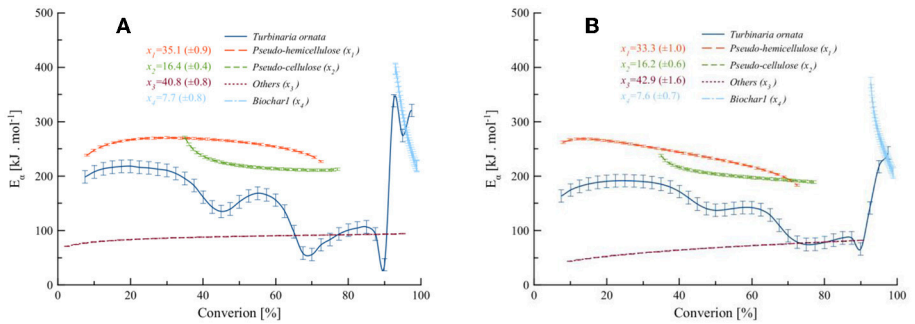

FIGURE 7 | Evolution of activation energies with the conversion from the **(A)** Friedman method and **(B)** KAS method.

TABLE 7 | Optimized kinetic parameters of pseudo-components.

β [°C·min^{-1}]		Pseudo-hemicellulose			Pseudo-cellulose			Others			Biochar				
		A [s^{-1}]	E_a [kJ·mol^{-1}]	*n* [–]	*A* [s^{-1}]	E_a [kJ·mol^{-1}]	*n* [–]	*A* [s^{-1}]	E_a [kJ·mol^{-1}]	*n* [–]	*A* [s^{-1}]	E_a [kJ·mol^{-1}]	*n* [–]	SSE [s^{-2}]	Fit [%]
Differential	5	1.9×10^{19}	223.9	2.52	5.1×10^{16}	224.6	1.48	0.02	23.7	1.10	2.2×10^{13}	309.7	1.79	1.3×10^{-6}	97.50
	10	1.4×10^{12}	151.8	1.79	3.4×10^{16}	223.1	1.28	0.04	25.4	0.97	1.6×10^{13}	304.9	2.44	6.0×10^{-7}	98.83
	15	3.9×10^{14}	176.1	2.10	1.8×10^{13}	186.2	1.12	0.08	27.1	1.09	9.6×10^{5}	158.6	1.24	1.1×10^{-6}	98.71
	30	2.2×10^{15}	182.8	1.97	2.5×10^{13}	186.8	1.14	0.12	27.0	0.96	5.0×10^{5}	187.3	1.31	2.1×10^{-6}	98.80
Integral	5	0.9×10^{19}	230.6	2.62	2.1×10^{15}	209.4	1.38	0.02	24.6	1.18	2.7×10^{10}	258.9	1.54	1.3×10^{-6}	97.43
	10	1.5×10^{20}	231.8	2.71	2.3×10^{15}	209.6	1.34	0.02	21.3	1.09	1.5×10^{10}	252.8	1.79	3.1×10^{-6}	97.49
	15	1.0×10^{13}	160.3	1.88	1.4×10^{15}	207.6	1.19	0.05	25.1	0.94	2.4×10^{10}	253.9	1.98	9.7×10^{-7}	98.78
	30	2.8×10^{16}	194.0	2.09	2.6×10^{13}	187.0	1.17	0.20	29.3	1.08	2.6×10^{6}	181.5	1.33	2.4×10^{-6}	98.73

activation energies with respect to conversion; these are shown in **Figure 7**.

It is clear from **Figure 7** that the primary decompositions overlap and that the interplay of the components causes the overall activation energy decrease until around 90% of the conversion. This aspect has been regarded by some researchers to the condensation of polymers at higher temperature to form char (Chorley, 1892; Basile et al., 2016; Anca-Couce and Scharler, 2017; Ciuta et al., 2018). The secondary conversion of *Biochar1* at a higher temperature with a higher activation energy, which drops as the conversion proceeds toward completion. Average activation energies of the pseudo-components and initial parameter values obtained from the Friedman and KAS methods were used to optimize the kinetic parameters via non-linear regression. The SB parameters m and p were absent, hence both order-based and SB models were found to be equivalent. The obtained parameters using differential and integral methods at different heating rates are presented in **Table 7**.

A summary of the key thermal and kinetic parameters is tabulated in **Table 8**. It is evident that the peak-maximum temperature (T_m) for the decomposition of pseudo-hemicellulose is 541.2 K for the differential Friedman method and 541.5 K for the integral KAS method. The T_m for pseudo-cellulose is 598.4 and 583.4 K using the Friedman and KAS methods, respectively. Pseudo-others decompose with a T_m of 641.8 to 634.2 K according to the Friedman and KAS methods. The decomposition at mild-to-high temperatures may also involve condensation of polymers. Depending on the heating rate, the

TABLE 8 | Thermal characteristics of the pseudo-components of Turbinaria ornata pyrolysis.

Components	Friedman method (Differential)						KAS method (Integral)					
	T_m (± SE) [K]	α_m (± SE) [%]	x_j (± SE) [–]	n (± SE) [–]	A (± SE) [s^{-1}]	E_a (± SE) [kJ.mol^{-1}]	T_m (± SE) [K]	α_m (± SE) [%]	x_j (± SE) [–]	n (± SE) [–]	A (± SE) [s^{-1}]	E_a (± SE) [kJ.mol^{-1}]
Pseudo-hemicellulose	541.2 (± 3.6)	26.6 (± 0.7)	0.351 (± 0.009)	2.09 (± 0.16)	4.7×10^{18} ($\pm 4.7 \times 10^{18}$)	183.7 (± 14.97)	541.5 (± 3.6)	26.6 (± 0.8)	0.333 (± 0.010)	2.33 (± 0.20)	5.9×10^{19} ($\pm 3.6 \times 10^{19}$)	204.2 (± 17.05)
Pseudo-cellulose	598.4 (± 5.3)	61.3 (± 0.0)	0.164 (± 0.004)	1.03 (± 0.07)	2.1×10^{16} ($\pm 1.3 \times 10^{16}$)	205.2 (± 10.8)	583.4 (± 14.2)	61.6 (± 0.0)	0.162 (± 0.006)	1.27 (± 0.05)	1.5×10^{15} ($\pm 0.5 \times 10^{15}$)	203.4 (± 5.5)
Others	641.8 (± 13.7)	70.9 (± 0.0)	0.408 (± 0.008)	1.03 (± 0.04)	0.06 (± 0.02)	25.8 (± 0.8)	634.2 (± 15.3)	71.8 (± 0.0)	0.429 (± 0.016)	1.07 (± 0.05)	0.07 (± 0.04)	25.1 (± 1.6)
Biochar1	963.9 (± 10.9)	96.0 (± 0.0)	0.077 (± 0.008)	1.69 (± 0.28)	9.5×10^{12} ($\pm 5.6 \times 10^{12}$)	240.1 (± 39.2)	964.2 (± 10.0)	96.1 (± 0.0)	0.076 (± 0.007)	1.66 (± 0.14)	1.6×10^{10} ($\pm 0.6 \times 10^{10}$)	236.8 (± 18.5)
Weighted Average		–	–	1.45	1.7×10^{18}	127.15		–	–	1.57	2.0×10^{19}	129.70

secondary decomposition of *Biochar1* occurs in a temperature range of 870–1,100 K with a T_m of 963.9 and 964.2 K using the Friedman and KAS methods, respectively.

The average reaction order (n) of the decomposition of pseudo-hemicellulose, pseudo-cellulose, others, and biochar was found to be 2.09, 1.03, 1.03, and 1.69 for the Friedman method and 2.33, 1.27, 1.07, and 1.66 for the KAS method, respectively. Similarly, the average pre-exponential factor (A) of the decomposition of pseudo-hemicellulose, pseudo-cellulose, others, and biochar was found to be 4.7×10^{18}, 2.1×10^{16}, 0.06, and 9.5×10^{12} s^{-1}, respectively, for the Friedman method and 5.9×10^{19}, 1.5×10^{15}, 0.07, and 1.6×10^{10} for the KAS method, respectively.

The average E_a of pseudo-hemicellulose obtained from the Friedman and KAS methods was 183.7 and 204.2 kJ.mol^{-1}, respectively. Similarly, the average E_a of pseudo-cellulose using the Friedman and KAS methods was 205.2 and 203.4 kJ.mol^{-1}, respectively. Pseudo-others decomposed with a lower average E_a of 25.8 and 25.1 kJ.mol^{-1}, as estimated from the Friedman and KAS methods, respectively. The average E_a of pseudo-others is very low, which may be due to the formation of polymers owing to the metal oxides from inherited inorganics taken up by *T. ornata* macro-algae. Jian et al. (2014) found that the E_a of metal oxides was low at higher heating rates, indicating oxygen transport to be a rate limiting step at high temperatures and high heating rates. This may induce a partial gasification phenomenon at this stage. The partial gasification, according to Equation (8), could be due to the inherited metal oxides present in the cell wall of the polysaccharide matrix of *T. ornata.* The average E_a was calculated for the degradation of *Biochar1*, which was 240.1 and 236.5 kJ.mol^{-1} using the Friedman and KAS methods, respectively. It can also be deduced that the variation in the values of A, n, and E_a was the greatest during the secondary decomposition of *Biochar1* in Zone (II) among the other pseudo-components. Moreover, the sharp decrease in the E_a of *Biochar1* is a mere indication of the spontaneity of the process.

CONCLUSIONS

Marine macro-algae contains inorganics, including heavy metals, the amount of which depends on the macro-algae's ability to uptake these as well as the concentration of inorganics dissolved in the marine environment. While this help mitigates the heavy metals, their disposal needs care. Pyrolysis offers not only a means to handle such materials but also the ability to use these to our benefit in the form of valuable products such as volatiles and biochar. The Red Sea is a rich source of many minerals, which are taken up by the organisms living there. The role of these organisms in this process is important and needs to be evaluated using complex models. A four-component independent-reaction model using a simple order-based mechanism for each reaction is sufficient to analyze the pyrolytic kinetics. This shows that three primary reactions proceed simultaneously, producing a solid product which degrades through a secondary decomposition reaction at a higher temperature. Interestingly, the activation energy drops considerably for the secondary reaction, hinting at the partial gasification and the catalytic effects of the minerals inherent in the macro-algae.

AUTHOR CONTRIBUTIONS

All authors listed have made a substantial, direct and intellectual contribution to the work, and approved it for publication.

REFERENCES

Abdallah, A. M. A., Abdallah, M. A., Beltagy, A., and Siam, E. (2006). Contents of heavy metals in marine algae from Egyptian Red Sea coast. *Toxicol. Environ. Chem.* 88, 9–22. doi: 10.1080/02772240500414911

Aboyade, A. O., Carrier, M., Meyer, E. L., Knoetze, J. H., and Görgens, J. F. (2012). Model fitting kinetic analysis and characterisation of the devolatilization of coal blends with corn and sugarcane residues. *Thermochim. Acta* 530, 95–106. doi: 10.1016/j.tca.2011.12.007

Adanez, J., Abad, A., Garcia-Labiano, F., Gayan, P., and de Diego, L. F. (2012). Progress in chemical-looping combustion and reforming technologies. *Prog. Energy Combust. Sci.* 38, 215–282. doi: 10.1016/j.pecs.2011.09.001

Agency, I. E. (2017). *Energy Technology Perspectives 2017: Catalysing Energy Technology Transformations*. OECD/IEA.

Ali, I., Naqvi, S. R., and Bahadar, A. (2018). Kinetic analysis of *Botryococcus braunii* pyrolysis using model-free and model fitting methods. *Fuel* 214, 369–380. doi: 10.1016/j.fuel.2017.11.046

Anca-Couce, A., and Scharler, R. (2017). Modelling heat of reaction in biomass pyrolysis with detailed reaction schemes. *Fuel* 206, 572–579. doi: 10.1016/j.fuel.2017.06.011

Baghel, R. S., Mantri, V. A., and Reddy, C., R. K. (2017). "A new wave of research interest in marine macroalgae for chemicals and fuels: challenges and potentials," in *Fuels, Chemicals and Materials from the Oceans and Aquatic Sources*, eds. F. M. Kerton, and N. Yan (John Wiley and Sons, Ltd), 43–63. doi: 10.1002/9781119117193.ch3

Basile, L., Tugnoli, A., Stramigioli, C., and Cozzani, V. (2016). Thermal effects during biomass pyrolysis. *Thermochim. Acta* 636, 63–70. doi: 10.1016/j.tca.2016.05.002

Behairy, A. K. A., and El-Sayed, M. M. (1983). *Biochemical Composition of Some Marine Brown Algae From Jeddah Coast, Saudi Arabia. IJMS Vol.12(3) [September 1983]*. Available online at: http://nopr.niscair.res.in/handle/123456789/38893 (Accessed December 17, 2017).

Bold, H. C., and Wynne, M. J. (1984). *Introduction to the Algae, 2nd Edn*. Englewood Cliffs, NJ: Prentice-Hall.

Bruckner, A., Rowlands, G., Riegl, B., Purkis, S., Williams, A., and Renaud, P. (2013). *Atlas of Saudi Arabian Red Sea Marine Habitats. Oceanography Faculty Books and Book Chapters*. Available online at: http://nsuworks.nova.edu/occ_facbooks/33

Chorley, C. (1892). The destructive distillation of wood. *J. Soc. Chem. Industry* 11, 872–874. doi: 10.1002/jctb.5000111104

Ciuta, S., Tsiamis, D., and Castaldi, M. J. (2018). "Chapter two - fundamentals of gasification and pyrolysis," in *Gasification of Waste Materials*, eds S. Ciuta, D. Tsiamis, and M. J. Castaldi (Academic Press), 13–36. doi: 10.1016/B978-0-12-812716-2.00002-9

Davis, T. A., Volesky, B., and Mucci, A. (2003). A review of the biochemistry of heavy metal biosorption by brown algae. *Water Res.* 37, 4311–4330. doi: 10.1016/S0043-1354(03)00293-8

Deepak, P., Sowmiya, R., Balasubramani, G., and Perumal, P. (2017a). Phytochemical profiling of Turbinaria ornata and its antioxidant and anti-proliferative effects. *J. Taibah Univ. Med. Sci.* 12, 329–337. doi: 10.1016/j.jtumed.2017.02.002

Deepak, P., Sowmiya, R., Ramkumar, R., Balasubramani, G., Aiswarya, D., and Perumal, P. (2017b). Structural characterization and evaluation of mosquito-larvicidal property of silver nanoparticles synthesized from the seaweed, Turbinaria ornata (Turner) J. Agardh 1848. *Artif. Cells Nanomed. Biotechnol.* 45, 990–998. doi: 10.1080/21691401.2016.1198365

Di Blasi, C. (2008). Modeling chemical and physical processes of wood and biomass pyrolysis. *Progr. Energy Combust. Sci.* 34, 47–90. doi: 10.1016/j.pecs.2006.12.001

Dussan, K., Dooley, S., and Monaghan, R. (2017). Integrating compositional features in model compounds for a kinetic mechanism of hemicellulose pyrolysis. *Chem. Eng. J.* 328, 943–961. doi: 10.1016/j.cej.2017.07.089

El-Naggar, M. E. E., and Al-Amoudi, O. A. (1989). Heavy metal levels in several species of marine algae from the Red Sea of Saudia Aabia. *J. King Abdulaziz Univ. Sci. J.* 1, 5–13. doi: 10.4197/Sci.1-1.1

Ferdouse, F., Holdt, S. L., Smith, R., Murúa, P., and Yang, Z. (2018). *The Global Status of Seaweed Production, Trade and Utilization*. Rome, Italy: Products, Trade and Marketing Branch, Fisheries and Aquaculture Policy and Resources Division, Food and Agriculture Organization of the United Nations Available online at: http://www.fao.org/in-action/globefish/publications/details-publication/en/c/1154074/ (Accessed Jan 26, 2019).

Friedman, H. L. (1964). Kinetics of thermal degradation of char-forming plastics from thermogravimetry. application to a phenolic plastic. *J. Polym. Sci. C Polym. Symp.* 6, 183–195.

Gámiz-González, M. A., Correia, D. M., Lanceros-Mendez, S., Sencadas, V., Gómez Ribelles, J. L., and Vidaurre, A. (2017). Kinetic study of thermal degradation of chitosan as a function of deacetylation degree. *Carbohydr. Polym.* 167, 52–58. doi: 10.1016/j.carbpol.2017.03.020

Ghadiryanfar, M., Rosentrater, K. A., Keyhani, A., and Omid, M. (2016). A review of macroalgae production, with potential applications in biofuels and bioenergy. *Renew. Sustain. Energy Rev.* 54, 473–481. doi: 10.1016/j.rser.2015.10.022

Grigiante, M., Brighenti, M., and Antolini, D. (2016). A generalized activation energy equation for torrefaction of hardwood biomasses based on isoconversional methods. *Renew. Energy* 99, 1318–1326. doi: 10.1016/j.renene.2016.07.054

Han, Z., Guo, Z., Zhang, Y., Xiao, X., Xu, Z., and Sun, Y. (2017). Pyrolysis characteristics of biomass impregnated with cadmium, copper and lead: influence and distribution. *Waste Biomass Valor* 2017, 1–8. doi: 10.1007/s12649-017-0036-5

Hong, Y., Chen, W., Luo, X., Pang, C., Lester, E., and Wu, T. (2017). Microwave-enhanced pyrolysis of macroalgae and microalgae for syngas production. *Bioresour. Technol.* 237, 47–56. doi: 10.1016/j.biortech.2017.02.006

Huang, Z., Deng, Z., He, F., Chen, D., Wei, G., Zhao, K., et al. (2017). Reactivity investigation on chemical looping gasification of biomass char using nickel ferrite oxygen carrier. *Int. J. Hydrogen Energy* 42, 14458–14470. doi: 10.1016/j.ijhydene.2017.04.246

Huang, Z., He, F., Feng, Y., Liu, R., Zhao, K., Zheng, A., et al. (2013). Characteristics of biomass gasification using chemical looping with iron ore as an oxygen carrier. *Int. J. Hydrogen Energy* 38, 14568–14575. doi: 10.1016/j.ijhydene.2013.09.022

Jian, G., Zhou, L., Piekiel, N. W., and Zachariah, M. R. (2014). Low effective activation energies for oxygen release from metal oxides: evidence for mass-transfer limits at high heating rates. *ChemPhysChem* 15, 1666–1672. doi: 10.1002/cphc.201301148

Kayalvizhi, K., Asmathunisha, N., Subramanian, V., and Kathiresan, K. (2014). Purification of silver and gold nanoparticles from two species of brown seaweeds (*Padina tetrastromatica* and *Turbinaria ornata*). *J. Med. Plants Stud.* 2, 32–37.

Keown, D. M., Favas, G., Hayashi, J., and Li, C. Z. (2005). Volatilisation of alkali and alkaline earth metallic species during the pyrolysis of biomass: differences between sugar cane bagasse and cane trash. *Bioresour. Technol.* 96, 1570–1577. doi: 10.1016/j.biortech.2004.12.014

Kissinger, H. E. (1957). Reaction kinetics in differential thermal analysis. *Anal. Chem.* 29, 1702–1706 doi: 10.1021/ac60131a045

Li, D., Chen, L., Yi, X., Zhang, X., and Ye, N. (2010). Pyrolytic characteristics and kinetics of two brown algae and sodium alginate. *Bioresour. Technol.* 101, 7131–7136. doi: 10.1016/j.biortech.2010.03.145

Liu, W. J., Li, W. W., Jiang, H., and Yu, H. Q. (2017). Fates of chemical elements in biomass during its pyrolysis. *Chem. Rev.* 117, 6367–6398. doi: 10.1021/acs.chemrev.6b00647

Liu, W. J., Tian, K., Jiang, H., Zhang, X. S., Ding, H. S., and Yu, H. Q. (2012). Selectively improving the bio-oil quality by catalytic fast pyrolysis of heavy-metal-polluted biomass: take copper (Cu) as an example. *Environ. Sci. Technol.* 46, 7849–7856. doi: 10.1021/es204681y

Liu, W. J., Zeng, F. X., Jiang, H., Zhang, X. S., and Yu, H. Q. (2011). Techno-economic evaluation of the integrated biosorption–pyrolysis technology for lead (Pb) recovery from aqueous solution. *Bioresour. Technol.* 102, 6260–6265. doi: 10.1016/j.biortech.2011.02.104

Maceiras, R., Rodri'guez, M., Cancela, A., Urréjola, S., and Sánchez, A. (2011). Macroalgae: raw material for biodiesel production. *Appl. Energy* 88, 3318–3323. doi: 10.1016/j.apenergy.2010.11.027

Manivannan, K., Thirumaran, G., Devi, G. K., Anantharaman, P., and Balasubramanian, T. (2009). Proximate composition of different group of seaweeds from Vedalai coastal waters (Gulf of Mannar): southeast coast of India. *Middle East J. Sci. Res.* 4, 72–77.

Millán, L. M. R., Vargas, F. E. S., and Nzihou, A. (2017). Kinetic analysis of tropical lignocellulosic agrowaste pyrolysis. *Bioenerg. Res.* 10, 832–845. doi: 10.1007/s12155-017-9844-5

Mohamed Ali, D., and Elnabawy Ward, F. M. (2016). Ecological and biochemical analyses of the brown alga Turbinaria ornata (Turner) J. Agardh from Red Sea coast, Egypt. *J. Coastal Life Med.* 4, 187–192. doi: 10.12980/jclm.4.2016j6-10

Mohammadi, M., Tajik, H., and Hajeb, P. (2013). Nutritional composition of seaweeds from the Northern Persian Gulf. *Iran. J. Fish. Sci.* 12, 232–240.

Mohan, D., Pittman Charles, U., and Steele, P. H. (2006). Pyrolysis of wood/biomass for bio-oil: a critical review. *Energy Fuels* 20, 848–889. doi: 10.1021/ef0502397

Oliveira, J. (2016). *An Integrated Use of Macroalgae as Bioproducts Source and Biosorbent for Environmental Applications*. Porto: Faculdade de Engenharia da Universidade do Porto.

Omar, H. H., Shiekh, H. M., Gumgumjee, N. M., El-Kazan, M. M., and El-Gendy, A. M. (2012). Antibacterial activity of extracts of marine algae from the Red Sea of Jeddah, Saudi Arabia. *Afr. J. Biotechnol.* 11, 13576–13585. doi: 10.5897/AJB12.780

Opfermann, J. R., Kaisersberger, E., and Flammersheim, H. J. (2002). Model-free analysis of thermoanalytical data-advantages and limitations. *Thermochimica Acta* 391, 119–127. doi: 10.1016/S0040-6031(02)00169-7

Orfão, J. J. M., Antunes, F. J. A., and Figueiredo, J. L. (1999). Pyrolysis kinetics of lignocellulosic materials—three independent reactions model. *Fuel* 78, 349–358 doi: 10.1016/S0016-2361(98)00156-2

Ortiz-Calderon, C., Silva, H. C., and Vásquez, D. B. (2017). "Metal removal by seaweed," in *Biomass Volume Estimation and Valorization for Energy*, ed J. S. Tumuluru (InTechOpen), 361–380.

Osman, A. I., Abdelkader, A., Johnston, C. R., Morgan, K., and Rooney, D. W. (2017). Thermal investigation and kinetic modeling of lignocellulosic biomass combustion for energy production and other applications. *Ind. Eng. Chem. Res.* 56, 12119–12130. doi: 10.1021/acs.iecr.7b03478

Özsin, G., and Pütün, A. E. (2017). Insights into pyrolysis and co-pyrolysis of biomass and polystyrene: thermochemical behaviors, kinetics and evolved gas analysis. *Energy Convers. Manage.* 149, 675–685. doi: 10.1016/j.enconman.2017.07.059

Patwardhan, P. R., Dalluge, D. L., Shanks, B. H., and Brown, R. C. (2011). Distinguishing primary and secondary reactions of cellulose pyrolysis. *Bioresour. Technol.* 102, 5265–5269. doi: 10.1016/j.biortech.2011.02.018

Perejón, A., Sánchez-Jiménez, P. E., Criado, J. M., and Pérez-Maqueda, L. A. (2011). Kinetic analysis of complex solid-state reactions. A new deconvolution procedure. *J. Phys. Chem. B* 115, 1780–1791. doi: 10.1021/jp110895z

Poletto, M., Zattera, A. J., and Santana, R. M. (2012). Thermal decomposition of wood: Kinetics and degradation mechanisms. *Bioresour. Technol.* 126, 7–12. doi: 10.1016/j.biortech.2012.08.133

Ponnan, A., Ramu, K., Marudhamuthu, M., Marimuthu, R., Siva, K., and Kadarkarai, M. (2017). Antibacterial, antioxidant and anticancer properties of Turbinaria conoides (*J. Agardh) Kuetz. Clin. Phytosci.* 3:5. doi: 10.1186/s40816-017-0042-y

Rajeshkumar, S., Malarkodi, C., Gnanajobitha, G., Paulkumar, K., Vanaja, M., Kannan, C., et al. (2013). Seaweed-mediated synthesis of gold nanoparticles using Turbinaria conoides and its characterization. *J. Nanostruct. Chem.* 3:44. doi: 10.1186/2193-8865-3-44

Ranzi, E., Debiagi, P. E. A., and Frassoldati, A. (2017). Mathematical modeling of fast biomass pyrolysis and bio-oil formation. note I: kinetic mechanism of biomass pyrolysis. *ACS Sustain. Chem. Eng.* 5, 2867–2881. doi: 10.1021/acssuschemeng.6b03096

Richardson, Y., Motuzas, J., Julbe, A., Volle, G., and Blin, J. (2013). Catalytic investigation of *in situ* generated Ni metal nanoparticles for tar conversion during biomass pyrolysis. *J. Phys. Chem. C* 117, 23812–23831. doi: 10.1021/jp408191p

Roesijadi, G., Jones, S., Snowden-Swan, L., and Zhu, Y. (2010). *Macroalgae as a Biomass Feedstock: A Preliminary Analysis*. U.S. Department of Energy. doi: 10.2172/1006310

Ross, A. B., Jones, J. M., Kubacki, M. L., and Bridgeman, T. (2008). Classification of macroalgae as fuel and its thermochemical behaviour. *Bioresour. Technol.* 99, 6494–6504. doi: 10.1016/j.biortech.2007.11.036

Roy, S., P, A., Attia, A. M., and Attia, A. A. A. (2017). Heavy Metals Accumulation of Different Parts of *Turbinaria* spp. along the Olaikuda Coast, Rameshwaram, Tamilnadu, India. *IARJSET* 4, 99–102. doi: 10.17148/IARJSET.2017.4319

Saha, B., and Orvig, C. (2010). Biosorbents for hexavalent chromium elimination from industrial and municipal effluents. *Coordinat. Chem. Rev.* 254, 2959–2972. doi: 10.1016/j.ccr.2010.06.005

Santoso, J., Gunji, S., Yoshie-Stark, Y., and Suzuki, T. (2006). Mineral contents of indonesian seaweeds and mineral solubility affected by basic cooking. *Food Sci. Technol. Res.* 12, 59–66. doi: 10.3136/fstr.12.59

Šesták, J., and Berggren, G. (1971). Study of the kinetics of the mechanism of solid-state reactions at increasing temperatures. *Thermochim. Acta* 3, 1–12 doi: 10.1016/0040-6031(71)85051-7

Sheldon, R. A. (2014). Green and sustainable manufacture of chemicals from biomass: state of the art. *Green Chem.* 16, 950–963. doi: 10.1039/C3GC41935E

Shuping, Z., Yulong, W., Mingde, Y., Chun, L., and Junmao, T. (2010). Pyrolysis characteristics and kinetics of the marine microalgae *Dunaliella tertiolecta* using thermogravimetric analyzer. *Bioresour. Technol.* 101, 359–365. doi: 10.1016/j.biortech.2009.08.020

Siddall, M., Smeed, D. A., Hemleben, C., Rohling, E. J., Schmelzer, I., and Peltier, W. R. (2004). Understanding the Red Sea response to sea level. *Earth Planet. Sci. Lett.* 225, 421–434. doi: 10.1016/j.epsl.2004.06.008

Šimon, P. (2011). Fourty years of the Šesták–Berggren equation. *Thermochim. Acta* 520, 156–157. doi: 10.1016/j.tca.2011.03.030

Spalding, M. D., Green, E. P., and Ravilious, C. (2001). *World Atlas of Coral Reefs*, *1st Edn*. Berkeley, CA: University of California Press.

Stranska-Zachariasova, M., Kurniatanty, I., Gbelcova, H., Jiru, M., Rubert, J., Nindhia, T. G., et al. (2017). Bioprospecting of turbinaria macroalgae as a potential source of health protective compounds. *Chem. Biodivers.* 14:201600192. doi: 10.1002/cbdv.201600192

Tenorio-Rodriguez, P. A., Murillo-Álvarez, J. I., Campa-Cordova, Á. I., and Angulo, C. (2017). Antioxidant screening and phenolic content of ethanol extracts of selected Baja California Peninsula macroalgae. *J. Food Sci. Technol.* 54, 422–429. doi: 10.1007/s13197-016-2478-3

Vyazovkin, S., Burnham, A. K., Criado, J. M., Pérez-Maqueda, L. A., Popescu, C., and Sbirrazzuoli, N. (2011). ICTAC Kinetics Committee recommendations for performing kinetic computations on thermal analysis data. *Thermochim. Acta* 520, 1–19. doi: 10.1016/j.tca.2011.03.034

Vyazovkin, S., and Wight, C. A. (1998). Isothermal and non-isothermal kinetics of thermally stimulated reactions of solids. *Int. Rev. Phys. Chem.* 17, 407–433. doi: 10.1080/014423598230108

Wang, J., Wang, G., Zhang, M., Chen, M., Li, D., Min, F., et al. (2006). A comparative study of thermolysis characteristics and kinetics of seaweeds and fir wood. *Process Biochem.* 41, 1883–1886. doi: 10.1016/j.procbio.2006.03.018

Wang, S., Dai, G., Yang, H., and Luo, Z. (2017). Lignocellulosic biomass pyrolysis mechanism: a state-of-the-art review. *Prog. Energy Combust. Sci.* 62, 33–86. doi: 10.1016/j.pecs.2017.05.004

Wei, X., Zhang, G., Cai, Y., Li, L., and Li, H. (2012). The volatilization of trace elements during oxidative pyrolysis of a coal from an endemic arsenosis area in southwest Guizhou, China. *J. Analyt. Appl. Pyrol.* 98, 184–193. doi: 10.1016/j.jaap.2012.08.015

Xu, T., Xu, F., Hu, Z., Chen, Z., and Xiao, B. (2017). Non-isothermal kinetics of biomass-pyrolysis-derived-tar (BPDT) thermal decomposition via thermogravimetric analysis. *Energy Convers. Manage.* 138, 452–460. doi: 10.1016/j.enconman.2017.02.013

Ye, N., Li, D., Chen, L., Zhang, X., and Xu, D. (2010). Comparative studies of the pyrolytic and kinetic characteristics of maize straw and the seaweed ulva pertusa. *PLoS ONE* 5:e0012641. doi: 10.1371/journal.pone.0012641

Zhao, H., Guo, L., and Zou, X. (2015). Chemical-looping auto-thermal reforming of biomass using Cu-based oxygen carrier. *Appl. Energy* 157, 408–415. doi: 10.1016/j.apenergy.2015.04.093

Zubia, M., Payri, C. E., Deslandes, E., and Guezennec, J. (2005). Chemical Composition of Attached and Drift Specimens of Sargassum mangarevense and *Turbinaria ornata* (Phaeophyta: Fucales) from Tahiti, French Polynesia. *Bot. Mar.* 46, 562–571. doi: 10.1515/BOT.2003.059

Conflict of Interest Statement: The authors declare that the research was conducted in the absence of any commercial or financial relationships that could be construed as a potential conflict of interest.

The handling Editor declared a shared affiliation at the time of review, though no other collaboration, with the authors.

frontiers in Energy Research

ORIGINAL RESEARCH
published: 19 March 2019
doi: 10.3389/fenrg.2019.00027

Catalytic Pyrolysis of Plastic Waste: Moving Toward Pyrolysis Based Biorefineries

Rashid Miandad[1], Mohammad Rehan[2], Mohammad A. Barakat[3,4], Asad S. Aburiazaiza[3], Hizbullah Khan[1], Iqbal M. I. Ismail[2], Jeya Dhavamani[2], Jabbar Gardy[5], Ali Hassanpour[5] and Abdul-Sattar Nizami[2]*

[1] Department of Environmental Sciences, University of Peshawar, Peshawar, Pakistan, [2] Centre of Excellence in Environmental Studies, King Abdulaziz University, Jeddah, Saudi Arabia, [3] Department of Environmental Sciences, Faculty of Meteorology, Environment and Arid Land Agriculture, King Abdulaziz University, Jeddah, Saudi Arabia, [4] Central Metallurgical R&D Institute, Helwan, Egypt, [5] School of Chemical and Process Engineering, University of Leeds, Leeds, United Kingdom

Pyrolysis based biorefineries have great potential to convert waste such as plastic and biomass waste into energy and other valuable products, to achieve maximum economic and environmental benefits. In this study, the catalytic pyrolysis of different types of plastics wastes (PS, PE, PP, and PET) as single or mixed in different ratios, in the presence of modified natural zeolite (NZ) catalysts, in a small pilot scale pyrolysis reactor was carried out. The NZ was modified by thermal activation (TA-NZ) at 550°C and acid activation (AA-NZ) with HNO_3, to enhance its catalytic properties. The catalytic pyrolysis of PS produced a higher liquid oil (70 and 60%) than PP (40 and 54%) and PE (40 and 42%), using TA-NZ and AA-NZ catalysts, respectively. The gas chromatography-mass spectrometry (GC-MS) analysis of oil showed a mixture of aromatics, aliphatic and other hydrocarbon compounds. The TA-NZ and AA-NZ catalysts showed a different effect on the wt% of catalytic pyrolysis products and liquid oil chemical compositions, with AA-NZ showing higher catalytic activity than TA-NZ. FT-IR results showed clear peaks of aromatic compounds in all liquid oil samples with some peaks of alkanes that further confirmed the GC-MS results. The liquid oil has a high heating value (HHV) range of 41.7–44.2 MJ/kg, close to conventional diesel. Therefore, it has the potential to be used as an alternative source of energy and as transportation fuel after refining/blending with conventional fuels.

Keywords: catalytic pyrolysis, pyrolysis based biorefineries, natural zeolite, plastic waste, aromatic compounds, modified natural zeolite, catalyst

OPEN ACCESS

Edited by:
Wei-Hsin Chen,
National Cheng Kung University, Taiwan

Reviewed by:
Gopalakrishnan Kumar,
University of Stavanger, Norway
Tzu-Hsien Hsieh,
CPC Corporation, Taiwan

****Correspondence:***
Mohammad Rehan
dr.mohammad_rehan@yahoo.co.uk

Specialty section:
This article was submitted to Bioenergy and Biofuels, a section of the journal Frontiers in Energy Research

Received: *15 November 2018*
Accepted: *22 February 2019*
Published: *19 March 2019*

Citation:
Miandad R, Rehan M, Barakat MA, Aburiazaiza AS, Khan H, Ismail IMI, Dhavamani J, Gardy J, Hassanpour A and Nizami A-S (2019) Catalytic Pyrolysis of Plastic Waste: Moving Toward Pyrolysis Based Biorefineries. Front. Energy Res. 7:27. doi: 10.3389/fenrg.2019.00027

INTRODUCTION

Plastic waste production and consumption is increasing at an alarming rate, with the increase of the human population, rapid economic growth, continuous urbanization, and changes in life style. In addition, the short life span of plastic accelerates the production of plastic waste on a daily basis. The global plastic production was estimated at around 300 million tons per year and is continuously increasing every year (Miandad et al., 2016a; Ratnasari et al., 2017). Plastics are made of petrochemical hydrocarbons with additives such as flame-retardants, stabilizer, and oxidants that make it difficult to bio-degrade (Ma et al., 2017). Plastic waste recycling is carried out in different ways, but in most developing

countries, open or landfill disposal is a common practice for plastic waste management (Gandidi et al., 2018). The disposal of plastic waste in landfills provide habitat for insects and rodents, that may cause different types of diseases (Alexandra, 2012). Furthermore the cost of transportation, labor and maintenance may increase the cost of recycling projects (Gandidi et al., 2018). In addition, due to rapid urbanization, the land available for landfills, especially in cities, is reducing. Pyrolysis is a common technique used to convert plastic waste into energy, in the form of solid, liquid and gaseous fuels.

Pyrolysis is the thermal degradation of plastic waste at different temperatures (300–900°C), in the absence of oxygen, to produced liquid oil (Rehan et al., 2017). Different kinds of catalysts are used to improve the pyrolysis process of plastic waste overall and to enhance process efficiency. Catalysts have a very critical role in promoting process efficiency, targeting the specific reaction and reducing the process temperature and time (Serrano et al., 2012; Ratnasari et al., 2017). A wide range of catalysts have been employed in plastic pyrolysis processes, but the most extensively used catalysts are ZSM-5, zeolite, Y-zeolite, FCC, and MCM-41 (Ratnasari et al., 2017). The catalytic reaction during the pyrolysis of plastic waste on solid acid catalysts may include cracking, oligomerization, cyclization, aromatization and isomerization reactions (Serrano et al., 2012).

Several studies reported the use of microporous and mesoporous catalysts for the conversion of plastic waste into liquid oil and char. Uemichi et al. (1998) carried out catalytic pyrolysis of polyethylene (PE) with HZSM-5 catalysts. The use of HZSM-5 increased liquid oil production with the composition of aromatics and isoalkanes compounds. Gaca et al. (2008) carried out pyrolysis of plastic waste with modified MCM-41 and HZSM-5 and reported that use of HZSM-5 produced lighter hydrocarbons (C_3–C_4) with maximum aromatic compounds. Lin et al. (2004) used different kinds of catalysts and reported that even mixing of HZSM-5 with mesoporous SiO_2-Al_2O_3 or MCM-41 led to the maximum production of liquid oil with minimal gas production. Aguado et al. (1997) reported the production of aromatics and aliphatic compounds from the catalytic pyrolysis of PE with HZSM-5, while the use of mesoporous MCM-41 decreased the aromatic compounds produced due to its low acid catalytic activity. The use of synthetic catalysts enhanced the overall pyrolysis process and improved the quality of produced liquid oil. However, the use of synthetic catalysts increased the cost of the pyrolysis process.

The NZ catalysts can be used to overcome the economic challenges of catalytic pyrolysis which comes with the use of expensive catalysts. In recent years, NZ has gained significant attention for its potential environmental applications. Naturally, NZ is found in Japan, USA, Cuba, Indonesia, Hungary, Italy, and the Kingdom of Saudi Arabia (KSA) (Sriningsih et al., 2014; Nizami et al., 2016). The deposit of NZ in KSA mostly lies in Harrat Shama and Jabbal Shama and mainly contain minerals of mordenite with high thermal stability, making it suitable as a catalyst in plastic waste pyrolysis. Sriningsih et al. (2014) modified NZ from Sukabumi, Indonesia by depositing transitional metals such as Ni, Co, and Mo and carried out pyrolysis of low-density polyethylene (LDPE). Gandidi et al. (2018) used NZ from Lampung, Indonesia for the catalytic pyrolysis of municipal solid waste.

This is the first study to investigate the effect of modified Saudi natural zeolite, on product quality and yield from catalytic pyrolysis of plastic waste. Saudi natural zeolite catalyst was modified via novel thermal activation (TA-NZ) at 550°C and acid activation (AA-NZ) with HNO_3 to enhance its catalytic properties. The catalytic pyrolysis of different types of plastics waste (PS, PE, PP, and PET) as single or mixed in different ratios, in the presence of modified natural zeolite (NZ) catalysts in a small pilot scale pyrolysis reactor, was carried out for the first time. The quality and yield of pyrolysis products such as liquid oil, gas, and char were studied. The chemical composition of the liquid oil was analyzed by GC-MS. Furthermore, the potential and challenges of pyrolysis-based biorefineries have been discussed.

MATERIALS AND METHODS

Feedstock Preparation and Reactor Start-Up

The plastic waste used as the feedstock in the catalytic pyrolysis process was collected from Jeddah and included grocery bags, disposable juice cups and plates, and drinking water bottles, which consist of polyethylene (PE), polypropylene (PP) polystyrene (PS), and polyethylene terephthalate (PET) plastics, respectively. The selection of these plastic materials was made based on the fact that they are the primary source of plastic waste produced in KSA. To obtain a homogenous mixture, all the waste samples were crushed into smaller pieces of around 2 cm^2. The catalytic pyrolysis was carried out using an individual or mixture of these plastic wastes in different ratios (**Table 1**). 1000 g of feedstock was used, with 100 g of catalyst in each experiment. Saudi natural zeolite (NZ), collected from Harrat-Shama located in the northwest of Jeddah city, KSA (Nizami et al., 2016), was modified by thermal and acid treatment and used in these catalytic pyrolysis experiments. NZ was crushed into powder (<100 nm) in a ball-milling machine (Retsch MM 480) for 3 h using 20 Hz/sec, before modification and its usage in pyrolysis. For thermal activation (TA), NZ was heated in a muffle furnace at 550°C for 5 h, while for acidic activation (AA) NZ was soaked in a 0.1 M solution of nitric acid (HNO_3) for 48 h and continuously shaken using an IKA HS 501 digital shaker with 50 rpm. Afterward, the sample was washed with deionized water until a normal pH was obtained.

The experiments were carried out in a small pilot-scale pyrolysis reactor at 450°C, using a heating rate of 10°C/min and reaction time of 75 min (**Figure 1**). The obtained yield of each pyrolysis product was calculated based on weight, after the completion of each experiment. The produced liquid oil characterization was carried out to investigate the effect of feedstock composition on the quality of liquid oil produced in the presence of modified NZ. TGA was carried out on feedstock to obtain the optimal process conditions such as temperature and reaction time (75 min) under controlled conditions. In TGA, a 10 μg of each type of plastic waste was taken and heated with a rate of 10°C from 25 to 900°C under a continuous flow of nitrogen (50

TABLE 1 | Experimental scheme.

Feedstock types	Feedstock quantity (g)	Catalyst QUANTITY (g)	Feedstock ratio (%)	Retention time (min)	Reaction temp (°C)	Heating rate (°C/min)
PS	1,000	100	100	75	450	10
PE	1,000	100	100	75	450	10
PP	1,000	100	100	75	450	10
PS/PE	1,000	100	50/50	75	450	10
PS/PP	1,000	100	50/50	75	450	10
PP/PE	1,000	100	50/50	75	450	10
PS/PE/PP	1,000	100	50/25/25	75	450	10
PS/PP/PE/PET	1,000	100	40/20/20/20	75	450	10

ml/min). The authors of this study have recently published work on the effect of feedstock composition and natural and synthetic zeolite catalysts without catalyst modification on different types of plastic waste (Miandad et al., 2017b; Rehan et al., 2017).

Experimental Setup

The small pilot scale reactor has the capability to be used as both a thermal and catalytic pyrolysis, using different feedstocks such as plastic and biomass materials (**Figure 1**). In this study, modified NZ catalysts were added in the reactor with the feedstock. The pyrolysis reactor can hold up to 20 L of feedstock and the maximum working safe temperature of up to 600°C can be achieved with the desired heating rates. Detailed parameters of the pyrolysis reactor were published earlier (Miandad et al., 2016b, 2017b). As the temperature increases above certain values, the plastic waste (organic polymers) converts into monomers that are transferred to the condenser, where these vapors are condensed into liquid oil. A continuous condensation system using a water bath and ACDelco Classic coolant was used to ensure the condensation temperature was kept below 10°C, and to ensure the maximum condensation of vapor to liquid oil. The produced liquid oil was collected from the oil collection tank, and further characterization was carried out to uncover its chemical composition and characteristics for other potential applications.

Analytical Methods

The pyrolysis oil was characterized using different techniques such as gas chromatography coupled with mass spectrophotometry (GC-MS), Fourier transform infrared spectroscopy (FT-IR),

Bomb Calorimeter and TGA (Mettler Toledo TGA/SDTA851) by adopting the standard ASTM methods. The functional groups in pyrolysis oil was analyzed by a FT-IR, Perkin Elmer's, UK instrument. The FT-IR analysis was conducted using a minimum of 32 scans with an average of 4 cm^{-1} IR signals within the frequency range of 500–4,000 cm^{-1}.

The chemical composition of oil was studied using a GC-MS (Shimadzu QP-Plus 2010) with FI detector. A capillary GC 30 m long and 0.25 mm wide column coated with a 0.25 μm thick film of 5% phenyl-methylpolysiloxane (HP-5) was used. The oven was set at 50°C for 2 min and then increased up to 290°C using a 5°C/min heating rate. The temperature of the ion source and transfer line were kept at 230, and 300°C and splitless injection was applied at 290°C. The NIST08s mass spectral data library was used to identify the chromatographic peaks, and the peak percentages were assessed for their total ion chromatogram (TIC) peak area. The high heating values (HHV) of produced liquid oil obtained from different types of plastic waste were measured following the standard ASTM D 240 method with a Bomb Calorimeter (Parr 6200 Calorimeter) instrument, while production of gas was estimated using the standard mass balance formula, considering the difference of weights of liquid oil and char.

RESULTS AND DISCUSSION

TGA Analysis of Feedstock

TGA was carried out for each type of plastic waste on an individual basis to determine the optimum temperature for thermal degradation. All types of plastic waste show similar degradation behavior with the rapid loss of weight of hydrocarbons within the narrow range of temperature (150–250°C) (**Figure 2**). The maximum degradation for each type of plastic waste was achieved within 420–490°C. PS and PP showed single step decomposition, while PE and PET showed a two-stage decomposition under controlled conditions. The single step decomposition corresponds to the presence of a carbon-carbon bond that promotes the random scission mechanism with the increase in temperature (Kim et al., 2006). PP degradation started at a very low temperature (240°C) compared to other feedstocks. Half of the carbon present in the chain of PP consists of tertiary carbon, which promotes the formation of carbocation during its thermal degradation process (Jung et al., 2010). This is probably the reason for achieving maximum PP degradation at a lower temperature. The PS initial degradation started at 330°C and maximum degradation was achieved at 470°C. PS has a cyclic structure, and its degradation under the thermal condition involves both random chain and end-chain scission, which enhances its degradation process (Demirbas, 2004; Lee, 2012).

PE and PET showed a two-stage decomposition process; the initial degradation started at lower temperatures followed by the other degradation stage at a higher temperature. PEs initial degradation started at 270°C and propagated slowly but gradually

FIGURE 1 | Small pilot scale pyrolysis reactor (Miandad et al., 2016b).

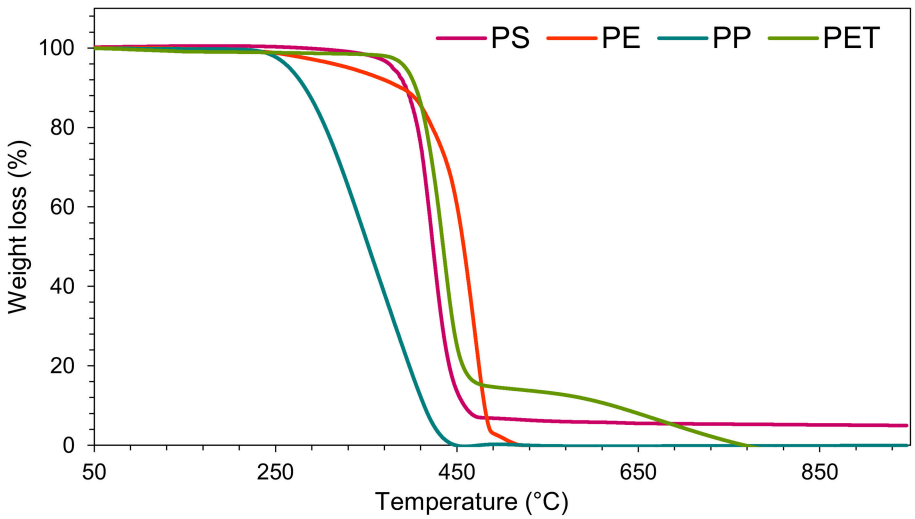

FIGURE 2 | Thermogravimetric analysis (TGA) of PS, PE, PP, and PET plastic waste.

until the temperature reached 385°C. After that temperature, a sharp degradation was observed, and 95% degradation was achieved with a further increase of around 100°C. A similar two-stage degradation pattern was observed for PET plastic and the initial degradation started at 400°C with a sharp decrease in weight loss. However, the second degradation started at a slightly higher temperature (550°C). The initial degradation of PE and PET may be due to the presence of some volatile impurities such as the additive filler used during plastic synthesis (Dimitrov et al., 2013).

Various researchers have reported that PE and PET degradation requires higher temperatures compared to other plastics (Dimitrov et al., 2013; Rizzarelli et al., 2016). Lee (2012) reported that PE has a long chain branched structure and that its degradation occurs via random chain scission, thus requiring a higher temperature, while PET degradation follows the ester link random scission which results in the formation oligomers (Dziecioł and Trzeszczynski, 2000; Lecomte and Liggat, 2006). The initial degradation of PET was perhaps due to the presence of some volatile impurities such as diethylene glycol (Dimitrov et al., 2013). Literature reports that the presence of these volatile impurities further promotes the degradation process of polymers (McNeill and Bounekhel, 1991; Dziecioł and Trzeszczynski, 2000). The difference in TGA curves of various types of plastics could be due to their mesoporous structure (Chandrasekaran et al., 2015). In addition, Lopez et al. (2011) reported that the use of catalysts decreases the process temperature. Therefore, 450°C could be taken as the optimum

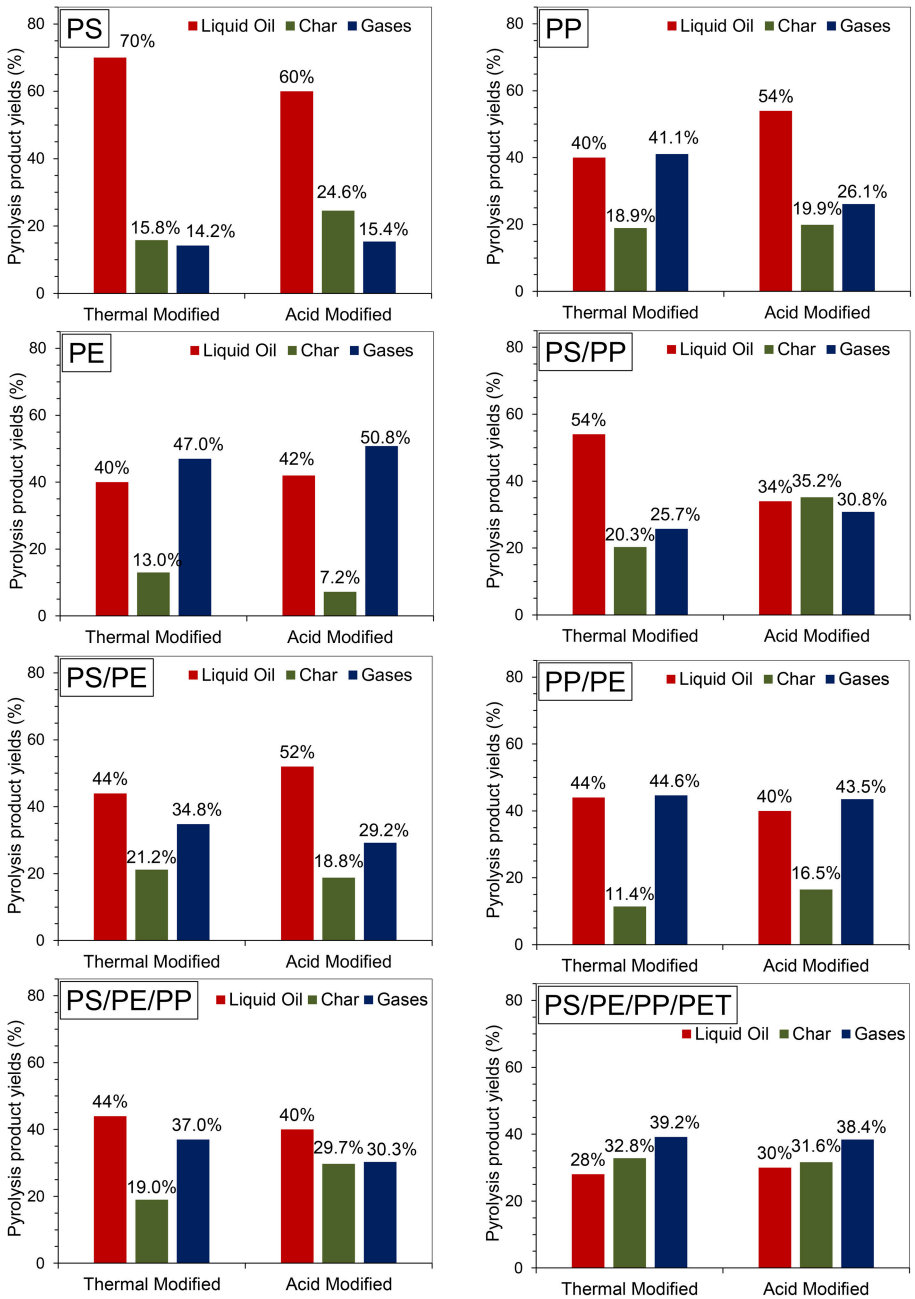

FIGURE 3 | Effect of TA-NZ and AA-NZ on the pyrolysis product yield.

temperature, in the presence of activated NZ, for catalytic pyrolysis of the aforementioned plastic waste.

Effect of Feedstock and Catalysts on Pyrolysis Products Yield

The effect of thermal and acid activation of NZ on the product yield of the pyrolysis process was examined (**Figure 3**). The catalytic pyrolysis of individual PS plastic using TA-NZ and AA-NZ catalysts showed the highest liquid oil yields of 70 and 60%, respectively, compared to all other types of individual and combined plastic waste studied. The high yield of liquid oil from catalytic pyrolysis of PS was also reported in several other studies (Siddiqui and Redhwi, 2009; Lee, 2012; Rehan et al., 2017). Siddiqui and Redhwi (2009) reported that PS has a cyclic structure, which leads to the high yield of liquid oil from catalytic pyrolysis. Lee (2012) reported that PS degradation occurred via both random-chain and end chain scissions, thus leading to the production of the stable benzene ring structure, which enhances further cracking and may increase liquid oil production. Furthermore, in the presence of acid catalysts, PS degradation

followed a carbenium mechanism, which further underwent hydrogenation (inter/intramolecular hydrogen transfer) and β-scission (Serrano et al., 2000). In addition, PS degradation occurred at a lower temperature, compared to other plastics such as PE, due to its cyclic structure (Wu et al., 2014). On the other hand, the catalytic pyrolysis of PS produced a higher amount of char (24.6%) with AA-NZ catalyst than with TA-NZ (15.8%) catalyst. Ma et al. (2017) also reported the high production of char from the catalytic pyrolysis of PS with an acidic zeolite (Hβ) catalyst. The high char production numbers were due to the high acidity of the catalyst, which favors char production via intense secondary cross-linking reactions (Serrano et al., 2000).

The catalytic pyrolysis of PP produced higher liquid oil (54%) with the AA-NZ catalyst than the TA-NZ catalyst (40%) (**Figure 3**). On the other hand, the TA-NZ catalyst produced large amounts of gas (41.1%), which may be due to the lower catalytic activity of the TA-NZ catalyst. According to Kim et al. (2002) catalyst with low acidity and BET surface areas with microporous structures, favor the initial degradation of PP which may lead to the maximum production of gases. Obali et al. (2012) carried out pyrolysis of PP with an alumina-loaded catalyst and reported the maximum production of gas. Moreover, formation of carbocation during PP degradation, due to the presence of tertiary carbon in its carbon chain, may also favor gas production (Jung et al., 2010). Syamsiro et al. (2014) also reported that catalytic pyrolysis of PP and PS with an acid (HCL) activated natural zeolite catalyst produced more gases than the process with a thermally activated natural zeolite catalyst, due to its high acidity and BET surface area.

The catalytic pyrolysis of PE with TA-NZ and AA-NZ catalysts produced similar amounts of liquid oil (40 and 42%). However, the highest amounts of gases (50.8 and 47.0%) were produced from PE, using AA-NZ and TA-NZ respectively, compared to all other types of plastic studied. The char production was lowest in this case, 7.2 and 13.0% with AA-NZ and TA-NZ, respectively. Various studies also reported the lower production of char from the catalytic pyrolysis of PE (Xue et al., 2017). Lopez et al. (2011) reported that catalysts with high acidity enhanced the cracking of polymers during the catalytic pyrolysis. The increase in cracking, in the presence of a high acidic catalyst, promotes the production of gases (Miandad et al., 2016b, 2017a). Zeaiter (2014) carried out catalytic pyrolysis of PE with HBeta zeolite and reported 95.7% gas production due to the high acidity of the catalyst. Batool et al. (2016) also reported the maximum production of gas from catalytic pyrolysis of PE, with highly acidic ZSM-5 catalyst. According to Lee (2012) and Williams (2006), PE has a long chain carbon structure, and its degradation occurs randomly into smaller chain molecules via random chain scission, which may promote gas production. During the pyrolysis of PE, which holds the C-H and C-C bonds only, initially, macromolecule backbone breaking occurred and produced stable free-radicals. Further, the hydrogenation steps occurred, leading to the synthesis of secondary free-radicals (new stable C-H bond), which resulted into β-scission and produced an unsaturated group (Rizzarelli et al., 2016).

The catalytic pyrolysis of PP/PE (50/50% ratio) did not show any significant difference in the overall product yields when using both AA-NZ and TA-NZ. The liquid oil produced from the catalytic pyrolysis of PP/PE was 44 and 40% from TA-NZ and AA-NZ catalysts, respectively. A slight decrease in the liquid oil yield from AA-NZ could be due to its high acidity. Syamsiro et al. (2014) reported that AA-NZ with HCl has high acidity compared to TA-NZ, produced less liquid oil yield and had high production of gases. Overall catalytic pyrolysis of PP/PE produced the maximum amount of gas with low amounts of char. The high production of gas may be due to the presence of PP. The degradation of PP enhances the carbocation process due to the presence of tertiary carbon in its carbon chain (Jung et al., 2010). Furthermore, the degradation of PE in the presence of catalyst also favors the production of gas with a low yield of liquid oil. However, when PP and PE catalytic pyrolysis was carried out separately with PS, a significant difference was observed in the product yield.

There was a significant difference in the liquid oil yield of 54 and 34% for catalytic pyrolysis of PS/PP (50/50% ratio) with TA-NZ and AA-NZ catalysts, respectively. Similarly, a significant difference in the char yield of 20.3 and 35.2% was observed, whereas the high yield of gases were 25.7 and 30.8% using TA-NZ and AA-NZ catalysts, respectively. Lopez et al. (2011) and Seo et al. (2003) reported that a catalyst with high acidity promotes the cracking process and produces maximum gas production. Furthermore, the presence of PP also enhances gas production due to the carbocation process during degradation (Jung et al., 2010). Kim et al. (2002) reported that PP degradation produces maximum gas in the presence of acid catalysts.

The catalytic pyrolysis of PS with PE (50/50% ratio) in the presence of TA-NZ catalyst produced 44% liquid oil, however 52% liquid oil was obtained using the AA-NZ catalyst. Kiran et al. (2000) carried out pyrolysis of PS with PE at different ratios and reported that an increase in the concentration of PE decreased the liquid oil concentration with the increase in gas. The presence of PS with PE promotes the degradation process due to the production of an active stable benzene ring from PS (Miandad et al., 2016b). Wu et al. (2014) carried out TGA of PS with PE and observed two peaks, the first one for PS at a low temperature, followed by PE degradation at a high temperature. Moreover, PE degradation follows a free radical chain process and hydrogenation process, while PS follows a radical chain process including various steps (Kiran et al., 2000). Thus, even when considering the degradation phenomena, PS resulted in higher degradation compared to PE and produced stable benzene rings (McNeill et al., 1990).

Catalytic pyrolysis of PS/PE/PP (50/25/25% ratio) showed slightly lower liquid oil yields as compared to catalytic pyrolysis of all individual plastic types. The oil yield from both catalysts, TA-NZ and AA-NZ, in this case, is similar, 44 and 40%, respectively. The char production was higher (29.7%) with the AA-NZ catalyst than (19.0%) with the TA-NZ catalyst, which may be due to polymerization reactions (Wu and Williams, 2010). Furthermore, the addition of PET with PS, PE and PP (20/40/20/20% ratio) reduced the liquid oil yields down to 28 and 30% overall, using TA-NZ and AA-NZ catalysts, respectively, with higher fractions of char and gas. Demirbas (2004) carried out pyrolysis of PS/PE/PP and reported similar results for the

product yield. Adnan et al. (2014) carried out catalytic pyrolysis of PS and PET using he Al-Al_2O_3 catalyst with ratios of 80/20% and reported only 37% liquid oil. Moreover, Yoshioka et al. (2004) reported the maximum production of gas and char with negligible liquid oil production from catalytic pyrolysis of PET. In addition, maximum char production was also reported when PET catalytic pyrolysis was carried out with other plastics (Bhaskar et al., 2004). The higher production of char from PET pyrolysis was due to the carbonization and condensation reactions during its pyrolysis at a high temperature (Yoshioka et al., 2004). In addition, the presence of the oxygen atom also favors the high production of char from catalytic pyrolysis of PET (Xue et al., 2017). Thilakaratne et al. (2016) reported that production of benzene-free radicals, with two activated carbons, is the precursor of catalytic coke from PET degradation.

Effect of Catalysts on the Composition of Liquid Oil

The chemical composition of liquid oil produced by the catalytic pyrolysis of different plastic waste using TA-NZ and AA-NZ catalysts were characterized by GC-MS (**Figures 4**, **5**). The produced liquid oil composition is affected by different types of feedstock and catalysts used in the pyrolysis process (Miandad et al., 2016a,b,c). The liquid oil produced from the individual plastic types such as PS, PP and PE contained a mixture of aromatics, aliphatic and other hydrocarbon compounds. The aromatic compounds found in oil, from PS and PE, were higher than PP using the TA-NZ catalyst. The aromatic compounds increased in oil from PS and PP but reduced in PE when using the AA-NZ catalyst. The mesoporous and acidic catalyst leads to the production of shorter chain hydrocarbon due to its high cracking ability (Lopez et al., 2011). However, microporous and less acidic catalysts favor the production of long chain hydrocarbons as the cracking process occurred only on the outer surface of the catalysts. Overall, in the presence of catalysts, PE and PP follow the Random-chain scission mechanism, while PS follows the unzipping or end chain scission mechanism (Cullis and Hirschler, 1981; Peterson et al., 2001). The end-chain scission results in monomer production while random chain scission produces oligomers and monomers (Peterson et al., 2001).

The liquid oil produced from the catalytic pyrolysis of PE, when using both catalysts, produced mainly Naphthalene, Phenanthrene, Naphthalene, 2-ethenyl-, 1-Pentadecene, Anthracene, 2-methyl-, Hexadecane and so on (**Figures 4A**, **5A**). These results agree with several other studies (Lee, 2012; Xue et al., 2017). The production of a benzene derivate reveals that TA-NZ enhances the process of aromatization compared to AA-NZ. Xue et al. (2017) reported that intermediate olefins produced from catalytic pyrolysis of PE, further aromatized inside the pores of catalysts. Nevertheless, the aromatization reaction further leads to the production of hydrogen atoms that may enhance the aromatization process. Lee (2012) reported that ZSM-5 produced more aromatic compounds compare to the mordenite catalyst, due to its crystalline structure.

There are two possible mechanisms which may involve the degradation of PE in the presence of a catalyst; hybrid ion abstraction due to the presence of Lewis sites or, due to the carbenium ion mechanism via the addition of a proton (Rizzarelli et al., 2016). Initially, degradation starts on the external surface of the catalysts and later proceeds with further degradation in the inner pores of the catalysts (Lee, 2012). However, microporous catalysts hinder the entrance of larger molecules and thus higher carbon chain compounds are produced from catalytic pyrolysis of PE with microporous catalysts. In addition, in the presence of acidic catalysts, due to carbenium mechanism, the formation of aromatic and olefin compound production may increase (Lee, 2012). Lin et al. (2004) reported highly reactive olefin production, as intermediate products during the catalytic pyrolysis of PE, that may favor the production of paraffin and aromatic compounds in produced liquid oil. Moreover, the presence of an acidic catalyst and free hydrogen atom may lead to alkylation of toluene and benzene, converting intermediate alkylated benzene to the production of naphthalene due to aromatization (Xue et al., 2017).

The liquid oil produced from catalytic pyrolysis of PS with TA-NZ and AA-NZ, contains different kinds of compounds. Alpha-Methylstyrene, Benzene, 1,1′-(2-butene-1,4-diyl)bis-, Bibenzyl, Benzene, (1,3-propanediyl), Phenanthrene, 2-Phenylnaphthalene and so on were the major compounds found in the produced liquid oil (**Figures 4A**, **5A**). The liquid oil produced from catalytic pyrolysis of PS, with both activated catalysts, mainly contains aromatic hydrocarbons with some paraffins, naphthalene and olefin compounds (Rehan et al., 2017). However, in the presence of a catalyst, the maximum production of aromatic compounds was achieved (Xue et al., 2017). Ramli et al. (2011) also reported the production of olefins, naphthalene with aromatic compounds from catalytic pyrolysis of PS with Al_2O_3, supported with Cd and Sn catalysts. PS degradation starts with cracking on the outer surface of the catalyst and is then followed by reforming inside the pores of the catalyst (Uemichi et al., 1999). Initially, the cracking of polymer is carried out by the Lewis acid site on the surface of catalysts to produce carbocationic intermediates, which further evaporates or undergoes reforming inside the pores of the catalyst (Xue et al., 2017).

The catalytic pyrolysis of PS mainly produces styrene and its derivate as the major compounds in the produced liquid oil (Siddiqui and Redhwi, 2009; Rehan et al., 2017). Conversion of styrene into its derivate was increased in the presence of protonated catalysts due to hydrogenation (Kim et al., 2002). Shah and Jan (2015) and Ukei et al. (2000) reported that hydrogenation of styrene increased with the increase of the reaction temperature. Ogawa et al. (1982) carried out pyrolysis of PS with the alumina-silica catalyst at 300°C and found the hydrogenation of styrene to its derivate. Ramli et al. (2011) reported the possible degradation mechanism of PS on acid catalysts that may occur due to the attack of a proton associated with Bronsted acidic sites, resulting in the carbenium ion mechanism, which further undergoes β-scission and is later followed by hydrogen transfer. Moreover, cross-linking reaction was favored by strong Bronsted acidic sites and when this reaction occurred the completing cracking may decrease to some extent and enhance the production of char (Serrano et al.,

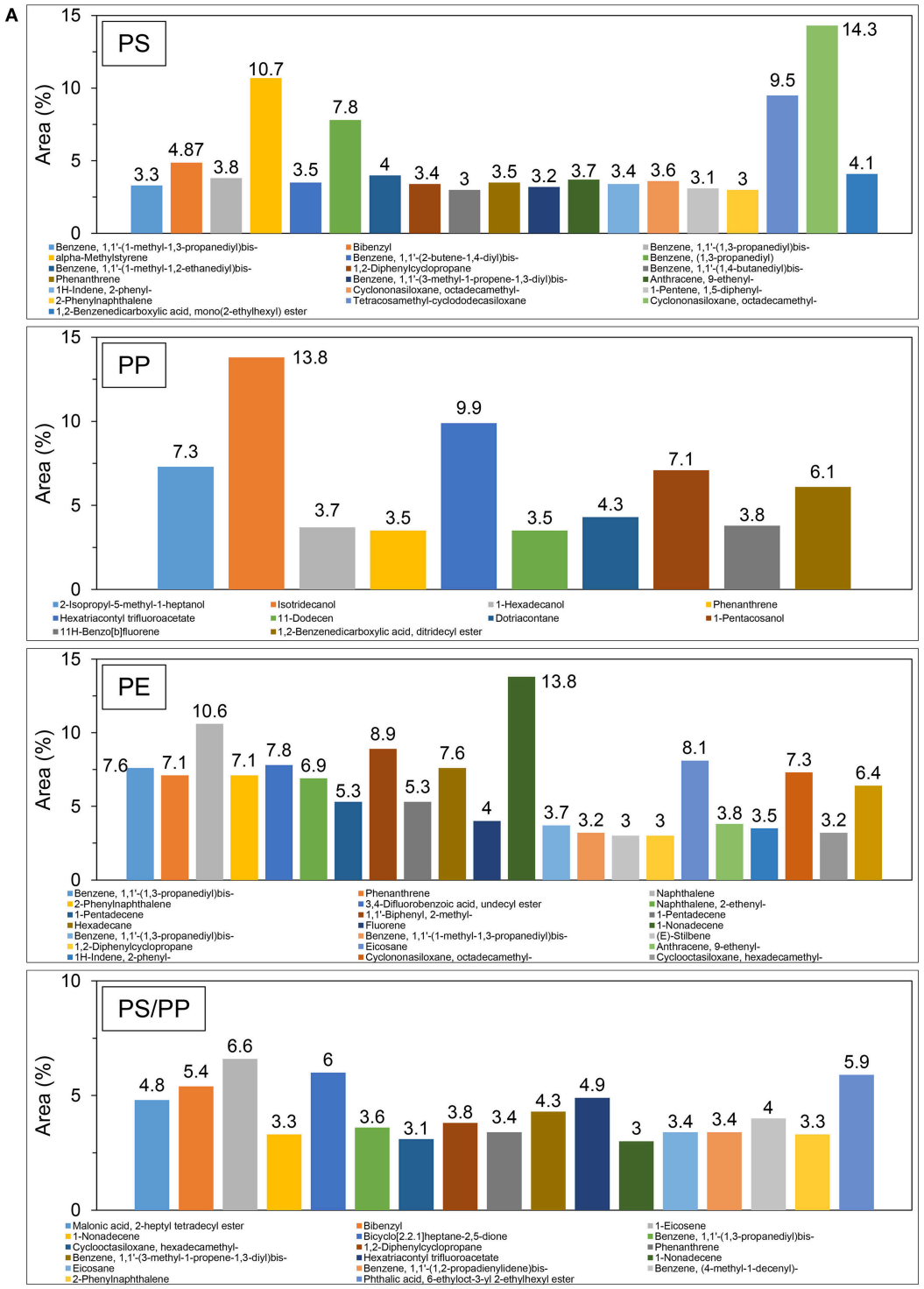

FIGURE 4 | Continued

2000). Furthermore, silica-alumina catalysts do not have strong Bronsted acidic sites, though it may not improve the cross-linking reaction but favor the hydrogenation process. Thus, it may be the reason that styrene was not found in the liquid oil, however, its derivate was detected at high quantities (Lee et al., 2001). Xue et al. (2017) also reported the dealkylation of styrene, due to the delay in evaporation inside the reactor, which may lead to an enhanced reforming process and result in the production of

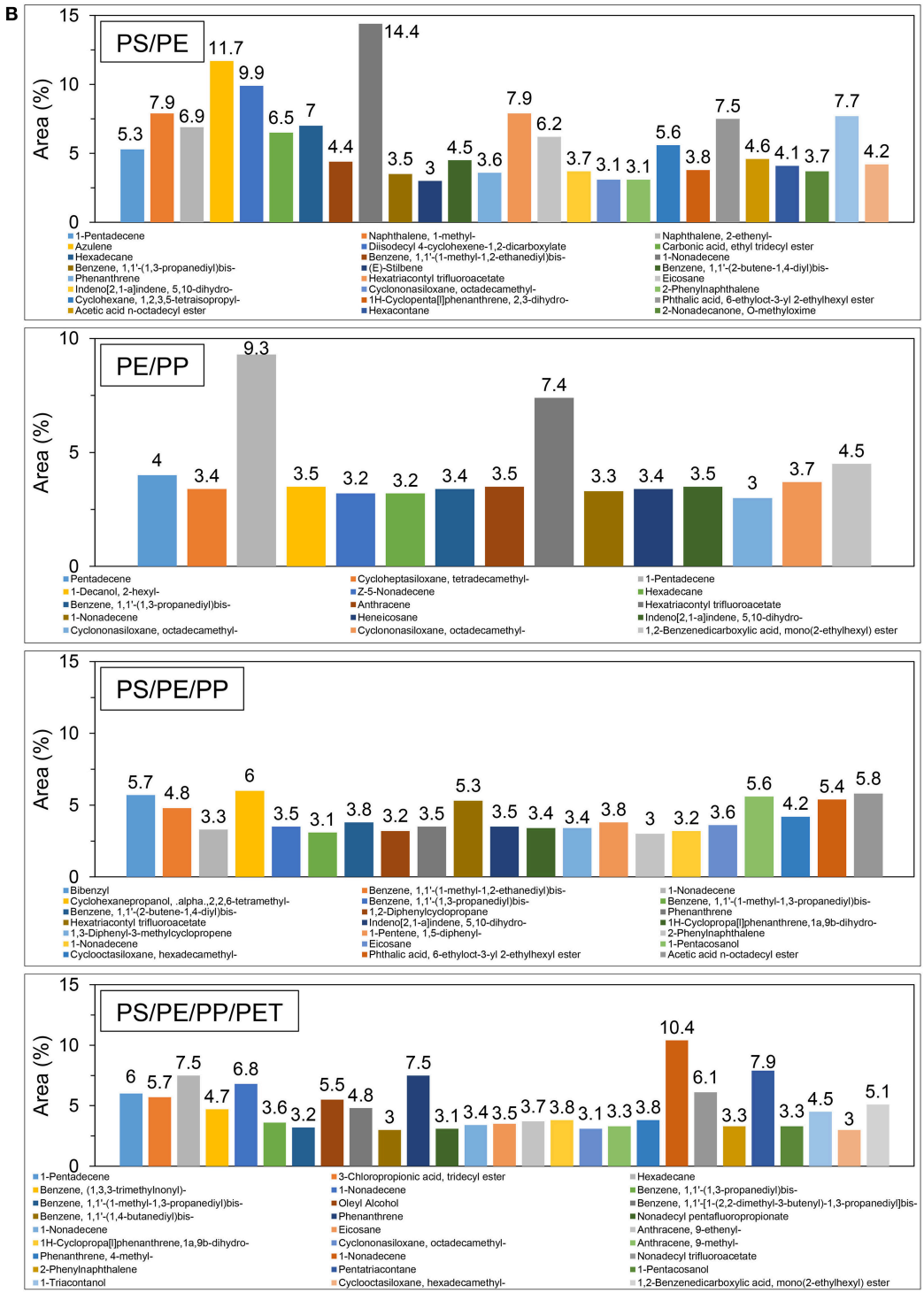

FIGURE 4 | (A,B) GC-MS of liquid oil produced from different types of plastic waste with TA-NZ.

a styrene derivate. TA-NZ and AA-NZ contain a high amount of alumina and silica that leads to the hydrogenation of styrene to its derivate, resulting in the production of styrene monomers instead of styrene.

The catalytic pyrolysis of PP produced a complex mixture of liquid oil containing aromatics, olefins and naphthalene compounds. Benzene, 1,1′-(2-butene-1,4-diyl)bis-, benzene, 1,1′-(1,3-propanediyl)bis-, anthracene, 9-methyl-, naphthalene,

2-phenyl-, 1,2,3,4-tetrahydro-1-phenyl-, naphthalene, phenanthrene etc. were the major compounds found in the liquid oil (**Figures 4A**, **5A**). These findings are in line with other studies that carried out catalytic pyrolysis of PP with various catalysts (Marcilla et al., 2004). Furthermore, degradation of PP with AA-NZ resulted in the maximum production of phenol compounds. The higher production was perhaps due to the presence of high acidic sites, as it favors phenol compound production. Moreover, the presence of a high acidic site on catalysts enhanced the oligomerization, aromatization and deoxygenation mechanism that led to the production of poly-aromatic and naphthalene compounds. Dawood and Miura (2002) also reported the high production of these compounds from the catalytic pyrolysis of PP with a high acidic modified HY-zeolite.

The composition of oil from the catalytic pyrolysis of PP with PE contains compounds found in the oil from both individual plastic type feedstocks. Miandad et al. (2016b) reported that feedstock composition also affects the quality and chemical composition of the oil. The produced liquid oil from catalytic pyrolysis of PE/PP contains aromatic, olefin, and naphthalene compounds. The major compounds found were; benzene, 1,1′-(1,3-propanediyl)bis-, mono(2-ethylhexyl) ester, 1,2-benzenedicarboxylic acid, anthracene, pentadecane, phenanthrene, 2-phenylnaphthalene and so on (**Figures 4B**, **5B**). Jung et al. (2010) reported that the aromatic production from PP/PE catalytic pyrolysis might follow the Diels–Alder reaction mechanism and is then followed by dehydrogenation. Furthermore, catalytic pyrolysis of PP and PE carried out individually with PS, mainly produced aromatic compounds due to the presence of PS. The produced liquid oil from PS/PP contains benzene, 1,1′-(1,3-propanediyl)bis, 1,2-benzenedicarboxylic acid, disooctyl ester, bibenzyl, phenanthrene, 2-phenylnaphthalene, benzene, (4-methyl-1-decenyl)- and so on (**Figures 4A**, **5A**). PS catalytic pyrolysis with PE mainly produced liquid oil with major compounds of azulene, naphthalene, 1-methyl-, naphthalene, 2-ethenyl, benzene, 1,1′-(1,3-propanediyl)bis-, phenanthrene, 2-phenylnaphthalene, benzene, 1,1′-(1-methyl-1,2-ethanediyl)bis- and some other compounds as well (**Figures 4B**, **5B**). Miskolczi et al. (2006) carried out pyrolysis of PS with PE with a ratio of 10 and 90%, respectively, and reported the maximum production of aromatics even at a very low ratio of PS. Miandad et al. (2016b) reported that thermal pyrolysis of PE with PS without a catalyst, resulted in the conversion of PE into liquid oil with a high composition of aromatics. However thermal pyrolysis of the only PE without a catalyst converted it into wax instead of liquid oil due to its strong long chain branched structure (Lee, 2012; Miandad et al., 2016b). Wu et al. (2014) carried out TGA of PS with PE and reported that the presence of PS favors the degradation of PE, due to the production of stable benzene rings.

The chemical composition of pyrolysis oil, by different functional groups, was studied using FT-IR. The obtained data revealed the presence of aromatics and aliphatic functional groups in the oil (**Figures 6**, **7**). A very strong peak at 696 cm^{-1} was observed in most of the liquid oils obtained using both catalysts, which corresponds to the high concentration of aromatic compounds. Two more peaks, that are obvious, were visible at around 1,456 and 1,495 cm^{-1} for C-C with single and double bonds, corresponding to aromatic compounds. Furthermore, at the end of the spectrum, strong peaks at 2,850, 2,923, and 2,958 cm^{-1} were observed in all types of liquid oils except the PS, corresponding to the C-H stretch of alkanes compounds. Overall, the liquid oil obtained from catalytic pyrolysis of different plastic waste using the AA-NZ catalyst, showed more peaks than the samples from the TA-NZ catalysts. These extra peaks corresponded to aromatics, alkanes and alkene compounds. This indicates that, as expected, the AA-NZ had better catalytic properties than the TA-NZ. Various researchers have reported similar results, that liquid oil produced from PS was dominant with aromatics. Tekin et al. (2012) and Panda and Singh (2013) also reported the presence of aromatics with some alkanes and alkenes from catalytic pyrolysis of PP. Kunwar et al. (2016) carried out the thermal and catalytic pyrolysis of PE and reported that produced liquid oil contained alkanes and alkenes as a major functional group. Overall, the FT-IR analysis provided more insight into the chemical composition of liquid oil produced, from catalytic pyrolysis of different plastic waste, using modified NZ catalysts and further confirmed our GC-MS results.

Potential Applications of Pyrolysis Products

The liquid oil produced from the catalytic pyrolysis of different types of plastic feedstock has a high number of aromatic, olefin, and naphthalene compounds that are found in petroleum products. Moreover, the HHV of the produced liquid oil has been found in the range of 41.7–44.2 MJ/kg (**Table 2**) which is very close to the energy value of conventional diesel. The lowest HHV of 41.7 MJ/ kg was found in liquid oil obtained from PS using the TA-NZ catalyst, whereas the highest HHV of 44.2 MJ/kg was from PS/PE/PP using the AA-NZ catalyst. Thus, the pyrolysis liquid oil produced from various plastic wastes has the potential to be used as an alternative source of energy. According to Lee et al. (2015) and Rehan et al. (2016), the production of electricity is achievable using pyrolysis liquid oil in a diesel engine. Saptoadi and Pratama (2015) successfully used pyrolytic liquid oil as an alternative in a kerosene stove. Moreover, the produced aromatic compounds can be used as raw material for polymerization in various chemical industries (Sarker and Rashid, 2013; Shah and Jan, 2015). Furthermore, various researchers utilized the produced liquid oil as transportation fuel after blending with conventional diesel at different ratios. The studies were carried out to explore the potential of produced liquid oil in the context of engine performance and vehicle exhaust emission. Nileshkumar et al. (2015) and Lee et al. (2015) reported that 20:80% blend ratio of pyrolytic liquid oil and conventional diesel, respectively, gave similar engine performance results than conventional diesel. Moreover, at the same blended ratio the exhaust emissions were also similar, however the exhaust emissions increased with the increase in the blended amount of pyrolysis oil (Frigo et al., 2014; Mukherjee and Thamotharan, 2014).

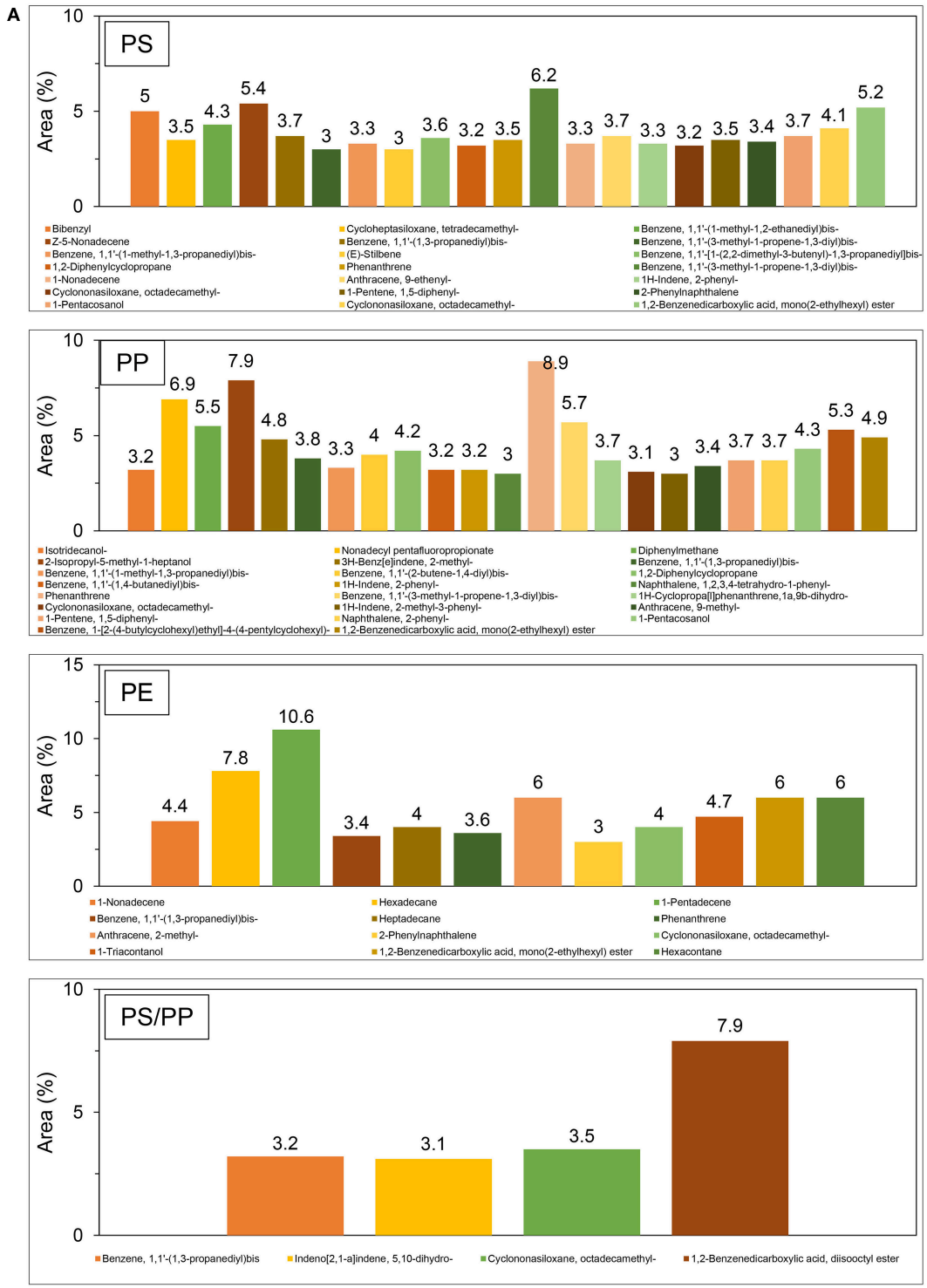

FIGURE 5 | Continued

The residue (char) left after the pyrolysis process can be utilized for several environmental applications. Several researchers activated the char via steam and thermal activation (Lopez et al., 2009; Heras et al., 2014). The activation process increased the BET surface area and reduced the pore size of the char (Lopez et al., 2009). Furthermore, Bernando (2011)

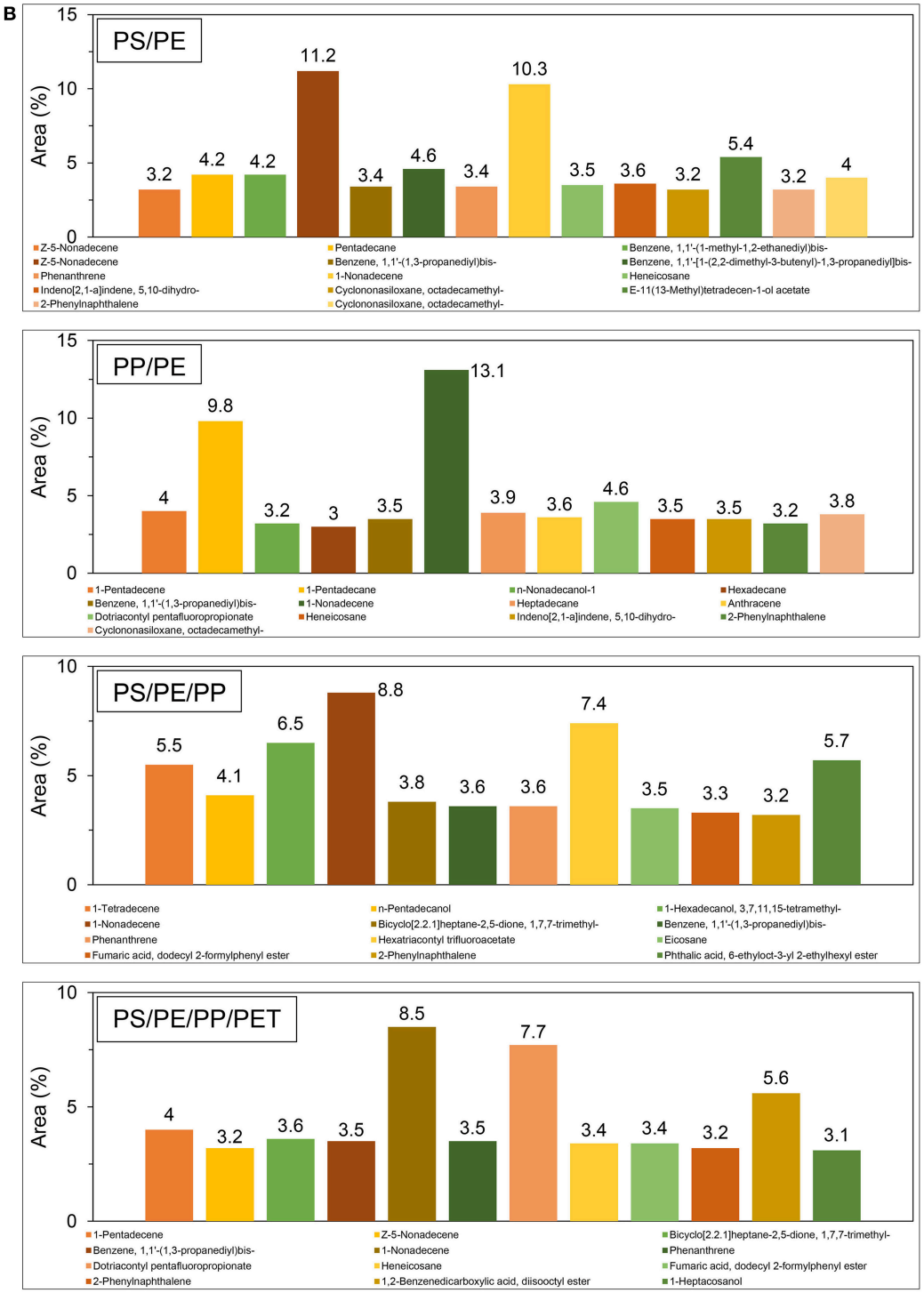

FIGURE 5 | (A,B) GC-MS of liquid oil produced from different types of plastic waste with AA-NZ.

upgraded the plastic char with biomaterial and carried out the adsorption (3.6–22.2 mg/g) of methylene blue dye from wastewater. Miandad et al. (2018) used the char obtained from pyrolysis of PS plastic waste to synthesize a novel carbon-metal double-layered oxides (C/MnCuAl-LDOs) nano-adsorbent for the adsorption of Congo red (CR) in wastewater. Furthermore, the char can be used as a raw material for the production of activated carbon as well.

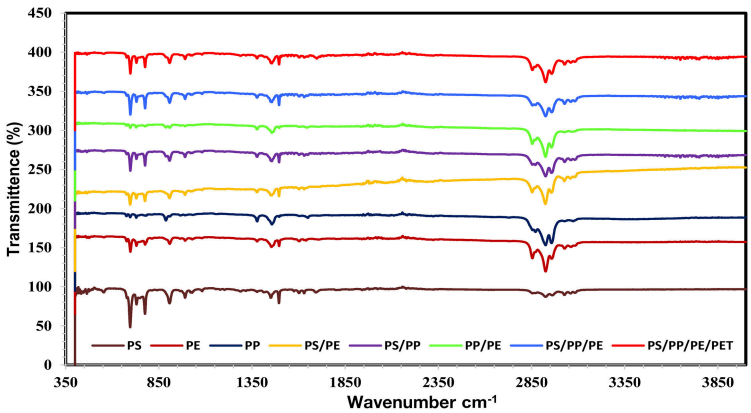

Peaks	PS	PP	PE	PS/PP	PS/PE	PE/PP	PS/PP/PE	PS/PP/PE/PET	Bond	Functional Group
696	✓	✓	✓	X	✓	X	X	X	C-H "oop"	Aromatics
1456	✓	✓	✓	✓	✓	✓	✓	✓	C-C stretch (in ring)	Aromatics
1495	✓	X	X	X	✓	X	X	X	ring C=C stretch	Aromatics
2850	X	X	✓	✓	✓	✓	X	✓	C-H stretch	Alkanes
2923	✓	✓	✓	✓	✓	✓	✓	✓	C-H stretch	Alkanes
2958	X	✓	X	✓	X	✓	✓	✓	C-H stretch	Alkanes

FIGURE 6 | FT-IR analysis of liquid oil produced from catalytic pyrolysis with TA-NZ.

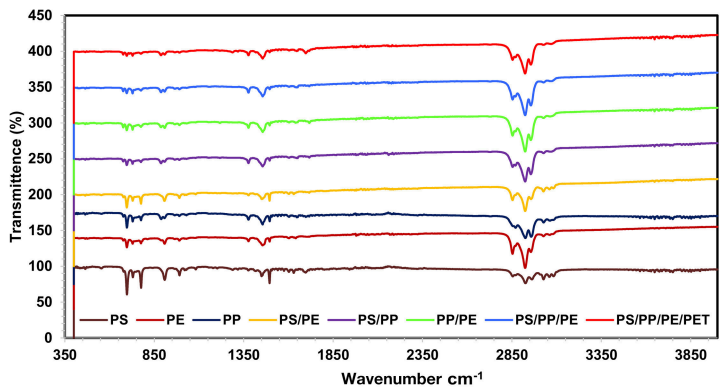

Peaks	PS	PP	PE	PS/PP	PS/PE	PE/PP	PS/PP/PE	PS/PP/PE/PET	Bond	Functional Group
696	✓	X	✓	✓	✓	X	✓	✓	C-H "oop"	Aromatics
776	✓	X	✓	✓	✓	X	✓	✓	=C-H bend	Alkenes
905	✓	✓	X	✓	X	X	✓	✓	=C-H bend	Alkenes
1375	X	X	X	X	X	X	X	X	=C-H bend	Alkenes
1452	X	X	✓	✓	X	X	✓	✓	C-C stretch (in ring)	Aromatics
1466	X	✓	X	X	X	X	X	X	ring C=C stretch	Aromatics
1495	✓	✓	✓	✓	✓	✓	✓	✓	ring C=C stretch	Aromatics
2850	X	✓	✓	✓	✓	✓	X	✓	C-H stretch	Alkanes
2923	X	✓	✓	✓	✓	✓	✓	✓	C-H stretch	Alkanes
2958	X	X	✓	✓	✓	✓	✓	✓	C-H stretch	Alkanes

FIGURE 7 | FT-IR analysis of liquid oil produced from catalytic pyrolysis with AA-NZ.

TABLE 2 | High Heating Values (HHV) of pyrolysis oil from various feedstocks using TA-NZ and AA-NZ catalysts.

Feedstock	TA-NZ (MJ/kg)	AA-NZ (MJ/kg)
PS	41.7	42.1
PP	43.4	42.9
PE	42.9	43.5
PS/PP	42.5	42.9
PS/PE	42.6	43.7
PP/PE	44.1	43.7
PS/PE/PP	42.4	44.2
PS/PE/PP/PET	41.9	43.7

Limitations of GC-MS Analysis of Pyrolysis Oil

There are some limitations in conducting the accurate quantitative analysis of chemical components in pyrolysis oil using GC-MS. In this study, we used the mass percentage of different chemicals found in oil samples, calculated based on the peak areas identified by a normal phase DP5-MS column and FID. The identified peaks were matched with the NIST and mass bank spectra library. The compounds were chosen based on the similarity index (SI $>$ 90%). Further comparison with known (CRM) standards enabled confirmation of the identified compounds. The used column and detectors were limited only with hydrocarbons. In reality however, oil from most plastic waste has a complex chemical structure and may contain other groups of unidentified chemicals such as sulfur, nitrogen, and oxygen-containing hydrocarbons. This is why a more in-depth and accurate qualitative chemical analysis is needed to fully understand the chemistry of pyrolysis oil, using advanced calibration and standardization and using different MS detectors like SCD and NCD as well as different GC columns.

The Potential and Challenges of Pyrolysis Based Biorefineries

Waste biorefineries are attracting tremendous attention as a solution to convert MSW and other biomass waste into a range of products such as fuels, power, heat and other valuable chemicals and materials. Different types of biorefineries, such as an agriculture-based biorefinery, animal waste biorefinery, wastewater biorefinery, algae-based biorefinery, plastic waste refinery, forestry-based biorefinery, industrial waste biorefinery, and Food waste biorefinery etc., can be developed depending on the type and source of waste (Gebreslassie et al., 2013; De Wild et al., 2014; Nizami et al., 2017a,b; Waqas et al., 2018). These biorefineries can play a significant role to reduce waste-related environmental pollution and GHG emissions. Furthermore, they generate substantial economic benefits and can help achieve a circular economy in any country.

A pyrolysis based biorefinery can be developed to treat a range of biomass waste and plastic waste to produce liquid and gas fuels, energy, biochar, and other higher value chemicals using an integrated approach. The integrated approach helps to achieve maximum economic and environmental benefits with minimal waste production. There are many challenges and room for improvement in pyrolysis-based biorefineries, that need to be addressed and optimized to ensure maximum benefits. Although pyrolysis oil holds more energy than coal and some other fuels, pyrolysis itself is an energy-intensive process, and the oil product requires more energy to be refined (Inman, 2012). This means that pyrolysis oil may not be much better than conventional diesel or other fossil-based fuels in terms of GHG emissions, though much detailed research studies on mass and energy balance across the whole process's boundaries are needed to confirm this. To overcome these process energy requirements, more advanced technologies can be developed using the integration of renewable energies such as solar or hydro with pyrolysis-based biorefineries, to achieve maximum economic and environmental benefits.

The availability of plastic and biomass waste streams as feedstocks for pyrolysis based biorefineries, is another major challenge, since recycling is not currently very efficient, especially in the developing countries. The gases produced from pyrolysis of some plastic waste such as PVC are toxic, and therefore pyrolysis emission treatment technology has to be further refined to achieve maximum environmental benefits. The pyrolysis oil obtained from various plastic types need to be cleaned significantly before it is used in any application, to ensure minimal environmental impact. The high aromatic contents of the pyrolysis oil is good and some aromatic compounds such as benzene, toluene, and styrene can be refined and sold in an already established market. However, some of the aromatic hydrocarbons are known carcinogens and can cause serious human health and environmental damage. Serious consideration is therefore needed in this regard.

Other aspects for optimization of pyrolysis based biorefineries, such as new emerging advanced catalysts including nano-catalysts, have to be developed and applied in pyrolysis processes in order to increase the quality and yield of products, and to optimize the overall process. The market for pyrolysis based biorefinery products should be created/ expanded to attract further interest and funding, in order to make this concept more practical and successful. Similarly, more focus is needed to conduct further research and development work on enriching the biorefinery concept and to tap into its true potential. Furthermore, it is vital to conduct a detailed economic and environmental impact assessment of biorefineries during a design stage, using specialized tools such as the life-cycle assessment (LCA). The LCA can analyze the environmental impact of the biorefinery and all products by conducting detailed energy and material balances of all life stages including raw material extraction and processing, manufacturing, product distribution, use, maintenance, and disposal/recycling. The outcomes of LCA will help to determine the sustainability of biorefineries, which is crucial in making the right decision.

CONCLUSIONS

Catalytic pyrolysis is a promising technique to convert plastic waste into liquid oil and other value-added products, using a modified natural zeolite (NZ) catalyst. The modification of NZ catalysts was carried out by novel thermal (TA) and acidic (AA) activation that enhanced their catalytic properties. The catalytic pyrolysis of PS produced the highest liquid oil (70 and 60%) compared to PP (40 and 54%) and PE (40 and 42%), using the TA-NZ and AA-NZ catalysts, respectively. The chemical composition of the pyrolysis oil was analyzed using GC-MS, and it was found that most of the liquid oil produced a high aromatic content with some aliphatic and other hydrocarbon compounds. These results were further confirmed by the FT-IR analysis showing clear peaks corresponding to aromatic and other hydrocarbon functional groups. Furthermore, liquid oil produced from different types of plastic waste had higher heating values (HHV) in the range of 41.7–44.2 MJ/kg similar to that of conventional diesel. Therefore, it has the potential to be used in various energy and transportation applications after further treatment and refining. This study is a step toward developing pyrolysis-based biorefineries. Biorefineries have a great potential to convert waste into energy and other valuable products and could help to achieve circular economies. However, there are many technical, operational, and socio-economic challenges, as discussed above, that need to be overcome in order to achieve the maximum economic and environmental benefits of biorefineries.

DATA AVAILABILITY

All datasets generated for this study are included in the manuscript and/or the supplementary files.

AUTHOR CONTRIBUTIONS

RM performed the pyrolysis experiments and helped in manuscript write up. HK, JD, JG, and AH have carried out the detailed characterization of the process products. MR and ASA have analyzed the data and written parts of the manuscript. MAB, MR, and A-SN have corrected and edited the manuscript. ASA and IMII supported the project financially and technically.

ACKNOWLEDGMENTS

MR and A-SN acknowledge the Center of Excellence in Environmental Studies (CEES), King Abdulaziz University (KAU), Jeddah, KSA and the Ministry of Education, KSA for financial support under Grant No. 2/S/1438. Authors are also thankful to Deanship of Scientific Research (DSR) at KAU for their financial and technical support to CEES.

REFERENCES

Adnan, A., Shah, J., and Jan, M. R. (2014). Polystyrene degradation studies using Cu supported catalysts. *J. Anal. Appl. Pyrol.* 109, 196–204. doi: 10.1016/j.jaap.2014.06.013

Aguado, J., Sotelo, J. L., Serrano, D. P., Calles, J. A., and Escola, J. M. (1997). Catalytic conversion of polyolefins into liquid fuels over MCM-41: comparison with ZSM-5 and amorphous SiO2–Al_2O_3. *Ener fuels* 11, 1225–1231. doi: 10.1021/ef970055v

Alexandra, L. C. (2012). *Municipal Solid Waste: Turning a Problem Into Resourceewaste: The Challenges Facing Developing Countries, Urban Specialist*. World Bank. 2–4 p.

Batool, M., Shah, A. T., Imran Din, M., and Li, B. (2016). Catalytic pyrolysis of low density polyethylene using cetyltrimethyl ammonium encapsulated monovacant keggin units and ZSM-5. *J. Chem.* 2016:2857162. doi: 10.1155/2016/2857162

Bernando, M. (2011). "Physico-chemical characterization of chars produced in the co-pyrolysis of wastes and possible routes of valorization," in *Chemical Engineering* (Lisboa: Universidade Nova de Lisboa), 27–36.

Bhaskar, T., Kaneko, J., Muto, A., Sakata, Y., Jakab, E., Matsui, T., et al. (2004). Pyrolysis studies of PP/PE/PS/PVC/HIPS-Br plastics mixed with PET and dehalogenation (Br, Cl) of the liquid products. *J. Anal. Appl. Pyrolysis* 72, 27–33. doi: 10.1016/j.jaap.2004.01.005

Chandrasekaran, S. R., Kunwar, B., Moser, B. R., Rajagopalan, N., and Sharma, B. K. (2015). Catalytic thermal cracking of postconsumer waste plastics to fuels. 1. Kinetics and optimization. *Energy Fuels* 29, 6068–6077. doi: 10.1021/acs.energyfuels.5b01083

Cullis, C. F., and Hirschler, M. M. (1981). *The Combustion of Organic Polymers*. Vol. 5. London: Oxford University Press.

Dawood, A., and Miura, K. (2002). Catalytic pyrolysis of c-irradiated polypropylene (PP) over HY-zeolite for enhancing the reactivity and the product selectivity. *Polym. Degrad. Stab.* 76, 45–52. doi: 10.1016/S0141-3910(01)00264-6

De Wild, P. J., Huijgen, W. J., and Gosselink, R. J. (2014). Lignin pyrolysis for profitable lignocellulosic biorefineries. *Biofuels Bioprod. Biorefining* 8, 645–657. doi: 10.1002/bbb.1474

Demirbas, A. (2004). Pyrolysis of municipal plastic wastes for recovery of gasoline-range hydrocarbons. *J. Anal. Appl. Pyrolysis* 72, 97–102. doi: 10.1016/j.jaap.2004.03.001

Dimitrov, N., Krehula, L. K., Siročić, A. P., and Hrnjak-Murgić, Z. (2013). Analysis of recycled PET bottles products by pyrolysis-gas chromatography. *Polym. Degrad. Stab.* 98, 972–979. doi: 10.1016/j.polymdegradstab.2013.02.013

Dziecioł, M., and Trzeszczynski, J. (2000). Volatile products of poly (ethylene terephthalate) thermal degradation in nitrogen atmosphere. *J. Appl. Polym. Sci.* 77, 1894–1901. doi: 10.1002/1097-4628(20000829)77:9<1894::AID-APP5>3.0.CO;2-Y

Frigo, S., Seggiani, M., Puccini, M., and Vitolo, S. (2014). Liquid fuel production from waste tyre pyrolysis and its utilisation in a Diesel engine. *Fuel* 116, 399–408. doi: 10.1016/j.fuel.2013.08.044

Gaca, P., Drzewiecka, M., Kaleta, W., Kozubek, H., and Nowinska, K. (2008). Catalytic degradation of polyethylene over mesoporous molecular sieve MCM-41 modified with heteropoly compounds. *Polish J. Environ. Stud.* 17, 25–35.

Gandidi, I. M., Susila, M. D., Mustofa, A., and Pambudi, N. A. (2018). Thermal–Catalytic cracking of real MSW into Bio-Crude Oil. *J. Energy Inst.* 91, 304–310. doi: 10.1016/j.joei.2016.11.005

Gebreslassie, B. H., Slivinsky, M., Wang, B., and You, F. (2013). Life cycle optimization for sustainable design and operations of hydrocarbon biorefinery via fast pyrolysis, hydrotreating and hydrocracking. *Comput. Chem. Eng.* 50, 71–91. doi: 10.1016/j.compchemeng.2012.10.013

Heras, F., Jimenez-Cordero, D., Gilarranz, M. A., Alonso-Morales, N., and Rodriguez, J. J. (2014). Activation of waste tire char by cyclic liquid-phase oxidation. *Fuel Process. Technol.* 127, 157–162. doi: 10.1016/j.fuproc.2014.06.018

Inman, M. (2012). Cooking up fuel. *Nat. Clim. Change* 2, 218–220. doi: 10.1038/nclimate1466

Jung, S. H., Cho, M. H., Kang, B. S., and Kim, J. S. (2010). Pyrolysis of a fraction of waste polypropylene and polyethylene for the recovery of BTX

aromatics using a fluidized bed reactor. *Fuel Process. Technol.* 91, 277–284. doi: 10.1016/j.fuproc.2009.10.009

Kim, H. S., Kim, S., Kim, H. J., and Yang, H. S. (2006). Thermal properties of bio-flour-filled polyolefin composites with different compatibilizing agent type and content. *Thermochim. Acta* 451, 181–188. doi: 10.1016/j.tca.2006.09.013

Kim, J. R., Yoon, J. H., and Park, D. W. (2002). Catalytic recycling of the mixture of polypropylene and polystyrene. *Polym. Degrad. Stab.* 76, 61–67. doi: 10.1016/S0141-3910(01)00266-X

Kiran, N., Ekinci, E., and Snape, C. E. (2000). Recyling of plastic wastes via pyrolysis. *Resour. Conserv. Recycl.* 29, 273–283. doi: 10.1016/S0921-3449(00)00052-5

Kunwar, B., Moser, B. R., Chandrasekaran, S. R., Rajagopalan, N., and Sharma, B. K. (2016). Catalytic and thermal depolymerization of low value post-consumer high density polyethylene plastic. *Energy* 111, 884–892. doi: 10.1016/j.energy.2016.06.024

Lecomte, H. A., and Liggat, J. J. (2006). Degradation mechanism of diethylene glycol units in a terephthalate polymer. *Polym. Degrad. Stab.* 91, 681–689. doi: 10.1016/j.polymdegradstab.2005.05.028

Lee, K. H. (2012). Effects of the types of zeolites on catalytic upgrading of pyrolysis wax oil. *J. Anal. Appl. Pyrol.* 94, 209–214. doi: 10.1016/j.jaap.2011.12.015

Lee, S., Yoshida, K., and Yoshikawa, K. (2015). Application of waste plastic pyrolysis oil in a direct injection diesel engine: For a small scale non-grid electrification. *Energy Environ. Res.* 5:18. doi: 10.5539/eer.v5n1p18

Lee, S. Y., Yoon, J. H., Kim, J. R., and Park, D. W. (2001). Catalytic degradation of polystyrene over natural clinoptilolite zeolite. *Polym. Degrad. Stab.* 74, 297–305. doi: 10.1016/S0141-3910(01)00162-8

Lin, Y. H., Yang, M. H., Yeh, T. F., and Ger, M. D. (2004). Catalytic degradation of high density polyethylene over mesoporous and microporous catalysts in a fluidised-bed reactor. *Polym. Degrad. Stab.* 86, 121–128. doi: 10.1016/j.polymdegradstab.2004.02.015

Lopez, A., Marco d, I., Caballero, B. M., Laresgoiti, M. F., Adrados, A., and Torres, A. (2011). Pyrolysis of municipal plastic waste II: influence of raw material composition under catalytic conditions. *Waste Manag.* 31, 1973–1983. doi: 10.1016/j.wasman.2011.05.021

Lopez, G., Olazar, M., Artetxe, M., Amutio, M., Elordi, G., and Bilbao, J. (2009). Steam activation of pyrolytic tyre char at different temperatures. *J. Anal. Appl. Pyrol.* 85, 539–543. doi: 10.1016/j.jaap.2008.11.002

Ma, C., Yu, J., Wang, B., Song, Z., Xiang, J., Hu, S., et al. (2017). Catalytic pyrolysis of flame retarded high impact polystyrene over various solid acid catalysts. *Fuel Process. Technol.* 155, 32–41. doi: 10.1016/j.fuproc.2016.01.018

Marcilla, A., Beltrán, M. I., Hernández, F., and Navarro, R. (2004). HZSM5 and HUSY deactivation during the catalytic pyrolysis of polyethylene. *Appl. Catal. A Gen.* 278, 37–43. doi: 10.1016/j.apcata.2004.09.023

McNeill, I. C., and Bounekhel, M. (1991). Thermal degradation studies of terephthalate polyesters: 1. *Poly (alkylene terephthalates). Polymer Degrad. Stab.* 34, 187–204. doi: 10.1016/0141-3910(91)90119-C

McNeill, I. C., Zulfiqar, M., and Kousar, T. (1990). A detailed investigation of the products of the thermal degradation of polystyrene. *Polym. Degrad. Stab.* 28, 131–151. doi: 10.1016/0141-3910(90)90002-O

Miandad, R., Barakat, M. A., Aburiazaiza, A. S., Rehan, M., Ismail, I. M. I., and Nizami, A. S. (2017b). Effect of plastic waste types on pyrolysis liquid oil. *Int. Biodeterior. Biodegrad.* 119, 239–252. doi: 10.1016/j.ibiod.2016.09.017

Miandad, R., Barakat, M. A., Aburiazaiza, A. S., Rehan, M., and Nizami, A. S. (2016a). Catalytic pyrolysis of plastic waste: a review. *Process Safety Environ. Protect.* 102, 822–838. doi: 10.1016/j.psep.2016.06.022

Miandad, R., Barakat, M. A., Rehan, M., Aburiazaiza, A. S., Ismail, I. M. I., and Nizami, A. S. (2017a). Plastic waste to liquid oil through catalytic pyrolysis using natural and synthetic zeolite catalysts. *Waste Manag.* 69, 66–78. doi: 10.1016/j.wasman.2017.08.032

Miandad, R., Kumar, R., Barakat, M. A., Basheer, C., Aburiazaiza, A. S., Nizami, A. S. et al. (2018). Untapped conversion of plastic waste char into carbon-metal LDOs for the adsorption of Congo red. *J Colloid Interface Sci.* 511, 402–410. doi: 10.1016/j.jcis.2017.10.029

Miandad, R., Nizami, A. S., Rehan, M., Barakat, M. A., Khan, M. I., Mustafa, A., et al. (2016b). Influence of temperature and reaction time on the conversion of polystyrene waste to pyrolysis liquid oil. *Waste Manag.* 58, 250–259. doi: 10.1016/j.wasman.2016.09.023

Miandad, R., Rehan, M., Nizami, A. S., Barakat, M. A. E. F., and Ismail, I. M. (2016c). "The energy and value- added products from pyrolysis of waste plastics," in *Recycling of Solid Waste for Biofuels and Bio- Chemicals*, eds O. P. Karthikeyan, K. H. Subramanian, and S. Muthu (Singapore: Springer), 333–355.

Miskolczi, N., Bartha, L., and Deak, G. (2006). Thermal degradation of polyethylene and polystyrene from the packaging industry over different catalysts into fuel-like feed stocks. *Polym. Degrad. Stab.* 91, 517–526. doi: 10.1016/j.polymdegradstab.2005.01.056

Mukherjee, M. K., and Thamotharan, P. C. (2014). Performance and emission test of several blends of waste plastic oil with diesel and ethanol on four stroke twin cylinder diesel engine. *IOSR J. Mech. Civil Eng.* 11, 2278–1684. doi: 10.9790/1684-11214751

Nileshkumar, K. D., Jani, R. J., Patel, T. M., and Rathod, G. P. (2015). Effect of blend ratio of plastic pyrolysis oil and diesel fuel on the performance of single cylinder CI engine. *Int. J. Sci. Technol. Eng.* 1, 2349–2784.

Nizami, A. S., Ouda, O. K. M., Rehan, M., El-Maghraby, A. M. O., Gardy, J., Hassanpour, A., et al. (2016). The potential of Saudi Arabian natural zeolites in energy recovery technologies. *Energy* 108, 162–171. doi: 10.1016/j.energy.2015.07.030

Nizami, A. S., Rehan, M., Waqas, M., Naqvi, M., Ouda, O. K. M., Shahzad, K., et al. (2017a). Waste biorefineries: enabling circular economies in developing countries. *Bioresour. Technol.* 241, 1101–1117. doi: 10.1016/j.biortech.2017.05.097

Nizami, A. S., Shahzad, K., Rehan, M., Ouda, O. K. M., Khan, M. Z., Ismail, I. M. I., et al. (2017b). Developing waste biorefinery in makkah: a way forward to convert urban waste into renewable energy. *Appl. Energy.* 186, 189–196. doi: 10.1016/j.apenergy.2016.04.116

Obali, Z., Sezgi, N. A., and Doğu, T. (2012). Catalytic degradation of polypropylene over alumina loaded mesoporous catalysts. *Chem. Eng. J.* 207, 421–425. doi: 10.1016/j.cej.2012.06.146

Ogawa, T., Kuroki, T., Ide, S., and Ikemura, T. (1982). Recovery of indan derivatives from polystyrene waste. *J. Appl. Polym. Sci.* 27, 857–869. doi: 10.1002/app.1982.070270306

Panda, A. K., and Singh, R. K. (2013). Experimental optimization of process for the thermo-catalytic degradation of waste polypropylene to liquid fuel. *Adv. Energy Eng.* 1, 74–84.

Peterson, J. D., Vyazovkin, S., and Wight, C. A. (2001). Kinetics of the thermal and thermo-oxidative degradation of polystyrene, polyethylene and poly (propylene). *Macromol. Chem. Phys.* 202, 775–784. doi: 10.1002/1521-3935(20010301)202:6<775::AID-MACP775>3.0.CO;2-G

Ramli, M. R., Othman, M. B. H., Arifin, A., and Ahmad, Z. (2011). Cross-link network of polydimethylsiloxane via addition and condensation (RTV) mechanisms. Part I: synthesis and thermal properties. *Polym. Degrad. Stab.* 96, 2064–2070. doi: 10.1016/j.polymdegradstab.2011.10.001

Ratnasari, D. K., Nahil, M. A., and Williams, P. T. (2017). Catalytic pyrolysis of waste plastics using staged catalysis for production of gasoline range hydrocarbon oils. *J. Anal. Appl. Pyrolysis* 124, 631–637. doi: 10.1016/j.jaap.2016.12.027

Rehan, M., Miandad, R., Barakat, M. A., Ismail, I. M. I., Almeelbi, T., Gardy, J., et al. (2017). Effect of zeolite catalysts on pyrolysis liquid oil. *Int. Biodeterior. Biodegrad.* 119, 162–175. doi: 10.1016/j.ibiod.2016.11.015

Rehan, M., Nizami, A. S., Shahzad, K., Ouda, O. K. M., Ismail, I. M. I., Almeelbi, T., et al. (2016). Pyrolytic liquid fuel: a source of renewable energy in Makkah. *Energy Sources A* 38, 2598–2603. doi: 10.1080/15567036.2016.1153753

Rizzarelli, P., Rapisarda, M., Perna, S., Mirabella, E. F., La Carta, S., Puglisi, C., et al. (2016). Determination of polyethylene in biodegradable polymer blends and in compostable carrier bags by Py-GC/MS and TGA. *J. Anal. Appl. Pyrolysis* 117,72–81. doi: 10.1016/j.jaap.2015.12.014

Saptoadi, H., and Pratama, N. N. (2015). Utilization of plastics waste oil as partial substitute for kerosene in pressurized cookstoves. *Int. J. Environ. Sci. Dev.* 6, 363–368. doi: 10.7763/IJESD.2015.V6.619

Sarker, M., and Rashid, M. M. (2013). Waste plastics mixture of polystyrene and polypropylene into light grade fuel using Fe2O3 catalyst. *Int. J. Renew. Energy Technol. Res.* 2, 17–28.

Seo, Y. H., Lee, K. H., and Shin, D. H. (2003). Investigation of catalytic degradation of high density, polyethylene by hydrocarbon group type analysis. *J. Anal. Appl. Pyrol.* 70, 383–398. doi: 10.1016/S0165-2370(02)00186-9

Serrano, D. P., Aguado, J., and Escola, J. M. (2000). Catalytic conversion of polystyrene over HMCM-41, HZSM-5 and amorphous SiO_2–Al_2O_3: comparison with thermal cracking. *Appl. Catal. B:Environ.* 25, 181–189. doi: 10.1016/S0926-3373(99)00130-7

Serrano, D. P., Aguado, J., and Escola, J. M. (2012). Developing advanced catalysts for the conversion of polyolefinic waste plastics into fuels and chemicals. *ACS Catal.* 2, 1924–1941. doi: 10.1021/cs3003403

Shah, J., and Jan, M. R. (2015). Effect of polyethylene terephthalate on the catalytic pyrolysis of polystyrene: Investigation of the liquid products. *J. Taiwan Inst. Chem. Eng.* 51, 96–102. doi: 10.1016/j.jtice.2015.01.015

Siddiqui, M. N., and Redhwi, H. H. (2009). Pyrolysis of mixed plastics for the recovery of useful products. *Fuel Process. Technol.* 90, 545–552. doi: 10.1016/j.fuproc.2009.01.003

Sriningsih, W., Saerodji, M. G., Trisunaryanti, W., Armunanto, R., and Falah, I. I. (2014). Fuel production from LDPE plastic waste over natural zeolite supported Ni, Ni-Mo, Co and Co-Mo metals. *Proc. Environ. Sci.* 20, 215–224. doi: 10.1016/j.proenv.2014.03.028

Syamsiro, M., Cheng, S., Hu, W., Saptoadi, H., Pratama, N. N., Trisunaryanti, W., et al. (2014). Liquid and gaseous fuel from waste plastics by sequential pyrolysis and catalytic reforming processes over indonesian natural zeolite catalysts. *Waste Technol.* 2, 44–51. doi: 10.12777/wastech.2.2.44-51

Tekin, K., Akalin, M. K., Kadi, C., and Karagöz, S. (2012). Catalytic degradation of waste polypropylene by pyrolysis. *J. Energy Ins.* 85, 150–155. doi: 10.1179/1743967112Z.00000000029

Thilakaratne, R., Tessonnier, J. P., and Brown, R. C. (2016). Conversion of methoxy and hydroxyl functionalities of phenolic monomers over zeolites. *Green Chem.* 18, 2231–2239. doi: 10.1039/c5gc02548f

Uemichi, Y., Hattori, M., Itoh, T., Nakamura, J., and Sugioka, M. (1998). Deactivation behaviors of Zeolite and Silica– Alumina catalysts in the degradation of polyethylene. *Ind. Eng. Chem. Res.* 37, 867–872. doi: 10.1021/ie970605c

Uemichi, Y., Nakamura, J., Itoh, T., Sugioka, M., Garforth, A. A., and Dwyer, J. (1999). Conversion of polyethylene into gasoline-range fuels by two-stage catalytic degradation using Silica–Alumina and HZSM-5 Zeolite. *Ind. Eng. Chem. Res.* 38, 385–390. doi: 10.1021/ie980341+

Ukei, H., Hirose, T., Horikawa, S., Takai, Y., Taka, M., Azuma, N., et al. (2000). Catalytic degradation of polystyrene into styrene and a design of recyclable polystyrene with dispersed catalysts. *Catal. Today* 62, 67–75. doi: 10.1016/S0920-5861(00)00409-0

Waqas, M., Rehan, M., Aburiazaiza, A. S., and Nizami, A. S. (2018). "Chapter 17-Wastewater Biorefinery based on the microbial electrolysis cell: opportunities and challenges," *in Progress and Recent Trends in Microbial Fuel Cells*, eds K. Dutta and P. Kundu (New York, NY: Elsevier Inc.), 347–374. doi: 10.1016/B978-0-444-64017-8.00017-8

Williams, P. T. (2006). "Yield and composition of gases and oils/waxes from the feedstock recycling of waste plastic." *In Feeds Tock Recycling and Pyrolysis of Waste Plastics: Converting Waste Plastics into Diesel and Other Fuels, eds J. Scheirs and W. Kaminsky (West Sussex: John Wiley & Sons Press),* 285–309.

Wu, C., and Williams, P. T. (2010). Pyrolysis–gasification of plastics, mixed plastics and real-world plastic waste with and without Ni–Mg–Al catalyst. *Fuel* 89, 3022–3032. doi: 10.1016/j.fuel.2010.05.032

Wu, J., Chen, T., Luo, X., Han, D., Wang, Z., and Wu, J. (2014). TG/FTIR analysis on co-pyrolysis behavior of PE, PVC and PS. *Waste Manag.* 34, 676–682. doi: 10.1016/j.wasman.2013.12.005

Xue, Y., Johnston, P., and Bai, X. (2017). Effect of catalyst contact mode and gas atmosphere during catalytic pyrolysis of waste plastics. *Energy Conv. Manag.* 142, 441–451. doi: 10.1016/j.enconman.2017.03.071

Yoshioka, T., Grause, G., Eger, C., Kaminsky, W., and Okuwaki, A. (2004). Pyrolysis of poly (ethylene terephthalate) in a fluidised bed plant. *Polym. Degrad. Stab.* 86, 499–504. doi: 10.1016/j.polymdegradstab.2004.06.001

Zeaiter, J. (2014). A process study on the pyrolysis of waste polyethylene. *Fuel* 133, 276–282. doi: 10.1016/j.fuel.2014.05.028

Conflict of Interest Statement: The authors declare that the research was conducted in the absence of any commercial or financial relationships that could be construed as a potential conflict of interest.

frontiers in Energy Research

ORIGINAL RESEARCH
published: 19 March 2019
doi: 10.3389/fenrg.2019.00022

Biorefining Waste Sludge From Water and Sewage Treatment Plants Into Eco-Construction Material

Wai Nam Cheng[1†], Haakrho Yi[2†], Chun-fai Yu[3], Ho Fai Wong[4], Guoxiang Wang[5], Eilhann E. Kwon[6] and Yiu Fai Tsang[1,5]*

[1] Department of Science and Environmental Studies, The Education University of Hong Kong, Tai Po, Hong Kong, [2] Department of Gwangyang Research Group, RIST, Gwangyang City, South Korea, [3] Environmental Science Program, Division of Science and Technology, BNU-HKBU United International College, Zhuhai, China, [4] Faculty of Science and Technology, Technological and Higher Education Institute of Hong Kong, Tsing Yi Island, Hong Kong, [5] School of Environment, Nanjing Normal University, Nanjing, China, [6] Department of Environment and Energy, Sejong University, Seoul, South Korea

This study aims to investigate the feasibility of using different waste sludge and coal combustion residuals in eco-concrete block production. The compressive strength of the eco-concrete blocks produced by waterworks sludge, bottom and fly ashes were 36 MPa, which comply with the standard specifications for paving blocks in Hong Kong. The optimal mixing proportion (by weight) of different materials in the blocks, such as aggregates, cementitious materials, water, and fly ash was 1.1:1.0:0.5:0.22, respectively. The environmental and toxicological impacts of the final products were then evaluated according to the toxicity characteristic leaching procedure (TCLP). While several heavy metals (i.e., Hg, Cu, and Pb) have been identified in the specimens, the levels of these contaminants complied with Standards (US 40 CFR 268.48). Waste materials generated from water and sewage treatment processes and power plants are feasible to be used as ingredients for paving concrete block production. These products are environmentally acceptable and mechanically suitable for resource recovery of waste materials.

Keywords: resource recovery, construction materials, sewage sludge, waterworks sludge, solidification

OPEN ACCESS

Edited by:
Mohammad Rehan, King Abdulaziz University, Saudi Arabia

Reviewed by:
Sidney Man Ngai Chan, Open University of Hong Kong, China
Na Duan, China Agricultural University, China

***Correspondence:**
Yiu Fai Tsang
tsangyf@eduhk.hk

[†]These authors have contributed equally to this work and are co-first authors

Specialty section:
This article was submitted to Bioenergy and Biofuels, a section of the journal Frontiers in Energy Research

Received: *31 October 2018*
Accepted: *14 February 2019*
Published: *19 March 2019*

Citation:
Cheng WN, Yi H, Yu C-f, Wong HF, Wang G, Kwon EE and Tsang YF (2019) Biorefining Waste Sludge From Water and Sewage Treatment Plants Into Eco-Construction Material. Front. Energy Res. 7:22. doi: 10.3389/fenrg.2019.00022

INTRODUCTION

In 2015, ~15,100 tons per day (TPD) of solid waste were disposed to landfill sites in Hong Kong. However, existing landfills will be filled up by 2020 (Environmental Protection Department (EPD), 2016a; 2016b). In terms of commingling of solid waste, waste sludge is the unavoidable by-product from water and sewage treatment processes. It is classified as special waste, which cannot be easily reduced at sources (Jordan et al., 2005; Tuan et al., 2013). The amount of sludge produced could significantly increase due to future urban development, such as the North East New Territories New Development Area. The government estimates that the sludge production will increase to ~2,000 TPD by 2030 due to the completion of the Harbor Area Treatment Scheme Phase 2B (Environmental Protection Department, 2016b). The sludge treatment facility was built to alleviate the mounting pressure faced by the landfill. The facility can process 90% of the sludge volume through high-temperature incineration. However, the remaining 10% of the waste residues are still disposed to the landfill (Environmental Protection Department, 2016b). Thus, reusing and recycling of the waste sludge are win-win strategies for mitigating the load of waste treatment facilities and reducing natural resources and energy consumption.

GRAPHICAL ABSTRACT | Concept of the study.

Several studies have demonstrated the feasibility of using sewage sludge for the production of eco-construction materials, such as cement (Monzó et al., 2004; Cyr et al., 2007), lightweight aggregate (Liu et al., 2017), and ceramic tile (Jordan et al., 2005). Utilizing sewage sludge as ingredients in construction materials not only could reduce the production cost but also provide ecological and energy saving advantages (Wang et al., 2008; Liu et al., 2011; Tyagi and Lo, 2013). Despite an estimated 10,000 TPD of waterworks sludge generated globally, few studies have focused on its resource recovery (Babatunde and Zhao, 2007). In Hong Kong, ∼60 TPD waterworks sludge is discarded to the landfill (Environmental Protection Department, 2016a). There is a need to find ways on how to effectively reuse waterworks sludge due to the shortage of landfill space (Tang et al., 2014; Tsang, 2015). Huang and Wang (2013) illustrated the possibility of reusing waterworks sludge in the production of lightweight aggregate. Power plant contractors also face the problem of disposing of coal combustion residuals. Considering different pozzolanic properties along with the issues of cost and environment, fly ash is mainly used in cement manufacturing, while bottom ash is utilized mainly in construction materials (Meij and Berg, 2001; Tsang, 2015). Several studies reported the feasibility of using bottom ash for different engineering purposes, such as blocks (Arenas et al., 2011) and concrete (Lee et al., 2010; Kim and Lee, 2011). Bottom ash has better performance compared with sand, in fact, the compressive strength of 100% aggregate replacement was even higher than that of reference blocks (Andrade et al., 2007). The coliform population of the sludge can also be reduced by the addition of coal fly ash (Papadimitriou et al., 2008). Supplementing with coal combustion residuals may

Abbreviations: A/C, aggregate to cement; BA, bottom ash; CEDD, Civil Engineering and Development Department; EPD, Environmental Protection Department; FA, fly ash; ICP-AES, inductively coupled plasma-atomic emission spectrometry; ICP-MS, inductively coupled plasma-mass spectrometry; LoD, limit of detection; PC, Portland cement; S/S, solidification/stabilization; SA, sludge incineration residuals; SS, sewage sludge; SSWTWs, Sheung Shui Water Treatment Works; STSTWs, Shatin Sewage Treatment Works; TCLP, toxicity characteristic leaching procedure; TPD, tons per day; W/C, water to cement; WS, waterworks sludge.

facilitate the utilization of waste sludge as ingredients in concrete blocks. Meanwhile, Wang (2005) demonstrated the use of waste materials, such as red mud and building sand, to produce non-sintered and non-clay blocks. The resulting blocks are considered as an environmentally friendly construction material because of low cement content.

Aside from paving blocks, the Chinese Government has implemented related economic policies to encourage and regulate the production and use of new wall materials (Mohurd, 2012). These policies aim to promote the innovation of wall materials and energy-saving buildings. The Ministry of Finance and the State Administration of Taxation has made clear that enterprises using effluent, exhausted gases, waste residues, and other waste materials as primary feedstock for producing wall materials can avail of income tax reduction or exemption within 5 years. Eco-construction materials development is the trend of construction materials production. In fact, there were not many researches focus on eco-concrete block produced from mentioned waste materials. And previous researches demonstrated the feasibility of using waste materials for eco-construction materials production. These successful experiences could be applied to eco-concrete block production. Moreover, the government also supports green product production. Eco-construction materials could be developed in the future. In this study, the feasibility to reuse dewatered sludge, dried sludge, and coal combustion residues as sand and aggregate replacements for paving concrete blocks production to reduce the sludge quantities for disposal or further treatment was investigated. The ratios of different waste materials were optimized to meet the standard specifications for paving blocks. Toxicity and mechanical performance were also examined to evaluate the environmental acceptance and feasibility of the engineering view of the products.

MATERIALS AND METHODS

Raw Materials

Waterworks sludge (WS), sewage sludge (SS), and sludge incineration residuals (SA) were selected to investigate the possibility of producing concrete blocks due to the properties more similar to traditional constituents. WS and SS were collected from Shaiin Sewage Treatment Works (STSTWs) and Sheung Shui Water Treatment Works (SSWTWs) in Hong Kong, respectively. SA were collected from sludge treatment facility adopted incineration at 850°C in Tune Mun, Hong Kong. WS was the aluminum-rich sludge generated in local drinking water treatment process, in which alum is used as the coagulant in coagulation-flocculation process. SS was the sludge generated from a typical secondary wastewater treatment plant. Coal combustion residuals [i.e., bottom ash (BA) and fly ash (FA)] were collected from Castle Peak Power Plant. Ordinary Portland cement (PC) equivalent to BS EN197-1:2000 sourced commercially in Hong Kong were used as cementitious materials and partially substituted by fly ash. The moisture content of waste materials was similar to typical value. Beside of waste sludge and coal combustion residuals, red mud, coal gangue, waste glass were used to produce non-sintered blocks. Red mud that is insoluble waste residual was produced during extraction and purification of aluminum oxide and consisted of fine particles and coarse granules. Coal gangue is a solid waste that generated during the process of coal mining and washing.

Experimental Design

This study was separated into two parts (**Graphical Abstract**). In Part one, specimens with various mixing proportion (**Table 1**) were produced to evaluate the feasibility of utilizing waste materials as substitutes in concrete blocks. The leachability of heavy metals (i.e., Hg, Cu, and Pb) in the eco-concrete blocks with different mixing proportions was also determined. In Part two, the mechanical performance of the specimens was evaluated according to the standard specifications for paving blocks published by Hong Kong SAR.

The water to cement (W/C) and aggregate to cement (A/C) ratios obtained during determining the effective ratio. W/C and A/C were 0.3 and 1.1, respectively. The ratios of waste material substitution to natural material varied from 20 to 100%, while the ratios of bottom ash to sewage sludge (BA/SS) varied between 1.0 and 2.4. In Series 4, moisture was provided from the SS; therefore no tap water was added to the concrete mix. Effective mixing proportion obtained from Part one would be used for the production of specimens in Part two. Different type of waste materials would substitute the natural resources in the specimens to evaluate various waste materials, which would present acceptable mechanical performance.

Coarse aggregate and fine aggregate were replaced by WS and BA, respectively. Coal combustion FA and SA would work as cementitious materials to substitute part of cement. The coarse aggregate to fine aggregate ratio was amended to 50% to 50%. The detailed information of mixing proportion of Part two is shown in **Tables 2**, **3**. Series 5 would determine the effect of varying materials on compressive strength. In order to maximize the amount of waste materials reusing, effect of increasing A/C ratio would evaluate in series 6. Given that no standards or regulations exist to produce eco-concrete blocks in Hong Kong, and the materials used in this study were different from traditional materials in terms of physical or chemical characteristics, the W/C and A/C ratios were different from the typical ratios used. Besides, series 7 would evaluate the mechanical performance of specimens produced by waste materials. In this mix series, cement was also replaced by coal fly ash.

Materials Preparation

All waterworks sludge used in this study was oven-dried at 105°C for at least 2 days before mixing to obtain harden character to simulate the character of natural coarse aggregate. Sewage sludge cakes mixed with other materials without pretreatment to determine the effect of utilizing sludge cake to replace natural aggregate. Bottom ashes are porosities and would absorb water to reduce the free-water content for cement hydration. To maintain W/C, saturated surface-dry condition for aggregate was needed to obtain (Marsh, 1997). In this study, 18% by weight of water was added to bottom ash to reach the saturated surface-dry condition. For materials used in series 7, two-grain sizes of coal gangue and waste glass were selected, which were between 0.35 and

TABLE 1 | Mixing proportion used in the Part one study[a].

Mix		Mixing proportion (kg/m^3)					Ratio	
		Water	PC	BA	SS	Sand	BA/SS	% of waste
Control	HM-0	214	762	0	0	1,086	0	0
Series 1	HM-I-20	214	762	88	108	815	1	20
	HM-I-40	214	762	176	216	543	1	40
	HM-I-70	214	762	264	324	272	1	70
	HM-I-100	214	762	352	432	0	1	100
Series 2	HM-II-20	214	762	120	73	815	1.6	20
	HM-II-40	214	762	232	143	543	1.6	40
	HM-II-70	214	762	352	216	272	1.6	70
	HM-II-100	214	762	468	290	0	1.6	100
Series 3	HM-III-20	214	762	132	54	815	2.4	20
	HM-III-40	214	762	264	108	543	2.4	40
	HM-III-70	214	762	396	162	272	2.4	70
Series 4	HM-NW-100	214	762	587	359	0	1.6	100

[a]*Specimens with various mixing proportion for evaluating the feasibility of utilizing waste materials as substitutes in concrete blocks.*

TABLE 2 | Mixing proportion used in the Part two study[a].

Mix		Mixing proportion (kg/m^3)								Ratio
		Water	PC	FA	BA	[b]CWS	[c]FWS	SS	SA	A/C
Series 5	E-BA/CW	380	633	266	500	500	Nil	Nil	Nil	1.1
	E-BA/FW	380	633	266	500	Nil	500	Nil	Nil	1.1
	E-CW/SS	380	633	266	Nil	500	Nil	500	Nil	1.1
	E-CW/SA	380	633	266	Nil	500	Nil	Nil	500	1.1
Series 6	E-A/C1.1	380	633	266	500	500	Nil	Nil	Nil	1.1
	E-A/C1.3	380	633	183	541	541	Nil	Nil	Nil	1.3
	E-A/C1.5	380	633	125	570	570	Nil	Nil	Nil	1.5

[a]*Acceptable mechanical performance for the substitutability of different types of waste material in the specimens.*
[b]*Coarse waterworks sludge.*
[c]*Fine waterworks sludge.*

0.5 mm (medium size) and over 0.5 mm (coarse size). The ratio between medium-size particles and coarse-size particles was 6:4. Coal gangue and waste glass were mixed to prepare the aggregate mixture for series 7.

Effective Ratios

Waste materials properties either physically or chemically were different to natural materials utilized in the traditional concrete block. The curing performance may differ to traditional materials. More cement may be needed for concrete mix production, therefore effective ratios were needed to determine. The optimal A/C ratio for waste materials concrete mix would determine before concrete block production. Typical A/C is in the range of 3:1 to 6:1 (Shackel, 1990) and the preliminary study of A/C ratio and W/C ratio for waste materials start with 4:1 and 0.6, respectively. For W/C ratio, it is not the critical factor at this part; the typical value was applied here. Preliminary study for effective ratio would proceed until specimens' cure successfully on Day 1.

Specimens Preparation

Hundred wooden molds fabricated according to Civil Engineering and Development Department (CEDD) standard for the concrete paving block (i.e., L × W × H: 200 × 100 × 60 mm) were used in parts one and two studies (CEDD, 2006). The concrete mixtures were prepared by the hand-mixing method and vibrate manually to eliminate the air trapped in the mixture. The specimens were removed from the molds and cure in water for 28 days on day 1. In series 7, the sizes of specimens were in the shape of a cylinder with 40 mm (diameter) and 13.2 mm (height).

Analytical Methods

Leachability of heavy metals was determined by Toxicity Characteristic Leaching Procedures (TCLP, USEPA Method 1311, 1992), which is common practice to evaluate leachability of waste and contaminated soils. According to USEPA and Hong Kong TCLP limits, the selected analytes included Cd, Cr, Cu, Pb, Hg, Ni, Zn, and As (Environmental Protection Department, 2011).

TABLE 3 | Mixing proportion used in non-sintered and non-clay block.

Mix		Mixing proportion (kg/m^3)						% of CG
	Plaster	PC	FA	QL	[a]RM	[b]CG		
Series 7	E-CG20	36	18	486	180	721	360	20
	E-CG30	36	18	432	180	595	540	30
	E-CG40	36	18	342	180	504	721	40

[a]*Red mud.*
[b]*Coal gangue and waste glass.*

Samples were leached with 0.5 M glacial acetic acid at liquid to solid ratio of 20 L/kg and rotated for 18 h at 30 rpm. The sample solutions after extraction were analyzed by inductively coupled plasma-atomic emission spectrometry (ICP-AES) (Perkin Elmer Optima 3300DV, USA) and inductively coupled plasma-mass spectrometry (ICP-MS) (Agilent 7900, USA). In addition, 2 mg/L standard solution was analyzed every 10 samples and after the whole sequence of determination for QA/QC. All samples were determined in triplicate (Li et al., 2017)

For other analytical methods on mechanical performance, compressive strength test was complied with local civil engineering works standard. Water absorption test was condcuted according to AS/NZS 4456.14 ($n = 3$). Compressive strength test was determined by automatic compression machines (36-5165/01, ELE International, UK) with compression speed 6,800 N per second and "non-standard" for size setting ($n = 3$). The compressive strength was calculated by determining the breaking load of the specimens. The compressive strength of specimens in series 7 would be evaluated according to GB5101-2003, which is a collection of current common sintered brick's national standards in the People's Republic of China.

RESULTS AND DISCUSSION

Effective Ratios

W/C ratio and A/C ratio for waste materials utilized in the concrete mix were determined. The A/C ratio for waste materials was dramatically lower than typical A/C ratio, and a relatively high amount of cementitious materials was needed. A/C ratio for waste materials was 1.1, which can cure successfully on Day 1. The high amount of cementitious materials was needed may due to bottom ash, which is porous materials and representing of large surface area compare to natural aggregate (Singh and Siddique, 2013). In this study, The A/C ratio and W/C ratio of effective mixing proportion is 1.1 and 0.5. And the A/C ratio in this study was higher than Poon and Lam (2008) mentioned. The author recommended A/C ratio with 3 is suitable for eco-friendly concrete block production. Regarding W/C ratio, it is like the typical value, 0.6 (Jiménez et al., 2014). It may vary due to the difference of a characteristic of materials.

Leachability of Heavy Metals

In Part one study, leachability of heavy metals in specimens was determined through TCLP to evaluate the environmental impacts of specimens produced by waste materials, including different types of sludge and ashes. The results of the TCLP are summarized in **Table 4**. The concentrations of Cd, Cr, Ni, As, and Zn were below the limit of detection (LoD). However, Pb, Cu, and Hg were detected from both specimens and raw materials. Compared with the specimens, the relatively high concentrations of heavy metals were detected from raw materials. However, the concentrations of metal leached from the specimens were lower than those from raw materials samples. It may be due to the immobilization of heavy metals during cement hydration reaction.

TABLE 4 | TCLP results.

Mix		Heavy metals (ppm)		
		Pb	Cu	Hg
TCLP limit (HK)		50	250	1
TCLP limit (US)		5	25	0.1
Raw materials	Sludge	0.067 ± 0.006	0.181 ± 0.001	0.150 ± 0.017
	Stone	0.063 ± 0.010	0.402 ± 0.001	[a]-
	Sand	0.030 ± 0.001	0.185 ± 0.001	[a]-
	Bottom Ash	[a]-	0.166 ± 0.001	[a]-
Control	HM-0	0.027 ± 0.009	0.205 ± 0.001	[a]-
Series 1	HM-I-20	0.017 ± 0.003	0.206 ± 0.001	[a]-
	HM-I-40	0.012 ± 0.005	0.119 ± 0.001	[a]-
	HM-I-70	0.005 ± 0.001	0.122 ± 0.001	[a]-
	HM-I-100	0.012 ± 0.005	0.128 ± 0.001	[a]-
Series 2	HM-II-20	0.017 ± 0.007	0.147 ± 0.001	[a]-
	HM-II-40	0.005 ± 0.007	0.120 ± 0.001	[a]-
	HM-II-70	0.010 ± 0.008	0.121 ± 0.001	[a]-
	HM-II-100	0.010 ± 0.007	0.120 ± 0.001	[a]-
Series 3	HM-III-20	0.020 ± 0.003	0.174 ± 0.001	[a]-
	HM-III-40	0.009 ± 0.003	0.124 ± 0.001	[a]-
	HM-III-70	0.004 ± 0.007	0.117 ± 0.001	[a]-
Series 4	HM-NW-100	0.012 ± 0.001	0.116 ± 0.001	[a]-

[a]*Below limit of detection = 0.001 ppm.*

Solidification/stabilization (S/S) is the commonly used technique in the world to reduce the toxicity of the waste materials for treatment of contaminated soil and sludge (Li et al., 2001; Valls and Vàzquez, 2002; Malviya and Chaudhary, 2006; Chen et al., 2009; ÖzverdI and Erdem, 2010). Solidification converts waste material from liquid phase to solid phase and strength development (Hills and Pollard, 1997; Chen et al., 2009). Due to this technique not only solidification but also reduce the toxicity and leachability through insolubilize and immobilize the waste materials, it become non-hazardous or less hazardous to achieve waste materials stabilization (Hills and Pollard, 1997; Malviya and Chaudhary, 2006). Cement-based S/S processes are suitable for treating heavy metal-contaminated sludge or soils because hazardous components are difficult to leach from concrete materials (Marion et al., 2005; Malliou et al., 2007; Qiao et al., 2007). Moreover, some studies demonstrated the possibility of using cement to treat heavy metals. Hills and Pollard (1997) found that the concentration of zinc in the specimen has reduced about 99% on Day 28. In addition, Antemir et al. (2010)

have conducted a series test about the long-term performance of S/S and the test up to 16 years. The results indicated that the contaminants leach from the S/S soil was not excess the specific limit and the contaminant was immobilized in the solid for a long period of time. On the other hands, Marion et al. (2005) have studied the leaching behavior of paving concrete mixing with slag and reported there is no systematic correlation between the heavy metal content and the leached heavy metal from concrete. And authors comment that there is no significant risk of contamination of soil and water. Based on these previous studies, cement-based S/S processes are available to treat heavy metal.

Compressive Strength Test

The compressive strength test was conducted on Day 28 in Part two study. Compressive strength was calculated according to local civil engineering standard for concrete paving blocks (**Table 5**). In this part, different types of materials were utilized to replace coarse and fine aggregate. The results were indicated that the series, which were consisting of sewage sludge cake and sludge incineration residuals was failed to cure on Day 1. The texture of specimens consist of sewage sludge cake was sponge-like and soft. The strength of the cement matrix, aggregate and interfacial bond between the cement matrix and aggregate are the factors affecting the strength of concrete (Poon et al., 2004). Fail to may be attributed to the type of aggregate and interfacial bond between the cement matrix and aggregate. Whereas, the texture of specimens consists of sludge incineration residuals was cracked on Day 1. Thermal expansion may become the reason for cracking. When deformation of concrete is restrained, thermal stress will occur. Thermal stress is greater than tensile strength consequently cracking of the concrete (McCarthy et al., 2015; Siddiqui and Fowler, 2015). Another researcher also points out thermal stress is affecting durability and the life of concrete due to thermal stress generated by cement hydration greater than loading of concrete (Siddiqui and Fowler, 2015). Therefore, series mixed with sewage sludge and sludge incineration residuals were rejected and no further analysis to evaluate the mechanical performance. Dewatered sewage sludge and sludge incineration residuals may not be suitable for substitute into the concrete mix without pretreatment and admixture addition to improving the early strength of the specimens. Weak initial strength results in thermal expansion cracking due to generated by cement hydration (Hoang et al., 2016).

In series 5, only concrete mix E-BA/CW, which was consisting of bottom ash and coarse waterworks sludge, reached the local concrete paving block standard, 30 MPa (**Table 5**). On the other hands, the compressive strength of concrete mix E-BA/FW was 18.7 MPa. It may because the coarse aggregate was replaced by fine waterworks sludge. The appearance like mortar but not concrete, which is similar to the results obtained by Wang et al. (2015). Coarse aggregate presented a significant effect on compressive strength. Compressive strength was increased with increasing amount of coarse aggregate. In order to optimize the amount of reusing waste materials, the correlation between different A/C ratios and compressive strength was also determined in series 6. E-A/C1.1 and E-A/C1.3 represent the satisfied compressive strength, which was 33.9 ± 1.3 and 36.3 ± 0.85, respectively (**Table 5**). When A/C ratio increased to 1.5, the compressive strength was begun to decrease. It may due to increasing of bottom ash and need more cementitious materials for concrete production. However, the previous study indicated that the compressive strength of concrete mixture, which was replace fine aggregate by coal bottom ash was greater than concrete mix consists of sand. Because of the pozzolanic effect of coal bottom ash begun affecting the chemical reaction inside the concrete and enhancing the properties of concrete after the curing period (Singh and Siddique, 2014). It would be possible to utilizing waster sludge and coal combustion residuals to produce eco-concrete blocks with A/C ratio 1.5.

TABLE 5 | Compressive strength and water absorption tests.

Mix		Compressive strength (MPa)	Water absorption (%)
Series 5	E-BA/CW	33.95 ± 1.32	4.2 ± 0.1
	E-BA/FW	18.73 ± 1.30	8.4 ± 0.6
	E-CW/SS	Rejected	Rejected
	E-CW/SA	Rejected	Rejected
Series 6	E-A/C1.1	33.95 ± 1.32	4.2 ± 0.1
	E-A/C1.3	36.33 ± 0.85	1.3 ± 0.4
	E-A/C1.5	29.27 ± 0.87	2.0 ± 0.1
Series 7	E-CG20	10.20 ± 0.15	Not available
	E-CG30	10.70 ± 0.25	Not available
	E-CG40	10.60 ± 0.15	Not available

Regarding the preliminary study of non-sintered and non-clay standard size block, the compressive strength of all concrete mixes was reached MU10 mentioned in GB5101-2003. The results for these concrete mixes are summarized in **Table 5**. From **Figure 1**, the trend of the difference of compressive strength for concrete mix E-CG20 and E-CG40 become stability on Day 28 and tendencies for increasing of compressive strength of E-CG30 was slightly greater than E-CG40 and E-CG20. Therefore, the compressive strength of E-CG30 would keep rising in the following days. E-CG30's tendency for increasing of compressive strength is greater than E-CG20 and E-CG40, which means that according to the average natural curing period (28 days), the compressive strength of E-CG30's blocks, would increase more significantly than the others, and the final compressive strength may be higher.

Water Absorption Test

Water absorption test was conducted, and the procedure was complying with local civil engineering standard. The results of water absorption test are summarized in **Table 5**. Excepting concrete mix E-BA/FW, every concrete mix was below 6% and not exceeds the standard limit. Specimens in concrete mix E-BA/CW not only have the highest strength but also have the lowest water absorption value. Compare to another study, the result of water absorption test was lower with similar coal bottom

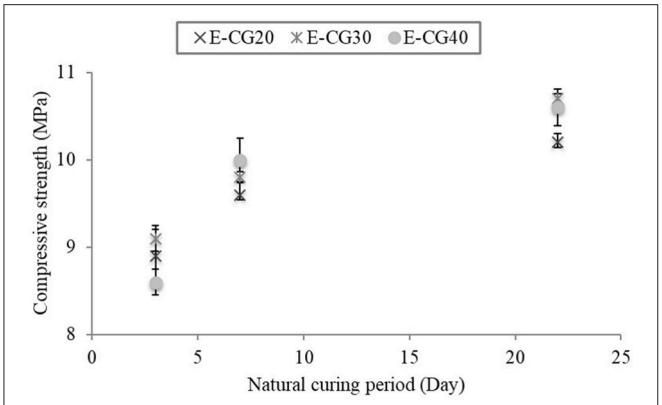

FIGURE 1 | Change of theoretical compressive strength.

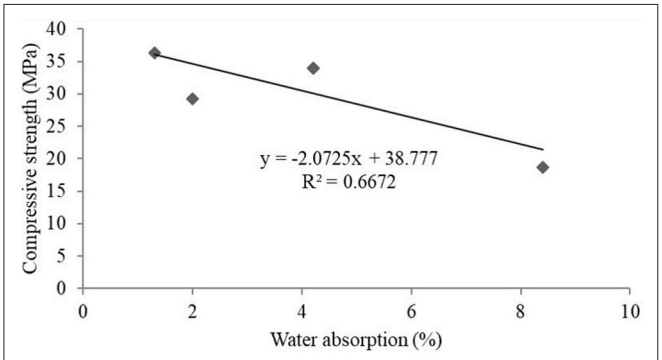

FIGURE 2 | Relationship between compressive strength and water absorption.

ash substitution. Singh and Siddique (2015) obtained the water absorption was fall in the range from 4.7 to 5.6% on Day 28. In addition, the author also found that the voids of bottom ash were filled Ettringites needle and a high amount of calcium silicate hydrate (CSH) gel in the bottom ash concrete on Day 90. Concrete mix E-BA/FW may reach the satisfied water absorption value on Day 90.

Correlation of Compressive Strength and Water Absorption

In this study, the strong correlation of compressive strength and water absorption test was found. From the **Figure 2**, when decreasing of compressive strength of concrete mix E-BA/FW and E-A/C1.5, the water absorption value of these concrete mixes were increased simultaneously. When conducted water absorption test, a lot of air bubbles occurred during the early stage of this test. It reflects that there were some spaces presences inside the concrete block. A similar result was obtained from another study, Singh and Siddique (2014) found that the compressive strength of bottom ash concrete was lower than river sand concrete at early curing age. Authors summarized the increased porosity of concrete was one of the reasons for that. Whereas, authors also found that the pozzolanic effect of coal bottom ash was begun to react with calcium hydroxide and form C-S-H gel and this gel was filled up the void of bottom ash on Day 14. Coal bottom ash could enhance the compressive strength of bottom ash concrete after the curing age and bottom ash reach the almost similar properties to river sand with more extended curing age were summarized by Singh and Siddique.

CONCLUSIONS

In this study, different kinds of waste materials, which are the unavoidable by-products from wastewater treatment and power generation processes, were utilized to produce eco-concrete blocks. The results indicated that eco-concrete blocks consisting of waterworks sludge (in coarse size) and coal bottom ash were feasible for use in eco-concrete blocks production. The specimens reached the requirements stated in the General Specifications from the Hong Kong Government and did not exceed the toxicity characteristic leaching procedure standards. The mixing proportion of eco-concrete block production was dramatically different compared with concrete produced from raw materials. The A/C and W/C ratios were 1.1 and 0.5, respectively. Aside from eco-concrete paving blocks, non-sintered and non-clay blocks production from wastes (i.e., sludge and incinerated residues) was evaluated from an engineering viewpoint. The results showed that non-sintered and non-clay blocks produced with large fractions in waste materials reached MU10 in GB5101-2003. The proposed method will provide potentially inexpensive sources of environmentally friendly construction materials with desirable properties through the exploration of novel and advanced routes for resource recovery. It not only converts such wastes into useful materials but also helps alleviate the shortage of landfill sites. Hence, the practice of reusing waste materials is a win-win strategy that can alleviate raw material consumption during urban development in China. It not only reduces the quantity of sludge and incinerated residues for further treatment, but also provides a cost-effective and energy-efficient method for eco-construction materials production.

AUTHOR CONTRIBUTIONS

WC: analysis and interpretation of the data/Drafting of the article/Critical revision of the article for important intellectual content/Collection and assembly of data/Administrative, technical, or logistic support/Final approval; HY: analysis and interpretation of the data/Drafting of the article/Critical revision of the article for important intellectual content/Collection and assembly of data/Final approval; CY: conception and design/Analysis and interpretation of the data/Critical revision of the article for important intellectual content/Administrative, technical, or logistic support/Final approval; HW: analysis and interpretation of the data/Critical revision of the article for important intellectual content/Collection and assembly of data/Administrative, technical, or logistic support/Final approval; GW: critical revision of the article for important intellectual content/Obtaining of funding/Final approval;

EK: drafting of the article/Critical revision of the article for important intellectual content/Administrative, technical, or logistic support/Final approval; YT: conception and design/Analysis and interpretation of the data/Drafting of the article/Critical revision of the article for important intellectual content/Collection and assembly of data/Obtaining of funding/Administrative, technical, or logistic support/Final approval of the article.

ACKNOWLEDGMENTS

This work was financially supported by the Research Grants Council of the Hong Kong SAR, China (No.: 18202116), the Research Cluster Fund (RG50/2017-2018R), the Dean's Research Fund (No.: DRF/SFRS-8 and DSRAF-6 SP1), and the Internal Research Grant (No.: RG 78/2015-2016R and RG 34/2017-2018R) of The Education University of Hong Kong.

REFERENCES

Andrade, L. B., Rocha, J. C., and Cheriaf, M. (2007). Evaluation of concrete incorporating bottom ash as a natural aggregates replacement. *Waste Manage.* 27, 1190–1199. doi: 10.1016/j.wasman.2006.07.020

Antemir, A., Hills, C. D., Carey, P. J., Gardner, K. H., Bates, E. R., and Crumbie, A. K. (2010). Long-term performance of aged waste forms treated by stabilization/solidification. *J. Hazard. Mater.* 181, 65–73. doi: 10.1016/j.jhazmat.2010.04.082

Arenas, C. G., Marrero, M., Leiva, C., Solís- Guzmán, J., and Arenas, L. V. (2011). High fire resistance in blocks containing coal combustion fly ashes and bottom ash. *Waste Manage.* 31, 1783–1789. doi: 10.1016/j.wasman.2011.03.017

Babatunde, A. O., and Zhao, Y. Q. (2007). Constructive approaches towards water treatment works sludge management: an international review of beneficial re-uses. *Crit. Rev. Env. Sci. Tech.* 37, 129–164. doi: 10.1080/10643380600776239

CEDD (2006). *General Specification for Civil Engineering Works.* Civil Engineering and Development Department, HKSAR. Available online at: http://www.cedd.gov.hk/eng/publications/standards_handbooks_cost/doc/stan_gs_2006/GS%202006%20Vol%202%20Rev%2016-161230.pdf

Chen, Q. Y., Tyrer, M., Hills, C. D., Yang, X. M., and Carey, P. (2009). Immobilisation of heavy metal in cement-based solidification/stabilisation: a review. *Waste Manage.* 29, 390–403. doi: 10.1016/j.wasman.2008.01.019

Cyr, M., Coutand, M., and Clastres, P. (2007). Technological and environmental behavior of sewage sludge ash (SSA) in cement-based materials. *Cement Concrete Res.* 37, 1278–1289. doi: 10.1016/j.cemconres.2007.04.003

Environmental Protection Department (2011). *Practice Guide for Investigation and Remediation of Contaminated Land.* Environmental Protection Department, HKSAR. Available online at: http://www.epd.gov.hk/epd/sites/default/files/epd/gn_pdf/GN2014P244-2011c-e.pdf

Environmental Protection Department (2016a). *Monitoring of Solid Waste in Hong Kong 2015.* Environmental Protection Department, HKSAR. Available online at: https://www.wastereduction.gov.hk/sites/default/files/msw2015.pdf

Environmental Protection Department (2016b). *Sludge Treatment Facility (STF). Waste – Problem and Solutions.* Environmental Protection Department, HKSAR. Available online at: http://www.epd.gov.hk/epd/english/environmentinhk/waste/prob_solutions/Sewage_Sludge.html

Hills, C. D., and Pollard, S. J. T. (1997). The influence of interference effects on the mechanical, microstructural and fixation characteristics of cement-solidified hazardous waste forms. *J. Hazard. Mater.* 52, 171–191. doi: 10.1016/S0304-3894(96)01806-7

Hoang, K., Justnes, H., and Geiker, M. (2016). Early age strength increase of fly ash blended cement by a ternary hardening accelerating admixture. *Cement Concrete Res.* 81, 59–69. doi: 10.1016/j.cemconres.2015.11.004

Huang, C. H., and Wang, S. Y. (2013). Application of water treatment sludge in the manufacturing of lightweight aggregate. *Constr. Build. Mater.* 43, 174–183. doi: 10.1016/j.conbuildmat.2013.02.016

Jiménez, C., Barra, M., Valls, S., Aponte, D., and Vázquez, E. (2014). Durability of recycled aggregate concrete designed with the equivalent mortar volume (EMV) method: validation under the Spanish context and its adaptation to bolomey methodology. *Mater. Construct.* 64:313. doi: 10.3989/mc.2013.00913

Jordan, M. M., Almendro-Candel, M. M., Romero, M., and Rincon, J. M. (2005). Application of sewage sludge in the manufacturing of ceramic tile bodies. *Appl. Clay Sci.* 30, 219–224. doi: 10.1016/j.clay.2005.05.001

Kim, H. K., and Lee, H. K. (2011). Use of power plant bottom ash as fine and coarse aggregates in high-strength concrete. *Constr. Build. Mater.* 25, 1115–1122. doi: 10.1016/j.conbuildmat.2010.06.065

Lee, H. K., Kim, H. K., and Hwang, E. A. (2010). Utilization of power plant bottom ash as aggregates in fiber-reinforced cellular concrete. *Waste Manage.* 30, 274–284. doi: 10.1016/j.wasman.2009.09.043

Li, J. S., Beiyuan, J., Tsang, D. C., Wang, L., Poon, C. S., Li, X. D., et al. (2017). Arsenic-containing soil from geogenic source in Hong Kong: leaching characteristics and stabilization/solidification. *Chemosphere* 182, 31–39. doi: 10.1016/j.chemosphere.2017.05.019

Li, X. D., Poon, C. S., Sun, H., Lo, I. M. C., and Kirk, D. W. (2001). Heavy metal speciation and leaching behaviors in cement based solidified/stabilized waste materials. *J. Hazard. Mater.* 82, 215–230. doi: 10.1016/S0304-3894(00)00360-5

Liu, M., Xu, G., and Li, G. (2017). Effect of the ratio of components on the characteristics of lightweight aggregate made from sewage sludge and river sediment. *Process Saf. Environ. Prot.* 105, 109–116. doi: 10.1016/j.psep.2016.10.018

Liu, Z. H., Chen, Q. Y., Xie, X. B., Xue, G., Du, F. F., Ning, Q. Y., et al. (2011). Utilization of the sludge derived from dyestuff-making wastewater coagulation for unfired bricks. *Constr. Build. Mater.* 25, 1699–1706. doi: 10.1016/j.conbuildmat.2010.10.012

Malliou, O., Katsioti, M., Georgiadis, A., and Katsiri, A. (2007). Properties of stabilized/solidified admixtures of cement and sewage sludge. *Cement Concrete Comp.* 29, 55–61. doi: 10.1016/j.cemconcomp.2006.08.005

Malviya, R., and Chaudhary, R. (2006). Factors affecting hazardous waste solidification/stabilization: a review. *J. Hazard. Mater.* 137, 267–276. doi: 10.1016/j.jhazmat.2006.01.065

Marion, A. M., De Lanève, M., and De Grauw, A. (2005). Study of the leaching behaviour of paving concretes: quantification of heavy metal content in leachates issued from tank test using demineralized water. *Cement Concrete Res.* 35, 951–957. doi: 10.1016/j.cemconres.2004.06.014

Marsh, B. K. (1997). *Design of Normal Concrete Mixes, 2nd Edn.* England: Building Research Establishment Ltd

McCarthy, L. M., Gudimettla, J. M., Crawford, G. L., Guercio, M. C., and Allen, D. (2015). Impacts of variability in coefficient of thermal expansion on predicted concrete pavement performance. *Constr. Build. Mater.* 93, 711–719. doi: 10.1016/j.conbuildmat.2015.04.058

Meij, R., and Berg, J. (2001). "Coal fly ash management in Europe trends, regulations and health and safety aspects," in *International Ash Utilization Symposium*. Available online at: http://www.flyash.info/2001/keynote/108meij.pdf

Mohurd. (2012). *Special Guideline for Building Energy Conservation during Twelfth Five-Year Plan Period.* Retrieved from: http://www.gov.cn/zwgk/2012-05/31/content_2149889.htm

Monzó, J., Paya, J., Borrachero, M. V., and Girbes, I. (2004). Reuse of sewage sludge ashes (SSA) in cement mixtures: the effect of SSA on the workability of cement mortars. *Waste Manage.* 23, 373–381. doi: 10.1016/S0956-053X(03)00034-5

ÖzverdI, A., and Erdem, M. (2010). Environmental risk assessment and stabilization/solidification of zinc extraction residue: I. Environmental risk assessment. *Hydrometallurgy* 100, 103–109. doi: 10.1016/j.hydromet.2009.10.011

Papadimitriou, C. A., Haritou, I., Samaras, P., and Zouboulis, A. I. (2008). Evaluation of leaching and ecotoxicological properties of sewage sludge–fly ash mixtures. *Env. Res.* 106, 340–348. doi: 10.1016/j.envres.2007.04.007

Poon, C. S., and Lam, C. S. (2008). The effect of aggregate to cement ratio and types of aggregate on the properties of pre-cast concrete blocks. *Cement Concrete Comp*. 30, 283–289. doi: 10.1016/j.cemconcomp.2007.10.005

Poon, C. S., Shui, Z. H., Lam, L., Fok, H., and Kou, S. C. (2004). Influence of moisture states of natural and recycled aggregates on the slump and compressive strength of concrete. *Cement Concrete Res*. 34, 31–36. doi: 10.1016/S0008-8846(03)00186-8

Qiao, X. C., Poon, C. S., and Cheeseman, C. R. (2007). Investigation into the stabilization/solidification performance of Portland cement through cement clinker phases. *J Hazard. Mater*. 139, 238–243. doi: 10.1016/j.jhazmat.2006.06.009

Shackel, B. (1990). *Design and Construction of Interlocking Concrete Block Pavements*. London: Elsevier Applied Science

Siddiqui, M. S., and Fowler, D. W. (2015). A systematic optimization technique for the coefficient of thermal expansion of Portland cement concrete. *Constr. Build. Mater*. 88, 204–211. doi: 10.1016/j.conbuildmat.2015.04.008

Singh, M., and Siddique, R. (2013). Effect of coal bottom ash as partial replacement of sand on properties of concrete. *Resour. Conserv. Recy*. 72, 20–32. doi: 10.1016/j.resconrec.2012.12.006

Singh, M., and Siddique, R. (2014). Strength properties and micro-structural properties of concrete containing coal bottom ash partial replacement of fine aggregate. *Constr. Build. Mater*. 50, 246–256. doi: 10.1016/j.conbuildmat.2013.09.026

Singh, M., and Siddique, R. (2015). Properties of concrete containing high volumes of coal bottom ash as fly aggregate. *J. Clean. Prod*. 91, 269–278. doi: 10.1016/j.jclepro.2014.12.026

Tang, Y. Y., Chan, S. W., and Shih, K. M. (2014). Copper stabilization in beneficial use of waterworks sludge and copper-laden electroplating sludge for ceramic materials. *Waste Manage*. 34, 1085–1091. doi: 10.1016/j.wasman.2013.07.001

Tsang, Y. F. (2015). "Environmental protection and pollution management in China," in *The Entrepreneurial Rise in Southeast Asia–The Quadruple Helix Influence on Technological Innovation*, eds S. Sindakis and C. Walter (New York, NY: Palgrave Macmillan), 309–336

Tuan, B. L. A., Hwang, C. L., Lin, K. L., Chen, Y. Y., and Young, M. P. (2013). Development of lightweight aggregate from sewage sludge and waste glass powder for concrete. *Constr. Build. Mater*. 47, 334–339. doi: 10.1016/j.conbuildmat.2013.05.039

Tyagi, V. K., and Lo, S. L. (2013). Sludge: a waste or renewable source for energy and resources recovery? *Renew. Sust. Energ. Rev*. 25, 708–728. doi: 10.1016/j.rser.2013.05.029

Valls, S., and Vàzquez, E. (2002). Leaching properties of stabilised/solidified cement-admixtures-sewage sludges systems. *Waste Manage*. 22, 37–45. doi: 10.1016/S0956-053X(01)00027-7

Wang, H. L., Brown, S. L., Magesan, G. N., Slade, A. H., Quintern, M., Clintion, P. W., et al. (2008). Technological options for the management of biosolids. *Env. Sci. Poll. Res*. 15, 308–317. doi: 10.1007/s11356-008-0012-5

Wang, L., Kwok, S. H. J., Tsang, C. W. D., and Poon, C. S. (2015). Mixture design and treatment methods for recycling contaminated sediment. *J. Hazard. Mater*. 283, 623–632. doi: 10.1016/j.jhazmat.2014.09.056

Wang, M. (2005). *Research on Producing Non-Fired Bricks by Red Mud and Fly Ash*. Wuhan: Huazhong University of Science and Technology, 1–64.

Conflict of Interest Statement: The authors declare that the research was conducted in the absence of any commercial or financial relationships that could be construed as a potential conflict of interest.

frontiers in Energy Research

ORIGINAL RESEARCH
published: 17 December 2018
doi: 10.3389/fenrg.2018.00137

Potential of Acid-Activated Bentonite and SO_3H-Functionalized MWCNTs for Biodiesel Production From Residual Olive Oil Under Biorefinery Scheme

Hadi Rahimzadeh[1], Meisam Tabatabaei[2,3], Mortaza Aghbashlo[4]*, Hamed Kazemi Shariat Panahi[5], Alimorad Rashidi[6], Sayed Amir Hossein Goli[7], Mostafa Mostafaei[8], Mehdi Ardjmand[1] and Abdul-Sattar Nizami[9]*

[1] Department of Chemical Engineering, South Tehran Branch, Islamic Azad University, Tehran, Iran, [2] Department of Microbial Biotechnology, Agricultural Biotechnology Research Institute of Iran, Agricultural Research, Extension, and Education Organization, Karaj, Iran, [3] Biofuel Research Team, Karaj, Iran, [4] Engineering and Technology, College of Agriculture and Natural Resources, University of Tehran, Karaj, Iran, [5] Department of Microbial Biotechnology, School of Biology and Centre of Excellence in Phylogeny of Living Organisms, College of Science, University of Tehran, Tehran, Iran, [6] Nanotechnology Research Center, Research Institute of Petroleum Industry, Tehran, Iran, [7] Department of Food Science and Technology, College of Agriculture, Isfahan University of Technology, Isfahan, Iran, [8] Department of Mechanics and Biosystems Engineering, Agricultural Faculty, Razi University, Kermanshah, Iran, [9] Center of Excellence in Environmental Studies, King Abdulaziz University, Jeddah, Saudi Arabia

OPEN ACCESS

Edited by:
Saurabh Dhiman,
South Dakota School of Mines and Technology, United States

Reviewed by:
Jaime Puna,
Instituto Superior de Engenharia de Lisboa, Portugal
Konstantinos Moustakas,
National Technical University of Athens, Greece

***Correspondence:**
Meisam Tabatabaei
meisam_tab@yahoo.com;
meisam_tabatabaei@abrii.ac.ir
Mortaza Aghbashlo
maghbashlo@ut.ac.ir

Specialty section:
This article was submitted to Bioenergy and Biofuels, a section of the journal Frontiers in Energy Research

Received: 22 September 2018
Accepted: 28 November 2018
Published: 17 December 2018

Citation:
Rahimzadeh H, Tabatabaei M, Aghbashlo M, Panahi HKS, Rashidi A, Goli SAH, Mostafaei M, Ardjmand M and Nizami A-S (2018) Potential of Acid-Activated Bentonite and SO_3H-Functionalized MWCNTs for Biodiesel Production From Residual Olive Oil Under Biorefinery Scheme. Front. Energy Res. 6:137. doi: 10.3389/fenrg.2018.00137

Application of acid-activated bentonite and SO_3H-functionlized multiwall carbon nanotubes (SO_3H-MWCNTs) for lowering free fatty acids (FFAs) content of low-quality residual olive oil, prior to alkali-catalyzed transesterification was investigated. The used bentonite was first characterized by Scanning Electron Microscopy (SEM), Inductively Coupled Plasma mass spectrometry (ICP-MS), and X-ray fluorescence (XRF), and was subsequently activated by different concentrations of H_2SO_4 (3, 5, and 10 N). Specific surface area of the original bentonite was measured by Brunauer, Emmett, and Teller (BET) method at 45 m^2/g and was best improved after 5 N-acid activation (95–98°C, 2 h) reaching 68 m^2/g. MWCNTs was synthesized through methane decomposition (Co-Mo/MgO catalyst, 900°C) during the chemical vapor deposition (CVD) process. After two acid-purification (HCl, HNO_3) and two deionized-water-neutralization steps, SO_3H was grafted on MWCNTs (concentrated H_2SO_4, 110°C for 3 h) and again neutralized with deionized water and then dried. The synthesized SO_3H-MWCNTs were analyzed using Fourier-Transform Infrared Spectroscopy (FTIR) and Transmission Electron Microscopy (TEM). The activated bentonite and SO_3H-MWCNTs were utilized (5 wt.% and 3 wt.%, respectively), as solid catalysts in esterification reaction (62°C, 450 rpm; 15:1 and 12:1 methanol-to-oil molar ratio, 27 h and 8 h, respectively), to convert FFAs to their corresponding methyl esters. The results obtained revealed an FFA to methyl ester conversion of about 67% for the activated bentonite and 65% for the SO_3H-MWCNTs. More specifically, the acid value of the residual olive oil was decreased significantly from 2.5 to 0.85 and 0.89 mg KOH/g using activated bentonite and SO_3H-MWCNTs, respectively. The total FFAs in the residual olive oil after esterification was below 0.5%,

which was appropriate for efficient alkaline-transesterification reaction. Both catalysts can effectively pretreat low-quality oil feedstock for sustainable biodiesel production under a biorefinery scheme. Overall, the acid-activate bentonite was found more convenient, cost-effective, and environment-friendly than the SO_3H-MWCNTs.

Keywords: acid-activated bentonite, SO_3H-functionlized multiwall carbon nanotube (SO_3H-MWCNTs), waste olive oil, high free fatty acid, biodiesel production, biorefinery

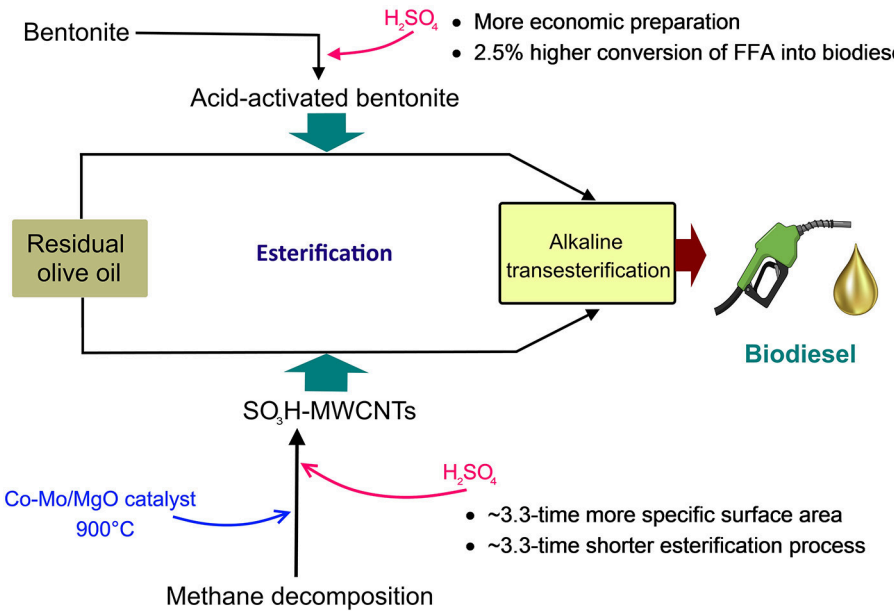

GRAPHICAL ABSTRACT

INTRODUCTION

Clay, particularly bentonites (clay mineral with different colors) are very popular in various industries (Christidis, 2013). Bentonite, has been applied as adsorbent, bleaching earth, and catalyst, as well as in eutrophication management and remediation of pollutions (Önal, 2006; Jeenpadiphat and Tungasmita, 2014; Copetti et al., 2016; El Korashy et al., 2016; Rezende and Pinto, 2016). Smectites are major clay minerals in bentonite with a 2:1 structure, or in another word, two silica tetrahedral sheets sandwich, an aluminum octahedral sheet or, a three-layer structure in which an aluminum octahedral sheet is located between two silica tetrahedral sheets. Replacement of some trivalent ions such as Al^{3+}, by some divalent ions like Fe^{2+} or Mg^{2+} in the octahedral layer, or substitution of Si^{4+} with Al^{3+} in the tetrahedral layer generates a net negative electric charge on the surface of clay. This negative charge is balanced by either Ca^{2+} or Na^{+} cations on the surface of clay in Na-type bentonite or Ca-type bentonite, respectively, (Shen, 2001; Önal, 2006; Önal and Sarıkaya, 2007).

Bentonites, by virtue of montmorillonite, have high absorption capacity for exchanging some certain cations from solutions with their own molecules. Bentonite quality and properties (i.e., clay minerals loading, cation exchange capacity (CEC), porosity, selectivity, surface acidity, surface area) are very important in industrial applications and could be modified by activation methods (Önal and Sarıkaya, 2007). In another word, prior to effective application of bentonite in industry, some of its properties should be improved through activation or treatment procedures. There are four major ways to activate bentonite and improve many of its properties. Those include (i) chemical, (ii) physical, (iii) pillaring, and (iv) thermal procedures. Bentonite is activated by the application of inorganic acids (such as H_2SO_4 or HCl) for replacing the exchangeable ions of bentonite during chemical procedure. Physical procedure involves mechanical improvement of bentonite's surface area by crushing it into smaller pieces. Similarly, pillaring procedure also improve bentonite's surface area as well as adsorption capacity. However, during pillaring procedure, these improvements are obtained through intercalating some elements or metal hydroxides

Abbreviations: BET, Brunauer, Emmett and Teller; CEC, Cation exchange capacity; CNT, Carbon nanotube; CVD, Chemical vapor deposition, FFA, Free fatty acid; FTIR, Fourier-Transform Infrared Spectroscopy; ICP-MS, Inductively Coupled Plasma mass spectrometry; SEM, Scanning Electron Microscopy, SO_3H-MWCNT, SO_3H-functionlized multiwall carbon nanotube, TEM, Transmission Electron Microscopy; XRF, X-ray fluorescence.

between the lamellar structures of bentonite creating pillars. In the last procedure, crystalline structure, or chemical composition of bentonite is thermally modified by heating bentonite at appropriate temperatures depending on its type. Amongst the aforementioned procedures, chemical treatment is the most common, and convenient method. It is worth mentioning that acid-activated bentonite could be used as solid acid catalyst in various reactions, such as esterification of oil for biodiesel production.

Carbon nanotubes (CNTs), first synthesized in 1991, have many applications as fillers, chemical sensors, hydrogen storage, electronic devices, catalyst supports, and etc., due to their unique properties including chemical stability, electrical, and thermal properties, high surface area, mechanical characteristic, etc. (Ham et al., 2004). CNTs are divided into single-wall CNTs and multi-wall CNTs (MWCNTs), arranged like a single rolled-up graphite sheet and like multiple layers of graphite rolled-up on themselves to form a tube shape, respectively (Kalamkarov et al., 2006). These structures can provide good support for various functional groups of specific features.

Oil feedstocks could be converted into biodiesel through the transesterification reaction (Aghbashlo et al., 2018b,c); however, food vs. fuel debate prevents the application of edible oils for this purpose (Hasheminejad et al., 2011; Aghbashlo et al., 2015, 2017b; Sahafi et al., 2018). On the other hand, ∼70–88% of the total biodiesel production cost arises from the cost of raw material (Haas et al., 2006). Therefore, biodiesel may be synthesized under a waste-oriented biorefinery scheme to address the aforementioned issues (Aghbashlo et al., 2018a, 2019). Under this concept, non-edible oils, such as waste cooking oils, and vegetable oil refinery waste oil that are either generated during processing oily crops into edible oil or their subsequent residuals from food processing sectors could be recycled into biodiesel (Aghbashlo et al., 2017a; Hajjari et al., 2017). For example, 0.11–0.22 billion liters a year residual olive oil is recovered from olive cake (Pütün et al., 2005). Therefore, one prominent feedstock for the reduction of biodiesel production cost is such waste/residual oil resources such as residual olive oil. The main drawbacks of such oil feedstock are; however, their high water, and free FFA contents, lowering the yield of direct alkaline-catalyzed transesterification of oil into biodiesel due to the consumption of high amounts of catalyst and the formation of soap.

Alternatively, biodiesel may be produced from high FFA oil feedstock through acid-catalyzed (trans) esterification reaction, in which FFAs and triglyceride simultaneously react with alcohol to produce methyl ester (biodiesel) (Pan et al., 2017). The main disadvantage of this strategy is the lengthy process that requires high methanol-to-oil molar ratios. Therefore, often acids are only used as a pretreatment (esterification) method only to lower FFA or acid value to the acceptable points (0.5% or 1 mg KOH/g, respectively), prior to the commencement of the alkaline-catalyzed transesterification reaction (Montefrio et al., 2010; Hasheminejad et al., 2011). Homogeneous acids (such as HCl, H_2SO_4, H_3PO_4) have been widely applied as catalyst for esterification of high FFA oil feedstocks (Photaworn et al., 2017; Murad et al., 2018). Overall, the main shortcomings of using homogeneous acids include high quantity of alcohol consumed, and that the acid used could not be recovered and should be neutralized as well. Moreover, the corrosive nature of some of these acids, for example H_2SO_4, could increase the maintenance costs by damaging the equipment.

Hydrophobic solid acid catalysts could be used to overcome the above-mentioned drawbacks of the homogeneous acid catalysts. Carbonized vegetable oil asphalt, ferric sulfate supported on silica, and tolune-4-sulfonic monohydrate acid are some solid acid catalysts investigated for pretreating low-quality oil feedstock for biodiesel production (Hayyan et al., 2010; Shu et al., 2010; Dokic et al., 2012). Unfortunately, despite their comparatively high catalytic activity, they suffer from high production cost, complexity of preparation methods, or harsh operating conditions.

Having considered the disadvantages of the acid pretreatment methods discussed above, searching for more efficient, less expensive, and easier to operate strategies is inevitable. Considering that, this study was set to investigate the catalytic performance of acid-activated bentonite in converting FFAs of low-quality, high FFA-containing residual olive oil into methyl esters. This could be regarded as a pretreatment step for FFA removal prior to basic-catalyzed transesterification reaction. To achieve that, bentonite was characterized, acid-activated, and its performance in decreasing FFA content of residual olive oil through conversion to methyl esters was evaluated. Moreover, MWCNTs were also synthesized, SO_3H functionalized, and their performance in FFA removal from residual olive oil was evaluated and compared with that of the acid-activated bentonite.

MATERIALS AND METHODS

Chemicals

Raw bentonite with the following physicochemical properties was used: surface area of 45 $m^2.g^{-1}$, mean pore diameter of 7.7 nm, total pore volume of 0.0898 $cm^3.g^{-1}$, swelling index of 15 mL/2 g, and CEC of 58 meq/100 g. Residual olive oil was purchased from an olive oil refinery and its FFA profiles and physical properties were investigated. All the chemicals used in this study were purchased either from Merck (Germany) or Sigma-Aldrich (Germany).

Bentonite Preparation, Activation, and Characterization

A uniform sample of bentonite with the size of about 130 μm was obtained by passing it through different sieves with appropriate mesh sizes. Then, aliquots of 50 g were weighted for the acid activation step.

Three different concentrations of H_2SO_4 (i.e., 3, 5, and 10 N) were used for the activation of 50 g bentonite. The treatment was conducted in a water bath (95–98°C, atmospheric pressure) and 250 ml H_2SO_4 was slowly added while the mixture was agitated at 400 rpm using a magnetic stirrer. After 2 h, samples were washed (i.e., pH 7) with deionized water until reaching a neutral pH. The remaining slurry was subsequently dried in an oven at 130°C for 2 h. The dried bentonites were kept in a desiccator until further use. The acid-activated bentonite was characterized by Scanning Electron Microscopy (SEM)

(Tescan Vega3, Czech Republic), Inductively Coupled Plasma Mass Spectrometry (ICP-MS) (Agilent, United States), and X-ray fluorescence (XRF) (Spectro, Germany). The specific area of the bentonite was measured by BET technique with N_2 adsorption, at 77 K, using BELSORB Mini instrument (Bel Japan, Inc.) based on the ASTM 4567.

MWCNTs Synthesis and Characterization

MWCNTs were synthesized through methane decomposition (900°C, atmospheric pressure, 20–50 min) over cobalt-molybdenum nanoparticles supported by nanoporous magnesium oxide during a chemical vapor deposition (CVD) process as described previously (Rashidi et al., 2007). Briefly, the reaction was performed using a flow of methane (50 mL/min) as carbon source and a flow of hydrogen (250 mL/min) as career gas at 900°C for 30 min. Upon the completion of the reaction, the furnace was cooled under a nitrogen atmosphere and then the product was purified. To achieve that, the resultant material was first dissolved in HCl solution (18%) for a duration of 16 h at ambient temperature (25°C ± 1) followed by filtration and several rounds of rinsing by distilled water. Subsequently, the product was dissolved in a nitric acid solution (6 M) for 6 h at 70°C. The slurry was then filtered, dried, and heated in a furnace at 400°C for 30 min. Then, the synthesized MWCNTs were subsequently sulfonated with 98% H_2SO_4 (110°C for 3 h), and neutralized (pH 7) by washing with deionized water. The sulfonated MWCNTs (SO_3H-MWCNTs) were dried and kept until further use.

The prepared MWCNTs were characterized by transmission electron microscopy (TEM, CM30, Philips, Netherland) for morphology determination. For FTIR analysis, the samples were milled with KBr to form a very fine powder, followed by their compression into pellets. FTIR spectra were recorded on a Thermo Nicolet Nexus 670 FT-IR ESP (Thermo Nicolet Corp., Madison, WI, United States). The specific area of the MWCNTs was measured by same BET technique used for bentonite, but was analyzed by an ASAP 2010 (Micromeritics, United States).

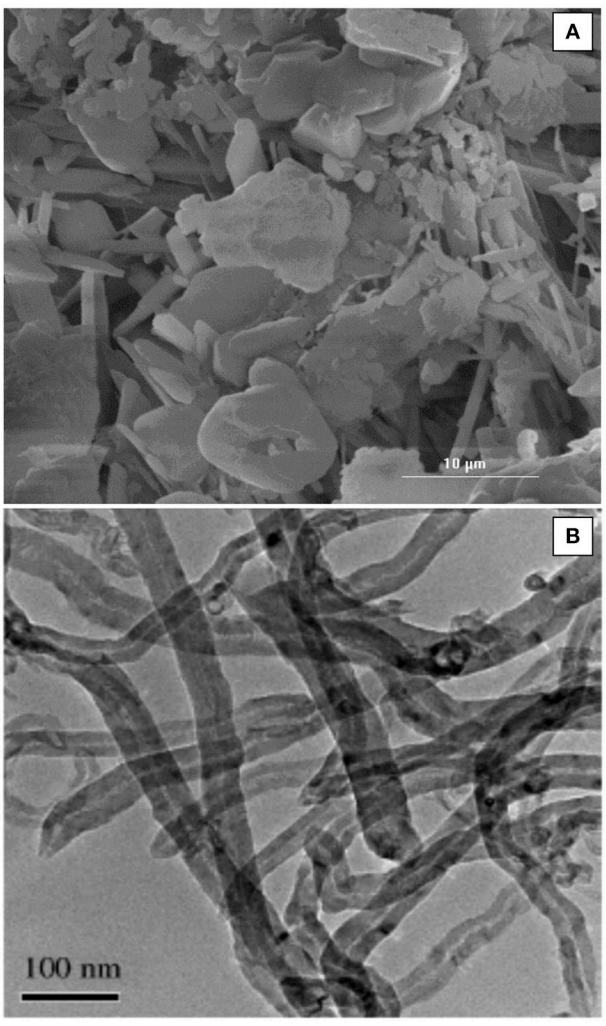

FIGURE 1 | (A) SEM micrograph of the bentonite used and **(B)** TEM micrograph of the synthesized MWCNTs.

Catalytic Activity of the Catalysts

Catalytic activities of the acid-activated bentonite (5 wt.% of oil) and SO_3H-MWCNTs (3 wt.% of oil) were calculated in respect to the esterification reaction with methanol-to-oil molar ratio

TABLE 1 | Inductively coupled plasma mass spectrometry (ICP-MS) and X-ray fluorescence (XRF) results for the used bentonite as well as surface area data obtained using BET technique for bentonite samples activated by different concentration of H_2SO_4.

Element	Concentration (ppm)	Element	Concentration (ppm)
ICP-MS ANALYSIS			
Ag	<0.01	Li	0.04
Al	270	Mg	22.8
As	0	Mn	1.4
B	99	Mo	0.1
Ba	9	Na	94
Be	<0.01	Ni	0.3
Ca	68	Pb	0.3
Cd	<0.01	Sb	0.0
Co	0.03	Sc	0.0
Cr	0.17	Se	<0.02
Cu	0.06	Sr	0.7
Fe	125	Ti	11.0
K	32	V	0.2
La	0.04	Zn	0.3
XRF ANALYSIS (WT.%)			
L.O.I.[a]	8.37	K_2O	0.94
Na_2O	3.17	MgO	0.95
CaO	2.38	TiO_2	0.46
Al_2O_3	12.75	Fe_2O_3	4.46
SiO_2	64.13		
BET SURFACE AREA ANALYSIS (m^2/g)			
Raw bentonite			45
3N acid-activated bentonite			62
5N acid-activated bentonite			68
10N acid-activated bentonite			66

[a] *Loss On Ignition (L.O.I.).*

of 15:1 and 12:1, respectively. The reaction was conducted in a magnetic stirred tank reactor (450 rpm) equipped with an alcohol reflux system at 62°C. The acid value was determined at certain intervals and the pretreatment step was continued until the value reached about 0.5 mg KOH/g. Samples were withdrawn and immediately placed in an ice bath to stop the reaction, followed by centrifugation (3,500 rpm, 5 min). Then, these samples were used for FFA reduction measurements.

Determination of FFA Conversion

The composition of the methyl esters produced by esterification of residual olive oil and methanol in the presence of acid-activated bentonite or SO_3H-MWCNTs as solid acid catalyst was determined using gas chromatography (GC; Claus 580 GC model, Perkin Elmer Co., United States). The conversion of the waste oil into methyl esters was determined by using the following equation:

$$conversion(\%) = \frac{\sum A \times A_{IS}}{A_{IS}} \times \frac{m}{M} \times 100 \quad (1)$$

where $\sum$A is the total area of the peaks, A_{IS} is the peak of the internal standard (C17:0), m is weight of internal standard, and M is the sample weight.

Acid value of the samples was also measured according to the method of Cd 3d-63 provided by American Oil Chemists' Society.

TABLE 2 | Free fatty acid profile and physical properties of residual olive oil used in the present study.

Fatty Acid composition	**Wt.%**
Palmitic (C16:0)	12.29
Palmitoleic (C16:1)	0.61
Stearic (C18:0)	2.44
Oleic (C18:1)	73.67
Linoleic (C18:2)	9.42
Linolenic (C18:3)	0.40
Arachidic (C20:0)	0.36
Others	0.82
Characteristic	**Value**
Free Fatty Acid (wt. %)	1.3
Mean Molecular weight (g/mol)	885.4
Viscosity (mPa.s)	34.52
Density (g/cm^3)	0.89
Acid value (mg KOH/g)	2.5
Iodine No.	94

RESULTS AND DISCUSSION

Characterization of the Acid-Activated Bentonite

The morphology of the natural bentonite as shown by SEM are presented in **Figure 1A**. The CEC of natural bentonite (58 meq/100 g) was, to a certain extent, lower than the expected range for smecite (80–150 meq/100), showing the presence of some impurities. The characterizations of the acid-activated bentonite synthesized in this study are presented in **Table 1**. The results of ICP-MS revealed that the bentonite used was of Na-type. Moreover, XRF data indicated that the bentonite structure was mostly composed of Al_2O_3 and SiO_2, providing good structure stability. It was expected that H_3O^+ ions replaced some of these elements (such as Na and calcium) as a result of acid pretreatment (Rezende and Pinto, 2016). Bentonite activation was performed with three different concentration of H_2SO_4 (3, 5, and 10 N), in order to investigate the impact of acid concentration on the surface area. Compared with natural bentonite, acid-activated bentonite displayed about 38–51% larger surface area (**Table 1**). It can be deduced from the BET data tabulated in **Table 1**,

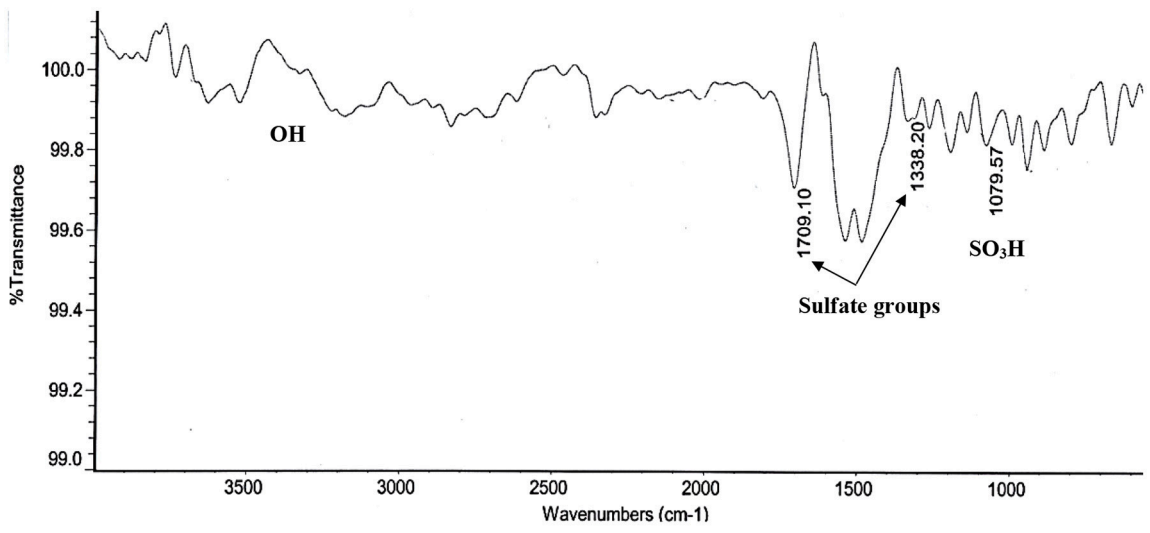

FIGURE 2 | FTIR spectroscopy of the SO_3H-MWCNTs.

TABLE 3 | The impact of 5 N acid-activated bentonite and SO_3H-functionalized MWCNT as catalyst in the esterification reaction (methanol-to-oil molar ratio of 15:1 and 12:1, respectively), on FFA removal through its conversion into methyl esters and acid value over time.

Time	Final FFA conc. (wt.%)*		Conversion of FFA(%)		Acid value (mg KOH/g)	
	Acid-activated bentonite	SO_3H-functionalized MWCNTs	Acid-activated bentonite	SO_3H-functionalized MWCNTs	Acid-activated bentonite	SO_3H-functionalized MWCNTs
20 min	1.27	–	2.3	–	2.45	–
40 min	1.21	–	6.9	–	2.39	–
1 h	1.18	1.2	9.2	7.7	2.30	2.4
2 h	1.14	1.14	12.3	12.3	2.27	2.27
3 h	1.03	0.98	20.8	24.6	2.04	1.95
4 h	0.99	0.81	23.8	37.7	1.97	1.6
5 h	0.97	0.71	25.4	45.4	1.91	1.41
6 h	0.95	0.68	26.9	47.7	1.95	1.35
7 h	–	0.60	–	53.8	–	1.20
8 h	–	0.47	–	64.4	–	0.89
23 h	0.51	–	60	–	1.00	–
25 h	0.53	–	59.2	–	1.08	–
27 h	0.43	–	66.9	–	0.85	–

**Initial FFA content = 1.3 (wt.%).*

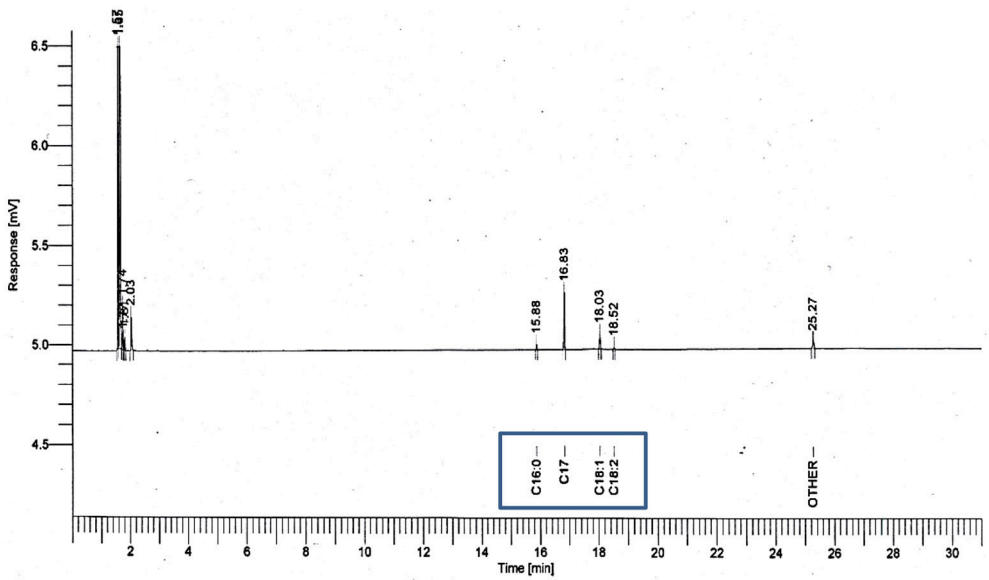

FIGURE 3 | GC chromatograms used for calculating methyl ester yield through the esterification reaction, with 5 N acid-activated bentonite and the SO_3H-MWCNTs as catalyst.

that the activation of bentonite with 5 N solution of H_2SO_4 triggered the largest surface area. In another word, increasing acid concentration from 3 to 5 N had a positive impact on the surface area, and consequently, on the number of hydrogen ions anchored on bentonite's surface. However, further elevation of acid concentration to 10 N must have damaged bentonite structure by collapsing some of its layers by dissolving them. In fact, the lower surface area obtained through the activation by 10 N H_2SO_4 solution signifies that fewer hydrogen ions were anchored, and thus, less catalytic activity was achieved. On this basis, bentonite sample activated by 5 N acid solution was selected for the FFA reduction experiment.

Characterization of the Synthesized SO_3H-MWCNTs

The BET surface area of the synthesized SO_3H-MWCNTs was measured at 230 m^2/g, with the pore volume and diameter recorded at 0.76 cm^3/g and 11 nm, respectively. This high BET surface area was because of inducing the repulsion force between SO_3H and COOH groups on the MWCNTs surface (Shuit et al.,

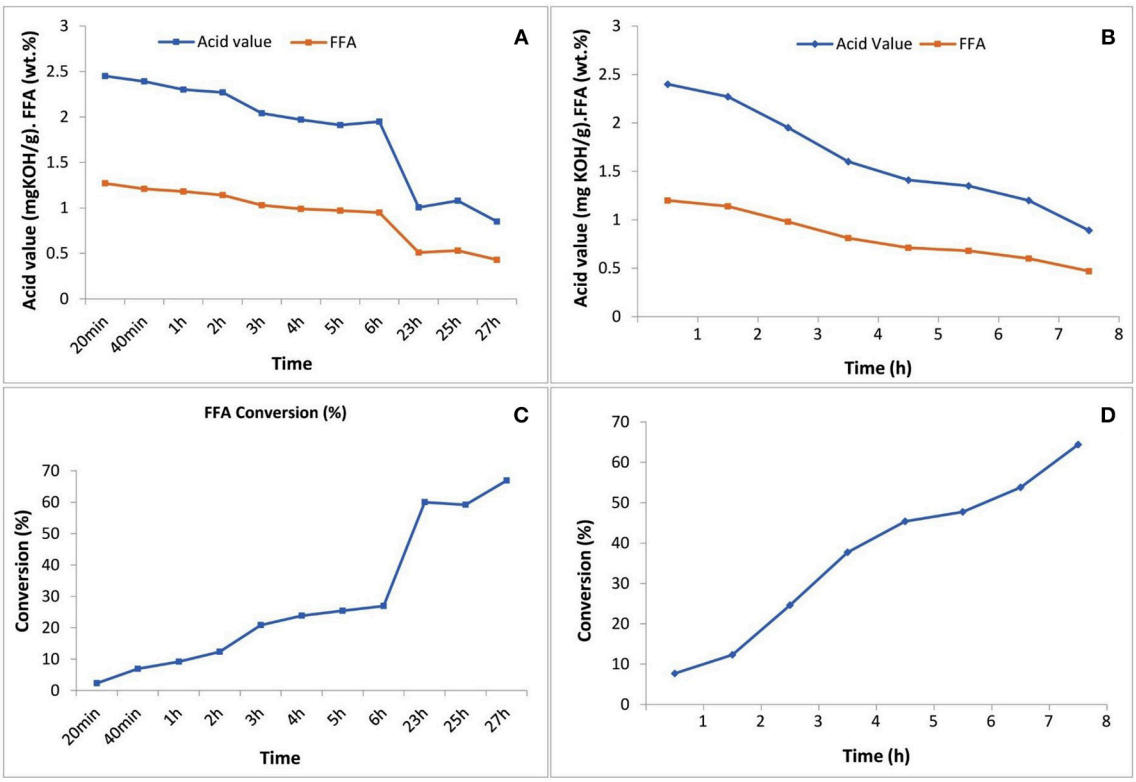

FIGURE 4 | Acid value and FFA content reduction through the esterification reaction **(A)** with 5 N acid-activated bentonite and **(B)** with SO_3H-MWCNTs, as catalyst vs. time; and diagrams of FFA conversion to methyl esters **(C)** using 5N acid-activated bentonite and **(D)** using SO_3H-MWCNTs.

2015), The morphology of the SO_3H-MWCNTs as shown by TEM are presented in **Figure 1B**. As it can be observed, the sidewalls of SO_3H-MWCNTs are not smooth due to the oxidizing effect of HNO_3. FTIR data confirmed successful functionalization of the MWCNTs with SO_3H (**Figure 2**). As revealed in the figure, a strong peak representing the stretch vibration of the SO_3H functional group anchored on the MWCNTs appeared at around 1,000–1,080 cm^{-1}. Moreover, a broad band in the region 3,100–3,400 cm^{-1} was assigned to OH group caused by the purification step implemented. In addition, the strong band observed at 1,709 cm^{-1}, and the weak band at 1,338 cm^{-1} could be attributed to the stretching modes of sulfate groups.

Impacts of the Synthesized Catalysts on FFA Conversion

The characteristics of the residual olive oil used in this study, i.e., FFA profiles and physicochemical properties are presented in **Table 2**. Respectively, the applications of 5 N acid-activated bentonite and SO_3H-MWCNTs efficiently decreased the FFA content of residual olive oil to 0.43 and 0.47% that were less than the maximum acceptable value of 0.5% (**Table 3**). Intriguingly, original bentonite sample used as control did not show any positive impacts on FFA reduction. The results related to the FFA content reduction as determined by GC analysis (**Figure 3**), through their conversion to methyl esters are shown in **Table 3** and **Figure 4**. These findings well demonstrate the catalytic activity of the acid-activated bentonite and the SO_3H-MWCNTs.

The acid-activated bentonite acted as a solid acid catalyst due to the hydrogen ions already anchored among its smectite's layers during the activation process. In another word, acid-activated bentonite acted as a proton donor catalyst expediting the esterification reaction. As seen in **Figure 4**, ∼67% of the FFAs contained in the residual olive oil were converted to methyl esters within the 27 h experimental period. It is worth mentioning that a methyl ester yield of 1.3% would be achieved from 100% conversion of the total FFA. However, the total methyl ester measured was 2.06% from 67% conversion of total available FFAs. This unexpected difference implies that some of the methyl ester yield (∼1.1 out of 2.06%) arose from acid-transesterification of triglycerides and not from the esterification of FFAs. This indicates that, although very minor, the active sites present on the surface of acid-activated bentonites could also attack the huge triglyceride molecules, and converted them into methyl esters.

Moreover, SO_3H-MWCNTs was shown to possess favorable catalytic activity as 65% of the contained FFAs were converted, reaching the final concentration of 0.47%, in just 8 h of

TABLE 4 | Comparison of some studies in which acid-activated bentonites and SO_3H-functionlized multiwall carbon nanotubes (MWCNT) were used as catalysts in FFA esterification process.

Study	Catalyst	Preparation	Characteristics features			Feedstocks (molar ratio)	Esterification conditions	FFA conversion yield (%)
			Surface area (m^2/g)	Pore diameter (nm)	Pore volume (cm^3/g)			
Shuit et al., 2015	SO_3H-MWCNTs	10 wt.% $(NH_4)_2SO_4$, ultrasonication (10 min), heating (235°C, 30 min)	92.37	12.3	0.25	Palm fatty acid distillate + methanol (1:20)	2 wt.% catalyst, 170°C, 1 MPa, 3 h	84.9
Current study	SO_3H-MWCNTs	Concentrated H_2SO_4, 110°C, 3 h	230	11 nm	0.76	Residual olive oil + methanol (1:12)	3 wt.% catalyst, 450 rpm, 62°C, 8 h	64.4
Rezende and Pinto, 2016	Acid-activated bentonite	10% w/v suspension of clay, H_2SO_4 (4 $mol.L^{-1}$), 90°C, 2 h	137	56.6	0.21	Fatty acids from residual palm oil + methanol (1:3) methanol	50 g catalyst/mol fatty acid, 100°C, 4 h	89
Jeenpadiphat and Tungasmita, 2014		H_2SO_4 or HNO_3 (bentonite-to acid ratio of 1 g/30 mL), 120°C, 1 h	42	21	0.16	Oleic acid in palm oil + methanol (1:23)	10 wt.% catalyst, 60°C, 1 h	99
Current study	Acid-activated bentonite	5 N H_2SO_4 (??? wt.%), 95–98°C, 400 rpm, 2 h	68	–	–	Residual olive oil + methanol (1:15)	5 wt.% catalyst, 450 rpm, 62°C, 27 h	66.9

esterification reaction (**Figure 4**). From the performance point of view, SO_3H-MWCNTs were found as a better choice in comparison with acid-activated bentonite, as it led to slightly higher FFA reduction within 3-fold shorter time period (**Table 3**). This could be ascribed to its stronger acidic functional group (SO_3H).

Table 4 compares some studies in which acid-activated bentonites and SO_3H-MWCNTs were used as catalysts in FFA esterification process. These studies differ in terms of the procedures used for catalyst preparation though. Shuit et al. (2015) used 10 wt.% $(NH_4)_2SO_4$ solution and ultrasonication (10 min), followed by a heating step (°C, 30 min) to synthesize SO_3H-MWCNTs for biodiesel production. This process was more advantageous than the procedure used in the present study in terms of synthesis time and being H_2SO_4 free; however, about 2.1-time higher temperature was required. Moreover, the synthesized SO_3H-MWCNTs had very lower surface area (92.37 vs. 230 m^2/g, respecively) and pore volume (0.25 vs. 0.76 cm^3/g, respectiely) making it a less efficient catalyst. The acid-activated bentonite produced herein showed about 62% higher surface area than that prepared by Jeenpadiphat and Tungasmita (2014). Both catalysts prepared in the current study, especially SO_3H-MWCNTs, could decrease mass transfer limitation due to their high surface area. Nevertheless, and despite their characteristic advantages, lower FFA conversion yields were obtained by these catalysts in comparison with those listed in **Table 4**. This could be attributed to the fact that esterification process was not optimized in this study. Instead, a common mild-esterification reaction was targeted to only evaluate the catalytic performance of prepared catalysts.

CONCLUDING REMARKS AND FUTURE PROSPECTS

This study showed that bentonite could be applied as an efficient raw material for synthesizing solid acid catalyst, through a simple chemical (i.e., acid) activation method, for using in solid acid catalyzed-esterification of high FFA oils. The application of this natural clay may encourage the production of sustainable fuels, as there is no requirement for sophisticated methods, and environmental hazardous chemicals as well. Acid activation of benonite using 5 N H_2SO_4 was found to considerably improve its acidity as well as its specific surface area (more than half-time), and in turn, its catalytic activity for FFA content reduction of residual olive oil to <0.5 wt.%. It should also be noted that bentonite is very abundant and cheap (<20 USD/ton) and therefore, 5 N acid-activated bentonite could serve as a promising pre-treatment process for esterification of low-quality oil feedstock prior to alkali-catalyzed transesterification. Moreover, SO_3H-MWCNTs were also synthesized and their catalytic performance was characterized. It showed excellent specific surface area (230 m^2/g), and good pore diameter (11 nm) and pore volume (0.76 cm^3/g), enhancing mass transfer of reaction. Compared with the acid-activated bentonite, SO_3H-MWCNTs provided better catalytic performance. Despite more favorable economic preparation of the 5 N acid-activated

bentonite and its relatively similar performance in terms of FFA reduction with the SO_3H-MWCNTs, the latter catalyst proved more feasible for industrial application. This feasibility can be attributed to its considerably shorter reaction time due to more than 3.3 times higher specific surface area, significantly lowering mass transfer limitation. Further optimization of the esterification reaction conditions would be necessary for full exploitation of these two catalysts for FFA conversion into biodiesel. Overall, both of the prepared catalysts could be used for effective pretreatment of low-quality residual olive oil for sustainable biodiesel production under a biorefinery scheme.

AUTHOR CONTRIBUTIONS

HR performed the bentonite catalyst production, SG and MM assisted with GC analyses, MeA assisted with some characterizations, MT and AR developed the idea and led the research. MT, MoA, and A-SN wrote the manuscript. HP as of substantial help during the revision process.

ACKNOWLEDGMENTS

We are thankful to Biofuel Research Team (BRTeam) for supporting this study.

REFERENCES

Aghbashlo, M., Hosseinpour, S., Tabatabaei, M., and Dadak, A. (2017a). Fuzzy modeling and optimization of the synthesis of biodiesel from waste cooking oil (WCO) by a low power, high frequency piezo-ultrasonic reactor. *Energy* 132, 65–78. doi: 10.1016/j.energy.2017.05.041

Aghbashlo, M., Hosseinpour, S., Tabatabaei, M., and Soufiyan, M. M. (2019). Multi-objective exergetic and technical optimization of a piezoelectric ultrasonic reactor applied to synthesize biodiesel from waste cooking oil (WCO) using soft computing techniques. *Fuel* 235, 100–112. doi: 10.1016/j.fuel.2018.07.095

Aghbashlo, M., Tabatabaei, M., and Hosseinpour, S. (2018a). On the exergoeconomic and exergoenvironmental evaluation and optimization of biodiesel synthesis from waste cooking oil (WCO) using a low power, high frequency ultrasonic reactor. *Energy Convers. Manage.* 164, 385–398. doi: 10.1016/j.enconman.2018.02.086

Aghbashlo, M., Tabatabaei, M., Jazini, H., and Ghaziaskar, H. S. (2018b). Exergoeconomic and exergoenvironmental co-optimization of continuous fuel additives (acetins) synthesis from glycerol esterification with acetic acid using Amberlyst 36 catalyst. *Energy Convers. Manage.* 165, 183–194. doi: 10.1016/j.enconman.2018.03.054

Aghbashlo, M., Tabatabaei, M., Mohammadi, P., Khoshnevisan, B., Rajaeifar, M. A., and Pakzad, M. (2017b). Neat diesel beats waste-oriented biodiesel from the exergoeconomic and exergoenvironmental point of views. *Energy Convers. Manage.* 148, 1–15. doi: 10.1016/j.enconman.2017.05.048

Aghbashlo, M., Tabatabaei, M., Mohammadi, P., Pourvosoughi, N., Nikbakht, A. M., and Goli, S. A. H. (2015). Improving exergetic and sustainability parameters of a DI diesel engine using polymer waste dissolved in biodiesel as a novel diesel additive. *Energy Convers. Manage.* 105, 328–337. doi: 10.1016/j.enconman.2015.07.075

Aghbashlo, M., Tabatabaei, M., Rastegari, H., Ghaziaskar, H. S., and Shojaei, T. R. (2018c). On the exergetic optimization of solketalacetin synthesis as a green fuel additive through ketalization of glycerol-derived monoacetin with acetone. *Renew. Energy* 126, 242–253. doi: 10.1016/j.renene.2018.03.047

Christidis, G. (2013). "Assessment of industrial clays," in *Handbook of Clay Science. Part B. Techniques and Applications,* eds F. Bergaya and G. Lagaly (Amsterdam: Elsevier), 425–449.

Copetti, D., Finsterle, K., Marziali, L., Stefani, F., Tartari, G., Douglas, G., et al. (2016). Eutrophication management in surface waters using lanthanum modified bentonite: a review. *Water Res.* 97, 162–174. doi: 10.1016/j.watres.2015.11.056

Dokic, M., Kesic, Z., Krstic, J., Jovanovic, D., and Skala, D. (2012). Decrease of free fatty acid content in vegetable oil using silica supported ferric sulfate catalyst. *Fuel* 97, 595–602. doi: 10.1016/j.fuel.2012.03.039

El Korashy, S. A., Elwakeel, K. Z., and El Hafeiz, A. A. (2016). Fabrication of bentonite/thiourea-formaldehyde composite material for Pb (II), Mn (VII) and Cr (VI) sorption: a combined basic study and industrial application. *J. Cleaner Prod.* 137, 40–50. doi: 10.1016/j.jclepro.2016.07.073

Haas, M. J., McAloon, A. J., Yee, W. C., and Foglia, T. A. (2006). A process model to estimate biodiesel production costs. *Bioresour. Tech.* 97, 671–678. doi: 10.1016/j.biortech.2005.03.039

Hajjari, M., Tabatabaei, M., Aghbashlo, M., and Ghanavati, H. (2017). A review on the prospects of sustainable biodiesel production: a global scenario with an emphasis on waste-oil biodiesel utilization. *Renew. Sustain. Energy Rev.* 72, 445–464. doi: 10.1016/j.rser.2017.01.034

Ham, H. T., Koo, C. M., Kim, S. O., Choi, Y. S., and Chung, I. J. (2004). Chemical modification of carbon nanotubes and preparation of polystyrene/carbon nanotubes composites. *Macromol. Res.* 12, 384–390. doi: 10.1007/BF03218416

Hasheminejad, M., Tabatabaei, M., Mansourpanah, Y., and Javani, A. (2011). Upstream and downstream strategies to economize biodiesel production. *Bioresour. Tech.* 102, 461–468. doi: 10.1016/j.biortech.2010.09.094

Hayyan, A., Alam, M. Z., Mirghani, M. E., Kabbashi, N. A., Hakimi, N. I. N. M., Siran, Y. M., et al. (2010). Sludge palm oil as a renewable raw material for biodiesel production by two-step processes. *Bioresour. Tech.* 101, 7804–7811. doi: 10.1016/j.biortech.2010.05.045

Jeenpadiphat, S., and Tungasmita, D. N. (2014). Esterification of oleic acid and high acid content palm oil over an acid-activated bentonite catalyst. *Appl. Clay Sci.* 87, 272–277. doi: 10.1016/j.clay.2013.11.025

Kalamkarov, A. L., Georgiades, A., Rokkam, S., Veedu, V., and Ghasemi Nejhad, M. (2006). Analytical and numerical techniques to predict carbon nanotubes properties. *Int. J. Solids Struct.* 43, 6832–6854. doi: 10.1016/j.ijsolstr.2006.02.009

Montefrio, M. J., Xinwen, T., and Obbard, J. P. (2010). Recovery and pre-treatment of fats, oil and grease from grease interceptors for biodiesel production. *Appl. Energy* 87, 3155–3161. doi: 10.1016/j.apenergy.2010.04.011

Murad, P. C., Hamerski, F., Corazza, M. L., Luz, L. F., and Voll, F. A. (2018). Acid-catalyzed esterification of free fatty acids with ethanol: an assessment of acid oil pretreatment, kinetic modeling and simulation. *React. Kinet. Mech. Catal.* 123, 505–515. doi: 10.1007/s11144-017-1335-3

Önal, M. (2006). Physicochemical properties of bentonite: an overview. *Commun. Fac. Sci. Univ. Ankara Seri. B* 52, 7–21. doi: 10.1501/Commub_0000000349

Önal, M., and Sarıkaya, Y. (2007). Preparation and characterization of acid-activated bentonite powders. *Powder Technol.* 172, 14–18. doi: 10.1016/j.powtec.2006.10.034

Pan, H., Zhang, H., and Yang, S. (2017). "Production of Biodiesel via Simultaneous Esterification and Transesterification," in *Production of Biofuels and Chemicals with Bifunctional Catalysts,* eds Z. Fang, J.R. Smith, and H. Li (Singapore: Springer), 307–326. doi: 10.1007/978-981-10-5137-1_10

Photaworn, S., Tongurai, C., and Kungsanunt, S. (2017). Process development of two-step esterification plus catalyst solution recycling on waste vegetable oil possessing high free fatty acid. *Chem. Eng. Process.* 118, 1–8. doi: 10.1016/j.cep.2017.04.013

Pütün, A. E., Uzun, B. B., Apaydin, E., and Pütün, E. (2005). Bio-oil from olive oil industry wastes: pyrolysis of olive residue under different conditions. *Fuel Process. Tech.* 87, 25–32. doi: 10.1016/j.fuproc.2005.04.003

Rashidi, A. M., Akbarnejad, M. M., Khodadadi, A. A., Mortazavi, Y., and Ahmadpourd, A. (2007). Single-wall carbon nanotubes synthesized using organic additives to Co-Mo catalysts supported on nanoporous MgO. *Nanotechnology* 18:315605. doi: 10.1088/0957-4484/18/31/315605

Rezende, M. J., and Pinto, A. C. (2016). Esterification of fatty acids using acid-activated Brazilian smectite natural clay as a catalyst. *Renew. Energy* 92, 171–177. doi: 10.1016/j.renene.2016.02.004

Sahafi, S. M., Ahmadibeni, A., Talebi, A. F., Goli, S. A. H., Aghbashlo, M., and Tabatabaei, M. (2018). Seed oils of *Sisymbrium irio* and *Sisymbrium sophia* as a potential non-edible feedstock for biodiesel production. *Biofuels* 1–9. doi: 10.1080/17597269.2018.1457315

Shen, Y. H. (2001). Preparations of organobentonite using nonionic surfactants. *Chemosphere* 44, 989–995. doi: 10.1016/S0045-6535(00)00564-6

Shu, Q., Nawaz, Z., Gao, J., Liao, Y., Zhang, Q., Wang, D., et al. (2010). Synthesis of biodiesel from a model waste oil feedstock using a carbon-based solid acid catalyst: reaction and separation. *Bioresour. Technol.* 101, 5374–5384. doi: 10.1016/j.biortech.2010.02.050

Shuit, S. H., Ng, E. P., and Tan, S. H. (2015). A facile and acid-free approach towards the preparation of sulphonated multi-walled carbon nanotubes as a strong protonic acid catalyst for biodiesel production. *J. Taiwan Inst. Chem. Eng.* 52, 100–108. doi: 10.1016/j.jtice.2015.02.018

Conflict of Interest Statement: The authors declare that the research was conducted in the absence of any commercial or financial relationships that could be construed as a potential conflict of interest.

frontiers in Energy Research

ORIGINAL RESEARCH
published: 10 January 2019
doi: 10.3389/fenrg.2018.00143

Effect of Pretreatment and Substrate Ratios in Biorefinery Employing Co-digestion of Plant Biomass and Poultry Waste

Fayyaz Ali Shah[1], *Naim Rashid*[2], *Qaisar Mahmood*[1]* *and Arshad Ali*[3]

[1] *Department of Environmental Sciences, COMSATS University Islamabad, Abbottabad Campus, Abbottabad, Pakistan,* [2] *Department of Chemical Engineering, COMSATS University Islamabad, Lahore Campus, Lahore, Pakistan,* [3] *Military College of Engineering (MCE), National University of Sciences and Technology (NUST), Risalpur Campus, Risalpur, Pakistan*

The current study investigated the optimization of biogas generation during co-digestion of various plant biomasses with poultry waste at different ratios and pretreatment of plant biomass. The biochemical tests were executed at 35°C in a thermostat. Water hyacinth was found as the suitable substrate for mono and co-digestion due to high volatile solids (VS) and total soluble contents. However, poultry waste was appropriate only if it was co-digested with other biomasses. The experiments evaluating biogas generation at different ratios of plant biomasses and poultry waste demonstrated that water hyacinth and poultry (50:50) produced 262 mL g^{-1}VS, giant reed and poultry (80:20) produced 235 mL g^{-1}VSwhile maize and poultry (60:40) generated 193 mL g^{-1}VS. However, the pretreating the plant biomass with either Fenton's or Fenton's plus ultrasonic had no effect on biogas generation. The volumes of biogas generated after various pretreatment were low as compared to condition without pretreatment. The codigestion can be classified as WH:P (50:50 > GR:P (80:20) > M:P (60:40). So, these ratios can be applied at decentralized scale for better waste management and biogas generation due to balanced C:N ratio of plant biomass and poultry manure. Co-digestion can also be applied at large scale with optimized ratio in Pakistan and other developing countries for biogas generation and waste management and reduce the methane emission through landfills.

Keywords: anaerobic digestion, co-digestion, giant reed, maize, pretreatment, water hyacinth

OPEN ACCESS

Edited by:
Abdul-Sattar Nizami,
King Abdulaziz University, Saudi Arabia

Reviewed by:
Md Mofijur Rahman,
Central Queensland University, Australia
Mohammad Rehan,
King Abdulaziz University, Saudi Arabia

***Correspondence:**
Qaisar Mahmood
mahmoodzju@gmail.com

Specialty section:
This article was submitted to Bioenergy and Biofuels, a section of the journal Frontiers in Energy Research

Received: *06 August 2018*
Accepted: *10 December 2018*
Published: *10 January 2019*

Citation:
Shah FA, Rashid N, Mahmood Q and Ali A (2019) Effect of Pretreatment and Substrate Ratios in Biorefinery Employing Co-digestion of Plant Biomass and Poultry Waste. Front. Energy Res. 6:143. doi: 10.3389/fenrg.2018.00143

INTRODUCTION

Currently, the world is facing problems like environmental contamination and shortage of energy. Exploring non-conventional and eco-friendly sources of energy is serious consideration of many developing nations (Owamah et al., 2014). In this scenario, the need and exploration of alternative biofuels is a need of the hour. Even exploitation of methanogenesis during anaerobic digestion (AD) is quite old (Triolo et al., 2011). The advantages of AD are multi-dimensional; it not only reduces wastes from the environment but also helps in nutrient turn over along generation of biomethane as an important energy source. The industrial viability of AD demands an appropriate low-cost amalgamation of physicochemical parameters for the optimum functioning of this process (Owamah et al., 2014). For a sustainable and productive AD process, appropriate amounts of various macro and micronutrients including N, P, S, Fe, Ni, Se, W, Co, Mo, among many others is

quite desirable (Chen et al., 2008; Demirel and Scherer, 2008; Hinken et al., 2008). The role of co-digestion, pretreatment and digester design for the enhancement of biogas have been thoroughly reviewed by Shah et al. (2015).

Co-digestion involves the use of two different substrates in a mixture at different ratios. Previously, it was iterated that methanogenesis could significantly be enhanced and optimized if feedstocks were co-digested with animal wastes (Cavinato et al., 2010). In view of few drawbacks of feed stocks for mono-digestion (Hinken et al., 2008; Pobeheim et al., 2010), the codigestion of various substrates always resulted in enhanced biogas generation. Considering the nature, strength flow rate of the substrate used and the biogas generation could be enhanced in range of 25–400% (Callaghan et al., 2002; Alatrwaste-Mondragón et al., 2006).

Researchers reported different results for the screening of diverse biomasses for methanogenesis in mono-digestion and co-digestion. An increase of 400% was noted in methanogenesis when pig manure was co-digested with glycerol under mesophilic conditions (Astals et al., 2012). Co-digestion of algal biomass and fats, oils, and waste grease resulted in increased biogas production with gradual rise in organic loadings (Park et al., 2012). Stable biogas generation of 621 L/kgVS was observed at HRT of 42 days by digesting 50% slurry and whey mixture (Comino et al., 2012). The combination of waste paper, cow dung, and *Eichhornia crassipes* was evaluated for methanogenesis and the results were promising to reduce waste paper and enhancing biogas yield (Comino et al., 2012). In addition to increased methanogenesis, co-digestion of various substrates may present many advantages like high OLR, better biodegradability, balance of nutrients, suitable C:N ratio and lowering of toxicity of some substrates (Khalid et al., 2011; Wang et al., 2012, 2013). The preference of co-digestion was also advocated by (De Varies, 2012). AD of sewage sludge with poultry manure was also found beneficial (Bujoczek et al., 2000).

Biogas production was also found plentiful when substrates containing lignocelluloses was digested anaerobically (Zheng et al., 2014). In case of substrates containing high lignocellulose contents, pretreatment of biomasses with various techniques can be useful (Zheng et al., 2014) which reduce lignin, crystallinity but increase surface area. However, the richness of lignocellulose contents in the feedstock of AD may pose a barrier to microbial action on these substrates thus limiting the performance of AD (Fernández-Cegrí et al., 2012). In view of promising results obtained for co-digestion of different substrates, the importance of poultry waste in providing phosphorus for AD has never been realized to treat water hyacinth and other substrates. Water hyacinth is an abundant biomass that grows prolifically in all tropical and sub-tropical regions of the world. We anticipated that better biogas yield might be resulted by co-digestion of plant biomasses with poultry waste along with pretreatments. Pretreatment may be useful in view of fibrous nature of substrates which might have high cellulose and lingo-cellulosic materials. Based on above published reports, the aim of the current research was to evaluate the effects of pretreatment and co-digestion of various plant wastes with poultry litter for biogas generation.

METHODOLOGY

Sampling

Various substrates were collected for the experimentation from various non-contaminated places of Khyber Pakhtoonkhwa province of Pakistan. Prior to feeding into bioreactor, the plant biomasses and poultry wastes were air and oven dried at 35°C. The plant biomasses were chopped and ground for further experimentation.

Experimental Design

All the experiments were carried out in triplicates in a flask of volume of 500 ml for 30 days. The active volume was 100 ml with headspace of 400 ml for ratio experiment. The reactors were operated at temperature of 35°C as given in the **Figure 1**. Inoculum to substrate ratio (I/S) of 2:1 was administered to the bioreactor. The contents of the bioreactors were purged

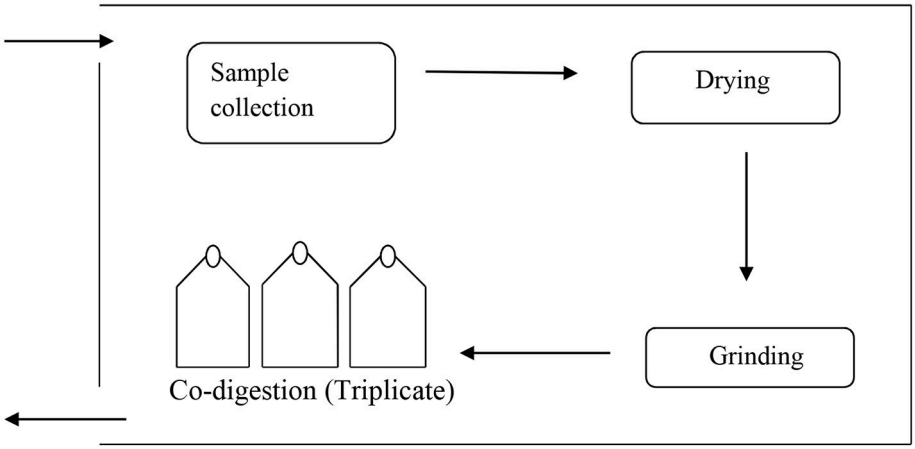

FIGURE 1 | Schematic diagram of the experiment.

with nitrogen gas for 5 min to generate anaerobic conditions for microbes and subsequently sealed using butyl rubber stoppers. An outlet in the stopper was used for collecting biogas in inverted graduated cylinder and biogas was measured daily by water displacement as previously described by Shah et al. (2015). The pH of liquid in the inverted cylinder was kept acidic using 0.01 M HCl to avoid carbon dioxide absorption from biogas. A blank reactor was also run containing inoculum and distilled water, incubated at the same temperature to measure the background biogas produced from the inoculum and for pretreatment, which was subtracted from the total biogas production. All the digesters were monitored daily for biogas production. Experimental design for biomass ratio was given in the **Table 1** and pretreatment design was shown in the **Table 2**.

Biogas Unit

A schematic diagram of experimental set up was adapted from Shah et al. (2015). It consisted of a temperature controlled water bath at 35°C containing digesters for the experiment. Each digester was connected to a graduated gas collector by means of a connecting tube. The experimental set up was shown in **Figure 1**. Biogas evolved was collected by downward water displacement as described above.

Seed Inoculum

Anaerobic sludge was used from the already running experiment. Therefore, it was assumed as microbiologically adequate to treat various substrates proposed for the BMP assays. Similarly, the amount of inoculum used in the test bottles was determined based on amount of organic substrate available for degradation, i.e., inoculum-to-substrate (I/S) ratio (on VS basis), which was equivalent to the inverse value of the food-to-microorganisms (F/I) ratio.

TABLE 1 | Experimental design for different biomass ratio test.

Different Biomass ratio	Poultry (g)	Giant Reed (g)	Maize (g)	Water hyacinth (g)	Inoculum (mL)	Water (mL)
50:50	5	5	5	5	20	10
80:20	8	2	2	2	20	10
20:80	2	8	8	8	20	10
60:40	6	4	4	4	20	10
40:60	4	6	6	6	20	10

TABLE 2 | Experimental design for pretreatment of plant biomass for biogas production.

Plant biomass	Weight (g)	Pretreatment conditions			
		Frequency (Khz)	Power (W)	Time (minutes)	Temperature (°C)
Giant Reed	10	40	2.7	10	30
Maize	10	40	2.7	10	30
Water Hyacinth	10	40	2.7	10	30

Statistical Analysis

All determinations were performed in triplicates and mean values were presented in the results. Statistical comparisons of the mean values were performed by two-way analysis of variance (ANOVA) using Sigma Plot^{TM} v.12.

RESULTS AND DISCUSSION

Effect of Different Biomass Ratios

A batch experiment was carried out to test co-digestion of different biomasses such as giant reed (GR), water hyacinth (WH), maize (M), and poultry (P) along with monodigestion. Poultry and plant biomass had no naturally occurring microbes and therefore, needed ample inoculation for startup of AD. The biomasses were co-digested at various ratios (50:50. 80:20, 60:40, 40:60, and 20:80) to test its potential for biogas generation. The biomasses were also characterized chemically to evaluate biogas generation through anaerobic mono and co-digestion. In case of mono-digestion, water hyacinth was the leading substrate among all the four selected substrates. The specific biogas production was the highest for WH (234 mL g^{-1}VS) followed by GR (107 mL g^{-1}VS), M (92 mL g^{-1}VS), and P (49 mL g^{-1}VS) for mono-digestion. The chemical composition distinctly showed that WH had high volatile solids and soluble contents make the basis for highest cumulative biogas yield and daily biogas production as shown in **Figures 2**, **3**.

Various ratios of water hyacinth and poultry (WH: P) were presented in **Figure 4**. The 50:50 ratios of WH and P showed the highest biogas yield than rest of ratios of the same biomasses. The maximum biomethane yields from *E. crassipes* were 8.54 kJ g^{-1} dry biomass and 853.9 GJ $ha^{-1}y^{-1}$ which were 2.9 times higher than other crops (Yeong-Song et al., 2011). The total CO_2 emission reduced the bioenergy production of *E. crassipes* and replacing coal, fossil oil and natural gas with *E. crassipes* would reduce the CO_2 emission of 15.2–23.7 ton per year (Yeong-Song et al., 2011). Water hyacinth can be rich in nitrogen, up to 3.2% of DM and have a C:N ratio around 15. Water hyacinth was recommended as a substrate for compost or biogas production (Gunnarsson and Petersen, 2007).

On volatile solids (VS) basis, different ratios of water hyacinth and poultry 50:50, 80:20, 20:80, 60:40, and 40:60 produced specific biogas values of 262, 170, 164, 148, and 116 mL g^{-1} VS, respectively. The ratio of 50:50 produced the highest biogas production which might be due to the better C:N ratio ranging between 15 and 30 which seemed to be suitable range for microbial growth (Haug, 1993). Lower amounts of biogas produced at other ratios might be due to imbalanced C:N ratio. As it shown in the **Table 1**, water hyacinth contained 21.34 ppm nitrogen and poultry contained 16 ppm nitrogen. So, the excessive N in other different ratio affected the C:N ratio thereby affected the biogas production. At very high C:N ratio, accumulation of VFAs occurs which leads to inhibition of anaerobic digestion. For all tested ratios of water hyacinth and poultry substrate, the biogas generation at 50:50 ratio

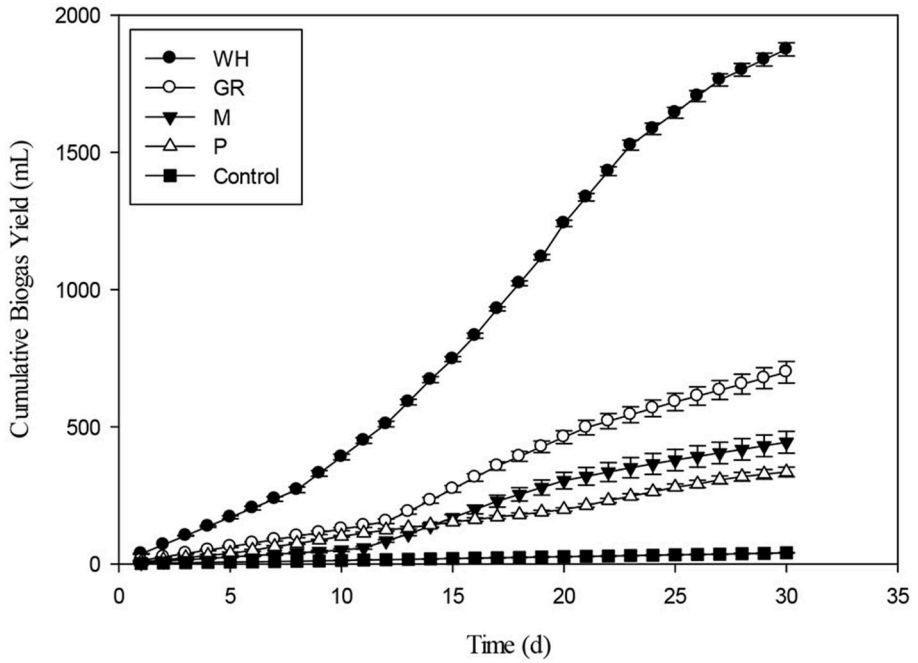

FIGURE 2 | Single substrate anaerobic mono-digestion of Water Hyacinth, Giant Reed, Maize, and Poultry.

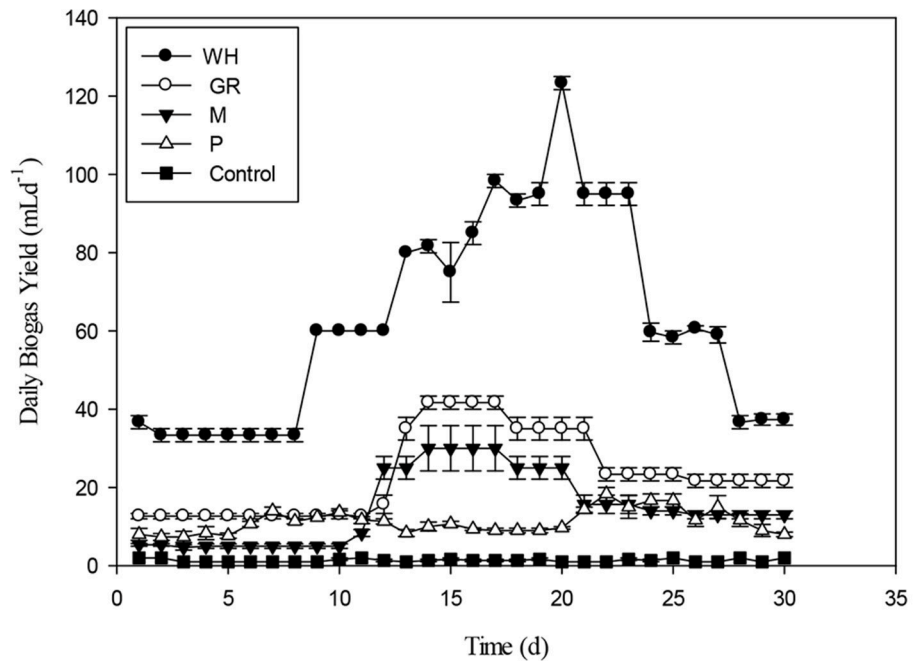

FIGURE 3 | Daily biogas production of water hyacinth, Giant Reed, Maize, and Poultry for ratio test.

was significantly different from other ratios during 30 days of experiment.

The daily biogas production of water hyacinth and poultry at different ratios were shown in the **Figure 5**. A ratio of 50:50 had the most stable biogas production and was significantly different from rest of tested ratios until day 15. The 20:80 ratio of WH: P had less biogas production up to 10th day in comparison to other ratios. On VS basis, 40% of water hyacinth with poultry waste

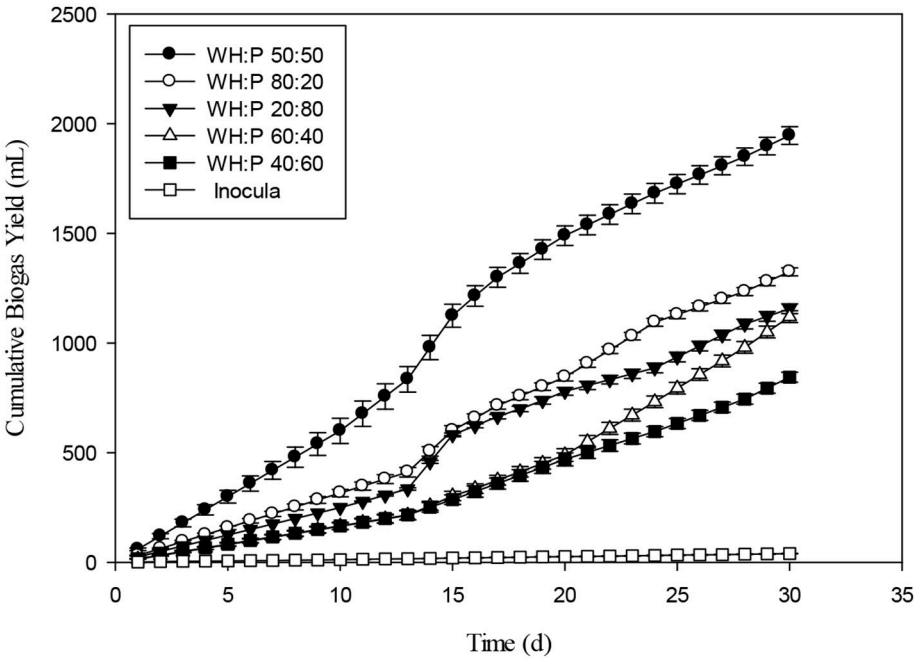

FIGURE 4 | Cumulative biogas production of different ratio of Water hyacinth and Poultry (WH:P).

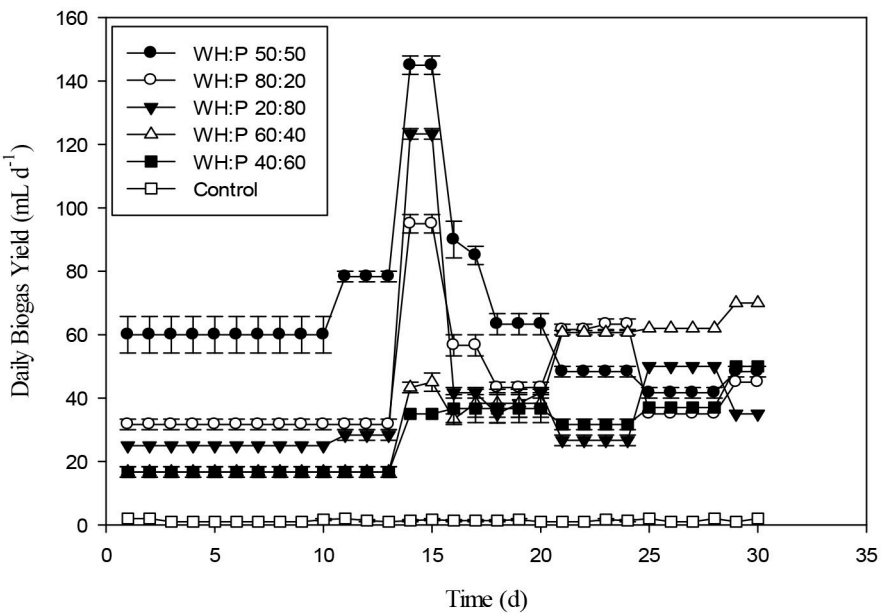

FIGURE 5 | Daily biogas production of different ratio of water hyacinth and poultry (WH:P).

had better contribution for biogas generation. Almost similar contribution on VS basis (35%) of was shown by raw sludge and food waste which enhanced the anaerobic digestion process as compared to mono-digestion (Koch et al., 2015). The co-digestion of APW with DM increased the biogas and methane yield by 11.7–28.6 and 18.9–43.7%, respectively, compared with the mono-digestion of APW. However, the ratio of 3:1 for Aloe peel waste and dairy manure (APW/DM) depicted the optimal performance leading to the highest cumulative methane yield (195.1 mL g^{-1} VS) (Huang et al., 2016). **Figure 6** showed the results of cumulative biogas production for different ratios for giant reed and poultry. For all the 80:20 and 20:80 mixing ratios

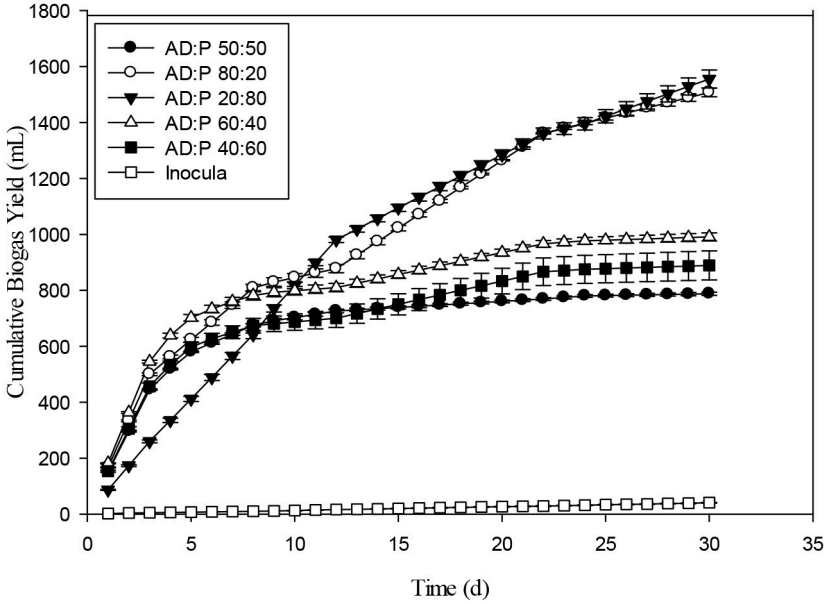

FIGURE 6 | Cumulative biogas production of different ratio of Giant reed and Poultry (GR:P).

of Giant reed (GR), and Poultry (P), better results were recorded as compared with all other ratios. The biogas production for 80:20 and 20:80 were 235 and 229 mL g^{-1}VS compared to monodigestion of GR 107 mL g^{-1} VS. The 50:50 ratios of GR and P had least biogas production as compared to all other ratios. The pH of the 50:50 was 5.5. Lower pH might be due to the aggregation of VFAs. The C/N ratio may be a major factor behind such results; the impact of the C/N ratio on AD has been investigated at the optimum C/N ratio of 20–25 (Mshandete et al., 2004; Yen and Brune, 2007). With the higher C:N ratio, VFAs may accumulate. If C:N was lower than the appropriate range, methanogens may be inhibited by the high ammonia concentration (Gong et al., 2011; Banks et al., 2012).

The daily rate of biogas production for various ratios of giant reed and poultry substrates were presented in **Figure 7**. In the beginning of the experiment 60:40 ratio of the GR and P had the highest biogas production peak. The most stable biogas production rates were given by 60:40 from day 13 to day 23. By comparing the monodigestion of GR the overall daily biogas production was <40 mL d^{-1}. The co-digestion of giant reed and poultry resulted in improved daily biogas production.

The biogas production at various ratios of maize and poultry substrate was presented in the **Figure 8**. For all the ratios of M and P, the 40:60 has the highest cumulative biogas production. However, 80:20 had the lowest biogas production by comparing with all other ratio. On basis of VS, 40:60 produced 193 mL g^{-1} VS, 20:80 gave 172 mL g^{-1} VS, 60:40 gives 153 mL g^{-1} VS, 50:50 generated 136 mL g^{-1}VS, and 80:20 produced 121 mL g^{-1} VS. The order of biogas production on VS basis was 40:60> 20:80> 60:40>50:50 and 80:20. The primary reason may be for production of less biogas production from mixing ratio of Maize and Poultry of 50:50 and 80:20 seemed high VFAs volatile fatty acids and reduced pH, which might have caused process instability.

The stability of anaerobic digestion was often expressed as the ratio of VFA to alkalinity. A ratio of <0.4 was generally regarded as optimal for anaerobic digestion, whereas a ratio exceeding 0.6 was regarded as indicative of overfeeding (Brown and Li, 2013). The results showed that acidogenesis was dominant over acetogenesis.

The production of long chain fatty acids causes slight inhibition of biogas production. However, a study evaluated the dairy manure and switch grass which presented best results at 50:50 ratio (Zheng et al., 2015). The positive effects of co-digestion can be accredited to manifold factors, including proportional nutrient composition, accelerated synergistic effects of microbial composition, an associated increase in buffering capacity and a decreased effect of toxic compounds on the digestion process (Wang et al., 2012). **Figure 9** presents the daily biogas production rate for different ratios of Maize and poultry waste (M:P). Initially, the 80:20 ratio had the highest biogas production. However, during the latter stages of the experiment 40:60 and 20:80 had the highest and stable biogas production than 80:20 and 60:40 ratios. The biogas production was decreasing with the passage of due to substrate utilization during the 30 day, experiment. During last 10 days, biogas production was minimal as compared to early days of the experiment. The comparison of present study with the previous ones was presented in **Table 3**.

Effect of Various Pretreatments

The effect of Fenton and Fenton plus ultrasonication pretreatment on biogas generation of WH was shown in the **Figure 10**. The biogas produced by WH biomass treated with Fenton's and Fenton's plus ultrasonic was lesser than

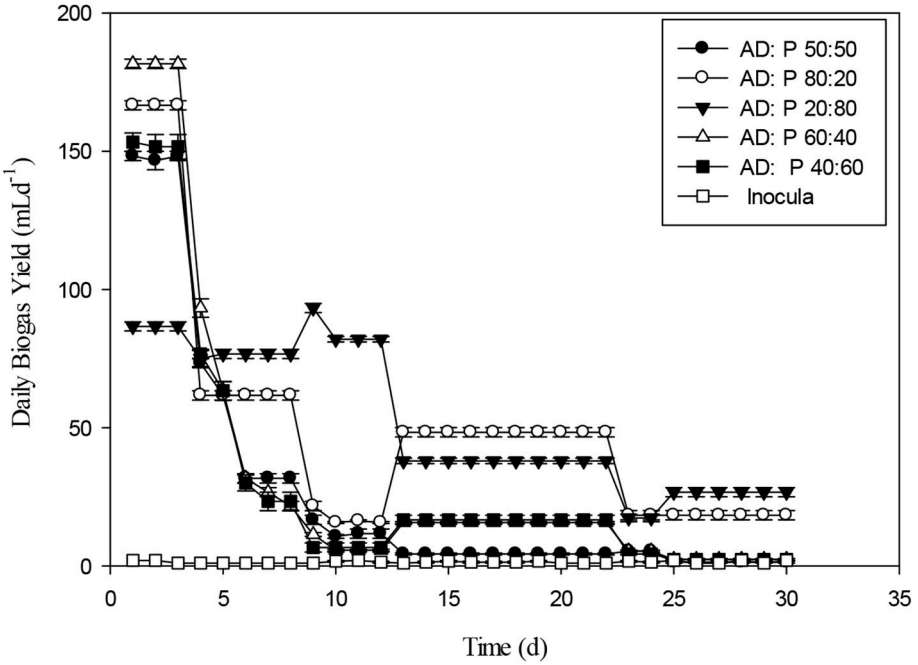

FIGURE 7 | Daily biogas rate of different ratio of Giant reed and Poultry (GR:P).

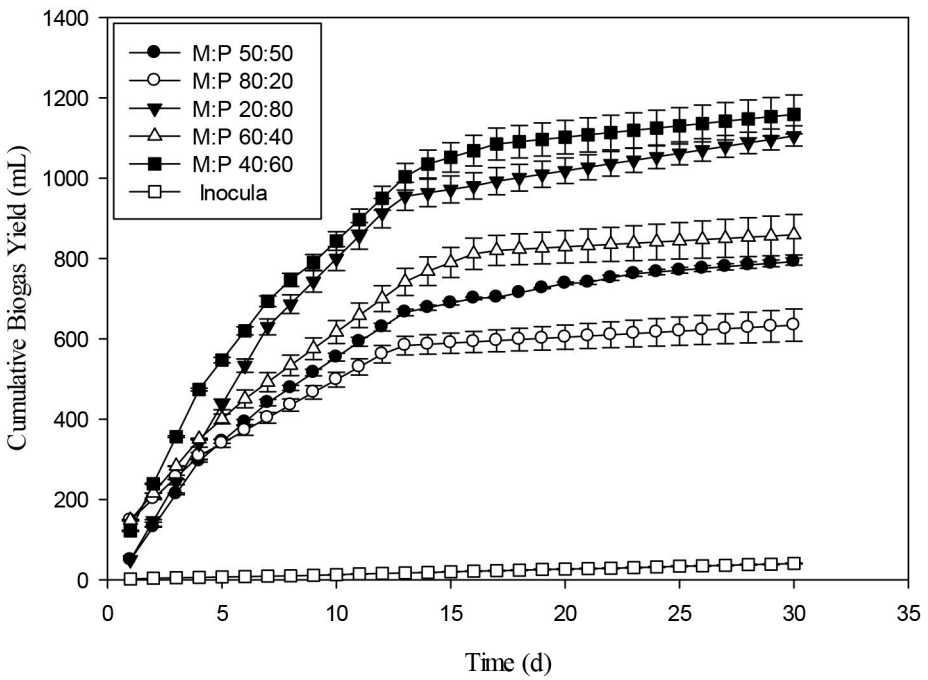

FIGURE 8 | Cumulative biogas production of different ratio of Maize and Poultry (M:P).

control. The reason for less biogas production in the present study from the chemical pretreatment might be due to the less target of ligno-cellulosic part of the WH. However, in literature the thermal pretreatment of the water hyacinth was quite effective for biogas optimization (Barua and Kalamdhad, 2017). The biochemical study unveiled that the cumulative methane production of hot air oven pretreated WH (3039 $\pm$ 32 mL CH_4 g^{-1} VS) at 90°C for 1 h was way higher than the cumulative

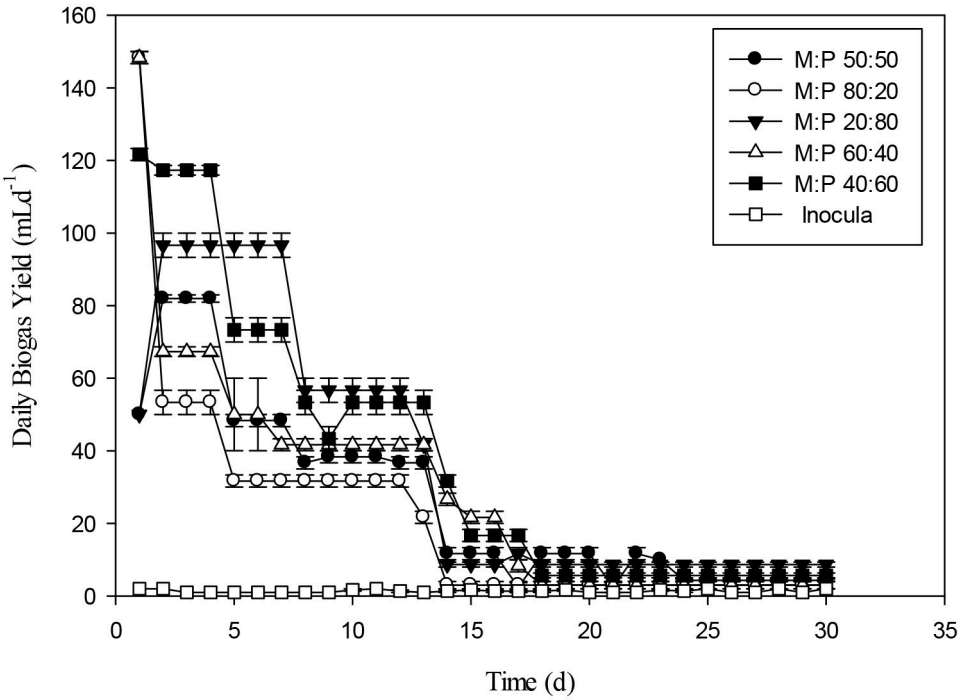

FIGURE 9 | Daily biogas rate of different ratio of Maize and Poultry (M:P).

methane production of untreated substrate 2396 ± 19 mL CH_4 g^{-1} VS on the 35th day (Barua and Kalamdhad, 2017). The cumulative biogas production from day second to day 8th the WH pretreated with Fenton's and Fenton's plus ultrasonic were not significantly different ($p > 0.05$). The **Figure 11** presents the pretreatment effect of Fenton's and Fenton's plus ultrasonic on daily biogas production. From the beginning, there was no significant effect of both pretreatment on biogas production with the control. However, Fenton pretreatment was comparatively better than Fenton's and Fenton's plus ultrasonic pretreatment. The less biogas production may due to the low energy application of ultrasound where no cell lysis occurred and COD solubilisation was due to exo-polymer dissolution, resulting in low methane production. However, at higher energies the disruption of the cell contributed to enhanced methane production (González-Fernández et al., 2012). The ultrasound pretreatment was recommended and effective when the lignocellulosic material to mix with water (Rodriguez et al., 2017). For daily biogas production, the control and both pretreatments were significantly different ($p < 0.05$) on day first; however, control and both pretreatments were significantly not different ($p > 0.05$) on day sixth. From day seventh to day 27th control and both pretreatments were significantly different ($p < 0.05$).

The cumulative biogas production from Maize with pretreatments such as Fenton's and Fenton's plus ultrasonic was shown in the **Figure 12**. On VS basis, the cumulative biogas production from maize under the mentioned pretreatments was 61 mL g^{-1}VS and 30 mL g^{-1}VS. Both the pretreatments were effective for biogas production up to 15 days. By comparing with control the Fenton pretreatment was more efficient than Fenton's plus ultrasonic. The cumulative biogas production for maize pretreatment with Fenton's and Fenton's plus ultrasonic with control were not significantly different ($p > 0.05$). However, from day 20th to day 30th control vs. pretreatments were significantly different ($p < 0.05$). The current ultrasonic pretreatment was carried out at 30°C. Temperature has crucial influence in the samples used for sonication because other studies showed that it has a great influence on the changing of different properties of the liquid medium, such as viscosity, surface tension, and mainly vapor pressure, which influence cavitation (Karray et al., 2015). As the temperature of the liquid increases, its vapor pressure, and consequently the vapor pressure inside the bubble, also increases when implosion occurs. It can be seen that the ultrasonication pre-treatment results in the solubilization of carbohydrates. However, the current results for biogas production at 30°C were not fruitful as compared to the other results conducted experiments with macro algal biomass (Karray et al., 2015). In the most recent article published by Rodriguez et al. (2017) it was recommended that plant biomass must be mixed with water for optimum results.

The daily biogas production of Maize after pretreatment with Fenton's and Fenton's plus ultrasonic was represented in the **Figure 13**. In the beginning, biogas production from the pretreated biomass was lesser. However, on the 5th day onwards, biogas production from pretreated biomass was higher than biomass pretreated with Fenton's and from control. The daily biogas production was stable on 15th day onwards until 30th

TABLE 3 | The comparison of current study with those previous researches.

Co-substrates	Experimental Conditions					
	RT	T	RS (substrate ratio) yield	pH	Methane/biogas	
Poultry (P) and Hog Wastes (H)	13	35	(P:H) 100:0, 80:20,60:40, 40:60, 20:80, 0:100	Initial P = 6 Initial H = 5 Remaining = 7–7.5	Biogas yield H80 = 200 mL g^{-1} VS CH_4 = 130 mL g^{-1} VS	Magbanua et al., 2001
CM with Cattle slurry (CS)	21	35	CS:CM 100:0, 70:30,50:50, 25:75, 10:90	7.8-8	CH_4 =0.12 m^3kg^{-1} VS	Callaghan et al., 2002
Diluted Chicken manure+ Whey	18	35	Whey in CM = 15%, 25%, 35%, 50% v/v	Manure:7.4 Whey:3.5	Biogas production:1.5 to 2.5 Ld^{-1}	Gelegenwas et al., 2007
CM or dairy or Swine manure with Switch grass	62	55	CM:Switch grass 0.95:2	6.9	CH_4 2mL g^{-1} VS	Ahn et al., 2010
CM:DM and Wheat Straw (WS)	30	35	DM:CM 100:0, 0:100, 50:50 and WS added to the DM:CM mixture to adjust C/N ratio to 1/25	7.03-7.34	234.7 mL g^{-1} VS	Wang et al., 2012
CM with *Spartina alternefloria* residues	–	35	CM:SAR 1:4,4:1, 2:3,3:2,0:5,5:0 based on TS	–	Biogas 107.25 mL g-1 TS 76.92 % CH_4	Chen et al., 2012
CM and Corn Stover (CS)	30	37	CS:CM 1:0,3:1,1:1, 1:3, 0:1 (based on VS)	7.9	Methane yield=205 mL g^{-1} VS	Li et al., 2013
CM, Cattle manure and Maize silage	37	35	CM:Cattle manure: Maize silage (1:1:1) based on VS	7.4- 8.3	CH_4 693 mL g^{-1} VS	Yangin-Gomec and Ozturk, 2013
Water hyacinth and Poultry (W: P)	30	35			Biogas (mL $g^{-1}VS$)	Current study
			60:40	6.5	148	
			40:60	6	116	
			80:20	6	170	
			20:80	6.5	164	
			50:50	7	262	
Giant Reed and Poultry (GR:P)	30	35			Biogas (mL $g^{-1}VS$)	Current study
			60:40	6.5	148	
			40:60	6	125	
			80:20	7	235	
			20:80	7	229	
			50:50	6	117	
Maize and Poultry (M:P)	30	35			Biogas (mL $g^{-1}VS$)	Current study
			60:40	6.5	193	
			40:60	6	153	
			80:20	6	121	
			20:80	6.5	172	
			50:50	6	136	

day. **Figure 14** depicts the cumulative biogas production of giant reed with Fenton's and Fenton's plus ultrasonics pretreatment. The giant reed pretreated with Fenton's was comparatively better for biogas production than the giant reed pretreated with Fenton's plus ultrasonic. However, both pretreatments giant reed produced lower biogas than the control. Lower biogas production might be due to chemical effect of pretreatment on the microbial guilds of the batch system. The cumulative biogas production from day 1st to day 12th both pretreatment and control were not significantly different ($p > 0.05$).

The daily biogas production for the pretreated giant reed with Fenton's and Fenton's plus ultrasonic were shown in the **Figure 15**. In the early stages, daily biogas production for Fenton plus ultrasonic was lesser than control and giant reed biomass pretreated with Fenton. After day 3, biogas production from both pretreatment was almost at same level until day 19th. After 20th day the daily biogas production for both pretreatment were different. The daily biogas production from day 1st, day 3rd, were significantly different ($p < 0.05$).

The above-mentioned findings are quite practical in enhancing biogas production from various biomasses rich in cellulosic or lignocellulosic contents. There were two objectives of this investigation viz. the balancing of nutrients by the codigestion process and secondly the overcoming of toughness of lingo-cellulosic materials through physic-chemical pretreatment. The results produced are very promising and quite practical in the sense that we recommend co-digestion of WH, giant reed, and poultry waste in order to enhance

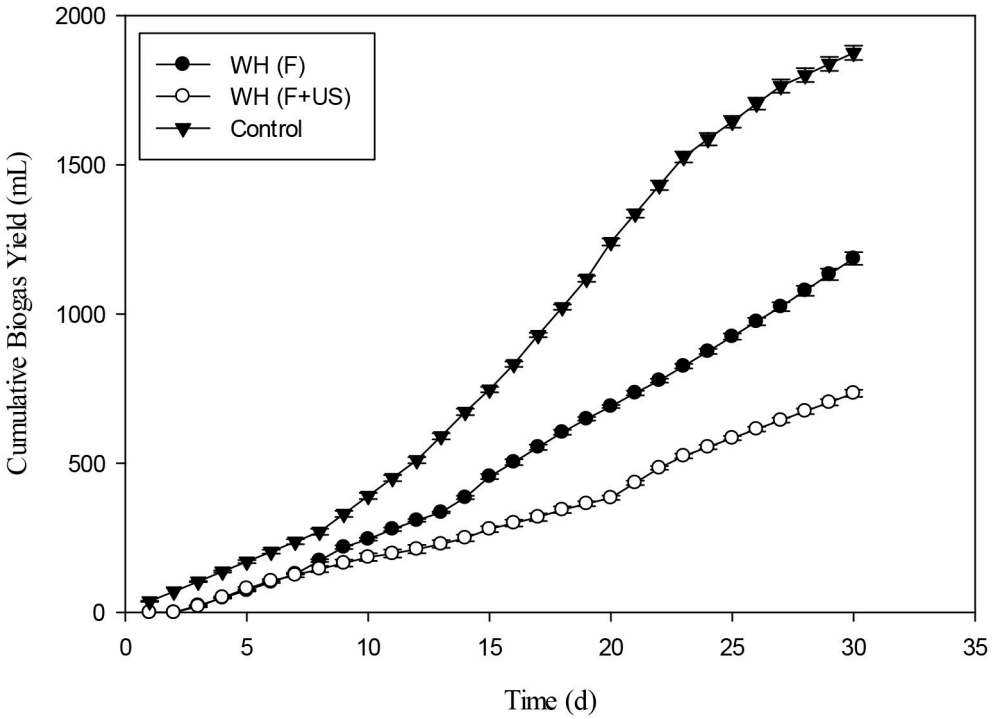

FIGURE 10 | Effect of Fenton's and ultrasound (Fenton's + Ultrasonication) on biogas generation of water hyacinth.

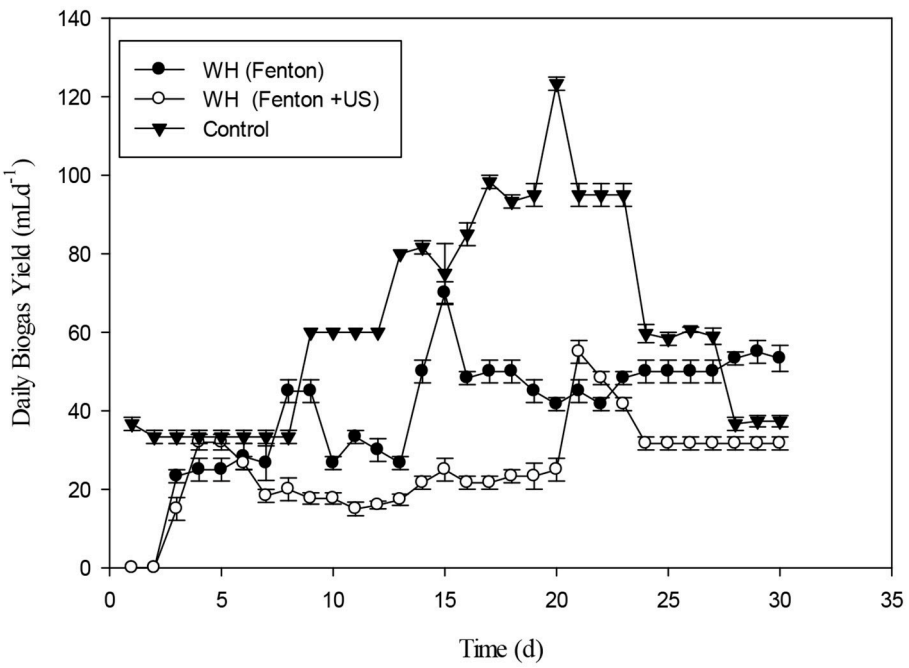

FIGURE 11 | Daily biogas rate of water hyacinth pretreatment with Fenton's and Fenton's plus ultra-sonication.

biogas yield per gram VS basis. Water hyacinth and poultry codigestion was the most promising in enhancing biogas production. Poultry waste could be a rich source of phosphorus which could satisfy the nutrient deficiency and to optimize C:N:P for an optimum methanogenesis. The codigestion can be classified as WH:P (50:50) > GR:P (80:20) > M:P

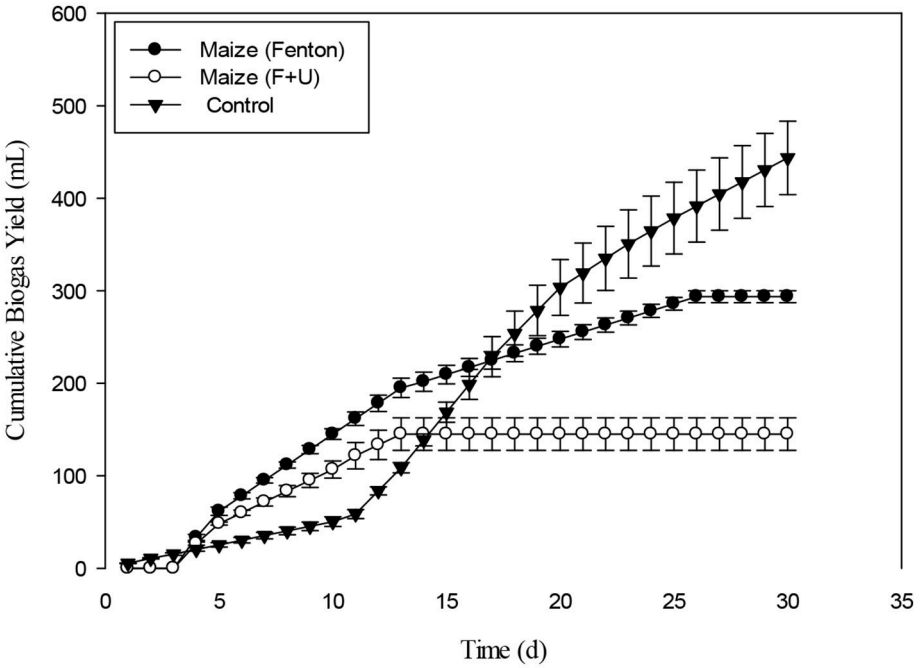

FIGURE 12 | Cumulative biogas production from Maize with Fenton's and Fenton's plus ultrasound pretreatment.

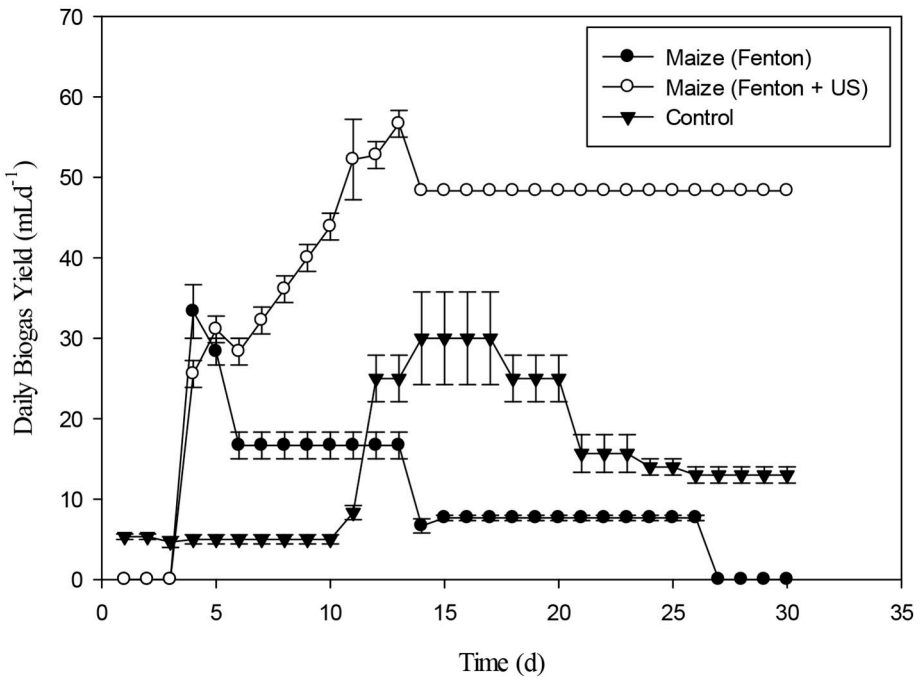

FIGURE 13 | Daily Biogas production of Maize with pretreatment of Fenton's and Fenton's plus Ultrasonic.

(60:40). So, these ratios can be applied at decentralized scale for better waste management and biogas generation due to balanced C:N ratio of plant biomass and poultry manure. Co-digestion can also be applied at large scale with optimized ratio in Pakistan and other developing countries for biogas generation and waste management and reduce the methane emission through landfills. Co-digestion can be applied at home scale by operating through pickle barrel digester to

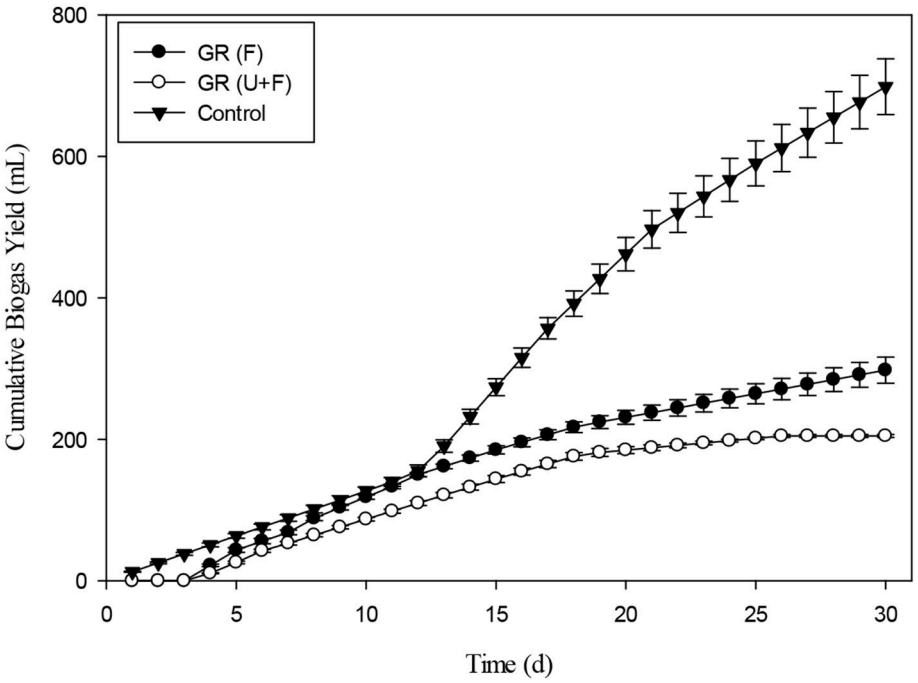

FIGURE 14 | Cumulative biogas production from Giant reed (GR) with Fenton's (F) and Fenton's plus ultrasound (F + US) pretreatment.

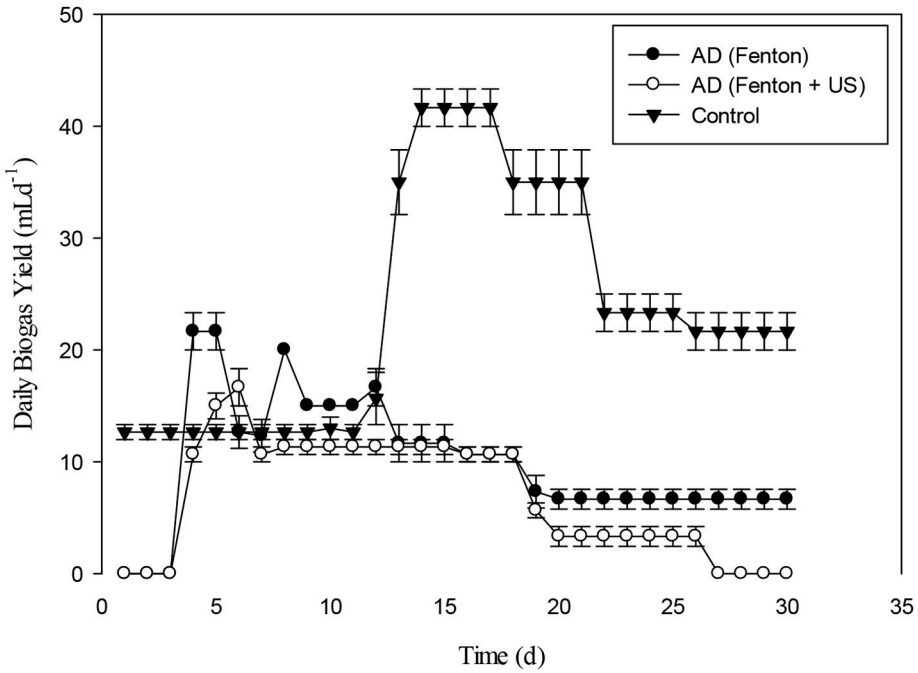

FIGURE 15 | Daily Biogas production of giant reed (G:R) with pretreatment of Fenton's (F) and Fenton's plus (F+US) Ultrasonic.

play a key role against the global warming to avoid the open dumping of waste. The present study does not recommend the use of pretreatment as discussed above. The use of various chemicals especially Fenton reagent may disturb pH and chemical composition of feedstock and thus disturb optimum conditions for AD. The chemical structure of the

feedstock may also be affected which resulted in lower biogas yields.

CONCLUSION

The batch experiments were conducted with various ratios and pretreatment of water hyacinth, giant reed, maize, and poultry substrates. The incubated biomasses were optimized at different ratios. The ratios experiments involving various selected plant biomasses and poultry wastes concluded that water hyacinth and poultry (50:50) produced 262 mL g^{-1}VS, Giant reed and Poultry produced (80:20) produced 235 mL g^{-1}VS, while Maize and Poultry (60:40) produced 193 mL g^{-1}VS. So, these ratios can be applied at decentralized scale for better waste management and biogas generation due to balanced C:N ratio of plant biomass and poultry manure. However, the Fenton and Fenton's plus ultrasonic pretreatments of plant biomasses were not suitable for biogas optimization as compared to co-digestion.

AUTHOR CONTRIBUTIONS

All authors listed have made a substantial, direct and intellectual contribution to the work, and approved it for publication.

REFERENCES

Ahn, H. K., Smith, M., Kondrad, S., and White, J. (2010). Evaluation of biogas production potential by dry anaerobic digestion of switchgrass–animal manure mixtures. *Appl. Biochem. Biotechnol.* 160, 965–975. doi: 10.1007/s12010-009-8624-x

Alatrwaste-Mondragón, F., Samar, P., Cox, H. H., Ahring, B. K., and Iranpour, R. (2006). Anaerobic codigestion of municipal, farm, and industrial organic wastes: a survey of recent literature. *Water Environ. Res.* 78, 607–636. doi: 10.2175/106143006X111673

Astals, S., Nolla-Ardèvol, V., and Mata-Alvwerez, J. (2012). Anaerobic co-digestion of pig manure and crude glycerol at mesophilic conditions: biogas and digestate. *Bioresour. Technol.* 110, 63–70. doi: 10.1016/j.biortech.2012.01.080

Banks, C. J., Zhang, Y., Jiang, Y., and Heaven, S. (2012). Trace element requirements for stable food waste digestion at elevated ammonia concentrations. *Bioresour. Technol.* 104, 127–135. doi: 10.1016/j.biortech.2011.10.068

Barua, V. B., and Kalamdhad, A. S. (2017). Effect of various types of thermal pretreatment techniques on the hydrolyswas, compositional analyswas and characterization of water hyacinth. *Bioresour. Technol.* 227, 147–154. doi: 10.1016/j.biortech.2016.12.036

Brown, D., and Li, Y. (2013). Solid state anaerobic co-digestion of yard waste and food waste for biogas production. *Bioresour. Technol.* 127, 275–280. doi: 10.1016/j.biortech.2012.09.081

Bujoczek, G., Oleszkiewicz, J., Sparling, R., and Cenkowski, S. (2000). High solid anaerobic digestion of chicken manure. *J. Agricul. Eng. Res.* 76, 51–60 doi: 10.1006/jaer.2000.0529

Callaghan, F. J., Wase, D. A. J., Thayanithy, K., and Forster, C. F. (2002). Continuous codigestion of cattle slurry with fruit and vegetable wastes and chicken manure. *Biomass Bioenergy* 27, 71–77 doi: 10.1016/S0961-9534(01)00057-5

Cavinato, C., Fatone, F., Bolzonella, D., and Pavan, P. (2010). Thermophilic anaerobic co-digestion of cattle manure with agro-wastes and energy crops: comparwason of pilot and full scale experiences. *Bioresour. Technol.* 101, 545–550. doi: 10.1016/j.biortech.2009.08.043

Chen, G., Chang, Z., Ye, X., Du, J., Xu, Y., and Zhang, J. (2012). Methane production by anaerobic co-digestion of chicken manure and Spartina alterniflora residue after producing methane. *Huan jing ke xue* 33, 203–207. doi: 10.1016/S0960-8524(01)00133-X

Chen, Y., Cheng, J. J., and Creamer, K. S. (2008). Inhibition of anaerobic digestion process: review. *Bioresour. Technol.* 90, 4044–4064. doi: 10.1016/j.biortech.2007.01.057

Comino, E., Riggio, V. A., and Rosso, M. (2012). Biogas production by anaerobic co-digestion of cattle slurry and cheese whey. *Bioresour. Technol.* 114, 46–53. doi: 10.1016/j.biortech.2012.02.090

De Varies, J. M. (2012). Comparing environmental consequences of anaerobic mono and codigestion of pig maure to produce bioenergy. A life cycle perspective. *Bioresour. Technol.* 125, 239–248. doi: 10.1016/j.biortech.2012.08.124

Demirel, B., and Scherer, P. (2008). Production of methane from Sugar Beet Silage without Manure addition by a single-stage anaerobic digestion process. *Biomass Bioener.* 32, 203–209. doi: 10.1016/j.biombioe.2007.09.011

Fernández-Cegrí, V., De la Rubia, M. Á., Raposo, F., and Borja, R. (2012). Effect of hydrothermal pretreatment of sunflower oil cake on biomethane potential focusing on fibre composition. *Bioresour. Technol.* 123, 424–429. doi: 10.1016/j.biortech.2012.07.111

Gelegenwas, J., Georgakakwas, D., Angelidaki, I., and Mavrwas, V. (2007). Optimization of biogas production by co-digesting whey with diluted poultry manure. *Renew. Energy* 32, 2147–2160 doi: 10.1016/j.renene.2006.11.015

Gong, L., Lewicki, R., Griffin, R., Flynn, J., and Lefer, B. (2011). Atmospheric ammonia measurements in Houston, TX using an external-cavity quantum cascade laser-based sensor. *Atmos. Chem. Phys.* 11, 9721–9733. doi: 10.5194/acp-11-9721-2011

González-Fernández, C., Sialve, B., Bernet, N., and Steyer, J. (2012). Comparwason of ultrasound and thermal pretreatment of Scenedesmus biomass on methane production. *Bioresour. Technol.* 110, 610–616. doi: 10.1016/j.biortech.2012.01.043

Gunnarsson, C. C., and Petersen, C. M. (2007). Water hyacinths as a resource in agriculture and energy production: a literature review. *Waste Manag.* 27, 117–129. doi: 10.1016/j.wasman.2005.12.011

Haug, R. T. (1993). *The Practical Handbook of Compost Engineering*. CRC Press.

Hinken, L., Urban, I., Haun, E., Urban, I., Weichgrebe, D., and Rosenwinkel, K. H. (2008). The valuation of malnutrition in the mono-digestion of maize silage by anaerobic batch tests. *Wat. Sci. Technol.* 58, 1458–1459. doi: 10.2166/wst.2008.491

Huang, X., Yun, S., Zhu, J., Du, T., Zhang, C., and Li, X. (2016). Mesophilic anaerobic co-digestion of aloe peel waste with dairy manure in the batch digester: focusing on mixing ratios and digestate stability. *Bioresour. Technol.* 218, 62–68. doi: 10.1016/j.biortech.2016.06.070

Karray, R., Hamza, M., and Sayadi, S. (2015). Evaluation of ultrasonic, acid, thermo-alkaline and enzymatic pre-treatments on anaerobic digestion of Ulva rigida for biogas production. *Bioresour. Technol.* 187, 205–213. doi: 10.1016/j.biortech.2015.03.108

Khalid, A., Arshad, M., Anjum, M., Mahmood, T., and Dawson, L. (2011). The anaerobic digestion of solid organic waste. *Waste Manag.* 31, 1737–1744 doi: 10.1016/j.wasman.2011.03.021

Koch, K., Helmreich, B., and Drewes, J. E. (2015). Co-digestion of food waste in municipal wastewater treatment plants: effect of different mixtures on methane yield and hydrolyswas rate constant. *Appl. Energy* 137, 250–255. doi: 10.1016/j.apenergy.2014.10.025

Li, Y., Zhang, R., Chen, C., Liu, G., He, Y., and Liu, X. (2013). Biogas production from co-digestion of corn stover and chicken manure under anaerobic wet, hemi-solid, and solid state conditions. *Bioresour. Technol.* 149, 406–412. doi: 10.1016/j.biortech.2013.09.091

Magbanua, B. S. Jr., Adams, T. T., and Johnston, P. (2001). Anaerobic codigestion of hog and poultry waste. *Bioresour. Technol.* 76, 165–168 doi: 10.1016/S0960-8524(00)00087-0

Mshandete, A., Kivawasi, A., Rubindamayugi, M., and Mattiasson, B. (2004). Anaerobic batch co-digestion of swasal pulp and fwash wastes. *Bioresour. Technol.* 95, 19–24. doi: 10.1016/j.biortech.2004.01.011

Owamah, H. I., Alfa, M. I., and Dahunsi S. O. (2014). Optimization of biogas from chicken droppings with Cymbopogon citrates. *Renew. Energy* 68, 366–371. doi: 10.1016/j.renene.2014.02.006

Park, C., Park, S., Kim, C., and Lee, S. (2012). Effects of EGR on performance of engines with spark gap projection and fueled by biogas–hydrogen blends. *Int. J. Hydr. Energy* 37, 14640–14648. doi: 10.1016/j.ijhydene.2012.07.080

Pobeheim, H., Munk, B., Johansson, J., and Guebitz, G. M. (2010). Influence of trace elements on methane formation from a synthetic model substrate for maize silage. *Bioresour. Technol.* 101, 836–839. doi: 10.1016/j.biortech.2009.08.076

Rodriguez, C., Alaswad, A., Benyounwas, K., and Olabi, A. (2017). Pretreatment techniques used in biogas production from grass. *Renew. Sustain. Energy Rev.* 68, 1193–1204. doi: 10.1016/j.rser.2016.02.022

Shah, F. A., Mahmood, Q., Rashid, N., Pervez, A., Raja, I. A., and Shah, M. M. (2015). Co-digestion, pretreatment and digester design for enhanced methanogeneswas. *Renew. Sustain. Energy Rev.* 42, 627–642. doi: 10.1016/j.rser.2014.10.053

Triolo, J. M., Sommer, S. G., Møller, H. B., Wewasbjerg, M. R., and Jiang, X. (2011). A new algorithm to characterize biodegradability of biomass during anaerobic digestion: Influence of lignin concentration on methane production potential. *Bioresour. Technol.* 102, 9395–9402 doi: 10.1016/j.biortech.2011.07.026

Wang, X., Yang, G., Li, F., Feng, Y., Ren, G., and Han, X. (2013). Evaluation of two statistical methods for optimizing the feeding composition in anaerobic co-digestion mixture design and central composite design. *Bioresour. Technol.* 131, 172–178 doi: 10.1016/j.biortech.2012.12.174

Wang, X., Yang, Y., Feng, Y., Ren, G., and Han, X. (2012). Optimizing feeding composition and carbon-nitrogen ratios for improved methane yield during anaerobic codigestion of dairy, chicken manure and wheat straw. *Bioresour. Technol.* 120, 78–83 doi: 10.1016/j.biortech.2012.06.058

Yangin-Gomec, C., and Ozturk, I. (2013). Effect of maize silage addition on biomethane recovery from mesophilic co-digestion of chicken and cattle manure to suppress ammonia inhibition. *Energy Conver. Manag.* 71, 92–100. doi: 10.1016/j.enconman.2013.03.020

Yen, H.-W., and Brune, D. E. (2007). Anaerobic co-digestion of algal sludge and waste paper to produce methane. *Bioresour. Technol.* 98, 130–134. doi: 10.1016/j.biortech.2005.11.010

Yeong-Song, C., Chyi-How, L., Biswarup, S., Chin-Chao, C., Gopalakrishnan, K., Jou-Hsien, W., et al. (2011). Biohydrogen and biomethane from water hyacinth *(Eichhornia crassipes)* fermentation: effects of substrateconcentration and incubation temperature. *Int. J. Hydrogen Energy* 36, 14191–14203. doi: 10.1016/j.ijhydene.2011.04.188

Zheng, Y., Zhao, J., Xu, F., and Li, Y. (2014). Pretreatment of lignocellulosic biomass for enhanced biogas production. *Prog. Energy Combust. Sci.* 42, 35–53. doi: 10.1016/j.pecs.2014.01.001

Zheng, Z., Liu, J., Yuan, X., Wang, X., Zhu, W., Yang, F., et al. (2015). Effect of dairy manure to switchgrass co-digestion ratio on methane production and the bacterial community in batch anaerobic digestion. *Appl. Energy* 151, 249–257. doi: 10.1016/j.apenergy.2015.04.078

Conflict of Interest Statement: The authors declare that the research was conducted in the absence of any commercial or financial relationships that could be construed as a potential conflict of interest.

frontiers in Energy Research

ORIGINAL RESEARCH
published: 08 November 2018
doi: 10.3389/fenrg.2018.00116

Anaerobic Co-digestion of Catering and Agro-Industrial Waste: A Step Forward Toward Waste Biorefinery

Muzammil Anjum, Samia Qadeer and Azeem Khalid*

Department of Environmental Sciences, PMAS Arid Agriculture University, Rawalpind, Pakistan

In the present study, a biorefinery system is proposed using catering and agro industrial waste for biogas and low phytotoxic digestate. Anaerobic co-digestion of catering waste with partially pre-treated (microwave 800 J/g/min + steam 121 °C 40 min) maize crop residues was conducted under different composition (20–50%) of feedstock. The results showed that the biogas production was increased by 2.03 times in co-digestion experiment (40% partially pre-treated maize crop residue + 60% catering waste: TCM3) as compared to catering waste alone (control). The increment in accumulative methane 116.7 m^3 t^{-1} was recorded in TCM3 which is due to improvement in biodegradation under co-digestion process. The post digestion byproduct (residual digestate) was evaluated for its phytotoxicity which is supplied with aerobic post treatment. The post treatment has improved the digestate quality by decreasing VS/TS ratio from 259 to 173 g/L and slightly increase the pH from 7.29 to 8.32. Seed germination assay showed that the germination percentage (G%), germination index (GI) and vigor index (VI) were relatively higher with post treated digesate as compared to un-treated digestate. In the germination test using wheat seeds, the post treated digestate (5% sol. extract) achieved higher values of GI and VI (46 and 609) whereas in un-treated, values for these indices were 14 and 62, respectively. Overall the findings of the present study identify the significance co-digestion based waste biorefinery, in order to development of value added bio-products such as biogas and biofertilizers.

Keywords: anaerobic digestion, biorefinery, bioenergy, digestate, phytotoxicity, organic waste

OPEN ACCESS

Edited by:
Abdul-Sattar Nizami, Center of Excellence in Environmental Studies, King Abdulaziz university, Saudi Arabia

Reviewed by:
Vivekanand Vivekanand, Malaviya National Institute of Technology, Jaipur, India
Qaisar Mahmood, COMSATS University Islamabad, Pakistan
Mohammad Rehan, King Abdulaziz University, Saudi Arabia

****Correspondence:***
Muzammil Anjum
muzammilanjum@gmail.com

Specialty section:
This article was submitted to Bioenergy and Biofuels, a section of the journal Frontiers in Energy Research

Received: *07 August 2018*
Accepted: *18 October 2018*
Published: *08 November 2018*

Citation:
Anjum M, Qadeer S and Khalid A (2018) Anaerobic Co-digestion of Catering and Agro-Industrial Waste: A Step Forward Toward Waste Biorefinery. Front. Energy Res. 6:116. doi: 10.3389/fenrg.2018.00116

INTRODUCTION

The advancement in living standard has risen the generation of organic waste at substantial rates. One of the signific sources of organic wastes in municipalities is from catering services which are generated excessively in hotels, canteens, restaurants, and the aviation industry (Ayomoh et al., 2008; Jiang et al., 2018). Catering waste may contain vegetables, fruit, meat, baked goods, dairy, and animal by-products which are not only rich in nutrients, but also a variety of amino acids, proteins, carbohydrates, and vitamins are also present. According to an estimate of UN Food and Agriculture Organization, about 1.3 billion tons of these kinds of waste are lost during the food supply chain (Jiang et al., 2018). Catering wastes are problematic to treat due their high moisture content, it can involve in the transmission of pathogen microorganisms that possibly cause diseases in humans and also pollute drinking water (Chen et al., 2017). Hence, it requires being dealt in an environmentally safe method (Zhang et al., 2005; Izumi et al., 2010; Anjum et al., 2016). On the

other hand, agriculture is another major source of organic waste in the form of crop residues. Maize is known as one of the major crops in Pakistan, which produce thousands of tons of post harvesting residues. These residues are difficult to degrade through a biological process due to high content of lignocellulose (Surra et al., 2018).

The organic waste when disposed in landfills creates problems of leachate and biogas production that not only create nuisance in the landfill area, but also results in the loss of huge resource potential. Thus, an effective management system (biorefinary) is required to ensure the integration of organic waste management with energy recovery and reuse of byproduct formulation. Competence of biological waste treatment in this regard is well established option both in terms of scope and applicability, as it encompasses a wide variety of organic wastes ranging from food waste (Kuczman et al., 2018) and agro-allied industries (Alvarez et al., 2010) to waste activated sludge (Bolzonella et al., 2012; Bundhoo et al., 2016).

Among biological treatment anaerobic digestion has received special interest in the past few years, which results in the production of two byproducts that is biogas and digestate (Chen et al., 2018). However, some interventions are still needed for the provision of balanced nutrients and stable conditions for creating efficient digestion systems (Sosnowski et al., 2003). Recently, anaerobic co-digestion has been reported to improve the digestion process and energy production by improving the nutrient availability and organic load, while lowering the toxicity of the inhibitory compounds by dilution (Anjum et al., 2012, 2016; Serrano et al., 2013).

In anaerobic digestion most of the studies highlighting the anaerobic treatment of organic waste have made significant improvements to enhance the energy recovery as a factor of biogas production. Where mere efforts have been made to utilize anaerobic digestate which is an enriched nutrient source(Abdullahi et al., 2008; Trzcinski and Stuckey, 2011). The digestate effluents carry vital nutrients capable of promoting plant growth (Tornwall et al., 2017). Application of such high nutrient entities to the soil not only ensure the sound disposal of anaerobic byproducts, but also is an appealing solution to declining soil nutrient balance, which has identified as an important soil health problem worldwide (Galvez et al., 2012; Da Ros et al., 2018). However, the characteristic phytotoxicity limits the applications of anaerobic digestate as soil conditioner (Coelho et al., 2018). The fertilizer value of digestate can be enhanced by reducing its phytotoxic effects. Therefore, an appropriate pre-treatment is required that ensures sound application of anaerobic digestate to the soil. Aerobic "polishing" is identified as competent option for the reduction of toxic effects of anaerobic digestate through reduction in moisture, odor, carbon and pathogens in the digestate.

In view of above mention concerns the present study was conducted with the aims to: (1) partial pretreatment of maize crop residue to improve its digestibility in co-digestion with catering waste, (2) Optimizing substrate ratio in co-digestion catering waste and partial pre-treated maize crop residues to maximum digestibility and biogas production, (3) to test and prepare a low pytotoxic digestate as an organic conditioner for plants.

MATERIALS AND METHODS

Feedstock Material and Physico-Chemical Characterization

The raw materials used for the preparation of digestate were catering waste and crop residues maize crop residues. The catering waste samples were taken from local food restaurants and banquet halls of Rawalpindi city, while the maize residues were collected from PMAS Arid Agriculture University Research Farm located at Koont, Pakistan. The initial physico-chemical characterization of catering waste and maize crop residues are described in **Table 1**.

Pre-treatment of Maize Crop Residues

Prior to anaerobic digestion maize crop residues were supplied with the pretreatment steps, which were selected based on a partial level of treatment with minimal energy prerequisite, and that avoids the complete degradation (Taherzadeh and Karimi, 2008). Sequential physical pretreatments, microwave irradiation and steam water were applied to the maize crop residues in order to enhance the accessibility of lignocellulose of maize crop residues for biological degradation. For microwave irradiation pretreatment a household-type DW-105-G microwave oven (Dawlance, Pakistan). Maize crop residues (50 g of each) were placed in the microwave oven for 3 min supplying energy of 800 J/g/min. Subsequently, irradiated substrate was placed in a high-pressure steam unit (Nanolytik Nanoclave 1, Germany) for 40 min at 121°C for steam treatment (Anjum et al., 2016). After pretreatments, maize crop residues were dried in air for 6 h, and later in a digital oven for 12 h prior to use in co-digestion.

Anaerobic Co-digestion Experiment

Anaerobic digestion experiments were performed in two steps. First, the optimization of feeding composition was performed and secondly the analysis of optimized co-digestion treatment was conducted during biogas production. At first set of experiment anaerobic co-digestion experiments were performed using catering waste as a main substrate mixed with partially pre-treated maize crop residues at different compositions. Maize crop residues (M) were used in 20, 30, 40, and 50% of total fraction with catering waste, while similar experiments were repeated

TABLE 1 | Physico-chemical characteristics of substrates.

Parameters	Units	Catering waste	Maize crop residues
Volatile solids	g/L	913 ± 18.9	946 ± 19.93
Total dissolve solids	g/L	5.81 ± 0.36	0.31 ± 6.32
Fixed solids	g/L	87 ± 10.7	30 ± 3.11
Total solids	g/L	143 ± 5.71	874 ± 21.5
Carbon	%	51 ± 1.78	62 ± 4.32
C/N ratio	–	25 ± 1.05	53 ± 3.45
COD	g/L	30.8 ± 0.39	34.5 ± 0.36
pH	–	3.91 ± 0.06	5.01 ± 0.05
Electrical conductivity	dS/m	3.00 ± 0.15	5.36 ± 0.71

with untreated maize crop residues. Anaerobic glass batch bottles of 500 ml capacity were used with total substrate volume of 350 and 150 ml empty head space. All mixtures of substrates were prepared on the basis of total solids. The seed anaerobic microorganisms were applied using previously digested organic waste added at a rate of 100 g/L (Anjum et al., 2012). A suitable amount of water was added keeping the moisture content of reactors fixed between ranges of the 70 and 75%. Co-digestion experiment took place for 6 weeks 42 at mesophilic temperature 30 ± 1°C. To examine the degradation efficiency of co-digestion, samples were analyze at different interval changes in COD and VS.

In the second set of experiment, selected treatments (40 % maize crop residues and 60% catering waste) (TEM3) was subjected to biogas production in a lab scale, anaerobic static batch reactor and compared with control. Two similar reactor of dimensions 13 × 30 cm (diameter × width) each, having capacity of 2,500 ml were designed. One reactor was used for co-digestion (TEM3), while the second was used as control reactor having catering waste only. About 2,000 ml of the reactor volume was

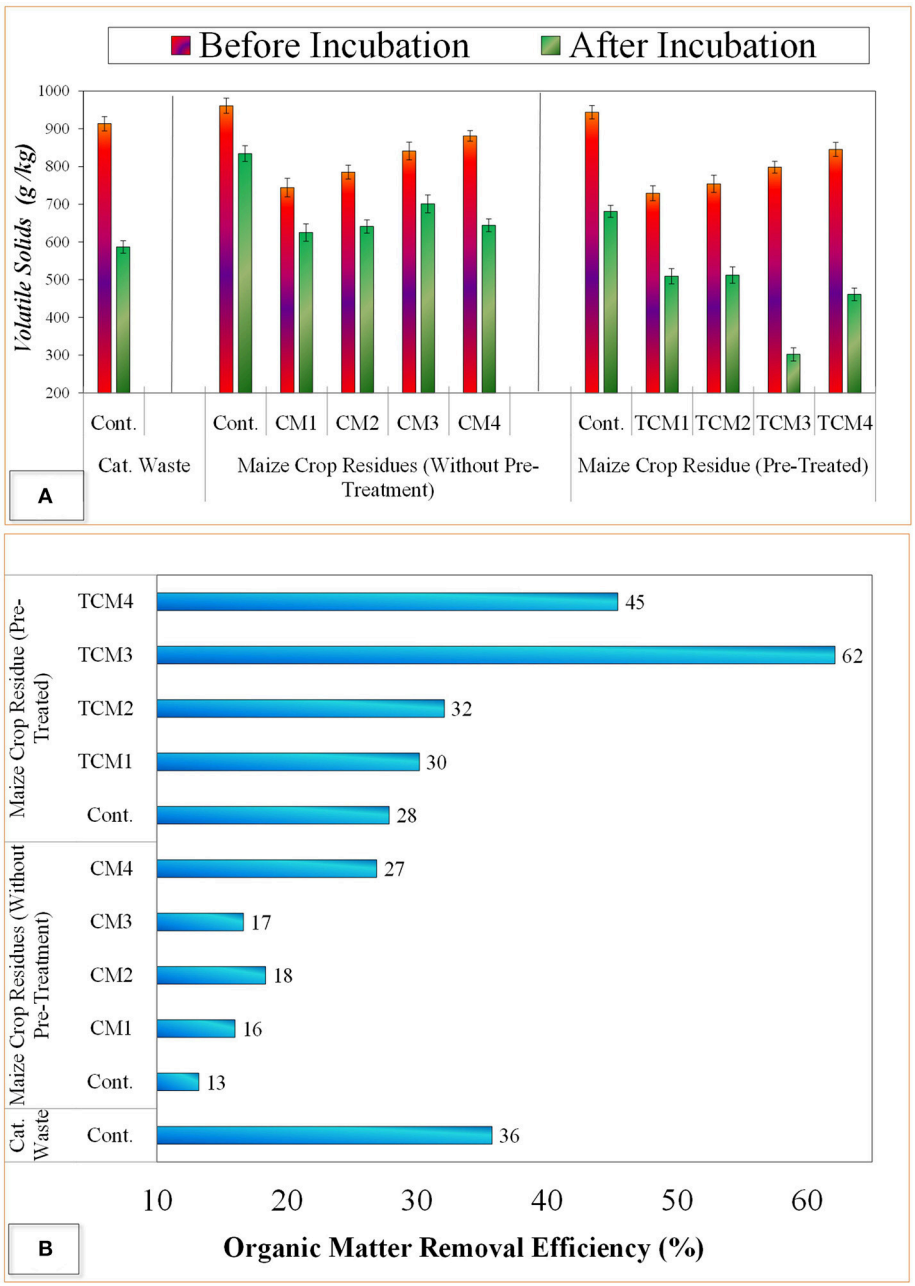

FIGURE 1 | Anaerobic co-digestion test of catering waste with maize crop residues; **(A)** Effect on VS degradation, **(B)** Organic matter removal efficiency.

filled with the substrates, while 500 ml head space was left empty for biogas accumulation. Biogas was collected in biogas collection bag connected at the top biogas valve, through the flow tube built in with an internal valve to control the one-way flow of biogas. The digestate samples were taken from the lower part of the reactor where a sampling valve was set. Both reactors were placed in an incubator at fixed temperature 30 ± 1°C. The biogas was analyzed using liquid displacement apparatus.

Aerobic Post Treatment of Digestate

Two digestate samples were collected from anaerobic co-digestion of catering waste and maize crop residues. One digestate sample is supplied with an aerobic post treatment in order to reduce toxic substances exist in digestate, while second digestate sample did not supply with any post treatment. Aerobic pretreatment was performed using continuous stirred aerobic reactor supplied by continuous air diffusion from the bottom and string of 150 rpm. The temperature was maintained in range of 32–35°C and reaction was continued for 20 days. The digestate quality was analyzed by measuring carbon content, volatile solids, pH and EC using standard methods. The digestate was dried in a digital oven for 24 h at 70°C. The final obtained digestate materials were preserved in the cold storing unit at temperature >50°C for further utilization in experiments.

Phytotoxicity Test

The phytotoxicity test of both digestate was conducted by using 72 h seed germination assay. Germination assay is a rapid and widely applied method for evaluating phytotoxicity of organic product (Da Ros et al., 2018). Three dilution of each digestate material (post treated and untreated digestate) were prepared using 5, 10, and 20 g of dried digestate in 100 ml of distilled water.

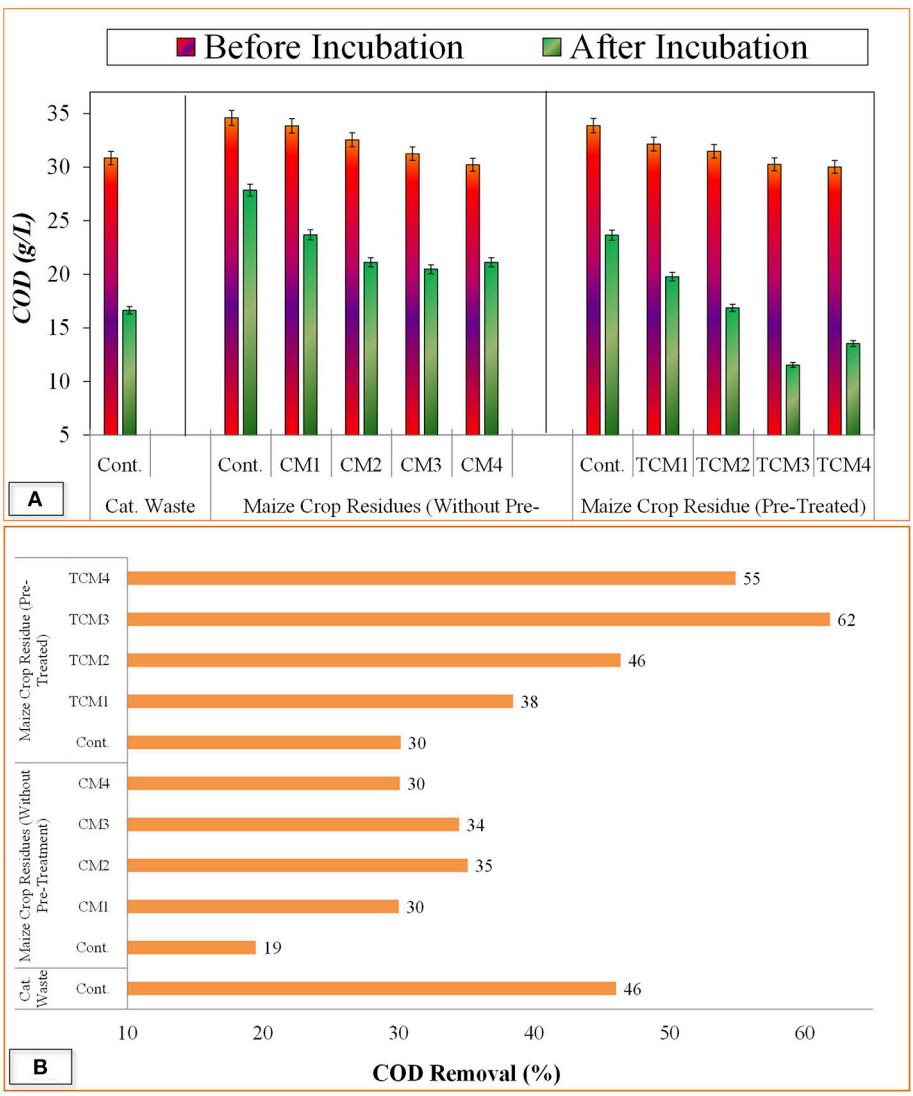

FIGURE 2 | Anaerobic co-digestion test of catering waste with maize crop residues; **(A)** Effect on COD, **(B)** COD removal efficiency.

Wheat seed were used to testing seed germination assay. For the germination assay, Petri dishes of 10 cm diameter were lined with watt man filter paper. Each dish received 5 ml of the digestate solution using a micropipet. Ten wheat seeds (sterilized) were placed in each petri dish and sealed with the parafilm. The petri dishes were incubated at 25°C for 72 h in the dark conditions. The germinated seeds were counted and, root length and shoot length were measured were at regular interval during 72 h. The seed germination percentage (G%), germination index (GI) and vigor index (VI) were analyzed to estimate the phytotoxicity of digestate.

Anatical Methods

Chemical oxygen demand (COD) was analyzed using the closed, reflux titrimetric method applying the standard method of American Public Health Association (APHA (American Public Health Association), 2005). COD was calculated using the following equation (Equation 1):

$$COD\ (mg/L) = \frac{(X - B)\ \times\ M\ \times\ 8000)}{Vol.\ of\ samle} \quad (1)$$

The factor X-B is ml of FAS used for blank subtracted from ml of FAS used for sample. M denotes the molarity of FAS, whereas the value 8,000 is the weight of oxygen mill equivalent 1,000 ml/l. Solid fractions i.e., TS and VS were analyzed using the standard method # 1684 (US EPA, 2001). TS was determined by measuring the difference in mass of the sample before and after drying in oven at temperature 105°C, whereas VS was measured as an ignition loss at high temperature (550°C) in the muffle

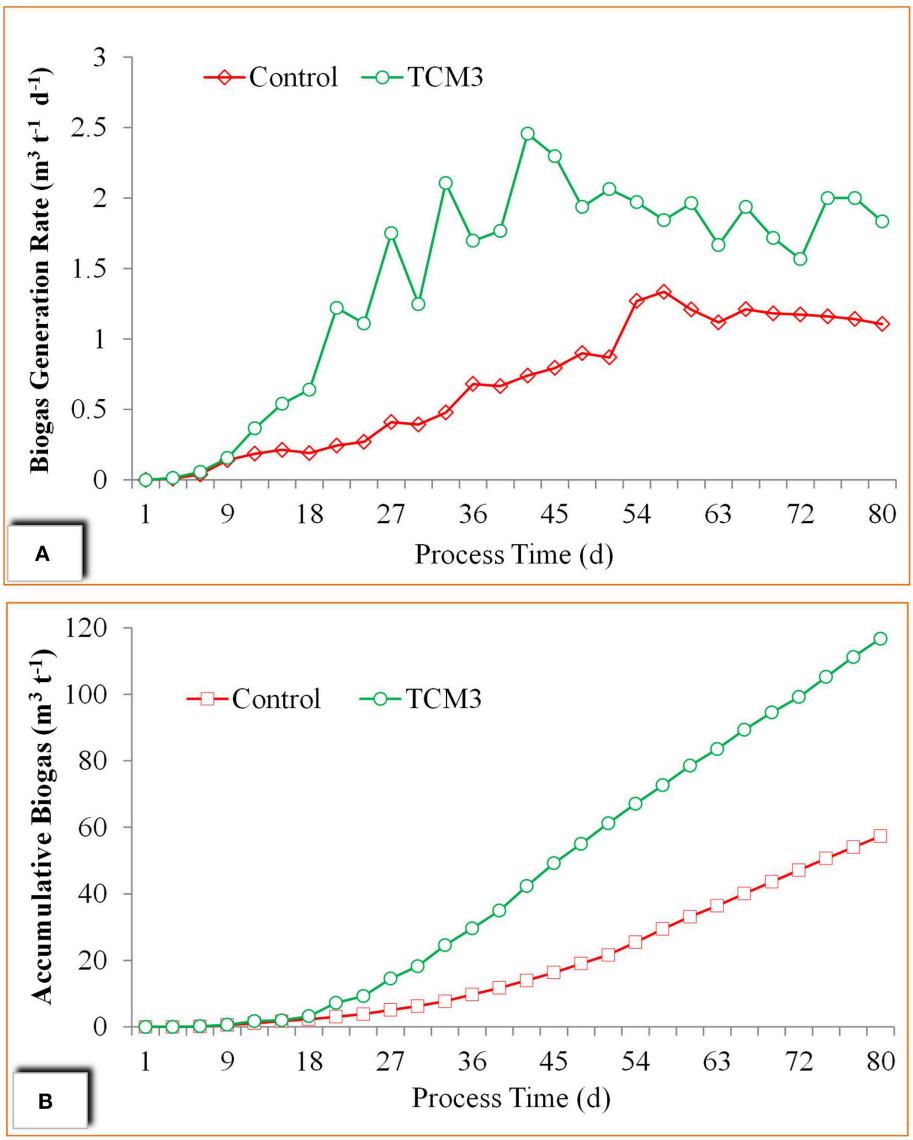

FIGURE 3 | Anaerobic co-digestion of catering waste with partial pre-treated maize crop residues at optimum mixing ratio for biogas production; **(A)** Biogas production rate, **(B)** Accumulative biogas production.

furnace. The C:N ratio was calculated by taking the total mass of carbon divided by mass of nitrogen in grams (Smith and Holtzapple, 2011; Anjum et al., 2012). pH, EC, and TDS values were recorded on Crison Multimeter (Model number: "CRISON MM-40þ"). In anaerobic digesters, the biogas production was measured as methane production through liquid a displacement methods for duration of 80 days using the method described by Elaiyaraju and Partha (2012). During phytotoxicity experiment, seed germination assay was conducted where seed germination index, germination percentage, seedling length, and vigor index were measured. The germination index (GI) was calculated using the following formula (Equation 2) (Mitelut and Popa, 2011):

$$GI = \frac{G}{G_o} \times \frac{L}{L_o} \times 100 \quad (2)$$

where L_o and G_o are root growth and germination percentage. Data interpretation, calculation, averages and standard deviations were calculated using MS Office Excel 2010.

RESULTS AND DISCUSSION

Anaerobic Co-digestion Test of Catering Waste With Maize Crop Residues

Optimization of Substrate Ratio and Effect of Pretreatment of Maize Crop Residues

For optimization of the substrate ratio, the co-digestion experiments were conducted using catering waste as main substrate and maize crop residues as co-substrates (untreated and pre-treated with microwave-steam) for a duration of 42 days. The

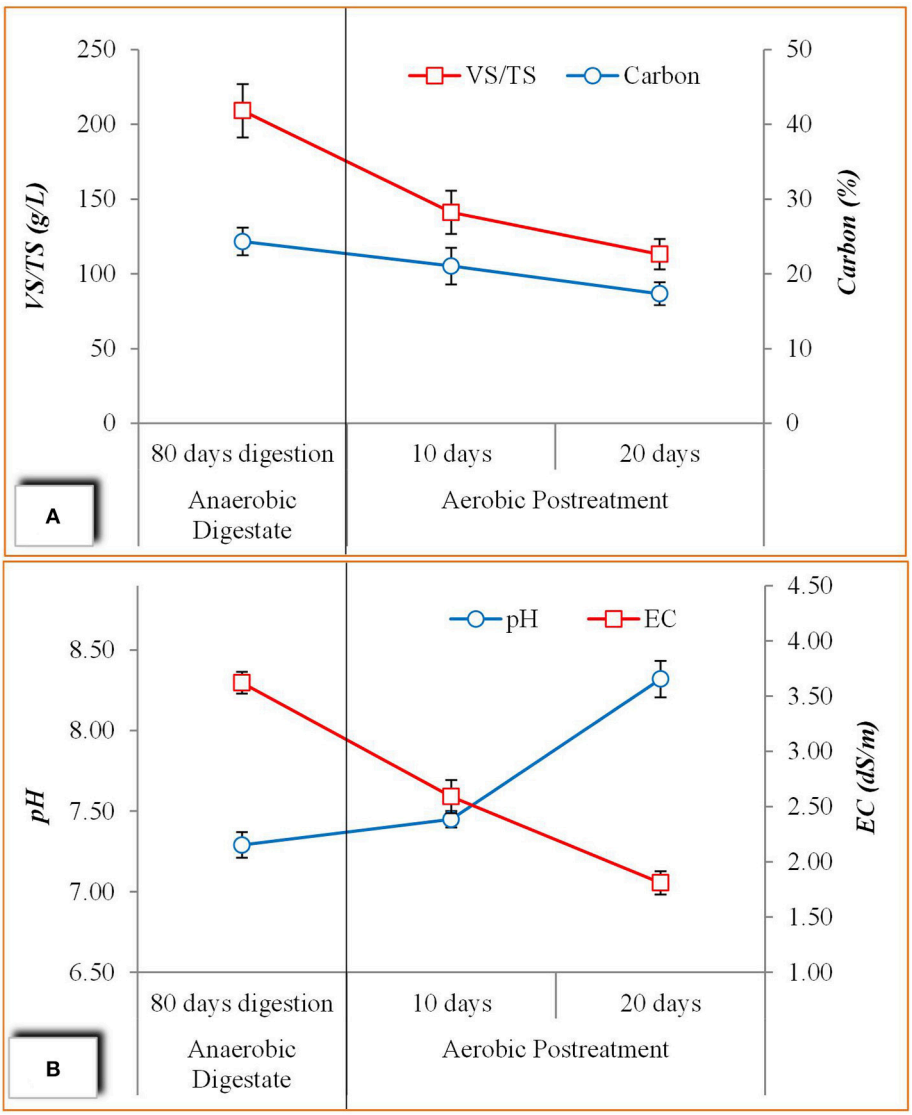

FIGURE 4 | Post treatment of anaerobic co-digested digestate for bio-product formulation; **(A)** Effect on VS and Carbon content, **(B)** Effect on EC and pH.

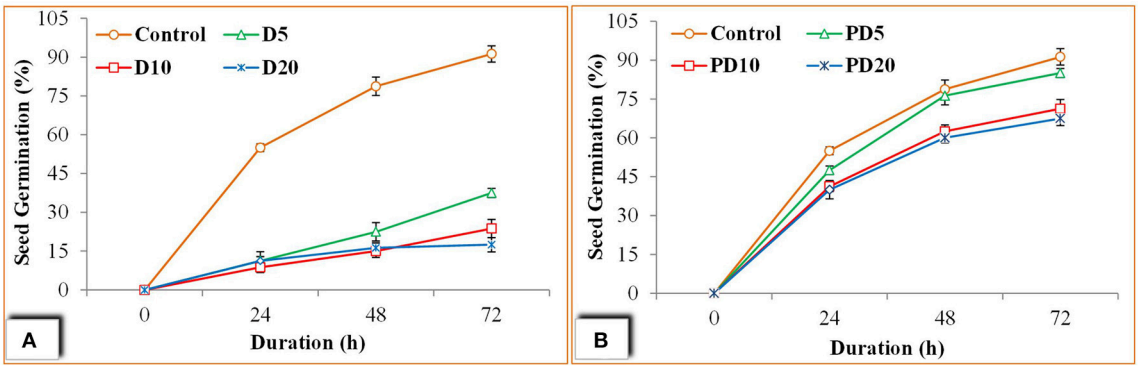

FIGURE 5 | Seed germination assay; **(A)** Seed germination percentage using un-treated digestate, **(B)** Seed germination percentage using aerobic post treated digestate.

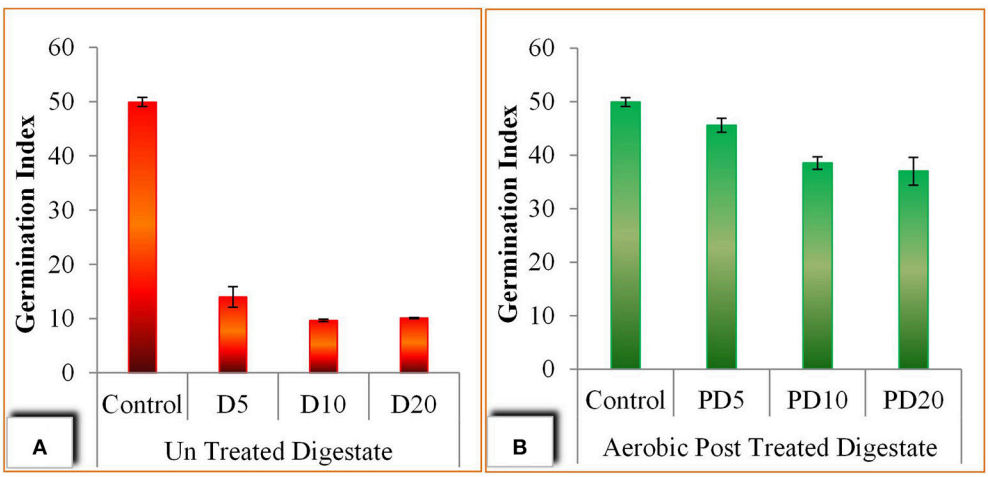

FIGURE 6 | Seed germination assay; **(A)** Seed germination index using un-treated digestate, **(B)** Seed germination index using aerobic post treated digestate.

results regarding organic matter removal efficiency (VS content basis) and change in COD are explained as under:

The results regarding VS content and organic matter removal efficiency are described in **Figure 1** which showed that the co-digestion experiments with pre-treated maize crop residues showed more reduction in VS as compared to untreated maize crop residues. The maximum reduction in VS was shown by CM4 (50% untreated crop residue ratio) where VS content was lowered to 644 g/kg from 881 g/kg after 42 days of incubation. However, maximum degradation in case of pre-treated maize crop residues was observed in TCM3 (40% ratio), with the VS reduction of 302 g/kg from 798 g/kg. The organic matter removal efficiency was achieved up to maximum 62% in TEM3 compared to the TEM4 (45%). The increased in organic matter removal efficiency is probably due to the increase in lignin loss under the influence of pretreatment of maize crop residues as reported by Yuan et al. (in press). The fact that pre-treatment enhance the degradation of lignocellulose and hemicellulose material of maize crop residues which are actually recalcitrant in nature (Surra et al., 2018). After applying pre-treatment these material partially degraded and become available to microorganisms. Overall, these outcomes revealed that the pretreatment of maize crop residues has enhanced the degradation in co-digestion process with catering waste.

The variation in COD values during anaerobic digestion of catering waste and pre-treated maize crop residues is presented in **Figure 2** COD is used as a sole indicator of optimization of anaerobic digestion process. After 42 days of the co-digestion process, the highest decrease in COD (30.2–11.5 g/L) was observed at 40% maize crop residues (TCM3), which means that insoluble COD (51%) was probably transformed soluble organic matter to final mineralized products (**Figure 2B**). In untreated maize crop residues the maximum degradation COD from 31.2 g/L (day1) to 20.4 g/L (day 42) was achieved at 40% fraction ration with catering waste (CM3). The lowest COD removal (31%) was observed in CM1 and CM4 in case of untreated maize crop residues which is even lower than catering waste alone (control) where COD removal of 46% was found. The improved COD degradation with pre-treated maize crop residue was due to the fact that pretreatment provides more organics in

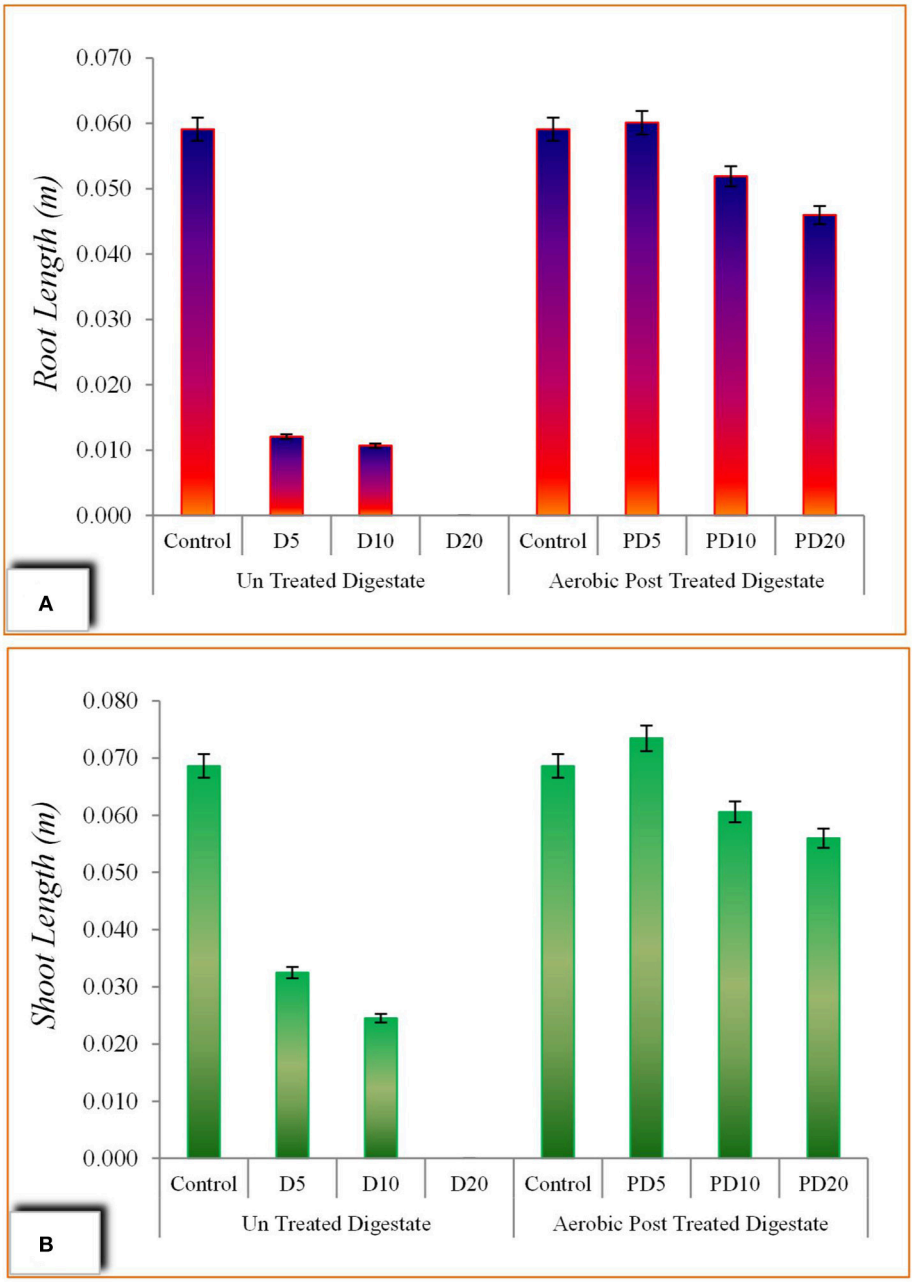

FIGURE 7 | Seed germination assay using un-treated and aerobic post treated digestate; **(A)** Root length, **(B)** Shoot length.

solubilized form (sCOD) and thus more available to anaerobic bacteria (Anjum et al., 2018). Overall, these results showed that use of pre-treated crop residues is more promising with catering waste co-digestion where optimum mixing ration was found at 40% maize crop residue with 60% catering waste and labeled as TCM3.

Biogas Production

To observe the biogas potential of mixed catering waste and maize crop residues, anaerobic digestion was performed in two static batch reactors. One is for co-digestion containing both substrates in ratio as optimized in previous experiment (TCM3), while second reactor was taken as control containing catering waste alone. The results showed that the addition of pre-treated maize crop residues in catering waste, significantly increase the methane production potential as compared to that in catering waste alone (**Figure 3A**). During the anaerobic digestion process of 80 days, TCM3 co-digestion reactor showed an increasing trend in biogas production up 27–42 days where highest methane generation rate of 2.46 m^3 d^{-1} t^{-1} was

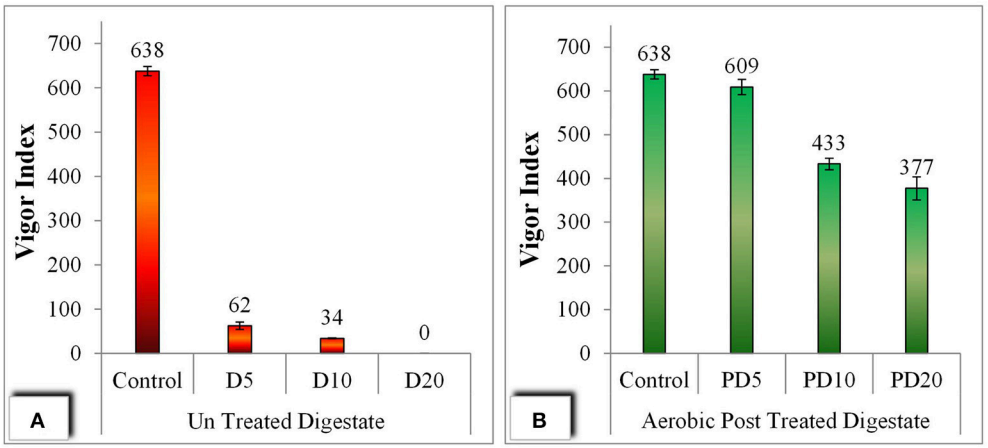

FIGURE 8 | Seed germination assay; **(A)** Vigor Index with un-treated digestate, **(B)** Vigor Index with aerobic post treated digestate.

recorded. The incremented methane production was due to the influence of pretreatment of lignocellulosic biomass, where the pretreatment degrade the lignocellulose and increase the cellulose component (Rajput and Visvanathan, 2018). Furthermore, it is well reported that the co-digestion has ability to provide more balance nutrients such as optimum C/N (Wang et al., 2014) and increased P (Medvedeff et al., 2014) content which ultimately improve the growth of methanogens and biogas production.

On the other hand, control bioreactor showed the highest methane production rate of between after 54–60 days. Thereafter, the methane production rate was become stable in TEM3 co-digestion reactor till 80 days. In control bioreactor the methane production rate was slightly decrease after 60 days, which is due to slow and incomplete degradation rate. The lowering in methane production in catering waste alone may be due the accumulation of volatile fatty acids, as acidic pH range was found during the anaerobic digestion process. Moreover, the inhibition in biogas production may be cause due to accumulation of ammonia within the system which cause lowering in C/N ratio below the optimum range (25–30 required for methanogens Wang et al., 2014. The accumulation of volatile fatty acids inhibit the methanogenic activity and longer the acetogenic phase, thus reduces overall efficiency of the system Chen et al., 2014; Yang et al., 2015; Jiang et al., 2018. Overall, the accumulative methane production was more in TEM3 as compared to catering waste alone (**Figure 3B**). The maximum accumulative methane of 116.7 m^3 t^{-1} was recorded in TCM3 reactor i.e., 2.03 times more as compared to control reactor. The addition of the co-substrate in anaerobic digestion process has influence the provision of more balanced nutrients such as C/N ratio and, organic load, thus creating more suitable conditions for microbial activity (Sosnowski et al., 2003; Zou et al., 2018).

Effect of Aerobic Post Treatment of Digestate

In order to prepare anaerobic digestate bio-product as low phytotoxic organic fertilizer, aerobic post treatment was applied to the anaerobic digestate of co-digested catering waste and wheat crop residues (TCM3). **Figure 4A** expressed the results regarding effect on VS and carbon content due aerobic post treatment. VS in the digestate was decreased from 209 g/L to 113 g/L after 20 days where as carbon content was lowered to 17% from 24% in fresh digestate. The lowering in VS and carbon content is attributed degradation of toxic organic compound especially organic acids produced during anaerobic digestion process. The lowering in VS content in post treatment make digestate more stable (Wojnowska-Baryła et al., 2018). These means that aerobic post treatment for 20 days could lower the phytotoxic compounds in digestate and make more feasible bio-product for soil application.

In case of pH, aerobic post treatment increases an overall pH of the digestate up 8.32 which is very favorable for soil application (**Figure 4B**). The basic reason of low pH in anaerobic digestion production of organic acid in high quantity which inhibit the digestion process (Yang et al., 2015; Zhang et al., 2018), but in the present study the pH of 7.29 showed that there were limit accumulation of organic acids and aerobic post treatment has further improved the pH of the digestate. Electrical conductivity is another important indicator of quality of digestate which mainly represents the concentration of salts and ions. EC values of 3.62 dS/m was found in anaerobic fresh digestate which is further lowered to 1.81 dS/m after aerobic digestion process (**Figure 4B**). EC can influence seed germination in contact with digestate, where lower EC is more favorable for seed germination (Coelho et al., 2018). This showed that EC of the digestate could be improved by post treatment of digestate in order to cause least negative effect in soil due to higher EC.

Phytotoxicity Analysis of Digestate

Phytotoxicity is widely applied and promising parameter to evaluate digestate application on plants which describes the index its overall eco-toxicological impact (Da Ros et al., 2018). The phytotoxicity test of both untreated and post treated digestate at varying digestate solution (5, 10, and 20 g per 100 ml water)

was performed using seed germination assay on wheat seeds. The results regarding seed germination percentage are described in **Figure 5**. Seed germination was continuously increased in case of control (Water only) where after 72 h 91% of seed were observed fully germinated. When digestate was applied G% was lowered where only 17 % of germination was found even after 72 h in D20 (20 g untreated digestate/100 ml water) (**Figure 5A**). However, a slightly higher G% (38 and24%) was found in D5 and D10, respectively after 72 h. This shows that the digested without post treatment cause swear toxicity to wheat seed which in increased as the concentration of digestate increase.

In case of post treated digestate an improvement in G% was observed with up to 85% seed germination was attained after 72 h in PD5 (5 g/100 ml) (**Figure 5B**). These finding also confirmed by the Germination Index (GI) values with a maximum GI of 46 was shown by PD5 and followed by PD10 (GI = 39) and PD20 (GI = 37) (**Figure 6**). However, the lower germination index values in un-treated digestate was observed which is probably due to low high EC values (Tang et al., 2018).

The seedling length was measured after 72 h of incubation and illustrated in **Figure 7**. Both shoot length and rood length were significantly increased with post treated digestate solution. A maximum root length of 6.01 cm and 5.19 cm were achieved by PD5 and PD10 which were 4.9 and 4.8 times higher than respective treatments with untreated digestate. Similarly, shoot length of 7.34 cm was the highest in PD5 with the slight lowing in PD10 (6.06 cm) and PD20 (5.60 cm). The improvement in seedling length is attributed to the post treatment of digestate which supply more plants essential nutrients [N, P, and K (Coelho et al., 2018)] to seedling with least effect of toxic materials.

Vigor index is one the known indicator used in analyses toxicity in plants (Shaikh et al., 2013). The vigor of seeds was described as a vigor index (VI) as illustrated in **Figure 8**. Seeds treated with post treated digestate showed the higher VI i.e., up to 609 in PD5, where with the increase in concentration of digestate from 5 g/100 ml to 20 g/100 ml, VI was decreased to 377. On the other hand the seed grown with untreated digestate shows significantly lower vigor i.e., even with a value of zero with D20 (20 g/100 ml).

CONCLUSION

The present study demonstrates the successful application of anaerobic co-digestion process for catering waste with partially pre-treated maize crop residues to produce biogas and biofertilizer production. The co-digestion of catering waste partially pre-treated maize crop residues at 40 % mixing ratio (TCM3) showed a significant degradability, where, 2.03 times higher methane production was achieved compared to control reactor.

Thereafter, the quality of digestate was improved by applying aerobic post treatment. The phytoxic analysis showed that improved G% (85%) while maximum GI of 46 and VI of 609 were achieved. Overall, the present study proposed a biorefinery concept in which co-digestion can be used as waste management approach for multiple outcomes such as energy recovery and biofertilizer production.

AUTHOR CONTRIBUTIONS

MA conducted the basic experimental work and prepared the initial draft. AK supervised the work and provided technical and scientific assistance. The final draft was revised by both AK and SQ.

ACKNOWLEDGMENTS

This work was conducted and supported by Environmental Science Lab, Department of Environmental Sciences, PMAS Arid Agriculture University, Rawalpindi Pakistan.

REFERENCES

Abdullahi, Y. A., Akunna, J. C., White, N. A., Hallett, P. D., Wheatley, R. (2008). Investigating the effects of anaerobic and aerobic post-treatment on quality and stability of organic fraction of municipal solid waste as soil amendment. *Bioresour. Technol.* 99, 8631–8636. doi: 10.1016/j.biortech.2008.04.027

Alvarez, J. A., Otero, L., Lema, L. J. (2010). A methodology for optimising feed composition for anaerobic co-digestion of agro-industrial wastes. *Bioresour. Technol.* 101, 1153–1158. doi: 10.1016/j.biortech.2009.09.061

Anjum, M., Khalid, A., Mahmood, T., and Arshad, M. (2012). Anaerobic co-digestion of municipal solid organic waste with melon residues to enhance biodegradability and biogas production. *J. Mater. Cycles Waste Manag.* 14, 388–395. doi: 10.1007/s10163-012-0082-9

Anjum, M., Khalid, A., Mahmood, T., and Aziz, I. (2016). Anaerobic co-digestion of catering waste with partially pretreated lignocellulosic crop residues. *J. Clean. Prod.* 117, 56–63. doi: 10.1016/j.jclepro.2015.11.061

Anjum, M., Kumar, R., Al-Talhi, H. A., Mohamed, S. A., and Barakat, M. A. (2018). Valorization of biogas production through disintegration of waste activated sludge using visible light ZnO-ZnS/Ag_2O-Ag_2S photocatalyst. *Proc. Safety Environ. Protect.* 119, 330–339. doi: 10.1016/j.psep.2018.08.022

APHA (American Public Health Association) (2005). Standard *Methods for the Examination of Water and Wastewater*, *21st Edn*. Washington, DC: APHA-AWWA-WEF.

Ayomoh, M. K., Oke, S. A., Adedeji, W. O., and Charles-Owaba, O. E. (2008). An approach to tackling the environmental and health impacts of municipal solid waste disposal in developing countries. *J. Environ. Manag.* 88, 108–114. doi: 10.1016/j.jenvman.2007.01.040

Bolzonella, D., Cavinato, C., Fatone, F., Pavan, P., Cecchi, F. (2012). High rate mesophilic, thermophilic, and temperature phased anaerobic digestion of waste activated sludge: a pilot scale study. *Waste Manag.* 32, 1196–1201. doi: 10.1016/j.wasman.2012.01.006

Bundhoo, Z. M. A., Mauthoor, S., and Mohee, R. (2016). Potential of biogas production from biomass and waste materials in the Small Island Developing State of Mauritius. *Renew. Sustain. Energy Rev.* 56, 1087–1100. doi: 10.1016/j.rser.2015.12.026

Chen, H., Shen, H., Su, H. F., Chen, H. Z., Tan, F. R., Lin, J. F. (2017). High-efficiency bioconversion of kitchen garbage to biobutanol using an enzymatic cocktail procedure. *Bioresour. Technol.* 245 (Pt A) 1110–1121. doi: 10.1016/j.biortech.2017.09.056

Chen, X., Yan, W., Sheng, K., and Sanati, M. (2014). Comparison of high-solids to liquid anaerobic co-digestion of food waste and green waste. *Bioresour. Technol.* 154, 215–221. doi: 10.1016/j.biortech.2013.12.054

Chen, Y-D., Ho, S-H, Nagarajan, D., Ren N-Q, and, Chang, J. S. (2018). Waste biorefineries—integratanaerobic digestion and microalgae cultivation for bioenergy production. *Curr. Opin. Biotechnol.* 50, 101–110. doi: 10.1016/j.copbio.2017.11.017

Coelho, J. J., Prieto, M. L., Dowling, S., Hennessy, A., Casey, I., Woodcock, T., et al. (2018). Physical-chemical traits, phytotoxicity and pathogen detection in liquid anaerobic digestates. *Waste Manag.* 78, 8–15. doi: 10.1016/j.wasman.2018.05.017

Da Ros, C, Libralato, G., Ghirardini, A. V., Radaelli, M., Cavinato, C. (2018). Assessing the potential phytotoxicity of digestate from winery wastes. *Ecotoxicol. Environ. Safety* 150, 26–33. doi: 10.1016/j.ecoenv.2017.12.029

Elaiyaraju, P., and Partha, N. (2012). Biogas production from co-digestion of orange peel waste and jatropha de-oiled cake in an anaerobic batch reactor. *African J. Biotechnol.* 11, 3339–3345. doi: 10.5897/AJB11.2622

Galvez, A., Sinicco, T., Cayuela, M. L., Mingorance, M. D., Fornasier, F., and Mondini, C. (2012). Short term effects of bioenergy by-products on soil C and N dynamics, nutrient availability and biochemical properties. *Agric. Ecosyst. Environ.* 160, 3–14. doi: 10.1016/j.agee.2011.06.015

Izumi, K., Okishio, Y. K., Nagao, N., Niwa, C., Yamamoto, S., and Toda, T. (2010). Effects of particle size on anaerobic digestion of food waste. *Int. Biodeterior. Biodegrad.* 64, 601–608. doi: 10.1016/j.ibiod.2010.06.013

Jiang, Y., Dennehy, C., Lawlor, P. G., Hu, Z., McCabe, M., Cormican, P., et al. (2018). Inhibition of volatile fatty acids on methane production kinetics during dry co-digestion of food waste and pig manure. *Waste Manag.* 79, 302–311. doi: 10.1016/j.wasman.2018.07.049

Kuczman, O.,Gueri, M. V. D., De Souza, S. N. M., Schirmer, W. N., Alves, H. J., Secco, D., et al. (2018). Food waste anaerobic digestion of a popular restaurant in Southern Brazil. *J. Clean. Prod.* 196, 382–389. doi: 10.1016/j.jclepro.2018.05.282

Medvedeff, C. A., Inglett, K. S., and Inglett, P. W. (2014). Evaluation of direct and indirect phosphorus limitation of methanogenic pathways in a calcareous subtropical wetland soil. *Soil Biol. Biochem.* 69, 343–345. doi: 10.1016/j.soilbio.2013.11.018

Mitelut, A. C., and Popa, M. E. (2011). Seed germination bioassay for toxicity evaluation of different composting biodegradable materials. *Romanian Biotechnol. Lett.* 16, 121–129.

Rajput, A. A., and Visvanathan, C. (2018). Effect of thermal pretreatment on chemical composition, physical structure and biogas production kinetics of wheat straw. *J. Environ. Manag.* 221, 45–52. doi: 10.1016/j.jenvman.2018.05.011

Serrano, A., Siles, J. A., Chica, A. F., and Martín, M. A. (2013). Agri-food waste valorization through anaerobic co-digestion: fish and strawberry residues. *J. Clean. Prod.* 54, 125–132. doi: 10.1016/j.jclepro.2013.05.002

Shaikh, I. R., Shaikh, P. R., Shaikh, R. A., and Shaikh, A. A. (2013). Phytotoxic effects of heavy metals (Cr, Cd, Mn and Zn) on wheat (*Triticum aestivum* L.) seed germination and seedlings growth in black cotton soil of Nanded, India. *Res. J. Chem. Sci.* 3, 14–23.

Smith, A. D., and Holtzapple, M. T. (2011). Investigation of the optimal carbon–nitrogen ratio and carbohydrate-nutrient blend for mixed-acid batch fermentations. *Bioresour. Technol.* 102, 5976–5987. doi: 10.1016/j.biortech.2011.02.024

Sosnowski, P., Wieczorek, A., and Ledakowicz, S. (2003). Anaerobic co-digestion of sewage sludge and organic fraction of municipal solid wastes. *Adv. Environ. Res.* 7, 609–616. doi: 10.1016/S1093-0191(02)00049-7

Surra, E., Bernardo, M., Lapa, N., Esteves, I., Fonseca, I., Motab, J. P., et al. (2018). Maize cob waste pre-treatment to enhance biogas production through co-anaerobic digestion with OFMSW. *Waste Manag.* 72, 193–205. doi: 10.1016/j.wasman.2017.11.004

Taherzadeh, M. J., and Karimi, K. (2008). Pretreatment of lignocellulosic wastes to improve ethanol and biogas production: a review. *Int. J. Mol. Sci.* 9, 1621–1651. doi: 10.3390/ijms9091621

Tang, Y., Li, X., Dong, B., Huang, J., Wei, Y., Dai, X., et al. (2018). Effect of aromatic repolymerization of humic acid-like fraction on digestate phytotoxicity reduction during high-solid anaerobic digestion for stabilization treatment of sewage sludge. *Water Res.* 143, 436–444. doi: 10.1016/j.watres.2018.07.003

Tornwall, E., Pettersson, H., Thorin, E., Schwede, S. (2017). Post-treatment of biogas digestate-an evaluation of ammonium. *Energy Procedia* 142, 957–963. doi: 10.1016/j.egypro.2017.12.153

Trzcinski, A. P., and Stuckey, D. C. (2011). Parameters affecting the stability of the digestate from a two-stage anaerobic process treating the organic fraction of municipal solid waste. *Waste Manag.* 31, 1480–1487. doi: 10.1016/j.wasman.2011.02.015

US EPA (2001). *Total, Fixed, and Volatile Solids in Water, Solids, and Biosolids (Method 1684)*. Washington, DC: US Environmental Protection Agency.

Wang, X., Lu, X., Li, F., and Yang, G. (2014). Effects of temperature and carbon-nitrogen (C/N) ratio on the performance of anaerobic co-digestion of dairy manure, chicken manure and rice straw: focusing on ammonia inhibition. *PloS ONE* 9:97265. doi: 10.1371/journal.pone.0097265

Wojnowska-Baryła, I., Bernat, K., and Sartowska, S. (2018). Biological stability of multi-component agri-food digestates and post-digestates. *Waste Manag.* 77, 140–146. doi: 10.1016/j.wasman.2018.05.016

Yang, L., Huang, Y., Zhao, M., Huang, Z., Miao, H., Xu, Z., et al. (2015). Enhancing biogas generation performance from food wastes by high-solids thermophilic anaerobic digestion: effect of pH adjustment. *Int. Biodeteriorat. Biodegrad.* 105, 153–159. doi: 10.1016/j.ibiod.2015.09.005

Yuan, H., Lan, Y., Zhu, J., Wachemo, A. C., Li, X., and Yu, L. (in press). Effect on anaerobic digestion performance of corn stover by freezing-thawing with ammonia pretreatment. *Chin. J. Chem. Eng.* doi: 10.1016/j.cjche.2018.04.021

Zhang, B., Zhang, L. L., Zhang, S. C., Shi, H. Z., and Cai, W. M. (2005). The influence of pH on hydrolysis and acidogenesis of kitchen wastes in two-phase anaerobic digestion. *Environ. Technol.* 26, 329–339. doi: 10.1080/09593332608618563

Zhang, W., Xing, W., and Li, R. (2018). Real-time recovery strategies for volatile fatty acid-inhibited anaerobic digestion of food waste for methane production. *Bioresour. Technol.* 265, 82–92. doi: 10.1016/j.biortech.2018.05.098

Zou, H., Chen, Y., Shi, J., Zhao, T., Yu, Q., Yu, S., et al. (2018). Mesophilic anaerobic co-digestion of residual sludge with different lignocellulosic wastes in the batch digester. *Bioresour. Technol.* 268, 371–381. doi: 10.1016/j.biortech.2018.07.129

Conflict of Interest Statement: The authors declare that the research was conducted in the absence of any commercial or financial relationships that could be construed as a potential conflict of interest.

frontiers in Energy Research

ORIGINAL RESEARCH
published: 04 March 2019
doi: 10.3389/fenrg.2019.00014

Role of Biochar in Anaerobic Digestion Based Biorefinery for Food Waste

Carol W. Wambugu, Eldon R. Rene, Jack van de Vossenberg, Capucine Dupont and Eric D. van Hullebusch*

Department of Environmental Engineering and Water Technology, UNESCO-IHE Institute for Water Education, Delft, Netherlands

The effect of biochar addition on the anaerobic digestion (AD) of food waste was evaluated. From the five biochars tested, Fe, Co, Ni, and Mn were leached in very small quantities (<10 mg/kg), while a high amount of K (1,510 and 1,969 mg/kg) was leached from treated waste wood and willow tree pyrochar, respectively. AD batch experiments were performed at an inoculum:substrate ratio of 1:1, at 30°C and under agitating conditions. The results showed that the biogas volume produced by the treatments with the brewery residue hydrochar and treated waste wood pyrochar was lower than the amount of biogas produced by the control with only food waste. The food waste supplemented with 1.5 mL of trace elements yielded the highest biogas of 588 mL/g COD (CH_4 content−48%). Furthermore, two identical upflow anaerobic sludge blanket (UASB) reactors, i.e., control reactor and biochar amended reactor, were operated at 30°C, at organic loading rates (OLR) varying from 3.4 to 7.8 g COD/L.day. The average COD removal efficiencies of the control and the biochar-amended reactor were 47 and 77% at an OLR of 6.9–7.8 g COD/L.day, respectively. These study results clearly indicate that the type of biochar and trace elements concentration in biochar play a key role in determining the effectiveness of the biochar in enhancing biogas production from food waste.

Keywords: anaerobic digestion (AD), biochar, trace elements, food waste, leaching

OPEN ACCESS

Edited by:
Abdul-Sattar Nizami, King Abdulaziz University, Saudi Arabia

Reviewed by:
Muzammil Anjum, Pir Mehr Ali Shah Arid Agriculture University, Pakistan
Rajendra Prasad Singh, Southeast University, China

****Correspondence:***
Eldon R. Rene
e.raj@un-ihe.org

Specialty section:
This article was submitted to Bioenergy and Biofuels, a section of the journal Frontiers in Energy Research

Received: *15 November 2018*
Accepted: *04 February 2019*
Published: *04 March 2019*

Citation:
Wambugu CW, Rene ER, van de Vossenberg J, Dupont C and van Hullebusch ED (2019) Role of Biochar in Anaerobic Digestion Based Biorefinery for Food Waste. Front. Energy Res. 7:14. doi: 10.3389/fenrg.2019.00014

INTRODUCTION

Food waste accounts for about 32–62% of the municipal solid waste (MSW) fraction and is expected to increase due to the increasing population and urbanization around the world (Xu et al., 2018). Food waste generation is higher in developed countries, e.g., 98 million tons per annum in the European Union (EU) countries (Xu et al., 2018) and about 43.6 million tons of food is reported to have been thrown away in the U.S.A (Zhang et al., 2007). The methods commonly used for food waste disposal include incineration, landfilling and aerobic composting (Zhang et al., 2014). However, landfilling has been banned in most of the developed countries, leaving incineration as the preferred method. Incineration is energy intensive (Zhang et al., 2014) and an expensive technology to implement, especially in developing countries, incineration possesses environmental risks such as air pollution. Incineration of food waste is also not favorable because food waste contains high level of water.

In contrast, AD is emerging as a most efficient technology for food waste treatment and disposal. The high amount of the organic food waste fraction in MSW presents sufficient raw material for the AD process, which does not only remove the waste from the environment but is a promising source of renewable energy as well (Meyer-Kohlstock et al., 2016; Xu et al., 2018). The biogas produced from AD consists of about 65–70% methane (CH_4) and 35–40% carbon dioxide (CO_2) (Xu et al., 2018), which can be converted into a compressed natural gas (CNG), and electric energy. However, the AD process is quite sensitive to disturbance due to the presence of a variety of microorganisms that are involved in the four distinct stages such as hydrolysis, acidogenesis, acetogenesis, and methanogenesis (Fagbohungbe et al., 2017).

The first step is the hydrolysis, where the macromolecules (proteins, fats, and carbohydrates) are broken down into smaller molecules (peptides, fatty acids, and saccharides). It is catalyzed by exo-enzymes called hydrolyses produced by the fermentative bacteria, as shown in Equation (1) (Kondusamy and Kalamdhad, 2014). Example of these bacteria include *Bacterioides succinogenes* and *Clostridium thermocellum*.

$$nC_6H_{10}O_5 + nH_2O \rightarrow nC_6H_{12}O_6 \quad (1)$$

The second step is acidogenesis, where the smaller molecules are converted into volatile fatty acids (VFA) such as propionic, acetic and butyric acid, and other by-product gases like ammonia, carbon dioxide, hydrogen sulfide, alcohols, and aldehydes by acidogenic bacteria (*Clostridium butyricum*) as shown in Equation (2) (Kondusamy and Kalamdhad, 2014; Zhang et al., 2014).

$$nC_6H_{12}O_6 \rightarrow 3nCH_3COOH \quad (2)$$

The third and fourth steps, i.e., the acetogenesis and methanogenesis, involve the conversion of acetic acid into acetate, which is then converted into carbon dioxide and methane (Equation 3) by acetoclastic methanogens such as *Methanosarcina* and *Methanosaeta*. The hydrogenotrophic methanogens also produce CH_4 by using CO_2 as a carbon source and hydrogen as a reducing agent (Equation 4) (Kondusamy and Kalamdhad, 2014; Lü et al., 2016).

$$CH_3COOH \rightarrow CH_4 + CO_2 \quad (3)$$

$$CO_2 + H_2 \rightarrow CH_4 + 3H_2O \quad (4)$$

Long-term AD of food waste is characterized by poor stability due to accumulation of volatile fatty acids (VFA), which is mostly caused by the deficiency of essential trace elements such as manganese (Mn), cobalt (Co), nickel (Ni), zinc (Zn), and iron (Fe) (Zhang and Jahng, 2012). Trace elements are very important in the methanogenesis step of AD that involves the action of acetyl-CoA synthase and methyl coenzyme M reductase to catalyze key metabolic steps and require sufficient amount of Fe, Ni, and Co (van Hullebusch et al., 2016), while some methanogens may require molybdenum (Mo), tungsten (W), copper (Cu), and selenium (Se) (Molaey et al., 2018). The inefficiency of the methanogenesis step leads to low CH_4 production. AD metabolic by-products like ammonia (NH_3) also inhibit the methanogenesis step. Several solutions have been provided to improve the long-term stability of the AD process. These include, (i) co-digestion with other substrates such as cattle manure and sewage sludge (Xu et al., 2018) due to their high buffering capacity, (ii) addition of trace elements (Banks et al., 2012), and (iii) multi-digestion steps to separate the acidogenic and methanogenic phase of AD. One of the emerging trends in AD is the use of biochar as an additive for enhanced biogas production. A few researchers have reported that biochar can help to alleviate this effect when used as an additive in AD (Mumme et al., 2014; Lü et al., 2016; Wang et al., 2017).

Biochar is a carbon-rich compound that is produced through thermochemical decomposition of biomass in the absence of oxygen (Cha et al., 2016). It is produced through different processes such as pyrolysis (300–700°C; N_2; atmospheric pressure) and hydrothermal carbonization (170–250°C; water above saturated pressure) (Cha et al., 2016). The energy required for biochar production varies depending on the type of biomass used. For wood biomass used in the present study, approximately 160 MJ would be utilized for an effective pyrolysis process as illustrated in **Figure 1** (Joseph et al., 2018).

Recent studies have shown that the addition of biochar in AD of food waste increased the biogas yield (Fagbohungbe et al., 2016; Meyer-Kohlstock et al., 2016; Sunyoto et al., 2016; Wang et al., 2017). Sunyoto et al. (2016) added pine sawdust biochar (produced at 650°C) to AD of aqueous carbohydrate food waste made from white bread and observed increased CH_4 production by 41.6%. The addition of 8.3 g/L biochar to the food waste produced higher methane (from 55 to 78%), while 33.3 g/L biochar addition resulted in the lowest yield. It is hypothesized that the biochar creates a surface area for colonization by the microbial flora in the AD and acts as an adsorbent for compounds such as limonene (Fagbohungbe et al., 2016) and ammonia (Lü et al., 2016), that would otherwise inhibit the performance of the AD. Wang et al. (2017) added vermicompost based biochar (500°C) to mixed kitchen waste and observed that the biochar acted as a buffer and increased CH_4 production due to 15–20% (*w/w*) biochar addition. Meyer-Kohlstock et al. (2016) added Holm oak residue biochar (produced at 650°C) to municipal bio-waste and observed an increase of CH_4 production per organic dry matter (ODM) by 5% (257–272 NL/kg_{ODM}) due to 5% (*w/w*) biochar addition and 3% (252–267 NL/kg_{ODM}) due to 10% (*w/w*) biochar addition.

Recent studies have been carried out to evaluate the role of trace elements and biochar in the AD of food waste, independently, mostly in single-stage anaerobic systems. However, these studies have not addressed the role of biochar in improving the trace elements bioavailability in AD. The role of biochar in continuous AD process has also not yet been reported. Therefore, the objectives of the present study were to: (i) evaluate the ability of different types of biochar to leach trace elements, (ii) evaluate the effect of biochar and trace elements addition on the AD of food waste in batch reactors, and (iii) evaluate the effect of biochar addition on continuous AD of food waste using an upflow anaerobic sludge blanket (UASB) reactor.

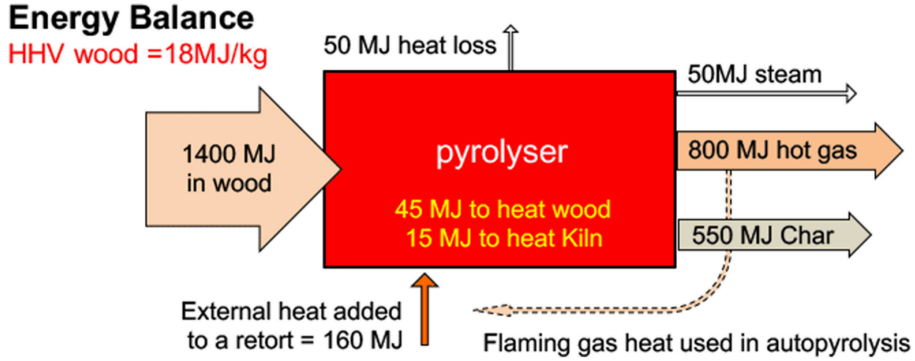

FIGURE 1 | Energy balance for biochar production from wood biomass. HHV is the higher heating value, a measure of energy content, including the latent heat of vaporization of water in the biomass (adapted from Joseph et al., 2018).

MATERIALS AND METHODS

Food Waste, Inoculum, and Biochar

The food waste was simulated using potatoes (30%), white bread (44%), spinach (10%), tomatoes (10%), and soya beans (6%). The total solids (TS) and volatile solids (VS) of the individual fractions of the food waste was analyzed, and the VS/TS ratio was used to select the required amounts used for this study. Shredding and dicing was done using a kitchen knife to reduce the size to ∼2 mm. Small portion of the food waste was blended using a kitchen blender (Proline, MIX55) with frequent addition of de-ionized water (total of 2 L), which resulted in a thick paste that was used in the batch experiments. Some of the paste was stored at −20°C until further use in continuous experiments. Anaerobic granular sludge was collected from Veolia Water Technologies Techno Center Netherlands B.V. (Biothane). The sludge was stored at 4°C until use. Before every batch test and the continuous experiment, the sludge was maintained at 30°C for 24 h, in order to acclimatize the sludge to the experimental conditions. The biochar used was (i) treated waste wood (600°C, ETIA, France), (ii) spruce wood (650°C, CIRAD, France), (iii) scots pine bark (475°C, VTT, Finland), (iv) willow tree (475°C, VTT, Finland), and (iv) brewery residue (260°C, VTT, Finland).

Trace Elements Leaching From Biochar

Biochar samples were weighed and dried in an oven at 105°C for 24 h. The moisture content was calculated using the gravimetric method for total solid analysis. The biochar samples (0.5 g) were placed in 250 mL bottles, and 20 mL of demi-water added. The bottles were agitated at 200 rpm on an orbital shaker (Innova^{TM} 2100 platform shaker), for 48 h at 30°C, and samples were collected at intervals of 0, 24, and 48 h, respectively. The mixture was filtered using a vacuum pump (Knf laboport, N816.3KT.45.18) to obtain the leachate. The electrical conductivity (WTW EC meter) and volume of the leachate were measured. Concentrated nitric acid (5% per L of filtered volume) was added to acidify the leachate for trace metal analysis by an inductively coupled plasma mass spectrometry (ICP-MS, X series 2 by Thermo Scientific). The amount of trace elements leached was expressed in mg/kg, according to the calculations described in the EN12457-4 standard (Dutch Standardization Institute, 2002).

Batch AD Experiments

Batch AD tests were carried out in 250 mL glass bottles having a working volume of 150 and 170 mL headspace, respectively. The inoculum/substrate (ISR) ratio 1:1 (VSS inoculum/VS food waste) was used for all the batch experiments. The batch experiments were carried out in three treatments as summarized in **Table 1**. All the batch experiments were performed and analyzed in triplicates. The food waste paste used in treatments A and B had an organic load of 18 g COD/$L_{(wetbasis)}$, while the food waste used in treatment C had an organic load of 6 g COD/$L_{(wetbasis)}$. The trace elements solution was composed of Fe, Co, Ni, and Zn, each with a concentration of 1,000 mg/L. The headspace was purged with pure nitrogen gas for 2 min, and the bottles were tightly covered using a metallic ring cap fitted with a rubber septum. The reactors were incubated on an orbital shaker (Innova^{TM} 2100 platform shaker), at 150 rpm and 30°C, for 6 days. The daily increment of headspace gas pressure in the bottles was measured using a manometer (LEO 1 Keller, model: LEO 1/-1 to 3 bar/81000.2) and was used to calculate the biogas volume, according to the procedure described by de Lemos Chernicharo (2007). The biogas was expressed in mL/g COD.

Continuous AD Experiments With UASB Reactors

Two identical UASB reactors made of perspex glass were used for continuous experiments. **Figure 2** shows the schematic of the UASB reactor set up. The working volume was 2.25 L with a height of 91.5 cm and a diameter of 5.6 cm. One reactor was used as a control and the second one with biochar amendment as the test reactor. The granular sludge volume was maintained at 600 mL, which was about 30% of the reactors working volume in both reactors. The treated waste wood pyrochar was sieved to obtain 800 μm particle size fractions. The pyrochar was added to the granular sludge bed in the test reactor at a concentration of

TABLE 1 | Experimental design for batch experiments.

Treatment	Biochar source	Biochar amount (g)	Food waste (mL)	Granular sludge (mL)	Trace elements mix (mL)	pH adjustment
A	(i) Brewery residue	0, 0.1, 0.2, 0.3, 0.4, 0.5, 0.75, 1.2	76	74	0	1 M NaOH
	(ii) Treated waste wood	0, 0.1, 0.2, 0.3, 0.4, 0.5, 0.75, 1.2	76	74	0	1 M NaOH
B	(i) Brewery residue	0, 0.2, 1.2	76	74	0	1 M $NaHCO_3$
	(ii) Treated waste wood	0, 0.3, 1.2	76	74	0	
	(iii) Biochar only	1.2	0	74	0	
C	(i) Brewery residue	0, 0.2, 1.2	25 + 51 mL water	74	0	4 M $NaHCO_3$
	(ii) Treated waste wood	0, 0.3, 1.2	25 + 51 mL water	74	0	
	(iii) Brewery residue	0.2	25 + 51 mL water	74	1.5	
	(iv) Treated waste wood	1.2	25 + 51 mL water	74	1.5	
	(v) Food waste + TE	0	25 + 51 mL water	74	1.5	

M, molarity; NaOH, sodium hydroxide; Na_2HCO_3, sodium bicarbonate; TE, trace elements solution.

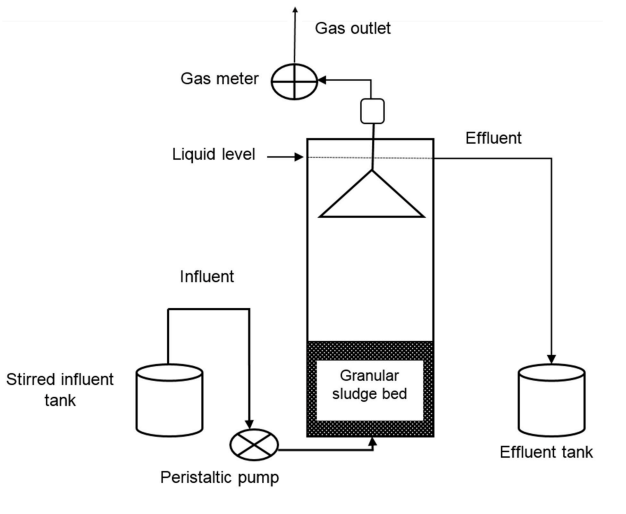

FIGURE 2 | Schematic of the UASB reactor.

8 g/L of the reactors working volume. The control contained the granular sludge only.

The mixed food waste paste was diluted with deionized water to the desired g COD/L and the pH adjusted to 7.0–7.5 using 1 M $NaHCO_3$. The diluted food waste was continuously fed into the reactor using a peristaltic pump (Masterflex, by Cole-Parmer; Model: 7528-30), at a rate of 2.6 L.day and an upflow velocity of 0.04 m/h. The organic loading rate of the diluted food waste was increased stepwise from 3.4 to 7.8 g COD/L.day and the hydraulic retention time (HRT) maintained at 24 h throughout the operational period. The reactors were operated at 30°C for 40 days. On day 25 of the UASB reactor operation, the biomass in the two reactors was reduced to about 20% of the total reactor working volume. The effluent of both the reactors was sampled daily and analyzed for COD, NH_4-N, pH, and VFA.

Analytical Methods

The analysis of different parameters was done according to the standard protocols adopted by the IHE Delft laboratory (Kruis, 2014). Total solids, volatile solids, and volatile suspended solids were analyzed using the gravimetric (oven method). The COD, total nitrogen, total phosphorous, and ammonia-nitrogen concentration were measured using a Perkin Elmer, UV/VIS Lambda 365 spectrophotometer at 600, 655, 880, and 655 nm, respectively. VFA was measured using a gas chromatograph (Varian 430-GC, CP-8400) as well as the CH_4 composition (Scion 456-GC). The trace elements were analyzed using microwave digestion method with concentrated nitric acid and the concentration measured using an ICP-MS (ICP-MS, X series 2 by Thermo Scientific).

RESULTS AND DISCUSSION

Feedstock Characteristics

The initial feedstock characteristics play an important role in AD. The selection of the mixed food waste recipe used for this research was inspired by research done on AD of kitchen waste (Qiang et al., 2013; Sunyoto et al., 2016). The food waste and inoculum were first characterized before the start of the AD and **Table 2** illustrate the properties. The C:N ratio of the mixed food waste was 21.07, which was in line with the findings of Kondusamy and Kalamdhad (2014) who reported that a C:N ratio of 20–30 was sufficient for the AD process. The VS/TS ratio (organic content) was 97%, which indicates a very high potential for microbial treatment as reported by Xu et al. (2018). Trace elements concentration of important elements like Fe, Co, Ni, and Zn should be present in sufficient supply for a successful AD. The trace elements concentration in the food waste was very low and could not be detected by the ICP-MS used for the analysis. The minimum detection limits were (μg/L): Fe 200; Co 0.5; Ni 3.0; Zn 20; Cu 10; Mn 100; Na 6,000 and K 3,000. Hence supplementation was necessary for this food waste. The granular sludge used as the inoculum contained 842.5, 2.43, 8.02, and 186.35 μg/ (g d.w.) of Fe, Co, Ni, and Zn respectively which may have played a role in enhancing the AD process.

The characteristics of the biochar used for the AD are summarized in **Table 3**. The brewery residue hydrochar had a 4% ash content, which was lower than that of the treated

TABLE 2 | Characteristics of the mixed food waste and the inoculum used for the AD process.

Parameter	Unit	Food waste	Inoculum
pH		5.40	7.20
Moisture content $_{(wet)}$	%	61.82 ± 0.34	–
Total solids (TS) $_{(wet)}$	%	38.18 ± 0.34	–
Volatile solids (VS) $_{(wet)}$	%	36.97 ± 0.42	–
VS/TS	%	97	–
Volatile solids (VS) (d.w.)	g/g	0.37	–
Total suspended solids (TSS)	g/L	–	44.67 ± 8.08
Volatile suspended solids (VSS)	g/L	–	39.67 ± 7.20
COD (d.w.)	g/g	1.22 ± 0.01	0.48 ± 0.05
NO_3-N $_{(wet)}$	g/L	–	B.D.L.
NO_2-N $_{(wet)}$	g/L	–	B.D.L.
Phosphorous (d.w.)	g/g	8.85	–
Total nitrogen (NH_4-N, d.w.)	g/g	0.15	0.10
Total organic carbon (d.w.)	%	3.16	–
C/N ratio		21.07	–
Iron (d.w.)	μg/g	B.D.L.	842.50 ± 43.13
Cobalt (d.w.)	μg/g	B.D.L.	2.43 ± 0.01
Nickel (d.w.)	μg/g	B.D.L.	8.02 ± 0.14
Zinc (d.w.)	μg/g	B.D.L.	186.35 ± 12.14
Copper (d.w.)	μg/g	B.D.L.	B.D.L.
Manganese (d.w.)	μg/g	B.D.L.	B.D.L.
Sodium (d.w.)	μg/g	B.D.L.	B.D.L.
Potassium (d.w.)	μg/g	B.D.L.	B.D.L.

-, Not analyzed; (d.w.), dry weight basis; B.D.L., below detection limit; g/L, gram per liter; g/g, gram per gram; μg/g, microgram per gram; %, percentage; COD, chemical oxygen demand; NO_3-N, nitrate-nitrogen; NO_2-N, nitrite-nitrogen; C/N, carbon/nitrogen.

TABLE 3 | Characteristics of biochar used for the AD process.

Parameter	Brewery residue hydrochar	Treated waste wood pyrochar
Particle size	**Powder**	**Powder**
Temperature (°C)	260	600
pH	6	8
Electrical conductivity (μS/cm)	117	300
Moisture content (%)	1	29
Ash (%)	4	20
Volatile matter (%)	12	18
Fixed carbon (%)	83	33

waste wood pyrochar, which had 20%. This was in line with the hypothesis from literature by Kambo and Dutta (2015) who reported that hydrothermal carbonization produced a product with a lower ash content compared to slow pyrolysis. The ash content is an indicator of the amount of alkali metals that remained in the biochar after production (Kambo and Dutta, 2015). Poerschmann et al. (2015) reported a 6.3% ash content from HTC of brewer's spent grain, which is another term used to refer to the brewery residue. The pH of the brewery residue hydrochar was 6 while that of the treated waste wood pyrochar was 8. Poerschmann et al. (2015) also reported a pH of 6.9 of the produced hydrochar. The pH is important in that the biochar can provide buffering to the AD when used as an additive.

Trace Elements Leaching From Biochar

The essential trace elements (Fe, Co, Ni, and Zn) were leached out in very small rates as illustrated in **Table 4** in all the biochar used in the leaching test. This can be explained by the fact that they were also in almost negligible amounts in the initial biomass. Only Na and K ions were leached out in high amounts. The Na and K ions released into the leachate were responsible for the increase in the EC in the leachate of all the biochars tested as illustrated in **Figure 3**. The treated waste wood pyrochar with the highest EC had the highest Na and K amount while the brewery residue hydrochar had the second lowest EC and Na, and the least K within 48 h. This finding corresponds to Kambo and Dutta (2015) who reported that pyrolyzed biochar contained higher ash content, which signifies a high amount of alkali metals in the end product.

The percentage of the leached trace and macro elements from the biochar about the original biomass composition was also calculated. The data for the brewery residue hydrochar and the treated waste wood pyrochar was not available for the initial biomass composition. The scots pine bark leached out 85% of the amount of Ni and 45.4% K. Cu was not detected in any of the biochar. The willow pyrochar leached 38.6% Na and 68.3% K, while the spruce wood pyrochar leached 33% Zn and 30% Fe.

Effect of Biochar on AD in Batch Reactors

Treatment A: pH Adjustment With 1 M NaOH

In the batch reactors treated with the brewery residue hydrochar, the addition of small doses of hydrochar, i.e., 0.2 g (332 mL/g COD) and 0.1 g (332 mL/g COD) increased the biogas production by 35 and 30%, respectively, when compared to the control which produced 215 mL/g COD (**Figure 4A**). The addition of a higher dose (1.2 g) produced the same biogas volume as the control (215 mL/g COD). This indicated that the addition of small amounts of the brewery residue hydrochar was enough to enhance the volume of the biogas produced. However, the CH_4 percentage in all the treatments was only 7–10%.

In the batch reactors with the treated waste wood pyrochar, the addition of 1.2 g (262 mL/g COD) pyrochar increased the biogas production by 18%. The lowest production was by the addition of 0.3 g (191 mL/g COD) pyrochar, which was 11% lower than the control (**Figure 4C**). This indicated that a higher amount of the treated waste wood pyrochar was required to enhance the volume of the produced biogas. The CH_4 percentage in all the treatments was between 15 and 27%. The biogas volume was higher in the treatments with the brewery residue hydrochar, but the CH_4 percentage in the biogas was higher in the treated waste wood pyrochar treatments.

The pH of the treatments with both the brewery residue hydrochar and the treated waste wood pyrochar decreased from 7.0 to below 4.5. This was caused by the rapid accumulation of VFA. Acetic (3.2–9.8 g/L) and propionic acids (1.4 to 2.1 g/L) were the most dominant in these treatments (**Figures 4B,D**). The pre-treatment of the food waste by blending made it highly biodegradable; hence, the rate of VFA production rate exceeded

TABLE 4 | Trace element concentration within 24 h of leaching from different biochar.

	0 h					24 h				
	BR	**SR**	**SPB**	**TWW**	**WIL**	**BR**	**SR**	**SPB**	**TWW**	**WIL**
	mg/kg	**mg/kg**	**mg/kg**	**mg/kg**	**mg/kg**	**mg/kg**	**mg/kg**	**mg/kg**	**mg/kg**	**mg/kg**
Mn (d.w.)	0.6 ± 0.4	1.0	0.4	1.0	B.D.L.	2.3 ± 1.6	6.4	0.8 ± 0.3	B.D.L	1.3
Fe (d.w.)	1.9 ± 1.4	1.9	1.9	1.9 ± 0.3	1.9	2.0 ± 1.4	3.9	B.D.L.	1.2	B.D.L.
Co (d.w.)	B.D.L.	B.D.L.	B.D.L.	B.D.L.	B.D.L.	B.D.L.	B.D.L.	B.D.L.	B.D.L.	B.D.L.
Ni (d.w.)	1.4 ± 1.6	0.7	0.5	1.0	0.4	3.4 ± 1.5	0.4	1.7 ± 2.1	0.4 ± 0.3	0.2
Cu (d.w.)	B.D.L.	B.D.L.	B.D.L.	B.D.L.	B.D.L.	0.5 ± 0.4	2.3	B.D.L.	B.D.L.	B.D.L.
Zn (d.w.)	0.9 ± 0.3	0.7 ± 0.1	0.5 ± 0.1	1.2 ± 0.5	0.7	3.0 ± 2.6	13.2	1.5 ± 1.4	1.3 ± 0.5	0.4 ± 0.2
Na (d.w.)	37.5	22.3 ± 3.2	20.7	294.6 ± 24.9	21.5 ± 2.1	50.1 ± 5.5	46.6 ± 1.9	43.7 ± 6.5	454 ± 14.7	55.7 ± 0.2
K (d.w.)	27.6 ± 1.9	128.3 ± 64.5	178.5 ± 27.4	1048.4 ± 3.6	470.1	34.2 ± 19.6	420.2 ± 47.4	967.7 ± 27.4	1510.3 ± 3.8	1969.3 ± 43.4

BR, brewery residue; SR, spruce wood; SPB, scots pine bark; WIL, willow tree; Mn, manganese; Fe, iron; Co, cobalt; Ni, nickel; Cu, copper; Zn, zinc; Na, sodium; K, potassium; B.D.L., below detection limit.

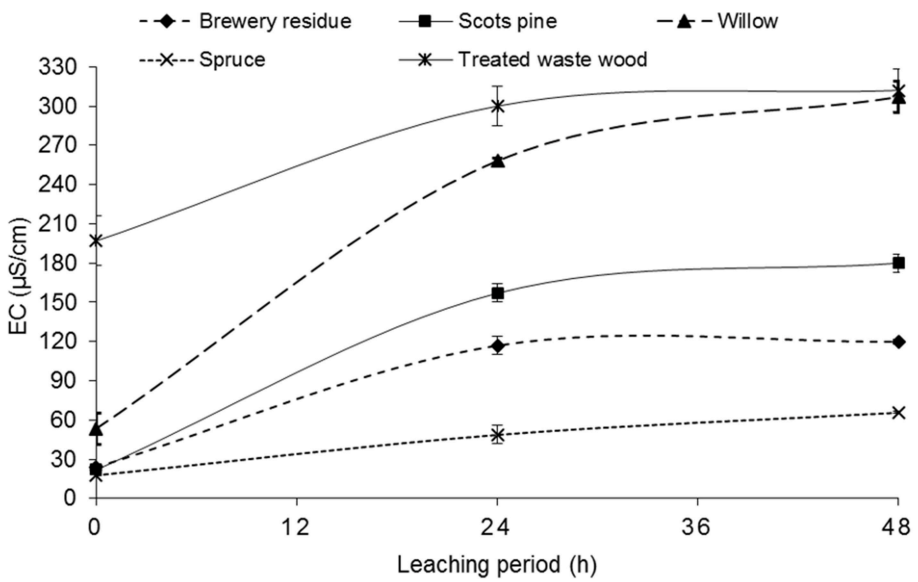

FIGURE 3 | Increase in electrical conductivity (EC) over the 48 h leaching period.

the consumption rate (Ren et al., 2018). The methanogenesis step was inhibited by the high VFA concentration leading to a low CH_4 percentage in the biogas. This was in line with the findings of Sunyoto et al. (2016) who used pine sawdust biochar on AD of white bread without pH buffering and observed accumulation of VFA in their cultures that led to low pH of about 4.9. The hydrochar and the pyrochar did not provide buffering against the high VFA concentration as reported in the literature by Wang et al. (2017).

Treatment B: pH Adjustment With 1 M $NaHCO_3$

1 M $NaHCO_3$ was used as a buffer to adjust the pH to 7.0. Two brewery residue hydrochar and treated waste wood pyrochar doses were used for this set instead of the seven used in the treatments adjusted with NaOH (treatment A). The doses that produced the highest and lowest biogas yield in treatment A were used for this set, together with two controls (With biochar only and with food waste only). The 0.2 and 1.2 g brewery residue hydrochar, and 0.3 and 1.2 g treated waste wood pyrochar doses were used.

The treatment with 0.2 g hydrochar dose produced 325 mL/g COD which was an increase in biogas production by 3% when compared to the control which produced 315 mL/g COD (**Figure 5A**). This volume by the 0.2 g dose was 2% lower than the amount produced with 1 M NaOH pH buffering. The 1.2 g hydrochar dose (317 mL/g COD) increased the biogas production by only 0.6%. However, the volume produced by the 1.2 g dose in the buffered treatment was 32% more than in the treatment with NaOH (treatment A). The biogas produced by the control with hydrochar only (12 mL/g COD) could be attributed to the digestion of the organic carbon still present in the hydrochar as reported by Kambo and Dutta (2015). The CH_4

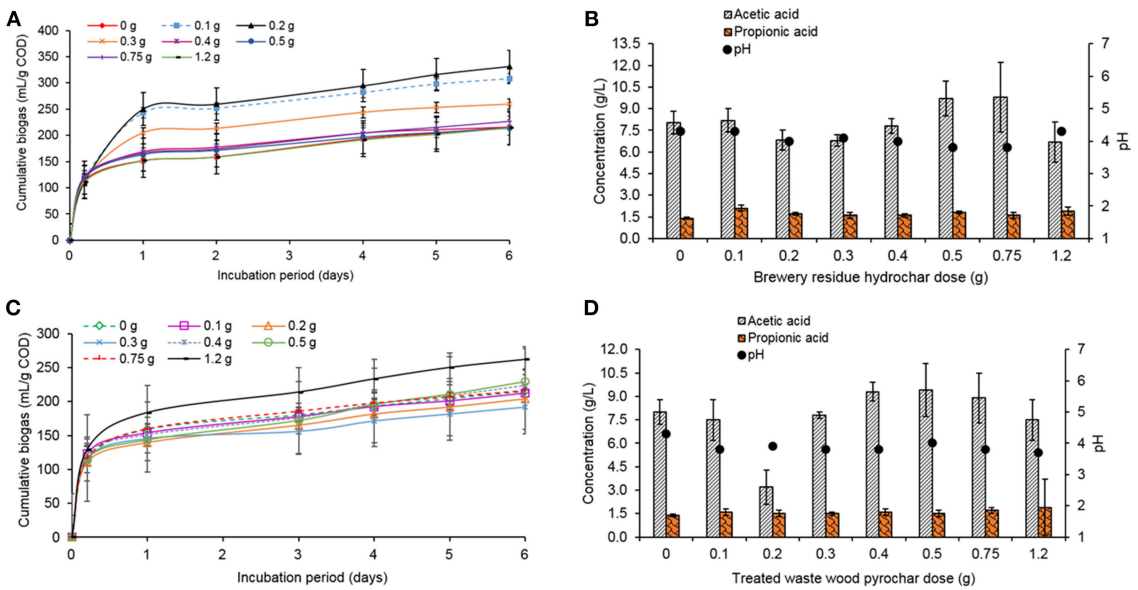

FIGURE 4 | (A) Cumulative biogas production during the treatment with different doses of the brewery residue hydrochar, with 1 M NaOH, **(B)** Production of acetic and propionic acid in the treatments with the brewery residue hydrochar, with 1 M NaOH (incubation period: 6 days), **(C)** Cumulative biogas production during the treatment with different doses of the treated waste wood pyrochar, with 1 M NaOH, and **(D)** Production of acetic and propionic acid in the treatments with the treated waste wood pyrochar, with 1 M NaOH.

percentage in the biogas was 23 and 24% for the treatments with the hydrochar and control, respectively, an increase from 7 to 10% reported in the treatment with NaOH (treatment A). The treatment with 1.2 g treated waste wood pyrochar dose (328 mL/g COD) increased the biogas production by 4%, but the volume was 20% higher than in the treatment with NaOH (treatment A). The CH_4 percentage in the biogas with the treated waste wood pyrochar treatments was 24%, a slight increase for the 0.3 g dose that had 16% in the treatment with NaOH (treatment A).

The pH in all the biochar treatments and the control without biochar, reduced from 7.0 to 4.0 due to the accumulation of VFA in the reactors. Acetic acid was produced in high concentrations (more than 8 g/L) in all the treatments with the hydrochar, pyrochar, and the control without biochar. Butyric acid was the second highest concentration with more than 3 g/L in all the treatments. The highest concentration of propionic acid was 2.6 g/L in the 0.3, and 1.2 g treated waste wood dose treatment while 0.2 g brewery residue hydrochar dose had the lowest concentration of 1.7 g/L. The 6.9 and 7.2 pH in the hydrochar control without the food waste and the treated waste wood pyrochar respectively was an indicator that the organic load from the food waste was contributing to the high VFA production in the reactors (Hobbs et al., 2018).

The addition of the 1 M $NaHCO_3$ pH buffer enhanced the volume of biogas produced in all the treatments, but the high VFA concentration quickly reduced its effect. At high organic load, a higher concentration of the pH buffer is required (Gao et al., 2015). The hydrochar and the pyrochar could not provide sufficient buffering to counter the effect of acidification from the VFA.

Treatment C: pH Adjustment With 4 M $NaHCO_3$

The treatment with 4 M $NaHCO_3$ was aimed at addressing the effect of the hydrochar and pyrochar on AD on a reduced organic load of the food waste. The food waste paste was diluted by reducing the amount of food waste from 76 to 25 mL and then adding 51 mL of de-ionized water to top up the volume to 76 mL, which was the required amount for the 1:1 ISR (**Table 1**). The same hydrochar and pyrochar doses used in the treatment with 1 M $NaHCO_3$ (treatment B), were used in treatment C, together with a control without biochar, food waste with 1.5 mL mixed trace elements supplement (1,000 mg/L of Fe, Co, Ni, and Zn) and a combination of biochar doses with trace elements supplement. The $NaHCO_3$ buffer concentration was increased to 4 M in treatment C.

In the batch reactors with the brewery residue hydrochar, the food waste with trace element supplement produced 588 mL/g COD which was an increase in biogas production by 9% when compared to the control without biochar, which had a biogas production of 538 mL/g COD as illustrated in **Figure 5B**. The biogas production by the control was 60 and 41% more compared to the treatment with NaOH (treatment A) and 1 M $NaHCO_3$ (treatment B) treatments, respectively. The 0.2 g hydrochar dose biogas production (435 mL/g COD), was 24–25% higher than in the treatments with NaOH and 1 M $NaHCO_3$, respectively. The 1.2 g hydrochar dose production (438 mL/g COD) was 51–28% more than in treatments A and B, respectively. The production was also higher than that of the 0.2 g hydrochar in treatments A and B. The 0.2 g hydrochar dose with trace elements supplement produced 4% more biogas compared to

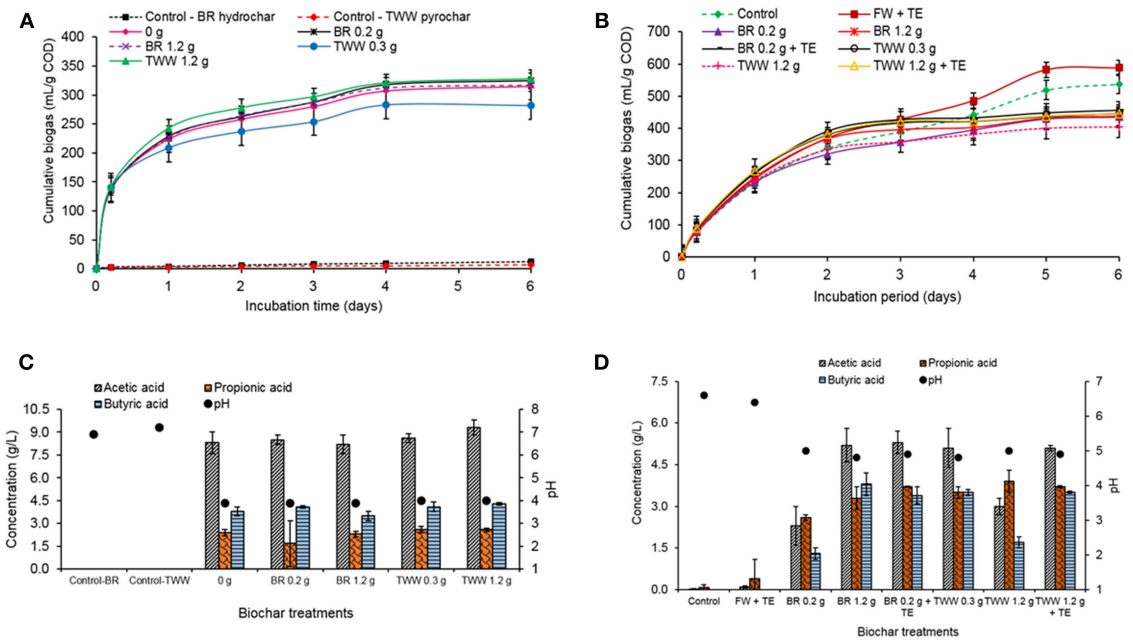

FIGURE 5 | (A) Cumulative biogas production during the treatment with different doses of the brewery residue (BR) hydrochar and the treated waste wood (TWW) pyrochar, with 1 M $NaHCO_3$, **(B)** Cumulative biogas production during treatment with the brewery residue hydrochar and the treated waste wood pyrochar (FW, food waste; TE, trace element; BR, brewery residue; TWW, treated waste wood), with 1 M $NaHCO_3$, **(C)** VFA production in the treatments with different doses of the brewery residue (BR) hydrochar and the treated waste wood (TWW) pyrochar (incubation period: 6 days), with 1 M $NaHCO_3$, and **(D)** VFA production in the treatments with the brewery residue hydrochar and the treated waste wood pyrochar (incubation period: 6 days; FW, food waste; TE, trace element; BR, brewery residue; TWW, treated waste wood), with 1 M $NaHCO_3$.

the hydrochar treatments without the supplement, and 22% lower than the treatment with the trace elements supplement without biochar addition. However, the hydrochar treatments still produced lower biogas when compared to the control without hydrochar.

The 0.3 g treated waste wood pyrochar dose treatment production (447 mL/g COD) was higher by 57–37% when compared to the treatment with NaOH (treatment A) and 1 M $NaHCO_3$ (treatment B) treatments, respectively. The 1.2 g pyrochar dose production (405 mL/g COD) increased by 35–19% compared to treatments A and B. The 1.2 g pyrochar dose with trace elements supplement produced 9% more biogas than the treatments without the supplement but was 24% lower compared to the treatment with the trace elements supplement without biochar addition. This could be due to the adsorption of the trace elements ions by the hydrochar and the pyrochar as reported by Fagbohungbe et al. (2017) and Li et al. (2017). The trace elements were therefore not available for the enzymatic activity of the microorganisms. The CH_4 composition in the biogas was 48% in the control and food waste with trace element supplement treatments, which was higher than in the treatments with the hydrochar and the pyrochar (36–38%). The biogas volume and CH_4 composition improved with the high buffer concentration in this treatment compared to the treatment with NaOH (treatment A) and 1M $NaHCO_3$ (treatment B) treatments. The addition of 4 M $NaHCO_3$ provided good buffering capacity in the batch reactors as reported by Gao et al. (2015), wherein the authors used 1,000 mg/L $NaHCO_3$ in the AD of kitchen waste and reported a 48% improvement in CH_4 yield.

Even with a pH buffer, the pH of the treatments with the hydrochar and pyrochar reduced to between 4.8 and 5.0 due to VFA accumulation (**Figures 5C,D**). The propionic acid concentration was higher (2.6 to 3.9 g/L) in all the hydrochar and pyrochar treatments. This explains the rapid decline in the pH because the accumulation of propionic acid consumes the highest alkalinity in the AD, thus inhibiting the degradation of acetic acid, which was also very high (2.3 to 5.3 g/L). The high propionic acid concentration in the treatment with 4 M $NaHCO_3$ (treatment C) could also be due to Na^+ toxicity to the propionic utilizing microorganisms than the acetic acid utilizing ones (Gao et al., 2015). The pH buffer used contained a higher concentration of Na^+. The control and the food waste with trace elements supplement had very low total VFA production of <0.7 g/L. Hence, the pH remained around neutral. The high VFA accumulation and low final pH observed in the three treatments are in line with the findings of Wang et al. (2017). The authors used kitchen waste and vermicompost biochar for the batch AD and after incubation recorded 0.4 g/L acetic acid, 5 g/L butyric and 1 g/L propionic acid at pH 4.9. The higher biogas volume and CH_4 percentage in this treatment (C), for both the brewery residue hydrochar and the treated waste wood pyrochar, shows that the methanogenesis step was relatively successful compared to treatments A and B, due to the good buffering capacity provided by the addition of 4 M $NaHCO_3$. However, the

TABLE 5 | Oxidation-reduction reactions in anaerobic digestion.

	Oxidation reactions	ΔG_0 (kJ/mole)
Propionate → acetate	$CH_3CH_2COO^- + 3H_2O \rightarrow CH_3COO^- + HCO^- + H^+ + H_2$	+76.1
Butyrate → acetate	$CH_3CH_2CH_2COO^- + 2H_2O \rightarrow 2CH_3COO^- + H^+ + H_2$	+48.1
	Reduction Reactions	
Bicarbonate → acetate	$2HCO_3^- + 4H_{2+}\ H^+ \rightarrow CH_3COO^- + 4H_2O$	−104.6
Bicarbonate → methane	$HCO_3^- + 4H_{2+}\ H^+ \rightarrow CH_4 + 3H_2O$	−135.6

Modified from de Lemos Chernicharo (2007). ΔG_0, Gibb's free energy; kJ, kilojoules.

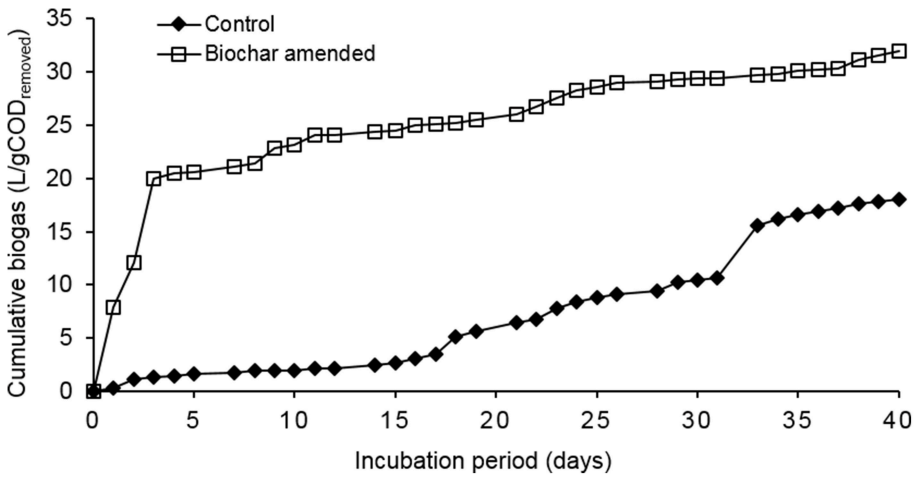

FIGURE 6 | Cumulative biogas production in the control and biochar amended UASB reactors.

hydrochar and pyrochar treatments did not enhance the biogas production and composition when compared to the control.

From the trace elements leaching experiments, the hydochar and pyrochar used in the batch AD released negligible amounts of the trace elements into the batch reactors. This explains the inability of the biochar to enhance the biogas production as there was a deficiency of the required trace elements for utilization by the methanogens. The conversion of the organic matter in the food waste in the AD process takes place following the oxidation and reduction reactions as illustrated in **Table 5**. The oxidation reactions have a $\Delta G_0 > 0$; hence, the degradation of propionate and butyrate cannot occur under standard conditions and the reactions cannot shift to the right due to high amount of hydrogen (H^+) ions. There was more hydrogen production in the batch experiments evidenced by the reduced pH due to high VFA concentration at the end of the incubation period, which inhibited the conversion of propionic and butyric acids into acetic acid, and CH_4. The continuous removal of hydrogen from the AD system would ensure efficient completion of the process (de Lemos Chernicharo, 2007). This can be achieved by the addition of alkalinity (electron acceptors) in the form of bicarbonate to complete the methanogenesis step. The results from the three batch AD treatments indicate that even with the addition of a higher buffer concentration, the pH of the treatments with the brewery residue hydrochar and the treated waste wood pyrochar reduced to levels that inhibited the methanogenesis step, due to high VFA concentration. The pH of the biochar did not influence the AD process, but it led to the acidification in the reactors.

The NH_4-N in the batch reactors of the three treatments (A, B, and C) was below 200 mg NH_4-N/L. It is reported in the literature that concentrations in this range can be beneficial to the AD process, while more than 3,000 mg NH_4-N/L can cause complete inhibition of methanogenic activity at any pH level (Rajagopal et al., 2013).

Effect of Biochar on AD in a Continuous UASB Reactor

The reactor with biochar (treated waste wood pyrochar) amendment produced the highest cumulative biogas (32 L/g $COD_{removed}$) with an average of about 0.86 L/g $COD_{removed}$ per day. The highest volume was within the first 3 days with a production of 20 L/g $COD_{removed.}$ This may have been due to the low amount of particles in the influent caused by some particles settling in the influent pipes. The diluted food waste was therefore easily digested owing to the high activity of the granular sludge at the beginning of the operation. The biogas production remained steady for the rest of the operation time. The control reactor cumulative biogas production was 18 L/g $COD_{removed}$ with an average of 0.45 L/g $COD_{removed}$ per day. The biogas production in the control was also steady during the operation time with the highest production of 5 L/g $COD_{removed}$ on day 32 (**Figure 6**). On

day 29, the pH of the control reduced to 5.8, which reduced the activity of the granular sludge. This led to the accumulation of organic matter in the sludge bed, and once the pH was restored to 7.0, the activity and COD removal recovered causing a sharp increase in the biogas volume.

The COD removal efficiency (RE) was higher in the reactor with the biochar amendment than in control (**Figure 7**). For both reactors, the RE increased to 75% up to day 4 when the organic loading rate (OLR) was 3.4 g COD/L.day. The OLR was increased to 4.4 g COD/L.day on day 5. The RE of both reactors decreased to 33 and 25% for the control and the reactor with biochar amendment, respectively, between day 6 and 9. This was due to a design problem of the influent pipes, which led to clogging of the pipes hence the diluted food waste could not reach the granular sludge bed. This led to a sharp decrease in the pH (**Figure 8**) and reduced the activity of the microorganisms. The influent pipes were replaced with a smaller size, which allowed efficient pumping of the influent. The pH was adjusted to 7.0 using 1 M $NaHCO_3$ and the reactors recovered on day 10. Apart from day 8 and 9, the pH of the two reactors remained stable (around neutral) up to day 40. The OLR was maintained at 4.4 to 5.2 g COD/L.day from day 5 to 29. The average RE of the control was 38–59% for the reactor with biochar amendment during this period. The CH_4 percentage in the biogas was 28% for the control and 63% for the biochar amended reactor in this period.

During the operation, the granular sludge bed was rising to the top of the reactors (**Figure 9**). The produced gas was trapped within the sludge bed causing it to float, and because the diameter of the reactor was very narrow (5.6 cm); the granules could not fall back to the bottom without manual manipulation. Therefore, the biomass was reduced to about 20% of the reactors working volume on day 25. After the reduction, the granules were able to rise and fall back.

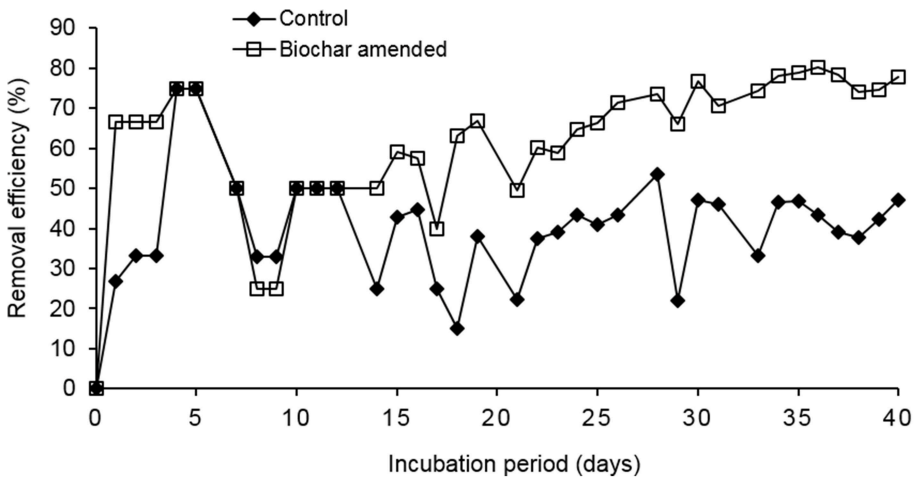

FIGURE 7 | Comparison of the COD removal efficiencies (RE) of the control and biochar amended UASB reactors.

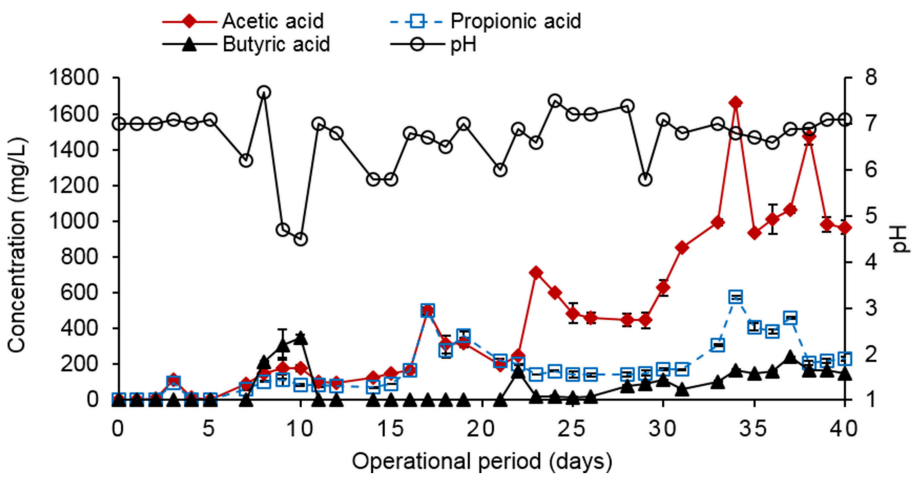

FIGURE 8 | VFA production in the control UASB reactor.

The OLR was later increased to 6.9–7.8 g COD/L.day on day 30–40. The average RE for the control was 47–77% for the reactor with biochar amendment during this period. The average CH_4 percentage in the biogas during this period was 39% for the control and 65% for biochar amended reactor. The high CH_4 percentage in the biogas produced by the biochar amended reactor was in line with the findings of Latif et al. (2012) who reported a 63% CH_4 composition in the treatment of liquidized food waste at an OLR of 12.5 g COD/L.day, and a COD removal efficiency of 75%, but without biochar amendment. The control (R1) is more comparable to the findings of these authors and the CH_4 percentage, and COD removal efficiency was 38–37% lower, respectively. The results indicate that the COD, RE and CH_4 percentage increased in both reactors when the OLR was increased to 6.9–7.8 g COD/L.day. The treated waste wood biochar amendment in the test reactor enhanced the COD removal and increased the CH_4% by 37–47% respectively when compared to the control. The high carbon content in the biochar enhanced the C:N ratio of the diluted food waste paste hence the better performance of AD in the test reactor.

The VFA production in control was slightly higher than in the reactor with the biochar amendment during the operation period (**Figures 8**, **10**). The total VFA concentration in control was below 500 mg/L up to day 24 when it started increasing up to a high of 1,660 mg/L of acetic acid on day 34. This corresponds to the fluctuating pH level of the reactor. The total VFA concentration in the reactor with the biochar amendment was below 350 mg/L during the operation period. This indicated that the AD process in the biochar amended reactor was relatively stable. A total VFA concentration of between 50 and 250 mg/L would indicate a stable AD system (Ren et al., 2018). The VFA concentration in both reactors was below the inhibitory 2 g/L level as reported by Kondusamy and Kalamdhad (2014). The NH_4-N concentration in both reactors was below 200 mg NH_4-N/L and was below the inhibitory levels as reported by Rajagopal et al. (2013).

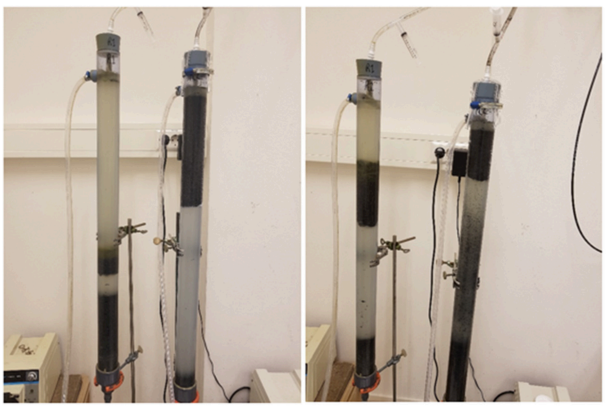

FIGURE 9 | Photograph of the floating granular sludge during the operation period.

Practical Implications of This Research

The results of this research show that biochar addition can be used to enhance the AD process especially in the UASB reactor. However, some of the challenges faced in this research can be stated as follows:

(i) The pH drop in the batch reactors with the different biochars was caused by the accumulation of VFA.
(ii) The high particulate matter in the food waste used in the UASB reactors led to reactor failure at the start of the operations. Besides, the design of the reactors, less inner diameter and the fluctuation of the pH during the night also affected the performance of the reactor.
(iii) The physical and chemical properties of the pyrochar and hydrochar used in this research could not be compared to previous literatures because the available literature is on different types of biochar produced from a wide variety of biomass sources, i.e., different physico-chemical properties, which makes a direct comparison of the results difficult.

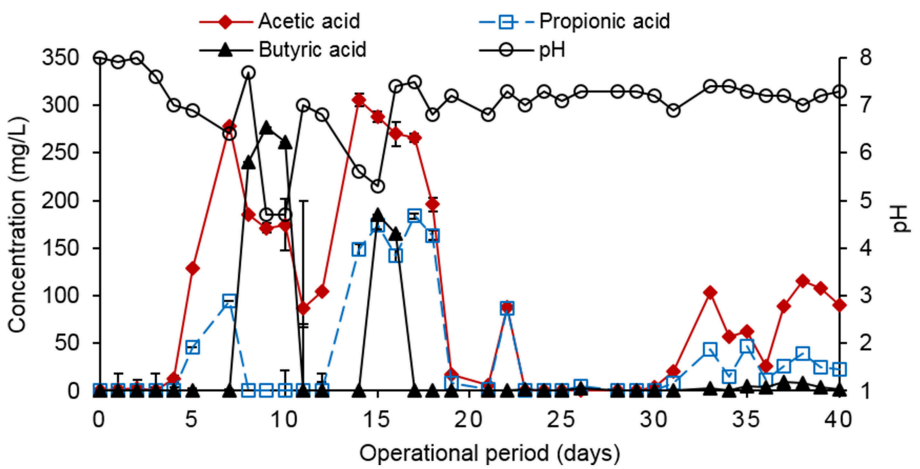

FIGURE 10 | VFA production in the UASB reactor amended with biochar.

The effect of the biochar of this food waste in the batch reactors should further be investigated using different inoculum: substrate ratios, and trace elements concentration to establish the right ratios in case of future applications in large-scale applications to avoid VFA accumulation. The applicability of the UASB reactors in the AD of food waste requires research to establish the suitable design due to the high particulate matter present in the food waste. The reactors should be designed with an optimum height: diameter ratio than the ones used in this research to create more space for the granules to rise and release the gas with ease and fall back. The operation of the UASB at a large-scale level should be automated to ensure continuous pH monitoring and buffer dosing, which will prolong the longevity of the operations. The relationship between the initial biomass trace elements concentration will need to be established and the bioavailable amount at the end of the biochar production for AD applications. A database of suitable biomass and production temperature/process should be put in place to act as a guide for future AD applications. Biochar production at the industrial level for use in AD applications requires careful planning involving the integration of different policies. These include Waste Management, Renewable Energy, European GMO policy, Clean Development Mechanism (CDM) of the Kyoto Protocol, United Nations Framework Convention for Climate Change (UNFCCC), and Economic Policies. Some of the standards that need to incorporate the biochar include; the REACH (Registration, Evaluation, Authorization & Restriction of Chemicals) regulation (Regulation 1907/2006/EC), use of fertilizer regulation, soil remediation and protection regulations, and regulation of biodiversity (Van Laer et al., 2015). The International Biochar Initiative (IBI) has developed standards for biochar properties and testing of biochar, while the Delinat Institute defines on top of the biochar properties also the required properties of the feedstock used for the production of the biochar more in detail (Van Laer et al., 2015). The available standards are meant for the application of biochar in soils, hence, there is an urgent need to develop and integrate standards that apply to the use of biochar for AD processes.

CONCLUSIONS

The biochar used in this research leached very small quantities of trace elements because the initial biomass used for their production also had low quantities of Fe, Co, Ni, Zn, Cu, and Mn. The high amount of K leached from the treated waste wood (1,510 mg/kg) and the willow tree pyrochar (1,969 mg/kg), and relatively high amount of Na and K from the other biochars caused an increase of the EC in the leachate. Even with the addition of a buffer, the pH of the biochar treatments reduced to levels that inhibited the methanogenesis step (pH 3.8–5.0), at both higher (18 g COD/L) and lower (6 g COD/L) organic load of the food waste in the batch reactors. The biogas volume produced by the treatments with the brewery residue hydrochar and treated waste wood pyrochar was lower than that produced by the control with food waste only (538 mL/g COD). Trace elements supplementation enhanced the biogas production of the food waste without biochar addition (588 mL/g COD) by 8.5%. The combination of the 0.2 g brewery residue hydrochar and 1.2 g treated waste wood pyrochar with trace elements supplement in the batch AD enhanced the biogas production compared to the treatments without the supplement, but the biogas volume and composition was still lower when compared to the control. The treated waste wood pyrochar enhanced the COD removal efficiency and CH_4 composition in the test UASB reactor by 37–47% respectively, compared to the control. This shows that addition of treated waste wood pyrochar can enhance the performance of a UASB reactor for the AD of food waste.

AUTHOR CONTRIBUTIONS

CW performed the laboratory experiments, data analysis, and wrote the manuscript. ER assisted in designing the laboratory experiments, as well as in writing the manuscript. JV and CD offered technical guidance, supported in data analysis and worked on the completed manuscript. EH provided overall guidance, supervision, and scientific knowledge support for this research work.

ACKNOWLEDGMENTS

CW thanks UNESCO-IHE Institute for Water Education and the Dutch government for financially supporting the MSc programme through the Nuffic fellowship. The authors thank the UNESCO-IHE laboratory staff members, ETIA (France), RAGT (France), VTT (Finland), CIRAD (France), and Veolia Water Technologies Techno Center, Netherlands B.V. (Biothane) for providing analytical support, the bio/pyrochars, and inoculum used in this study.

REFERENCES

Banks, C. J., Zhang, Y., Jiang, Y., and Heaven, S. (2012). Trace element requirements for stable food waste digestion at elevated ammonia concentrations. *Bioresour. Technol.* 104, 127–135. doi: 10.1016/j.biortech.2011.10.068

Cha, J. S., Park, S. H., Jung, S.-C., Ryu, C., Jeon, J.-K., Shin, M.-C., et al. (2016). Production and utilization of biochar: a review. *J. Indus. Eng. Chem.* 40, 1–15. doi: 10.1016/j.jiec.2016.06.002

de Lemos Chernicharo, C. A. (2007). "Anaerobic Reactors," in *Biological Wastewater Treatment in Warm Climate Regions*, Vol. 1, eds M. von Sperling and C. A. de Lemos Chernicharo (London: IWA Publishing), 659–827.

Dutch Standardization Institute, N. (2002). "One stage batch test at a liquid to solid ratio of 10 L/kg for materials with particle size below 10 mm (Without or with size reduction)," in *Compliance test for leaching of granular waste materials and sludges, Vol. NEN-EN 12457-4 (en). NNI Delft* (Delft).

Fagbohungbe, M. O., Herbert, B. M., Hurst, L., Ibeto, C. N., Li, H., Usmani, S. Q., et al. (2017). The challenges of anaerobic digestion and the role of biochar in optimizing anaerobic digestion. *Waste Manage.* 61, 236–249. doi: 10.1016/j.wasman.2016.11.028

Fagbohungbe, M. O., Herbert, B. M., Hurst, L., Li, H., Usmani, S. Q., and Semple, K. T. (2016). Impact of biochar on the anaerobic digestion of citrus peel waste. *Bioresour. Technol.* 216, 142–149. doi: 10.1016/j.biortech.2016.04.106

Gao, S., Huang, Y., Yang, L., Wang, H., Zhao, M., Xu, Z., et al. (2015). Evaluation the anaerobic digestion performance of solid residual kitchen waste by $NaHCO_3$ buffering. *Energy Convers. Manage.* 93, 166–174. doi: 10.1016/j.enconman.2015.01.010

Hobbs, S. R., Landis, A. E., Rittmann, B. E., Young, M. N., and Parameswaran, P. (2018). Enhancing anaerobic digestion of food waste through biochemical methane potential assays at different substrate: inoculum ratios. *Waste Manage.* 71, 612–617. doi: 10.1016/j.wasman.2017.06.029

Joseph, S., Taylor, P., and Cowie, A. (2018). *Basic Principles and Practice of Biochar Production and Kiln Design*. Available online at: https://biochar.international/guides/basic-principles-of-biochar-production/#introduction (Accessed 24.12.2018).

Kambo, H. S., and Dutta, A. (2015). A comparative review of biochar and hydrochar in terms of production, physico-chemical properties and applications. *Renew. Sustain. Energy Rev.* 45, 359–378. doi: 10.1016/j.rser.2015.01.050

Kondusamy, D., and Kalamdhad, A. S. (2014). Pre-treatment and anaerobic digestion of food waste for high rate methane production - a review. *J. Environ. Chem. Eng.* 2, 1821–1830. doi: 10.1016/j.jece.2014.07.024

Kruis, F. (2014). *Environmental Chemistry: Selected Methods for Water Quality Analysis*. UNESCO-IHE Laboratory Manual, Delft.

Latif, M. A., Ahmad, A., Ghufran, R., and Wahid, Z. A. (2012). Effect of temperature and organic loading rate on upflow anaerobic sludge blanket reactor and CH_4 production by treating liquidized food waste. *Environ. Prog. Sustain. Energy* 31, 114–121. doi: 10.1002/ep.10540

Li, H., Dong, X., da Silva, E. B., de Oliveira, L. M., Chen, Y., and Ma, L. Q. (2017). Mechanisms of metal sorption by biochars: Biochar characteristics and modifications. *Chemosphere* 178, 466–478. doi: 10.1016/j.chemosphere.2017.03.072

Lü, F., Luo, C., Shao, L., and He, P. (2016). Biochar alleviates combined stress of ammonium and acids by firstly enriching *Methanosaeta* and then *Methanosarcina*. *Water Res.* 90, 34–43. doi: 10.1016/j.watres.2015.12.029

Meyer-Kohlstock, D., Haupt, T., Heldt, E., Heldt, N., and Kraft, E. (2016). Biochar as additive in biogas-production from bio-waste. *Energies* 9:247. doi: 10.3390/en9040247

Molaey, P., Bayrakdar, A., Sürmeli, R. O., and Calli, B. (2018). Influence of trace element supplementation on anaerobic digestion of chicken manure: linking process stability to methanogenic population dynamics. *J. Clean. Product.* 181, 794–200. doi: 10.1016/j.jclepro.2018.01.264

Mumme, J., Srocke, F., Heeg, K., and Werner, M. (2014). Use of biochars in anaerobic digestion. *Bioresour. Technol.* 164, 189–197. doi: 10.1016/j.biortech.2014.05.008

Poerschmann, J., Weiner, B., Koehler, R., and Kopinke, F. D. (2015). Organic breakdown products resulting from hydrothermal carbonization of brewer's spent grain. *Chemosphere* 131, 71–77. doi: 10.1016/j.chemosphere.2015.02.057

Qiang, H., Niu, Q., Chi, Y., and Li, Y. (2013). Trace metals requirements for continuous thermophilic methane fermentation of high-solid food waste. *Chem. Eng. J.* 222, 330–336. doi: 10.1016/j.cej.2013.02.076

Rajagopal, R., Massé, D. I., and Singh, G. (2013). A critical review on inhibition of anaerobic digestion process by excess ammonia. *Bioresour. Technol.* 143, 632–641. doi: 10.1016/j.biortech.2013.06.030

Ren, Y., Yu, M., Wu, C., Wang, Q., Gao, M., Huang, Q., et al. (2018). A comprehensive review on food waste anaerobic digestion: research updates and tendencies. *Bioresour. Technol.* 247, 1069–1076. doi: 10.1016/j.biortech.2017.09.109

Sunyoto, N. M. S., Zhu, M., Zhang, Z., and Zhang, D. (2016). Effect of biochar addition on hydrogen and methane production in two-phase anaerobic digestion of aqueous carbohydrates food waste. *Bioresour. Technol.* 219, 29–36. doi: 10.1016/j.biortech.2016.07.089

van Hullebusch, E. D., Guibaud, G., Simon, S., Lenz, M., Yekta, S. S., Fermoso, F. G., et al. (2016). Methodological approaches for fractionation and speciation to estimate trace element bioavailability in engineered anaerobic digestion ecosystems: an overview. *Critic. Rev. Environ. Sci. Technol.* 46, 1324–1366. doi: 10.1080/10643389.2016.1235943

Van Laer, T., De Smedt, P., Ronsse, F., Ruysschaert, G., Boeckx, P., and Verstraete, W., et al. (2015). Legal constraints and opportunities for biochar: a case analysis of EU law. Review. *GCB Bioenergy* 7, 14–24. doi: 10.1111/gcbb.12114

Wang, D., Ai, J., Shen, F., Yang, G., Zhang, Y., Deng, S., et al. (2017). Improving anaerobic digestion of easy-acidification substrates by promoting buffering capacity using biochar derived from vermicompost. *Bioresour. Technol.* 227, 286–296. doi: 10.1016/j.biortech.2016.12.060

Xu, F., Li, Y., Ge, X., Yang, L., and Li, Y. (2018). Anaerobic digestion of food waste – challenges and opportunities. *Bioresour. Technol.* 247, 1047–1058. doi: 10.1016/j.biortech.2017.09.020

Zhang, C., Su, H., Baeyens, J., and Tan, T. (2014). Reviewing the anaerobic digestion of food waste for biogas production. *Renew. Sustain. Energy Rev.* 38, 383–392. doi: 10.1016/j.rser.2014.05.038

Zhang, L., and Jahng, D. (2012). Long-term anaerobic digestion of food waste stabilized by trace elements. *Waste Manage.* 32, 1509–1515. doi: 10.1016/j.wasman.2012.03.015

Zhang, R., El-Mashad, H. M., Hartman, K., Wang, F., Liu, G., and Choate, C., et al. (2007). Characterization of food waste as feedstock for anaerobic digestion. *Bioresour. Technol.* 98, 929–935. doi: 10.1016/j.biortech.2006.02.039

Conflict of Interest Statement: The authors declare that the research was conducted in the absence of any commercial or financial relationships that could be construed as a potential conflict of interest.

frontiers in Energy Research

ORIGINAL RESEARCH
published: 26 October 2018
doi: 10.3389/fenrg.2018.00112

Fuzzy Cognitive Map-Based Modeling of Social Acceptance to Overcome Uncertainties in Establishing Waste Biorefinery Facilities

Konstantinos Kokkinos[1], *Evangelia Lakioti*[2], *Elpiniki Papageorgiou*[1,3], *Konstantinos Moustakas*[4]* *and Vayos Karayannis*[2]

[1] Department of Computer Science, University of Thessaly, Lamia, Greece, [2] Department of Environmental Engineering, Western Macedonia University of Applied Sciences, Kozani, Greece, [3] Department of Electrical Engineering, University of Applied Sciences of Thessaly, Larissa, Greece, [4] Unit of Environmental Science & Technology, School of Chemical Engineering, National Technical University of Athens, Athens, Greece

OPEN ACCESS

Edited by:
Abdul-Sattar Nizami,
Centre of Excellence in Environmental Studies, King Abdulaziz University, Saudi Arabia

Reviewed by:
Giuseppe Mancini,
Università degli Studi di Catania, Italy
Alok Satlewal,
Indian Oil Corporation, India
Ta Yeong Wu,
Monash University Malaysia, Malaysia

***Correspondence:**
Konstantinos Moustakas
konmoust@central.ntua.gr

Specialty section:
This article was submitted to Bioenergy and Biofuels, a section of the journal Frontiers in Energy Research

Received: 07 August 2018
Accepted: 04 October 2018
Published: 26 October 2018

Citation:
Kokkinos K, Lakioti E, Papageorgiou E, Moustakas K and Karayannis V (2018) Fuzzy Cognitive Map-Based Modeling of Social Acceptance to Overcome Uncertainties in Establishing Waste Biorefinery Facilities. Front. Energy Res. 6:112. doi: 10.3389/fenrg.2018.00112

Sustainable Waste Biorefinery Facilities (WBFs) represent multifactorial systems that necessitate the organization, cooperation and the acceptance of different social stakeholders. However, these attempts have become targets of environmental, social and legal oppositions despite their obvious economic benefits. The variety of ambivalent and heterogeneous external effects of such projects result in either local support or opposition to the facility, which in turn becomes a critical factor affecting facility location decisions, and subsequent success of a WBF. Research has shown that simple surveys do not sufficiently measure social acceptance of such endeavors, and in most cases, local community factors dominate other external valuable impacts. In the current study, a novel Fuzzy Cognitive Map (FCM) modeling approach is proposed in order to analyze the socio-economic implications and to overcome multiple uncertainties occurring in sustainable WBF development and implementation. The primary investigation relates to the factors that influence the development of organic or chemical treatment of waste by the local communities and the competent authorities. The determination of concepts involved in the FCM modeling depends on a hybrid approach where both experts' opinion and statistical results from questionnaires distributed to stakeholders participate in the concept circumscription, thus identifying the centrality of each node in the model. Several steady state and dynamic analysis scenarios show the influence of driver concepts to receiver concepts on the social aspect FCM constructed.

Keywords: waste biorefinery facility (WBF), social acceptance, uncertainty, fuzzy cognitive map (FCM), modeling

INTRODUCTION

Our society well-being remains heavily dependent on non-renewable fossil sources that provide heat, electricity, pharmaceuticals, transportation and food production. The major problem is though that our reliance on non-renewable energy sources has important negative environmental impacts, such acidification of oceans and global warming. To safeguard present livelihoods and

offer development pathways for non-industrialized societies, energy sustainability is needed. Thus, the requirement to use renewable resources and to minimize waste becomes apparent. For that reason, an increasing number of individuals, companies, organizations and governments turn toward the development of biorefineries and biofuel production (Halder et al., 2012). This rapid growth is predominantly supported by major associations, such as central and local agencies whose primary goal is to promote policies, regulations and R&D initiatives that will lead to the increased production and use of sustainable biofuels. For the biorefinery industry the selection of the installation location is of great importance, as this is the major parameter impacting the initial capital of the project, the transportation costs for the raw materials and the produced fuel, which in turn become secondary factors affecting the retail price of the product. It must be noted here that a major role affecting the decision on the installation location is the acceptance of the local community at a first level and the approval of the local competent authorities at a second level. The immediate social acceptance drastically diminishes installation time delays and indirectly decreases the installation costs. On the other hand, companies believe that they are the ones that should decide where to locate the plants, arguing on the assumption that producers are economic free agents, evaluating sites as if all counties are contenders for their business, weighing the availability of feedstocks along with their infrastructure needs, operating without ties to localities, and being subject to enticement from policy incentives (Walter and Gutscher, 2011; Tigges and Noble, 2012; Fortenbery et al., 2013; Nizami et al., 2017a,b). Regardless of any minor disadvantages in relation to bioeconomy, the vast majority of researchers support the broad participation of various stakeholder groups and citizen associations, in order to "chart a strategic plan" to promote crucial importance of Waste Biorefinery Facility (WBF) growth. To be more specific, the following important impacts necessitate the urgency to open up the discussion about WBFs into the general public and include all affected stakeholders and major citizen groups (McGuire et al., 2017):

- The engagement of local citizens and stakeholders in relation to WBF growth are established at the regional level and mostly at the places where the establishments are meant to be built.
- The bigger the interaction with the major stakeholder groups, the bigger the increase of mutual understanding and agreement when dealing with collisions and conflicts of various social groups of citizens.
- The benefits of the local and regional rural economy are maximized when the WBF growth is "mainstreamed" and the vast majority of local citizens get advantage of it.
- The engagement of the general public and the major stakeholder groups makes better use of good practices in relation to the efficient use of waste-based resources.
- The mutual decision making process among all affected stakeholder groups, scientists, researchers, and non-governmental organizations ensures an integrated methodology resulting in a sustainable bioeconomy.

Certainly, there are also negative effects emanating by WBF growth. However, appropriate management of such inverse impacts ends up in promoting new sustainability standards and a better policy making framework than the existed one. On the other hand, high levels of public acceptance are essential if local authorities plan substantial increases in new renewable energy power plants for a certain area, as such projects may impose both positive and negative externalities on the local communities concerned. Apart from the increase of local jobs created and the stimulation of the local economy, such attempts positively affect local tax revenues, while at the same time purchases of local goods and services are also boosted. Nevertheless, the most common phenomenon occurring is a social syndrome usually referred as "Not In My Back Yard (NIMBY)" (Dear, 1992; van der Horst, 2007), reflecting residents' opposition to a proposed development in their local area. This characteristic phenomenon often carries the connotation that local residents are only opposing the development of waste biorefinery plants because they are close to them, and that they would tolerate or support such installations if they were built further away (Haddad et al., 2009; Lambert, 2009; CTV Kitchener, 2012; Lakioti et al., 2017). Characteristic cases are the ones mentioned in Selfa (2010), which investigate the opposition to biofuel facilities by local communities in three different locations in Kansas and Iowa. Lambert (2009) also mentions a good practice by a consulting company, which has helped tremendously various WBF corporations to address the NIMBY wars triggered in 135 locations. However, more and more researchers lately tend to discard the NIMBY-thesis due to the limitations imposed relatively to the human attitudes in obscuring the actual reasons for rejecting any kind of land use and particularly any WBF related land use (Devine-Wright, 2009; Wolsink, 2012).

Similar thesis relative to land use (Brion, 2015; Ciment, 2015) is the "Locally Unwanted Land Use" (LULU) syndrome. This basically argues that there is a land use creating externality costs on those citizens living within close proximity and these costs include potential health hazards, poor aesthetics, or reduction in home values. Therefore, the development of such facilities, with an increased level of hazards, need to be created for the greater benefits of the society as a whole, in order to get global acceptance and supportiveness.

The design and control of engineering systems such as waste biorefineries is a complex decision-making process in which multiple conflicting objectives of social, economic, and environmental nature must be taken into account. The key sustainability factors that drive the development and management of WBF or change the status quo of an existing waste management system can be summarized and categorized into: (a) environmental (climate change, land use, depletion of natural resources etc.), (b) social (local demographics, public resistance/resilience, NIMBY-LULU, public participation in making policies etc.), (c) competent authorities (institutional and administrative policies for WBF development, regional and municipal politics and legislation, structural development etc.), (d) economic (development funding, structural efficiency in installation minimizing costs, pricing models, secondary materials market etc.), and (e) technological (collection and transfer system, treatment technologies, waste stream composition and change) (Bovea and Powell, 2006; den Boer and

Lager, 2007; Beigl et al., 2008; Graymore et al., 2008; Rehan et al., 2018).

The decision and policy making relatively to the development and sustainability of such large-scale waste biorefinery projects is done by stakeholders that influence these operations and sometimes their opinion is conflicting with others. *Stakeholders* include each of people or groups who are affected by technology developments or can affect that. Many of the barriers to access a successful performance of the projects could be the result of lack of acceptance of such projects by these social groups (Hosseini et al., 2018). From a socio-political point of view, acceptance of projects by core stakeholders and political actors has critical importance. When challenge is programming and increasing pub1ic participation incentive, cooperation with stakeholders and policy makers and also analysis of the acceptance level is important. For that reason, the decision-making model that will be adopted should provide quantifiable metric enabling systematic comparisons of the effect of different compromise solutions on the dissatisfaction of the stakeholders. With that model, it must be possible to make a thorough analysis relatively to the fairness of the decision taken and how decisions affect the opinions of specific stakeholder communities. Because of the diversity of stakeholder perceptions and attitudes, the model should also be able to analyze if a certain stakeholder or subset of stakeholders fully dictates the nature of a decision and therefore dissatisfaction of the rest of the stakeholders occurs. Stakeholder opinions along with polling procedures are the main tools that can be used for the development of such decision and policy making models, as they alleviate the conflicts created due to the way the information is presented and processed by the stakeholders (Cucek et al., 2013; Geraili and Romagnoli, 2015; Liew et al., 2015; Dowling et al., 2016).

Even though there is not an exact consensus on all environmental, economic and social impacts of building and managing WBFs, in the current paper we outline how an understanding of the processes of bridging cognitive and socio-political legitimacy can be used in the formation of a Fuzzy Cognitive Map (FCM) as a decision and policy making tool for the management of WBFs. Unlike all previous attempts of modeling such a problem, this study primarily depends on the local society stakeholder perceptions, opinions, attitudes and expectations to model the installation of new sites in rural and suburban areas.

The structure of the paper is as follows: In the next section, all the material and methods related to WBFs and FCMs are presented. More specifically, the integration of stakeholders in the WBF management decision process, the multi-criteria analysis and the scenario-based analysis methodologies are reviewed. Also, the characteristics of the FCM including the most popular activation and transformation functions as well as the algorithm of FCM construction from experts and the development of FCM from learning and training techniques are quoted. In section three, the application of FCMs in analyzing Social Acceptance for WBFs, developing a decision making FCM for a case study of WBF development in Thessaly, Greece, is discussed. Furthermore, due to the amount of concepts and the FCM complexity generated, the social part of the FCM is focused, by discussing its steady and dynamic state analysis and how the driver concepts influence the social acceptance. In the final section, conclusions and future challenges on the issue are highlighted.

MATERIALS AND METHODS

Integration of Stakeholders in the WBF Development Decision Making Process

Analyzing waste biorefinery development and management decision making has been a challenge in the recent years along with other similar problems (Lin and Yang, 2018; Stadler et al., 2018). Most of the researchers initially based their analyses on science, consensus, structured and multi-criteria decision making approaches according to Gregory et al. (2012). With a focus on methods to involve citizens and other stakeholders in decision-making processes Van Asselt and Rijkens-Klomp (2002) identified eight different methods such as focus groups, scenario analysis, scientific stakeholder workshops, policy exercises, participatory modeling building, citizens' juries, consensus conferences, and participatory planning. However, when it comes to make decisions, the integration of stakeholders along with the opinion differences created between them and the experts in co-producing knowledge forces the analysts to use more widely approved methodologies. Among these methods, multi-criteria analysis, scenario analysis and rationality theory analysis are the ones to bring stakeholders and experts together in triggering learning processes that can make science more sensitive for societal problems (Mielke et al., 2016).

Multi-Criteria Analysis

The basic idea behind Multi-Criteria Analysis (MCA) is to set up measurable parameters that affect the process under study and to identify well established units for these impacts along with a clear ranking methodology. This formalized procedure allows decision makers to select the most desirable alternative among all available choices. Whenever there exist trade-offs between various alternatives, MCA clarifies values associated with decisions and evaluates these different alternatives including additional criteria. More specifically, the alternatives are further classified and clustered into criteria, which are weighted separately and then recombined back together onto the initial grading scale. Munda (2004, 2008). MCA methodologies utilize predominantly quantitative data. On the other hand, when the incorporate of stakeholders' perspectives into the decision process is attempted, their input usually consists of qualitative information making MCA methods insufficient to integrate this input. To overcome this problem, researchers synthesize traditional social research techniques (surveys, discourse based evaluation, narrative analysis, and value integration methods) with MCA for addressing the integration of stakeholders' perspectives. Thus, alternative MCA methodology variants have been developed to overcome the aforementioned challenge (Stirling, 2006; Yatsalo et al., 2007). For our case, the most important variant is the one that corresponds to Social Multi-Criteria Evaluation (SMCE), as emphasis is given mostly to stakeholder engagement in making decisions and also on the

operational framework useful to answer the following question: how can the local society and the local competent authorities integrate a plurality of technical aspects and social views into its ex-ante impact assessment in a coherent and transparent manner for the development and management of WBFs. According to Scolobig and Lilliestam (2016) the phases of SMCE are: (a) institutional analysis, (b) alternatives and criteria, (c) assessment of the criteria, and d) identification of the most desirable alternative. Finally, the most critical parameter in this impact assessment technique is to produce a decision policy based on the following three main objectives:

1. Effectiveness: the degree to which the policy objectives are achieved (in terms of goals or levels of output) and the problems identified are solved,
2. Efficiency: making sure that the local society of experts and stakeholders has expressed its commitment to ensure that its proposals meet policy goals at minimum cost and/or taking into account an analysis of costs and benefits and their distribution among the stakeholders affected, and
3. Coherence: with other existing local society rules and policies.

Scenario-Based Decision Making

In general, the Scenario-Based methodology simply presents all the alternative scenarios evaluating the impacts they impose in decision making without the inclusion of a decision-making directive. After evaluating the impacts of each scenario, the decision maker should be able to make a decision related to the problem at hand, evaluating the less expensive alternative. A critical task in this process is the involvement of stakeholders in suggesting different scenarios for evaluation, or evaluating the existing ones, or setting scenario boundary conditions together with the decision makers (Kok et al., 2015; Trutnevyte et al., 2016). Furthermore, as we already explained, the difficulty stands on the fact that all the qualitative information coming from the stakeholders' input needs to be converted into quantitative. Therefore, it is useful to incorporate Fuzzy Logic techniques to achieve this defuzzificaton process. To summarize, the key steps of the engagement of the stakeholders in scenario-based approaches (Scolobig and Lilliestam, 2016) are: (a) the elicitation of stakeholders' perspectives, (b) quantification of inputs to feed the model parameters and (c) the scenario ranking and identification of actions to enact a particular scenario.

Plural Rationality Decision Making

In this case, decision and policy making is based on a solution as a result of a compromising process among multiple "voices" through extraction of multiple stakeholder perspectives. This methodology is based on the theory of plural rationality, which suggests that all stakeholder perspectives are organized and relate to five different issues, namely the hierarchical, the egalitarian, the individualistic, the fatalistic, and the autonomous. These categories share common attitudes and views of stakeholders. Thus, for this method, the key steps that need to be taken are: (a) the elicitation of stakeholder perspectives, (b) the creation of technical-policy alternatives, (c) the construction of focus groups to discuss these alternatives and prioritize the actions needed to be taken, and finally (d) a thorough discussion to reach a decision.

Experts and Stakeholders

The increasing number of decision making models that can incorporate both expert opinions and a diverse collection of stakeholder perspectives creates inevitably a confusion in selecting the best analytic-deliberative-adaptive methodology for developing and managing WBFs. For this reason, we choose to base our approach on the inclusive definition of all the concepts made primarily by experts. At the same time, the model scrutiny will also utilize systematic and transparent procedures including as wide a range of stakeholders as possible. However, it must be noted that priority must be given to the quality of the enquiry for those responsible for waste biorefinery management and policy formulation for this kind of projects. For such systems, the efficiency of decision-making depends largely on the ability of decision-makers to analyse the complex cause and effect relationships and take productive actions based on the analysis. More specifically, the dynamics of large scale complex WBF reveal different components which affect each other, and these cause and effect relations show system behavior. All aforementioned arguments guide us to use system conceptualization graphs to understand all of the system aspects, such as FCMs.

Fuzzy Cognitive Mapping (FCM)

FCM is a qualitative or rather semi-quantitative and dynamic method to structure expert knowledge that aims to capture a person's perception of a particular issue in a diagrammatic format. FCM graphs provide both the modeler and the interviewee with an informal structured process having the ability to give additional beliefs, insights and concepts about a certain domain. Furthermore, the interrelations and interdependencies of these concepts are also revealed, providing information about how the change of one issue can affect the others. The selection of the FCM methodology to investigate the development and management of WBF is due to following advantages according to Ozesmi and Ozesmi (2004): (a) FCMs are well structured to imprint the complexity and the reason for the waste biorefinery model, (b) FCMs are capable to represent the quantitative and qualitative information obtained from the stakeholders' opinion, overcoming the lack of quantitative reliability of data due to uncertainty, and (c) FCMs are suitable to illustrate the effects of factor changing for the whole systems even though they are not able to make quantitative predictions. Therefore, FCMs are allowed to predict the effects of the policy taken under the "*what-if*" scenario, having assumed that, since the real world is complex, knowledge can be obtained from the perception of people involved into a certain issue (Kosko, 1986, 1987).

Basic Concepts for FCMs

More rigorously, an FCM is a graphical representation of a system used to illustrate the cause and effect relations between nodes, thus giving us the opportunity to describe its behavior in a simple and symbolic way. In FCM graphs, nodes represent concepts, and arcs represent the perceived relationships between

these concepts (Axelrod, 1976). These relationships in a FCM are logically imposed by connecting concepts via semantic or otherwise meaningful directed linkages showing the causality between them (Novak and Cañas, 2008). According to Gray et al. (2014), this causality in representing cognition by weighted arcs in a structural map is derived from constructivist psychology, which suggests that individuals interactively and collectively construct experience/knowledge developing internal associative representations that help to catalog, interpret, and assign meaning to environmental stimuli and experiences (Raskin, 2002). Another view of the FCMs is from the Neural Networks and Fuzzy Logic point of view. For that reason, learning techniques and algorithms can be borrowed and utilized to train the FCMs and adjust the weights of the concept interconnections.

In order to ensure the operation of the system, FCMs embody the accumulated knowledge and experience from experts who acquaint how the system operates under different conditions. For experts to conclude on which concepts to integrate, stakeholders give firstly feedback prior to knowledge extraction. Especially for decision policies made, this knowledge extraction is succeeded transforming all linguistic variables into numeric values via a defuzzification process. This produces a set of concepts denoted as C_i $(i = 1, 2, \ldots n)$ (graph nodes) with their interrelations denoted as w_i (graph directed edges). After the defuzzification, concepts are assigned a value within the range [0, 1] and weights are assigned values in the range [−1, 1] to capture negative and positive causality. A positive value of the weight w_{ij} indicates that an increase (decrease) in the value of concept C_i results to an increment (decrement) of the concept's value C_j. Similarly, a negative weight w_{ij} indicates that an increase (decrease) in the value of concept C_i results to a decrement (increment) of the concept's value C_j, while a zero weight denotes the absence of relationship between concepts C_i and C_j, respectively. **Figure 1** depicts a typical FCM.

Taking into consideration the interrelations between the concepts of a FCM, the corresponding adjacency matrix can easily be formed. Every concept C_i in the graph has a value A_i that expresses the quantity of its corresponding physical value derived after the defuzzification described above. The value A_i of C_i is computed in each simulation step and it basically indicates the influence of all other concepts C_j to C_i (inference). The most popular inference rules are: (a) Kosko's inference, (b) Modified Kosko's inference, and (c) Rescale inference, as shown in the following three activation functions, respectively.

$$A_i(k+1) = f\left(\sum_{j=1,\, j\neq i}^{N} w_{ji} \times A_j(k)\right)$$

$$A_i(k+1) = f\left(A_i(k) + \sum_{j=1,\, j\neq i}^{N} w_{ji} \times A_j(k)\right)$$

$$A_i(k+1) = f\left((2 \times A_i(k) - 1) + \sum_{j=1,\, j\neq i}^{N} w_{ji} \times (2 \times A_j(k) - 1)\right)$$

Also $f(.)$ is the threshold (transformation) function that can be: (a) bivalent, (b) trivalent, (c) sigmoid or (d) hyperbolic, as shown in the following four equations, respectively.

$$f(x) = \begin{cases} 1 & x > 0 \\ 0 & x \leq 0 \end{cases}$$

$$f(x) = \begin{cases} 1 & x > 0 \\ 0 & x = 0 \\ -1 & x < 0 \end{cases}$$

$$f(x) = \frac{1}{1 + e^{-\lambda x}}$$

$$f(x) = \tanh(\lambda \times x)$$

where λ is a real positive number ($\lambda > 0$) that determines the steepness of the continuous function f and x is the value $A_i(k)$ on the equilibrium point. It should be noted that the sigmoid threshold function ensures that the calculated value of each concept will belong to the interval [0, 1]. When the values of concepts can be negative and their values belong to the interval [−1, 1], the hyperbolic tangent function can be used instead.

FCM Development Using Expert Knowledge

Experts can use their knowledge in the area under study to develop an FCM by firstly identifying the main concepts involved and secondly indicating the causal relationships among these concepts. The final step is the calculation of the causal relationships strengths using either crisp numeric values within the range [−1, 1] or using linguistic variables and values that at second stage are defuzzified into numeric. Furthermore, experts can improve an existed FCM by collectively analysing the key characteristics of the system under study and reevaluating the structure and the interconnections of the graph using fuzzy conditional statements or fuzzy rules. The algorithm used for the development of a FCM is depicted below (Groumpos and Anninou, 2017):

Step 1 : Experts select the concepts C_i that constitute the FCM graph.

Step 2 : Each expert defines the causal relationship between any two concepts, if there exists one (positive, negative, neutral).

Step 3 : Experts carefully determine the value of the relationship between the two concepts.

Step 4 : Experts describe initially the causal influence using linguistic variables, such as "low," "medium," "high" etc. The sign of each weight (+ or –) represents the type of influence between concepts. There are three types of interconnections between two concepts C_i and C_j:

- $w_{ij} \geq 0$ means that an increase or decrease in concept C_i causes the same result in concept C_j.
- $w_{ij} \leq 0$ means that an increase or decrease in concept C_i causes the opposite result in concept C_j.
- $w_{ij} = 0$ means that there is no relation between concepts C_i and C_j.

The degree of influence between the two concepts is indicated by the absolute value of w_{ij}. During the simulation, the value of each

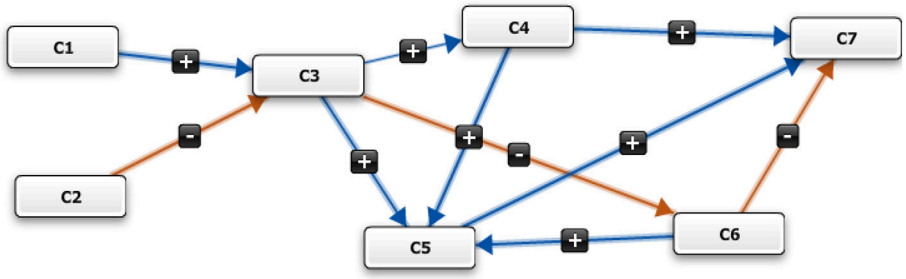

FIGURE 1 | A typical FCM graph depicting positive and negative causalities between concepts.

concept is calculated using the following rule:

$$A_i(k) = f\left(k_1 A_i(k-1) + \sum_{j=1,\, j\neq i}^{N} w_{ji} \times A_j(k-1)\right)$$

Learning Process in a FCM

In general, the manual process for developing an FCM described in section FCM Development Using Expert Knowledge can be used only when there is at least one expert with expertise on the problem under study. However, in some situations, a FCM could not be constructed because of the following reasons:

- There is no expert or stakeholders with direct interest to define a FCM.
- The experts' knowledge is different or with each other and they draw drastically different FCMs or even FCMs with minimum overlap of concepts.
- There are large amount of concepts and connections between them, which could not be drawn without mistakes (it occurs in high complexity problems).

For such extreme cases there has been developed a systematic way of constructing the FCM using a learning process, i.e., a process that will automatically determine the weights of the FCM, which best fits the decision-making and prediction problems. Diverse learning methods have been proposed by many researchers and they are based on the same techniques that used to train neural networks. These techniques are of three basic types namely: (a) Hebbian-based, (b) Population-based, and (c) Hybrid. Hebbian oriented learning requires data to be used alomg with a learning formula that regulates the adjustment of the cognitive map weights. The initial map before FCM learning in this case is established using experts' knowledge. Population-based learning algorithms on the other hand use evolution strategies to learn FCMs from data such as particle swam optimization (Koulouriotis et al., 2001), real-coded genetic algorithms (Stach et al., 2005), and the well-known big bang-big crunch algorithm (Yesil and Dodurka, 2013). Finally, hybrid learning approaches make use of both the effectiveness of Hebbian learning and the global search capability of evolutionary-based algorithms. Even though the hybrid approaches can learn FCMs with high accuracy, these approaches still suffer from the problem of converging to undesired states for the output concept values (Zhu and Zhang, 2008).

In the case of unsupervised learning algorithms, Hebbian-based methods use available data and a learning formula that is based on several modifications of Hebbian law, to iteratively adjust FCM weights. Typical Hebbian-based methods have been reported in the literature (Dickerson and Kosko, 1994; Huerga, 2002; Papageorgiou et al., 2003, 2004; Konar and Chakraborty, 2005; Stach et al., 2007, 2008).

In the case of population-based algorithms, such as simulated annealing, evolution-based and particle swarm optimization, the basic idea is to use the available input datasets in order to discover models that mimic the input data. It should be noticed that this method uses an objective criterion or a function to be optimized, thus making the method computationally intensive (for the genotype development and management). The primary goal is to find a near-optimal weight matrix based on the functional characteristics of the FCMs. Typical population-based methods have been published by many researchers (Koulouriotis et al., 2001; Papageorgiou et al., 2004; Mateou et al., 2005; Petalas et al., 2005; Stach et al., 2005; Alizadeh et al., 2007).

Finally, the hybrid method is implemented combining the previous two learning techniques using the coupling of differential evolution algorithm and nonlinear Hebbian learning algorithm, by using both the global search capabilities of evolutionary strategies and the effectiveness of the NHL rule (Papageorgiou and Groumpos, 2005). This hybrid learning module was applied successfully in real-world problems. Moreover, through the experimental analysis, the results showed that this hybrid strategy was capable to train FCM effectively, thus leading the system to desired states and determining an appropriate weight matrix for each specific problem (Zhu and Zhang, 2008).

APPLICATION OF FCMS IN ANALYZING SOCIAL ACCEPTANCE FOR WBFS –STEADY AND DYNAMIC STATE ANALYSIS

Description of the Case Study

The knowledge relating to FCM was applied in a case study considering a hypothetical development of a WBF. This study was supposedly applied to the district of Thessaly, Greece. Thessaly region is located in the central part of Greece (Coordinates: 39.6103° N, 22.0476° E) and has one of the two largest plains in Greece covering a total area of 14,037

km^2. Also, there exist four major cities generating a huge amount of municipal solid waste among other types of waste making the area an ideal candidate for developing a WBF. The hypothetical location chosen was near the existed one, i.e., near the Parapotamos of Tempi municipality. The reason the location chosen were nearby the real location was not to create any opposition and prejudice in answering questionnaires by the local stakeholders and residents. Furthermore, we assumed that the heat and cooling customer was a local community. The main goal for the study was to assess the community attitudes toward the development and management of a WBF, measuring the degree of this acceptability. Apart from the site selection we also tried to keep the other characteristics of the hypothetical study as close as possible to the real case and only altering the ones that deal with the social issues. That is, our polling methods avoided to deal with: (a) the selection of energy conversion technologies and processes, (b) the product management policies, (c) the technological improvement, and (d) the economic and environmental sustainability. Even though we included a plethora of concepts relating to environmental, health, governmental, economic and technological issues, we primarily concentrated on the social concepts affecting the acceptance proposition or opposition of WBFs.

In order to draw the FCM, a diverse team of stakeholders and experts were interviewed to express their perceptions toward the environmental, health, social, governmental, economic and technological aspects relating to the development and management of WBFs. The diversity of the group imposed the inclusion of stakeholders such as local citizens, consumers, competent authority's government employees, institution representatives, farmers etc. Two experts were also interviewed, one with socio-economic and the other with chemical process engineering expertise. The experts were showed similar research works on the subject such as of Lopolito et al. (2009) and Sacchelli (2014). This is the reason that some of the concepts involved in the creation of the FCM were similar to the ones used in these two works. The total number of stakeholders raised to 23 and complemented by the interviews of the two experts. In total, the experts have identified 43 concepts, as it is explained in the following subsection focusing on the social acceptance of WBF operations. We must say that the number 43 resulted after the merging of similar concepts that were practically the same but with different linguistic description/labeling. It should also be noted that some concepts were dominant for most of the stakeholders and experts, but others were depended of their area of interest and expertise. The age of the involved participants in the study was between 29 and 59 years. The weight of the answers was calculated differently for the stakeholders and the experts though. More specifically, 40% of the weighted average of the answers was due to experts and the rest of 60% to the stakeholders following a widely known practice in developing and drawing FCMs. Relatively to the interviewing process, at first we described to the stakeholders the most relevant concepts to WBF and also the causal relationships between concepts using mostly natural language, so they could understand, digest and share among themselves the new information. Once the participants were given an assessment example of a similar problem, they were able to assign negative or positive causality. The values assigned to causality (weights) were of the fuzzy range [very high, high, medium to high, medium, medium to low, low, very law] and similarly on the negative scale. After the collection of interviews, the results were defuzzified and entered in the online software "Mental Modeler" (2018)[1] to draw the FCM, which is depicted in **Figure 2**, and calculate the following:

- Total number of components
- Total number of connections
- Indegree and Outdegree of each component
- Connections per component
- Type of component (driver, ordinary, receiver)
- Centrality: absolute value of either a) overall influence in the model (all + and –relationships indicated, for entire model) or b) influence of individual concepts as indicated by positive (+) or negative (-) values placed on connections between components; indicates a) the total influence (positive and negative) to be in the system or b) the conceptual weight/importance of individual concepts (Kosko, 1986, 1987). The higher the value, the greater is the importance of all concepts or the individual weight of a concept in the overall model[1].
- C/N: number of connections divided by number of variables (concepts)
- Complexity: ratio of receiver variables to transmitter variables
- Density: connections number compared to all possible connections number.

FCM Steady State Analysis

Table 1 shows the general statistics of the FCM and **Table 2** the concept individualized properties described above. The complexity of the resulting FCM comes from the large amount of connections, but this is due to the nature of the concepts identified. It should be noted that we categorized these concepts into five classes, namely: (a) Environmental-Health, (b) Social, (c) Government-Laws, (d) Economics, and (e) Technological. An apparent similarity and increased interdependence of the concepts belonging to the same class can be observed. However, there is also an increased number of interconnections between concepts of different classes. This is because of the correlation of environment and health with societal issues and how these affect the decisions of local citizens when it comes to altering their lives.

It must be noticed that experts and stakeholders from the local community (citizens, consumers) referred to the social issues (Risk perception, Public Trust, Well-being of citizens, Inclusiveness) as the most crucial factors influencing the operation and management of such facilities, and regarded the technological and economics issues as secondary. On the other hand, experts and stakeholders coming from competent authorities such as government employees, institution representatives and chemical engineers gave extensive weight to the potential consequences of using WBF products and by-products and also to the resulting economic benefits (new investment and business plans, profit analysis for the

[1] www.mentamodeler.org (Accessed July 7, 2018).

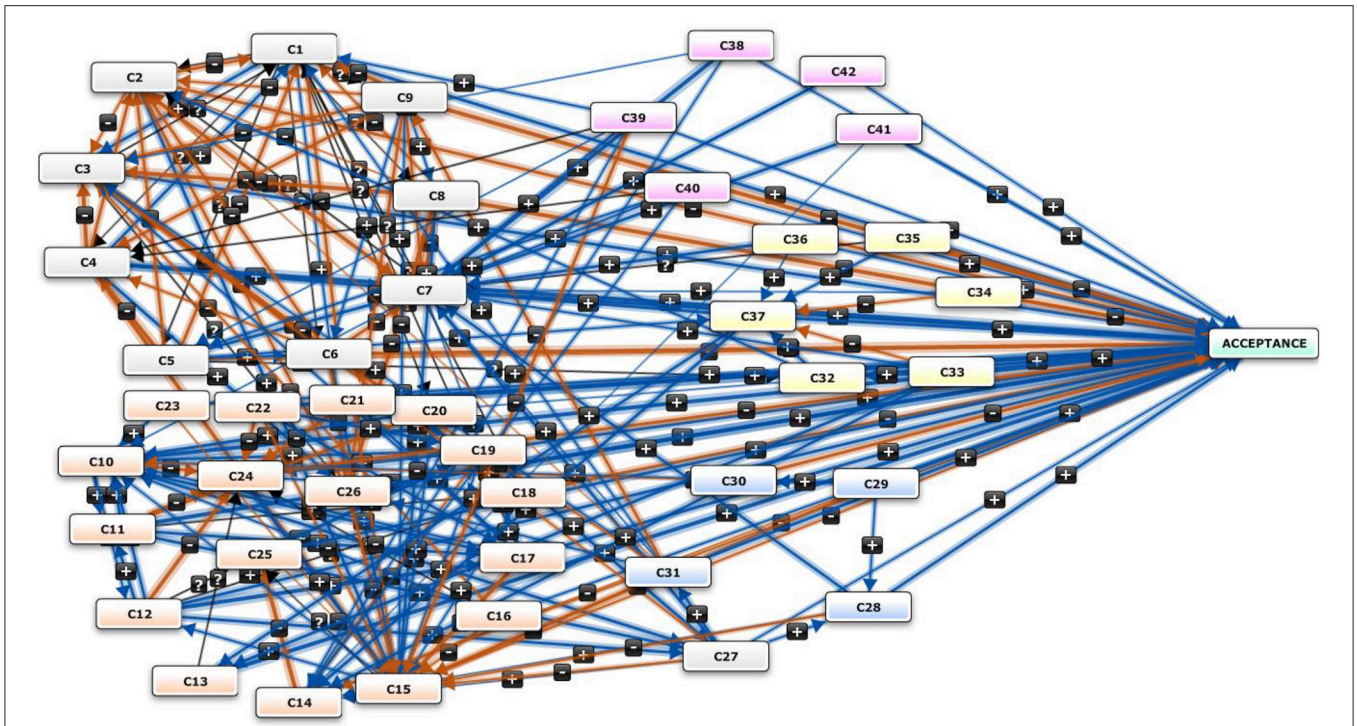

FIGURE 2 | The resulting FCM from the experts and stakeholder analysis.

TABLE 1 | General FCM statistics.

FCM properties	Value
Total components	43
Total connections	209
Density	0.115725
Connections per Component	4.860465
Number of driver components	14
Number of receiver components	1
Number of ordinary components	28
Complexity score	0.071429

companies involved etc.). Respectively, the average number of connections was 158, ranging from 123 to 209 according to different participants. For the merged FCM shown in **Figure 2**, a density of 0.115725 is deduced, with average Connections per Component raised up to 4.860465.

Another structural measure of FCM is the Hierarchy Index which is defined by the following equation and depends on the out degree (*od*) of each concept (node) in an FCM of *N* concepts (MacDonald, 1983).

$$h = \frac{12}{(N-1)\,N(N+1)} \sum_i \left[\frac{od\,(v_i) - (\sum od\,(v_i))}{N} \right]^2$$

When h is equal to 1, the mapping is completely hierarchical, and when it is equal to 0, the mapping is completely democratic (Ozesmi and Ozesmi, 2004). The hierarchy index of the FCM was calculated to be 0.137, making it very close to 0 and therefore highly democratic. Of course there is diversification of the hierarchy index in the case of the individual FCMs as opposed to the merged one. Obviously, the collective case increases the number of nodes, as it affects the in-degree and out-degree of these nodes, making the FCM more democratic and its system's steady state more resistant to the alterations of individual concepts. The concept with the highest centrality, as expected, was the "Acceptance" with a very high score of 24.83. Furthermore, the most central concepts directly affecting the Acceptance concept were the following, in decreasing order of their complexity: WBF Product Certification 11.32, Risk perception 11.08, Equity of decision making processes 6.64, Uncertainty toward the settlement of the new industry 6.51 and Well-being of citizens 6.09. This depicts the direct association of the social issues (primarily) and the environmental issues (secondly) to affect this decision.

To the best of the authors' knowledge, there does not exist any relevant research that could establish the current state and values of the environmental, health, social, governmental, economic and technological oriented concepts involved in the creation of the FCM depicted in **Figure 2**. For this reason, we consider the steady state of the FCM model as the initial scenario to start our analysis. In order to make evaluations and draw conclusions, we examined the worst case and the best case scenario as compared to the steady state. The worst case scenario is set up with all driver concepts to have the value of 0.1. On the opposite side the best case scenario is set up with all driver concepts to have

TABLE 2 | Categorization, InDegree, OutDegree, Centrality and Type of Concepts in the FCM.

	Conc. num.	Conc. name	In	Out	Centrality	Type
Environmental and Health	C1	Local Climate Status	4.66	1.87	6.53	ordinary
	C2	WBF bi-product production hazards	2.65	4.6	7.25	ordinary
	C3	Local Tourism	6.25	0.5	6.75	ordinary
	C4	Gas (CO2) emission reduction	1.98	5.5	7.48	ordinary
	C5	WBF raw material preprocessing	0.3	3.73	4.03	ordinary
	C6	Transport emissions	1.32	5.49	6.81	ordinary
	C7	WBF Product Certification	10.48	0.84	11.32	ordinary
	C8	Smell / Noice	0.22	4.78	5	Ordinary
	C9	Traffic	0.51	5.64	6.15	ordinary
Social	C10	Stakeholder participation	4.08	4.6	8.68	ordinary
	C11	Stakeholder specific knowledge	1.06	4.49	5.55	ordinary
	C12	Exposure on previous WBF projects	0.65	4.55	5.2	ordinary
	C13	Local job generation	1.33	0.99	2.32	ordinary
	C14	Intervention of non-local businessman	2.27	1.67	3.94	ordinary
	C15	Risk perception	9.95	1.13	11.08	ordinary
	C16	Mass media publicity	0	1.39	1.39	driver
	C17	Public Trust	4.76	2.44	7.2	ordinary
	C18	Bias	0.35	1.61	1.96	ordinary
	C19	Equity of decision making processes	3.03	3.61	6.64	ordinary
	C20	Consumer/citizen awareness	0.68	1.08	1.76	ordinary
	C21	Inclusiveness	0	3.28	3.28	driver
	C22	Flexibility	0	3.4	3.4	driver
	C23	Stakeholder Training	0	0.69	0.69	driver
	C24	Uncertainty toward the settlement of the new industry	4.87	1.64	6.51	ordinary
	C25	Equity in sharing WBF product profit	0.98	1.79	2.77	ordinary
	C26	Well-being of citizens	4.61	1.48	6.09	ordinary
Government-Laws	C27	WBF policies	2.82	2.58	5.4	ordinary
	C28	Permanence of policies	0.81	1.42	2.23	ordinary
	C29	Competent authority participation	0	2.06	2.06	driver
	C30	Bureaucracy	0.19	0.82	1.01	ordinary
	C31	Geographic dispersion of WBF sources	0.55	3.15	3.7	ordinary
Economic	C32	Power of Plant	0.52	1.06	1.58	ordinary
	C33	WBF product availability	0	2.41	2.41	driver
	C34	Project installation cost	0	0.54	0.54	driver
	C35	Land cost	0	0.53	0.53	driver
	C36	Agricultural sector profitability	0	1.27	1.27	driver
	C37	WBF product profit	1.73	2.83	4.56	ordinary
Technological	C38	Project structure efficiency	0	1.65	1.65	driver
	C39	Well known technology used	0	2.01	2.01	driver
	C40	Experience in setting up WBFs	0	1.06	1.06	driver
	C41	Innovation	0	1.19	1.19	driver
	C42	Adoption of technology by the consumers	0	1.07	1.07	driver
	C43	ACCEPTANCE	24.83	0	24.83	receiver

the value of 1. In **Figure 3** we depict the analysis where in the worst case scenario a decrease of about 1% is shown in the "Social Acceptance" receiver concept when it is compared to the original steady state scenario which was set as the base for the analysis. In the same figure, we also observe the biggest decrease in the "WBF Product Certification" concept rising up to 18% with the "Intervention of non-local businessman" to follow having an overall 11% decrease. These two values show

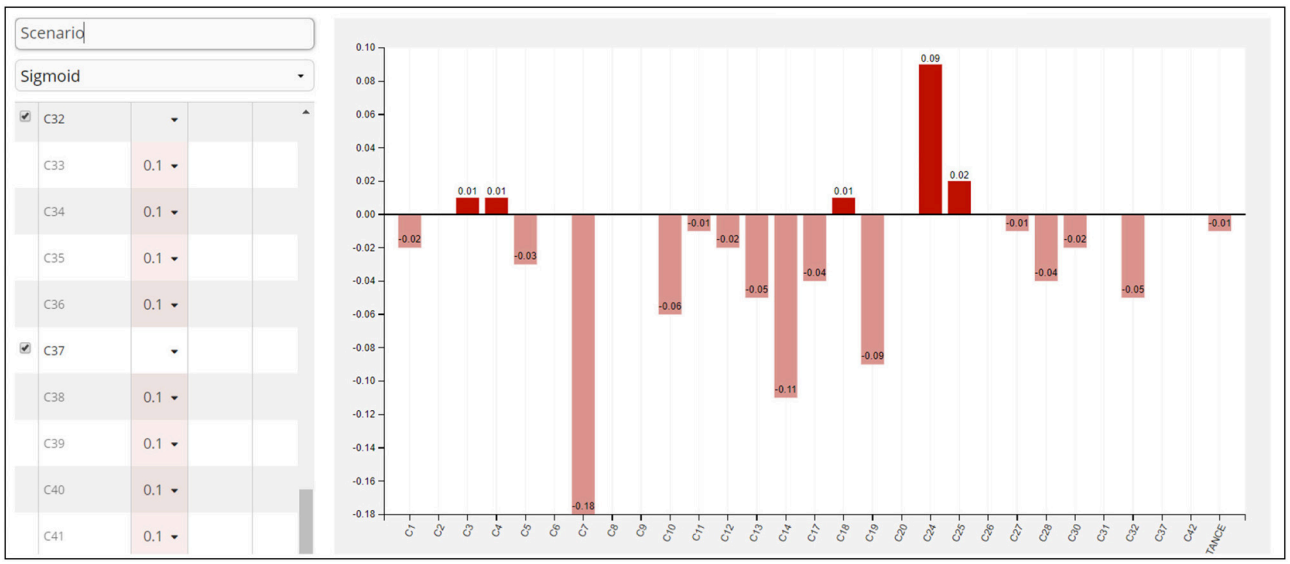

FIGURE 3 | The effect of the driver concepts in the full FCM for the worst case scenario compared to the steady state.

that the relation of the driver concepts for this FCM to the "WBF Product Certification" and the "Intervention of non-local businessman" concepts is driven by what we call negative causality. The meaning of this great decrease of concept C7 and C14, respectively is that a small increase of the driver concepts causes the highest irrelevance to them. Therefore, these two concepts are the ones that they are the least affected in positive changes of the driver concepts in the FCM. The values of 18 and 11% decrease, respectively are not significant but the fact of the greater negatively causality is of great importance. The highest increases appear on the "Uncertainty toward the settlement of the new industry" and "Equity in sharing WBF product profit" scoring a 9 and 2% increase, respectively.

On the opposite side, the best case scenario is set up with all driver concepts to have the value near the value of 1. That means that we set up our model so that driver concepts are the ones that primarily affect the FCM as opposed to the rest of the ordinary concepts. Similarly in this case and after setting up all the driver concepts in the steady analysis to the value of 1 we observe the difference on the ordinary and receiver concepts giving special priority on the final receiver concept of the "Social Acceptance" (see **Figure 4**). We observe a 10% increase in the "Social Acceptance" receiver concept when it is compared to the original steady state scenario which was set as the base for the analysis. Also several ordinary concepts behave in a similar way with representative the "Intervention of non-local businessman" with an increase of 10% and the "Consumer/citizen awareness" with an increase of 9%. In the inverse side concept C15 in **Figure 4** which is the "Risk perception" is decreased as expected with a decrease of 12% and concept C24 (Uncertainty toward the settlement of the new industry) performs accordingly with a decrease of 7%. The significance of the highest decrease of concept C15 in this Figure is similar as in **Figure 3** for the negative causality between the driver concepts and the concepts C15 and C24, respectively. The highest the increase of the driver concept makes the concepts C15 and C24 to be insignificant for the social acceptance receiver concept. The values of the decrease are as much important as the fact of signifying the least relevant ordinary concepts C15 and C24 in the model. For this case also, it was expected that the biggest increase of the driver concepts will decrease the risk (for example the bigger the Mass media publicity the smaller the risk reception and similarly this holds for the rest of the driver concepts).

Dynamic Scenario Analysis of the Social Issues

The size and complexity of the FCM conducted in sections Description of the Case Study and FCM Steady State Analysis however make the dynamic simulations needed for scenario analysis of the model less efficient. Such simulations on the extreme case (all concepts used as variables with semi-continuity on the values assigned between 0 and 1) run for long time periods to converge. Furthermore, the combinations of fixed value and variable value concepts are of exponential nature in this case, thus making us unable to explore the dynamic interactions between all concepts in the merged FCM. For this reason, we developed a second FCM based only on the concepts related to the social issues, trying to discover how only these aspects affect the social acceptance of WBFs. The graph achieved is shown in **Figure 5**, and from now on, it will be denoted as Social_FCM.

For this case, the total number of concepts including "Social Acceptance" rises up to 18, with the total number of associations between concepts to be 60. For this case again, the only receiver concept is the "Social Acceptance," with 7 Driver components and 10 Ordinary. The hierarchy index for this case was calculated to 0.0023, making the FCM slightly "more democratic" than the previous one. The general statistics of the Social_FCM are shown

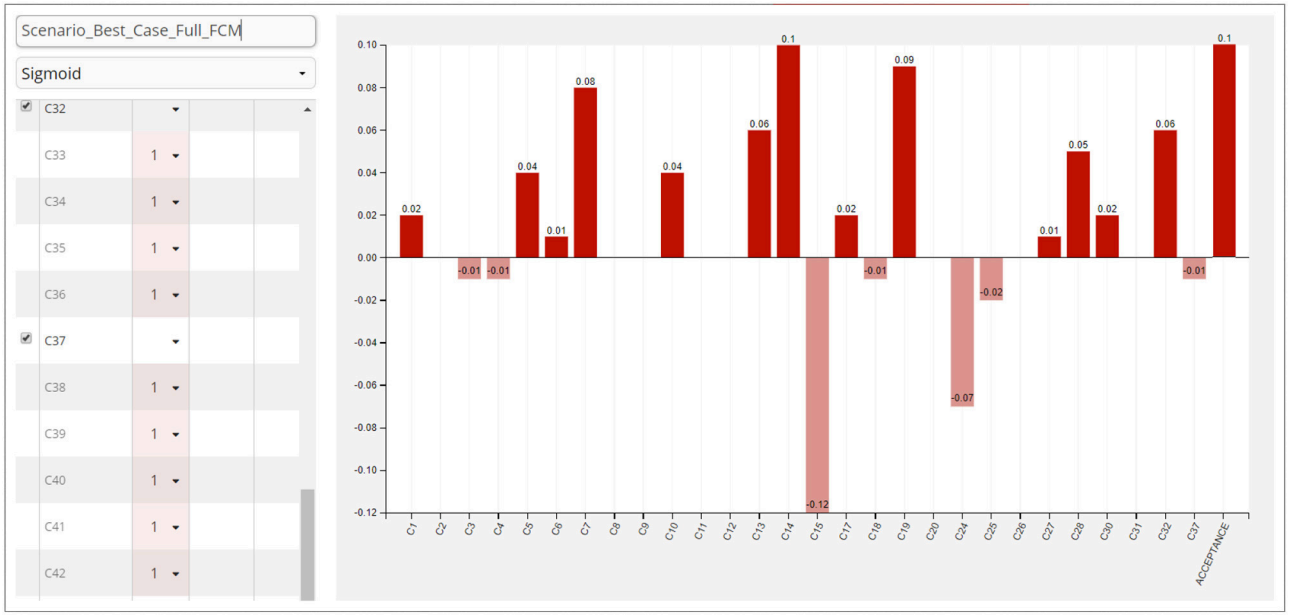

FIGURE 4 | The effect of the driver concepts in the full FCM for the best case scenario compared to the steady state.

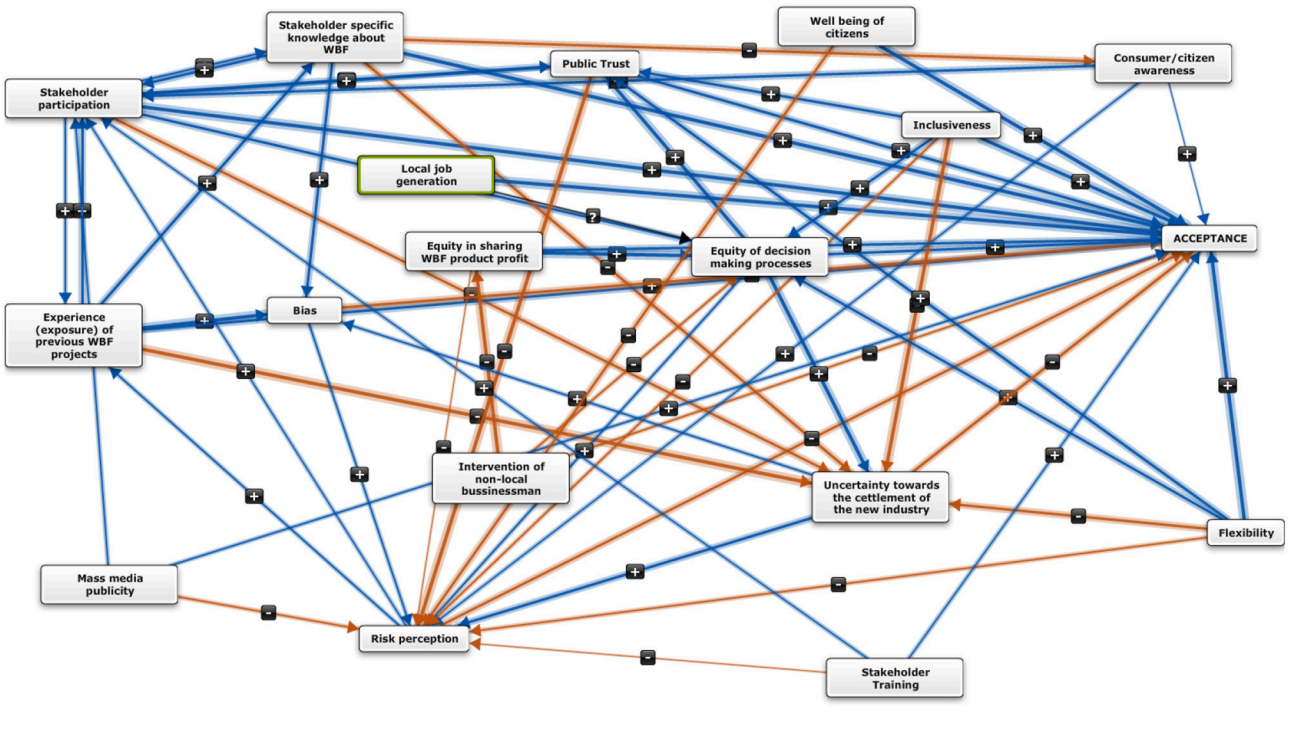

FIGURE 5 | The FCM emanating from only the social aspects affecting acceptance of WBFs.

in **Table 3** and the degrees and centralities of all the concepts in **Table 4**.

For the resulted FCM, we run a significant amount of simulations to explore the nature of the associations between the related concepts in the map and the importance of one concept (defuzzified concept value). We focused on the convergence of the FCM after a certain number of iterations, using the clamping process as stated by Kosko (1986). According to clamping, a

TABLE 3 | General Social_FCM Statistics.

Social_FCM properties	Value
Total components	18
Total connections	60
Density	0.1960784314
Connections per component	3.33333333
Number of driver components	7
Number of receiver components	1
Number of ordinary components	10
Complexity score	0.1428571429

TABLE 4 | InDegree, OutDegree, Centrality and Type of Concepts in the Social_FCM.

Conc. num.	Conc. name	In	Out	Centrality	Type
C1	Stakeholder participation	3.42	3.86	7.28	ordinary
C2	Stakeholder specific knowledge	1.06	3.83	4.89	ordinary
C3	Exposure on previous WBF projects	0.65	3.84	4.49	ordinary
C4	Local job generation	0	0.99	0.99	driver
C5	Intervention of non-local businessman	0	1.65	1.65	driver
C6	Risk perception	4.45	1.15	5.6	ordinary
C7	Mass media publicity	0	1.01	1.01	driver
C8	Public Trust	3.1	2.03	5.13	ordinary
C9	Bias	2	1.09	3.09	ordinary
C10	Equity of decision making processes	3.03	3.01	6.04	ordinary
C11	Consumer/citizen awareness	0.68	1.08	1.76	ordinary
C12	Inclusiveness	0	3.24	3.24	driver
C13	Flexibility	0	3.46	3.46	driver
C14	Stakeholder Training	0	0.65	0.65	driver
C15	Uncertainty toward the settlement of the new industry	4.93	1.69	6.62	ordinary
C16	Equity in sharing WBF product profit	0.98	1.81	2.79	ordinary
C17	Well-being of citizens	0	1.46	1.46	driver
C18	ACCEPTANCE	11.55	0	11.55	receiver

subset of the concepts is selected to be studied, i.e., to change values as opposed to the rest, in order to understand their effect in reaching the equilibrium end states. We may use all the ordinary and driver concepts for this process, although the receiver concepts cannot be included. However, it is intuitively logical to clamp only the driver concepts, as they primarily participate on the influence of the social acceptance receiver concept. According to this process, each of the concepts is increased or decreased accordingly, and the resulting concept value vector is compared to the steady state vector of the FCM (Vasslides and Jensen, 2016). For our case, the changes are compared to the initial Social_FCM steady state. **Figure 6** shows an indicative simulation of the Social_FCM, with all 18 concepts ranging from 0 to 1 along with their final converged values, and the corresponding curves of concept activation levels per each iteration. Simulations are run for all cases of activation functions available in combination to the available transformation functions, as described with the equations in section Basic Concepts for FCMs. Furthermore, any other combination and mixture of variable and ordinary concepts can easily produce individualized effects of specific concepts to Social Acceptance.

Similarly to the previous subsection, we consider the steady state of the Social_FCM model as the initial scenario to start our analysis. Again, in order to draw conclusions for the effect of the driver concepts to the receiver and ordinary concepts of the Social_FCM, we examined the worst case and the best case scenario as compared to the steady state. The worst case scenario is set up with all driver concepts to have the value of 0.1 as in the full FCM use case before. On the opposite side, the best case scenario is set up with all driver concepts to have the value of 1. In **Figure 7**, we depict the analysis where in the worst case scenario a decrease of about 3% is shown in the "Social Acceptance" receiver concept when it is compared to the original steady state scenario that was set as the base for the analysis. In the same figure, we also observe the biggest decrease in the "Public Trust" concept rising up to 8%, with the "Equity of decision making processes" to follow having an overall 16% decrease. The highest increases appear on the "Risk perception," "Uncertainty toward the settlement of the new industry" and "Equity in sharing WBF product profit," recording a 16, 8, and 8% increase, respectively.

It must be noted that **Figure 7** does not depict absolute concept values, but only the increase or the decrease of these values relatively to the corresponding values of the steady state. For the case of the worst scenario explained previously, the concept values after convergence, as well as the curves of activation levels as they relate to the number of iterations, are shown in **Figure 8**.

On the opposite side, the best case scenario was run using the same activation function to be comparable with the previous scenario. For the best case, all seven driver concepts are set to value 1 and we study the decrease or increase of the ordinary and receiver concepts relatively to the steady state. It should be noted that, on **Figure 9**, we have: increase on the "Stakeholder participation," decrease of the "Risk perception," increase on "Public trust," decrease on "Bias," increase on "Equity of decision making processes," decrease on "Uncertainty toward the settlement of the new industry," decrease on the "Equity in sharing WBF product profit," and finally an increase on the "Social acceptance." It should also be noticed that these increases or decreases are relatively to the worst case scenario.

All increases and decreases are judged logical expect the concept of "Equity of decision making processes." This and only misbehavior of the FCM is minor for two reasons: firstly the concept affected is ordinary and secondly the receiver concept is not affected. Similarly, on **Figure 10** the curves of activation levels as they relate to the number of iterations are shown.

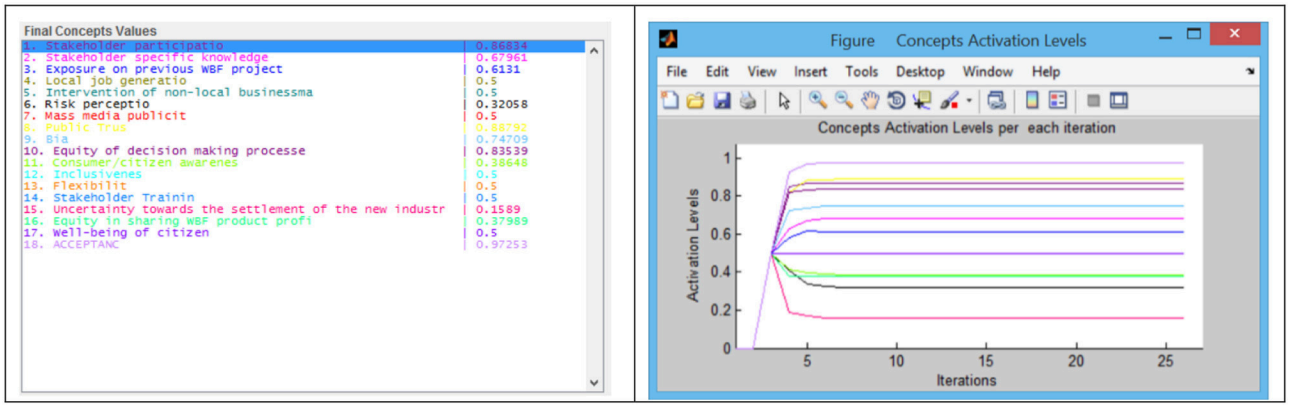

FIGURE 6 | Indicative dynamic simulation of the Social_FCM with the converged values of the social concepts and the corresponding curves of concept activation levels per each iteration.

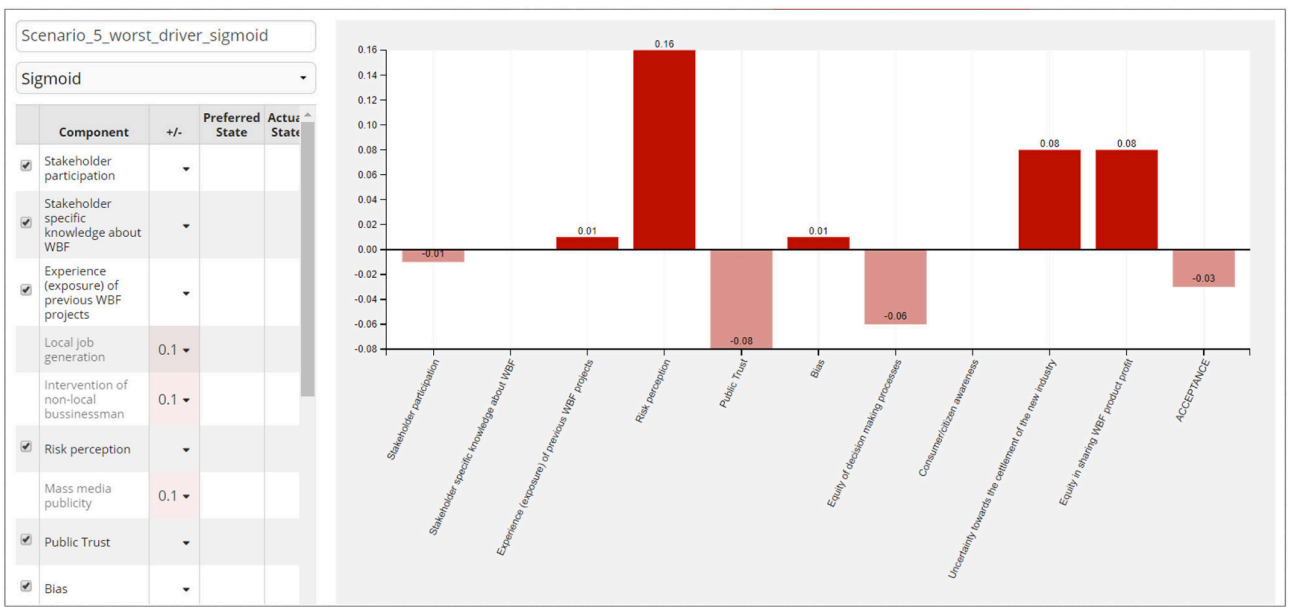

FIGURE 7 | The effect of the driver concepts in the Social_FCM for the worst case scenario compared to the steady state.

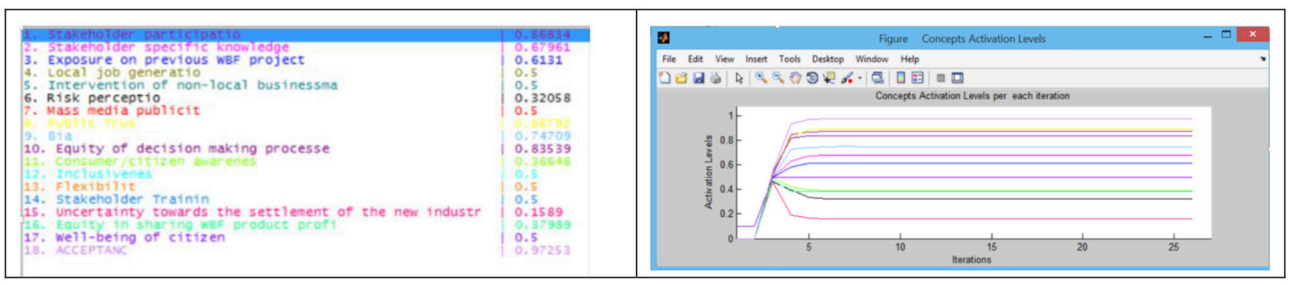

FIGURE 8 | Converged concept values and activation curves for the worst case scenario of the Social_FCM.

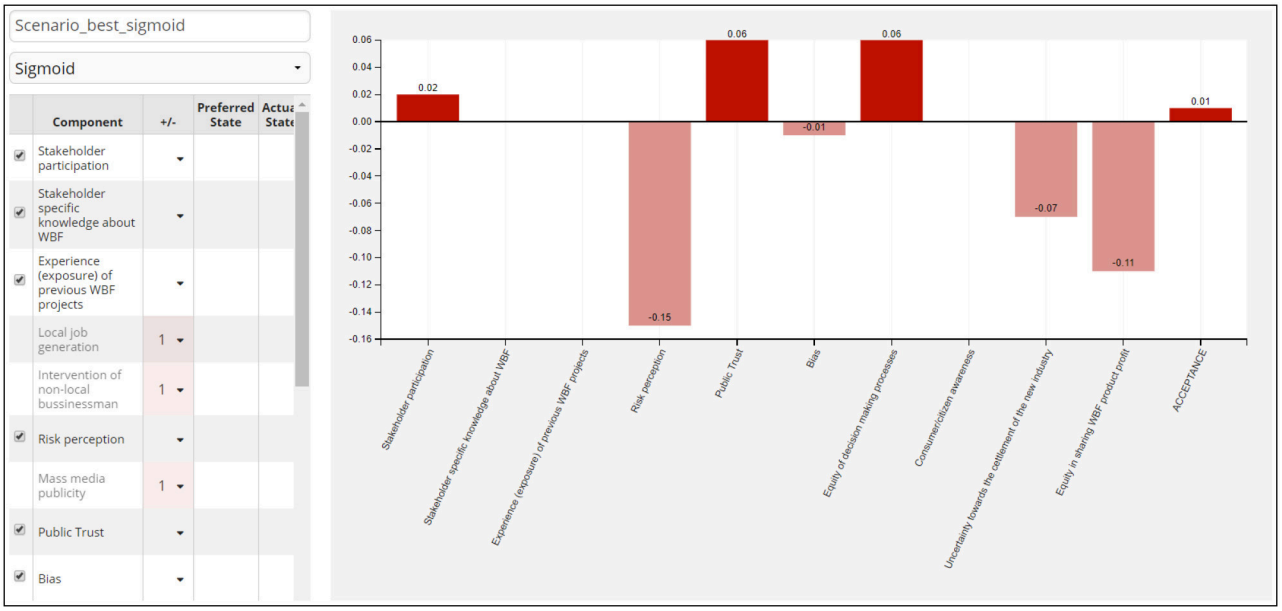

FIGURE 9 | The effect of the driver concepts in the Social_FCM for the best case scenario compared to the steady state.

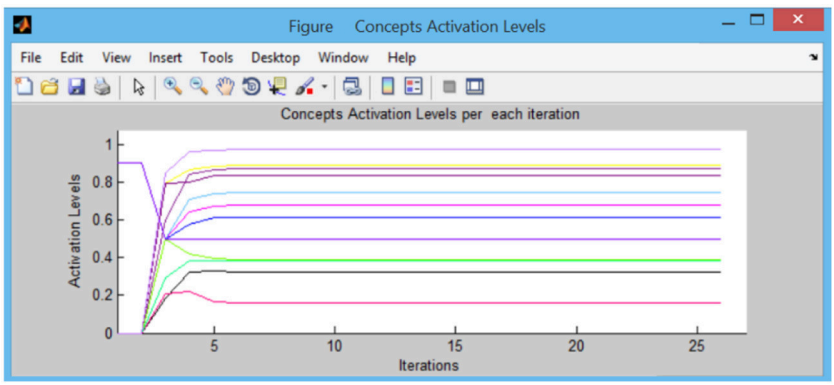

FIGURE 10 | Concept activation curves per each iteration for the best case scenario of the Social_FCM.

CONCLUSIONS AND FUTURE CHALLENGES

Waste biorefinery facilities (WBFs) development and sustainable waste management are still in infancy in the Southern Europe countries, due to limited allocated assets given, resulting in ischemic infrastructure and maintenance facilities. On the other hand, waste management is an enormously critical aspect because of the environmental, economical, technological and social consequences. For that reason, such large scale operations necessitate the coalition of large social bodies, stakeholders of diversified interest and competent authority policy makers.

Our methodology was two fold in relation to identifying the most important aspects that affect the social acceptance of WBF. Firstly, a Fuzzy Cognitive Map (FCM) was developed, which captures the interoperation of environmental, health, social, technological and economic concepts that influence the social acceptance of WBFs. Since the complicated structure of the resulted FCM did not allow any definite conclusion regarding the most influential concepts to the social acceptance, in the second phase we modeled the impacts of just the social aspects to "social acceptance" for WBFs. For this purpose, of smaller FCM was used, to show treads and general directions in identifying the most determinant factors affecting the public opinion. Our analysis was also twofold: a) Steady State, where the FCM resulted as an amalgamation of stakeholder and expert knowledge, identifying five major classes of issues and b) Dynamic scenario analysis, after extracting only the social components, resulting in a much smaller FCM. For the second case, we were able to highlight the effect of the driver concepts, comparing the worst case and best case scenarios with the steady state analysis results. Various simulations were tried also, with a combination

of activation and transformation functions selected as well as a variety of value levels between the worst and best case scenarios for a subset of ordinary and driver components.

More specifically, the analysis revealed that concepts such as "Uncertainty toward the settlement of the new industry," "Risk perception," "Stakeholder participation," "Consumer/Citizen awareness," "Equity of decision making processes" are the most influential factors to "Social Acceptance." This was what the dynamic scenario analysis has verified for the Social_FCM part of the FCM that was originally developed. However, there are some shortcomings to this study, which should be taken into account. First, the representation of the model and its dynamic behavior was focused only on the social aspects. This happened because the preliminary analysis of the full FCM resulted in a complicated structure increasing tremendously the state space of the FCM. For that reason, around 25 issues/concepts were cut from the original FCM overcoming the inability to provide dynamic scenario analysis with so many concepts. This concept reduction process also diminishes several indirect interrelations of the social concepts with the concepts of the other classes (environmental, economic, technological etc.). Thus, these interrelations and their impacts are not taken into consideration and their result in increase or decrease of the "Social Acceptance" cannot be revealed in the second version of the FCM. Secondly, the impact of the number of experts/stakeholders deployed to the developing task of the FCMs was not examined. There are studies that highlight the fact that, the greater the expert body the more stable the version of the FCM produced. Also, the improvement of the conceptual model describing the WBFs social acceptance is shown to be dependent of learning methodologies used.

Based on our discussion above and the input received from stakeholders, there are several recommended areas of focus as industry moves toward the optimization of WBF application. However, the most important issue is to design a competitive waste-biorefinery concept by systematic participation of all the factors that affect the decision and policy making in WBF application. The technology knowledge must be transmitted to various stakeholders in the wider society and the final decision must integrate not only the technological and economic advantages but also health and social acceptance. For that reason, social acceptance must always be present alongside life-cycle assessment and economic value and environmental impact analysis tools for the WBF application. The bottom line is that it is critical to engage local communities in the development and management of WBFs in order to elicit the view of lay people, as a means to amend burdens relating to social factors and to avoid the "NIMBY" phenomenon. We believe therefore that the enlargement of the present study with further investigation in this research area can provide a valuable tool for competent authorities and policy makers in developing WBFs.

AUTHOR CONTRIBUTIONS

All authors listed have made a substantial, direct and intellectual contribution to the work, and approved it for publication.

REFERENCES

Alizadeh, S., Ghazanfari, M., Jafari, M., and Hooshmand, S. (2007). Learning FCM by tabu search. *Int. J. Comput. Sci.* 2, 142–149.

Axelrod, R. (1976). "The analysis of cognitive maps," in *Structure of Decision: The Cognitive Maps of Political Elites*, ed R. Axelrod (Princeton, NY: Princeton University Press), 55–73

Beigl, P., Lebersorger, S., and Salhofer, S. (2008). Modelling municipal solid waste generation: a review. *J. Waste Manag.* 28, 200–214. doi: 10.1016/j.wasman.2006.12.011

Bovea, M. D., and Powell, J. C. (2006). Alternative scenarios to meet the demands of sustainable waste management. *J. Environ. Manage.* 79, 115–132. doi: 10.1016/j.jenvman.2005.06.005

Brion, D. J. (2015). An essay on LULU, NIMBY, and the problem of distributive justice. *Boston College Environ. Affairs Law Rev.* 15, 1–68.

Ciment, J. (2015). *Social Issues in America: An Encyclopedia. Business & Economics.*

CTV Kitchener (2012). *Group of Elmira Residents Protesting Biofuel Plant*. Published Sunday, April 15, 2012 5:35PM EDT. Available online at: http://kitchener.ctvnews.ca/group-of-elmira-residents-protestingbiofuel-plant-1.796466 [Last accessed June 21st 2018].

Cucek, L., Klemes, J. J., Varbanov, P. S., and Kravanja, Z. (2013). Dealing with high-dimensionality of criteria in multi-objective optimization of biomass energy supply network. *Ind. Eng. Chem. Res.* 52 , 7223–7239. doi: 10.1021/ie302599c

Dear, M. (1992). Understanding and overcoming the NIMBY syndrome. *J. Am. Plann. Assoc.* 58, 288–300. doi: 10.1080/01944369208975808

den Boer, E., and Lager, J. (2007). LCA-IWM: a decision support tool for sustainability assessment of waste management systems. *J. Waste Manage.* 27, 1032–1045. doi: 10.1016/j.wasman.2007.02.022

Devine-Wright, P. (2009). Rethinking NIMBYism: the role of place attachment and place identity in explaining place-protective action. *J. Commun. Appl. Soc. Psychol.* 19, 426–441. doi: 10.1002/casp.1004

Dickerson, J. A., and Kosko, B. (1994). Virtual worlds as fuzzy cognitive maps. *Presence* 3, 173–189. doi: 10.1162/pres.1994.3.2.173

Dowling, A. W., Ruiz-Mercado, G., and Zavala, V. M. (2016). A framework for multi-stakeholder decision-making and conflict resolution. *Comp. Chem. Eng.* 90, 136–150. doi: 10.1016/j.compchemeng.2016.03.034

Fortenbery, T., Randall, D., Steven, C., and Amiel, L. (2013). The location decisions of biodiesel refineries. *Land Econ.* 89, 118–136. doi: 10.3368/le.89.1.118

Geraili, A., and Romagnoli, J. A. (2015). A multi-objective optimization framework for design of integrated biorefineries under uncertainty. *AIChE J.* 61 3208–3222. doi: 10.1002/aic.14849

Gray, S. A., Zanre, E., and Gray, S. R. J. (2014). "Fuzzy cognitive maps as representations of mental models and group beliefs: theoretical and technical issues," in *Fuzzy Cognitive Maps for Applied Sciences and Engineering—From Fundamentals to Extensions and Learning Algorithms.* Papageorgiou, E. I. ed (Heidelberg: Springer), 29–48.

Graymore, M. L. M., Sipe, N. G., and Rickson, R. E. (2008). Regional sustainability: how useful are current tools of sustainability assessment at the regional scale? *J. Ecol. Econom.* 67, 362–372. doi: 10.1016/j.ecolecon.2008.06.002

Gregory, R., Failing, L., Harstone, M., Long, G., McDaniels, T., and Ohlson, D. (2012). *Structured Decision Making: A Practical Guide to Environmental Management Choices.* (New York, NY: Wiley).

Groumpos, P., and Anninou, A. (2017). A critical overview of modeling methods and decision support systems for complex dynamic systems. *Ann. Faculty Eng. Hunedoara* 15, 17–26.

Haddad, M. A., Gary, T., and Francis, O. (2009). Locational choices of the ethanol industry in the Midwest Corn Belt. *Econ. Dev. Q.* 24, 74–86. doi: 10.1177/0891242409347722

Halder, P., Prokop, P., Chang, C.-Y., Usak, M., Pietarinen, J., Havu-Nuutinen, S., et al. (2012). International survey on bioenergy knowledge, perceptions, and attitudes among young citizens. *Bioenergy Res.* 5, 247–261. doi: 10.1007/s12155-011-9121-y

Hosseini, A., Zolfagharzadeh, M. M., Asghar Sadabadi, A., Aslani, A., and Jafari, H. (2018). Social acceptance of renewable energy in developing countries: challenges and opportunities. *Distribut. Gener. Alternat. Energy J.* 33, 31–48. doi: 10.1080/21563306.2018.11969264

Huerga, A. V. (2002). *A Balanced Differential Learning Algorithm in Fuzzy Cognitive Maps*. 16th International Workshop Qualitat. Reason., Catalonia, Spain.

Kok, K., Bärlund, I., Flörke, M., Holman, I., Gramberger, M., Sendzimir, J., et al. (2015). European participatory scenario development: strengthening the link between stories and models. *Climate Change* 128, 187–200. doi: 10.1007/s10584-014-1143-y

Konar, A., and Chakraborty, U. K. (2005). Reasoning and unsupervised learning in a fuzzy cognitive map. *Inf. Sci.* 170, 419–441. doi: 10.1016/j.ins.2004.03.012

Kosko, B. (1986). Fuzzy cognitive maps. *Int. J. Man Mach. Stud.* 24, 65–75. doi: 10.1016/S0020-7373(86)80040-2

Kosko, B. (1987). "Adaptive inference in fuzzy knowledge networks," in *Proceedings of the First IEEE International Conference on Neural Networks,* vol. II, San Diego, California, 261–268.

Koulouriotis, D. E., Diakoulakis, I. E., and Emiris, D. M. (2001). "Learning fuzzy cognitive maps using evolution strategies: a novel schema for modeling and simulating high-level behavior," in *Proceedings IEEE Congress. Evoluation Computer*, 364–371.

Lakioti, E. N., Moustakas, K. G., Komilis, D. P., Domopoulou, A. E., and Karayannis, V. G. (2017). Sustainable solid waste management: Socio-economic considerations. *Chem. Eng. Trans.* 56, 661–666. doi: 10.3303/CET1756111

Lambert, E. (2009). Nimby wars. Published Jan. 29th 2009. Available online at: http://www.forbes.com/forbes/2009/0216/098.html [Last accessed June 21st 2018].

Liew, W. H., Hassim, M. H., Ng, D. K. S., and Chemmangattuvalappil, N. (2015). Systematic framework for sustainability assessment of biodiesel production: preliminary engineering stage. *Ind. Eng. Chem. Res.* 54, 12615–12629. doi: 10.1021/acs.iecr.5b02894

Lin, Y., and Yang, W. (2018). Application of multi-objective genetic algorithm based simulation for cost-effective building energy efficiency design and thermal comfort improvement. *Front. Energy Res.* 6:25. doi: 10.3389/fenrg.2018.00025

Lopolito, A., Prosperi, M., and Sisto, R. (2009). *Socio-Economic Implications of the Development of a Bio-Refinery: An Analysis with Fuzzy Cognitive Maps*. Available online at: http://unifg.academia.edu/AntonioLopolito/Papers/1053338/Socio-Economic_Implications_Of_The_Development_Of_A_BioRefinery_An_Analysis_With_Fuzzy_Cognitive_Maps.

MacDonald, N. (1983). *Trees and Networks in Biological Models*. New York, NY: John Wiley.

Mateou, N. H., Moiseos, M., and Andreou, A. S. (2005). "Multi-objective evolutionary fuzzy cognitive maps for decision support," in Proceedings IEEE Congress Evoluation Computer vol. 1, Edinburgh 824–830. Mental Modeler Manual, 2018. Available online at: www.mentamodeler.org [Last accessed 23rd of June, 2018].

McGuire, J. B., Leahy, J. E., Marciano, J. A., Lilieholm, R. J., and Teisl, M. F. (2017). Social acceptability of establishing forest-based biorefineries in Maine, United States. *Biomass Bioenergy* 105, 155–163. doi: 10.1016/j.biombioe.2017.06.015

Mielke, J., Vermaßen, H., Ellenbeck, S., Fernandez Milan, B., and Jaeger, C. (2016). Stakeholder involvement in sustainability science—A critical view. *Energy Res. Soc. Sci.* 17, 71–81. doi: 10.1016/j.erss.2016.04.001

Munda, G. (2004). Social multi-criteria evaluation: methodological foundations and operational consequences. *Eur. J. Oper. Res.* 158, 662–677. doi: 10.1016/S0377-2217(03)00369-2

Munda, G. (2008). *Social Multi Criteria Evaluation for a Sustainable Economy*. Berlin:Springer.

Nizami, A. S., Rehan, M., Waqas, M., Naqvi, M., Ouda, O. K. M., Shahzad, K., et al. (2017a). Waste biorefineries: enabling circular economies in developing countries. *Bioresour. Technol.* 241, 1101–1117. doi: 10.1016/j.biortech.2017.05.097

Nizami, A. S., Shahzad, K., Rehan, M., Ouda, O. K. M., Khan, M. Z., Ismail, I. M. I., et al. (2017b). Developing waste biorefinery in Makkah: a way forward to convert urban waste into renewable energy. *Appl. Energy* 186, 189–196. doi: 10.1016/j.apenergy.2016.04.116

Novak, J. D., and Cañas, A. J. (2008). *The theory underlying concept maps and how to construct and use them*. Technical Report IHMC CmapTools 2006-01 Rev 01-2008. Florida Institute for Human and Machine Cognition, Pensacola, Florida. Available online at: http://cmap.ihmc.us/publications/researchpapers/theoryunderlyingconceptmaps.pdf

Ozesmi, U., and Ozesmi, S. L. (2004). Ecological models based on people's knowledge: a multistep fuzzy cognitive mapping approach. *Ecol. Modell.* 176, 43–64. doi: 10.1016/j.ecolmodel.2003.10.027

Papageorgiou, E., Stylios, C. D., and Groumpos, P. P. (2003). "Fuzzy cognitive map learning based on nonlinear Hebbian rule," in *Proceedings Australasian Joint Conference on Artificial Intelligence* (Perth, WA), 256–268.

Papageorgiou, E., Stylios, C. D., and Groumpos, P. P. (2004). Active Hebbian learning algorithm to train fuzzy cognitive maps. *Int. J. Approx. Reason.* 37, 219–249. doi: 10.1016/j.ijar.2004.01.001

Papageorgiou, E. I., and Groumpos, P. P. (2005). A weight adaptation method for fine-tuning fuzzy cognitive map causal links. *Soft Comput. J.* 9, 846–857. doi: 10.1007/s00500-004-0426-z

Petalas, Y. G., Papageorgiou, E. I., Parsopoulos, E. I., Groumpos, P. P., and Vrahatis, M. N. (2005). "Fuzzy cognitive maps learning using memetic algorithms," in *Proceedings Conference Computational Methods in Sciences and Engineering,* Loutraki 1420–1423.

Raskin, J. D. (2002). "Constructivism in psychology: personal construct psychology, radical constructivism, and social constructionism," in *Studies in Meaning: Exploring Constructivist Psychology* ed Raskin, J. D., and Bridges, S. K. (New York, NY: Pace University Press), 1–25.

Rehan, M., Gardy, J., Demirbas, A., Rashid, U., Budzianowski, W. M., Pant, D., et al. (2018). Waste to biodiesel: a preliminary assessment for Saudi Arabia. *Bioresour. Technol.* 250, 17–25. doi: 10.1016/j.biortech.2017.11.024

Sacchelli, S. (2014). Social acceptance optimization of biomass plants: a fuzzy cognitive map and evolutionary algorithm application. *Chem. Eng. Trans.* 37, 181–186. doi: 10.3303/CET1437031

Scolobig, A., and Lilliestam, J. (2016). Comparing approaches for the integration of stakeholder perspectives in environmental decision making. *Resources* 5:37. doi: 10.3390/resources5040037

Selfa, T. (2010). Global benefits, local burdens? The paradox of governing biofuels production in Kansas and Iowa. *Renewable Agric. Food Syst.* 25, 129–142. doi: 10.1017/S1742170510000153

Stach, W., Kurgan, L., and Pedrycz, W. (2007). "Parallel learning of large fuzzy cognitive maps," in *Proceedings International Joint Conference Neural Network* (Orlando, FL), 1584–1589.

Stach, W., Kurgan, L., and Pedrycz, W. (2008). "Data driven nonlinear Hebbian learning method for fuzzy cognitive maps," in *Proceedings IEEE World Congress on Computational Intelligence*, Hong Kong, 1975–1981.

Stach, W., Kurgan, L. A., Pedrycz, W., and Reformat, M. (2005). Genetic learning of fuzzy cognitive maps. *Fuzzy Sets Syst.* 153, 371–401. doi: 10.1016/j.fss.2005.01.009

Stadler, P., Girardin, L., Ashouri, A., and Maréchal, F. (2018). Contribution of model predictive control in the integration of renewable energy sources within the built environment. *Front. Energy Res.* 6:22. doi: 10.3389/fenrg.2018.00022

Stirling, A. (2006). Analysis, participation and power: justification and closure in participatory multi-criteria analysis. *Land Use Policy* 23, 95–107. doi: 10.1016/j.landusepol.2004.08.010

Tigges, L. M., and Noble, M. (2012). Getting to yes or bailing on no: the site selection process of ethanol plants in Wisconsin. *Rural Sociol.* 77, 547–568. doi: 10.1111/j.1549-0831.2012.00092.x

Trutnevyte, E., Guivarch, C., Lempert, R., and Strachan, N. (2016). Reinvigorating the scenario technique to expand uncertainty consideration. *Climate Change* 135, 373–379. doi: 10.1007/s10584-015-1585-x

Van Asselt, M., and Rijkens-Klomp, N. (2002). A look in the mirror: Reflection on participation in integrated assessment from a methodological

perspective. *Glob. Environ. Chang.* 12, 167–184. doi: 10.1016/S0959-3780(02)00012-2

van der Horst, D. (2007). NIMBY or not? Exploring the relevance of locations and the politics of voiced opinions in renewable energy citing controversies. *Energy Policy* 35 2705–2714. doi: 10.1016/j.enpol.2006.12.012

Vasslides, J. M., and Jensen, O. P. (2016). Fuzzy Cognitive Mapping in support of integrated ecosystem assessments: developing a shared conceptual model among stakeholders. *J. Environ. Manage.* 166, 348–356. doi: 10.1016/j.jenvman.2015.10.038

Walter, G., and Gutscher, H. (2011). *Public Acceptance of Wind Energy and Bioenergy Projects in the Framework of Distributive and Procedural Justice Theories: Insights from Germany, Austria and Switzerland*. Zurich: The Advisory House.

Wolsink, M. (2012). "Wind power: basic challenge concerning social acceptance," in *Encyclopedia of Sustainability Science and Technology,* ed Meyers, R.A. New York, NY: Springer, 12218–12254.

Yatsalo, B. I., Kiker, G. A., Kim, J., Bridges, T. S., Seager, T. P., Gardner, K., et al. (2007). Application of multi-criteria decision analysis tools to two contaminated sediment case studies. *Integr. Environ. Assess. Manag.* 3, 223–233. doi: 10.1897/IEAM_2006-036.1

Yesil, E., and Dodurka, M. F. (2013). "Goal-oriented decision support using big bang-big crunch learning based fuzzy cognitive map: An ERP management case study," in *Proceedings 2013 IEEE International Conference on Fuzzy Systems (FUZZ-IEEE)*, 1–8.

Zhu, Y., and Zhang, W. (2008). "An integrated framework for learning fuzzy cognitive map using RCGA and NHL algorithm," in *Proceedings International Conference on Wireless Communications, Networking and Mobile Computing* (Dalian), 26, 10773–11195.

Conflict of Interest Statement: The authors declare that the research was conducted in the absence of any commercial or financial relationships that could be construed as a potential conflict of interest.

Advantages of publishing in Frontiers

OPEN ACCESS
Articles are free to read for greatest visibility and readership

FAST PUBLICATION
Around 90 days from submission to decision

HIGH QUALITY PEER-REVIEW
Rigorous, collaborative, and constructive peer-review

TRANSPARENT PEER-REVIEW
Editors and reviewers acknowledged by name on published articles

Frontiers
Avenue du Tribunal-Fédéral 34
1005 Lausanne | Switzerland

Visit us: www.frontiersin.org
Contact us: info@frontiersin.org | +41 21 510 17 00

REPRODUCIBILITY OF RESEARCH
Support open data and methods to enhance research reproducibility

DIGITAL PUBLISHING
Articles designed for optimal readership across devices

FOLLOW US
@frontiersin

IMPACT METRICS
Advanced article metrics track visibility across digital media

EXTENSIVE PROMOTION
Marketing and promotion of impactful research

LOOP RESEARCH NETWORK
Our network increases your article's readership